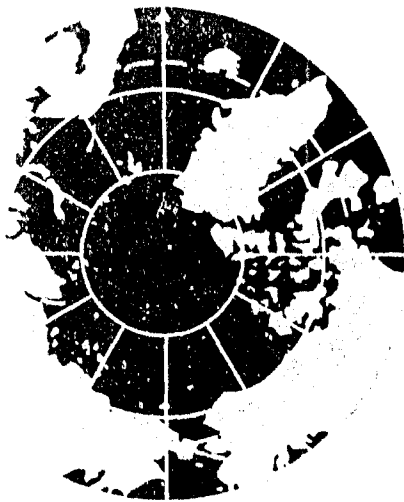


AD-A253 028

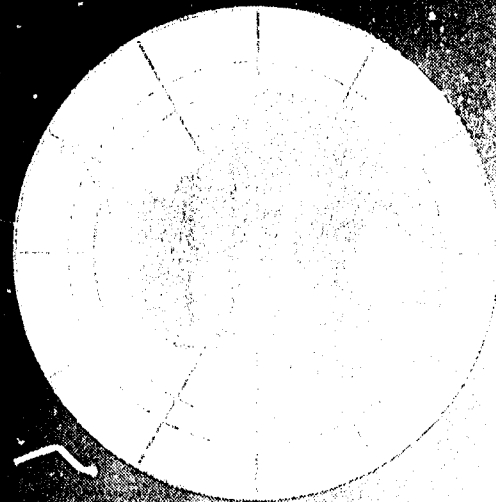


International Conference on the Role of the Polar Regions in Global Change

Vol. II



DTIC
ELECTE
APR 20 1992



This document has been approved
for public release and sale; its
distribution is unlimited.



Proceedings of a Conference
June 11-15, 1990 at the
University of Alaska Fairbanks

Alaska's Land, Sea and
Space Grant Institution
1917 75 years 1992

Best Available Copy

**Best
Available
Copy**

COMPONENT PART NOTICE

THIS PAPER IS A COMPONENT PART OF THE FOLLOWING COMPILATION REPORT:

TITLE: Proceedings of the International Conference on the Role of the Polar
Regions in Global Change Held in Fairbanks, Alaska on 11-15 June
1990. Volume 2.

TO ORDER THE COMPLETE COMPILATION REPORT, USE AD-A253 028.

THE COMPONENT PART IS PROVIDED HERE TO ALLOW USERS ACCESS TO INDIVIDUALLY AUTHORED SECTIONS OF PROCEEDING, ANNALS, SYMPOSIA, ETC. HOWEVER, THE COMPONENT SHOULD BE CONSIDERED WITHIN THE CONTEXT OF THE OVERALL COMPILATION REPORT AND NOT AS A STAND-ALONE TECHNICAL REPORT.

THE FOLLOWING COMPONENT PART NUMBERS COMPRISE THE COMPILATION REPORT:

AD#: AD-P007 311 thru AD-P007 367
 AD#: _____ AD#: _____
 AD#: _____ AD#: _____

Accession For	
NTIS CRA&I	<input checked="" type="checkbox"/>
DTIC TAB	<input type="checkbox"/>
Unannounced	<input type="checkbox"/>
Justification _____	
By _____	
Distribution /	
Availability Codes	
Dist	Avail and/or Special
A-1	

DTIC
ELECTE
JUL 08 1992
S A D

This document has been approved
 for public release and sale; its
 distribution is unlimited.

PAGES _____
ARE
MISSING
IN
ORIGINAL
DOCUMENT

International Conference on the Role
of the Polar Regions in Global Change:
Proceedings of a Conference Held June 11-15, 1990
at the University of Alaska Fairbanks

Volume II

Edited by

Gunter Weller
Cindy L. Wilson
Barbara A. B. Severin

Published by

Geophysical Institute
University of Alaska Fairbanks

and

Center for Global Change and Arctic System Research
University of Alaska Fairbanks
Fairbanks, Alaska 99775

December, 1991



Accession For	
NTIS CRA&I	<input checked="" type="checkbox"/>
DTIC TAB	<input type="checkbox"/>
Unannounced	<input type="checkbox"/>
Justification	
By	
Distribution /	
Availability Codes	
Dist	Avail and/or Special
A-1	

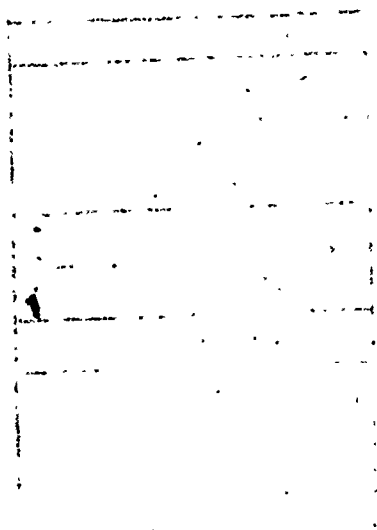


DEFENSE TECHNICAL INFORMATION CENTER



9209871

92 4 00 203



ISBN 0-915360-09-8 (Volume II)
ISBN 0-915360-10-1 (2-Volume Set)

REPORT DOCUMENTATION PAGE			Form Approved OMB No. 0704-0188	
Public reporting burden for this collection of information is estimated to average 1 hour per response, including the time for reviewing instructions, searching existing data sources, gathering and maintaining the data needed, and completing and reviewing the collection of information. Send comments regarding this burden estimate or any other aspect of this collection of information, including suggestions for reducing this burden, to Washington Headquarters Services, Directorate for Information Operations and Reports, 1215 Jefferson Davis Highway, Suite 1204, Arlington, VA 22202-4302, and to the Office of Management and Budget, Paperwork Reduction Project (0704-0188), Washington, DC 20503.				
1. AGENCY USE ONLY (Leave blank)		2. REPORT DATE March 1992		3. REPORT TYPE AND DATES COVERED Final 1 May 1990-30 April 1991
4. TITLE AND SUBTITLE International Conference on the Role of the Polar Regions in Global Change Volume <u>II</u>			5. FUNDING NUMBERS DAAL03-90-G-0126	
6. AUTHOR(S) Gunter Weller (principal investigator on project)				
7. PERFORMING ORGANIZATION NAME(S) AND ADDRESS(ES) University of Alaska Geophysical Institute Fairbanks, AK 99775-0800			8. PERFORMING ORGANIZATION REPORT NUMBER	
9. SPONSORING/MONITORING AGENCY NAME(S) AND ADDRESS(ES) U. S. Army Research Office P. O. Box 12211 Research Triangle Park, NC 27705-2211			10. SPONSORING/MONITORING AGENCY REPORT NUMBER ARO 27859.2-GS-CF	
11. SUPPLEMENTARY NOTES The view, opinions and/or findings contained in this report are those of the author(s) and should not be construed as an official Department of the Army position, policy, or decision, unless so designated by other documentation.				
12a. DISTRIBUTION/AVAILABILITY STATEMENT Approved for public release; distribution unlimited.			12b. DISTRIBUTION CODE	
13. ABSTRACT (Maximum 200 words)				

The International Conference on the Role of the Polar Regions in Global Change took place on the campus of the University of Alaska Fairbanks on June 11-15, 1990. It was co-sponsored by several national and international scientific organizations, as listed on the preceding page. The host institutions were the Geophysical Institute and the Center for Global Change and Arctic System Research, both at the University of Alaska Fairbanks.

The goal of the conference was to define and summarize the state of knowledge on the role of the polar regions in global change, and to identify gaps in knowledge. To this purpose experts in a wide variety of relevant disciplines were invited to present papers and hold panel discussions. While there are numerous conferences on global change, this conference dealt specifically with the polar regions which occupy key positions in the global system.

continued on reverse side

14. SUBJECT TERMS Conference, Global Change, Polar Regions, Global System			15. NUMBER OF PAGES 778	
			16. PRICE CODE	
17. SECURITY CLASSIFICATION OF REPORT UNCLASSIFIED	18. SECURITY CLASSIFICATION OF THIS PAGE UNCLASSIFIED	19. SECURITY CLASSIFICATION OF ABSTRACT UNCLASSIFIED	20. LIMITATION OF ABSTRACT UL	

Over 400 scientists from 15 different countries attended and presented 200 papers on research in the Arctic and Antarctic. The papers were distributed among seven major themes and sessions, each having about three invited papers, a dozen contributed papers, and 15-20 poster papers. These papers, or their abstracts, are contained in the two proceedings volumes. In publishing the papers we did not distinguish between invited, contributed, or poster papers, but gave them all equal weight. On the final day of the conference three panels met to discuss problems and priorities in polar research. A summary of their recommendations follows the final section of papers.

Section D:

**Effects on Biota
and Biological Feedbacks**

Chaired by

V. Alexander
University of Alaska Fairbanks
U.S.A.

G. Hempel
Alfred-Wegener Institut
Germany

Effects of Global Change on Net Ecosystem Carbon Flux of Arctic Tussock Tundra

W. C. Oechel

Department of Biology, San Diego State University, San Diego, California, U.S.A.

ABSTRACT

Arctic ecosystems contain vast quantities of carbon as soil organic matter and, depending on future climatic conditions, have the potential to act as major sources or sinks for atmospheric CO₂. Cold, moist soils and the presence of permafrost allow increased ecosystem production following global change to be stored on a continuing basis over long periods of time. Arctic ecosystems are one of the few ecosystems capable of long-term increased carbon storage. On the other hand, increases in the depth of the active layer, melting of the permafrost, and/or decreases in soil moisture could result in increased rates of soil decomposition and net CO₂ efflux from the tundra.

Recent evidence indicates that tussock tundra is currently losing substantial carbon, possibly in response to warming and drying of arctic soils within the last century. At Toolik Lake, Alaska, the rate of net CO₂ loss from the tundra is on the order of 3 g m⁻² d⁻¹. This rate of loss, if occurring over the circumpolar arctic, could account for the net loss of 0.1 to 0.2 x 10⁹ metric tons of carbon per year from tussock tundra alone.

Field manipulations and phytotron experiments indicate that the response of net primary production or net ecosystem carbon assimilation of tussock tundra to elevated CO₂ is limited by environmental conditions in the arctic. However, the combination of elevated atmospheric CO₂ and increased air temperature can result in a major increase in net primary production and net ecosystem carbon sequestering in tussock tundra.

Global change could cause the arctic to contribute up to 55 x 10⁹ metric tons of soil carbon to the atmosphere. On the other hand, conditions of elevated CO₂ and a moist, poorly aerated soil horizon, could result in long-term carbon sequestering and negative feedback on the rise of atmospheric CO₂. Likely effects depend on the nature of global change and the areas of arctic tundra considered.

The Role of Tundra and Taiga Systems in the Global Methane Budget

W. S. Reeburgh and Stephen C. Whalen

Institute of Marine Science, University of Alaska Fairbanks, Fairbanks, Alaska, U.S.A.

ABSTRACT

Tundra and boreal forest soils contain some 30% of the terrestrial soil carbon reservoir. A large fraction of this soil carbon is immobilized in permafrost and peat. This soil carbon reservoir could be susceptible to biogeochemical conversion to CO_2 and CH_4 under warmer, wetter climate. Both of these gases are radiatively active, and could be responsible for a positive climate feedback.

We performed weekly measurements of CH_4 flux at permanent sites to evaluate the importance of tundra and taiga systems in the present global CH_4 budget and to gain insights into the processes important in modulating emissions under present and modified climate. Our CH_4 flux time-series at tundra sites in the UAF Arboretum covers over 3.5 years and indicates that water table level, transport by vascular plants and microbial oxidation at the water table are important in modulating tundra CH_4 emissions. Emission of CH_4 essentially ceases during frozen periods. Our study at permanent taiga sites covers less than one year. All taiga sites consumed atmospheric methane in fall 1989, indicating that these soils could be a sink for atmospheric CH_4 during part of the year.

Integrated annual emission from the seasonal time-series measurements and results from a detailed survey along the Trans-Alaska Pipeline Haul Road led to independent estimates of the global tundra CH_4 flux of 19–33 and 38 Tg yr^{-1} , respectively. The road transect estimate for the global taiga CH_4 contribution is 15 Tg yr^{-1} .

The Influence of Sea Ice on the Structure and Function of Southern Ocean Ecosystems

C. W. Sullivan

Department of Biological Sciences, University of Southern California, Los Angeles, California, U.S.A.

ABSTRACT

The presence of sea ice and its seasonal dynamics has a profound influence on plants and animals that inhabit the Southern Ocean. Sea ice is a habitat for organisms at all trophic levels. The ice habitat covers approximately 20 million square kilometers of the sea surface during the austral winter, but is rapidly and dramatically reduced by 80% during the ensuing spring and summer. These dynamic processes characteristic of the physical environment result in cyclic changes in the horizontal and vertical distributions of the biomass and activities of organisms. Most notable among these changes are the spatial and temporal characteristics of productivity and the coupled process of sedimentation. These changes may in turn influence both tropho-dynamic relationships and biogeochemical cycles of matter that are unique to the polar regions of the world ocean. The presumed sensitivity of the sea ice ecosystem to global warming suggests that it may be an early indicator of both physical and biological oceanographic consequences of global change.

92-17815



AD-P007 311



Methane Emissions from Alaska Arctic Tundra in Response to Climatic Change

Gerald P. Livingston and Leslie A. Morrissey

TGS Technology, Inc., NASA Ames Research Center, Earth Systems Science Division, Moffett Field, California, U.S.A.

ABSTRACT

In situ observations of methane emissions from the Alaska North Slope in 1987 and 1989 provide insight into the environmental interactions regulating methane emissions and into the local- and regional-scale response of the arctic tundra to interannual environmental variability. Inferences regarding climate change are based on *in situ* measurements of methane emissions, regional landscape characterizations derived from Landsat Multispectral Scanner satellite data, and projected regional-scale emissions based on observed interannual temperature differences and simulated changes in the spatial distribution of methane emissions.

Our results suggest that biogenic methane emissions from arctic tundra will be significantly perturbed by climatic change, leading to warmer summer soil temperatures and to vertical displacement of the regional water table. The effect of increased soil temperatures on methane emissions resulting from anaerobic decomposition in northern wetlands will be to both increase total emissions and to increase interannual and seasonal variability. The magnitude of these effects will be determined by those factors affecting the areal distribution of methane emission rates through regulation of the regional water table. At local scales, the observed 4.7°C increase in mid-summer soil temperatures between 1987 and 1989 resulted in a 3.2-fold increase in the rate of methane emissions from anaerobic soils. The observed linear temperature response was then projected to the regional scale of the Alaska North Slope under three environmental scenarios. Under moderately drier environmental conditions than observed in 1987, a 4°C mid-summer increase in soil temperatures more than doubled regional methane emissions relative to the 1987 regional mean of 0.72 mg m⁻² hr⁻¹ over the 88,408 km² study area. Wetter environmental conditions led to a 4- to 5-fold increase in mid-summer emissions. These results demonstrate the importance of the interaction between the relative areal proportion of methane source areas and the magnitude of summer substrate temperatures in determining whether emissions from decomposition processes in northern ecosystems represent a significant global source and a potential positive feedback to climatic change.

INTRODUCTION

The northern high latitudes face a potentially unprecedented rate of climatic warming as a direct consequence of global increases over the past century in the atmospheric concentrations of infrared-absorbing gases such

as carbon dioxide (CO₂), methane (CH₄), and nitrous oxide (N₂O) [Bolin et al., 1986; Dickinson and Cicerone, 1986; Ramanathan et al., 1987]. As a direct result of the past and anticipated continued atmospheric inputs of these "greenhouse gases," current global circulation models project that

mean annual temperatures for the Arctic may increase between 3–8°C within the next century [Hansen et al., 1988; Post, 1990]. This climatic change is expected to result in earlier spring thaws, longer growing seasons, and 2–4°C elevated summer temperatures. Precipitation patterns may also change, although current projections are still highly uncertain. If these organic-rich and temperature-limited ecosystems [Chapin, 1984] respond to climatic change by releasing substantially greater quantities of CO₂ and CH₄, the climatic warming trend may be enhanced [Lashof, 1989] and the global carbon cycle significantly affected [Miller, 1981; Billings, 1987].

Empirical and atmospheric modeling studies indicate that the northern high latitude wetlands may represent one of the largest natural sources of CH₄ globally as a result of seasonal anaerobic microbial decomposition of organic materials in the active thaw layer. More than half of the wetlands area of the earth lies in the boreal region north of 50°N latitude [Mathews and Fung, 1987; Aselmann and Crutzen, 1989] and over 20% of the earth's total organics may be stored in these ecosystems as frozen or recalcitrant materials in the soils and peats [Post et al., 1985; Gorham, 1988]. Seasonal CH₄ emissions from these ecosystems are estimated to currently account for 6–10% of all CH₄ sources and 16–63% of all natural wetland sources [Aselmann and Crutzen, 1989]. If subjected to climatic warming, these ecosystems may respond by releasing substantially greater quantities of carbon to the atmosphere as a consequence of increased rates of decomposition operating over longer seasons of biological activity and on increasing quantities of organic materials as the permafrost thaws. Examination of arctic methane emissions under variable interannual meteorological conditions may provide insight into the response of northern ecosystems to anticipated climatic change.

In this paper we address observed and projected CH₄ emissions from arctic tundra in relation to anticipated climatically induced changes in soil temperature and water table position. Our conclusions are based upon measured *in situ* CH₄ emissions during the summers of 1987 and 1989 from the North Slope of Alaska, regional land cover characterizations derived from satellite observations, and estimated regional-scale emissions derived from observed interannual temperature differences and simulated changes in water table position.

METHODS

The region of study is an 88,408 km² area representative of the Arctic Coastal Plain and Foothill provinces of the Alaska North Slope (Figure 1). Estimates of mid-summer regional CH₄ emission rates for select climatic scenarios were derived through integration of satellite-based land cover characterizations and *in situ* observations of CH₄ emissions from early August of 1987 and 1989.

At the regional scale, digital classifications of Landsat Multispectral Scanner (MSS) data [Morrissey and Ennis, 1981; Walker et al., 1982] defined the land cover categories and their relative areal proportions subsequently used to calculate regional emission estimates. The spectrally based classification corresponded to vegetation type and density as well as to the presence or absence of surface water. These land cover classes nominally represented "Dry Tundra," "Moist Tundra," "Wet Tundra," "Very Wet Tundra," and

"Water" at 50 m² spatial resolution.

In situ sample allocations differed between 1987 and 1989. In 1987 the allocation was defined to regionally represent both the Arctic Coastal Plain and Arctic Foothills physiographic provinces of the North Slope. More specifically, each land cover class was sampled in proportion to its relative areal representation and to anticipated variances in emissions at the regional scale. Within each site sampled, a secondary allocation represented the microtopography and location of the local water table relative to the surface on a spatial scale of approximately 0.5 m². Ten microtopographic features were identified for sampling, e.g., "low center polygonal basins," "rims," "troughs," "sedge meadows," "high centered polygonal basins," "frost boils," "sedge tussocks," "inter-tussock areas," "lake-over emergent vegetation," and "lake-open water." The location of the water table was categorized as "below" ($z \leq -5$ cm), "at" ($-5 > z \geq 0$ cm), or "above" ($z > 0$ cm) the surface. In total, the area of study was represented by 122 emissions observations representing 57 spatially independent sites. Additional details of the sample allocation are given in Morrissey and Livingston [1991].

The regional mean rate of CH₄ emissions (F) was estimated on the basis of a two-tiered stratified approach [Cochran, 1953] using the relative areal proportions of the local and regional categorizations as the weighting terms:

$$F = \sum_{i=1}^m \sum_{j=1}^n (p_{ij} f_{ij}) \quad (1)$$

where p_{ij} represents the relative areal proportion of land cover class i and local-scale microtopographic feature j , and f_{ij} the measured rate of CH₄ emissions.

In 1989, the sample allocation was defined to assess the seasonal variability in emissions at anaerobic (waterlogged) organic sites on the Arctic Coastal Plain. Only data from the two years that were complementary in time (August 1–14) were included in this analysis. To estimate regional-scale emissions for 1989, we initially assumed no net change in the vegetation or hydrological regimes at the regional scale of the North Slope between 1987 and 1989. As such, in this "reference scenario," differences in estimated regional-scale emissions over the 3-year period reflect only observed interannual differences in the rates of emissions at the local scale. The 1989 CH₄ emission rates for each land cover class were thus calculated as:

$$E_{1989} = \left(\frac{e_{1989}}{e_{1987}} \right) (E_{1987}) \quad (2)$$

where E represents the ecosystem CH₄ emissions rate and e the *in situ* emission rate from anaerobic organic soils.

The sensitivity of regional CH₄ emissions to interaction between the observed interannual differences in the emission rates and changes in the areal representation of the methane source areas was explored in a simulation exercise and subsequently interpreted in light of the potential impacts of climatic change. Two scenarios were examined in addition to the reference scenario described above. "Dry" and "Wet" environmental conditions were simulated by assuming arbitrary shifts in the relative areal proportions of the regional land cover classes. The "Dry" climate scenario

was simulated by a 1/3 proportional loss in inundated surface area over the North Slope, represented as a shift from "Very Wet Tundra" to "Wet Tundra," "Wet Tundra" to "Moist Tundra," and "Moist Tundra" to "Dry Tundra." In the "Wet" climate scenario, an increase in surface inundation was simulated by a 1/3 areal proportional shift from "Wet Tundra" to "Very Wet Tundra" only. The areal extent of well-drained soils ("Moist Tundra") was assumed to be unaffected by a moderate elevation of local water tables. Similarly, the areal proportion of impounded lakes ("Water") was assumed unchanged in both the "Dry" and "Wet" scenarios.

Hydrology plays a major role in defining arctic ecosystem structure and function, thus providing the basis for the scenarios examined. Over large areas of arctic tundra, topography is known to vary on a scale of centimeters to meters. In such areas, even moderate vertical displacement of the local water table on seasonal to decadal time scales can result in substantial shifts in the areal extent of inundated (anaerobic) and drained (aerobic) substrates. The significance of this lies in the well-documented correspondence between the position of the local water table relative to the surface and microtopographic relief, substrate temperature profiles, nutrient and organic contents, ecosystem composition and productivity, and the mode (aerobic vs. anaerobic) of organic degradation [Bunnell et al., 1980; Webber et al., 1980; Walker, 1985]. Moreover, the position of the local water table in these ecosystems has been directly related to the processes of CO_2 and CH_4 production, uptake, and release to the atmosphere [Peterson et al., 1984; Svensson and Rosswall, 1984; Sebach et al., 1986; Crill et al., 1988; Conrad, 1989; Moore and Knowles, 1989; Morrissey and Livingston, 1991].

Emissions Measurements

In situ measurements of CH_4 emissions were made using enclosed chambers deployed over a 15- to 30-minute period within which the atmospheric concentration of CH_4 was monitored over time. Samples were collected in 10-ml glass syringes and analyzed within 12 hours using isothermal gas chromatography and a flame ionization detector. Net rate of emissions was calculated as the average rate of change in CH_4 concentration within the chambers normalized for the molar volume of the chambers at the ambient near-surface temperature. The minimal detectable rate of emissions averaged less than $0.14 \text{ mg CH}_4 \text{ m}^{-2} \text{ hr}^{-1}$. Details of the sampling protocol and analysis are given in Morrissey and Livingston [1991].

RESULTS

Observed Interannual Differences

Summer temperature regimes for the North Slope differed significantly between 1987 and 1989. Whereas mean monthly air temperatures at Prudhoe Bay for July and August of 1987 differed little from the 30-year mean, 1989 temperatures represented record highs [NOAA, 1987, 1989]. Mid-summer (July and August) mean daily air temperatures averaged 7.7 and 11.8°C in 1987 and 1989 respectively. By mid-August, cumulative daily temperatures above 0°C for the two years differed by nearly 600 degree-days (713 compared to $1302^\circ\text{C}\cdot\text{da}$ in 1989). Soil temperatures in anaerobic soils also differed significantly at 10 cm depths, averaging

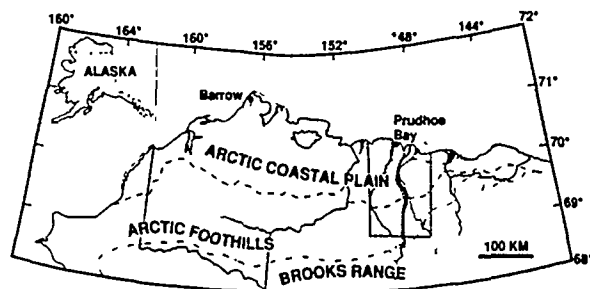


Figure 1. The Alaska North Slope. Regional estimates of emissions were calculated for that area ($88,408 \text{ km}^2$) represented by Landsat MSS digital data (shaded).

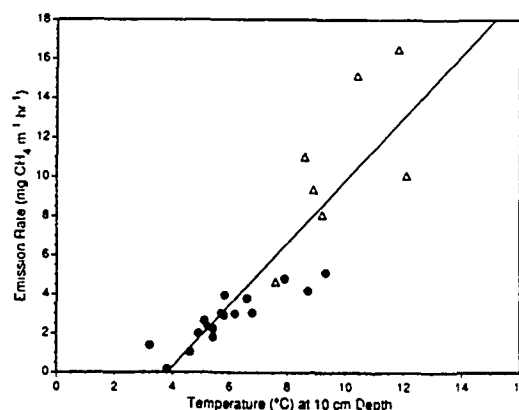


Figure 2. Mid-summer rates of methane emissions from anaerobic organic soils as a function of substrate temperatures at 10 cm depth. Filled symbols represent spatially independent observations over August 1-13, 1987; open symbols represent the average between spatially paired observations between August 2-4 and August 9-11, 1989.

4.7 and 9.4°C in 1987 and 1989. Mid-summer thaw depths ranged mostly between 35 and 45 cm with no clear relation to coincident soil temperatures at 10 cm depths and no measurable difference between years ($p > 0.2$; t-test).

Mid-summer rates of CH_4 emissions from anaerobic (waterlogged) organic soils on the North Slope were linearly related to ambient substrate temperatures at 10 cm depths both within and between years (Figure 2). As a consequence, local-scale rates of emissions differed dramatically between the summers of 1987 and 1989. Over the total observed temperature range of 3.1 to 14.9°C , CH_4 emissions (E) from anaerobic organic soils ranged between 1.6 and $23.6 \text{ mg m}^{-2} \text{ hr}^{-1}$ corresponding to a temperature ($T^\circ\text{C}$) response from spatially independent sites of: $E = 1.590T - 6.094$, $r^2 = 0.77$, $n = 24$. Local-scale methane emissions from anaerobic sites in early August of 1989 were over four times greater than in 1987, averaging $11.7 \text{ mg m}^{-2} \text{ hr}^{-1}$, 1.4 std. err., $n = 9$ and $2.8 \text{ mg m}^{-2} \text{ hr}^{-1}$, 0.3 std. err., $n = 17$ respectively. Within 1989, emission rates for repeatedly observed sites also demonstrated a temperature response between the first and second weeks of August ($p = 0.0001$, paired t-test, $n = 9$), averaging 9.1 and $14.4 \text{ mg m}^{-2} \text{ hr}^{-1}$ on 7.7 and 11.1°C soils. As expected, the relation between depth of thaw and emission rates was poorly defined ($r^2 = 0.24$, $p = 0.03$).

CLASS	Reference Climate	"Dry" Climate	"Wet" Climate
DRY TUNDRA	0	0.204	0
MOIST TUNDRA	0.618	0.479	0.618
WET TUNDRA	0.196	0.161	0.131
VERY WET TUNDRA	0.089	0.060	0.154
WATER	0.098	0.098	0.098

Table 1. Areal proportions of Landsat MSS land cover classes used in the calculation of Alaska North Slope regional CH₄ emissions under observed and simulated climatic regimes.

CLASS	1987	1989 Lower Estimate	1989 Upper Estimate
DRY TUNDRA	0	0	0
MOIST TUNDRA	0.39	0.39	1.59
WET TUNDRA	1.02	4.17	4.17
VERY WET TUNDRA	2.59	10.58	10.58
WATER	0.47	0.47	1.92
NORTH SLOPE TOTAL	0.72	2.05	2.93

Table 2. Mid-summer methane emission rates for Landsat MSS land cover classes used in the calculation of North Slope regional emissions under the reference scenario. Units of emission are in mg CH₄ m⁻² hr⁻¹. Total area represented is 88,408 km².

Projected Regional-Scale Emissions

Simulation parameters and results of the 1987 and 1989 regional emissions estimates and climatic change simulations are summarized in Tables 1 and 2, and Figure 3. Local-scale mid-summer emission rates were based upon actual 1987 and 1989 observations. Regional (88,408 km²)-scale projections are based upon three water table scenarios derived from the Landsat MSS regional characterization. Regional-scale 1987 mid-summer CH₄ emissions from the North Slope totaled 63,654 kg hr⁻¹, averaging 0.72 mg CH₄ m⁻² hr⁻¹. Under the assumption of no change in the regional water table (the reference scenario), mid-summer 1989 regionally averaged emissions were estimated between 2.05 and 2.93 mg CH₄ m⁻² hr⁻¹ (Figure 3, lines b and c). This represents the potential for a more than doubling in CH₄ emission rates at the regional scale for only a 2°C increase in mid-summer substrate temperatures at 10 cm depth. Both poorly and well-drained land cover classes are expected to contribute to the increased regional emissions at the higher substrate temperatures, although their relative contributions are temperature dependent. Given substrate temperatures comparable to those observed in 1989, "Moist Tundra," "Wet Tundra," and "Very Wet Tundra" are expected to contribute approximately equally (34, 28, and 32% respectively) to the regional emissions total despite a more than 2-fold difference in their relative areal proportions (Table 1).

Because of its vast areal extent both on the Alaska North Slope (Table 1) and globally, "Moist Tundra" will play a

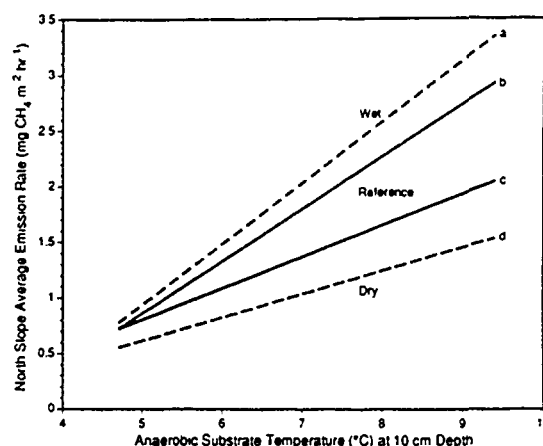


Figure 3. Mean mid-summer regional-scale methane emission rates projected for the Alaska North Slope. Solid lines (b and c) represent upper and lower projected emissions based upon observed 1987 and 1989 ecosystem parameters (reference scenario). Dashed lines represent projected emission rates under simulated "Wet" (a) and "Dry" (d) climatic regimes.

significant role in the arctic response to climatic change. The interaction between areal extent and emission rates for "Moist Tundra" is demonstrated in the range of the projected regional emissions estimates in the reference scenario (Figure 3, lines b and c). The difference in the regional estimates is due almost entirely to uncertainty in the emissions response of "Moist Tundra" to increased temperatures (Table 2). The lower estimate for the 1989 reference scenario assumes that carbon limitations and microbial CH₄ consumption from the shallow organic and aerobic soils characterizing "Moist Tundra" will result in no net increase in CH₄ emission rates even under warmer environments. No increased emission rates from "Water" is also assumed. The upper estimate for the reference scenario assumes that the CH₄ emissions-temperature response of "Moist Tundra" will be proportionally similar to the more anaerobic and organic-rich classes characteristic of the Coastal Plain. Emissions from "Water" also may be expected to increase under warmer environments, perhaps in response to increased ebullition transport of CH₄ to the surface. However, in a regional context, "Water" represents less than 10% of the total area, and combined with its low emission rate, is expected to contribute only about 6% of the regional CH₄ emissions total even under warm environments.

The interaction between substrate temperatures and the relative areal proportion of inundation is critical in determining both regional and annual CH₄ emissions. As both factors vary on seasonal and interannual scales, so will regional CH₄ emissions. For example, if midsummer substrate temperatures differ little from those observed in 1987, regional CH₄ emission rates are not expected to vary greatly even with moderate changes in the areal distribution of the contributing land cover classes. Projected regional CH₄ emission rates for "Dry" and "Wet" scenarios at 4.7°C (1987) substrate temperatures are between 0.55 and 0.82 mg m⁻² hr⁻¹ (Figure 3, lines a and d), representing about a 50% range. The difference in regional CH₄ emission rates under

"Dry" and "Wet" environments are projected to increase linearly thereafter with increased substrate temperatures. Subject to a doubling in temperatures at 10 cm depth, as observed between 1987 and 1989, regional CH₄ emissions rates could vary between 1.53 and 3.34 mg m⁻² hr⁻¹ depending on whether the "Dry" or "Wet" scenario is realized. This represents more than a 2-fold increase in emission rates from arctic tundra even under drier environmental conditions than observed in 1987. Moderately wetter conditions could result in a 4.6-fold increase in regional CH₄ emissions rates.

DISCUSSION

Methane emissions from the northern high latitudes will be significantly perturbed by climatic changes, leading to warmer mid-summer substrate temperatures and to changes in the areal distribution of the CH₄ source areas resulting from vertical displacement of the regional water table. The effect of increased soil temperatures on CH₄ emissions resulting from anaerobic decomposition in northern wetlands will be two fold. If soil temperatures at 10 cm depth are increased 2–4°C above observed 1987 temperatures, CH₄ emission rates are expected to increase several fold. The magnitude of the increase at the regional scale, however, will be determined by the relative areal representation of the sources and sinks. Even under moderately drier environmental conditions, the rate of CH₄ emissions at the regional scale could more than double. The interaction between substrate temperature and areal contributions are expected also to significantly increase the variability in CH₄ emissions on seasonal and interannual time scales.

Currently, *in situ* observations on the interannual variability of CH₄ emissions from northern ecosystems are limited [Whalen and Reeburgh, 1988], yet the results presented here show that an understanding of the magnitude of this variability may be an integral component in assessing the role of CH₄ emissions in climatic change. The critical factors in estimating regional-annual CH₄ emissions are the regional and seasonal characterization of CH₄ emission rates and the length of the growing season. Projections based upon *in situ* observations from the Alaska North Slope in 1987 and 1989 indicate that interannual differences in mid-

summer regional CH₄ emission rates may approach a factor of 3 due to temperature differences alone. Variability in the spatial distribution of CH₄ emissions due, for example, to interannual differences in the amount or timing of summer precipitation is expected to increase this interannual variability in CH₄ emissions even more, perhaps to a factor of 4 to 5 relative to 1987 emissions.

Interannual variability in regional CH₄ emissions related to increased soil temperatures were found to exceed expected variability in emissions due to the length of the growing season. Thirty-year climate records [Tieszen et al., 1980] indicate that thaw season lengths vary by only a factor of 2. Even ignoring seasonal temperature effects, this, at most, contributes a factor of 2 to the interannual variability in CH₄ emissions. Although the global impact of climate-related increases in growing season length is expected to be significant [Lashof, 1989], these results demonstrate that the magnitude of the summer soil temperatures in response to climatic change may be far more significant in determining the rate of CH₄ emissions in northern ecosystems.

Future CH₄ emissions measurement and modeling efforts must account for ecosystem spatial dynamics. Quantitative and dynamic estimation approaches, integrating empirical or process level correspondence between rates of emissions, and environmental parameters with regional-scale characterizations of ecosystem parameters will be required to fully understand the magnitude and variability of CH₄ emissions on regional to global scales. The integration of *in situ* and satellite-based observations demands further attention towards that goal.

ACKNOWLEDGMENTS

The authors are grateful to BP Exploration, Inc. for permitting access to research sites in the Prudhoe Bay region and to the numerous management and staff members who supported this effort. Acknowledgment is also given to Drs. W. Reeburgh and S. Whalen, University of Alaska Fairbanks, for their open discussions on the methane emissions issues and for sharing their facilities. This research was supported by the National Aeronautics and Space Administration Terrestrial Ecosystems and Interdisciplinary Research in Earth Science Programs under RTOPs 677-21-22 and 176-20-34.

REFERENCES

- Aselmann, I., and P. J. Crutzen, Global distribution of natural freshwater wetlands and rice paddies, their net primary productivity, seasonality and possible methane emissions, *J. Atmos. Chem.*, 8, 307–358, 1989.
- Billings, W. D., Carbon balance of Alaskan tundra and taiga ecosystems: Past, present, and future, *Quart. Sci. Rev.*, 6, 165–167, 1987.
- Bolin, B., B. Doos, J. Jager, and R. Warrick (Eds.), *The Greenhouse Effect, Climate Change, and Ecosystems*, John Wiley & Sons, Chichester, 1986.
- Bunnell, F. L., O. K. Miller, P. W. Flanagan, and R. E. Benoit, The microflora: composition, biomass, and environmental relations, in *An Arctic Ecosystem, The Coastal Tundra at Barrow, Alaska*, edited by J. Brown, P. Miller, L. Tieszen, and F. Bunnell, pp. 255–290, Dowden, Hutchinson, and Ross, Inc., Stroudsburg, PA, 1980.
- Chapin, F. S. III, The impact of increased air temperature on tundra plant communities, in *The Potential Effects of Carbon Dioxide-Induced Climatic Changes in Alaska, Proceedings of a Conference*, edited by J. H. McBeath, pp. 143–148, Misc. Pub. 83-1, University of Alaska Fairbanks, 1984.
- Cochran, W. G., *Sampling Techniques*, John Wiley & Sons, New York, 1953.
- Conrad, R., Control of methane production in terrestrial ecosystems, in *Exchange of Trace Gases between Terrestrial Ecosystems and the Atmosphere*, edited by M. O. Andreae and D. S. Schimel, pp. 39–58, John Wiley & Sons, New York, 1989.
- Crill, M. P., K. B. Bartlett, R. C. Harriss, E. Gorham, E. S. Verry, D. I. Sebacher, L. Madzar, and W. Sanner, Methane flux from Minnesota peatlands, *Global Biogeochemical Cycles*, 2, 371–384, 1988.

- Dickinson, R. E., and R. J. Cicerone, Future global warming from atmospheric trace gases, *Nature*, 319, 109-115, 1986.
- Gorham, E., Biotic impoverishment in northern peatlands, in *Biotic Impoverishment*, edited by G. M. Woodwell, Cambridge University Press, 1988.
- Hansen, J., I. Fung, A. Lacis, S. Lebedeff, D. Rind, R. Ruedy, G. Russell, and P. Stone, Global climate changes as forecast by the GISS 3-D model, *J. Geophys. Res.*, 93, 9341-9364, 1988.
- Lashof, D. A., The dynamic greenhouse: Feedback processes that may influence future concentrations of atmospheric trace gases and climatic change, *Climatic Change*, 14, 213-242, 1989.
- Matthews, E., and I. Fung, Methane emission from natural wetlands: Global distribution, area, and environmental characteristics of sources, *Global Biogeochemical Cycles*, 1, 61-86, 1987.
- Miller, P. C. (Ed.), *Carbon balance in northern ecosystems and the potential effect of carbon dioxide induced climatic change, Report of a Workshop*, San Diego, CA, March 7-9, 1980, CONF-8003118, U.S. Dept. of Energy, Washington, DC, 1981.
- Moore, T. R., and R. Knowles, The influence of water table levels on methane and carbon dioxide emissions from peatland soils, *Can. J. Soil Sci.*, 69, 33-38, 1989.
- Morrissey, L. A., and R. A. Ennis, Vegetation mapping of the National Petroleum Reserve in Alaska using Landsat digital data, *U.S. Geological Survey Open File Report 81-315*, 25 pp, Reston, VA, 1981.
- Morrissey, L. A., and G. P. Livingston, Methane flux from tundra ecosystems in Arctic Alaska; an assessment of local spatial variability, *J. Geophys. Res.*, 1991, In press.
- NOAA, *Local climatological data, monthly summary*, Environmental Data and Information Service, National Climatic Center, Asheville, NC, 1987, 1989.
- Peterson, K. M., W. D. Billings, and N. D. Reynolds, Influence of water table and atmospheric CO₂ concentration on the carbon balance of Arctic tundra, *Arctic and Alpine Research*, 16, 331-335, 1984.
- Post, W. M., *Report of a workshop on climate feedbacks and the role of peatlands, tundra, and boreal ecosystems in the global carbon cycle*, Environmental Sciences Division Publication No. 3289, Oak Ridge National Laboratory, Oak Ridge, TN, 1990.
- Post, W. M., J. Pastor, P. J. Zinke, and A. G. Stangenberger, Global patterns of soil nitrogen, *Nature*, 317, 613-616, 1985.
- Ramanathan, V., L. Callis, R. Cess, J. Hansen, I. Isaksen, W. Kuhn, A. Lacis, F. Luther, J. Mahlman, R. Reck, and M. Schlesinger, Climate-chemical interactions and effects of changing atmospheric trace gases, *Rev. Geophys.*, 25, 1441-1482, 1987.
- Sebach, D. I., R. C. Harriess, K. B. Bartlett, S. M. Sebach, and S. S. Grice, Atmospheric methane sources: Alaskan tundra bogs, an Alpine fen and a subarctic boreal marsh, *Tellus*, 38, 1-10, 1986.
- Svensson, B. H., and T. Roswall, In situ methane production from acid peat in plant communities with different moisture regimes in a subarctic mire, *Oikos*, 43, 341-350, 1984.
- Tieszen, L. L., P. C. Miller, and W. C. Oechel, Photosynthesis, in *An Arctic Ecosystem, The Coastal Tundra at Barrow, Alaska*, edited by J. Brown, P. C. Miller, L. L. Tieszen, and F. L. Bunnell, pp. 102-139, Dowden, Hutchinson, and Ross, Inc., Stroudsburg, PA, 1980.
- Walker, D. A., Vegetation and environmental gradients of the Prudhoe Bay region, Alaska, *CRREL Report 8514*, U.S. Army Cold Regions Research and Engineering Laboratory, Hanover, NH, 1985.
- Walker, D. A., W. Acevedo, K. R. Everett, L. Gaydos, J. Brown, and P. J. Webber, Landsat-assisted environmental mapping in the Arctic National Wildlife Refuge, Alaska, U.S. Cold Regions Research and Engineering Laboratory, Hanover, NH, 1982.
- Webber, P. J., P. C. Miller, F. S. Chapin III, and B. H. McCown, The vegetation: pattern and succession, in *An Arctic Ecosystem: The Coastal Tundra at Barrow, Alaska*, edited by J. Brown, pp. 186-218, Dowden, Hutchinson and Ross, Inc., Stroudsburg, PA, 1980.
- Whalen, S. C., and W. S. Reeburgh, Methane flux time-series for tundra environments, *Global Biogeochemical Cycles*, 2, 399-409, 1988.

92-17816



AD-P007 312



The Toolik Lake Project: Terrestrial and Freshwater Research on Change in the Arctic

J. E. Hobbie, B. J. Peterson, and G. R. Shaver

The Ecosystems Center, Marine Biological Laboratory, Woods Hole, Massachusetts, U.S.A.

W. J. O'Brien

Department of Systematics and Ecology, University of Kansas, Lawrence, Kansas, U.S.A.

ABSTRACT

The Toolik Lake research project in the foothills of the North Slope, Alaska, has collected data since 1975 with funding from the NSF's Division of Polar Programs and from the Long Term Ecological Research Program and Ecosystems Research Program of the Division of Biotic Systems and Resources. The broad goal is to understand and predict how ecosystems of tundra, lakes, and streams function and respond to change.

One specific goal is to understand the extent of control by resources (bottom-up control) or by grazing and predation (top-down control). The processes and relationships are analyzed in both natural ecosystems and in ecosystems that have undergone long-term experimental manipulations to simulate effects of climate and human-caused change. These manipulations include the fertilization of lakes and streams, the addition and removal of lake trout from lakes, the changing of the abundance of arctic grayling in sections of rivers, the exclusion of grazers from tundra, and the shading, fertilizing, and heating of the tussock tundra.

A second specific goal is to monitor year-to-year variability and to measure how rapidly long-term change occurs. The measurements include: for lakes, measurements of temperature, chlorophyll, primary productivity; for streams, nutrients, chlorophyll on riffle rocks, insect and fish abundance, and water flow; and for the tundra, amount of flowering, air temperature, solar radiation, and biomass.

A third specific goal is to understand the exchange of nutrients between land and water. Measurements include the flow of water in rivers, the concentration of nitrogen and phosphorus in streams, lakes, and soil porewater, and the effect of vegetation on nutrient movement through the tundra soils. A dynamic model of nutrient fluxes in the entire upper Kuparuk River watershed is being constructed that will interact with geographically referenced databases. Eventually the model and process information will be extrapolated to the larger region; this will allow prediction of the export of nutrients from the whole of the North Slope of Alaska under future conditions of changed temperature and precipitation.

INTRODUCTION

Description of Site. Field research is based at Toolik Lake, Alaska, in the northern foothills of the Brooks Range

(68°38'N, 149°43'W, 760 m) (Figure 1). The Toolik Lake Research Camp is operated by the University of Alaska. Tussock tundra is the dominant vegetation type but there are

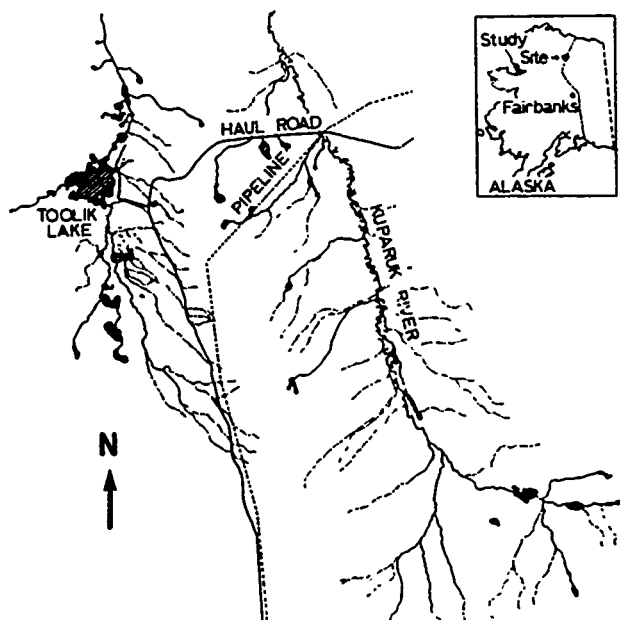


Figure 1. Location of arctic LTER research site at Toolik Lake, Alaska.

extensive areas of drier heath tundra on ridge tops and other well-drained sites as well as areas of river-bottom willow communities.

The mean annual air temperature is -7°C and the total precipitation 250–350 mm. The tundra is snow-free from late May to mid-September while the sun is continuously above the horizon from mid-May until late July. Lakes are ice-free from mid- to late June until late September. The entire region is underlain by continuous permafrost which exerts a major influence on the distribution, structure, and function of both terrestrial and aquatic ecosystems.

Terrestrial research in the Toolik area began in 1976 with descriptive and baseline vegetation studies of many sites along the length of the Dalton Highway and at Toolik Lake. The next phase, research on the response of plants to disturbances of pipeline and road construction, led to studies of plant demography and population dynamics. From 1979 to 1982, plant growth and its controls were analyzed and a number of long-term experiments (fertilization, light, temperature) were set up. The present studies emphasize the soil element cycling and have the goal of evaluating the lateral N and P fluxes in soil water moving downslope across the surface of the permafrost. Budgets of N and P for the various ecosystems through which the water flows have been developed and linked with a hydrologic model.

The primary focus of the streams research is the Kuparuk River, a fourth-order stream where it crosses the Dalton Highway (Figure 1). Intensive research on the Kuparuk River began in 1978, and its water chemistry, flow, and major species populations have been monitored for over 10 years. For much of this time, a section of the river has been fertilized by the continuous addition of phosphate. Recently, the abundance of the single type of fish in the river, the arctic grayling, was manipulated in various sections of the river to examine the effects of crowding and predation. In

1989, a monitoring program in Oksrukuyik Creek, a slightly smaller third-order stream about 15 km to the northeast, was begun with the intention of developing a long-term comparison and contrast with the Kuparuk River.

Toolik Lake has a surface area of 150 ha and a maximum depth of 25 m. Research began in 1975 with surveys of the biota, chemistry, and processes ranging from primary productivity to nutrient budgets. Dozens of other nearby lakes were also surveyed. In the 1980s the research concentrated on the question of controls of populations, community structure, and processes. Large (60 m^3) plastic bags were set up for manipulations of nutrients and predators; entire lakes and divided lakes were fertilized and lake trout, the top predator, removed and added to various lakes. More recently the survey work has been extended to parts of the Arctic coastal plain and Brooks Range, as well as the northern foothills region.

Goals of the Toolik Lake Project are:

- To understand how tundra, streams and lakes function in the Arctic and to predict how they respond to changes including climate change.

To reach this objective the project will:

- Determine year-to-year ecological variability in these systems and measure long-term changes;
- Understand the extent of control by resources (bottom-up control) or by grazing and predation (top-down control); and
- Measure rates and understand the controls of the exchange of nutrients between land and water.

Long-term data sets. To keep track of the observations, the Toolik Lake project maintains a computerized data base at the Marine Biological Laboratory which contains a wide variety of long-term data sets.

Kuparuk River: discharge, NH_4 , NO_3 , PO_4 , temperature, pH, conductivity, pCO_2 , seston (chlorophyll *a*, particulate C, N, P), epilithion (chlorophyll, primary production), insect abundance (*Orthocladius*, *Baetis*, *Brachycentrus*, black flies, small chironomids, drift density), grayling (growth of adults and young, population estimates), rate of N cycling with ^{15}N , major cations and anions.

Toolik Lake: climate data (temperature, relative humidity, wind, radiation), rain (volume, chemistry), lake temperature, oxygen, light, lake level (continuous record), lake and in-flow stream chemistry (NH_4 , NO_3 , PO_4), sedimentation rates, chlorophyll *a*, primary production, zooplankton (composition, density), *Lymnaea* density, fish length and weight (lake trout, sculpin, grayling, white fish).

Tundra: soil temperature, rain and runoff nutrients, soil extract, resin bag data, ^{15}N of plants, biomass (control plots, fertilize, shade, greenhouse plots), vegetation production.

ECOLOGICAL VARIABILITY AND LONG-TERM CHANGES

Terrestrial research. Can we detect long-term changes in the arctic climate? Are terrestrial ecosystems changing in response? These questions are being addressed through long-term monitoring and manipulation of both climate and key ecosystem processes. For example, growth and flowering of *Eriophorum vaginatum*, one of the most common and often dominant plant species throughout the Arctic, has been monitored at 34 sites along the climatic gradient between Fairbanks and Prudhoe Bay since 1976.

The combination of these approaches has allowed us to distinguish [Shaver et al., 1986] the effects of annual

variation in weather from broad regional differences in climate at two time scales: In the long term, we can show that genetically based, ecotypic variation between populations accounts for much of the variation in plant size and growth rate that we observe in the field, and that this variation is correlated with long-term average growing-season temperatures. In the short-term, we can show that growth and especially flowering vary uniformly from year to year over most of Alaska, but these annual fluctuations are not clearly correlated with annual variation in any climatic variable. Short-term plant responses to climate must be strongly "buffered," or constrained, by other limiting factors such as nutrient availability, and that longer-term responses are constrained genetically. Detection and explanation of multi-year trends in plant growth in relation to climate, then, requires linking climatic changes to changes in soil nutrient cycling processes and nutrient availability.

Lake Studies. What are the long-term trends in primary productivity of arctic lakes and how are these trends related to potential climate changes? In the context of climatic change, the master variable for controlling productivity appears to be temperature. Temperature regulates weathering rates, decomposition, and the depth of thaw in terrestrial ecosystems, all of which alter the flux of nutrients through terrestrial landscapes and into lakes. Temperature also regulates the strength and extent of thermal stratification and thus the zone of highest productivity in the lake.

Under the present climatic regime, algal primary productivity is controlled by the amount of phosphorus entering the lake which in turn is controlled by the amount of stream-flow. In Toolik Lake there was a positive correlation ($r^2 = 0.52$) between 14 years of summer primary productivity and the discharge of the nearby Kuparuk River [Miller et al., 1986].

Stream Studies. What is the variability in annual water discharge and nutrient flux from the Kuparuk watershed and is there a discernible long-term trend related to climatic change? The flow of water through the landscape affects many key biogeochemical processes that will potentially change if the hydrologic cycle is significantly changed by either long-term trends or changing annual variability in discharge. For example, increased water flow will likely increase weathering rates of soils in the watershed and increase the export of dissolved cations, anions, nutrients and dissolved organic materials from land to rivers and lakes. Higher discharge will also lead to greater streambank erosion which captures peat. When discharge is low, the flux of materials from land to water is decreased and the balance between autotrophic and heterotrophic processes in streams and lakes is probably shifted in favor of autotrophy. If climatic change does change either the amount of water flow through arctic watersheds or the timing of these flows, we expect large changes in nutrient fluxes and in biotic activity in rivers. Our monitoring program is designed to document these changes.

CONTROL BY RESOURCES VS. CONTROL BY GRAZING AND PREDATION

Terrestrial Studies. What is the relative importance of changes in air temperature, changes in light intensity (due to changes in cloudiness), and changes in soil nutri-

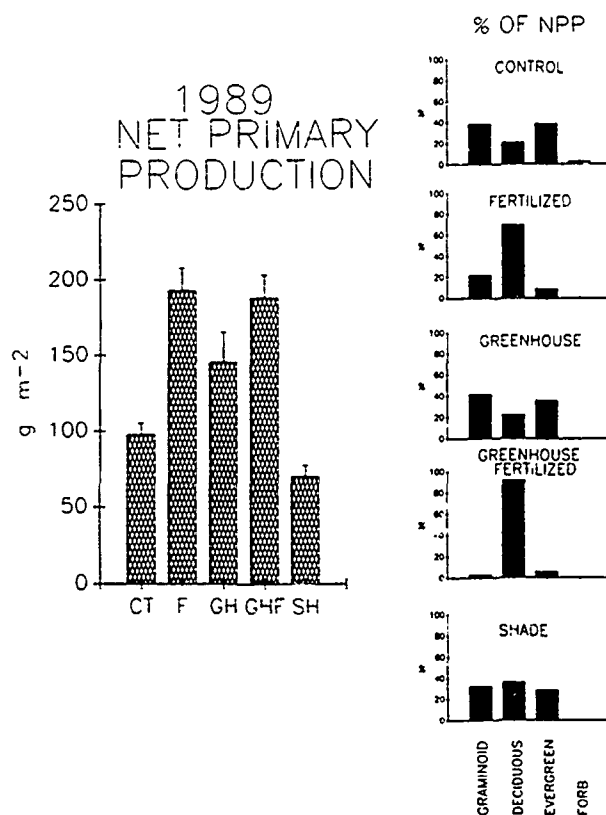


Figure 2. Effects of nine-year field treatments on net primary production and plant growth form composition in moist tussock tundra at Toolik Lake, Alaska. Symbols: CT = control; F = fertilized (N+P); GH = greenhouse; GHF = greenhouse + fertilizer; SH = shaded. Vertical lines are ± 1 S.E. ($n = 4$).

ent availability on terrestrial ecosystems, and how might these changes interact? In a series of short- and long-term experiments that began in 1976, we have manipulated air temperature by building small greenhouses over the tundra, light intensity by shading, and nutrient availability by fertilization. Changes in nutrient availability have effects on productivity and composition of tundra vegetation that are far greater than changes in either air temperature or light (Figure 2). The main effect of increased air temperature is to speed up the changes due to fertilizer alone. Without fertilizer the effect of increased temperatures on the vegetation is slight even after 9 years, and probably results from small increases in soil temperatures and increased nutrient mineralization. These results are consistent with results of our monitoring studies, and again lead to the prediction that effects of climate change on nutrient cycling processes are the key to understanding climate change in the Arctic.

Lake Studies. How much of the structure and function of the lake ecosystem is controlled by resources (bottom-up control), such as the rate of nutrient input, and how much is controlled by grazing and predation (top-down control)? To isolate the effects of nutrient availability on productivity we initiated process-oriented studies on the effects of fertilization. These studies began in 1983 using large limnocorrals and have been expanded to whole systems with our current experiments in divided lakes. Nutrient additions enhance primary production almost immediately, but the transfer of carbon to higher trophic levels proceeds more slowly. Additions of tracer amounts of ^{15}N to a whole

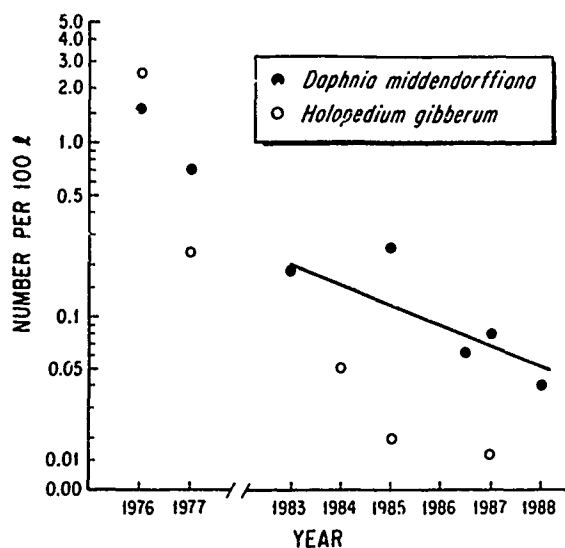


Figure 3. The numbers per 100 liters of two species of zooplankton in Toolik Lake, 1976–1988.

lake also indicated a time lag of at least one growing season in the incorporation of new phytoplankton production into the benthic food chain. Thus in the scenario of increased nutrient supply due to rising temperature we would expect rapid changes in primary productivity and a delayed, more complex response from the higher trophic levels.

To investigate the higher trophic levels and their interactions with populations below them in the context of climate change, we have been both monitoring and experimentally manipulating a series of lakes. We have data on long-term variability in zooplankton and fish populations in several ponds and lakes. We also have data and models of fish feeding on zooplankton and how this might change in response to climate. In 1988 we began investigating the feedback of higher trophic levels on changes in primary and secondary productivity. The experiments consist of addition and removal of top predators in lakes that lie along a productivity gradient. Such experiments will help separate the influence of nutrients from shifts in trophic structure as patterns of energy flow are modified by climatic change. Finally, when added to results of our regional surveys our monitoring will enable us to predict effects of increasing water temperatures on species and populations of both zooplankton and fish.

One interesting observation is the virtual extinction of the large-bodied zooplankton in Toolik Lake (Figure 3). In the late 1970s, many large lake trout in Toolik Lake were removed by angling. This released the predation pressure on smaller fish and they both expanded in numbers and in feeding on zooplankton in the pelagic zone of the lake. This has caused the dramatic drop in the numbers of the two large-bodied zooplankton.

Stream Studies. If climate change accelerates chemical weathering and phosphorus export from the tundra, how will the life of streams and rivers be changed? How much is the ecosystem controlled by resources (bottom-up) vs. predation (top-down) control? The sequence of responses to phosphorus fertilization that we have measured

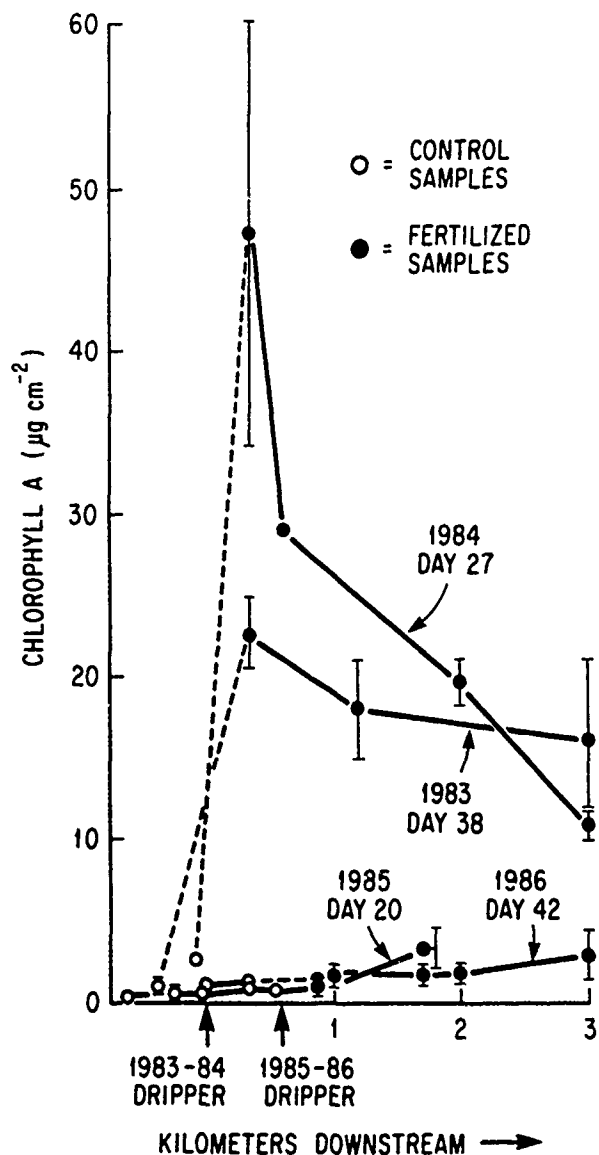


Figure 4. Chlorophyll concentration on riffle rocks of the Kuparuk in the control and fertilized (at 0 km in 1983-84) reaches of the river.

over the past seven years is as follows: Dissolved phosphate added to river water stimulates the growth of epilithic algae (Figure 4). Increases in algal production lead to sloughing and export of algal biomass and increased excretion and mortality. Increased algal excretion and mortality stimulate bacterial activity which is also stimulated directly by phosphorus addition. Increased bacterial activity and biomass make possible an increase in the rate of decomposition of refractory compounds such as lignocellulose and many components of the DOM pool. The increases in algal and bacterial biomass provide increased high quality food for filtering and grazing insects. The insects respond with increased growth rate and, in the case of *Baetis* and *Brachycentrus*, with increases in density. However, *Prosimulium* density in the fertilized reach declines due to competitive interaction with *Brachycentrus*. The increases in insects other than *Prosimulium* increase the available food for grayling;

both young-of-the-year and adult grayling grow faster and achieve better condition in the fertilized reach. In the long term, if the experimental nutrient addition were expanded to include the whole river, and barring other overriding but unknown population controls, we hypothesize that the fish population would increase. If so, it is possible that predation by fish would exert increased top-down control over insects such as *Baetis* or *Brachycentrus* which are vulnerable to fish predation when drifting and emerging. Experimental evidence from bioassays using insecticides indicates that grazing insects control algal biomass (also, in Figure 4 the low algal biomass in 1985 and 1986 is due to growth and grazing of insects). Finally, increases in epilithic algae and bacteria are responsible in part for uptake of added phosphorus and ammonium and for uptake of naturally abundant nitrate. Thus, the bottom-up effects of added nutrients are paralleled by several top-down effects of fish on insects, insects on insects, insects on epilithic algae, and epilithon on dissolved nutrient levels.

In summary, the entire biological system in the river is responsive to added phosphorus. The bottom-up effects propagate to all levels in the food web. Also both top-down effects and competitive interactions are clearly important in the response of the ecosystem to fertilization.

RATES AND CONTROLS OF THE EXCHANGE OF NUTRIENTS AND ORGANIC MATTER BETWEEN LAND AND WATER

Research. Question. What controls the fluxes of nutrients and water over the arctic landscape and into aquatic ecosystems? This question of land-water interactions is fundamental to our understanding of stream ecology and to predictions of climate change on arctic ecosystems. At the Toolik Lake site we already have many small plot measurements of nutrients in soil water and their interactions with plants. We also have large-scale data on the flux of nutrients out of entire watersheds. In the next few years we will construct a dynamic model of the movement of nutrients into streams and combine this with a geographic information system (GIS) to test our understanding of the system and to estimate the nutrient output from larger watersheds.

Terrestrial Research. In this research our principal aim is to evaluate the magnitude and relative importance of lateral N and P fluxes in soil water moving across the surface of the permafrost, between terrestrial ecosystem types and from terrestrial to aquatic systems. Our study site is a toposequence of six contrasting ecosystem types in a tundra river valley (Figure 5). To estimate N and P fluxes in soil

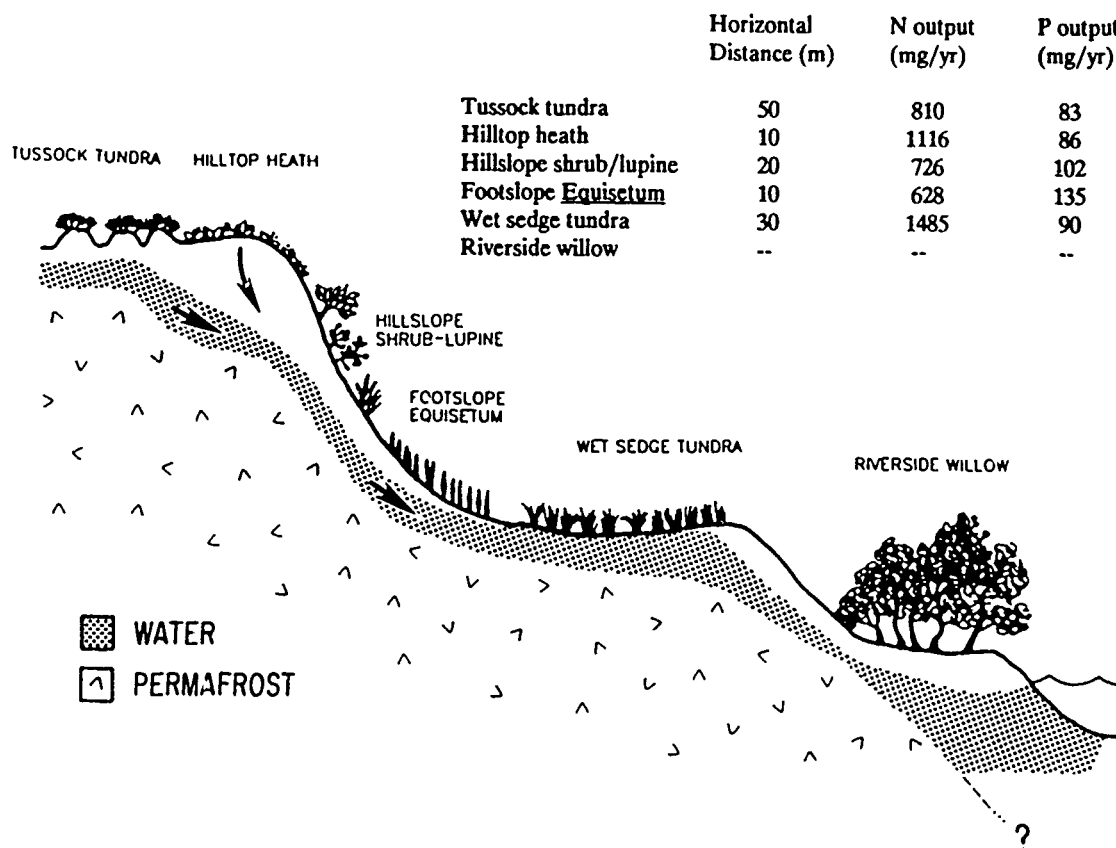


Figure 5. Ecosystem sites along a toposequence (a 1-m-wide strip) leading down to an arctic river and the amounts of N and P (mg ecosystem⁻¹ yr⁻¹) transported through each ecosystem annually.

water at this site we have had to develop and compare overall N and P budgets for all six ecosystems, and to link these budgets with a hydrologic model.

Our major conclusions are that the net uptake of N or P from moving soil water is small relative to internal fluxes such as annual plant uptake or N mineralization. However, each of the six ecosystem types has a major and very different effect on the total amounts of NO_3 , NH_4 , and PO_4 in soil water (Figure 5). This has important implications for the inputs of these nutrients to aquatic systems. Some ecosystem types, like tussock tundra and dry heath, are major sources of N to soil water. Other systems, particularly those occurring under or below late-thawing snowbanks, are important N sinks and P sources to soil water. Poorly drained wet sedge tundra is a P sink with a remarkably high N mineralization rate.

We have also learned a great deal about patterns and controls over N and P cycling processes along our toposequence. Among our most important discoveries, we have shown that nitrification is much more important along our toposequence than we suspected based on earlier research, and many plant species show high nitrate reductase activity. We have strong evidence from stable isotope analyses that different plant species are using isotopically different N sources, and that these species differences are maintained across sites. The relative amounts of different forms of organic and inorganic P in soils also vary dramatically across sites.

In sum, our work has shown that different terrestrial ecosystems differ strongly in their chemical interactions with the soil water, and thus have highly variable effects on the chemistry of water entering aquatic systems. This work is important in the context of global change, because if either the composition of the landscape mosaic changes, or the biogeochemistry of individual landscape units changes, the chemistry of inputs to aquatic systems will also change.

Land-Water Interactions. To achieve one of our major long-term objectives of understanding controls of water and nutrient flux at the whole watershed and regional levels, we are focusing on four major questions:

- What is the role of various units of landscape in determining the amount and chemistry of water flowing from land to rivers and lakes?

- What is the specific role of the riparian zone in modifying the chemistry of water entering rivers and in determining the amount of allochthonous organic matter and light in rivers and lakes?

- What is the role of lakes in retaining and transforming organic matter and nutrients as this material moves downstream through a drainage?

- How do the communities of rivers and lakes change in response to changes in water quantity and quality caused by various units of landscape, riparian zones and up-stream lakes?

From our history of experiments on fertilization of lakes and rivers, we know that both lake and stream biota are very responsive to both short- or longer-term changes in phosphorus and nitrogen supply. Thus we have a large amount of information on question #4 and we know from current research on small plots that different terrestrial ecosystems will yield very different quality runoff water. In future research, we will focus on determining the relationships between larger landscape units (0.1 to 1 km^2) and water quality of runoff, the role of the riparian zone, and the role of lakes in determining river water quality.

Scaling to Watershed and Regional Level. The long-term plan is to make a model of nutrient processing and transfer which would follow nutrients from the interactions in the soil into a stream. This watershed model can be verified by the continuous measurements of nutrient flux from the watershed being made at the point where the Kuparuk River crosses the single road. Next, the watershed model would be calibrated to fit the different environments of northern Alaska. Finally, the model would be used to characterize the variability among Alaskan ecosystems so that statistical extrapolations could be made to the regional scale. The end result would be regional predictions of nutrient fluxes from land to rivers under various scenarios of climate change. The flux from an entire region to the Arctic Ocean could then be predicted.

REFERENCES

- Miller, M. C., G. R. Hater, P. Spatt, P. Westlake, and D. Yeakel, Primary production and its control in Toolik Lake, Alaska, *Arch. Hydrobiol./Suppl.*, 74, 97-131, 1986.
- Shaver, G. R., N. Fetcher, and F. S. Chapin, Growth and flowering in *Eriophorum vaginatum*: Annual and latitudinal variation, *Ecology*, 67, 1524-1535, 1986.

AD-P007 313



**Paleolimnologic Evidence of High Arctic Late
Quaternary Paleoenvironmental Change:
Truelove Lowland, Devon Island, N.W.T., Canada**

R. H. King and I. R. Smith

Department of Geography, University of Western Ontario, London, Ontario, Canada

R. B. Young

Environmental Applications Group Limited, Toronto, Ontario, Canada

ABSTRACT

Truelove Lowland (75°33'N, 84°40'W) is a small area (43 km²) of relatively high biological diversity in the midst of the more typical Polar Desert of the Canadian High Arctic. Much of the Lowland is presently covered by freshwater lakes some of which are sufficiently deep (7–8.5 m) to contain stratified lake sediments. Sediment cores (≈ 2 m long) from the larger lakes have been analyzed for diatoms and chemical composition and reveal a stratigraphic record that spans the last 10,600 years.

This record indicates that lake development in the Lowland began as a series of shallow marine lagoons isolated from the sea as a result of glacio-isostatic rebound and the progressive emergence of the Lowland from the sea. Following isolation, the timing of which was strongly controlled by elevation and the relative rate of isostatic uplift, the lakes have been flushed with freshwater. Since that time the lakes have remained oligotrophic and lake sedimentation has been dominated by variations in non-biogenic factors and particularly by variations in the influx of allochthonous materials from within the lake catchments. Over time, the progressive stabilization of surface materials and pedogenesis within the lake catchments has been marked by decreasing amounts of Cr, As and Na in the sediments and an increase in allochthonous Fe and Mn.

INTRODUCTION

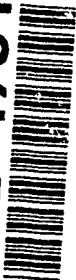
Under existing climatic conditions the Canadian High Arctic is a polar desert, characterized by low biological diversity and low productivity and underlain by continuous permafrost. However, in widely scattered locations small areas of relatively high biological diversity and productivity occur as terrestrial oases in the midst of the regional polar desert. An example of such an area is the Truelove Lowland (75°33'N, 84°40'W), one of a series of lowlands located on the northeastern coast of Devon Island, N.W.T. (Figure 1).

Because of their ecologic significance these polar oases have been the object of considerable scientific interest in recent years. Truelove Lowland was chosen as the location for one of fourteen major ecosystem studies within the Tun-

dra Biome component of the International Biological Program (IBP) and the only one out of a total of four major arctic projects that was conducted within the High Arctic [Bliss, 1977].

Although a considerable amount of detailed information on the characteristics and performance of this ecosystem was amassed by the IBP project over a four year period, 1970–1974, it provides only a small picture of changes, both environmental and ecological, experienced by the Lowland since it has been in existence. What has been lacking until now have been details of the changes experienced by the Lowland over the relatively longer term of the postglacial period. A major problem in obtaining such information has been the apparent absence of a stratigraphic record of such

92-17817



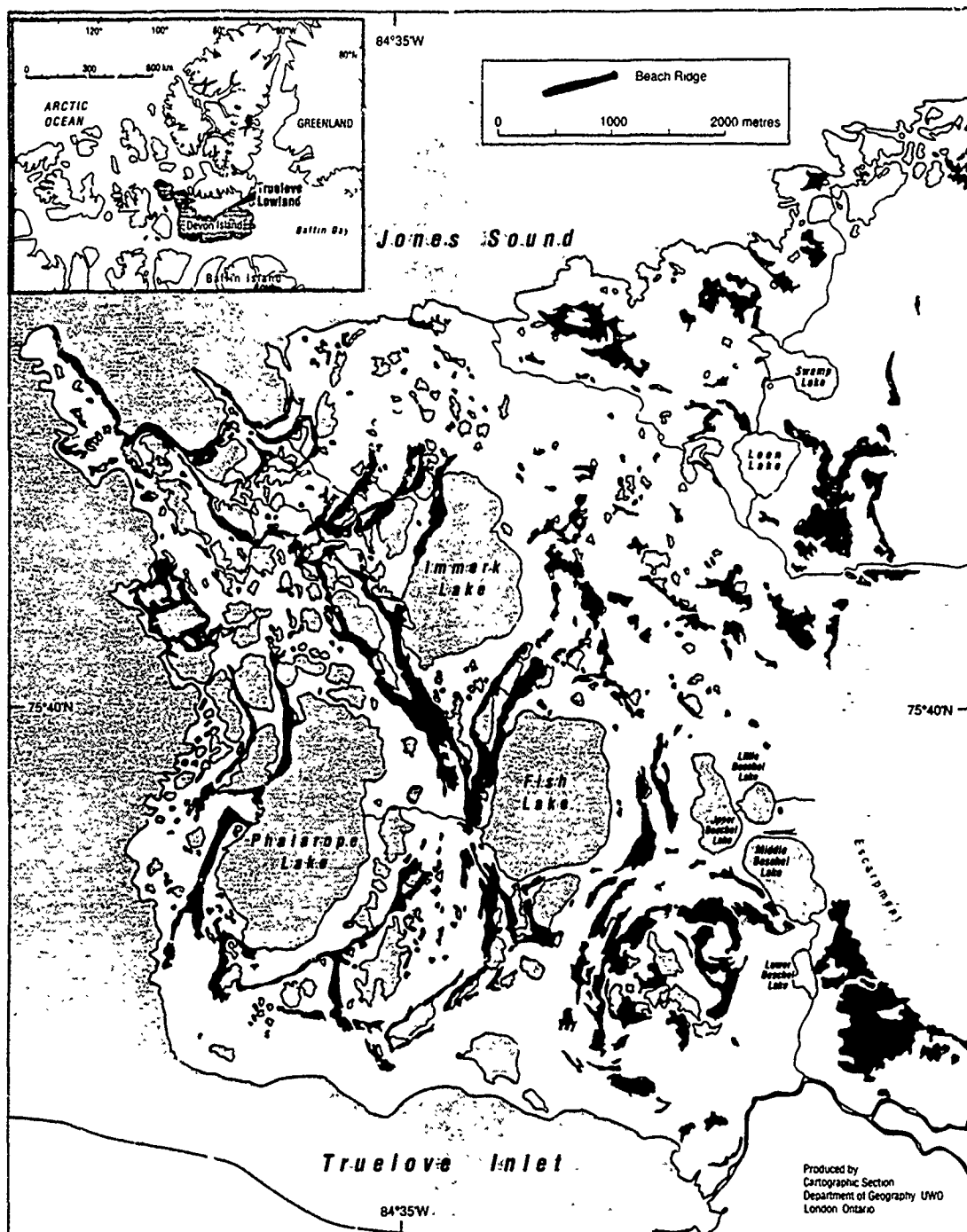


Figure 1. Location of the study area on the northeastern coast of Devon Island, N.W.T., Canada.

changes. However, recent research on the sediments in the larger lakes in the Truelove Lowland has revealed the presence of such a record. This paper examines the nature and significance of this record.

STUDY AREA

Truelove Lowland today is essentially an emerged platform of marine abrasion mantled with a complex sequence of Quaternary deposits [King, 1969]. Although the age of the emerged platform is uncertain, it obviously predates the present mantle of deposits. Local relief in the Lowland is

provided by Precambrian rock outcrops and a series of raised marine beaches rising inland from the present-day coastline to an elevation of approximately 86 m. Approximately 350 lakes, with a mean depth of 3 m, presently cover 22% of the Lowland. The four largest lakes are Phalarope Lake, Immerk Lake, Fish Lake and Middle Beschel Lake, with surface areas of 1.92 km², 1.25 km², 1.13 km² and 0.36 km², maximum depths of 6.8, 8.0, 7.0 and 10.5 m and elevations above sea level of 4.53 m, 13.71 m, 21.00 m, and 30.19 m respectively. These lakes are presently fresh, slightly alkaline, bicarbonate ion dominated and oligotrophic [Scheibli, 1990].

Lake ice begins to form in early September in an average year, reaches a maximum thickness of approximately 2 m and lasts into late July or early August. To a large extent, the presence of an ice pan controls the degree to which lake water mixing occurs. Throughflow of lighter water immediately beneath the lake ice appears to be greatest when the ice pan is most extensive. As an ice-free moat develops and as the fetch increases, the potential for turbulent mixing of the lake water by the wind also increases. Consequently the shallower lakes, which warm up rapidly during the early summer, tend to be well mixed and the sediments poorly stratified.

METHODS

Sediment coring has concentrated on the largest and deepest lakes in the Lowland since it was believed that the longest, most complete stratigraphic record of environmental changes was most likely to occur there [Young, 1987; Young and King, 1989]. Sediment cores have been collected using a modified Livingstone piston corer with an internal diameter of 5.75 cm and the lake ice in early June as a coring platform. Cores are initially extruded in 20- to 24-cm sections in the field and subsampled in 2-cm sections. Core samples have been analyzed in the following ways. Chemical compositional data was obtained using Instrument Neutron Activation Analysis (INAA). In particular, trace elements including As, Cr, Mo, U, and selected macro elements such as Fe (Fe_1) were determined. In addition, total organic carbon was determined using the modified Walkley-Black technique [Nelson and Summers, 1982] and biogenic silica was determined colorimetrically [after DeMaster, 1981] using a Pye-Unicam model 5620 visible spectrophotometer. Fe and Mn (Fe_d and Mn_d) were extracted using a citrate-bicarbonate-dithionite solution [Mehra and Jackson, 1960] and determined by atomic absorption spectrophotometry. Diatoms were mounted for microscopic identification in Hyrax (R.I. = 1.65) following sample preparation that included acidification with 10% HCl and peroxidation followed by extraction with concentrated H_2SO_4 and $K_2Cr_2O_7$ to remove organic matter. Diatoms were identified with reference to standard keys [Cleve-Euler, 1951-1955; Patrick & Freese, 1961; Foged, 1972-1974, 1981; Germain, 1981; Lichti-Federovich, 1983; Peragallo and Peragallo, 1897-1908]. In addition, selected bulk sediment core samples have been dated by accelerator mass spectrometry (AMS) at the Isotrace Laboratory, University of Toronto.

RESULTS AND DISCUSSION

This paper focuses on the results obtained from two sediment cores obtained in late June, 1986 from Fish Lake (FL3) and Phalarope Lake (PL2). The cores are generally similar, ranging in length from 78 cm (FL3) to 80 cm (PL2). Most of the cores comprised black (5Y 2.5/1 [Munsell, 1975]), olive (5Y 5/4) or dark olive grey (5Y 3/2) jellylike algal gyttja clay, except for the basal section of the FL3 core which was comprised of greyish brown (2.5Y 5/2) sand. Although present throughout both cores, laminations of alternating black and dark olive grey material tended to be restricted to the top and bottom parts of the cores. On exposure to the air oxidation of the material occurred rapidly resulting in the development of a more uniform olive brown

(2.5Y 4/4) color. Basal sediments from a depth of 79-80 cm in the PL2 core from Phalarope Lake and from a depth of 76-78 cm in the Fish Lake core FL3 yielded ^{14}C (AMS) dates of $10,620 \pm 160$ years B.P. (TO-564) and $10,570 \pm 200$ years B.P. (TO-566) respectively. An examination of the diatom assemblages present within the cores provides further evidence of the major environmental changes experienced by these lake systems. Although the diatom content in the basal sample of the FL3 core is extremely low (16 valves), the diatoms present are marine, benthic littoral forms such as *Cocconeis costata*, *Diploneis subsinica* and *Grammatophora angulosa* (Figure 2). The presence of this diatom assemblage indicates that the basal core section in FL3 represents a marine deposit. The basal date of $10,570 \pm 200$ years B.P. indicates that this part of the core was deposited at a time when this portion of the Lowland was inundated by the sea and prior to the subsequent coastal emergence that resulted in the creation of the raised beach sequence and isolated the lakes from marine influence.

The basal part of the FL3 core is overlain by a section of the core between 66 and 72 cm containing brackish tolerant diatom species (Figure 2) such as *Diploneis interrupta*, *Navicula digitoradiata*, *N. protracta* var. *elliptica* and *N. salinarium* suggesting that this portion of the core contains a record of the isolation of the lake from marine influence and a significant inflow of fresh water to the system. At that time the lake probably existed as a marine lagoon, separated from the sea by an offshore bar. The remainder of the core is dominated by *Fragilaria*, in particular, *F. pinnata*. This diatom, together with *F. construens*, has often been interpreted as representing a colonizing phase of benthic alkaliphils analogous to early postglacial limnological conditions [Florin and Wright, 1969; Bradbury and Whiteside, 1980; Smol, 1983]. Wolfe [1989] also reports that the *Fragilaria pinnata-construens* complex dominates the modern benthic and littoral sediments of the larger and deeper freshwater lakes in the Truelove Lowland. This suggests that the presence of *Fragilaria* indicates the post-brackish freshwater phase of lake development that followed coastal emergence.

Diatom preservation in Phalarope Lake, on the other hand, as represented by core PL2, is not as complete as it is in Fish Lake (Figure 2). Nevertheless, an environmental record similar to that in Fish Lake appears to be present. The top 4 cm of the core is dominated by *Fragilaria*, in particular, *F. pinnata*, *F. construens* and *F. construens* var. *subsalina*, but the core section from 4 to 42 cm is nearly devoid of diatoms. Underlying this section of the core, between 42 to 80 cm, the diatom assemblage consists of a mixture of euryhaline, brackish and marine forms such as *Achnanthes brevipes*, *Amphora libyca* var. *baltica*, *A. terroris*, *Cocconeis scutellum*, *C. costata*, *Navicula digitoradiata*, *N. protracta* var. *elliptica* and *N. salinarium*. A similar diatom assemblage exists in the benthic and littoral sediments of brackish lakes and ponds in the Lowland today [Wolfe, 1989]. The presence of such an assemblage in much of the PL2 core suggests that the period of brackish conditions persisted much longer in Phalarope Lake than it did in Fish Lake and that the freshwater phase of lake development is a comparatively recent event. Together, these two lakes appear to contain a record of the progressive emergence of the Truelove Lowland from the sea, beginning with lake isolation as a marine lagoon, followed by the inflow of fresh-

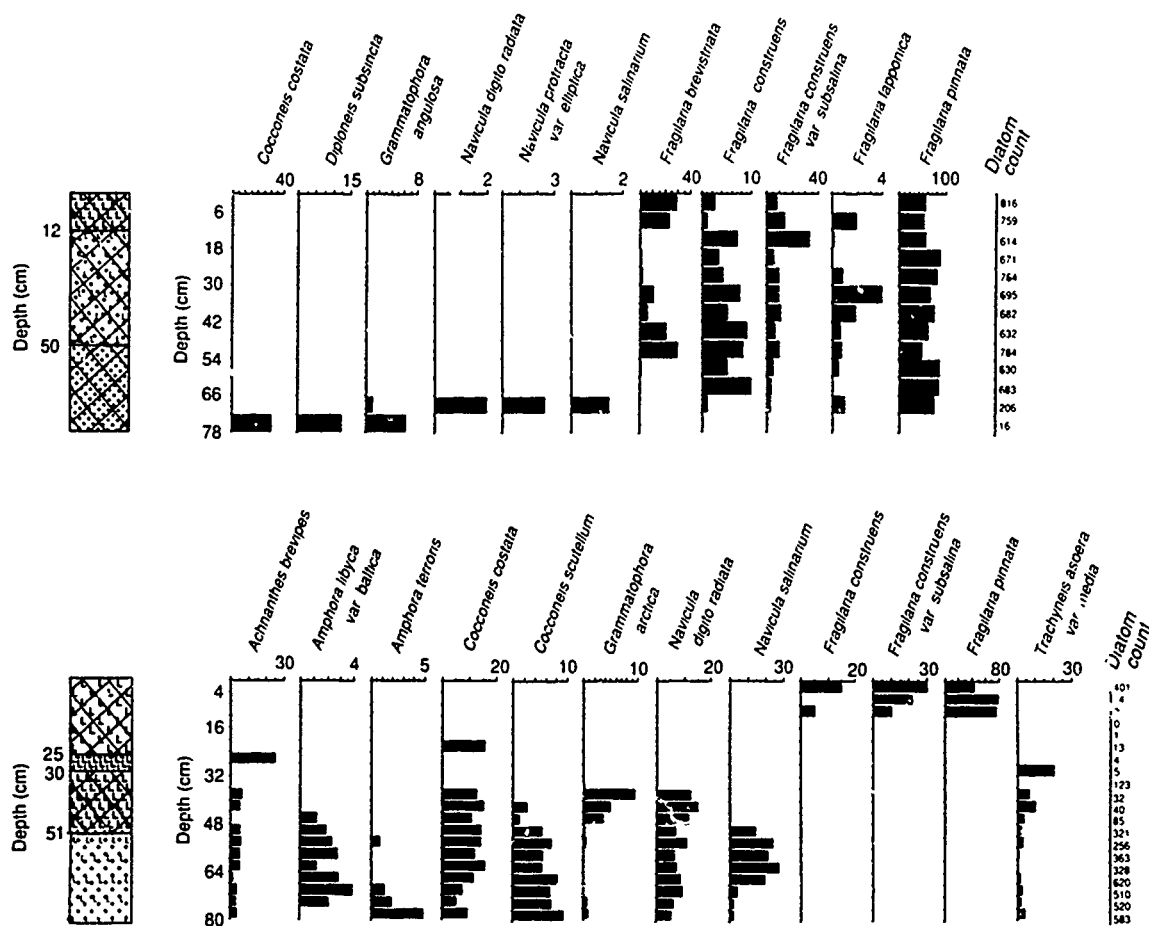


Figure 2. Diatom stratigraphy of the FL3 core from Fish Lake and the PL2 core from Phalarope Lake in percentage of diatom sum.

water derived from snow and ice melt diluting the seawater and the progression of the lake to a freshwater condition. Such an interpretation is supported by the geochemical data, especially that from the FL3 core (Figures 3 and 4). For example, Cr, Fe, U and Mo in the sediments of the FL3 core appear to be associated with the isolation phase when the marine lagoons were first isolated from the sea. At this time lake sedimentation would be strongly affected by the high energy environment associated with beach development and is sensitive to the presence of brackish water and erosion within the catchment. The geochemical data from the PL2 core are more difficult to interpret and this may reflect the much longer time taken for lake isolation to occur. Whereas in Fish Lake isolation of the lake appears to have been quickly accomplished at a time of relatively rapid isostatic uplift, in the case of Phalarope Lake, being lower in elevation, its isolation took much longer due to a much slower rate of isostatic uplift at that time. The relatively high concentrations of erosional indicators such as U, and allochthonous Mn and Fe (Mn_d and Fe_d) in the brackish zone of the PL2 core (Figure 3) lends further support to the idea that the isolation of Phalarope Lake was protracted.

Given that Mo is concentrated at the point in both cores where the diatom flora indicate that brackish conditions prevailed, the period of transition from marine to freshwater conditions appears to have been associated with the development of hypolimnetic anoxia. Such conditions are believed to have resulted in the precipitation of Mo as MoS_2

and the presence of a distinctive black layer in the sediments. However, biologic productivity, as indicated by the concentration of biogenic silica and organic matter (Figure 3), remains high in this region of the PL2 core, suggesting that the duration of such a hypolimnetic anoxia would have been short lived. Calculations of the residence time of water in the deeper lakes in the Lowland [Scheibler, 1990] suggest that the persistence of such anoxic conditions would be very short lived; in the order of approximately 20 to 30 years at most. In the case of Phalarope Lake which, despite its area, is comparatively shallow and thermally well mixed in summer, the persistence of such conditions would have been much less than in the deeper lakes.

The presence of basal marine deposits of similar age in both Fish Lake and Phalarope Lake supports the idea that by approximately 10,600 years B.P. much of the Lowland was covered by the sea. It is possible that the Lowland was inundated by a marine transgression which progressively covered the Lowland shortly before approximately 10,600 years B.P. up to an elevation of approximately 86 m a.s.l., this being the present field elevation of an easily identified marine limit at the base of the escarpment bounding the Lowland to the east. The marine transgression could have been the result of a general eustatic rise in sea level. Such a scenario assumes that the Lowland was already deglaciated prior to the marine transgression. On the other hand, it is equally possible that the Lowland was inundated by the sea considerably before 10,600 years B.P. Evidence in support

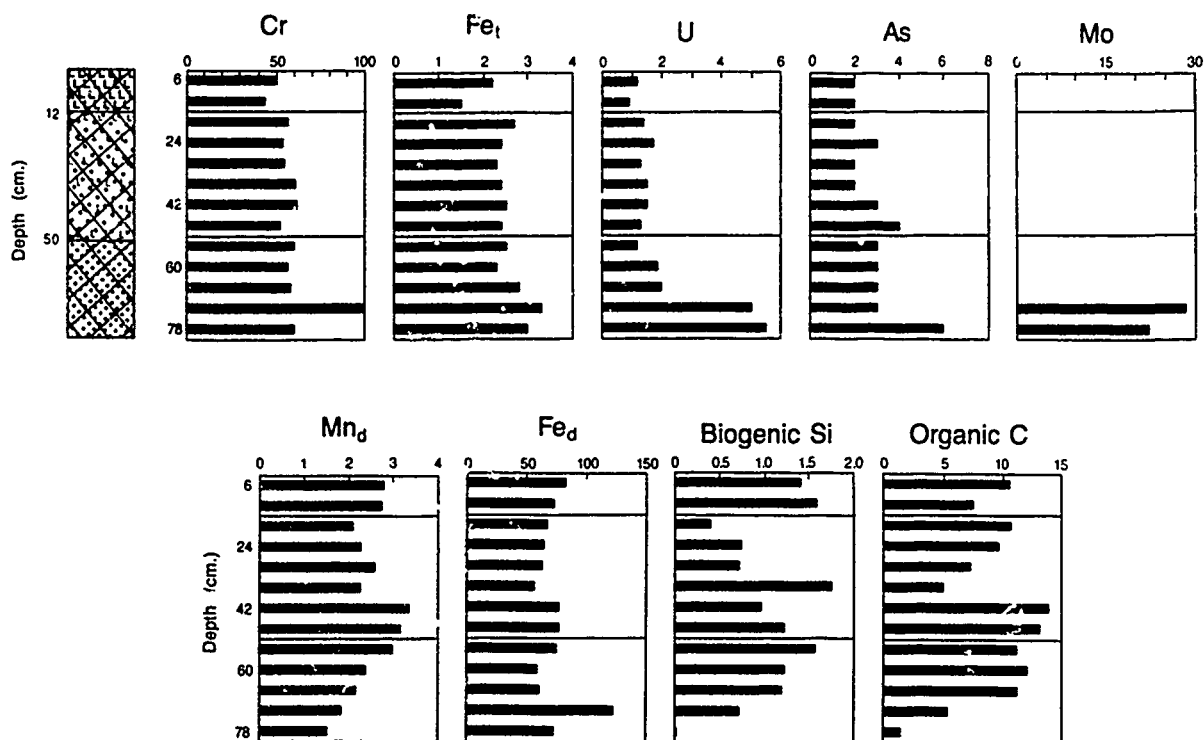


Figure 3. Chemical stratigraphy of the FL3 core from Fish Lake reported in $\mu\text{g g}^{-1}$ (oven dried weight), with Fe_t, Organic C reported in %.

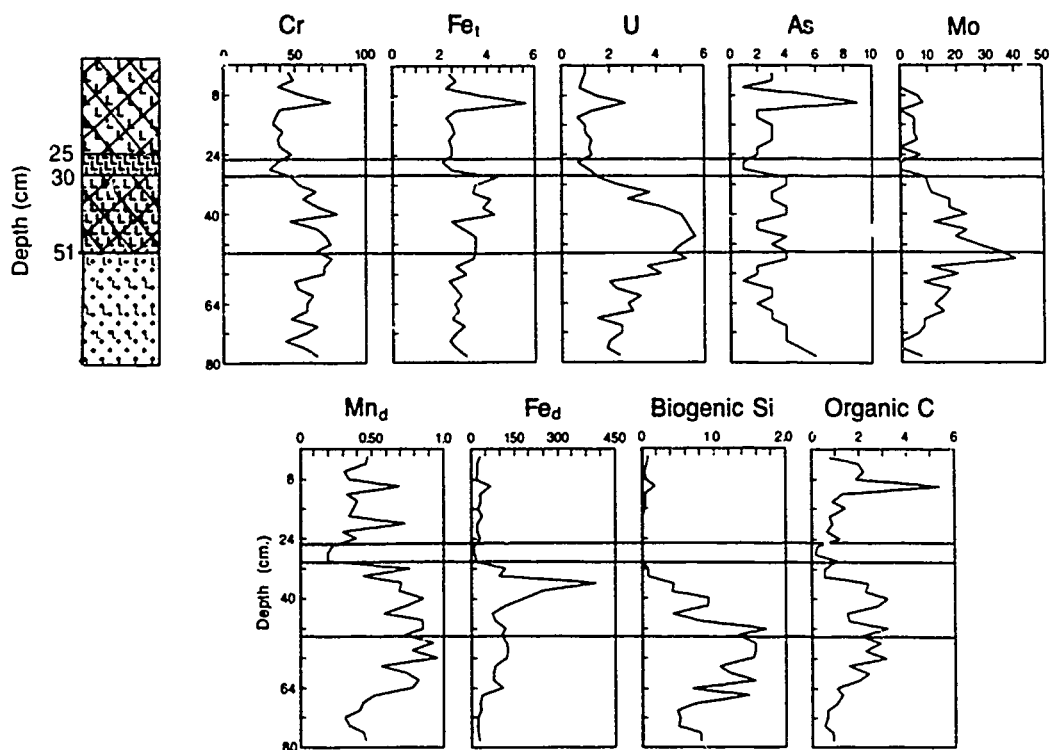


Figure 4. Chemical stratigraphy of the PL2 core from Phalarope Lake reported in $\mu\text{g g}^{-1}$ (oven dried weight), with Fe_t, Organic C reported in %.

of this idea is provided by Barr [1971] who reported the presence of marine shells with an age of approximately 30,000 years B.P. at an elevation of 36 m on Wolf Hill.

The record of paleoenvironmental change preserved in these lake sediments is not restricted to major changes in the development of the Truelove Lowland related to coastal emergence. During the early post-isolation phase in Fish Lake the response of the lake biota to an influx of nutrients is reflected in an increase in biogenic silica and organic carbon in the lake sediments (Figure 3). In the case of Phalarope Lake, where the process of lake isolation took much longer, a similar response took place much later.

Throughout the Holocene the isolated lakes in the lowland, such as Fish Lake, have remained very dilute and oligotrophic and lake sedimentation has been dominated by variations in non-biogenic factors and particularly by variations in the influx of allochthonous materials derived from within the lake catchments. Over time, the progressive mobilization of surface materials and pedogenesis within the lake catchments has been marked by decreasing $\delta^{13}C$, $\delta^{15}N$ and U in the sediments and an increase in allochthonous Mn and Fe (Mn_4 and Fe_2). Aggrading permafrost conditions have

the lake catchments followed lake isolation and the emergence of the Lowland. One consequence of this would have been lower soil redox potentials resulting from the development of a water-saturated active layer and the consequent mobilization and translocation of Fe as Fe^{2+} and Mn as Mn^{3+} to the lake sediments. There is every indication that the stratigraphic record provided by the sediments in these lakes will ultimately provide more information on the processes and changes occurring within the lake catchments than about events taking place within the lakes themselves.

ACKNOWLEDGMENTS

This research has been supported by the Natural Sciences and Engineering Research Council of Canada through an operating grant to R. H. King, I. R. Smith and R. B. Young were supported by grants from the Northern Scientific Training Program of the Department of Indian Affairs and Northern Development, Canada. Logistic support was provided by the Polar Continental Shelf Project of the Department of Energy, Mines and Resources, Canada and base camp facilities were provided by the Arctic Institute of North America.

REFERENCES

- Barr, W., Postglacial isostatic rebound in northeastern Devon Island: A reappraisal, *Arctic*, 21, 249-268, 1971.
- Bliss, L. C., Introduction, in *Truelove Lowland, Devon Island, Canada: A High Arctic Ecosystem*, edited by L. C. Bliss, pp. 1-11, University of Alberta Press, Edmonton, 1977.
- Bradbery, J. P., and M. C. Whiteside, Paleolimnology of two lakes in the Klondike Glacier Region, Yukon Territory, Canada, *Quat. Res.*, 14, 149-168, 1980.
- Canada Soil Survey Committee, The Canadian System of Soil Classification, *Canada Department of Agriculture Publication 1646*, 164 pp., Supply and Services Canada, Ottawa, 1978.
- Cleve-Euler, A., Die Diatomeen Von Schweden Und Finnland. I-V. Kungl. Svenska Vetenskaps Akademiens Handlingar, Fjarde Serien, Band 2:1, 4:1, 5, 5:4, 3:3, Almqvist & Wiksell's Boktryckeri AB, Uppsala, 1951-1955. (Reprinted in 1968 as *Bibliotheca Phycologica*, Band 5, Verlag Van J. Cramer, Vaduz.)
- DeMaster, D. J., The supply and accumulation of silica in the marine environment, *Geochim. Cosmochim. Acta*, 45, 1715-1732, 1981.
- Florin, M. B., and H. E. Wright, Jr., Diatom evidence for the persistence of stagnant glacial ice in Minnesota, *Geol. Soc. Am. Bull.*, 80, 695-704, 1969.
- Foged, N., The diatoms in four postglacial deposits in Greenland, *Meddelelser Om Gronland*, 194, 66 pp., 1972.
- Foged, N., Diatoms from southwest Greenland, *Meddelelser Om Gronland*, 194, 84 pp., 1973.
- Foged, N., *Freshwater Diatoms in Iceland*, 273 pp., Verlag Van J. Cramer, Vaduz, 1974.
- Foged, N., *Diatoms in Alaska*, *Bibliotheca Phycologica* Band 53, 317 pp., Verlag Van J. Cramer, Vaduz, 1981.
- Germain, H., *Flora des Diatomees*, 444 pp., Societe Nouvelle Des Editions Boubée, Paris, 1981.
- King, R. H., Periglaciation on Devon Island, N.W.T., Unpublished Ph.D. dissertation, 470 pp., Department of Geography, University of Saskatchewan, 1969.
- Licht-Federovich, S., A Pleistocene diatom assemblage from Ellesmere Island, Northwest Territories, *Geological Survey of Canada Paper* 83-9, 59 pp., 1983.
- Mehra, D. P., and M. L. Jackson, Iron oxide removal from soils and clays by a dithionitecitrate system buffered with sodium bicarbonate, *7th National Conference on Clays and Clay Minerals*, pp. 317-327, 1960.
- Munsell soil color charts, Kollmorgen Corporation, Baltimore, Maryland, 1975.
- Nelson, D. W., and L. E. Summers, Total carbon, organic carbon and organic matter, in *Methods of Soil Analysis. Part 2: Chemical and Microbiological Properties*, edited by A. L. Page, pp. 539-579, American Society of Agronomy, Madison, Wisconsin, 1982.
- Patrick, R., and L. R. Freese, Diatoms (Bacillariophyceae) from northern Alaska, *Proceedings of the Academy of Natural Sciences, Philadelphia*, 112, 129-293, 1961.
- Peragallo, H. and M. Peragallo, *Diatomees Marines de France*, 491 pp., Koeltz Scientific Books, 1897-1908.
- Scheibler, F. J., The physical and chemical limnology of three High Arctic lakes, Truelove Lowland, Devon Island, N.W.T., Unpublished M.Sc. thesis, 298 pp., Department of Geography, University of Western Ontario, 1990.
- Smol, J. P., Paleophycology of a High Arctic lake near Cape Herschel, Ellesmere Island, *Can. J. Botany*, 61, 2195-2204, 1983.
- Wolfe, A. P., Modern diatom assemblages and their limnological significance, Truelove Lowland, Devon Island, N.W.T., Unpublished B.Sc. thesis, 107 pp., Department of Geography, University of Western Ontario, 1989.
- Young, R. B., Paleolimnology of two high arctic isolation basins, Truelove Lowland, Devon Island, N.W.T., Unpublished M.Sc. thesis, 148 pp., Department of Geography, University of Western Ontario, 1987.
- Young, R. B., and R. H. King, Sediment chemistry and diatom stratigraphy of two high arctic isolation lakes, Truelove Lowland, Devon Island, N.W.T., Canada, *J. Paleolimnol.*, 2, 207-225, 1989.

Effect of Global Climate Change on Forest Productivity: Control Through Forest Floor Chemistry

K. Van Cleve, J. Yarie, and E. Vance

Forest Soils Laboratory, University of Alaska Fairbanks, Alaska, U.S.A.

ABSTRACT

Forest floor chemistry interacts with temperature and moisture to restrict or enhance the supply of nutrients for tree growth. In sub-arctic forests of interior Alaska, this control of element supply is manifest in dramatically different rates of nutrient cycling among the principal forest types. Slow-growing forests developing on cold, wet soils produce organic detritus that is slow to decompose because of its chemical composition. Consequently, element supply is restricted in these ecosystems. Productive forests developing on warm, drier soils produce organic detritus that decays more rapidly because of favorable chemical composition. Element supply is enhanced in these forest ecosystems.

Using the compartment model Linkages, we evaluate several scenarios that propose altered temperature and precipitation regimes for their influence on forest floor chemistry, element supply and the consequence to forest productivity.

92-17818



AD-P007 314



The Sensitivity of Ecosystem CO₂ Flux in the Boreal Forests of Interior Alaska to Climatic Parameters

Gordon B. Bonan

National Center for Atmospheric Research, Boulder, Colorado, U.S.A.

ABSTRACT

An ecophysiological model of carbon uptake and release was used to examine CO₂ fluxes in 17 mature forests near Fairbanks, Alaska. Under extant climatic conditions, ecosystem CO₂ flux ranged from a loss of 212 g CO₂ m⁻² yr⁻¹ in a black spruce stand to an uptake of 2882 g CO₂ m⁻² yr⁻¹ in a birch stand. Increased air temperature resulted in substantial soil warming. Without concomitant increases in nutrient availability, large climatic warming reduced ecosystem CO₂ uptake in all forests. Deciduous and white spruce stands were still a sink for CO₂, but black spruce stands became, on average, a net source of CO₂. With increased nutrient availability that might accompany soil warming, enhanced tree growth increased CO₂ uptake in conifer stands.

INTRODUCTION

The circumpolar boreal forest is the largest reserve of soil carbon and is second only to broadleaf humid forests in terms of carbon stored in live vegetation [Lashof, 1989]. Not surprisingly, boreal forests appear to play a significant role in the seasonal dynamics of atmospheric CO₂ [D'Arrigo et al., 1987]. With its wide range in site conditions, interior Alaska is a unique location to examine atmosphere-biosphere exchange of CO₂ in boreal forests. In mature forests, above-ground woody biomass ranges from 2.6 kg m⁻² in black spruce (*Picea mariana* (Mill.) B.S.P.) forests growing on cold, wet, nutrient-poor soils to 24.6 kg m⁻² in white spruce (*Picea glauca* (Moench.) Voss) forests growing on warmer, mesic soils [Van Cleve et al., 1983]. Forest floor mass ranges from an average of 2.2 kg m⁻² in mature balsam poplar (*Populus balsamifera* L.) forests to an average of 7.6 kg m⁻² in mature black spruce forests [Van Cleve et al., 1983].

Interactions among soil temperature, soil moisture, the forest floor, litter quality, nutrient availability and fire control stand productivity and organic matter decomposition in these forests [Van Cleve and Viereck, 1981; Van Cleve et al., 1983, 1986]. I have developed a process-oriented, ecophysiological model of carbon uptake and release that quantifies these relationships [Bonan, 1991b]. The purpose of this paper is to use this model to examine atmosphere-

biosphere exchange of CO₂ in boreal forests and its sensitivity to climatic parameters.

THE MODEL

Bonan [1991b] describes the calculation of the CO₂ fluxes. The model simulates daily CO₂ fluxes during plant growth and forest floor decomposition (Figure 1). Mosses form a significant component of many boreal forests [Oechel and Van Cleve, 1986], and moss photosynthesis and respiration are additional CO₂ fluxes. Tree photosynthesis is a function of the CO₂ diffusion gradient, bulk boundary layer resistance, stomatal resistance, and mesophyll resistance. Stomatal resistance is a function of irradiance, foliage temperature, vapor pressure deficit, and foliage water potential. Mesophyll resistance includes rate limitations imposed by the diffusion of CO₂ within cells and the effects of foliage temperature, irradiance, and foliage nitrogen on the biochemical process of photosynthesis. Tree respiration is partitioned into maintenance and growth respiration. Maintenance respiration is an exponential function of foliage temperature; growth respiration is a function of the efficiency with which tissue is synthesized. Moss photosynthesis is limited by irradiance, temperature, and moisture content. Moss respiration is also an exponential function of temperature and the efficiency with which new tissue is synthesized. Based on data from Schlentner and Van Cleve

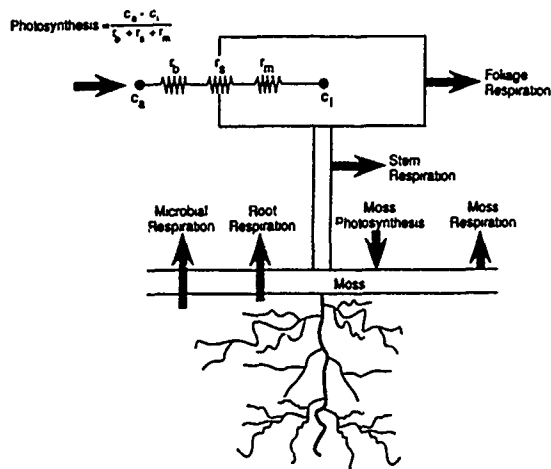


Figure 1. Simulated CO₂ fluxes. Tree fluxes are photosynthesis, and foliage, stem, and root respiration. Moss fluxes include photosynthesis and respiration. Microbial respiration during forest floor decomposition is an additional CO₂ flux. Ecosystem CO₂ flux is the sum of these fluxes. Bonan [1991b] provides more details on the calculation of these fluxes.

[1985], microbial respiration under optimal substrate quality is a function of soil moisture and soil temperature. Decomposition in boreal forests is a linear function of forest floor nitrogen [Flanagan and Van Cleve, 1983], and microbial respiration is adjusted for substrate quality as a function of forest floor nitrogen.

Simulated microbial respiration is converted to dry matter decomposition by the factor 0.61 g dry matter per gram CO₂ respired. Simulated plant dry matter production is directly proportional to the difference between photosynthesis and maintenance respiration (0.44 g dry matter per g CO₂ assimilated). Annual tree production is partitioned into above- and below-ground components.

Required biophysical factors such as the bulk boundary layer resistance, foliage temperature, foliage water potential, irradiance, vapor pressure deficit, soil temperature, and soil moisture are simulated by solving the surface energy budget of a multi-layered forest canopy (Figure 2). A more detailed description and validation of the biophysical calculations has been presented elsewhere [Bonan, 1991a].

Required stand parameters for the model are canopy height, leaf area index, foliage nitrogen, forest floor mass, forest floor nitrogen, moss and humus thickness, and green moss, sapwood, and root biomass. Site parameters are aspect, slope, elevation, soil color, and drainage. These parameters were estimated for one aspen (*Populus trem-*

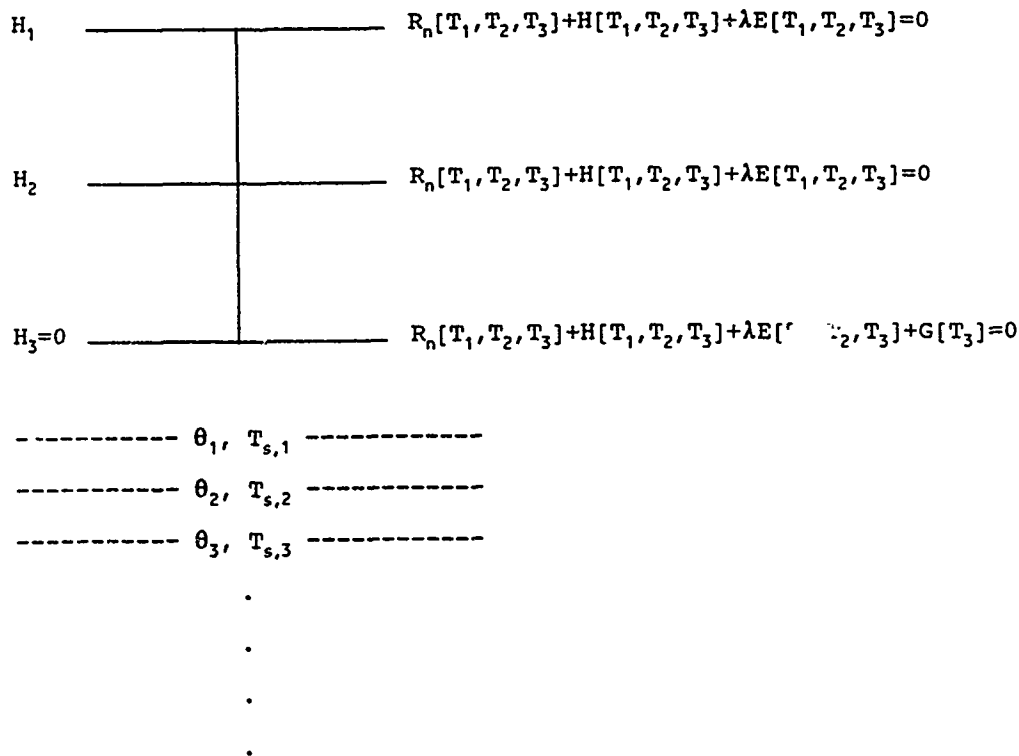


Figure 2. Schematic diagram of the surface energy budget for a forest divided into three layers. The net radiation R_n , sensible heat H , water vapor λE , and soil heat G fluxes in the upper canopy (height h_1), lower canopy (height h_2), and ground surface (height h_3) are a function of three unknown temperatures (T_1 , T_2 , T_3) at heights h_1 , h_2 , and h_3 , respectively. The surface energy budget of each canopy layer must sum to zero, and these three equations are solved simultaneously for the three unknown temperatures. Then, with the ground surface temperature, evapotranspiration, and snow melt known, soil temperature T_s and soil moisture θ in a multi-layered soil are updated. Bonan [1991a] provides more details for these calculations.

uloides Michx.), two birch (*Betula papyrifera* Marsh.), two balsam poplar, four white spruce, and eight black spruce mature stands located near Fairbanks, Alaska, based on observed stand descriptions [Viereck et al., 1983; Van Cleve et al., 1983]. Required climatic parameters were taken for a "typical" meteorological year [NOAA, 1981].

Daily CO₂ fluxes for each stand were simulated for one year with current climatic parameters to obtain control simulations. To evaluate the sensitivity of CO₂ fluxes to climatic parameters, the simulations were then repeated with 1°C, 3°C, and 5°C increases in daily air temperature. Each air temperature increase was repeated with current precipitation and 150% and 200% increases in daily precipitation. The model is not stochastic in any manner. Therefore, simulations are deterministic and differences among the simulations for a particular forest type reflect solely the change in climate parameters.

In addition to the direct effects of soil temperature on plant metabolism, tree photosynthesis increases with soil warming due to greater nutrient mineralization [Van Cleve et al. 1983, 1990]. The model does not simulate dynamic nutrient availability, and to examine this effect on CO₂ fluxes, the simulations for black spruce and white spruce, where current foliage nitrogen concentrations (0.7%) limit photosynthesis, were repeated but with increased foliage nitrogen concentrations (1.0%). This increase in foliage nitrogen reflects data from experimental heating of a cold soil [Van Cleve et al., 1983, 1990].

Bonan [1991a,b] provides detailed results of the control simulations. Simulated solar radiation, soil temperature, foliage water potential, evapotranspiration, and snow melt were consistent with observed data [Bonan, 1991a]. Simulated soil respiration, moss production, decomposition, and tree production were also consistent with observed data [Bonan, 1991b]. (Note: In contrast with the analyses of Bonan [1991b], here the ambient CO₂ concentration was 600 mg m⁻³ rather than 640 mg m⁻³).

RESULTS

The sensitivity of ecosystem CO₂ flux to climatic parameters varied with forest type. Without increased nutrient availability, the 1°C warming enhanced tree growth for the deciduous and white spruce stands (Tables 1 and 2). Decomposition also increased, but the net result was that these stands were a greater sink of CO₂ than in the control simulations. With increases in air temperature of 3°C and 5°C, tree production in these stands declined. Decomposition increased, and though these stands were a net sink for CO₂, they were less of a sink than in the control simulations. In contrast, the 1°C warming substantially reduced black spruce tree production (Table 3). Tree respiration exceeded photosynthesis in two of the eight black spruce stands, and ecosystem CO₂ uptake decreased from the control simulation. With the 3°C and 5°C warming, these stands became, on average, a source of CO₂ as net carbon uptake by trees and mosses was further reduced. With the 5°C warming, tree respiration exceeded photosynthesis in six of the eight stands.

Increased nutrient availability in the conifer stands enhanced tree growth compared to comparable nutrient-poor simulations (compare Table 4 with Tables 2 and 3). For black spruce, tree productivity and ecosystem CO₂ uptake

	Annual Productivity				
	SDD	Trees g m ⁻²	Moss g m ⁻²	Decomposition g m ⁻²	CO ₂ g m ⁻²
Control	1194	900	0	294	2376
1°C	1293	917	0	311	2421
150%	1301	915	0	317	2407
200%	1302	909	0	319	2381
3°C	1488	813	0	346	2027
150%	1505	819	0	354	2031
200%	1507	815	0	357	2013
5°C	1683	698	0	382	1588
150%	1705	702	0	391	1585
200%	1711	704	0	396	1584

Table 1. Deciduous forests: Simulated soil degree days (SDD) from May 20 to September 10 at 10 cm depth, annual above-ground tree productivity, annual moss productivity, annual forest floor decomposition, and annual ecosystem CO₂ flux with climatic warming and precipitation increases. A positive CO₂ flux indicates net uptake by the ecosystem. All values are averages for the five stands.

	Annual Productivity				
	SDD	Trees g m ⁻²	Moss g m ⁻²	Decomposition g m ⁻²	CO ₂ g m ⁻²
Control	997	366	111	202	851
1°C	1084	365	105	210	988
150%	1090	381	113	216	1053
200%	1091	378	113	220	1036
3°C	1251	274	86	227	620
150%	1275	295	70	239	703
200%	1283	297	74	244	706
5°C	1405	145	62	244	100
150%	1447	174	79	260	211
200%	1468	180	87	268	235

Table 2. Same as Table 1 but for four white spruce stands.

were enhanced for all climatic warmings when compared to the control simulation. For white spruce, tree productivity and ecosystem CO₂ uptake increased from the control simulation for the 1°C and 3°C warming, but decreased for the 5°C warming.

DISCUSSION

Under extant climatic conditions, mature boreal forests in interior Alaska range from a source of 212 g CO₂ m⁻² yr⁻¹ in a black spruce stand to a sink of 2882 g CO₂ m⁻² yr⁻¹ in a birch stand. This flux was extremely sensitive to air temperature increases. In all forest types, organic matter decomposition increased with increased air temperature. This reflected greater microbial activity with warmer soils. Moss productivity decreased with climatic warming because of increased dryness with a warmer climate. Indeed, for a

	<u>Annual Productivity</u>				
	SDD	Trees g m ⁻²	Moss g m ⁻²	Decomposition g m ⁻²	CO ₂ g m ⁻²
Control	642	113	98	107	196
1°C	692	68	91	110	146
150%	722	63	96	114	131
200%	717	55	96	116	100
3°C	787	40	68	114	0
150%	858	31	79	123	-26
200%	859	22	82	124	-52
5°C	852	-1	35	118	-217
150%	997	-14	52	130	-247
200%	1005	-22	59	133	-264

Table 3. Same as Table 1 but for eight black spruce forests.

given climatic warming, moss productivity increased with increases in precipitation.

Without increased nutrient availability, air temperature increases greater than 1°C caused annual above-ground tree productivity to decrease even though the soils became warmer. Though tree photosynthesis increased with climatic warming, tree respiration increased more. In particular, warmer soil temperatures greatly enhanced root respiration. For example, in a black spruce stand growing on a terrace at 468 m, annual CO₂ uptake during tree photosynthesis was 1531, 1559, 1657, and 1708 g m⁻² in the control, 1°C, 3°C, and 5°C simulations, respectively. However, annual tree respiration was 1379, 1462, 1651, and 1854 g CO₂ m⁻², respectively. Likewise, in a lowland white spruce stand at 120 m, annual tree photosynthesis was 3430, 3462, 3610, and 3679 g CO₂ m⁻² and annual tree respiration was 2491, 2652, 3040, 3505 g CO₂ m⁻² for the control, 1°C, 3°C, and 5°C simulations. Decreased net CO₂ uptake during tree growth reduced ecosystem uptake in all stands. With the 3°C and 5°C warmings, black spruce stands became, on average, a source of CO₂.

	<u>Black Spruce</u>		<u>White Spruce</u>	
	NPP g m ⁻²	CO ₂ g m ⁻²	NPP g m ⁻²	CO ₂ g m ⁻²
1°C	186	532	543	1541
3°C	164	405	461	1211
5°C	124	196	344	750

Table 4. Annual above-ground tree productivity (NPP) and annual ecosystem CO₂ flux with climatic warming and increased nitrogen availability. A positive CO₂ flux indicates uptake by vegetation. All values are averages for each forest type.

Nutrient availability increases with soil warming [Van Cleve et al., 1983, 1990]. When increased nutrient availability was included in the simulations, tree photosynthesis increased in the nutrient-poor conifer stands. The net effect was that these stands took up greater amounts of CO₂. This was most important in the black spruce stands, where increased nutrient availability promoted tree growth such that with 3°C and 5°C increases in air temperature, these sites were a sink rather than a source of CO₂.

These simulations examined the short-term (one year) response of boreal forests to climatic warming. The long-term effects of climatic warming on ecosystem CO₂ flux are likely to differ. For example, the equilibrium response of soil temperature to climatic warming will differ from the transient response. However, these analyses highlight the sensitivity of tree photosynthesis and respiration to climatic warming and the importance of nutrient availability in determining CO₂ fluxes with climatic warming.

ACKNOWLEDGMENTS

This manuscript was prepared while the author was a postdoctoral fellow in the Advanced Study Program at the National Center for Atmospheric Research. The National Center for Atmospheric Research is sponsored by the National Science Foundation.

REFERENCES

- Bonan, G. B., A biophysical surface energy budget analysis of soil temperature in the boreal forests of interior Alaska, *Water Resour. Res.*, 27, 767-781, 1991a.
- Bonan, G. B., Atmosphere-biosphere exchange of carbon dioxide in boreal forests, *J. Geophys. Res.*, 96, 7301-7312, 1991b.
- D'Arrigo, R., G. C. Jacoby, and I. Y. Fung, Boreal forests and atmosphere-biosphere exchange of carbon dioxide, *Nature*, 329, 321-323, 1987.
- Flanagan, P. W., and K. Van Cleve, Nutrient cycling in relation to decomposition and organic-matter quality in taiga ecosystems, *Can. J. For. Res.*, 13, 795-817, 1983.
- Lashof, D. A., The dynamic greenhouse: feedback processes that may influence future concentrations of atmospheric trace gases and climatic change, *Climatic Change*, 14, 213-242, 1989.
- NOAA, Typical meteorological year. Hourly solar radiation - surface meteorological observations, *User's manual TD-9734*, National Climatic Data Center, Asheville, NC, 1981.
- Oechel, W. C., and K. Van Cleve, The role of bryophytes in nutrient cycling in the taiga, in *Forest Ecosystems in the Alaskan Taiga*, edited by K. Van Cleve, F. S. Chapin, P. W. Flanagan, L. A. Viereck, and C. T. Dyrness, pp.121-137, Springer-Verlag, New York, 1986.
- Schlentner, R. E., and K. Van Cleve, Relationships between CO₂ evolution from soil, substrate temperature, and substrate moisture in four mature forest types in interior Alaska, *Can. J. For. Res.*, 15, 97-106, 1985.
- Van Cleve, K., and L. A. Viereck, Forest succession in relation to nutrient cycling in the boreal forest of interior Alaska, in *Forest Succession: Concepts and Application*, edited by D. C. West, H. H. Shugart, and D. B. Botkin, pp. 185-211, Springer-Verlag, New York, 1981.
- Van Cleve, K., L. Oliver, R. Schlentner, L. A. Viereck, and C. T. Dyrness, Productivity and nutrient cycling in taiga forest ecosystems, *Can. J. For. Res.*, 13, 747-766, 1983.
- Van Cleve, K., F. S. Chapin, P. W. Flanagan, L. A. Viereck, and C. T. Dyrness, *Forest Ecosystems in the Alaskan Taiga*, Springer-Verlag, New York 1986.
- Van Cleve, K., W. C. Oechel, and J. L. Hom, Response of black spruce (*Picea mariana*) ecosystems to soil temperature modification in interior Alaska, *Can. J. For. Res.*, 20, 1530-1535, 1990.
- Viereck, L. A., C. T. Dyrness, K. Van Cleve, and M. J. Foote, Vegetation, soils, and forest productivity in selected forest types in interior Alaska, *Can. J. For. Res.*, 13, 703-720, 1983.

Evolutionary History of Polar Regions

J. A. Crame

British Antarctic Survey, Natural Environment Research Council, Cambridge, United Kingdom

ABSTRACT

A traditional view of life on earth is that most major groups of plants and animals arose in the tropics and then disseminated to higher latitude regions. In some way, competitively less successful forms are displaced progressively towards mid- and high-latitude regions, with only the most tolerant forms reaching the poles. The latter are frequently cited as refugia.

However, we now know significantly more about the evolutionary history of polar regions than was the case when such theories were first promulgated. In particular, it is evident that, for long periods of geological time, vast areas of ice-free continent and continental shelf were present in the highest latitudes of both hemispheres. These undoubtedly served as the sites of origin for at least some of the components of the distinctive Mesozoic Boreal realm and its austral counterpart. Indeed it is likely that a distinctive biotic realm has characterized the southern high latitudes, at least intermittently, since the late Paleozoic.

In recent years it has become apparent that West Antarctica and its contiguous regions may have been the center of origin for a range of recent taxa. Here, the late Mesozoic and Cenozoic paleontological record contains the first occurrences of a number of prominent taxa in living Southern Hemisphere temperate forests. The same beds have also yielded first records of living marine invertebrate types such as decapod crustaceans, echinoids, bivalves, gastropods and brachiopods. It is even possible, at least within the marine realm, that the polar regions are still actively providing new taxa. In Antarctica, for example, certain groups of very closely related species (such as pycnogonids, buccinacean gastropods, certain echinoderms and notothenioid fish) seem to be the product of extensive Cenozoic adaptive radiations.

The polar regions may yet be shown to have been significant contributors to the global species pool.

AD-P007 315



92-17819



Possible Impacts of Ozone Depletion on Trophic Interactions and Biogenic Vertical Carbon Flux in the Southern Ocean

Harvey J. Marchant and Andrew Davidson
Australian Antarctic Division, Kingston, Tasmania, Australia

ABSTRACT

Among the most productive region of the Southern Ocean is the marginal ice edge zone that trails the retreating ice edge in spring and early summer. The timing of this near-surface phytoplankton bloom coincides with seasonal stratospheric ozone depletion when UV irradiance is reportedly as high as in mid-summer. Recent investigations indicate that antarctic marine phytoplankton are presently UV stressed. The extent to which increasing UV radiation diminishes the ability of phytoplankton to fix CO₂ and/or leads to changes in their species composition is equivocal. The colonial stage in the life cycle of the alga *Phaeocystis pouchetii* is one of the major components of the bloom. We have found that this alga produces extracellular products which are strongly UV-B absorbing. When exposed to increasing levels of UV-B radiation, survival of antarctic colonial *Phaeocystis* was significantly greater than colonies of this species from temperate waters and of the single-celled stage of its life cycle which produces no UV-B-absorbing compounds. *Phaeocystis* is apparently a minor dietary component of antarctic krill, *Euphausia superba*, and its nutritional value to crustacea is reportedly low. Phytoplankton, principally diatoms, together with fecal pellets and molted exoskeletons of grazers contribute most of the particulate carbon flux from the euphotic zone to deep water. If the species composition of antarctic phytoplankton was to shift in favor of *Phaeocystis* at the expense of diatoms, changes to pelagic trophic interactions as well as vertical carbon flux are likely.

INTRODUCTION

Stratospheric ozone over Antarctica and the Southern Ocean is markedly depleted during spring [Stolarski et al., 1986], resulting in UV flux rates similar to mid-summer conditions [Frederick and Snell, 1988]. Solar UV-B radiation penetrates oceanic water to depths that are able to influence the growth of macrophytes and phytoplankton [Jitts et al., 1976; Lorenzen, 1979; Calkins and Thordardottir, 1980; Worrest, 1983; Maske, 1984; Wood, 1987, 1989]. In addition, Trodahl and Buckley [1989] suggest that antarctic sea ice in early spring may be sufficiently transparent to UV for organisms living in and under it to receive levels of radiation high enough to have biological consequences.

The effect of UV-B radiation on antarctic marine phytoplankton is equivocal [Roberts, 1989]. El-Sayed et al.

[1990] concluded that antarctic phytoplankton are presently under UV stress and are likely to be seriously affected by any increase in UV-B radiation as would the higher trophic levels of the Southern Ocean food web. In contrast, Holm-Hansen et al. [1989] found that although the rate of photosynthesis by phytoplankton in the top meter of the water column was depressed by about 30%, organisms at depths greater than 20 m were unaffected by *in situ* exposure to UV. They concluded that increased UV irradiation would have little impact on the phytoplankton and higher trophic levels of the Southern Ocean. Species of phytoplankton differ in their ability to survive UV irradiation [Calkins and Thordardottir, 1980], and Karentz [1991] has argued that the most likely effect of elevated UV irradiation on antarctic marine phytoplankton is a shift in the species composition.

The principal primary producers in the Southern Ocean are diatoms. As well as contributing directly to the vertical flux of carbon, they are grazed by crustacea, especially euphausiids. The feces and molted exoskeletons of grazers constitute a major avenue of carbon to deep water [Nicol and Stolp, 1989]. Here we briefly review the spatial and temporal distribution of antarctic marine phytoplankton, especially *Phaeocystis pouchetii*. We discuss our finding of UV-B-absorbing pigments in this alga and the protection that they confer [Marchant et al., 1991] and consider the possible consequences on trophic interactions and biogenic vertical carbon flux of *Phaeocystis* surviving elevated levels of UV exposure.

SPRINGTIME SEA ICE RETREAT AND THE MARGINAL ICE EDGE ZONE

Meltwater released from the retreating sea ice generates a pycnocline at about 20 m depth above which phytoplankton bloom. Data from Jennings et al. [1984] indicate that 25–67% of the nutrient depletion in the Southern Ocean is due to phytoplankton production in the marginal ice edge zone [Smith and Nelson, 1986]. This southward-moving region of high productivity is coupled to higher trophic levels [Ainley et al., 1986], providing much of the carbon required to sustain the large populations of zooplankton, birds and mammals for which the Southern Ocean is noted [Ross and Quetin, 1986; Sakshaug and Skjoldal, 1989].

The most abundant components of the phytoplankton of the marginal ice edge zone are diatoms, principally of the genus *Nitzschia*, and the prymnesiophyte *Phaeocystis pouchetii* [Garrison et al., 1987; Fryxell and Kendrick, 1988; Garrison and Buck, 1989; Davidson and Marchant, 1991]. The massive deposits of diatomaceous ooze in Southern Ocean sediments, the species composition of which is dominated by the taxa found in the ice edge bloom [Truesdale and Kellogg, 1979] are thought to be due to reduced coupling of production and consumption in the marginal ice edge zone. Thus a substantial amount of the biogenic production sinks rapidly from the euphotic zone [Smith and Nelson, 1986] and while some is grazed, sedimentation is apparently the principal fate of much of this ice edge bloom [Smith and Nelson, 1986; Bodungen et al., 1986; Fischer et al., 1988].

THE ROLE OF PHAEOCYSTIS IN THE MARGINAL ICE EDGE ZONE

The cosmopolitan alga *Phaeocystis pouchetii* has two principal stages in its life cycle, free-swimming biflagellate unicells and a colonial phase in which cells are embedded in a mucilaginous matrix. Colonial *Phaeocystis* has been reported from the sea ice and the marginal ice edge zone where it is frequently one of the most abundant algae blooming in the top few meters of the water column. *Phaeocystis* apparently plays a pivotal role in the timing of the successional sequence of other autotrophs by mediating the availability of manganese [Davidson and Marchant, 1987; Lubbers et al., 1989]. Also, at least in antarctic waters, this alga provides substrates for heterotrophs by secretion of a large proportion of its photoassimilated carbon as particulate and dissolved organic matter [Davidson and Marchant, 1991]. In addition, *Phaeocystis* is reportedly the principal producer of dimethyl sulfide (DMS) in antarctic waters

[Gibson et al., 1990]. Oxidation of this DMS forms sulfate particles which constitute a major source of cloud condensation nuclei (CCN). Bates et al. [1987] and Charlson et al. [1987] propose that the abundance of CCN determines global albedo thereby establishing a mechanism for the regulation of climate by marine biological activity. Gibson et al. [1990] estimate that antarctic *Phaeocystis* may contribute as much as 10% of the total global flux of DMS to the atmosphere.

GRAZING ON PHAEOCYSTIS

Although *Phaeocystis* is grazed by herbivores including *Euphausia superba* [Sieburth, 1960; Marchant and Nash, 1986], the effect of grazing on this alga and its food value are equivocal [Verity and Smayda, 1989]. In an investigation on the impact of copepod grazing on a phytoplankton bloom in which *Phaeocystis* comprised about 97% of the biomass and the remainder was mainly diatoms, the diatoms accounted for some 74% of the copepod diet [Claustre et al., 1990]. Only 1.5% of the biomass of *Phaeocystis* was grazed by the copepods, the remainder apparently being lost to the pelagic food web. In addition, Claustre et al. [1990] reported that the low nutritional value of *Phaeocystis* was due to its fatty acid to chlorophyll *a* ratio being much lower than was found in diatoms. This was also the case for amino acids and vitamin C. *Phaeocystis* from antarctic sea ice has been found to have significantly lower concentrations of neutral lipids than diatom assemblages dominated by *Nitzschia* and *Navicula* [Priscu et al., 1990]. Antarctic euphausiids reportedly have a dietary preference for diatoms [Meyer and El-Sayed, 1983; Miller and Hampton, 1989]. We have found that at an antarctic inshore site very little of the carbon attributable to *Phaeocystis* is apparently utilized by metazoa [Davidson and Marchant, 1991] and, as was found by Claustre et al. [1990], most of the carbon was not used *in situ*.

VERTICAL CARBON FLUX IN THE SOUTHERN OCEAN

In addition to the direct contribution of the primary producers, fecal pellets of heterotrophs including protozoa [Nöthig and Bodungen, 1989; Buck et al., 1990] and metazoa, including krill [Wefer et al., 1988], contribute substantially to particulate carbon flux from surface waters of the Southern Ocean. In contrast to the marked seasonality of the sedimentation of primary producers and the feces of grazers, cast exoskeletons of *E. superba* are likely to constitute a major year-round flux of particulate organic carbon from the euphotic zone to deep water or the sediments [Nicol and Stolp, 1989].

UV-ABSORBING COMPOUNDS PRODUCED BY PHAEOCYSTIS

We have found that the mucilage of *Phaeocystis* colonies themselves as well as substances secreted into them absorb strongly in the UV region of the spectrum. Axenic cultures of this alga isolated from Prydz Bay, Antarctica, produce extracellular products that absorb strongly at 323 and 271 nm [Marchant et al., 1991]. Absorbance at 271 nm is unlikely to provide protection to the alga additional to that conferred by the attenuation of water [Smith and Baker, 1979]. The motile cells of *Phaeocystis* from Antarctica lack

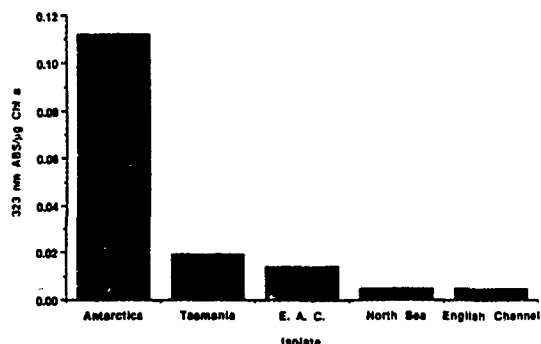


Figure 1. Concentration of 323 nm absorbing pigment per µg chlorophyll *a* from various isolates of *Phaeocystis*. E.A.C. = East Australian Current.

these UV-absorbing substances. Cultures of colonial cells of *Phaeocystis* from the East Australian Current, Tasmanian coastal waters, the North Sea and the English Channel possess these compounds but at substantially lower concentrations than found in antarctic material (Figure 1). The compounds are colorless, water soluble, labile and broken down by bacteria.

These UV-B-absorbing pigments confer a high level of protection to this alga. *Phaeocystis* cultures were exposed to increasing total irradiance using simulated sunlight or increasing UV-B irradiance alone while holding PAR and UV-A constant. Antarctic colonial *Phaeocystis* survived higher irradiances than colonial cells from the East Australian current or motile cells from Antarctica. While *Phaeocystis* has an effective UV-B protective screen, diatom species apparently differ in their level of UV-B screening. Some diatoms apparently lack UV-B-absorbing compounds [Yentsch and Yentsch, 1982]. In those species that do produce these compounds, their concentration is much lower than that found in *Phaeocystis* [J. Raymond, personal communication; A. Davidson, unpublished data]. Thus growth of the colonial stage of *Phaeocystis* rather than diatoms is likely to be favored under elevated levels of UV-B. In *Phaeocystis*-dominated blooms the colonial cell concentration can be very high, reaching 6×10^7 cells l^{-1} in ant-

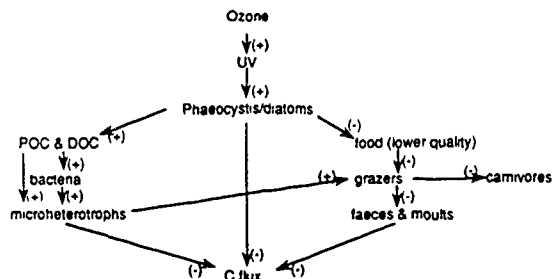


Figure 2. Conceptual diagram of the possible impacts of ozone depletion on Southern Ocean processes. The sign (+ or -) on the arrows indicates the direction of the possible change.

arctic coastal waters [Davidson and Marchant, 1991]. At such concentrations the absorbance in the water column at 323 nm would be about $80\% m^{-1}$ compared with $14\% m^{-1}$ in clear water [Jerlov, 1950] and is thus likely to mitigate UV exposure to co-occurring organisms.

The possible ramifications of increased dominance of *Phaeocystis* at the expense of diatoms in the marginal ice edge zone are indicated in Figure 2. Few data are available to indicate the consequences of such a change in species dominance. If however, as appears to be the case, crustacea selectively graze diatoms in preference to *Phaeocystis*, and diatoms are of greater food value, then there is the possibility that populations of krill and other grazers could be nutrient-limited with a consequent diminution of the food available to higher trophic levels. Reduced availability of more relatively nutritious food may reduce the fecundity of grazers [Verity and Smayda, 1989]. Any diminution in diatom growth is likely to reduce vertical carbon flux. In addition to the reduced flux of feces and molts of grazers that prefer diatoms there would be a decline in the flux of diatoms themselves. The high concentrations of slow-sinking POC and DOC produced by *Phaeocystis* provide substrates for bacteria and microheterotrophs in surface waters. Respiration by these organisms is likely to result in higher concentrations of CO_2 in the photic zone. Further, organisms of the microbial loop are more likely to produce smaller, slower-sinking particles than the feces and molts of grazers and thus constitute a lesser carbon flux than the larger, faster-sinking material.

REFERENCES

- Ainley, D. G., W. R. Fraser, C. W. Sullivan, J. J. Torres, T. L. Hopkins, and W. O. Smith, Antarctic mesopelagic micronekton: Evidence from seabirds that pack ice affects community structure, *Science*, 232, 847-849, 1986.
- Bates, T. S., R. J. Charlson, and R. H. Gammon, Evidence for the climatic role of marine sulphur, *Nature*, 329, 319-321, 1987.
- Bodungen, B. v., V. S. Smetacek, M. M. Tilzer, and B. Zeitzschel, Primary production and sedimentation during spring in the Antarctic Peninsula region, *Deep-Sea Res.*, 33, 177-194, 1986.
- Buck, K. R., P. A. Bolt, and D. L. Garrison, Phagotrophy and fecal pellet production by an athecate dinoflagellate in Antarctic sea ice, *Mar. Ecol. Prog. Ser.*, 60, 75-84, 1990.
- Calkins, J., and T. Thordardottir, The ecological significance of solar UV radiation on aquatic organisms, *Nature*, 283, 563-566, 1980.
- Charlson, R. L., J. E. Lovelock, M. O. Andreae, and S. G. Warren, Oceanic phytoplankton, atmospheric sulfur, cloud albedo and climate, *Nature*, 326, 655-661, 1987.
- Claustre, H., S. A. Poulet, R. Williams, J.-C. Marty, S. Coombs, F. Ben Mlih, A. M. Hapette, and V. Martin-Jezequel, A biochemical investigation of a *Phaeocystis* sp. bloom in the Irish Sea, *J. Mar. Biol. Ass. U.K.*, 70, 197-207, 1990.
- Davidson, A. T., and H. J. Marchant, Binding of manganese by antarctic *Phaeocystis pouchetii* and the role of bacteria in its release, *Mar. Biol.*, 95, 481-487, 1987.
- Davidson, A. T., and H. J. Marchant, Protist interactions and carbon dynamics of a *Phaeocystis*-dominated bloom at an Antarctic coastal site, *Polar Biol.* (submitted), 1991.

- El-Sayed, S. Z., F. C. Stephens, R. R. Bidigare, and M. E. Ondrusek, Effect of ultraviolet radiation on Antarctic marine phytoplankton, in *Antarctic Ecosystems. Ecological Change and Conservation*, edited by K. R. Kerry and G. Hempel, pp. 379-385, Springer-Verlag, Berlin, Heidelberg, 1990.
- Fischer, G., D. Fuetterer, R. Gersonde, S. Honjo, D. Ostermann, and G. Wefer, Seasonal variability of particle flux in the Weddell Sea and its relation to ice cover, *Nature*, 335, 426-428, 1988.
- Frederick, J. E., and H. E. Snell, Ultraviolet radiation levels during the antarctic spring, *Science*, 241, 438-440, 1988.
- Fryxell, G. A., and G. A. Kendrick, Austral spring microalgae across the Weddell Sea ice edge; spatial relationships found along a northward transect during AMERIEZ 83, *Deep-Sea Res.*, 35, 1-20, 1988.
- Garrison, D. L., K. R. Buck, and G. A. Fryxell, Algal assemblages in the antarctic pack ice and in ice-edge plankton, *J. Phycol.*, 23, 564-572, 1987.
- Garrison, D. L., and K. R. Buck, The biota of Antarctic pack ice in the Weddell Sea and Antarctic Peninsular regions, *Polar Biol.*, 10, 211-219, 1989.
- Gibson, J. A. E., R. C. Garrick, H. R. Burton, and A. R. McTaggart, Dimethylsulfide and the alga *Phaeocystis pouchetii* in antarctic coastal waters, *Mar. Biol.*, 104, 339-346, 1989.
- Holm-Hansen, O., B. G. Mitchell, and M. Vernet, Ultraviolet radiation in antarctic waters: Effects on rates of primary production, *Antarctic J. U.S.*, 24, 177-178, 1989.
- Jennings, J. C., L. I. Gordon, and D. M. Nelson, Nutrient depletion indicates high primary productivity in the Weddell Sea, *Nature*, 399, 51-54, 1984.
- Jerlov, N. G., Ultra-violet radiation in the sea, *Nature*, 166, 111-112, 1950.
- Jitts, H. R., A. Morel, and Y. Saijo, The relation of oceanic primary production to available photosynthetic irradiance, *Aust. J. Mar. Freshw. Res.*, 27, 441-454, 1976.
- Karentz, D., Ecological considerations of Antarctic ozone depletion, *Antarctic Science*, 3, 3-11, 1991.
- Lorenzen, C. J., Ultraviolet radiation and phytoplankton photosynthesis, *Limnol. Oceanogr.*, 24, 1117-1120, 1979.
- Lubbers, G. W., W. W. C. Gieskes, P. del Castilho, W. Salomons, and J. Bril, Manganese accumulation in the high pH microenvironment of *Phaeocystis* sp. (Haptophyceae) colonies from the North Sea, *Mar. Ecol. Prog. Ser.*, 59, 285-293, 1990.
- Marchant, H. J., and G. V. Nash, Electron microscopy of gut contents and faeces of *Euphausia superba* Dana, *Mem. Natl. Inst. Polar Res. Spec. Issue*, 40, 167-177, 1986.
- Marchant, H. J., A. T. Davidson, and G. J. Kelly, UV-B protecting pigments in the marine alga *Phaeocystis pouchetii* from Antarctica, *Mar. Biol.*, 1991, In press.
- Maske, H., Daylight ultraviolet radiation and the photo-inhibition of phytoplankton carbon uptake, *J. Plankton Res.*, 6, 351-357, 1984.
- Meyer, M. A., and S. Z. El-Sayed, Grazing of *Euphausia superba* Dana on natural populations, *Polar Biol.*, 1, 193-197, 1983.
- Miller, D. G. M., and I. Hampton, *Biology and Ecology of the Antarctic Krill (Euphausia superba Dana): A Review*, BIOMASS Scientific Series No. 9, 166 pp., SCAR & SCOR, Scott Polar Research Institute, Cambridge, 1989.
- Nöthig, E.-M., and B. v. Bodungen, Occurrence and vertical flux of faecal pellets of probably protozoan origin in the southeastern Weddell Sea (Antarctica), *Mar. Ecol. Prog. Ser.*, 56, 281-289, 1989.
- Nicol, S., and M. Stolp, Sinking rates of cast exoskeletons of Antarctic krill (*Euphausia superba* Dana) and their role in the vertical flux of particulate matter and fluoride in the Southern Ocean, *Deep-Sea Res.*, 36, 1753-1762, 1989.
- Priscu, J. C., L. R. Priscu, A. C. Palmisano, and C. W. Sullivan, Estimation of neutral lipid levels in Antarctic sea ice microalgae by Nile red fluorescence, *Antarctic Science*, 2, 149-155, 1990.
- Roberts, L., Does the ozone hole threaten antarctic life?, *Science*, 244, 288-289, 1989.
- Ross, R. M., and L. B. Quetin, How productive are Antarctic krill, *BioScience*, 36, 264-269, 1986.
- Sakshaug, E., and H. R. Skjoldal, Life at the ice edge, *Ambio*, 18, 60-67, 1989.
- Sieburth, J. McN., Acrylic acid, an "antibiotic" principle in *Phaeocystis* blooms in Antarctic waters, *Science*, 132, 676-677, 1960.
- Smith, R. C., and K. S. Baker, Penetration of UV-B and biologically effective dose-rates in natural water, *Photochem. Photobiol.*, 29, 311-323, 1979.
- Smith, W. O., Jr., and D. M. Nelson, Importance of ice edge phytoplankton production in the Southern Ocean, *BioScience*, 36, 251-257, 1986.
- Stolarski, R. S., A. J. Krueger, M. R. Schoeberl, R. D. McPeters, P. A. Newman, and J. C. Alpert, Nimbus 7 satellite measurements of the springtime Antarctic ozone decrease, *Nature*, 322, 808-811, 1986.
- Trodahl, H. J., and R. G. Buckley, Ultraviolet levels under sea ice during the antarctic spring, *Science*, 245, 194-195, 1989.
- Truesdale, R. S., and T. B. Kellogg, Ross Sea diatoms: modern assemblage distributions and their relationship to ecologic, oceanographic and sedimentary conditions, *Mar. Micropaleontol.*, 4, 13-31, 1979.
- Verity, P. G., and T. J. Smayda, Nutritional value of *Phaeocystis pouchetii* (Prymnesiophyceae) and other phytoplankton for *Acartia* spp. (Copepoda): ingestion, egg production, and growth of nauplii, *Mar. Biol.*, 100, 161-171, 1989.
- Wefer, G., G. Fischer, D. Fuetterer, and R. Gersonde, Seasonal particle flux in the Bransfield Strait, Antarctica, *Deep-Sea Res.*, 35, 891-898, 1988.
- Wood, W. F., Effect of solar ultra-violet radiation in the kelp *Ecklonia radiata*, *Mar. Biol.*, 96, 143-150, 1987.
- Wood, W. F., Photoadaptive responses of the coral red alga *Eucheuma striatum* Schmitz (Gigartinales) to ultra-violet radiation, *Aquatic Bot.*, 33, 41-51, 1989.
- Worrest, R. C., Impact of solar ultraviolet-B radiation (290-320 nm) upon marine microalgae, *Physiol. Plant.*, 58, 428-434, 1983.
- Yentsch, C. S., and C. M. Yentsch, The attenuation of light by marine phytoplankton with special reference to the absorption of near-UV radiation, in *The Role of Solar Ultraviolet Radiation in Marine Ecosystems*, edited by A. J. Calkins, pp. 691-706, Plenum, New York, 1982.

AD-P007 316



92-17820



Relationships Between Whale Hunting, Human Social Organization, and Subsistence Economies in Coastal Areas of Northwest Alaska during Late Prehistoric Times

R. K. Harritt

U.S. National Park Service, Alaska Region, Anchorage, Alaska, U.S.A.

ABSTRACT

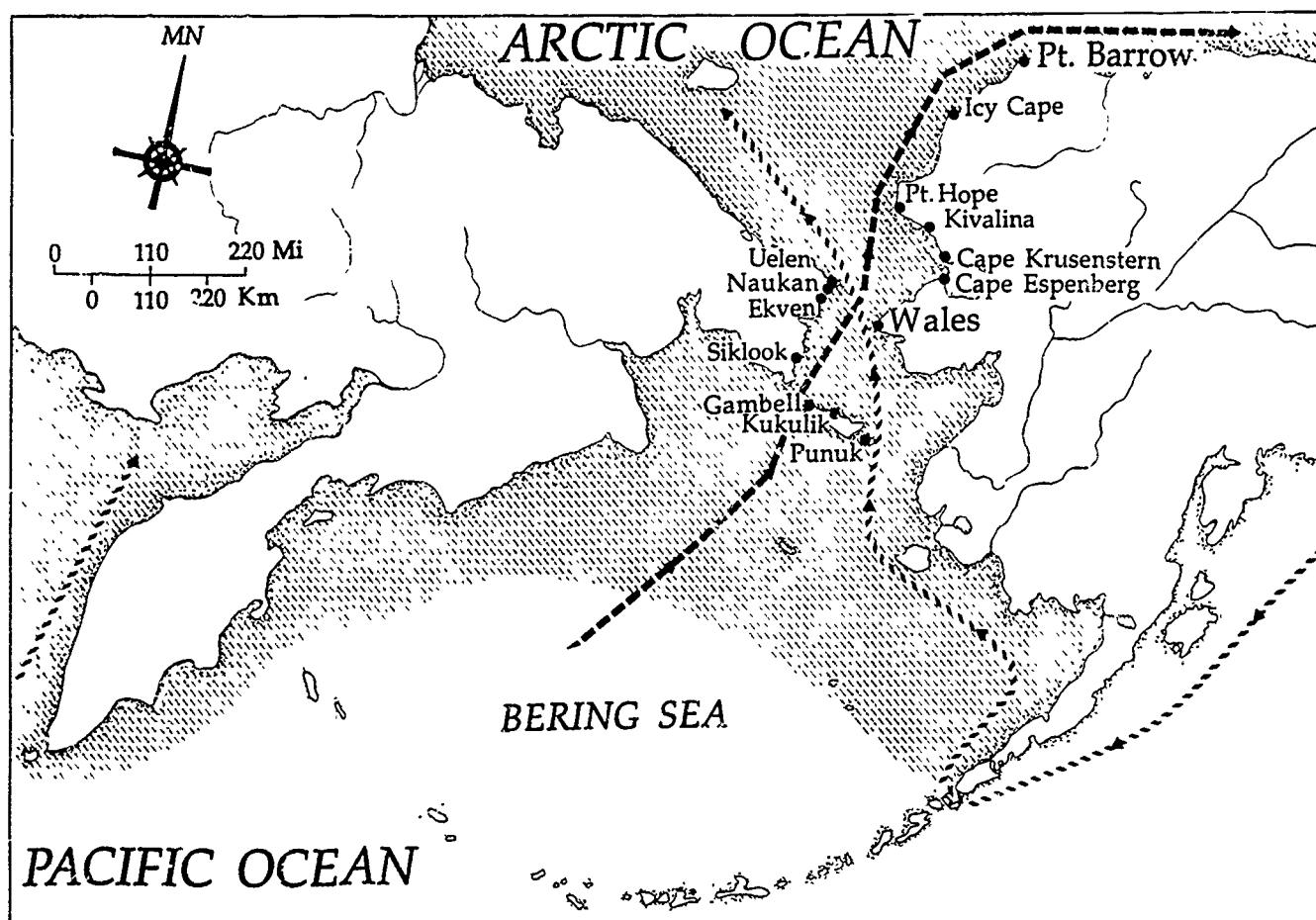
The florescence of Eskimo whaling on northwest Alaskan coasts during Western Thule times, A.D. 1000-1400, was followed by a shift to a more balanced subsistence pattern for human inhabitants of many coastal areas during Kotzebue Period times, from A.D. 1400-1900. The cause of this shift has been identified as a change in the migration routes of whales passing through Bering Strait which presented a circumstance prohibitive to effective whale hunting. Previous interpretations of social organization of the large whaling villages of the earlier portion of this period have suggested that whale hunting provided a basis for development of social ranking of village inhabitants with the umealik, or whaling captain, assuming the role of a chief. Concomitant explanations for the later, more diffuse settlement pattern encountered by early European explorers have not been previously presented. An alternative position presented here is that prehistoric Eskimo societies retained many egalitarian tenets throughout late prehistoric times. This social pattern provided flexibility in subsistence economies with nuclear families as the basic unit transferable from one permanent village to the next, and as a segment of society capable of effectively exploiting sparsely distributed seasonal resources. In this interpretation, social status can be construed as a seasonal phenomenon in which authority or rank was vested in an individual who had demonstrated special skills and abilities in organizing and carrying out successful hunts, and other food procurement expeditions. This status was relinquished as seasonal requirements for food acquisition changed.

INTRODUCTION

Differing interpretations of social and subsistence aspects of whaling by prehistoric and historic native inhabitants of northwest Alaskan coasts have been presented over the past 30 years. Here I present an alternative interpretation to one of these; a position taken by Sheehan [1985], who suggests that social ranking developed in late prehistoric and early historic Eskimo whaling villages. Sheehan argues that an abundance of food provided by whale harvesting enabled influential individuals who were good whale hunters to obtain and keep authority over less accomplished individuals within a village. Before discussing specific aspects of Sheehan's [1985] argument and my own, it is important to place Eskimo whaling in archaeological and historical context.

THE PREHISTORY OF WHALING

The earliest evidence of a substantial focus on whaling was found in Okvik/Old Bering sea components at the Ekven site on East Cape, Siberia, dating to the beginning of the first millennium A.D. [Ackerman, 1984:108-109; Krupnik et al., 1983:559; Stanford, 1976:91-92]. A second development of whaling techniques began by A.D. 500, when technology necessary for hunting large whales, including toggling harpoon heads, drag floats and umiaks, were obtained by the human inhabitants of Bering Strait [Bockstoe, 1979:93-95]. Evidence of this development appears on Siberian shores by the time of the Punuk tradition, sometime around A.D. 600 [Larsen and Rainey, 1948:37-39; Collins, 1964:94; Stanford, 1976:112-114; Bockstoe, 1979:86-88; Ackerman, 1984:108-109;



KEY: Beluga Distribution Gray Whale Spring Migration Route Bowhead Whale Spring Migration Route

Figure 1. Selected Siberian and Alaskan prehistoric and historic whale harvesting sites, and present-day migration routes of gray and bowhead whales; distribution of beluga whales is shown as well.

Anderson, 1986:110–111; Dumond 1987:124, 128–133]. By A.D. 800–1500, the Punuk aspect of Western Thule culture had developed an intense focus on whaling, reflected in large numbers of huge whale bones at Punuk sites on the coast of Chukotka and islands to the east [Ackerman, 1984:110–113; Dumond, 1987:128–131; Krupnik, 1987:18]. Bockstoe [1979:94] notes that the ability to hunt large whales was developed by inhabitants of St. Lawrence Island 1000 years before it developed on Alaskan shores. He further points out that although an effective technology for whale hunting existed on Alaskan shores by around A.D. 500, large whaling settlements did not develop until the advent of the Western Thule culture, dating to as early as A.D. 900. Therefore, although the means for harvesting large whales was developed and utilized by Punuk groups in Bering Strait by A.D. 600, the largely contemporaneous Birnirk inhabitants of Alaskan shores did not develop a focus on whaling [Bockstoe, 1979]. Changes that occurred on the coasts of northwest Alaska after A.D. 1000 include florescence of large whaling villages, such as those located at Wales, Cape Espenberg, Cape Krusenstern, Point Hope and Point Barrow (Utkiavik and Nuwuk) [Anderson, 1986:91–92; Dumond, 1987:128–139; Harritt, 1989]. In northwest

Alaska, the initial development of the large whaling settlement ranges from roughly A.D. 1000–1400 [Anderson, 1986]. Development of whaling villages at Cape Espenberg and Cape Krusenstern occurred after A.D. 1000, but whaling at these sites ceased around A.D. 1400 [loc cit.]. Some few new ones were established in later times, at locations such as Icy Cape and Kivalina [Anderson, 1986:323]. Kivalina is a good example of a recently adopted whale harvesting site. Villages such as Wales, and Point Barrow were established in prehistoric times and persist to present day [Anderson, 1984:92, 1986:323].

Archaeological analysis of prehistoric whaling settlements, such as those at Cape Espenberg and Cape Krusenstern, can provide insight into the nature of changing cultural patterns over long periods of time. In following this reasoning, the present discussion follows Anderson's [1986] recent interpretation of late prehistoric subsistence foci in the Kotzebue Sound area because it describes a prehistoric case of florescence and cessation of whaling.

Anderson's interpretation [1986:323] describes two basic patterns, represented by the Western Thule tradition, dated from A.D. 1000–1400 and the Kotzebue Period tradition, dated from A.D. 1400–1900. Remains of the Western Thule

traditions at Cape Krusenstern reflect the importance of whaling to this culture, with regard to settlement groupings [Giddings, 1967:98; Anderson, 1986:70-71, 91-92]. The advent of the Kotzebue Period may be related to shifts in prevailing wind direction and currents, sometime around A.D. 1400 [Anderson, 1986:323-324]. This environmental change apparently resulted in shifts in whale migration routes and ocean currents. This circumstance presented human hunters with difficult access to migrating whales, and resulted in the loss of opportunities for harvesting [Anderson, 1986:110-111]. Kotzebue Period inhabitants of the coast then turned to a more diverse approach to subsistence, one in which seasonal transhumancy across a tribal territory reflected variable distributions of resources within a region.

SOCIAL INTEGRATION

It is important to point out that general agreement exists among researchers on the importance of the nuclear family in subsistence pursuits and socio-political organization. There is also some agreement, at least, on the importance of the extended family in these respects [Burch, 1980; Ray, 1983:151,160-161; Spencer, 1984:331]. On this basis, it seems reasonable to accept Burch's [1980:266] interpretation of traditional Eskimo society as being comprised of local family segments. However, there is ongoing debate about the existence and nature of tribes which, although not crucial to this discussion, present questions about social integration above the level of the family [loc cit.].

These areas of disagreement can be briefly described as two extreme positions, derived from interpretations by Ray [1975:105-106, 1983:150-151], Burch [1980:279-282], Sheehan [1985] and Spencer [1959, 1984]. Ray, Burch, and Sheehan present arguments for the existence of formal tribes or societies. Burch is rather broad in his interpretation of tribes, suggesting that tribal territories changed and that the tribes themselves may have disappeared or been reorganized through time, in response to changing ecological conditions. In contrast, Spencer [1984:324] states flatly that the term "...tribe" has little or no validity, but rather that group names depend on local provenience within (native) territorial definitions...." Spencer [loc cit.] goes further to emphasize that the membership of a group shifted through time, and might at any point be made up of individuals who came from a number of different places.

THE PROBLEM OF RANKING IN WHALING GROUPS

It is difficult to accept Sheehan's [1985] interpretation of social ranking in whaling groups without reservations because of the preceding problems. Although Burch [1980:264-266] also suggests that ranking was present in such groups, he indicates that there were factors that militated against social integration, such as a tendency for divisiveness between local families within a village because of territoriality. A number of points could be made that counter the positions of Sheehan and Burch for ranking. But, here I will discuss only those areas that are most problematic in resolving the issue. These are: social integration, the relationship of population size to whaling, redistribution of resources, and a tendency of Eskimo groups to fission during periods of subsistence stress.

Integration. Perhaps the most basic assumption underlying the argument for ranking is that a degree of integration existed above the level of the local or extended family. Sheehan [1985:147-149] suggests that the whaling complex served as an organizing focus centered around the umealik, who attempted to recruit the best hunters for the crew of his umiak. This was a circumstance in which familial relations could be established with individuals with no actual affinal or consanguineous ties to the umealik. Such relationships comprised sharing partnerships and established connections between coastal and interior groups, to the mutual benefit of both with regard to exchange of goods [loc cit.]. However, in an alternative view, Burch [1980] suggests that umiak crews were made up primarily of members of a single family. Burch [1980:266] and Spencer [1984:331] both point out that political integration was based on kinship, primarily those of consanguineous relationships, while relatives of either spouse were treated in a less preferential manner.

In further support of his position, Burch suggests that a large traditional whaling village was made up of more than one local family whose affinal and consanguineous membership may include as many as 50 to 100 individuals [Burch, 1980:262-263; also, Spencer 1959:65-66]. Family groups organized themselves spatially in clusters or family "compounds" within the village, an arrangement in which a family maintained a degree of social distance as well as spatial separation from other families [loc cit.]. The social divisions between compounds were nearly on the order of divisions between tribes, with respect to perceptions of territoriality [Burch 1980:266].

Population size. Sheehan [1985:124] suggests that human populations increased in size after the advent of whaling and because of it, rather than prior to the time of its development. This differs from Bockstoce's [1979] interpretation, mentioned previously. Bockstoce suggests that relatively large numbers of hunters were necessary to effectively implement whaling techniques developed in Bering Strait, some 1000 years before intensive whaling appeared on Alaskan shores. Furthermore, it can generally be said that population sizes in almost all areas of Alaska increased from the earliest to latest prehistoric time.—this general trend most likely resulted from increasingly effective methods of exploiting available resources. It proceeded through late prehistoric times, both prior to and following the florescence of whaling [cf. Bockstoce, 1979:94-95; Dumond 1987:147-149]. By the time of initial European contact in the early nineteenth century, the populations of existing whaling villages were 500 at Wales, 400 at Point Hope, and 300 at Barrow [Oswalt 1967:90-99; Ray, 1975]. These settlements represent the large groupings necessary for traditional whaling.

Redistribution of resources. Sheehan [1985:131-133] suggests that the redistribution of whaling products was a major source of the political power held by the umealik. He [loc cit.] further suggests that this redistribution network "...involved the entire settlement and its outlying areas." In this interpretation, redistribution followed the composition of the crew—cross-cutting several families—rather than being confined to a single local family. This view varies with that of Burch [1980] and Spencer [1959:64-65] in which the extended family is principal sphere in which redistribution takes place. Burch [1980:268] goes so far as

to indicate that upon receiving his share of a whale, an unrelated hunter would then subdivide this in his family's redistribution system. Given the various interpretations of redistribution, the more conservative one would be Burch's position, in which the whale is divided among the family of the umealik first, and then among crew-members outside the umealik's family. This arrangement would accommodate distant relatives and formal sharing partners as well. In this interpretation, goods flow through a familial sharing system instead of directly from the umealik.

Fissioning tendencies of Eskimo groups. The economic basis for ranking suggested by Sheehan [1985:131-136] rests on an umealik's ability to control products of whaling over a long term. However, Burch [1980:265-266] suggests that even an "unusually gifted umealik" could not maintain organization of a large local family over more than one or two years in a diminished resource crisis. He further indicates that the family unit would fission at these times, dispersing in small family groups [1980:274]. It is evident that this tendency was in operation from Western Thule times through the Kotzebue Period, as well [cf. Anderson, 1986]. As Anderson [1986:113] notes, the basic shift in human distributions around Kotzebue Sound was from concentrations in large coastal settlements to small isolated settlements. Burch's [1980:263] suggestion that most of the small villages encountered by European explorers were single family settlements supports Anderson's interpretation. The tendency of Eskimo groups to fission is a social mechanism that would militate periods of environmental stress by reducing numbers of humans within a given area, and distribute human exploitation of resources more evenly across a region. The splitting up of village inhabitants militates against formal ranking in a village, beyond any that is present in each segment, or extended family.

DISCUSSION AND SUMMARY

Although the argument for ranking cannot be discounted, it is apparent that more conclusive evidence of its existence is needed. It is likely that opportunities for its development occurred sometime over the several centuries that Wales and Point Barrow were occupied. However, although circumstances of long-term occupation with apparent abundance of resources are evident in northwest Alaska in these two cases, it is curious that the social organizations of Wales and Barrow did not evolve into forms which set them clearly apart from those of the inhabitants of less productive locations. The potential would be high for such a development, if the processes described by Sheehan were operating over the course of several generations of umealiks in either of these villages. But the archaeological record shows no evidence of such developments. Instead, it reflects cases such as Cape Espenberg and Cape Krusenstern where the Western Thule remains of whale hunters are succeeded by those who pursued more diverse subsistence patterns.

The more rudimentary social organization, represented by the local family segment, was the most basic division which would be viable under the most stressful environmental conditions. Large aggregates such as whaling villages can be viewed as task groups which formed temporarily to accomplish large tasks, such as whale harvesting, more effectively than could single segments. These cultural tenets are at the core of the egalitarian society but they also form the basis for development of ranked society [cf. Fried, 1960]. With respect to traditional Eskimo socio-political organization, they were very likely at the threshold of a transformation. If militating factors had been overcome, the transformation would no doubt have been achieved.

CITATIONS

- Ackerman, R., Prehistory of the Asian Eskimo Zone. In Arctic. D. Damas, ed., *Handbook of North American Indians*, Vol. 5, W. Sturtevant, gen. ed., pp. 106-118, Smithsonian Institution, Washington, DC, 1984.
- Anderson, D., Prehistory of North Alaska. In Arctic. D. Damas, ed., *Handbook of North American Indians*, Vol. 5, W. Sturtevant, gen. ed., pp. 80-93, Smithsonian Institution, Washington, DC, 1984.
- Anderson, D., Beachridge archeology of Cape Krusenstern, *National Park Service Publications in Archeology* 20, pp. 311-325, U.S. Department of the Interior, Washington, DC, 1986.
- Bockstoce, J., The archaeology of Cape Nome, Alaska, *University of Pennsylvania, Museum Monograph* 38, The University Museum, Philadelphia, 1979.
- Burch, E., Traditional Eskimo societies in northwest Alaska, in Alaska Native Culture and History, edited by Y. Kotani and W. Workman, *Senri Ethnological Studies* 4, pp. 253-304, National Museum of Ethnology, Osaka, 1980.
- Collins, H., The Arctic and Subarctic, in *Prehistoric Man in the New World*, edited by J. D. Jennings and E. Norbeck, pp. 85-114, University of Chicago Press, Chicago, 1964.
- Dumond, D., *The Eskimos and Aleuts*, Revised Edition, Thames and Hudson, London, 1987.
- Fried, M., On the evolution of social stratification and the State, in *Culture in History*, edited by S. Diamond, pp. 713-731, Columbia University Press, New York, 1960.
- Giddings, J., *Ancient Men of the Arctic*, Alfred A. Knopf, New York, 1967.
- Harritt, R., Recent archaeology in Bering Land Bridge National Preserve: The 1988 season at Cape Espenberg, paper presented at 16th Annual Meeting of the Alaska Anthropological Association, Anchorage, March, 1989.
- Krupnik, I., The bowhead vs. the gray whale in Chukotkan aboriginal whaling, *Arctic*, 40, 16-32, 1987.
- Krupnik, I., L. Bogoslovskaya, and L. Botrogov, Gray whaling off the Chukotka Peninsula: Past and present status, *Report of the International Whaling Commission*, 33, 1983.
- Larsen, H., and F. Rainey, Ipiutak and the Arctic whale hunting culture, *Anthropological Papers of the American Museum of Natural History*, 42, New York, 1948.
- Oswalt, W., *Alaskan Eskimos*, Chandler Publishing Company, San Francisco, 1967.
- Ray, D., *The Eskimos of Bering Strait, 1650-1898*, University of Washington Press, Seattle, 1975.
- Ray, D., *Ethnohistory in the Arctic: The Bering Strait Eskimo*, edited by R. A. Pierce, The Limestone Press, Kingston, Canada, 1983.

Sheehan, G., Whaling as an organizing focus in north-western Alaskan Eskimo society, in *Prehistoric Hunter-Gatherers: The Emergence of Cultural Complexity*, edited by T. Price and J. Brown, pp. 123-154, Academic Press, New York, 1985.

Spencer, R., The North Alaskan Eskimo: A study in ecology and society, *Bureau of American Ethnology Bulletin 171*, Washington, DC, 1959.

Spencer, R., North Alaska Coast Eskimo. In Arctic. D. Damas, ed. *Handbook of North American Indians, Vol. 5*. W. Sturtevant, gen. ed., pp. 320-337, Smithsonian Institution, Washington, DC, 1984.

Stanford, D., The Walakpa Site, Alaska: Its place in the Birnirk and Thule cultures, *Smithsonian Contributions to Anthropology, No. 20*, Smithsonian Institution Press, Washington, DC, 1976.

92-17821



AD-P007 317



The Effect of Climatic Change on Farming and Soil Erosion in Southern Greenland During the Last Thousand Years

Bjarne Holm Jakobsen

Institute of Geography, University of Copenhagen, Copenhagen, Denmark

ABSTRACT

Soil studies in low-arctic South Greenland often reveal polysequence soil profiles. The study of these soils, dating of fossil surface horizons, study of land use, and use of paleoclimatic information from studies of ice cores show a complex interplay between climatic change, soil erosion and agricultural land use.

Two periods of agricultural land use are known in Greenland. From A.D. 985 to about 1450 Norsemen settled in Greenland, and about 1915 modern sheep breeding started in southern Greenland.

The Norsemen deserted the area in late 1400, and no exact knowledge exists about their fate. But soil profiles and large erosion areas of desolation tell us about their problems. Climatic fluctuations, soil erodibility factors and insufficient management response on environmental feedbacks probably caused the termination of the Norse era.

The expanding modern sheep breeding industry is facing the same problems as the Norsemen did. In spite of agricultural research and large investments in winter fodder production, stables and infrastructure, it seems difficult to practice a balanced land use as regards carrying capacity. Soil erosion accelerates, and the devastation of a unique landscape will be the consequence, if the really limiting factors for agricultural land use are not recognized.

INTRODUCTION

In the two periods of agricultural land use in Greenland, the basis has been grazing of the natural vegetation. In South Greenland luxuriant vegetation covers large areas in the inner parts of the fjord landscape. During the late 1970s and early 1980s it was planned to intensify the sheep breeding industry in these areas. At that time The Home Rule of Greenland and The Ministry of Greenland initiated interdisciplinary studies to evaluate the environmental impact of this change in land use. Special emphasis was laid on effects on soils and vegetation.

The study of soil profiles gave information on periods of serious soil erosion. The evaluation of consequences for the landscape caused by present-day changes in land use, therefore, also includes an evaluation of which role substantiated climatic fluctuations during the Holocene played in relation to soil erosion.

GEOGRAPHICAL CONDITIONS

The study area covers the ice-free landscape from the Davis Strait coast, through areas traversed by deep fjords, to the present margins of the Inland Ice (ca. 5000 km²).

The low-arctic climate shows a trend from an oceanic para-arctic type in the outer coast areas to a more continental paraboreal type in the inner regions. The low summer temperatures of 5–7°C, and foggy and moist conditions in the areas close to the Davis Strait are mainly due to the ice drift from the Polar Sea with the East Greenland current around Kap Farvel. Summer temperatures increase to about 10°C at the heads of the fjords, and the yearly precipitation here decreases to about 600 mm, whereas outer coast areas show an average of about 900 mm.

The climatic trend is the main factor for the vegetational zonation. Dwarf shrub heath, rich in mosses and lichens, covers the peninsulas and islands of the skerries landscape. Going east the vegetation changes, and in the continental

Hor.	Depth	Texture	%C	pH	CEC	%B.S.	Fe	Al	Si
Ah	0-5	Silt loam	9.8	5.6	36.3	32	3.0	0.9	0.1
E	5-12	Silt loam	3.3	5.0	17.9	19	3.2	1.0	0.1
Bs1	12-28	Sandy loam	1.3	4.5	22.4	7	9.7	2.7	0.2
Bs2	28-45	Sandy loam	1.0	4.8	12.2	6	2.7	3.0	0.3
C	45-	Loamy sand	0.4	5.3	5.8	9	1.4	1.9	0.4

Table 1. Textural and chemical characteristics for the dominating soil in the area. Soil horizon (Hor.) depth is in cm, pH values are measured in a 0.01 M CaCl₂ suspension, cation exchange capacity (CEC) is in meq/100 g and acid oxalate extractable Fe, Al and Si values are in per thousand by weight.

regions with warmer summer periods subarctic types take over. Subarctic birch forest and copses of willow are here interspersed with birch heath and open grassland communities. Fens and bog areas are found around lakes and along streams.

The climatic and vegetational zonation is clearly reflected in the geography of soils. Generally, the zonal soil type changes from a strongly leached, very acid Podzol type in the outer coast area to a moderately leached, weakly podzolized Brown Soil type in the warmer and more dry continental areas. In Table 1, data are presented from a characteristic soil. The distribution of Fe, Al, Si and CEC values in this moderately acid soil shows a translocation of Al-Fe-Silicate material into Podzol B horizons, probably mostly induced by inorganic processes [Jakobsen, 1989]. A very important characteristic is the two-sequential parent material. Generally, soils develop on coarse-textured tills or glaciofluvial materials, both covered by a mantle of late-glacial loess, whose thickness at different positions in the landscape generally varies from 5 to 40 cm. Therefore, the nutrient-rich and biologically active part of the soil is mostly developed in loess material.

CLIMATIC FLUCTUATIONS

Oxygen isotope analyses of ice cores from the Greenland ice sheet reveal a general climatic record of the past. The record shows medium-frequent climatic changes during the Holocene and confirms various kinds of historical information on a relatively warm mediaeval period followed by a cold period, "The Little Ice Age."

In addition to these long-term climatic changes, the climate varies markedly on a short term. These variations, especially length and warmth of the growing season and the soil water balance, have an immediate biological effect as they influence plant production. Figure 1 shows the seasonal variations in precipitation and temperature (1961-1989).

During the growing season, the soil water balance is primarily influenced by the frequency of strong, dry foehn winds from the Ice Cap.

Daily potential evapotranspiration of up to 15 mm has been measured in foehn situations and confirmed by measuring the rate of soil water loss. In Figure 2 variations in soil water balance are illustrated for the period 1985-1989. As most soils have a soil water storage of 75-100 mm at field capacity, it is evident that the water supply in some years is a limiting factor for plant production.

Based on NOAA-AVHRR satellite data, the calculation of Normalized Difference Vegetation Indices (NDVI) has been used for monitoring the biomass production [Hansen, 1991]. Using the integrated NDVI (iNDVI) as an estimator of the total biomass production during the growing season, calculations for the period 1985-1989—for a test area—show values of 1160, 910, 1080, 960 and 1050 kg ha⁻¹ (dry biomass), respectively. Based on results from this five-year period, warm summers generally give the highest plant production. Also the length of the growing season influences positively the total biomass production. Even though the vegetation in some areas suffers from water stress, the warmth and length of the growing season (amount of degree-days) is presumably the most important factor for the total, annual plant production.

FARMING AND SOIL EROSION

Farming was introduced for the first time in the history of Greenland when Norsemen around A.D. 985 settled in southern Greenland. They arrived at the end of a very favorable climatic period, and settled mainly in the interior, with its luxuriant vegetation and warm summers.

The Norsemen were farmers first of all, even though they supplemented the daily fare by hunting seal, fish and caribou. The agricultural system was based on sheep and cattle grazing the natural vegetation. During winter periods, stall-feeding of the cattle was necessary. Mainly hay from fenced, manured and irrigated homefields was used as feed. The clearing of copses and woods by fire and axes and the grazing of the natural vegetation caused a dramatic change of the landscape. Paleobotanical investigations by studies of pollen in accumulated organic-rich deposits [Fredskild, 1978] indicate a marked change from a landscape characterized by woods and copses interspersed with grassland to

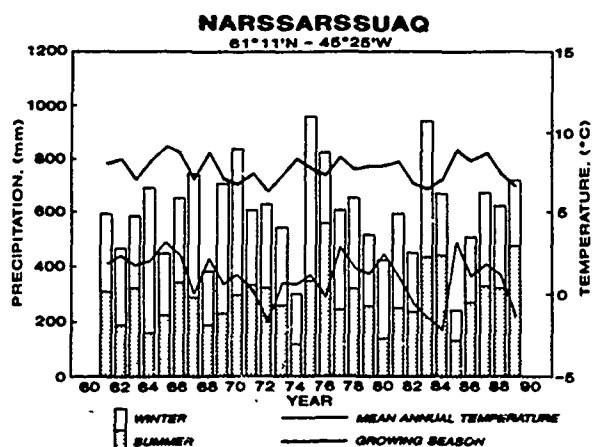


Figure 1. Variations in precipitation, mean annual temperature and mean temperature of the growing season for the period 1961-1989.

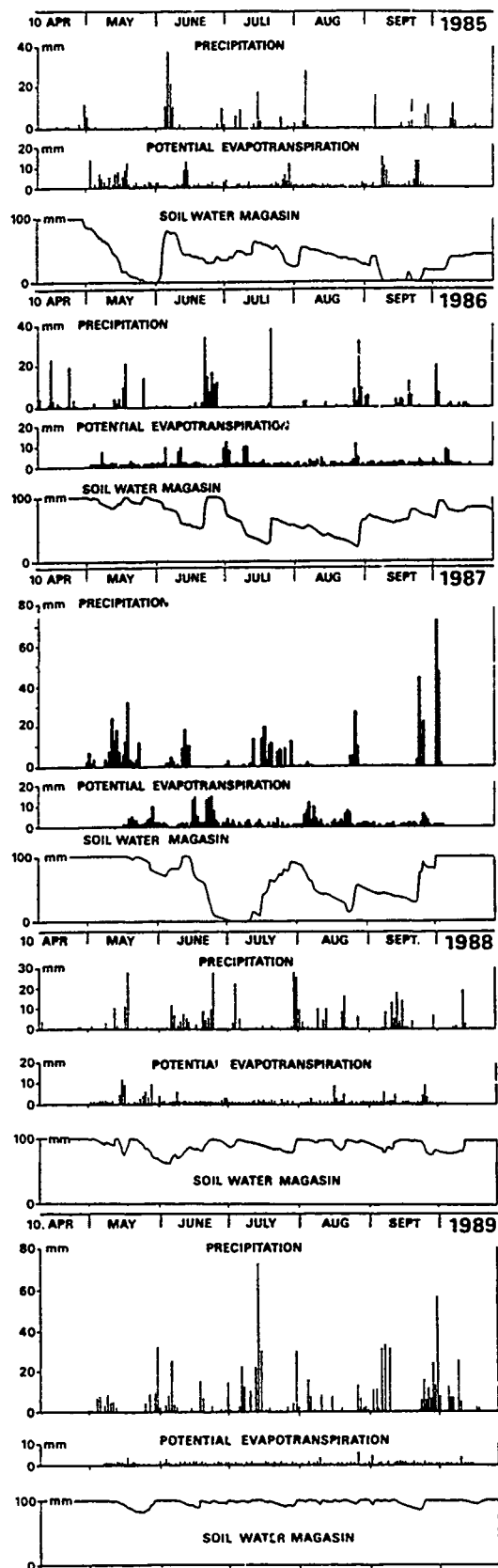


Figure 2. Variations in precipitation, potential evapotranspiration and soil water storage in the growing season for the period 1985-1989.

open-ground landscapes followed by a reflourishing of plants from the pioneer vegetation.

What factors caused the extinction of the Norsemen in the 15th century? Did a climatic cooling and the probable, resulting decrease in biomass production trigger a collapse of the Norse agricultural community? In this paper results from the study of soil profiles in the area are used to elucidate part of the complex interaction.

Soil profiles can be divided into four groups, each showing a characteristic sequence of soil horizons (Figure 3). In addition to these soils large erosion areas are seen in the valleys in the continental interior (Figure 4). The four soil profile groups have the following characteristics: Type 1, which is not notably affected by erosion/deposition features, is not very common in the area. It shows a distinct Podzol morphology developed in till/glaciofluvial material covered by late-glacial loess. Type 2 is normally found in the open landscape at some distance from Norse settlement sites. It shows a Podzol type 1 covered by loess and sandloess. The thickness—which spans from about 5 cm to over 1 m—and the mean grain size of this younger windblown material generally decrease from the continental interior to the skerries. Type 3 is found in homefield areas from the Norse period. In principle, it shows a similar morphology as type 2. But in contrast to this, charcoal fragments are observed in the younger aeolian material. In all type 3 soils studied, charcoal fragments were found from the A horizons of the buried Podzols and upwards. The upper part of the younger loess deposit was normally free of charcoal fragments (Figure 5). Type 4 represents a soil where deposits covering the Podzol also include layers of fluvial material. Furthermore, there is at some sites observed a second fossil humus-rich A horizon and a distinct Podzol morphology in the younger aeolian material. Charcoal fragments are confined to the lower part of the younger windblown material, down to the A horizon of the deepest-lying Podzol.

Nine ^{14}C -datings were carried out of larger charcoal fragments from type 3 and 4 profiles. All four datings of charcoal fragments from the A horizon of the buried Podzols gave dates at the very beginning of the Norse era. Two datings from distinct charcoal layers in the middle of the charcoal-containing aeolian material gave ages of about A.D. 1150 and 1225. Three datings of the uppermost charcoal fragments found in soil profiles gave ages of about 1300, 1350 and 1375, respectively.

These results indicate that apart from the late-glacial period, no erosion and deposition by wind of any importance occurred prior to the Norse era; soil formation until then took place on generally stable landscape surfaces in spite of medium-frequent climatic changes during the Holocene. The consequent occurrence of charcoal in the A horizons of the buried Podzols in all studied type 3 and type 4 profiles as well as the substantiated, extensive soil erosion less than 150 years after landnam indicate a very concentrated settlement period and the appearance of soil erosion early in the Norse era.

The soil horizon sequence of type 4 profiles indicates a decrease in soil erosion and a stabilization of landscape surfaces. This fossil, stable land surface shows a distinct Podzol. In consideration of the intensity of soil-forming processes in a moderately humid subarctic environment, this stabilization occurred shortly after the Norse era. A marked recovering of the vegetation and a stabilization of large ero-

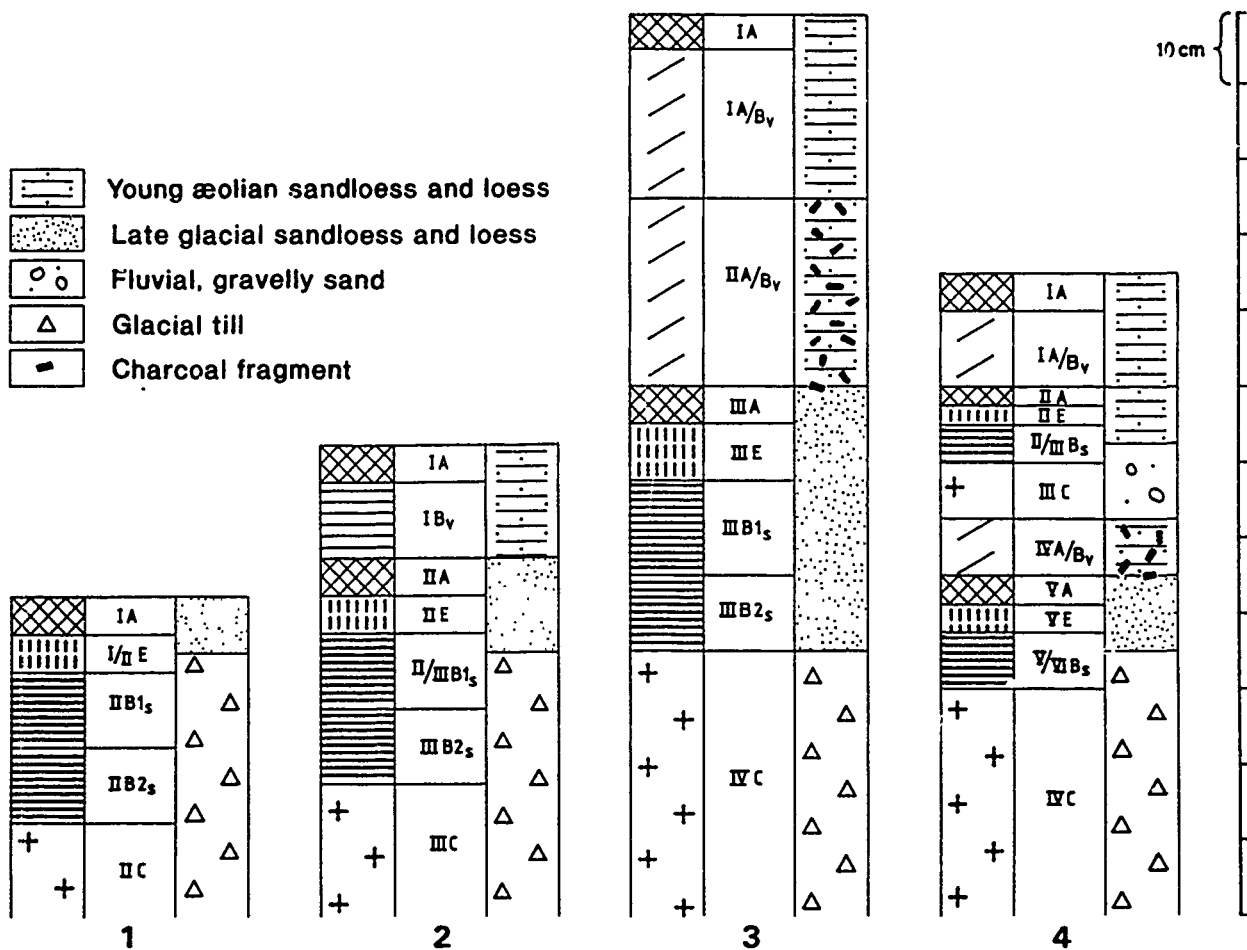


Figure 3. Characteristic soil profiles from southern Greenland.



Figure 4. Erosion border and deflation plain in a valley in the continental interior of southern Greenland.



Figure 5. A soil profile, type 3 (Figure 3).

sion areas thus took place in "The Little Ice Age," in spite of unfavorable climatic conditions. A renewed acceleration of soil erosion is seen at several sites, revealed by the cover of sandloess on land surfaces probably stable in the period A.D. 1600–1900 (II A in profile 4 in Figure 3). Recent studies of pollen and windblown material in lake sediments [Fredskild, personal communication] support the assumption of a reestablished ecosystem balance following the Norse era, and renewed accelerated soil erosion within the present century.

The second period of agricultural land use started about 1915. In most of the century more than 50,000 sheep have been grazing mainly in the areas densely settled during the Norse era. This extensive modern sheep-breeding developed in a period with warmer and favorable climate. The estimation of present grazing resources [Thorsteinsson, 1983] indicates sufficient summer grazing for at least 100,000 sheep. In spite of these favorable conditions, renewed extensive soil erosion characterizes the area today.

CONCLUSIONS

Beyond doubt, climatic fluctuations will reduce or increase the yearly biomass production and have an influence on the subarctic forest. Studies of annual biomass production (1985–1989) indicate variations up to 25%. But fluctuations in biomass production of this magnitude are hardly in themselves crucial for the success of the applied agricultural land use system. The soil characteristics emphasize the importance of understanding the impact of agriculture—in this case based on extensive grazing—on the ecological balance of this marginal subarctic environment with its characteristic, short-term climatic variations, before

the influence of long-term climatic changes can be properly analyzed.

During the Norse era the favorable continental interior was presumably densely settled after a few generations. Due to catastrophic years as regards the climate—especially high foehn activity—grazing beyond doubt broke the vegetation cover at exposed sites. Notwithstanding a climatic cooling or warming, it would probably have been impossible to achieve an ecological equilibrium as regards carrying capacity if extensive grazing of the natural vegetation was introduced in this marginal area. Therefore, in this case, the basic ecosystem, characterized by its geographical conditions, such as soils, erodibility factors, short-term climatic fluctuations and catastrophic events, directly determines the success of a specific land use system, much more than the influence of medium-frequent climatic changes.

Undoubtedly, the climatic cooling at the beginning of "The Little Ice Age" around 1300 worsened the problems for the Norsemen and accelerated the final collapse of their isolated community. They had to face somewhat shorter growing seasons, higher needs for yielding winter fodder, and a more isolated position as sailing probably was impeded by increased ice drift along the coast. Instability and tensions have also accentuated the general stress upon the community, especially when the centers for wealth and political power at the most favorable inland sites experienced the consequences of soil erosion.

In the main, modern sheep breeding practices the same land use system as the Norsemen and will therefore experience similar problems. Major parts of the South Greenland landscape will be further devastated. The apparently luxuriant vegetation and high, estimated grazing potential divert attention from the really limiting factors. Severe and spreading soil erosion will occur a long time before the limit will be reached for grazing the potential vegetation resources.

This conclusion is important for the agricultural management today. A balanced land use cannot be obtained by adjusting the number of sheep primarily to vegetation potentials. A recognition of the true Achilles' heel of the ecosystem requires a land use practice with very low grazing intensity and the protection of exposed areas. At the same time there exists political and economical pressure to expand the sheep breeding industry. Unfortunately, this conflict has a universal character.

REFERENCES

- Fredskild, B., Paleobotanical investigations of some peat deposits of Norse age at Qagssiarssuk, South Greenland, *Meddelelser om Grønland*, 204, 1–41, 1978.
- Fredskild, B. Personal communications. Grønlands Botaniske Undersøgelser. Botanical Museum, University of Copenhagen, Gothersgade 130, DK1123 Copenhagen K.
- Hansen, B. U., Monitoring natural vegetation in southern Greenland using NOAA AHVRR and field measurements, *Arctic*, 1991, In press.
- Jakobsen, B. H., Evidence for translocations into the B horizon of a subarctic Podzol in Greenland, *Geoderma*, 45, 317, 1989.
- Thorsteinsson, I., Undersøgelser af de naturlige græsgange i Syd-Grønland 1977–1981. Landbrugets Forskningsinstitut, Island. Forsøgsstationen Upernaviarssuk, Greenland, 1983.

Climate and Landscape Perestroykas

S. A. Zimov and V. I. Chuprynin

Pacific Institute of Geography, Far East Branch of the U.S.S.R. Academy of Science, Vladivostok, U.S.S.R.

ABSTRACT

Northern moss-lichen wood communities are becoming degraded progressively in many regions. That is why the question of their substitution to grass communities, ones less sensitive to mechanical and chemical loads, is widely discussed. The problem of landscape reorganization in Northeast Asia is interesting in this connection. Today, territories are over-moist and low productivity moss-lichen covers are distributed everywhere. But, a rich pasture ecosystem existed here in the Late Pleistocene. Many people relate the phenomenon of arid climate mammoth steppes and their destruction to replacement by humid conditions in the Holocene. But in Northeast Asia the climate is arid even now, since the radiation index of dryness is more than 1 and even reaches 3. In Lower Kolyma, grasses can evaporate 2-3 times annual rates of precipitation (4-6 times more than mosses and lichens evaporate). A mathematic model describing relations between various competitive plant communities depending on climate and activity of erosive-accumulative processes, pasture loads and CO₂ concentration is proposed. It is shown that the influence of these factors is more significant than that of climate alone. Maps of northern hemisphere plants in the Pleistocene are calculated, as well as maps forecasting plant distributions arising from future climatic and CO₂ changes. The possibilities of artificial regeneration of high-productivity pasture ecosystems are considered.

92-17822



AD-P007 318



Trajectory Analysis of the Atmospheric Carbon Dioxide Bimodal Distribution in the Arctic

Kaz Higuchi and Neil B. A. Trivett

RAGS Research Section, Atmospheric Environment Service, Downsview, Ontario, Canada

ABSTRACT

An examination of detrended atmospheric CO₂ time series from two arctic monitoring stations, Alert and Mould Bay, shows a very prominent seasonal cycle with a very broad maximum in the winter and a very sharp minimum in the late summer. The amplitude of the cycle is about 15 to 16 ppmv (parts per million by volume). This seasonal cycle is a reflection of the metabolic cycle of the land biota in the northern hemisphere. During the period of broad maximum concentration in winter, the time series of CO₂ shows, in some years, a bimodal feature with a relative minimum in late winter.

The bimodal distribution is difficult to explain in terms of (1) photosynthetic/respiratory cycle of terrestrial biospheric activities in the middle latitudes, and (2) anthropogenic activities. In this paper, we will speculate and discuss the bimodal feature in terms of the evolution of the atmospheric circulation in the Arctic.

INTRODUCTION

An examination of detrended atmospheric CO₂ concentration time series from two arctic monitoring stations, Alert and Mould Bay, shows a very prominent seasonal cycle with a very broad maximum in winter to early spring and a very sharp minimum during the late summer. The amplitude of the cycle is about 15 to 16 ppmv (parts per million by volume). It is believed that this seasonal cycle is a reflection of the photosynthetic/decay cycle of the land biota in the northern hemisphere. Composite average of the detrended seasonal cycle shows a gradual increase in the CO₂ concentration from late November to April, falling very rapidly thereafter. During this period of broad maximum in winter, the time series show, in some years at least, a bimodal feature, with a relative minimum in the latter half of winter (Figure 1a,b). This type of feature can also be seen in such chemical species as sulphate.

In this study, we show some preliminary evidence suggesting that the bimodal distribution can be explained, at least in part, by changes in the winter atmospheric circulation in the Arctic.

PROCEDURE

The CO₂ flask sampling programs at Alert and Mould Bay are described in Higuchi et al. [1987], Komhyer et al.

[1985], and Wong et al. [1984]. At Alert, the samples are obtained about once per week using evacuated 2-liter flasks. At Mould Bay, the samples are normally collected twice per week using 0.5-liter flasks that are pumped up to a pressure of 1.5–2 atm.

Nine years (1980–1988) of atmospheric CO₂ measurements from Alert and Mould Bay were chosen and analyzed. To each of the data sets, we applied the following steps:

(1) Equally spaced data were obtained by filling gaps in data by linear interpolation;

(2) A third-degree polynomial was then fitted to the CO₂ time series in a least square sense to remove secular trend; and

(3) A 28-day equally weighted running mean was applied to each of the detrended time series as a smoothing procedure.

Figure 1 shows the results of the application of these steps. There is a great deal of interannual variability in the way the CO₂ concentration evolves during the winter season. In particular, in some years there is a relative minimum lasting about half a month or so during late winter. To obtain an explanation for this phenomenon, we proceeded to examine the statistical distribution of trajectories arriving at Alert and Mould Bay. This is based on the assumption that

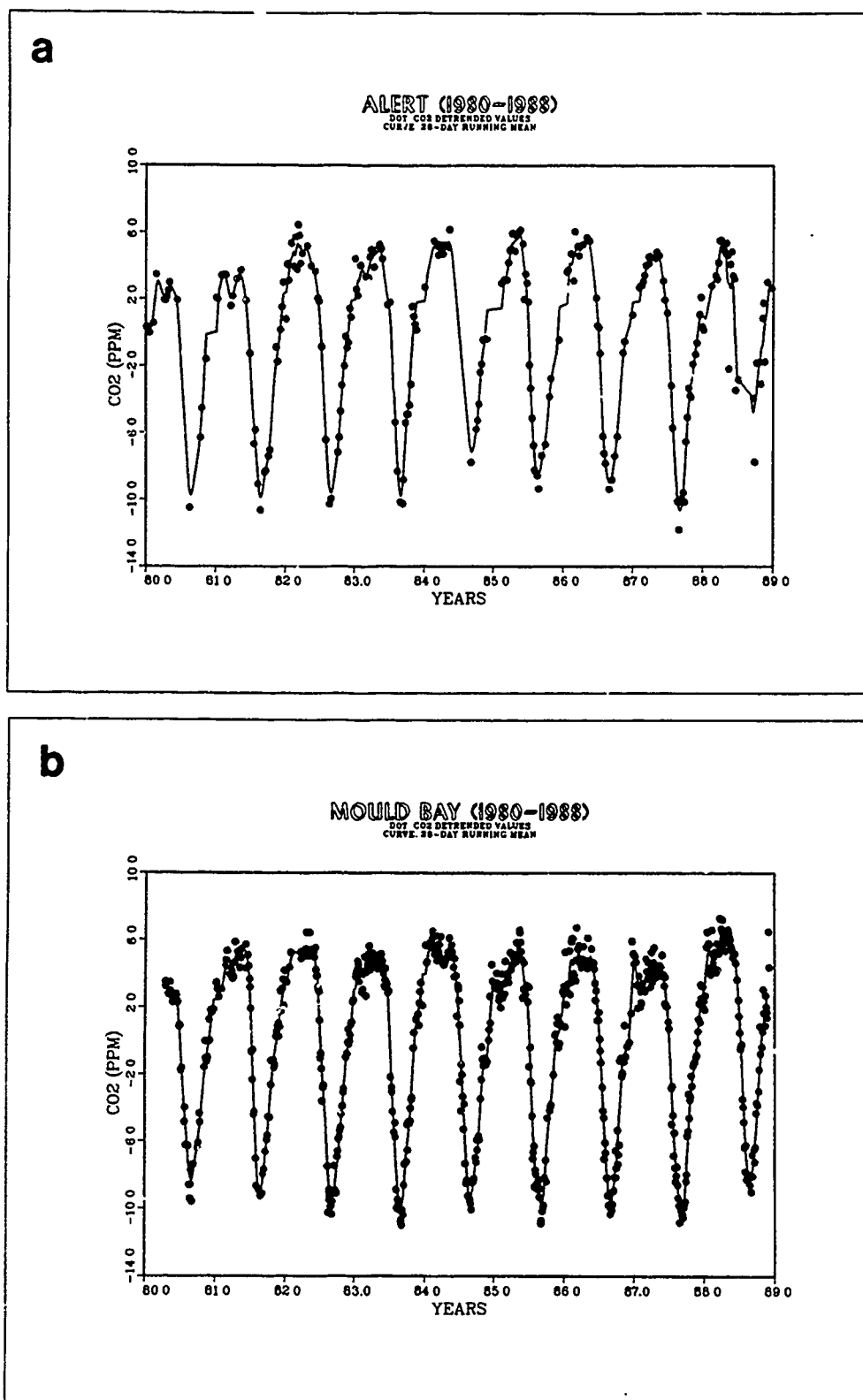


Figure 1. Detrended seasonal CO₂ cycle at (a) Alert, and (b) Mould Bay. Dots represent actual observed values minus the trend. Solid line is a 23-day running mean smoothing function. Note the interannual variability of the distribution of the winter concentration values.

the bimodal distribution produced by the relative minimum in the CO₂ concentration is due to a change in the atmospheric circulation pattern.

A 5-day back trajectory analysis was carried out using a constant acceleration, three-dimensional isobaric trajectory model. Three-dimensional trajectories were calculated for every day, when possible, from 1 November to 30 April for each of the years from 1980 to 1988. Trajectories originated from Alert and Mould Bay, starting at the 850 mb level, and at 00 GMT.

Positions of the 5-day back trajectory "origins" were categorized into six sectors, each 60° longitude wide (Figure 2). The number of times the trajectory "origins" fell within Sector 1 on November 1 from 1980 to 1987 were obtained and divided by the number of November 1 days for which the trajectories were calculated. In this way, a normalized frequency for November 1 was obtained, giving an indication of probability of a trajectory "origin" falling in Sector 1 on November 1. The above procedure was repeated for the remaining days (2 November to 30 April, 1980 to 1988) and for each of the sectors.

RESULTS AND DISCUSSION

The length of the data we used is too short to obtain conclusive evidence for what we are attempting to show. However, the following preliminary results do suggest a connection between the CO₂ bimodal feature and the atmospheric circulation pattern.

Sectors 1 and 2 are considered to be anthropogenic sources of CO₂ for the atmospheric carbon dioxide. Climatologically, air parcels arriving at Alert and Mould Bay from Sectors 1 and 2 will tend to give higher concentration values at these stations. When the atmospheric circulation

changes and air parcels arrive from other sectors, the concentration drops [Higuchi et al., 1987]. Figure 3 shows the 1980–1988 climatological frequency with which the trajectories "originate" in Sectors 1 and 2 for each day from 1 November to 30 April. For both Alert and Mould Bay, there is a drop in the frequency of air parcels arriving from Sectors 1 and 2 during January and the first half of February. This corresponds to the time when, in some years, the CO₂ concentration decreases.

To perform a specific case study of the proposed relationship between the CO₂ bimodal distribution and the atmospheric circulation change, we chose the winter of 1980–81. Figure 4 shows normalized frequency for Alert and Mould Bay. It appears that during most of January air parcels arriving at the monitoring stations "originated" from areas other than Sectors 1 and 2. This is consistent with relatively lower CO₂ values measured at the stations during the same period. Other years with the CO₂ bimodal feature during the winter season are under investigation.

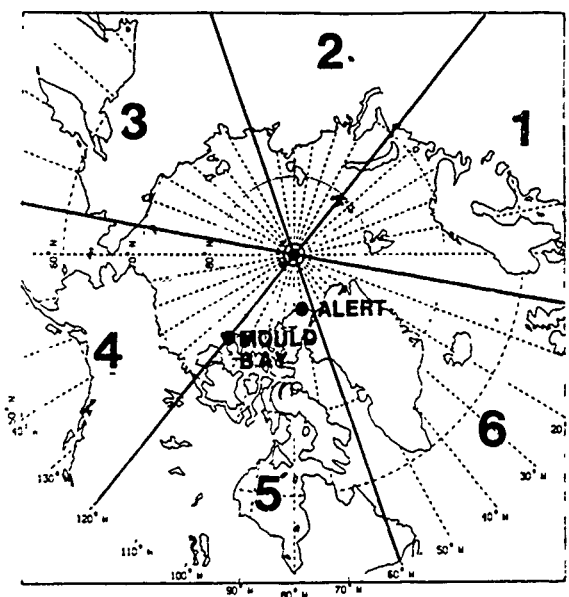


Figure 2. Six sectors into which 5-day back trajectory "origins" are categorized. Sectors 1 and 2 are major sources of anthropogenic CO₂.

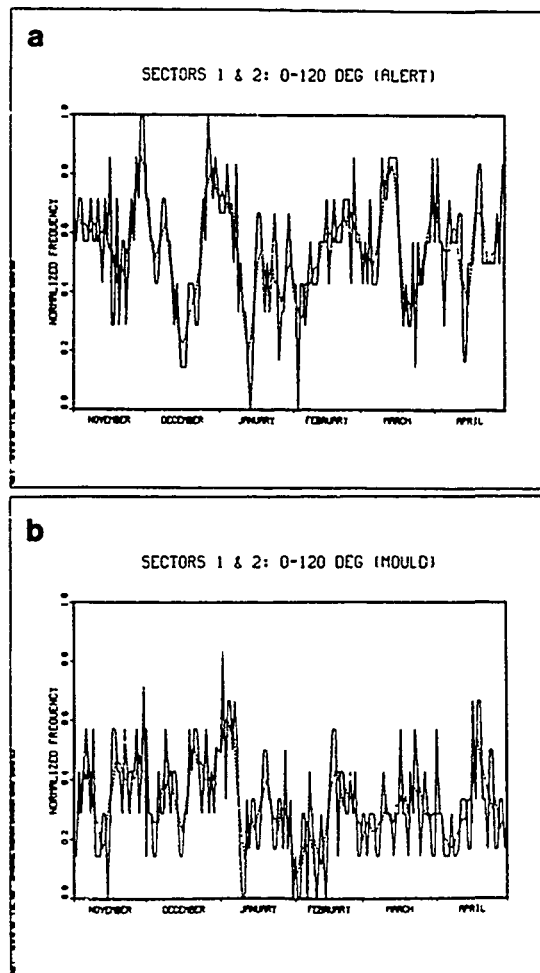


Figure 3. Normalized 1980–1988 climatological frequency with which the 5-day back trajectory "origins" fall within sectors 1 and 2 for (a) Alert, and (b) Mould Bay. Dashed line denotes 5-day running mean.

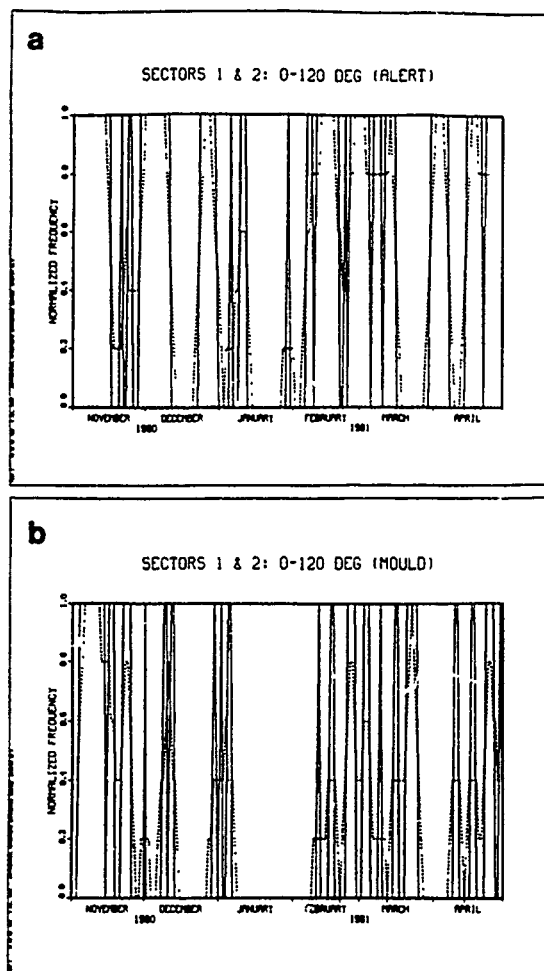


Figure 4. Same as Figure 3, except for the period 1 November to 30 April, 1980-1981.

CONCLUSION

Preliminary results of this study suggest that the bimodal distribution in the winter carbon dioxide concentration in the Arctic, when it occurs, is due at least partly to a change in the atmospheric circulation. Relatively low values of CO_2 concentration are likely to be observed when there is persistent lack of arrival, on a monthly time scale, of air parcels from Sectors 1 and 2, a major regional source of anthropogenic carbon dioxide in the Arctic.

ACKNOWLEDGMENTS

We would like to thank Tom Conway (NOAA/GMCC) and Kirk Thoning (CIRES) for providing us with the Mould Bay data, and to Dr. S. M. Daggupaty for useful discussions. Additional thanks to Buu Tran and Balbir Pabla for computational assistance.

REFERENCES

- Higuchi, K., N. B. A. Trivett, and S. M. Daggupaty, A preliminary climatology of trajectories related to atmospheric CO_2 measurements at Alert and Mould Bay, *Atmos. Environ.*, 21, 1915-1926, 1987.
- Komhyer, W. D., R. H. Gammon, T. B. Harris, L. S. Waterman, T. J. Conway, W. R. Taylor, and K. W. Thoning, Global atmospheric CO_2 distribution and variations from 1968-1982 NOAA/GMCC CO_2 flask sample data, *J. Geophys. Res.*, 90, 5567-5596, 1985.
- Wong, C. S., Y.-H. Chan, J. S. Page, R. D. Bellegay, and K. Petit, Trends of atmospheric CO_2 over Canadian WMO background stations at Ocean Weather P, Sable Island and Alert, *J. Geophys. Res.*, 89, 9527-9539, 1984.

Winter CO₂ Flux from Ecosystems in Northeast Asia

S. A. Zimov, G. M. Zimova, U. V. Voropaev, Z. V. Voropaeva, S. P. Davydov,
A. I. Davydova, S. F. Prosyannikov, and O. V. Prosyannikova

*North-Eastern Scientific Station of Pacific Institute of Geography, Far East Branch of the U.S.S.R. Academy of Science,
Yakut ASSR, Chersky, Malinovy Yar, U.S.S.R.*

ABSTRACT

To provide high concentrations and annual variations of CO₂ in the atmosphere at 70°N latitude, the existence of substantial winter sources is required. Winter activity of microbiota is low, thus a high flux of CO₂ from ecosystems is hardly to be expected. To address this contradiction a program of measurements of local CO₂ fluxes and CO₂ concentrations in soil in the low Kolyma has been initiated. The environments include maritime tundra territories, taiga, mountains, and lowland. An original express-method is proposed.

The analysis of materials demonstrates very high spatial and temporal variations of local fluxes as well as important contributions to local CO₂ variations produced by ecosystems in Northeast Asia.

Peat Accumulation Rates in Arctic Alaska: Responding to Recent Climatic Change?

D. M. Schell and B. Barnett

Water Research Center, University of Alaska Fairbanks, Fairbanks, Alaska, U.S.A.

ABSTRACT

The accumulation of peat in arctic Alaska has left deposits up to 2 meters in depth with basal ages of over 12,000 years B.P. The radiocarbon depressions in the peat serve as natural tracers of peat carbon movement in ecosystem processes. Many organisms collected from arctic Alaskan lakes and rivers show radiocarbon and stable isotope compositions that indicate that peat is being mobilized and acts as a major energy source to food webs. However, the large inputs of bomb radiocarbon from weapons testing in the late 1950s and early 1960s should be producing elevations in radiocarbon content, since decomposition of recent vegetation is presumed to be the primary source of particulate and dissolved organic matter in streams. All vegetation produced in the Northern Hemisphere since about 1958 has elevated radiocarbon concentrations. A net radiocarbon depression in consumers implies that the export of "old" peat carbon vastly exceeds that released from normal decay of recently grown plant material. Samples of dissolved organic carbon from tundra streams now being dated may help ascertain the source of carbon export.

Upland valley peats show a truncated radiocarbon profile at the top at 1000–2700 years B.P., indicating that peat accumulation has ceased. Cores from the coastal plain show that accumulation is still continuing, but decreases in soil carbon content in upper soil horizons imply slower rates. Peat cores were collected along a transect parallel to the Beaufort Coast near Prudhoe Bay and along a coast-to-foothills transect from Prudhoe Bay to Toolik Lake. Radiocarbon profiles of these cores are to be dated and should lead to a better understanding of the role of permafrost peatlands in carbon storage.

AD-P007 319



Microbial Mineralization in Soils and Plant Material from Antarctica

Manfred Bölker

Institute for Polar Ecology, University of Kiel, Germany

ABSTRACT

The process of microbial mineralization was analyzed in soil samples and plant material, mainly lichens, from the maritime and continental Antarctic (King George Island and Wilkes Land, resp.) to examine effects of temperature and moisture. Three methods were used: total CO₂-evolution and biological oxygen demand as a measure of general metabolic activity, and remineralization of ¹⁴C-labeled glucose (which may serve as a model for dissolved organic matter) as a measure of the activity of heterotrophic microorganisms. These methods are used as indicators for different fractions of organic material and microbial populations.

A comparison of the results of these methods showed that the portion of respired material from ¹⁴C-labeled glucose may even outcompete the totally metabolized material. These data differ with respect to the parent material and thus give an indication of its quality and the actual activity of the bacterial population which is considered to be mainly responsible for the turnover and mineralization of dissolved organic matter.

INTRODUCTION

Harsh environmental conditions in polar systems lead to several adaptive strategies at the level of microbial populations, such as metabolism at low temperatures, at low substrate concentrations, or survival during states of dormancy [Bailey and Wynn-Williams, 1982; Vincent, 1988; Wynn-Williams, 1990]. These adaptations are important for the survival of the organisms and the system itself which is governed by short time spans of possible metabolic activity. The organisms must communicate very effectively by short paths for the exchange of matter and information between producers and consumers.

This leads to distinct structures of the terrestrial microbial populations in terms of their close contact between both the individual organisms and their substrates. However, it reveals problems in estimating the metabolic rates of individual populations because it is difficult to separate them for detailed analyses. Thus, measurements of overall activity, such as CO₂-gas exchange, biological oxygen demand, enzymatic activities, or the use of model substrates have become important tools for analyzing the metabolic rates for these systems. Consideration of the specificity of these methods is required, i.e., that individual parts of the popula-

tion or parts of the organic matter show different results with respect to the methods used. Hence different methods of measuring respiration may show results due to different populations or processes detected.

This approach employs three methods which may be used to describe different parts of the population as well as different fractions of the organic matter:

- Total CO₂-evolution, a measure of the total actual metabolic activity under nearly undisturbed conditions;
- Biological oxygen demand, describing aerobic potential metabolic activity under water saturation;
- Remineralization of glucose, describing the potential heterotrophic activity of osmotrophic microorganisms, mainly bacteria.

These methods give information about the remineralization of organic matter in the soil ecosystems with special respect to microbial organisms on lichens.

MATERIAL AND METHODS

Samples

Samples of different soils and lichens were collected in the vicinity of Casey Station (Wilkes Land, Continental Antarctica) and of Arctowski Station (King George Island,

92-17823



Samples		n	LOI %	POC %	PCHO ppm	MCHO ppm	BBM µg C g-1
Casey:							
Soil	(med)	11	5.0	3.0	248.4	25.6	0.47
	(min)		1.6	0.5	56.4	0	0.06
	(max)		21.1	7.8	966.6	115.5	1.09
Lichens	(med)	4	80.1	25.4	1609	86.8	3.82
	(min)		39.4	18.2	0	0	9.04
	(max)		94.4	41.7	14987	1187	0.33
Arctowski:							
Soil	(med)	11	20.9	9.7	142.7	84.3	1.94
	(min)		3.4	0.8	9.8	12.2	0.63
	(max)		40.1	32.3	1337	641.8	11.00
Lichens	(med)	18	86.9	33.9	2655	1849	1.52
	(min)		11.9	4.5	188	209	15.90
	(max)		98.3	43.7	8697	6419	0.51

Table 1. Organic matter and bacterial biomass of soil samples and lichens. Data given are median values (med) and range (max: maximum, min: minimum). LOI = loss on ignition; POC = particulate organic matter; PCHO = particulate carbohydrates; MCHO = free monosaccharides; BBM = bacterial biomass.

Maritime Antarctic) during austral summer 1985/86 and 1986/87, respectively. The soil samples (surface horizons: depth 0–2 cm) comprise those of barren soils from sites on fjells, surface samples with dry moss cushions and crustose lichens, surface samples with layers of green algae, and samples from meadows with *Deschampsia antarctica* from Arctowski. Lichens are fruticose and crustose. Details of the samples are given in Tables 1–2, and Figures 2–3.

Methods

CO₂-evolution. Measurements of CO₂-gas exchange were performed in temperature-controlled flow chambers. The CO₂ was measured by an infrared gas analyzer at different temperatures and moisture conditions. The equipment used is a modified version of the device described in detail by Kappert et al. [1986].

¹⁴C-glucose mineralization. U-¹⁴C-glucose was used for measurements of uptake and respiration by using the non-kinetic approach. Twenty-six nanograms of this substrate were added to a water suspension (10 g soil/10 ml water) and incubated in time series. Subsamples were used to measure the respired ¹⁴CO₂ which was trapped in ethanolaniline and measured by liquid scintillation counting. For details see Harrison et al. [1971], Meyer-Reil [1978].

Oxygen consumption: 5–10 g soil were incubated in 50 ml water and apparent oxygen concentrations were measured by an oxygen probe after 12, 24 and 48 hours. These results are converted into stoichiometric equivalents of CO₂ according to the respiration equation.

Soil characteristics: Microbial biomass was estimated from bacterial counts by epifluorescence microscopy and converting biovolume into biomass [Zimmerman et al., 1978; Böter, 1990]. The actual glucose concentration (free monosaccharides, MCHO) and particulate monosaccharides (PCHO, measured after acid hydrolysis) were

Sample	Type*	5°C	15°C	25°C
C1	A	242.0	79.8	37.2
C8	B	1011.2	911.0	531.2
C11	C	21.6	22.4	15.5
C14	A	169.0	102.0	70.7
C17	C	0	0	0
C22	B	41.9	23.0	0.8
C25	C	0	61.1	0
C28	A	112.9	55.2	60.4
C29	B	78.1	28.9	25.8
C30	A	37.9	13.8	9.9

Table 2. Glucose mineralization (CO₂ production) of the soil samples of Casey in relation (%) to the data of the CO₂ gas exchange for three temperatures. *Type A: sand with dry moss cushion and crustose lichens; Type B: sand with green layer of algae; Type C: sand with no apparent organisms (lichens or algae).

determined according to Dawson and Liebezeit [1983]. Particulate organic carbon (POC) was analyzed by a CHN-analyzer (Heraeus Co., Germany).

RESULTS AND DISCUSSION

Table 1 gives an overview of the soil samples with regard to some constituents of the organic matter and the bacterial biomass as estimated by epifluorescence microscopy.

The surface samples show fairly high amounts of organic matter, due to their plant cover by moss cushions, crustose lichens and algae. There are considerable amounts of free glucose (MCHO), indicating an environment which is not limited by organic matter.

Considerable differences exist with regard to the individual fractions of organic matter as represented by POC

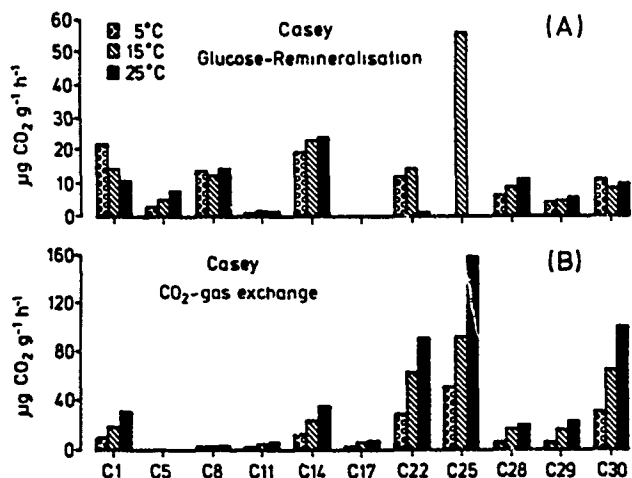


Figure 1. Apparent CO₂ production rates of soil samples from Casey measured by glucose remineralization (A) and total CO₂ gas exchange (actual water content) (B) at different temperatures. The nutrient states of these samples is given in Table 2.

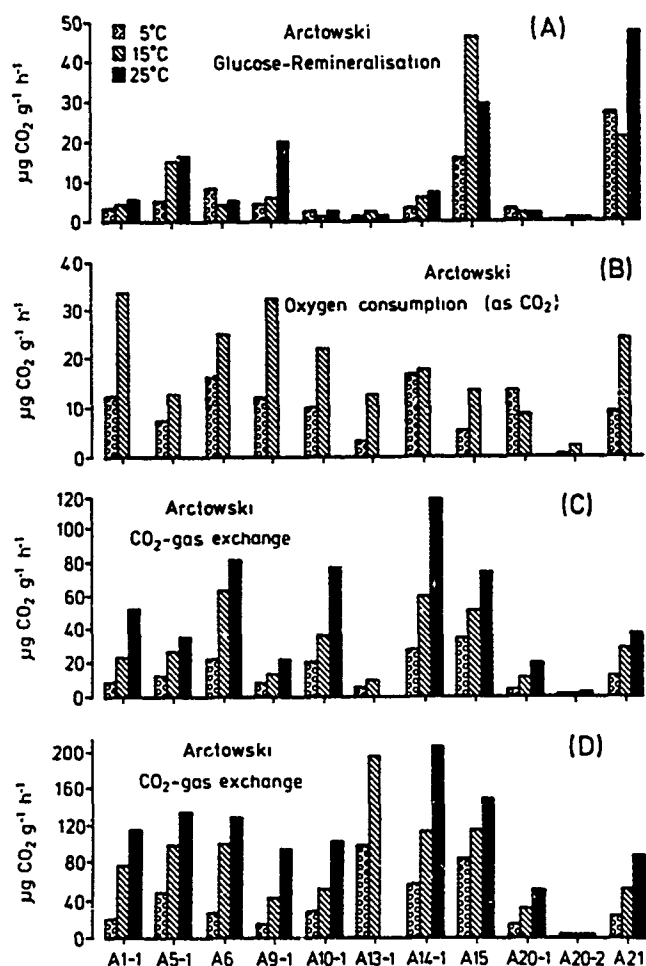


Figure 2. Apparent CO₂ production rates of soil samples from Arctowski measured for glucose remineralization (A), oxygen consumption (B), and gas exchange under actual water content (C) and enhanced water content (D) for different temperatures. Samples A1-1, A5-1, A6, A10-1, A13-1, A15, A20-1, A20-2, A21: dry moss cushion with sand and crustose lichens; A9-1, A14-1: soil with roots from *Deschampsia antarctica*.

(measured by CHN-analysis) and the loss on ignition (LOI, measured by combustion at 550°C). Few samples fulfill the assumption that approximately 50% of the LOI can be represented by POC, and most show a much wider span, indicating different qualities of the organic matter.

Data from the gross mineralization process (CO₂-gas exchange) are given in Figures 1–3. In order to estimate the effects of varying water content, the incubations of the samples from Arctowski were carried out using the ambient water content of the sample and under an increased water content of 50%. The effect of the elevated water content is evident for the overall respiration and acts as an enhancement of respiratory activity by more than double of the sample incubated under actual water conditions.

The data of the total CO₂-evolution show strong relationships to the concentrations of organic carbon and temperature. This is evident for both data sets, although it is difficult to establish functional relationships. As such, the amounts of organic matter are higher in the samples from the maritime Antarctic. However, this is not concomitant with the enhancement of the mineralization rates (cf. samples A14-1, A15 compared to samples C22, C25).

The response to increasing temperature is generally positive but shows different functional relationships among the individual samples.

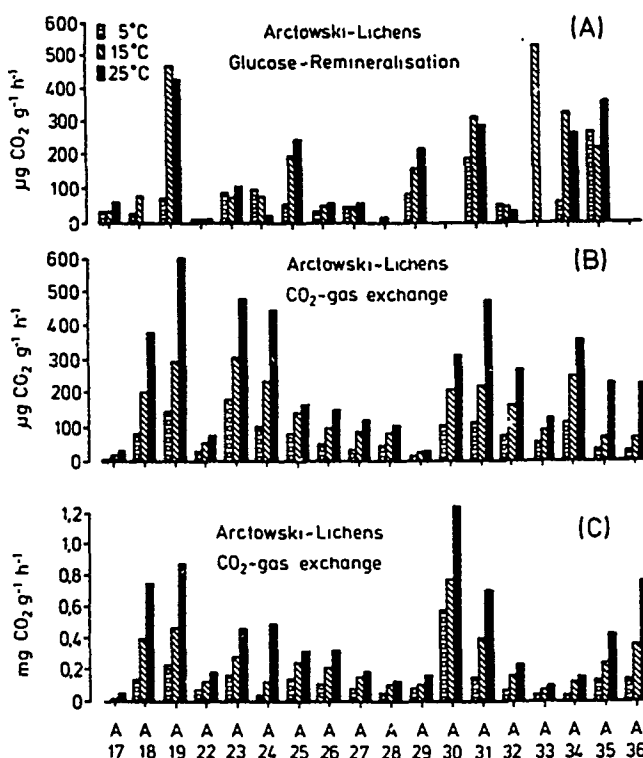


Figure 3. Apparent CO₂ production rates of lichens from Arctowski measured for glucose remineralization (A), CO₂-gas exchange under actual water content (B), and CO₂-gas exchange under enhanced water content (C). Samples: A17: crustose lichens (*Buellia* sp., *Ochrolechia* sp.); A18, A32: *Usnea antarctica*; A19, A31: *Alectoria* sp.; A22, A25: *Leptogium* sp.; A23: *Umbilicaria* sp.; A24: *U. fasciata*; A26, A27: *Ochrolechia* sp.; A28: *Placopsis* sp.; A29, A36: *Stereocaulon* sp.; A30: *Cornicularia* sp.; A33: *Ochrolechia* sp.; A34: undefined crustose lichens on dry moss cushion; A35: *Parmelia* sp.

Temperature:	5°C			15°C			25°C	
Method:	GR	GE	BOD	GR	GE	BOD	GR	GE
Samples								
Soils	43.0	214.4	62.8	17.0	235.6	74.8	9.2	201.9
Lichens	59.5	168.0		52.6	168.4		29.1	151.8

Table 3. Mean values of the CO₂ production (%) of the different methods in relation to the CO₂ production (gas exchange) measured under actual water content of the samples from Arctowski. GR: glucose remineralization; GE: CO₂-gas exchange (water content 50%); BOD: oxygen demand (recalculated for CO₂ production).

The CO₂-evolution by plant material, mainly crustose and fruticose lichens, is at least double that from soil samples. It also seems evident that the lichen samples show a significant contribution to glucose mineralization. This may be due to the epiphytic bacterial population which is consuming organic material produced by the lichen. The process of the "exudation," however, is still unclear. Tearle [1987] showed that high amounts of dissolved carbohydrates, mainly sugar alcohols, are released after the physical stress of freeze-thaw cycles during spring season.

The remineralization of dissolved organic matter (based on ¹⁴C-glucose) can be considered to be mainly due to osmotrophic organisms, i.e., bacteria and other small heterotrophs. The responses to temperature are not as clear as those from total CO₂-evolution. This may be a result of different active microbial populations and special problems of nutrient availability.

When comparing these data with those from total CO₂-evolution, it is possible to calculate the different relationships and note the great variability of individual samples. Table 2 shows the data for glucose remineralization by the soil samples from Casey in relation to the CO₂-gas exchange. Although the glucose remineralization is generally less than 100% of the gas exchange, there are exceptions, mainly samples with the highest contents of organic matter. The high values of samples C1, C8, C14 and C28 may reflect the actual available nutrients. Possible cofactors for metabolizing this material are probably at low concentrations. High levels of organic matter which can be found in samples of type A (moss cushions with crustose lichens) do not imply generally high total respiratory activity.

Table 3 presents the relationships between respired CO₂ as estimated from total CO₂-gas exchange under enhanced water content, glucose remineralization, and oxygen consumption in contrast to the data from the CO₂-gas exchange under actual water content. The increase in respiration (gas exchange) from actual to enhanced water content covers a range between approximately 2.0–2.1 for soil samples and 1.5–1.7 for lichens. Glucose remineralization, i.e., the use of free available moncarbohydrates, is at most about 60% of gas exchange. Highest levels are found for soil samples with high nutrient contents at low temperatures.

The following general results can be drawn from these tables:

- Gas exchange: The enhancement of mineralization shows no evident relationship with temperature. Highest rates can be found in soil samples with high (available)

nutrient content. Lowest rates can be shown for lichen samples.

- Glucose remineralization: High values can be obtained from soil samples with high (available) nutrients. The data show a decrease with increasing temperature. This also holds true for the lichen samples. Rather stable data can be shown for samples with low nutrient content, i.e., those from barren soils.

- Oxygen consumption: The rates from this method are intermediate between those from gas exchange and glucose remineralization.

CONCLUSION

Temperature, moisture and substrate quality considerably influence total microbial activity and mineralization processes. This is important for modeling purposes and overall description of this ecosystem. The data on mineralization do not show obvious adaptations by these organisms to low temperatures.

Temperature profiles of the different niches may illustrate this: The total range of temperature recordings was 0–20°C, although elevated temperatures may occur for short periods [Bölter, unpublished]. Temperatures in lichens growing on rock surfaces or moss surfaces show even higher values (to 40°C) [Smith, 1986; Bölter et al., 1989]. The activities show an adaptation to the whole environmental temperature span indicating that the microbial population can use this for active metabolic processes. However, both temperature and moisture show significant effects on microbial activity which also respond to substrate quality and availability. This holds true for all samples, soils and lichens.

The active total CO₂-evolution, oxygen consumption and glucose metabolism, i.e., the use of low molecular weight carbohydrates by small heterotrophs, shows that the microbial population is of great importance in these ecosystems. The results show that they can contribute to a considerable extent to the total mineralization.

This fact is especially important when taking into account the comparable data on plant material: Under the assumption that bacteria are a main constituent of the active population which is able to use glucose, then it produces a large part of the CO₂ which is normally considered to be of plant origin. This fact, however, needs further investigation by separating the epiphytic organisms from their source, and more detailed inspections of the surfaces of plants, detritus and inorganic matter.

REFERENCES

- Bailey, A. D., and D. D. Wynn-Williams, Soil microbiological studies at Signy Island, South Orkney Islands, *Br. Antarct. Surv. Bull.*, 51, 167-191, 1982.
- Bölter, M., Microbial activity in soils from Antarctica (Casey Station, Wilkes Land), *Proc. NIPR Symp. Polar Biol.*, 2, 146-153, 1989.
- Bölter, M., Microbial ecology of soils from Wilkes Land, Antarctica: II. Patterns of microbial activity and related organic and inorganic matter, *Proc. NIPR Symp. Polar Biol.*, 3, 120-132, 1990.
- Bölter, M., L. Kappen, and M. Meyer, The influence of microclimatic conditions on potential photosynthesis of *Usnea sphacelata*—a model, *Ecol. Res.*, 4, 297-307, 1989.
- Dawson, R., and G. Liebezeit, Determination of amino acids and carbohydrates, in *Methods of Seawater Analysis*, edited by K. Grasshoff, M. Ehrhardt, and K. Kremling, pp. 319-346, Verlag Chemie, Weinheim, 1983.
- Harrison, M. J., R. T. Wright, and R. Y. Morita, Method for measuring mineralisation of lake sediments, *Appl. Microbiol.*, 21, 223-229, 1971.
- Kappen, L., M. Bölter, and A. Kühn, Field measurements of net photosynthesis of lichens in the Antarctic, *Polar Biol.*, 5, 255-258, 1986.
- Meyer-Reil, L.-A., Uptake of glucose by bacteria in the sediment, *Mar. Biol.*, 44, 293-298, 1978.
- Smith, R. I. L., Plant ecological studies in the fellfield ecosystem near Casey Station, Australian Antarctic Territory, *Br. Antarct. Surv. Bull.*, 72, 81-91, 1986.
- Tearle, P. V., Cryptogamic carbohydrate release and microbial response during freeze-thaw cycles in Antarctic fellfield fines, *Soil Biol. Biochem.*, 19, 381-390, 1987.
- Vincent, W. F., *Microbial Ecosystems in Antarctica*, Cambridge Univ. Press, Cambridge, 1988.
- Wynn-Williams, D. D., Ecological aspects of Antarctic microbiology, *Adv. Microb. Ecol.*, 11, 71-146, 1990.
- Zimmerman, R., R. Iturriaga, and J. Becker-Birck, Simultaneous determination of the total number of aquatic bacteria and the number thereof involved in respiration, *Appl. Environ. Microbiol.*, 36, 926-935, 1978.

AD-P007 320



92-17824



Effects of Point Source Atmospheric Pollution on Boreal Forest Vegetation of Northwestern Siberia

T. M. Vlasova

Far North Institute for Agricultural Research, Noril'sk, U.S.S.R.

B. I. Kovalev

Bryansk All-Union Scientific Research Institute, Forest Resources Section, Bryansk, U.S.S.R.

A. N. Filipchuk

All-Union Scientific Research Institute, Forest Resources Section, Moscow, U.S.S.R.

ABSTRACT

Atmospheric pollution from the Noril'sk Mining-Metallurgical Complex, in the form of heavy metals and sulfur components, has resulted in damage to plant communities in the area. Vegetation on over 550,000 ha has been detrimentally affected by the pollution fallout, primarily sulfur dioxide. Forests (mainly *Larix sibirica*) and most lichens have been killed within a 300,000-ha zone around Noril'sk and extending about 50 km to the south and southeast. Less severe damage to lichens and vascular plants extends 170 km to the south and 80 km to the east of the pollution source consistent with prevailing winds during the period of plant growth. Tetracolous lichens are particularly vulnerable to the pollution products and among vascular plants *Larix gmelinii*, *Picea obovata*, *Ledum palustre*, *Calamagrostis* sp., and *Salix lanata* show least resistance.

INTRODUCTION

Growth in industrial production characterizes the modern world and has led to pollution of the environment with toxic substances, causing deterioration in the condition and loss of components of plant communities. Pollution effects on forest vegetation may be pronounced in regions with extreme climatic conditions—such as at forest ecotones in the Far North. A typical example of this phenomenon is furnished by the destruction of forest vegetation in the Noril'sk industrial region (NIR).

THE STUDY AREA

The NIR is located in North Krasnoyarsk Krai, on the right bank of the Yenisey River (Figure 1). The forests studied are those at the northern interface of taiga and tundra [Parmuzin, 1979; Chertovskii and Semenov, 1984]. They provide habitat for mammals and birds and the very important resource base for reindeer and hunting economies. Bodies of water in the region are rich in fish species. The ecosystems of such forest have little plasticity and restorative capability.

The NIR has a subarctic climate with an extended, cold winter and a short, cool summer with a vegetation growth period of about 60 days. Northerly winds prevail. Distribution of trees is in scattered small units or strips, large stands being infrequent. The average forest cover does not exceed 40%. The main tree species are *Larix sibirica*, shifting in the east to *L. gmelinii*, and also *Picea obovata* and *Betula pubescens*. Forested areas are concentrated mostly in river valleys and on watershed slopes. These same watersheds also include tundra vegetation. The forests have a low density with small tree crowns, about 25% of the forested area being represented by open stands. For every unit of plant biomass there are more photosynthesizing tissues than in the true taiga.

EMISSIONS PRODUCED BY THE NORIL'SK A.P. ZAVENIAGIN MINING AND METALLURGICAL INDUSTRIAL COMPLEX (NMMC)

The economic and social development and ecological state of the NIR are determined by the activities of the NMMC. It is the basis of development for the extensive

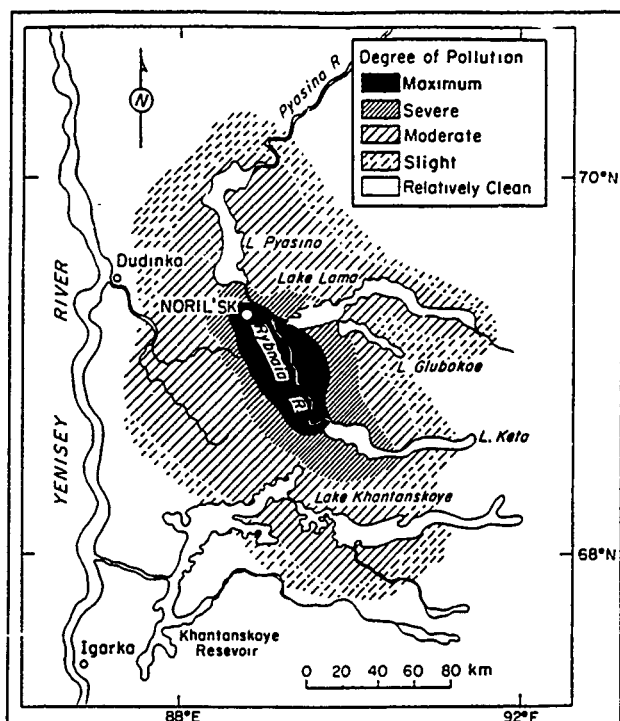


Figure 1. Distribution of atmospheric pollution from the Noril'sk industrial complex.

interriver region of the Siberian Yenisey and Lena rivers, from the Lower Tunguska in the south to the polar islands of Severnaya Zemlya to the north. Equal to the vastness of the region is the extent and negative effect of the complex on the environment. Atmospheric emissions rank first in terms of concern due to their negative consequences and their role as the most harmful form of anthropogenic influence on the region's biocoenosis [Kovalev and Filipchuk, 1990]. Processing polymetal ores containing large quantities of sulfur compounds, the enterprises of the NMMC annually give off around 4.5 million tons of harmful substances, including more than 2.2 million tons of sulfur anhydride (Table 1). These substances contribute not only to the regional background atmosphere, but also enter into air masses that diffuse over wide distances in the Arctic, negatively affecting the functioning of northern ecosystems as a whole [Kriuchkov, 1985].

Another source of pollution is the mining of ores used in the metallurgical processes. This includes the alteration of local relief and hydrological regimes, the disturbance of vegetative cover, and associated animal life.

A further source of pollution is discarded drainage water, the annual volume of which constitutes around 450 million cubic meters [Kriuchkov, 1985]. No more than 50% of this total volume is purified. After purification, drainage waters contain copper, nickel, titanium, iron, chromium, calcium, magnesium, sulfur substances, and petroleum products in quantities substantially exceeding the existing concentration levels deemed allowable.

EFFECTS ON THE VEGETATION

The greatest threat to forest vegetation is posed by the discharge of sulfur-containing gases. These are conventionally divided into two groups: strong autogenous process gases, readily convertible in the environment to sulfuric and sulfurous acids, and weak gases (containing less than 3% sulfur dioxide). Strong gases were first produced by the complex in 1981 with the introduction of the suspended fusion furnace [Kovalev and Filipchuk, 1990]. The portion of strong gases in the total volume of gaseous emissions in 1981 was 5%. In the period from 1981 to 1987 this amount increased from 5% to 38%, and with the change to autogenous fusion it will reach 50%. Compounding the situation, in recent years, raw materials with increased sulfur content have been brought to the complex for processing, which also influences the increased volume and concentration of sulfur-containing emissions. Thus, sulfur dioxide will become the main harmful ingredient in emissions into the atmosphere in the future and, despite an effort to decrease the volume of emissions, the concentration of sulfur dioxide will increase.

Plant response to sulfur dioxide, as a result of its concentration and the length of time of exposure by the leaves (needles), can be divided into five degrees: absence of damage, and hidden, chronic, severe, and catastrophic damage. A number of stands which were determined to be healthy at the time of observation may include trees with hidden damage, in which destruction of the physiological-biochemical processes was already occurring. Chronic damage to trees exists in all stands affected by emissions, and is manifested in decreased number of needles, dechromatization of needles and leaves, and the accumulation of an excessive number of phytotoxins [Kovalev and Filipchuk, 1990].

Indicators	Emissions, thousands of metric tons/year									
	1980	1981	1982	1983	1984	1985	1986	1987	1988	1989
Total quantity of harmful substances leaving all pollution sources	2349.0	2666.1	3707.3	3998.3	4723.4	4845.3	4738.6	4199.4	4385.5	4442.8
Solids	529.5	605.7	1114.8	1314.6	2008.5	2067.3	2369.1	1833.3	2074.8	2163.9
Gaseous	1819.5	2060.4	2592.5	2683.7	2714.9	2778.0	2369.5	2366.1	2310.7	2278.9
Amount of sulfur anhydride	1752.8	1994.9	2402.0	2567.7	2647.7	2724.3	2325.2	2244.3	2242.3	2216.4

Table 1. Total emissions of the Noril'sk Mining Metallurgical Complex during the period 1980-1989.

Severe and catastrophic damage are caused by the relatively short-lived influence of increased concentrations of phytotoxins during so-called "accidental" high level emissions of harmful substances. Such damage is indicated by extensive yellowing and needle and leaf loss on trees in limited areas in just a short time.

INSPECTION METHODS

Over the last 15 years (since 1976) a periodic aerial survey of the condition of the NIR's forest vegetation has been conducted by the Bryansk Specialized Forest-Organizational Section of the All-Union Scientific Research Institute. In the surveys, based on the total proportions of damaged (discolored foliage and low proportion of live branches) and dead trees, five categories of stand conditions were formulated: (1) healthy—damaged and dead trees in the stand constituting less than 10%; (2) weakened—10–25% of the trees were damaged or dead; (3) severely weakened—26–50% of trees were damaged or dead; (4) dying—damaged trees and dead trees constituted 51–80%; and (5) ruined—over 80% damaged or dead trees.

In 1987 a survey of forest conditions was conducted by the Moscow Aerocosmic Forest-Organizational Section using spectroscopic air photos with a 1:30,000 scale in the zone of totally damaged forest and shrub vegetation, and a 1:15,000 scale in the zone experiencing lesser degrees of

damage. On the whole, the data obtained using two independent and different survey methods were similar, which supports their reliability.

The Far North Institute for Agricultural Research has also collected vegetation specimens for chemical analysis. Fifty test plots were marked at various distances from the pollutant source, beginning at 7 km and continuing up to 25 km in the direction of prevailing winds during the period of vegetation growth. On the test plots a number of geobotanical and afforestation inspection tasks were performed, including a selection of 2500 specimens for chemical analysis and identification of visual indicators of damage to members of the plant community. To establish a connection between the level of pollution of an area and the plants' reaction to various toxin dosages, correlational analyses were conducted between the plants' content of heavy metals and sulfur dioxide, the distance from the pollutant source, and the degree of visible damage to the trees, shrubs, grasses, small shrubs, and lichens.

RESULTS

Response of the vegetation to pollutants

The constant pollution of the biosphere with sulfur and its compounds and other harmful substances comprising the NMMC's emissions has led to significant destruction of the forest biocoenoses, their destabilization, and substitution by

Survey Years	Weakened 1000 ha			Severely Weakened 1000 ha			Dying 1000 ha			Ruined 1000 ha			Total 1000 ha
	Tree Stands	Shrubs	Total	Tree Stands	Shrubs	Total	Tree Stands	Shrubs	Total	Tree Stands	Shrubs	Total	
1976	133.9	—	133.9	69.6	—	69.6	86.8	—	86.8	32.2	—	32.2	322.5
1978	177.9	—	177.9	66.8	6.7	73.5	86.3	—	86.3	60.0	—	60.0	397.7
Growth 1976-1978			+44.1			+3.9			-0.5			+27.8	+75.2
1980	133.3	0.5	133.8	21.9	—	21.9	137.9	15.2	154.9	114.9	1.4	116.3	424.9
Growth 1978-1980			-44.0			-51.6			+68.6			+56.3	+29.2
1982	93.4	2.4	95.8	66.5	2.0	68.5	116.2	15.2	151.4	118.4	1.4	119.8	435.5
Growth 1980-1982			-38.0			+46.6			-3.5			+3.5	+8.6
1984	104.9	3.6	108.5	69.6	2.0	71.6	92.3	12.1	104.4	151.6	9.2	160.8	445.3
Growth 1982-1984			+12.7			+3.1			+17.0			+41.0	+9.8
1986	66.1	3.8	69.9	98.9	2.6	101.5	38.7	4.7	43.4	231.0	10.8	241.8	456.6
Growth 1984-1986			-38.6			+29.9			-61.0			+81.0	+11.3
1987	114.2	—	114.2	128.0	9.9	137.9	Included in "Ruined" category			278.1	12.0	290.1	542.5
1989	89.7	4.1	93.8	104.4	2.7	107.1	59.8	2.8	62.6	283.2	18.4	301.6	565.1
Growth 1986-1989			+23.9			+5.6			+19.2			+57.8	+108.5
Growth 1987-1989			-20.4			-30.8						+74.1	+22.6

Table 2. Dynamics of forest and shrub vegetation in the study area that has been damaged by industrial emissions (data from the Moscow Aerocosmic Forest-organizational Section).

other plant associations, the development of pests and diseases, changes in the hydrologic and chemical composition of waters, soil erosion, and other negative consequences [Kriuchkov, 1985; Kovalev and Filipchuk, 1990].

According to the 1989 survey data, the total area of affected wood-shrub vegetation and other vegetation subject to various levels of damage constituted 565.1 thousand ha (Table 2). The increase in the damaged area from 1976 to 1989 was 242,000 ha, and in comparison to the 1986 survey, the affected area had grown between 1986 and 1989 by 108,000 ha or 44.7% of the total increase during the entire investigation period.

Weakened stands were evident on an area of 93.8 thousand ha, which made up 16.6% of the total area of damaged forest vegetation. In comparison to the previous survey, the area increased by 23.9 thousand ha at the cost of damage to tree stands where signs of phytotoxin influence were not noted earlier. In 1976 the southern border of such stands was at a distance of up to 90 km from Noril'sk. In recent years it has moved south to 170 km and east to 80 km.

Severely weakened stands were noted in an area of 107.1 thousand ha, which in comparison to 1986 is greater by 5.6 thousand ha. An analysis of the movement of the borders of weakened and severely weakened stands in previous years indicates that in the greater part of the area, formerly weakened tree stands had become severely weakened ones.

Next in terms of damage level zones and closer to the pollutant sources are dying tree stands, located on an area of 62.6 thousand ha. In comparison to 1986, their area has increased by 19.2 thousand ha. The movement of borders shows that in most cases, severely weakened tree stands pass into this category. Less severely impacted forest stands are not being closely monitored. It appears that the area of

these less severely affected forests varies depending upon the intensity of phytotoxin influence and associated climatic conditions prior to the period of analysis.

Ruined stands (301,000 ha) are located closer to pollutant sources than are stands subject to other degrees of damage. In the last three years, the area of ruined forests has grown by 59.8 thousand ha. More than all others, those trees that were dying in preceding years pass into the ruined category, and sometimes so do severely weakened tree stands. The boundary of ruined stands has moved from 20 to 120 km to the south of Noril'sk since 1976.

At a distance of more than 120 km to the south of Noril'sk, changes in forest vegetation conditions occurred less intensively in the period from 1976 to 1986, but after 1986, further weakening of the forests to the southeast, northeast, and east of Noril'sk has been noted. This has probably been brought about by more intensive assimilation of phytotoxins by the plants associated with the increase in "strong gases" in the emissions [Kovalev and Filipchuk, 1990].

Results of Chemical Analyses of Specimens

The results of chemical analyses showed that the contents of copper, zinc, cobalt, nickel, and sulfur in the plants varied greatly (Table 3), but all in all, for the majority of species, these quantities were inversely proportional to the distance from the emission source. A comparison of the visible damage of plants (the number of dead and damaged specimens, the presence or absence of needles and leaves, needle and leaf color, etc.) with their pollutant element contents did not reveal a direct dependency between these indicators.

An analysis of change in condition of the lichen cover versus the quantity of accumulated elements showed that the

Plant Groups	Elements				
	Copper	Nickel	Cobalt	Zinc	Sulfur
Trees	$\frac{530.0}{106.0} = 5.0^a$	$\frac{77.0}{28.8} = 2.5$	$\frac{3.0}{0.30} = 10.0$	$\frac{438.0}{48.7} = 9.0$	$\frac{2360}{9.1} = 260$
Shrubs	$\frac{480.0}{92.3} = 5.2$	$\frac{97.0}{12.9} = 7.5$	$\frac{4.0}{1.00} = 4.0$	$\frac{208.0}{13.9} = 15.0$	$\frac{2410}{2.7} = 880$
Small Shrubs	$\frac{300.0}{41.7} = 7.2$	$\frac{70.0}{14.0} = 5.0$	$\frac{3.0}{0.32} = 9.4$	$\frac{44.0}{9.2} = 4.8$	$\frac{2870}{3.4} = 850$
Sedges	$\frac{280.0}{46.7} = 6.0$	$\frac{147.0}{12.3} = 12.0$	—	$\frac{36.0}{2.8} = 13.0$	—
Grasses	$\frac{88.0}{11.8} = 6.8$	$\frac{22.0}{1.5} = 15.0$	—	$\frac{30.0}{2.1} = 14.1$	$\frac{1230}{1.2} = 1000$
Forbs	$\frac{280.0}{39.4} = 7.1$	$\frac{42.0}{2.5} = 17.0$	$\frac{1.5}{0.60} = 2.5$	$\frac{48.0}{2.2} = 22.0$	$\frac{8960}{5.6} = 1610$
Lichens	$\frac{220.1}{52.4} = 4.2$	$\frac{190.0}{95.0} = 2.0$	$\frac{4.1}{0.66} = 6.2$	$\frac{58.0}{8.9} = 6.5$	$\frac{2870}{38.9} = 80$
Plants of all groups	$\frac{530.0}{126.2} = 4.2$	$\frac{294.0}{147.0} = 2.0$	$\frac{10.0}{1.00} = 10.0$	$\frac{438.0}{91.3} = 4.8$	$\frac{8960}{112} = 80$

^a The contrast in pollution levels is shown as the product of the maximum value as the numerator and the minimum value as the denominator.

Table 3. Comparative variation between maximum and minimum levels of copper, nickel, cobalt, zinc, and sulfur in plants within the study area (mg kg⁻¹ air-dry substance).

number of species, the percentage of cover, and the phytomass reserve depends on copper, nickel and sulfur content [Kriuchkov, 1985]. Depending on the condition of the lichen cover, five zones characterizing pollution of the area were determined within the survey region: (1) areas of maximum pollution (lichen desert); (2) severe pollution; (3) average pollution; (4) slight pollution; and (5) relatively clean (Figure 1). The pattern of the zones is consistent with the direction of the pollution plumes, which confirms the importance of this factor in the transfer of polluted air masses. On the other hand, topographic features are also significant in influencing accumulation of pollutants. The terraces of the Putorana plateau, for example, prevent the penetration of toxins to the southeast and east; thus only along river valleys and lake basins open to the motion of winds blowing from the complex does pollution penetrate into the mountain regions.

The zone of maximum pollution (lichen desert) stretches for 50–55 km in a southeasterly direction, encompassing almost all of the Rybnaia River valley, and towards the southern area of Lake Pyasino up to 35 km to the northwest. The total area of the zone is around 300,000 ha. The forest cover is made up almost entirely of dead trees and strongly damaged shrubs (up to 60% of the above ground tissues dead). The portion of damaged small shrubs and grasses is 75%, and 50% of the rhizomes of grasses and sedges are dead. Lichen cover is absent.

The zone of severe pollution extends 50 km to the northwest and southeast 25–30 km beyond the preceding zone, occupying approximately 380,000 ha. The vegetation is characterized by the prevalence in the forest cover of ruined and dying trees, with 20–50% of the shrubs dying. There are less severe effects than in the preceding zone within the grass–small shrub layers. The number of damaged plants is 40% or less. Lichens appear, but their condition is unsatisfactory, not exceeding 1–5% of the ground cover and with some species exhibiting morphological changes.

The zone of average pollution is located in the northern area of the Khantayskoye reservoir, and it also occupies the western portions of lakes Lama, Glubokoe, and Keta. The zone's total area is about 420,000 ha. The forest cover is distinguished by the presence of up to 50% dead larch with yellowing spruce needles and birch leaves. The condition of the shrub and grass–small shrub layers is satisfactory with damaged plants constituting no more than 10%. Lichens include up to 34 species and cover ranges from 20–40%.

The zone of slight pollution encompasses a total area of 460,000 ha to the west of the Murovskiy Rock Range, to south of Lake Khantayskoye, and the eastern areas of lakes Lama and Glubokoe. The vegetation is practically without signs of damage, and only in the forest canopy are larch with yellowing needles noticeable. Lichens are well developed with plants of average size and cover increasing up to 70%; more than 34 lichen species were noted.

The boundaries of the weak pollution zone are not established, and these pass into a relatively clean zone where the plants show no visible signs of damage; lichen cover is distinguished by considerable species variety—up to 96 species—and cover reaches 80–90%. Metal content is almost at background level.

The defined zones have no clear boundaries in terms of distance, and between them there are some intermediate

strips which may be more or less extensive. The zones are not constant in terms of time, and their boundaries may blend together depending on variation in the volume of industrial emissions and the self-cleansing capability of natural communities. In the future, redistribution of the areas may occur both in terms of pollution levels and damage to plants.

CONCLUSIONS AND DISCUSSION

The aggregate effect of anthropogenic factors, primarily atmospheric emissions, has led to damage and destruction of the vegetative cover on the tundra and forest tundra in North Krasnoyarsk Krai in an area of 7.4 million ha [Kriuchkov, 1985]. The total area of dead and damaged forests in the NIR, which were previously important for hunting, as reindeer pastures, and as recreational zones for residents of Noril'sk, exceeded 0.5 million ha in 1990. The area of bodies of water that have lost their importance for fishing exceeds 200,000 ha, including Lake Pyasino and its system. The negative consequences of the atmospheric pollution do not stop with these losses due to the degradation and destruction of entire plant associations. Active circulation of accumulated pollutant microelements in natural mediums along the food chains will create a serious threat to living organisms, including man.

A combination of various survey techniques should be incorporated into local forest monitoring programs. These should include geobotanical, floral, and morphologic measurements as well as biochemical and physiological analyses of plant, soil, air, and water.

Visual signs of damage appear on the majority of plants with associated concentrations of chemically active harmful substances following a relatively long period of exposure to pollutants. Resumption of normal life processes for such plants or communities is often impossible, even with the removal of the pollution source. Therefore, to identify the early response of plants to the influence of industrial emissions, it is necessary to find suitable biological indicators that will reflect the presence of damage at different stages. Arboreal lichens are generally recognized as bioindicators of pollution levels, but their limited distribution in the NIR restricts their use in this capacity. According to the results of our research and that of others [Kriuchkov, 1985], it has been established that terricolous lichen species and *Larix gmelinii* are particularly sensitive to pollution. Other plant species that readily accumulate heavy metals and sulfur are *Picea obovata*, *Ledum palustre*, *Calamagrostis* sp., and *Salix lanata*.

The delineation of pollution zones based on the buildup of harmful microelements in lichens (as determined by chemical analyses) coincides with the categories of forest conditions determined on the basis of visual indicators. However, only the accumulation of elements in plant tissues may serve as a reliable indicator of areas of heavy metal and sulfur dioxide pollution. Assessment of atmospheric pollution levels according to surface damage indicators may not be totally reliable; however, the appearance of damage and apparent outward plant reaction are indicative of unfavorable ecological conditions.

LITERATURE CITED

Chertovskii, V. G., and B. N. Semenov, Pretundra Forests of the USSR, *Forestry*, 5, 26-33, (In Russian), 1984.
Kovalev, B. I., and A. N. Filipchuk, Forest conditions in the zone of the Noril'sk Mining and Metallurgical Complex's industrial influence, *Forest Management*, 5, 1-85 (In Russian), 1990.

Kriuchkov, V. V., Preservation of the North's Nature, in *Issues of Anthropogenous Effects on the Environment*, pp. 124-131, Nauka, Moscow, (In Russian), 1985.
Parmuzin, Iu. P., *Tundra-forests of the USSR*, 295 pp., Moscow, (In Russian), 1979.

Manuscript translated from the Russian by David A. Peterson, July 1990.

The Natural Background Disturbance in the Soviet Far East

V. P. Karakin

Pacific Geography Institute of the Far East Division of the U.S.S.R. Academy of Sciences, Vladivostok, U.S.S.R.

A. S. Sheinhouse

Institute of Regional Problems and Complex Analysis of the Far East Division of the U.S.S.R. Academy of Sciences, Khabarovsk, U.S.S.R.

ABSTRACT

The natural system development of the Soviet Far East dates back to the paleolith. It accelerated more and more, and strong anthropogenic pressure is now evident. The main parts of the ecosystems appear to have changed as a result. We have elaborated specific methods of ecosystem disturbance assessment. Measurement of a natural scale was adopted; this scale is based on the period necessary to the changed landscape restoration until climax. Assessments for the Amur, Kamchatka, Khabarovsk, Magadan, Prymorie, and Sakhalin regions have been made.

Sexual Reproduction of *Arctophila fulva* and Seasonal Temperature, Arctic Coastal Plain, Alaska

J. D. McKendrick

School of Agriculture and Land Resources Management, Agriculture and Forestry Experiment Station,
University of Alaska Fairbanks, Palmer, Alaska, U.S.A.

ABSTRACT

Arctophila fulva is an indigenous grass with circumpolar distribution. It occurs in Alaska's boreal and arctic environments, usually as an emergent aquatic. An intensive 5-year investigation of *Arctophila fulva* began in 1985 to determine its life history and environmental characteristics. Evaluations of environmental characteristics included recording hourly temperature means of soil/mud, water, and air during the growing season. Ten Coastal Plain Province sites and one Brooks Range foothills site were included in the 1986–1989 temperature monitoring project. Observations in the Alaska Range were done in 1987–1989.

Initial evaluation of sexual reproduction in 1985 indicated no seed formation occurred in *Arctophila fulva* colonies on the coastal plain during that year. Florets were in anthesis at or near the end of growing season. However, sexual reproduction occurred in the northern foothills of the Brooks Range where seeds matured before the coastal plain plants reached anthesis. Foothill stands of *Arctophila fulva* produced seed each growing season of our study. Low to no success in sexual reproduction continued for coastal plain stands of *Arctophila fulva* during 1986 and 1987. Seed formation was observed in plants on the coastal plain that were protected by a plexiglas shelter in 1988. During the 1988 growing season, few seeds were found in inflorescences from one natural stand on the coastal plain, and one stand on the margin of the foothills (about 35 miles inland) produced seed. In 1989, 25 stands of *Arctophila fulva* on the coastal plain produced seed, probably due to elevated growing season temperatures and perhaps extension of the growing season. During 1987–1989, sexual reproduction was consistently successful for *Arctophila fulva* growing in the Alaska Range.

Because sexual reproduction success for plants in the Arctic is often poor, plants in this region are believed to persist mainly by vegetative propagation. The lack of sexual reproduction may limit the gene recombination opportunities and genetic diversity. Also, the scarcity of seeds affects the rate and diversity of species available to colonize barren sites. It appears that warming of the Arctic could affect the quantity and perhaps the diversity of seed produced by indigenous arctic plants.

AD-P007 321



92-17825



In the Footsteps of Robert Marshall: Proposed Research of White Spruce Growth and Movement at the Tree Limit, Central Brooks Range, Alaska

Terry D. Droessler

ManTech Environmental Technology, Inc., US EPA Environmental Research Lab, Corvallis, Oregon, U.S.A.

ABSTRACT

The proposed research will quantify white spruce growth and document its latitudinal stability at the tree limit in the central Brooks Range over the life span of the living trees. The goal is to link tree growth and tree position to summer temperature and precipitation. Historical records from 1929 to 1938 from work by Robert Marshall have been used to identify tree limit sites and provide information to interpret the present location of the tree limit.

INTRODUCTION

Altitudinal and latitudinal tree limits represent temperature, precipitation or other barriers to species distribution. Tree limit is defined here as the last living white spruce (*Picea glauca*, Voss.) tree, regardless of form, that could be located at the farthest northern latitude or elevation in selected drainage of the central Brooks Range. The present tree limit may indicate the location of a temperature or moisture limitation that prohibits further species movement. A knowledge of temperature and moisture history and species movement and growth patterns is important for understanding the establishment and existence of the present tree limit. Studying growth and movement rates of trees in the vicinity of the tree limit will document tree response to temperature and moisture change over the life span of living trees. Predicting tree growth and tree movement in response to future temperature and precipitation scenarios may then be possible based on past tree growth and tree movement relationships to temperature and precipitation.

Indications of accelerated warming have been reported. Jones et al. [1986] show that the warmest near-surface temperatures over the land and oceans of both hemispheres between 1861-1984 have occurred since 1980. Jones et al. [1988] show overall rising global surface air temperature for 1901-1987. Lachenbruch and Marshall [1986] concluded that the depth to permafrost in the Alaska and Canadian Arctic has increased in recent decades. Houghton and Woodwell [1989] state that the greatest warming is expected to occur at higher latitudes in winter. The warming, accord-

ing to predictions from General Circulation Models (GCMs), will probably be at least twice the global average increase [IPCC, 1990].

Several studies of tree limit in the Arctic have shown stable to advancing conditions over the last few decades [Densmore, 1980; Goldstein, 1981; Odasz, 1983; Cooper, 1986; Lev, 1987]. If temperatures continue to increase and moisture is not limiting, the tree limit may advance in latitude and altitude until it is once again in equilibrium with temperature, moisture or other controlling factors.

One mechanism for tree limit movement is a change in sexual reproductive success. White spruce tree limit on the south slope and isolated clusters of balsam poplar (*Populus balsamifera*, L.) on the north slope of the Brooks Range, commonly reproduce by vegetative means only [Edwards and Dunwiddie, 1985; Lev, 1987]. Increases in temperature may allow sufficient time for sexual reproduction to take place. An increase in temperature would shift the 10°C July isotherm northward in latitude and higher in elevation. Movement rates could dramatically increase because seed dispersal distances are far greater than branch or root vegetative reproduction dispersal distances.

HISTORICAL STUDIES OF TREE LIMIT IN THE BROOKS RANGE

Work by Robert Marshall in the 1930s provides a historical basis for a study of tree growth and movement in the Brooks Range. Marshall undertook tree growth studies in the North Fork of the Koyukuk, Alatna, and John River

drainages north of the Arctic Circle near Wiseman, Alaska, from 1929 to 1939 [Retzlaf and Marshall, 1931; Marshall, 1933, 1970, 1979; Glover, 1986; Brown, 1988]. Marshall died before he was able to publish any results from his data collections. However, Robert's brother, George, donated the Robert Marshall Papers to The Bancroft Library, University of California, Berkeley, in 1979.

Marshall kept detailed field journals, including time and distance records and descriptions of locations where data were collected. Marshall recorded the location of tree limit as defined above. His documentation of tree limit locations have been used to define tree limit site locations that will be revisited in 1990 (see Table 1). Marshall collected tree growth and sample plot information at and below the tree limit. He hypothesized that tree growth was limited by moisture, solar radiation or temperature. Marshall's tree limit descriptions and historical data will help in interpreting data to be collected in 1990.

Marshall calculated the movement rate of trees from age and distance data he collected as he approached tree limit. White spruce produces seed at approximately age 50. Based on his observations (advancing tree limit) and calculation of movement rates, he decided that tree limit was not universally controlled by climatic factors. Rather, he hypothesized that spruce trees had insufficient time since the last glaciers receded to move to a temperature- or moisture-controlled tree limit.

Marshall attempted to advance tree limit by preparing white spruce seed plots beyond tree limit to see if seeds would germinate and grow; paired plots were established in three drainages (Grizzly, Kinnorutin and Barronland Creeks). The plots were established to verify that tree limit could still advance, albeit at a rate controlled by tree seed-bearing age and wind dispersal distances. For example, at Grizzly Creek, seed collected about six kilometers south of tree limit was sown approximately 19 kilometers north of tree limit in 1930. Marshall estimated that if the plots became established, he was advancing tree limit by about 3000 years (based on the estimated 50 years to reach seed-bearing age and a seed dispersal distance of 300–370 meters, roughly a movement rate of 1.6 kilometers in 250 years). The seed was sown on mineral soil (all vegetation removed) on one plot and on existing vegetation on a paired plot.

Marshall revisited the Grizzly Creek plots in 1938 and found no sign of germination. Samuel Wright visited the Kinnorutin Creek and Barronland Creek sites in 1966 and found no sign of tree growth [Wright, 1969, 1973, 1988]. Several explanations are possible, the foremost being that the seed source was inappropriate on two of the three plots. The Barronland Creek seed originated in the Chippewa National Forest near Cass Lake, Minnesota. The Kinnorutin Creek seed originated from the Ottawa National Forest and was obtained from the Hugo Sauer Nursery in Rhinelander, Wisconsin. In addition, seed viability was not established for two of the three seed sources. The seed may also have been sown above a temperature- or moisture-controlled tree limit.

Marshall [1970] described the Barronland Creek seed plot location as follows:

"The easterly plot is approximately 12x12 feet. The ground was sown as was found with white spruce seeds. About 20 feet upstream, the westerly plot is approximately 8x8 feet. Seed sown on mineral soil.

The seeds were collected at Chippewa NF near Cass Lake, Minn. When tested in autumn of 1938 they showed a germination rate of approximately 80 percent. The plots were established on July 7, 1939 at 2:15–3:00 PM. The spruce forest at the present moment has its outpost about a mile north of Amawek Creek. Previous studies made me calculate it was advancing at approximately a mile in 250 years. At this rate, and if my seeds developed, the present sowing would be anticipating nature by 2000 years."

Sam and Billie Wright obtained 100 four-year-old white spruce seedlings from Dr. Leslie Viereck at the Forestry Sciences Laboratory, University of Alaska, Fairbanks, in 1968 [Wright, 1973, 1988; Dr. Leslie Viereck, personal communication]. They were transported by bush plane to Summit Lake, approximately eight air miles northeast of Marshall's Barronland Creek site. The Wrights planted the white spruce seedlings within one of Marshall's original plots in 1968.

Sam Wright revisited the Barronland Creek planting site in 1989. He found five living seedlings, which were essentially the same size as at planting [Wright, personal communication].

PROPOSED WORK

I propose to revisit some of Marshall's tree limit sites and collect cores to determine tree age structure and growth rates. I propose to evaluate tree limit movement over the life span of living trees by analyzing the age structure from cores of tree limit trees. Marshall's data will be used to help interpret tree limit locations proposed for visitation in the summer of 1990. Enough time has elapsed since Marshall collected data that small seedlings at the tree limit could have matured to produce seed.

Hypotheses to be Addressed

Has the tree limit advanced, remained stable or retreated during the recent past (age of oldest living or dead trees)?

Has tree growth increased in response to temperature and moisture trends?

Tree Limit Sample Locations

Table 1 shows the approximate latitude and longitude of the proposed tree limit field sites.

Potential Usefulness of Marshall's Data

The potential usefulness of Marshall's data is dependent upon its quality. The actual cores no longer exist, so they can not be remeasured. Based on Marshall's notes, he traced the position of five-year growth and sometimes annual growth rings on paper and then measured the increment from the tracing with a ruler (to 0.0254 centimeter). The tree age recorded separately from the core tracings should be reliable.

Marshall's tree limit location descriptions have already been useful for planning research site locations and logistics. The tree core data is potentially useful for interpreting tree limit conditions. In the absence of physical evidence, mortality of tree limit trees (natural, caused by fire, etc.) in the last 60 years could be misinterpreted as an advancing tree limit if only young trees are found. Both Marshall's location descriptions and tree age data would be critical for realizing that mortality had occurred.

Location	Longitude (approximate)			Latitude		
Barronland Creek seedling plot	150°	30'	00"W	68°	00'	00"N
North Fork of the Koyukuk tree limit	150°	30'	00"W	67°	58'	30"N
Mouth of Ernie Creek	150°	50'	00"W	67°	50'	00"N
Ernie Creek tree limit	150°	50'	00"W	67°	58'	00"N
Hammond River tree limit	150°	11'	30"W	67°	55'	30"N
Clear River tree limit	150°	25'	00"W	67°	51'	30"N
Mouth of Kachwona Creek	150°	52'	00"W	67°	40'	00"N
Loon Lake tree limit	152°	40'	00"W	67°	57'	00"N
John River tree limit	152°	11'	00"W	67°	58'	00"N

Table 1. Proposed itinerary for August, 1990, in the central Brooks Range. (Additional sites not identified here may be selected while travelling between sites. A tree limit exists in many drainages, not just areas that Marshall sampled.)

Marshall's cores are also potentially important for interpreting tree movement over a considerable distance over the last 60 years. His data would provide information about the position and age of tree limit trees for comparison with newly collected cores at current tree limit. An advancement of more than a couple of miles may be prohibitive to sample given time and logistical constraints, so Marshall's location and age data would be essential for determining the extent of tree limit movement.

Data Collection

Marshall's recording of tree limit locations as well as more recent location information from quad maps will be used to arrange logistics to get to tree limit. Suitable aircraft (wheel or float planes are anticipated as available) will be used to locate tree limit from the air and to transport personnel and gear as close as possible to it. Substantial backpacking is anticipated as some of the locations are not close to landing areas.

Once a tree limit site has been located, the location will be recorded on quadrangle maps, a description will be recorded (location, slope, aspect, unique site characteristics) in the field journal and photographs will be taken. Starting with the last tree, tree cores will be extracted at (in the vicinity of) breast height and at the base from the cross-slope side of approximately twenty trees. Cores will be stored in labeled straws which will be stored in rigid containers.

Data Analysis

The goal is to link tree growth trends to temperature and precipitation trends. The historical data will be used to help interpret age and growth trends as described above. The data analysis will elicit the relationship between temperature, growth and tree limit movement. Specifically: (a) Are there temperature trends?; (b) Are there growth trends?; (c) Are there movement trends?; (d) Are there interactions?

The average monthly instrumented temperature and precipitation data from Bettles, Alaska (and other locations) will be plotted over time for the length of the record to see if any trends exist. A further breakdown using growing degree-days above 5°C or other temperature sums will be calculated. Adjusted temperature and precipitation using lapse-rate factors and interpolation may help account for the elevational and latitudinal differences between the temperature and precipitation at the sample sites and at the

instrumented sites.

Tree cores will be prepared, crossdated and measured using standard tree ring analyses. The age of tree limit trees will be determined from tree base cores and used to present the age structure in the vicinity of the tree limit. The age structure will indicate if trees have been advancing or stable. For example, if the age structure shows that trees at the tree limit are young and that maximum tree age increases in the vicinity south of the tree limit, the tree limit has advanced. If the age structure shows that the maximum tree age occurs at the tree limit, the tree limit has remained stable. The historical records will help clarify the age structure.

Growth indices and temperature and precipitation records will be analyzed for low-frequency trends. Growth indices will then be correlated with growing degree-day sums or other temperature sums and precipitation. Lev [1987] summarized average temperature and total precipitation into 73 five-day pentads throughout the year. Pentads are more flexible than monthly summaries. The pentads were combined into seasonal periods of flexible length based on the timing and the length of periods where tree growth was most strongly correlated with temperature and precipitation.

Gates of the Arctic National Park Support

National Park Service staff at Gates of the Arctic National Park and Preserve have expressed interest in the historical, educational and research aspects of this proposal. Logistical support and National Park Service employees will be provided to assist with travel and field work associated with the research. A research plan, a preliminary itinerary of tree limit field sites and a quality assurance plan for data collection and analysis will be completed for approval by the Environmental Protection Agency and the National Park Service before any work begins.

ACKNOWLEDGMENTS

The research described in this proposal has been funded by the U.S. Environmental Protection Agency (EPA). This document has been prepared at the EPA Environmental Research Laboratory in Corvallis, Oregon, through contract #68-C8-0006 to ManTech Environmental Technology, Inc. It has been subjected to the Agency's peer and administrative review and approved for publication. Mention of trade names or commercial products does not constitute endorsement or recommendation for use.

LITERATURE CITED

- Brown, W. E., *Gaunt Beauty . . . Tenuous Life*, National Park Service, Gates of the Arctic National Park, 1988.
- Cooper, D. J., Trees above and beyond tree limit in the Arrigetch Peaks region, Brooks Range, Alaska, *Arctic*, 39, 247-252, 1986.
- Densmore, D., Vegetation and forest dynamics of the upper Dietrich River Valley, Alaska, Master's Thesis, 183 pp., North Carolina State University, Raleigh, NC, 1980.
- Edwards, M. E., and P. W. Dunwiddie, Dendrochronological and palynological observations on *Populus balsamifera* in northern Alaska, U.S.A., *Arctic Alpine Res.*, 17, 271-278, 1985.
- Glover, J. M., *A Wilderness Original: The Life of Bob Marshall*, The Mountaineers, Seattle, 1986.
- Goldstein, G. H., Ecophysiological and demographic studies of white spruce (*Picea glauca* (Moench) Voss) at tree line in the central Brooks Range of Alaska, Ph.D. Thesis, 193 pp., University of Washington, Seattle, WA, 1981.
- Houghton, R. A., and G. M. Woodwell, Global climate change, *Scientific American*, 260, 36-44, 1989.
- Intergovernmental Panel on Climate Change (IPCC), Scientific assessment of climate change. Report for WGI Plenary Meeting, 1990.
- Jones, P. D., T. M. L. Wigley, and P. B. Wright, Global temperature variations between 1861 and 1984, *Nature*, 322, 430-434, 1986.
- Jones, P. D., T. M. L. Wigley, C. K. Folland, D. E. Parker, J. K. Angell, S. Lebedeff, and J. E. Hansen, Evidence for global warming in the past decade, *Nature*, 332, 790, 1988.
- Lachenbruch, A. H., and B. V. Marshall, Changing climate: Geothermal evidence from permafrost in the Alaskan Arctic, *Science*, 234, 689-696, 1986.
- Lev, D. J., Balsam poplar (*Populus balsamifera*) in Alaska: Ecology and growth response to climate, Master's Thesis, 69 pp., University of Washington, Seattle, WA, 1987.
- Marshall, R., *Arctic Village*, The Literary Guild, New York, 1933.
- Marshall, R., *Alaska Wilderness*, University of California Press, Berkeley and Los Angeles, 1970.
- Marshall, R., The Robert Marshall Papers. The Bancroft Library, University of California, Berkeley, 1979.
- Odasz, A. M., Vegetational patterns at the tree limit ecotone in the upper Alatna River Drainage of the Central Brooks Range, Alaska, Ph.D. Thesis, 224 pp., University of Colorado, Boulder, CO, 1983.
- Retzlaff, A., and R. Marshall, Journal of the exploration of the North Fork of the Koyukuk by Al Retzlaff and Bob Marshall, pp. 163-175, *The Frontier*, 1931.
- Wright, B., *Four Seasons North*, Harper and Row Publishers, San Francisco, 1973.
- Wright, S., A letter from the Arctic, *The Living Wilderness*, Spring, 4-6, 1969.
- Wright, S., *Koviashuvik*, Sierra Club Books, San Francisco, 1988.

USDA Forest Service Global Change Research: Monitored Ecosystems, Northern Linkages

D. V. Sandberg

Forestry Sciences Laboratory, Pacific Northwest Research Station, U.S.D.A. Forest Service, Seattle, Washington, U.S.A.

C. W. Slaughter

Institute of Northern Forestry, Pacific Northwest Research Station, U.S.D.A. Forest Service, Fairbanks, Alaska, U.S.A.

ABSTRACT

Foresters and natural resource managers have traditionally based long-term plans (i.e., 100+ year harvest cycles) on the assumption of stable landscapes and climate. Global climate change undercuts these assumptions and may alter or invalidate some accepted natural resource management practices and paradigms. Possible changes in biomass productivity, shifting of forest species' latitudinal or elevational limits, and rapid changes in forest community species and age class composition, all have major implications for management of the nation's forests.

The USDA Forest Service is undertaking a national research program to assess rates, significant processes, and management implications of possible climatic change for the nation's forests and related resources. Pacific Region Forest Service global change research places major emphasis on understanding and monitoring forest processes in the northern boreal forest and the sub-arctic taiga of Alaska, which is potentially "sensitive" to climatic warming and to shifts in precipitation regime. A major terrestrial carbon pool, taiga forests and organic soils may also be important in the flux of greenhouse gases between landscape and atmosphere.

Forest Service research emphasizes an ecosystem approach, incorporating landscape- and watershed-level field research with smaller-scale studies of forest ecosystem response mechanisms. Ecological monitoring is critical, and includes establishment of a monitoring mega-transect from northern latitudinal tree line to mediterranean/dry temperate forest/shrublands. Emphasis is placed on the most critical Pacific Region ecosystems: northern boreal forest (taiga), moist temperate forest, and mediterranean/dry temperate forest (chaparral/southern Ponderosa pine).

92-17826



AD-P007 322



Changes in the Source/Sink Relationships of the Alaskan Boreal Forest as a Result of Climatic Warming

J. Yarie and K. Van Cleve

Forest Soils Laboratory, University of Alaska Fairbanks, Fairbanks, Alaska, U.S.A.

ABSTRACT

A modified version of the LINKAGES ecosystem simulation model is used to access the changes in the role of forests in the interior of Alaska to act as a source or sink of carbon over a fifty-year period. The study area is the Tanana Valley State Forest (TVSF). The TVSF occupies an area of 5523 hectares along the Tanana River from the Canadian Border to the confluence of the Tanana River and the Yukon River.

The current inventory for the TVSF is used to develop a starting state for the model for ten vegetation classes. The model is run with the current climate until the current stand age for the various vegetation types is reached. Then a 5°C increase in mean annual temperature and a doubling in precipitation distributed evenly over the year is gradually added to the model.

The model was then used to develop an average estimate of the atmospheric carbon sequestering for the current vegetation distribution of the productive forest types in the TVSF. This value was estimated as 392 g m⁻² yr⁻¹ for a 490,000-hectare area of interior Alaska.

INTRODUCTION

The role of boreal forests in the global carbon cycle is unclear at this time. The boreal forest could either be a net source or sink for atmospheric CO₂. It has been suggested that the boreal forest could represent a large sink for atmospheric CO₂ [Tans et al., 1990]. Photosynthetic uptake by high arctic vegetation was thought to produce the large seasonal amplitude in atmospheric CO₂ measured at Barrow, Alaska [Peterson et al., 1986]. This uptake by the living plant material combined with the relatively slow decomposition rates found in the arctic and boreal forests [Flanagan and Van Cleve, 1983] could result in high latitude ecosystems acting as a net sink for atmospheric CO₂.

The problem of estimating the net effect of the boreal forest on the global carbon cycle becomes one of estimating the net uptake of carbon in vegetation, the release of carbon through decomposition, and the effect of periodic natural disturbance on the uptake/decomposition balance over large land areas. Direct estimates are not viable at this time; therefore ecosystem modeling approaches appear to be the best answer. These modeling approaches can then be applied to

the landscape which is derived from traditional forest inventories of the landscape in question.

Recent inventories of the vegetation of interior Alaska now give us the potential to start to develop precise estimates of the carbon budget over wide areas of the state. These inventories can be used to define the starting state of ecosystem models. By using actual inventories to define the starting state of the model we should be able to develop a more realistic estimate of the effect of global change on the carbon cycle for large land areas of the boreal forest. Recent forest inventories for interior Alaska have included the upper Yukon River drainage [Setzer, 1987], the Tanana River drainage [van Hees, 1984], and the Susitna River drainage [Setzer et al., 1984].

METHODS

The computer model LINKAGES2 [Pastor and Post, 1986] was used to estimate the change in carbon dynamics over a fifty-year period starting in approximately 1990 and ending in 2040. The starting climate of the model was set to the long-term average climate for Fairbanks. A linear

Forest Type	Size class	Current Age (years)	Ending Age (years)	Acreage (ha)	Carbon Balance*			
					1990 (Mg ha ⁻¹)	(Mg)	2040 (Mg ha ⁻¹)	(Mg)
White Spruce	Poletimber	70	120	21,909	1.2	26,291	1.0	21,909
	Sawtimber	150	200	12,182	1.1	13,400	0.8	9,746
Balsam Poplar/ White Spruce	Sapling	10	60	3,727	2.9	10,808	1.6	5,963
	Poletimber	50	100	12,545	10.5	131,722	-0.3	-3,764
	Sawtimber	125	175	3,591	1.6	5,746	-0.4	-2,298
Hardwood	Sapling	10	60	45,136	2.9	130,894	3.6	162,490
	Poletimber	75	125	115,045	2.6	299,117	-0.3	-34,514
Hardwood/ White Spruce	Sapling	10	60	111,545	2.5	278,862	3.4	379,253
	Poletimber	50	100	158,364	6.5	1,029,366	0.2	31,673
	Sawtimber	125	175	9,273	0.9	8,346	0.3	2,782
Totals				493,317		1,934,522		573,240
g C m ⁻²						392		116

*Positive values indicate a net uptake of carbon by the vegetation?

Table 1. Estimated Carbon Balance for Portions of the Tanana Valley State Forest in the years 1990 and 2040. These vegetation types represent 68% of the total forest area of 727,272 ha.

increase was applied to the mean annual temperature and total precipitation over the fifty-year period of the simulation. The climate was changed to represent a 5°C increase in mean annual temperature and a 100% increase in mean annual precipitation. The increase in temperature and precipitation was evenly distributed over the entire year.

LINKAGES2 was able to successfully reproduce stand development and current above-ground biomass, tree basal area, and foliage biomass for geographic regions in which the model was calibrated [Pastor and Post, 1986; Yarie, 1989]. This was accomplished by growing individual trees in relation to the environmental factors of light, moisture, temperature and nitrogen availability. Ecosystem carbon dynamics are then estimated by using a carbon concentration of 45% and applying it to the appropriate above-ground tree growth and decomposition processes.

The LINKAGES2 model currently does not estimate below-ground production. For the purposes of this analysis it was assumed that below-ground production was equal to above-ground production. This assumption has been shown to be generally applicable [Shipley, 1989].

The analysis reported here utilizes forest inventory statistics [State of Alaska, 1987] reported for the portion of the Tanana River drainage contained within the Tanana Valley State Forest (TVSF) to help define current vegetation structure and vegetation type distribution. Current vegetation structure was simulated to produce a stand of the appropriate age class (Table 1) prior to applying the climate change scenario. Ten vegetation classes were defined from the TVSF inventory report (Table 1). These ten classes represented 68% of the total area (727,272 ha) of the TVSF. The additional 32% was occupied by vegetation classes (Black Spruce (21.2%) and non-forest (10.8%)) that can not be adequately modeled by the current version of the LINKAGES2 model.

Fire was not included as a factor in the model runs. Although this restriction is unrealistic it was felt necessary because of our current inability to predict which vegetation types will burn over the next fifty years. The results will be discussed with regard to this restriction.

RESULTS

Changes in the carbon uptake and release are shown for the Hardwood/White Spruce Poletimber vegetation type in Figures 1 through 3. For this type the model was run for an initial 50 years to generate a hardwood-white spruce poletimber stand that could have developed over the past fifty years. This same procedure was followed for all of the vegetation types with climate change occurring at the current stand age (Table 1). The climate change scenario was applied over the fifty-year period from year 50 to 100. If root production is ignored, at stand age 70 this vegetation type switches from being a carbon sink to a carbon source (Figure 1). If root production is assumed to be equal to shoot production then this vegetation type is always a carbon sink (Figure 2). The importance of obtaining good estimates of root production can be seen from this analysis.

The carbon balance for the total area under study is calculated in Table 1. It is estimated that almost 2×10^{12} g of carbon will be removed from the atmosphere in 1990 over a land area of 493,300 ha in interior Alaska. This is equivalent to 392 g m⁻². As these systems age this figure drops to 116 g m⁻² in the year 2040 or a total of 6×10^{11} g of carbon in 2040. This later estimate represents an underestimate of the potential uptake by vegetation from the atmosphere because some of these systems will burn and revert back to a more productive state.

Stand development from 10 years following disturbance to stand age 60, with climate change included during this period, is shown in Table 2. The model predicts that at ten

HARDWOOD/WHITE SPRUCE POLETIMBER ABOVEGROUND BIOMASS ONLY

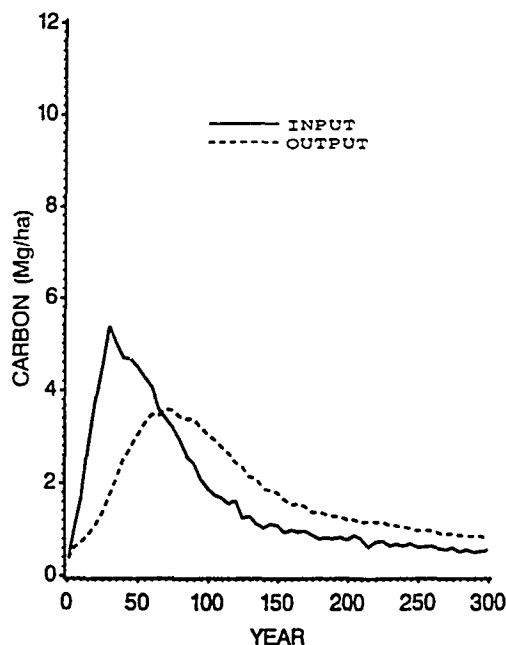


Figure 1. Net uptake of carbon by the above-ground vegetation (Input) and carbon release through decomposition (Output) for the hardwood/white spruce poletimber vegetation class. Climate change started in year 50 and ended in year 100. When input exceeds output the ecosystem acts as a sink for atmospheric carbon and when output exceeds input the ecosystem acts as a source for atmospheric carbon.

years following disturbance the Hardwood Sapling vegetation class will already be sequestering $2.5 \text{ Mg ha}^{-1} \text{ yr}^{-1}$ of atmospheric carbon. This sink goes to a maximum of almost $10 \text{ Mg ha}^{-1} \text{ yr}^{-1}$ at stand age 30 before dropping to $3.4 \text{ Mg ha}^{-1} \text{ yr}^{-1}$ at age 60. So for the first 60 years after disturbance this vegetation type acts as a net sink for atmospheric CO_2 .

DISCUSSION

The TVSF was not selected because it is typical of the interior of Alaska, but because inventory statistics were available for a relatively large land area. The black spruce vegetation type is under-represented in the forest and was not included in this modeling scenario. When compared to other forest types, black spruce sites pose more difficult problems in trying to predict the effects of climate change with potential vegetation type changes and significantly more complicated soil dynamics. This analysis can then only be considered to be representative of the more productive vegetation types within the interior of Alaska.

The importance of obtaining a good estimate of root production is obvious (Figures 1 and 2). Depending on the value assigned for below-ground productivity, the boreal forest can be shown to be either a source or sink for atmospheric carbon. For example in the case of the Hardwood/White Spruce Poletimber vegetation type a 15% reduction in the amount of root production results in this vegetation type switching from a net sink to a source for CO_2 at stand age 100.

Table 1 does not present the total accumulation of carbon over the fifty-year period but simply indicates the annual carbon balance for two specific years in the development of

HARDWOOD/WHITE SPRUCE POLETIMBER INCLUDING ROOT PRODUCTION

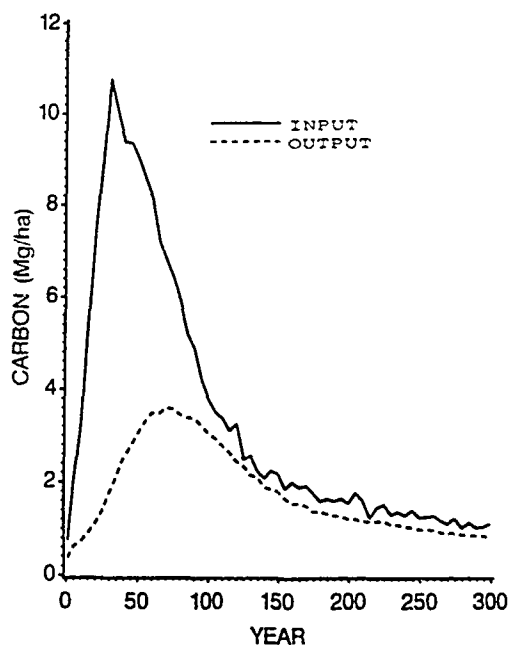


Figure 2. Net uptake of carbon by the above- and below-ground vegetation (Input) and carbon release through decomposition (Output) for the hardwood/white spruce poletimber vegetation class. Below-ground production was estimated as equal to above-ground production. Climate change started in year 50 and ended in year 100. When input exceeds output the ecosystem acts as a sink for atmospheric carbon and when output exceeds input the ecosystem acts as a source for atmospheric carbon.

Year	Carbon Balance (Mg ha^{-1})*
10	2.5
15	4.6
20	6.4
25	7.3
30	9.9
35	9.3
40	7.6
45	6.3
50	6.5
55	4.6
60	3.4

*A positive number indicates net uptake of atmospheric carbon by the ecosystem.

Table 2. Ecosystem carbon balance for the Hardwood/White Spruce Sapling Vegetation Class from age 10 (1990) to age 60 (2040).

these stands. The sapling size classes will accumulate much more carbon at the peak of the growth curve than indicated in Table 1. Table 2 shows the carbon balance values over the fifty-year period of interest for the Hardwood/White Spruce sapling vegetation class. From year 10 to 60 the average yearly balance is 620 g m^{-2} , almost two times higher than indicated for the two yearly estimates presented

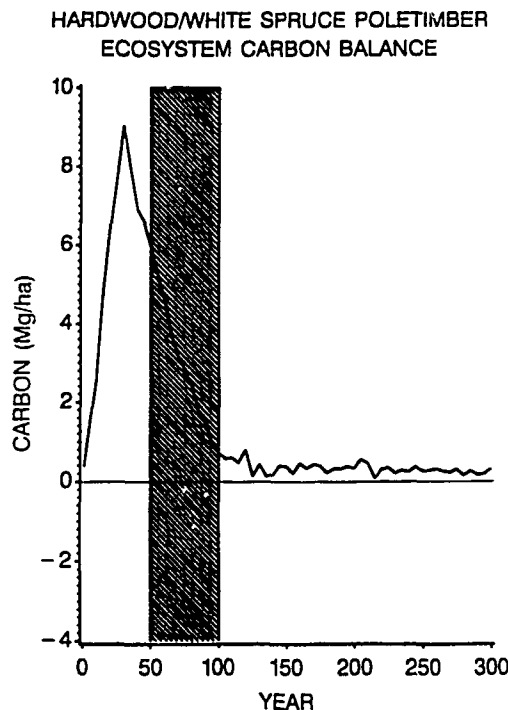


Figure 3. The ecosystem carbon balance (Input-Output from Figure 2) for the hardwood/white spruce poletimber vegetation class. Climate change begins in year 50 (1990) and ends in year 100 (2040), the shaded area. This vegetation type is a sink for atmospheric carbon for the next fifty years.

in Table 1. At the peak growth phase of this vegetation type it will capture almost $10 \text{ Mg ha}^{-1} \text{ yr}^{-1}$. The other two vegetation types that represent approximately 100% of the study area will capture about $6.5 \text{ Mg ha}^{-1} \text{ yr}^{-1}$ at age 50 for the Hardwood/White Spruce vegetation class and $2.5 \text{ Mg ha}^{-1} \text{ yr}^{-1}$ for the Hardwood poletimber vegetation class at year 75. The three sapling size class vegetation types will capture approximately 9 to $10 \text{ Mg ha}^{-1} \text{ yr}^{-1}$ 25 to 30 years after disturbance. These values represent a substantial sink for CO_2 in young developing vegetation types.

The effect of disturbance should be a positive one from the standpoint of carbon balance. A fire will not completely transform all standing carbon stores to a gaseous state. In fact the large majority of live standing carbon stores will remain on the site after disturbance. It is relatively rare that the tree boles will be destroyed in a fire, and the destruction of the forest floor will also be patchy.

The current area occupied by sapling size class types is 33% of the forest area (Table 1). Another 20% of the area is classified as black spruce sapling which was not included in this analysis. This percentage of the area represented by sapling size classes can be considered to be representative of the long-term fire-dominated age structure of the landscape. These values are also consistent with the age structure of other large areas of land within the interior of Alaska [Yarie, 1981]. The yearly estimates of carbon sequestering for the sapling size class of the modeled vegetation types is estimated to be close to 500 to 600 g m^{-2} . A true landscape average may be slightly lower than this value when black spruce types are included, but burning a black spruce type will result in an increase in CO_2 capture for that type by moving back in succession to a hardwood-dominated stage. Decomposition will increase some but still be primarily limited by the organic matter chemistry. Therefore old black spruce systems may be very close to at balance with the environment and have no effect on atmospheric CO_2 .

CONCLUSIONS

A modeling analysis was performed for a landscape area equal to 493,317 hectares of productive forest in interior Alaska. The analysis indicates that over the next fifty years, assuming a climate change of 5°C increase in mean annual temperature and a doubling in precipitation evenly dispersed over the year, the average rate of carbon sequestering by the vegetation should be between 392 and $116 \text{ g m}^{-2} \text{ yr}^{-1}$. The actual value should be closer to the upper limit reported here when the effect of periodic burning is considered.

LITERATURE CITED

- Flanagan, P. W., and K. Van Cleve, Nutrient cycling in relation to decomposition and organic-matter quality in taiga ecosystems, *Can. J. For. Res.*, 13, 795-817, 1983.
- van Hees, W. S., Timber resource statistics for the Tanana inventory unit, Alaska 1971-75, *Resource Bulletin PNW-109*, 36 pp., U.S. Department of Agriculture, Forest Service, Pacific Northwest Forest and Range Experiment Station, 1984.
- Pastor, J., and W. M. Post, Influence of climate, soil moisture, and succession on forest carbon and nitrogen cycles, *Biogeochemistry*, 2, 3-27, 1986.
- Peterson, J. P., W. D. Komhyr, L. S. Waterman, R. H. Gammon, K. W. Thorning, and T. J. Conway, Atmospheric CO_2 variations at Barrow, Alaska, 1973-1982, *J. Geophys. Res.*, 88, 3599-3608, 1986.
- Setzer, T. S., Timber resource statistics for the Porcupine Inventory Unit of Alaska, 1978, *Resource Bulletin PNW-RB-141*, 32 pp., U.S. Department of Agriculture, Forest Service, 1987.
- Setzer, T. S., G. L. Carroll, and B. R. Mead, Timber resource statistics for the Talkeetna Block, Susitna River Basin Multiresource Inventory Unit, Alaska, 1979, *Resource Bulletin PNW-115*, 47 pp., U.S. Department of Agriculture, Forest Service, 1984.
- Shipley, B., The use of above-ground maximum relative growth rate as an accurate predictor of whole-plant maximum relative growth rate, *Functional Ecology*, 3, 771-775, 1989.
- State of Alaska, *Tanana valley state forest; forest management plan - resource analysis*, 312 pp., Division of Forestry, Alaska Department of Natural Resources, 1987.
- Tans, P. P., I. Y. Fung, and T. Takahashi, Observational constraints on the global atmospheric CO_2 budget, *Science*, 247, 1431-1438, 1990.
- Yarie, J., Forest fire cycles and life tables: a case study from interior Alaska, *Can. J. Forest Research*, 11, 554-562, 1981.
- Yarie, J., A comparison of the nutritional consequences of intensive forest harvesting in Alaskan Taiga Forests as predicted by FORCTYE-10 and LINKAGES2, *IEA/BE Project A6 Report No. 1*, 59 pp., New Zealand Forest Research Institute, Rotorua, New Zealand, 1989.

AD-P007 323



Holocene Meltwater Variations Recorded in Antarctic Coastal Marine Benthic Assemblages

Paul Arthur Berkman

Byrd Polar Research Center, The Ohio State University, Columbus, Ohio, U.S.A.

ABSTRACT

Climate changes can influence the input of meltwater from the polar ice sheets. In Antarctica, signatures of meltwater input during the Holocene may be recorded in the benthic fossils which exist at similar altitudes above sea level in emerged beaches around the continent. Interpreting the fossils as meltwater proxy records would be enhanced by understanding the modern ecology of the species in adjacent marine environments. Characteristics of an extant scallop assemblage in West McMurdo Sound, Antarctica, have been evaluated across a summer meltwater gradient to provide examples of meltwater records that may be contained in proximal scallop fossils. Integrating environmental proxies from coastal benthic assemblages around Antarctica, over ecological and geological time scales, is a necessary step in evaluating the marginal responses of the ice sheets to climate changes during the Holocene.

INTRODUCTION

During the last 10,000 years ("the Holocene") the Antarctic ice sheet margins have retreated around the continent. In West Antarctica, the George VI Ice Shelf and Ross Ice Shelf retreated until 6000 years B.P. [Clapperton and Sugden, 1982; Denton et al., 1989]. In East Antarctica, the ice sheet along Wilkes Land also retreated during the middle Holocene [Domack et al., 1991]. The above ice sheet retreats could have been influenced by warmer temperatures in Antarctica, as suggested by the relatively negative $\delta^{18}\text{O}$ values recorded around 6000 years B.P. in the Dome C ice core from West Antarctica [Lorius et al., 1979].

This warming period that may have influenced the Antarctic ice sheets is thought to have been a global "climatic optimum" in the Holocene [Imbrie and Imbrie, 1979; Robin, 1983; Grove, 1988]. Although the impact of Holocene climate changes on the Antarctic ice sheets would be difficult to detect from the volume of meltwater in the Southern Ocean [Labeyrie et al., 1986], there may have been meltwater pulses along the continental margins that could be used to interpret ice sheet variations. The purpose of this paper is to consider a database that has yet to be developed to assess Antarctic ice sheet marginal melting during the last 10,000 years.

FOSSIL BENTHIC SPECIES IN AN EMERGED HOLOCENE COASTAL TERRACE AROUND ANTARCTICA

Fossil deposits in emerged Antarctic beaches have been recognized since the beginning of this century [David and Priestly, 1914] and have been used mainly for interpreting the emergence of coastal areas around the continent. Radiocarbon ages of these fossils have been derived from vertebrate species which are known to migrate onto land [Cameron and Goldthwait, 1961; Nichols, 1968], and species that are restricted to the marine environment (Table 1), primarily the bivalve molluscs *Adamussium colbecki* and *Laternula elliptica*. This latter group of species provide more accurate temporal constraints on beach emergence because their ranges are limited by sea level.

There are difficulties associated with correcting the "old" age of the radiocarbon reservoir in the Southern Ocean [Stuiver et al., 1981; Omoto, 1983; Domack et al., 1989]. There also are gross tectonic differences that exist around Antarctica [Craddock, 1972]. Because of these reasons, fossils in Antarctic beaches only have been interpreted regionally [Clapperton and Sugden, 1982; Yoshida, 1983; Adamson and Pickard, 1986; Denton et al., 1989]. The circumpolar distribution of the fossils (Table 1), however, may

Location	Height ¹ (m)	Age ² (¹⁴ C yr B.P.)	Reference
King George Island (62°S, 58°W)	3.5	8790-9670	Shotton et al., 1969
Antarctic Peninsula (72°S, 68°W)	---	6930-7200	Clapperton and Sugden, 1982
Syowa Coast (69°S, 39°E)	0.8-15	1450-10250	Omoto, 1977
Syowa Coast (69°S, 39°E)	0.8-15	2040-8370	Yoshida, 1983
Vestfold Hills (68°S, 78°E)	---	2410-7000	Adamson and Pickard, 1983
Vestfold Hills (68°S, 78°E)	3-15	3500-6000	Zhang and Peterson, 1984
Explorers Cove (77°S, 163°E)	0.5-8.1	4620-6350	Stuiver et al., 1981
Terra Nova Bay (74°S, 163°E)	---	7020	Stuiver et al., 1981
Terra Nova Bay (74°S, 163°E)	0.2-37	1840-6815	Baroni and Orombelli, 1989

Table 1. Emerged Holocene beach sites around Antarctica.

¹Dashes indicate no beach height measurements were made.

²Uncorrected radiocarbon ages determined from marine benthic invertebrate fossils in the emerged beaches (primarily the bivalves *Adamussium colbecki* and *Laternula elliptica* along with other molluscs, barnacles and calcareous worm tubes).

Location	Bivalve Densities ¹		Reference
	<i>A. colbecki</i> (# m ⁻²)	<i>L. elliptica</i> (# m ⁻²)	
Antarctic Peninsula (72°S, 68°W)	---	75	Stout and Shabica, 1970
Syowa Coast (69°S, 39°E)	112	---	Nakajima et al., 1982
Kerguelen Island (49°S, 68°E)	---	140	Beurois, 1987
Vestfold Hills (78°S, 68°E)	several	---	Tucker and Burton, 1987
Terra Nova Bay (74°S, 163°E)	10	---	Taviani and Amato, 1989
Explorers Cove (77°S, 163°E)	90	---	Stockton, 1984
Explorers Cove (77°S, 163°E)	55	---	Berkman, 1990

Table 2. Extant bivalve mollusc densities around Antarctica.

¹Dashes indicate no measurements were made.

provide a framework for assessing ice sheet marginal melting around the continent associated with climate changes during the Holocene.

ECOLOGY OF AN EXTANT SCALLOP POPULATION IN AN ANTARCTIC NEARSHORE MARINE ENVIRONMENT

Adjacent to fossil assemblages in the emerged beaches there are extant benthic assemblages which contain the same species, such as *Adamussium colbecki* and *Laternula elliptica* (Table 2). Explorers Cove (Figure 1), at the base of Taylor Valley in west McMurdo Sound, is a model habitat where *A. colbecki* occurs as a living population in the near-shore (less than 30 meters depth) marine environment and as fossils in the surrounding beaches.

During the summer, meltwater from the sea ice and nearby glaciers creates a buoyant hyposaline lens at Explorers Cove that extends 5 to 10 meters [Berkman, 1988]. Isolated measurements in this meltwater lens indicate that it has a salinity of 1.5 ‰ [Jackson et al., 1979] and temperature of -0.2°C [Stockton, 1984] in contrast to the underlying seawater which was 34.2 ‰ and -1.8°C.

Adamussium colbecki, the Antarctic scallop, was collected from above and below the hyposaline lens at Explorers Cove from 3 to 27 meters during the 1986-87 austral summer [Berkman, 1988, 1990]. These scallops provide information on the impacts of meltwater on nearshore polar benthic assemblages.

Scallop Population Characteristics

In general, scallop densities were higher and small scallops (<40 mm in shell height) were absent above 10 meters (Table 3a). A multiple discriminant analysis [Pielou, 1977] was used to reduce these data and to expose mutual relationships of the scallops at different depths.

This multivariate statistical technique is based on a data set composed of n variables and m measurements that is transformed into a new set of $k \leq n$ linearly independent and additive equations (discriminant functions) which can be used for classifying the measurements into groups [Green, 1971]. The A discriminant functions are created by subtracting the λ eigenvalues across the main diagonal of the B original variable vectors such that $A - \lambda B = 0$ [Strang, 1980]. Each of the discriminant functions is approximately distributed as a chi-square [Rao, 1952] and the first discriminant function is inclined in the direction which describes the greatest variability in the data set [Buzas, 1971].

The multiple discriminant model (Table 3b) of the scallop density and size variables in Table 3a was generated on an IBM-compatible personal computer with software developed by Statgraphics Inc. The relative contributions of the coefficients (variables) in the four discriminant functions are shown in Table 3c. This model indicates that there were two distinct scallop groups above and below 10 to 15 meters depth (Figure 2).

A corresponding depth change in the proportion of scallops (>65 mm in shell height) with epizootic macrofaunal species on their shells also was observed above 10 meters (Figure 3). This depth distribution of the epizootic species at Explorers Cove, including byssally attached small scallops which developed from planktotrophic larvae [Berkman et al., 1991], may have been influenced by hydrochemical gra-

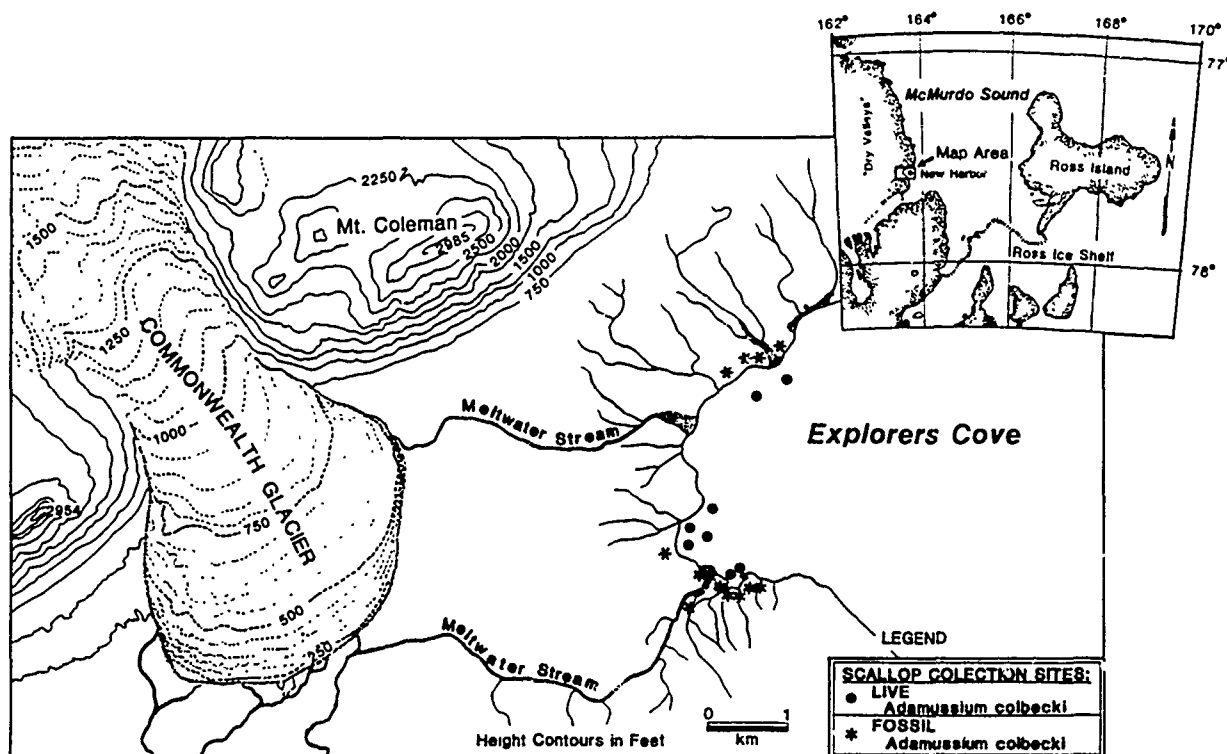


Figure 1. Modern and fossil scallop collections sites in Explorers Cove at the base of the Dry Valleys in West McMurdo Sound, Antarctica.

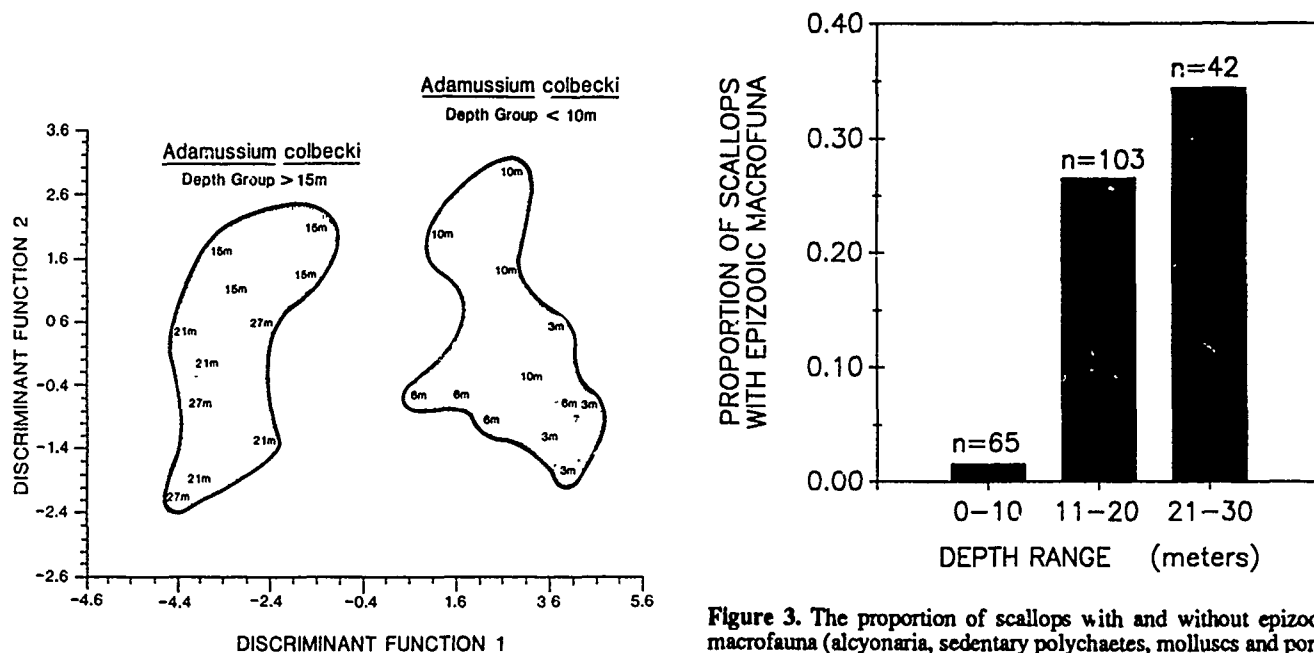


Figure 2. Multiple discriminant analysis of the scallop density and size variables (Table 3a) showing two distinct depth groups relative to discriminant function 1 which accounted for 82% of the variability in the data set. Together, discriminant functions 1 and 2 accounted for 92% of the variability with greater than 0.005% probability (Table 3b).

Figure 3. The proportion of scallops with and without epizooic macrofauna (alcyonaria, sedentary polychaetes, molluscs and porifera) from different depth ranges in the nearshore region at Explorers Cove, Antarctica, during January 1987. Between 11 to 20 meters and 21 to 30 meters depth, the occurrence of epizooic macrofauna on scallops was not significantly different ($X^2 = 3.4$, N.S.). However, compared to 0 to 10 meters, epizooic macrofauna were significantly more common at either 11 to 20 meters ($X^2 = 29.2$, $p < 0.001$) or 21 to 30 meters depth ($X^2 = 16.8$, $p < 0.001$).

Depth (m)	Density (# m ⁻²)	Mean (mm)	SIZE VARIABLES	
			Skewness (mm)	Range (mm)
3	40	74.0	-0.39	38.3 (53.4 - 91.7)
3	49	74.8	-1.42	51.0 (40.5 - 91.5)
3	37	74.2	-0.04	27.8 (61.2 - 89.0)
3	42	74.8	-0.67	36.1 (52.2 - 88.3)
6	36	80.3	-0.24	28.9 (63.4 - 92.3)
6	23	71.6	-0.80	46.6 (45.0 - 91.6)
6	27	76.8	-0.27	35.3 (57.2 - 92.5)
6	20	73.7	-0.70	33.1 (51.4 - 84.5)
10	8	76.4	-1.64	19.1 (63.5 - 82.6)
10	55	73.4	-2.90	76.7 (9.8 - 86.5)
10	44	74.4	-0.90	49.7 (42.8 - 92.5)
10	32	69.4	-2.54	80.9 (7.5 - 88.4)
15	24	69.4	-2.17	93.5 (4.0 - 97.5)
15	24	69.8	-1.80	87.6 (5.9 - 93.5)
15	38	69.2	-2.03	89.4 (4.3 - 93.7)
15	26	70.8	-2.36	78.5 (9.1 - 87.6)
21	19	64.6	-1.77	88.8 (4.5 - 93.3)
21	23	65.1	-1.45	87.1 (5.4 - 92.5)
21	28	59.4	-1.25	79.8 (6.6 - 86.4)
21	14	57.3	-0.97	76.9 (6.5 - 83.4)
27	24	64.8	-1.89	44.0 (42.7 - 86.7)
27	22	62.6	-1.26	59.0 (23.5 - 82.5)
27	20	55.7	-0.89	84.6 (5.4 - 90.0)
27	0		(zero scallops)	

Table 3a. *Adamussium colbecki* density and size characteristics at Explorers Cove, Antarctica, during 1986/1987.

Discriminant Function	Eigenvalue	Cumulative Percentage of Discrimination	X ²	D.F.	Probability
1	13.2965	82.07	76.91	20	<0.001
2	1.5876	91.87	31.69	12	<0.002
3	1.1657	99.07	15.53	6	<0.017
4	0.1512	100.00	2.39	2	<0.302

Table 3b. Multiple discriminant analysis of variables in Table 3a.

Coefficients	Discriminant Functions			
	1	2	3	4
Mean Size	0.18	-0.39	1.03	0.19
Size Range	-1.58	-0.09	1.19	0.71
Size Skewness	-0.40	-0.88	0.85	0.57
Scallop Density	1.27	-0.09	-0.83	0.57

Table 3c. Coefficients in the multiple discriminant model.

dients that inhibited their larval survival in shallow water.

The absence of small scallops and rarity of epizooic species, along with the transition between scallop depth groups above 10 meters, is reminiscent of a physical boundary influencing nearshore benthic zonation. In east McMurdo Sound, for example, the marked zonation of species in shallow water has been related to the presence of anchor ice [Dayton et al., 1969, 1970] which may vary over decadal time scales [Dayton, 1989]. Temperature-salinity gradients also can influence benthic zonation, as has been observed in estuaries [Carriker, 1951], fjords [Fleming, 1950] and the Arctic [Andersen et al., 1977; Kautsky, 1982]. If the melt-

water lens at Explorers Cove was influencing the nearshore benthic zonation in the mobile scallop population, then there may be corresponding physical-chemical differences in the scallops themselves.

Scallop Shell Growth Chronologies

Invertebrate growth chronologies, particularly in bivalve shells, produce patterns that can be interpreted in relation to environmental variation [Rosenberg, 1980; Lutz and Rhoads, 1980]. These growth chronologies also may be preserved in fossil bivalves, as has been observed in the Arctic [Andrews, 1971]. For these reasons, it is fortuitous that the bivalves *Adamussium colbecki* and *Lacuna elliptica* are the most common macrofossils in the emerged beaches around Antarctica (Table 1).

Seasonal shell growth patterns in *A. colbecki* from Explorers Cove indicate individuals that are 100 mm in shell height live about 12 years [Berkman, 1990]. These scallops grow faster during the summer than winter, and in each season there are approximately 12 smaller shell bands (Figure 4). These intra-seasonal shell bands may coincide with a bimonthly physical phenomenon, such as the fortnightly tidal cycle which has been observed around the continent [Robinson et al., 1975; Lutjeharms et al., 1985]. The intra-seasonal shell bands, which may be less than 100 mm in width during the winter (Figure 4), also can be resolved in fossil scallops from adjacent emerged beaches (Figure 5).

Scallop growth rate changes could be calculated as the first derivative of the exponential growth curve [Jones 1981; Equation 1]:

$$dy/dt = ae^{-kt} \quad (1)$$

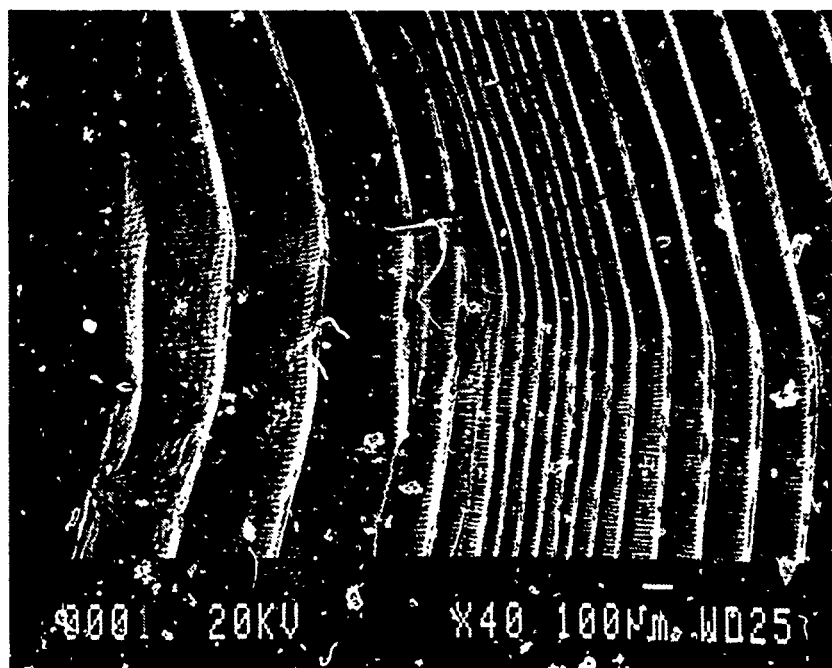


Figure 4. External summer (wide) and winter (narrow) shell growth bands from the Antarctic scallop, *Adamussium colbecki*, imaged with a JEOL JSM-820 scanning Electron Microscope.

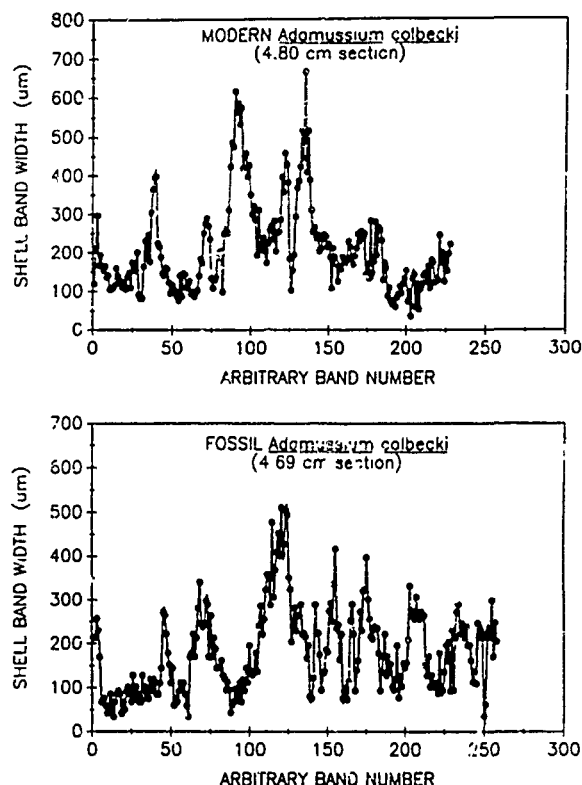


Figure 5. Resolution of shell-bands digitized across arbitrary sections of a modern shell from the nearshore marine environment and a fossil shell from the adjacent beach at Explorers Cove, Antarctica, based on JEOL JSM-820 Scanning Electron Microscope images.

where t is the time in years, y is the shell height, c is the base of the natural logarithm, k is a constant determined by curve fitting, and $a = ky_{\max}$ where y_{\max} is the maximum shell height. Studying shell growth chronologies may provide a basis for comparing inter-annual and intra-annual growth variability in nearshore environments around Antarctica during different periods in the Holocene.

Scallop Shell Composition

Preliminary crystalline and compositional characteristics of scallops from Explorers Cove have been determined to provide a basis for interpreting the elemental composition of the adjacent fossils in relation to meltwater variation. Shells (75 ± 5 mm in shell height) were scrubbed with a brush and all remaining epizooic species (such as foraminifera, bryozoans and barnacles) were scraped from the shell surface using a clean scalpel. The shells were then ultrasonicated in double distilled demineralized water. The samples were cut by a diamond surface low-speed rotary saw into 1-cm² fragments that then were systematically ground for several hours by an eccentric sliding disc mill. Each bulk shell sample provided approximately 4 cm³ of fine grained homogenized powder for analysis.

X-ray diffraction records of the shell crystalline characteristics were produced using a Philips 1316/90 goniometer with an XRG 3100 generator operating at 35 kV and 15 Ma with a Ni-filtered copper target [Berkman et al., In review]. Atomic absorption analysis of the shell compositional characteristics was produced on the Perkin-Elmer 1100B atomic absorption spectrophotometer with samples that had been acid digested according to United States Environmental Protection Agency SW846, Method 3050 (Springfield Environmental Inc., R. Liptak). Coulometric

analyses of the carbon phases in the Antarctic scallop shell were based on the CO₂ evolved during acid digestion (inorganic carbon phase) and ashing with a muffle furnace at 950°C (total carbon). The evolved CO₂ gas then was analyzed with the Model 5011 CO₂ Coulometer (Coulometrics, Inc.).

The crystalline characteristics of the Antarctic scallop shells are shown in Table 4a. Based on a comparison with a standard synthetic calcite specimen, which has unit cell dimensions of 4.9898 Å and 17.062 Å [Swanson and Fuyat, 1953], the principal carbonate phase of the Antarctic scallop shell was determined to be calcite. However, the larger average size of the unit cells in the Antarctic scallop suggests limited isomorphous substitution in the calcite lattice by cations with ionic radii larger than calcium [Berkman et al., In review]. As opposed to the interstitial spaces, the elements within the unit cells would be in the most stable positions in the calcite matrix. In addition, calcite itself is relatively stable over time compared to other carbonate phases such as aragonite [Lowenstam, 1954].

The coulometric analyses indicate that $11.5 \pm 0.2\%$ ($n = 24$) of the Antarctic scallop shell was carbon with organic carbon concentrations that were not detectable within the 0.3% precision limits of the analyses. The low organic carbon concentrations in the calcitic shells of modern Antarctic scallops suggest that shell decomposition would be minimal and that elemental signatures of environmental variation may be preserved in the shells of fossil scallops which occur in adjacent beaches.

The trace element characteristics of modern shells from Explorers Cove tended to decrease with depth (Table 4b), which would support the suggestion that there were physical-chemical gradients in the nearshore environment at

Unit Cell Axial Dimensions	Crystallite Diameter	Percent Calcite
a (Å)	c (Å)	(μm)
5.008 ± 0.008	17.14 ± 0.02	1.62 ± 0.03
		95.8 ± 2.5

Table 4a. Antarctic Scallop Shell Crystalline Characteristics from the Nearshore Environment at Explorers Cove (\pm Standard Error; $n = 6$).

Element	6 meters (ppm)	DEPTH	
		10 meters (ppm)	21 meters (ppm)
Iron	190.7 ± 41.2	75.4 ± 15.2	39.9 ± 0.9
Manganese	34.9 ± 7.2	18.1 ± 3.2	12.4 ± 1.0
Copper	12.1 ± 2.3	9.2 ± 0.3	7.8 ± 0.2
Zinc	7.0 ± 1.8	4.8 ± 0.5	3.0 ± 0.1
Lead	2.6 ± 0.1	6.7 ± 1.0	4.6 ± 0.6
Nickel	1.2 ± 0.1	2.7 ± 0.4	1.9 ± 0.2
Cadmium	0.3 ± 0.1	0.7 ± 0.1	0.5 ± 0.1

Table 4b. Antarctic Scallop Shell Elemental Composition from the Nearshore Environment at Explorers Cove (\pm Standard Error; $n = 8$).

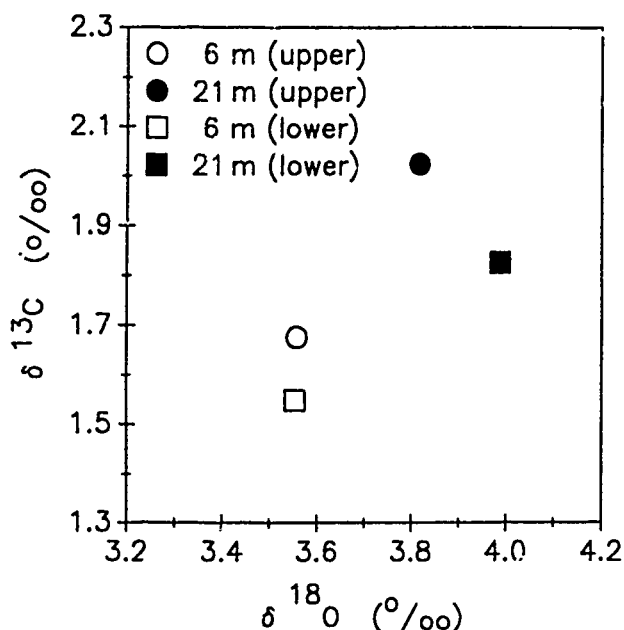


Figure 6. Carbon and oxygen isotopic values from homogenized samples of the outermost summer shell-band in the upper and lower shell valves of the Antarctic scallop, *Adamussium colbecki*, from 6 and 21 meters depth at Explorers Cove. These analyses were conducted in the laboratory of R. G. Fairbanks (Lamont-Doherty Geological Observatory) with a precision of ± 0.05 ‰ for the oxygen and ± 0.03 ‰ for the carbon isotopes ($n=13$).

Explorers Cove that were impacting the scallops. Further analysis of the elemental constituents across the growing margins of the shell with energy dispersive or wavelength dispersive spectrometry would complement the growth analyses and provide further resolution on inter-annual and intra-annual environmental variations.

Direct evidence for interpreting temperature and salinity variations may be reflected in the ratio of $^{18}\text{O}/^{16}\text{O}$ and $^{13}\text{C}/^{12}\text{C}$ in the shell carbonate of the scallops [Eisma et al., 1976]. However, unlike the $\delta^{18}\text{O}$ values which appear to be in equilibrium with the environment [Baroni et al., 1989; Barrera et al., 1990], the $\delta^{13}\text{C}$ values may be more difficult

to interpret because carbon is not incorporated in isotopic equilibrium [Broecker and Peng, 1982].

Oxygen and carbon isotopic values, based on homogenized samples of the outermost shell-bands from tagged scallops at Explorers Cove [Berkman, 1990], have been determined (Figure 6) and were similar to those reported for the shell margin by Barrera et al. [1990]. The relatively negative $\delta^{18}\text{O}$ values in the scallop at 6 meters suggests that it was exposed to warmer and fresher water than the scallop at 21 meters depth. As a preliminary paleoenvironmental interpretation, it has been suggested that $\delta^{18}\text{O}$ values from fossil scallops at Terra Nova Bay, Antarctica, reflect the impact of the climatic optimum during the middle Holocene [Baroni et al., 1989].

CONCLUSIONS

Meltwater introduced along the margins of the Antarctic ice sheets impacts nearshore marine benthic assemblages. The input of meltwater today, in areas such as Explorers Cove (Figure 7), is analogous to the influx of meltwater during periods of climate warming earlier in the Holocene.

Population, structural and compositional characteristics of the Antarctic scallop are examples of biological records that could be used for interpreting meltwater impacts. The presence of living and adjacent fossil benthic assemblages in coastal areas around Antarctica (Tables 1 and 2) provides a foundation for interpreting these biological records in relation to continent-wide meltwater variations during the last 10,000 years.

Integrating environmental proxies from coastal benthic assemblages in the polar regions, over ecological and geological time scales, can be used to assess the responses of the ice sheets to climate changes. This type of integration of biology and geology is necessary in developing international climate research efforts, such as the International Geosphere-Biosphere Program.

ACKNOWLEDGMENTS

I would like to thank R. G. Fairbanks for providing the isotope analyses and R. Liptak for providing the trace element analyses. I also would like to thank J. C. Nagy for his assistance with the illustrations. This research was generously supported by the Byrd Fellowship from the Byrd Polar Research Center at The Ohio State University (contribution 731).

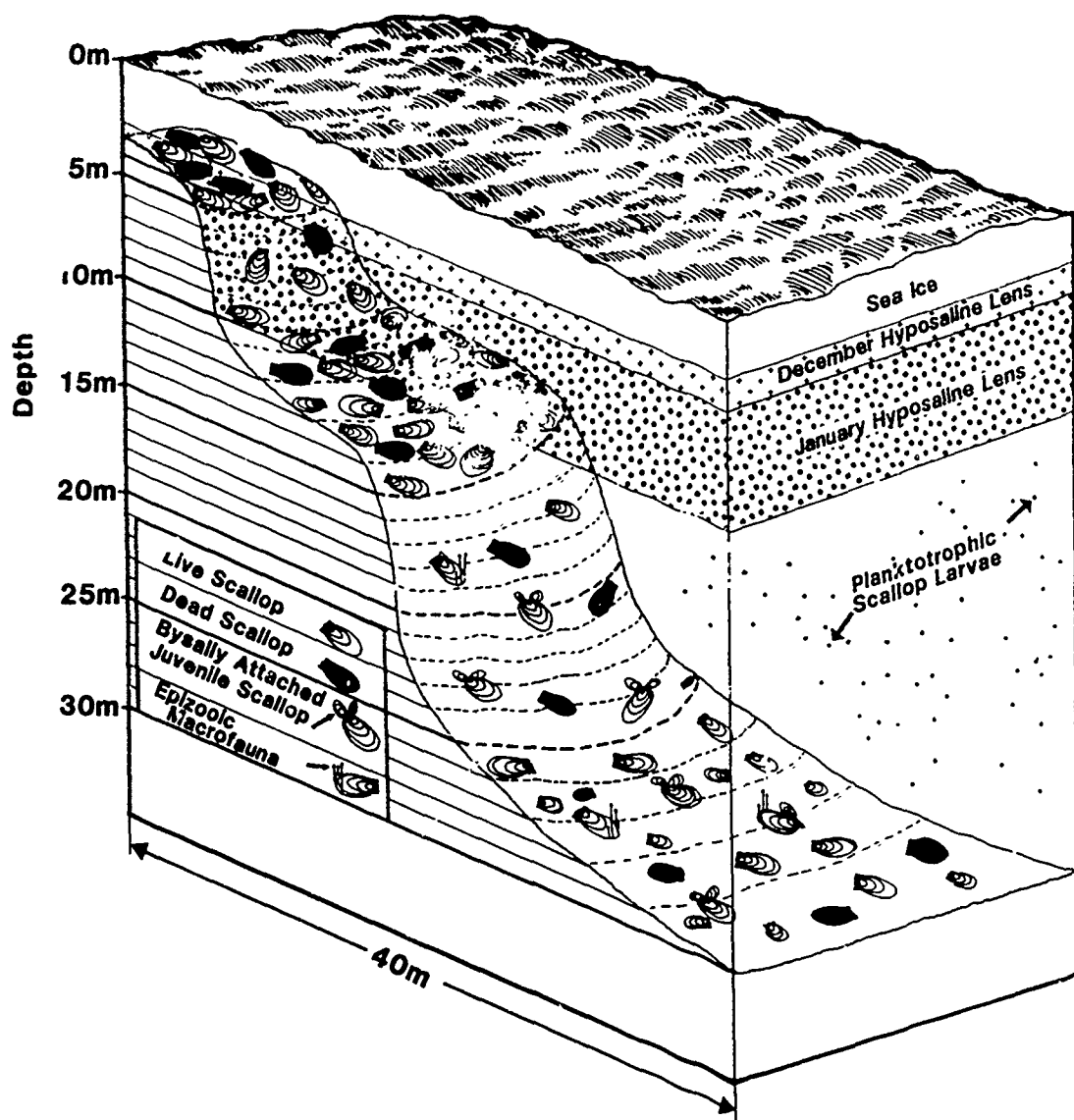


Figure 7. Summary illustration of possible hydrochemical impacts on a nearshore scallop population across the slope-bench topography at Explorers Cove caused by the stratification of relatively warm and fresh meltwater introduced from the sea ice and glaciers in the adjacent Dry Valleys. Only large scallops were encountered in and above the meltwater lens. Below the meltwater lens, which may have inhibited larval survival, there were byssally attached juvenile scallops and epizootic macrofauna which colonized the large scallop shells. The impact of this meltwater also may be reflected in the growth patterns, trace element signatures, and isotopic characteristics of the scallop shells.

REFERENCES

- Adamson, D., and J. Pickard, Late Quaternary ice movement across the Vestfold Hills, East Antarctica, in *Antarctic Earth Science*, edited by R. L. Oliver, P. R. James, and J. B. Jago, pp. 465-469, Cambridge University Press, 1983.
- Adamson, D., and J. Pickard, Cainozoic history of the Vestfold Hills, in *Antarctic Oasis: Terrestrial Environments and History of the Vestfold Hills*, edited by J. Pickard, pp. 99-139, Academic Press, New York, 1986.
- Andersin, A.-B., J. Lassig, and H. Sandler, Community structures of soft-bottom macrofauna in different parts of the Baltic, in *Biology of Benthic Organisms*, edited by B. F. Keegan, P. Oceidigh, and P. J. S. Boaden, pp. 7-20, Pergamon Press, New York, 1977.
- Andrews, J. T., Recent and fossil growth rates of marine bivalves, Canadian Arctic, and Late-Quaternary Arctic marine environments. *Palaeogeogr. Palaeoclimatol. Palaeoecol.*, 11, 157-176, 1971.
- Baroni, C., and G. Orombelli, Glacial geology and geomorphology of Terra Nova Bay (Victoria Land, Antarctica), *Mem. Soc. Geol. Ital.*, 33, 171-193, 1989.
- Baroni, C., B. Stenni, and A. Longinelli, Isotopic composition of Holocene shells from raised beaches and ice shelves of Terra Nova Bay (Northern Victoria Land, Antarctica), *3rd Meeting Scienze Della Terra in Antartide*, Siena, 4-6 October 1989, pp. 15-16, 1989.
- Barrera, E., J. S. Tevesz, and J. G. Carter, Variations in oxygen and carbon isotopic compositions and microstructure of the shell of *Adamussium colbecki* (Bivalvia), *Palaos*, 5, 149-159, 1990.
- Berkman, P. A., Ecology of the circumpolar Antarctic scallop, *Adamussium colbecki* (Smith 1902), Doctoral Dissertation, 215 pp., University of Rhode Island, 1988.
- Berkman, P. A., The population biology of the Antarctic scallop, *Adamussium colbecki* (Smith 1902) at New Harbor, Ross Sea, in *Antarctic Ecosystems: Ecological Change and Conservation*, edited by N. Kerry and G. Hempel, pp. 281-288, Springer-Verlag, Heidelberg, 1990.
- Berkman, P. A., T. R. Waller, and S. P. Alexander, Unprotected larval development in the endemic Antarctic scallop, *Adamussium colbecki* (Mollusca: Bivalvia: Pectinidae), *Antarct. Sci.*, 3, 151-157, 1991.
- Berkman, P. A., D. W. Foreman, and J. C. Mitchell, Interpreting the mineralogy of antarctic scallop shells based on X-ray diffraction analysis of their crystalline characteristics, *Antarct. Res. Ser.*, American Geophysical Union, Washington, DC, In review.
- Beurois, J., Invertébrés et algues benthiques exploitées ou exploitables, in *Actes du Colloque sur la Recherche Française Dans les Terres Australes*, edited by L. Lauber, S. Gauber, and I. Martin, pp. 221-228, Comité National Français des Recherches Antarctiques, Strasbourg, 1987.
- Broecker, W. S., and T.-H. Peng, *Tracers in the Sea*, 690 pp., Eldigio Press, New York, 1982.
- Buzas, M. A., An application of canonical analysis as a method for comparing faunal areas, *J. Anim. Ecol.*, 36, 563-577, 1967.
- Cameron, R. L., and R. D. Goldthwait, The US-IGY contribution to Antarctic geology, Union Géodésique et Géophysique, Association Internationale d'Hydrologie Scientifique, 55, 7-13, 1961.
- Carriker, M. B., Ecological observation on the distribution of oyster larvae in New Jersey estuaries, *Ecol. Monograph*, 21, 19-38, 1951.
- Clapperton, C. M., and D. E. Sugden, Late Quaternary glacial history of George VI Sound area, West Antarctica, *Quat. Res.*, 18, 243-267, 1982.
- Craddock, C., Antarctic tectonics, in *Antarctic Geology and Geophysics*, edited by R. J. Adie, pp. 449-455, Universitetsforlaget, Oslo, 1972.
- David, T. W. E., and R. E. Priestly, Glaciology, physiography, stratigraphy, and tectonic geology of South Victoria Land, *Rep. Scient. Invest. Brit. Antarct. Exped. 1907-1909 (Geology)*, 1, 1-319, 1914.
- Dayton, P. K., Interdecadal variation in an Antarctic sponge and its predators from oceanographic climate shifts, *Science*, 245, 1484-1486, 1989.
- Dayton, P. K., G. A. Robilliard, and A. L. DeVries, Anchor ice formation in McMurdo Sound, Antarctica, and its biological effects, *Science*, 163, 273-274, 1969.
- Dayton, P. K., G. A. Robilliard, and R. T. Paine, Benthic faunal zonation as a result of anchor ice at McMurdo Sound, Antarctica, in *Antarctic Ecology. Volume 1*, edited by M. W. Holdgate, pp. 244-258, Scientific Committee on Antarctic Research, London, 1970.
- Denton, G. H., J. G. Bockheim, S. C. Wilson, and M. Stuiver, Late Wisconsin and Early Holocene glacial history, Inner Ross Embayment, Antarctica, *Quat. Res.*, 31, 151-182, 1989.
- Domack, E. W., A. J. T. Jull, J. B. Anderson, T. W. Linick, and C. R. Williams, Application of Tandem Accelerator Mass-Spectrometer Dating to Late Pleistocene-Holocene sediments of the East Antarctic continental shelf, *Quat. Res.*, 31, 277-287, 1989.
- Domack, E. W., A. J. T. Jull, J. B. Anderson, and T. W. Linick, Mid-Holocene ice sheet recession from the Wilkes Land continental shelf, East Antarctica, in *Geologic Evolution of Antarctica*, edited by J. A. Crame and J. W. Thomson, pp. 693-698, Cambridge University Press, Cambridge, 1991.
- Eisma, D., W. G. Mook, and H. A. Das, Shell characteristics, isotopic composition and trace-element contents of some euryhaline molluscs as indicators of salinity, *Palaeogeogr. Palaeoclimatol. Palaeoecol.*, 19, 39-62, 1976.
- Fleming, C. A., The molluscan fauna of the fjords of Western Southland, *N.Z. J. Sci. Tech.*, 5, 20-40, 1950.
- Green, R. H., A multivariate statistical approach to the Hutchinsonian niche: bivalve molluscs of Central Canada, *Ecology*, 52, 543-555, 1971.
- Grove, J. M., *The Little Ice Age*, 458 pp., Methuen, London, 1988.
- Imbrie, J., and K. P. Imbrie, *Ice Ages: Solving the Mystery*, 224 pp., Enslow Publ., Short Hills, 1979.
- Jackson, T. L., T. W. Linick, R. L. Michel, and P. M. Williams, Tritium and carbon-14 distributions in McMurdo Sound, 1977, *Antarct. J. U.S.*, 13, 71-73, 1979.
- Jones, D. S., Annual growth increments in shells of *Spisula solidissima* record marine temperature variability, *Science*, 211, 165-167, 1981.
- Kautsky, N., Growth and size structure in a Baltic *Mytilus edulis* population, *Mar. Biol.*, 68, 117-133, 1982.

- Labeyrie, L. D., J. J. Pichon, M. Labracherie, P. Ippolito, J. Duprat, and J. C. Duplessy, Melting history of Antarctica during the past 60,000 years, *Nature*, 322, 701-706, 1986.
- Lorius, C., L. Merlivat, J. Jouzel, and M. Pourchet, A 30,000 yr isotope climatic record from Antarctic ice, *Nature*, 280, 644-648, 1979.
- Lowenstam, H., Factors affecting the aragonite/calcite ratios in carbonate-secreting marine organisms, *J. Geol.*, 62, 284-322, 1954.
- Lutjeharms, J. R. E., C. C. Stavropoulos, and K. P. Koltermann, Tidal measurements along the Antarctic coastline, in *Oceanology of the Antarctic Continental Shelf*, edited by S. S. Jacobs, pp. 273-289, American Geophysical Union, Washington, DC, 1985.
- Lutz, R. A., and D. C. Rhoads, Growth patterns within the molluscan shell: an overview, in *Skeletal Growth of Aquatic Organisms*, edited by D. C. Rhoads and R. A. Lutz, pp. 203-254, Plenum Press, New York, 1980.
- Nakajima, Y., K. Watanabe, and Y. Naito, Diving observations of the marine benthos at Syowa Station, Antarctica, *Mem. Nat. Inst. Polar Res. Spec. Issue* 23, 44-54, 1982.
- Nichols, R. L., Coastal geomorphology, McMurdo Sound, Antarctica, *J. Glaciol.*, 7, 449-478, 1968.
- Omoto, K., Geomorphic development of the Soya Coast, East Antarctica. Chronological Interpretation of raised beaches based on levelling and radiocarbon dating, *Sci. Rept. Tohoku Univ. 7th Ser.*, 27, 95-148, 1977.
- Omoto, K., The problem and significance of radiocarbon geochronology in Antarctica, in *Antarctic Earth Science*, edited by R. L. Oliver, P. R. James, and J. B. Jago, pp. 450-452, Cambridge University Press, Cambridge, 1983.
- Pielou, E. C., *Mathematical Ecology*, 384 pp., John Wiley and Sons, New York, 1977.
- Rao, C. R., *Advanced Statistical Methods in Biometrical Research*, 390 pp., Wiley, New York, 1952.
- Robin, G. de Q., *The Climate Record in Polar Ice Sheets*, 212 pp., Cambridge University Press, Cambridge, 1983.
- Robinson, E. S., R. T. Williams, H. A. C. Neuberg, C. S. Rohrer, and R. L. Ayers, Southern Ross Sea tides, *Antarct. J. U.S.*, 10, 155-157, 1975.
- Rosenberg, G. D., An ontogenetic approach to the environmental significance of bivalve shell chemistry, in *Skeletal Growth of Aquatic Organisms*, edited by D. C. Rhoads and R. A. Lutz, pp. 133-168, Plenum Press, New York, 1980.
- Shotton, F. W., D. J. Blundell, and R. E. G. Williams, Birmingham University radiocarbon dates III, *Radiocarbon*, 11, 263-270, 1969.
- Stockton, W. L., The biology and ecology of the epifaunal scallop *Adamussium colbecki* on the west side of McMurdo Sound, Antarctica, *Mar. Biol.*, 78, 171-178, 1984.
- Stout, W. E., and S. V. Shabica, Marine ecological studies at Palmer Station and vicinity, *Antarct. J. U.S.*, 5, 134-135, 1970.
- Strang, G., *Linear Algebra and Its Applications. 2nd Edition*, 414 pp., Academic Press, New York, 1980.
- Stuiver, M. L., G. H. Denton, T. J. Hughes, and J. L. Fastook, History of the marine ice sheet in West Antarctica during the last glaciation: a working hypothesis, in *The Last Great Ice Sheets*, edited by G. H. Denton and T. J. Hughes, pp. 319-436, John Wiley and Sons, New York, 1981.
- Swanson, H. E., and R. K. Fuyat, Standard X-ray diffraction powder patterns: carbonates, *Nat. Bur. Stand. Circ.* 539 (II), 51-54, 1953.
- Taviani, M., and E. Amato, Diving in Antarctica: Third Italian Expedition in Terra Nova Bay, *Boll. Oceano. Teorica Applic.*, 7, 43-53, 1989.
- Tucker, M. J., and H. R. Burton, A survey of the marine fauna in shallow coastal waters of the Vestfold Hills and Rauer Island, Antarctica, *Austral. Nat. Antarct. Res. Exped. Res. Notes*, 55, 1-24, 1987.
- Yoshida, Y., Physiography of the Prince Olav and the Prince Harald Coasts, East Antarctica, *Mem. Nat. Inst. Polar Res. C*, 13, 1-83, 1983.
- Zhang, Q., and J. A. Peterson, A geomorphology and Late Quaternary geology of the Vestfold Hills, Antarctica, *Austral. Nat. Antarct. Res. Exped. Rept.*, 133, 1-84, 1984.

EPOS—A New Approach to International Cooperation

G. Hempel

Alfred Wegener Institute for Polar and Marine Research, Bremerhaven, Germany

ABSTRACT

130 marine biologists and oceanographers from 11 Western European countries participated in the European Polarstern Study (EPOS) jointly organized by the Federal Republic of Germany (through Alfred Wegener Institute for Polar and Marine Research) and the European Science Foundation. The icebreaking research vessel *Polarstern* operated in the Weddell Sea from October 1988 to March 1989. Each of the three legs was headed by a German scientist in charge and by a foreign scientific advisor.

The first leg started under late winter conditions and was devoted to the role of the sea ice in the pelagic system and to the sea ice biota themselves. Leg 2 studied the retreating ice edge and the open water in front of it during spring, particularly the relation of the phytoplankton blooms to the physical structure and chemistry of the surface water and to the grazing by krill. Leg 3 concentrated on taxonomy and eco-physiology of invertebrates and fishes at the sea bed of the eastern Weddell Sea.

EPOS was meant to provide Antarctic research opportunities to European countries with little experience in Southern Ocean studies and to foster the exchange of knowledge and ideas between European marine biologists of different scientific background and interests. Therefore, the teams of the various projects on board were normally multi-national in order to ensure a maximum of interaction. This has been continued in a number of post-expedition workshops and by international fellowships.

Estimation of Matter Fluxes in the River-Sea and Ocean-Atmosphere Systems for Okhotsk and Bering Seas

V. V. Anikiev, A. V. Alekseev, A. N. Medvedev, and E. M. Shymilin

Pacific Oceanological Institute, Far East Branch, Academy of Sciences of the U.S.S.R., Vladivostok, U.S.S.R.

ABSTRACT

The matter fluxes from continental and anthropogenic sources to sea take place by river discharge and atmospheric precipitation.

The estimation of this flux may be done on the basis of a single concept, but it has its own specific character in both cases: (1) the time-space changeability of the matter distribution in sea components is connected with the complex gradients of hydrophysical, physico-chemical and hydrobiological characteristics of the water mass, by name "biological barrier"; (2) the "altitude" and stability of this biogeochemical barrier are determined by short-period (from seconds up to one year) geochemical processes; and (3) it is very interesting and important to estimate not only the matter fluxes on the continent under the motion of water and air, but also the intensity of accumulation on the biogeochemical barrier.

It is necessary to do the next complex of investigations on the coast and aquatory of the Okhotsk and Bering Seas. This will include: (1) the synchronous registration of physical, chemical and biological characteristics in the river-sea and ocean-atmosphere systems to determine the transport and transformation of existing forms of matter; (2) observations of the distribution of natural and pollutant matter (such as heavy metals, oil and polycyclic aromatic hydrocarbons, artificial radioisotopes, etc.) in the estuaries, atmosphere, shelf zones and open sea regions; and (3) calculations of the matter fluxes between the different components of the sea.

Investigations of Scales of Changeability of Biogeochemical Processes on the Okhotsk Sea Shelf

**V. V. Anikiev, O. V. Dudachev, T. A. Zadonskaya, A. P. Nedashkovski, A. V. Pervushin,
S. G. Sagalaev, D. A. Chochlov and V. V. Yarosh**

Pacific Oceanological Institute, Far Eastern Branch of the U.S.S.R. Academy of Sciences, Vladivostok, U.S.S.R.

ABSTRACT

Complex investigations of spatial-temporal changeability of biogeochemical processes and parameters were conducted on the north-eastern shelf of Sakhalin. They included: (1) transformation of the size and chemical composition of particulate matter by hydrophysical and biological factors; (2) the shift of equilibrium into the carbonate system of water masses in relation to variable physico-chemical and biological parameters; and (3) change of biomass and species phyto-zooplankton and the same amount of primary production connected with fluctuations of hydrophysical, physico-chemical and biological characteristics of water masses.

Observations conducted during the last 3 years in different seasons, apart from winter, were by way of polygon survey and daily stations. Mathematical treatment of the data made it possible to estimate quantitatively the correlation between separate parameters and to identify the influence of several external factors on their spatial-temporal changeability: seasonal variations; the significance of the Amur river discharge; tidal motion of waters; steady circulation; invasion of CO₂ from low-temperature hydrothermal sources on the sea bottom.

The obtained dependencies can be used for forecasting possible ecosystem changes during the industrial exploitation of the oilfield.

AD-P007 324



92-17828



Long-term Monitoring of Airborne Pollen in Alaska and the Yukon: Possible Implications for Global Change

J. H. Anderson

Institute of Arctic Biology, University of Alaska Fairbanks, Fairbanks, Alaska, U.S.A.

ABSTRACT

✓ Airborne pollen and spores have been sampled since 1978 in Fairbanks and 1982 in Anchorage and other Alaska-Yukon locations for medical and ecological purposes. Comparative analyses of pre- and post-1986 data subsets reveal that after 1986 (1) pollen is in the air earlier, (2) the multiyear average of degree-days promoting pollen onset is little changed while (3) annual variation in degree-days at onset is greater, (4) pollen and spore annual productions are considerably higher, and (5) there is more year-to-year variation in pollen production. These changes probably reflect directional changes in certain weather variables, and there is some indication that they are of global change significance, i.e., related to increasing atmospheric greenhouse gases. Correlations with pollen data suggest that weather variables of high influence are temperatures during specific periods following pollen dispersal in the preceding year and the average temperature in April of the current year. Annual variations in pollen dispersal might be roughly linked to the 11-year sunspot cycle through air temperature mediators. Weather in 1990, apparent pollen production cycles under endogenous control, and the impending sunspot maximum portend a very severe pollen season in 1991. The existing but unfunded aerospora monitoring program must continue in order to test predictions and hypotheses and as a convenient, economical indicator of effects of climate change on biological systems and human well-being in the North.

INTRODUCTION

The dominant trees and shrubs and the grasses, sedges and some other herbs in Alaska and the Yukon release large amounts of pollen for aerial transport. The less conspicuous but ubiquitous molds and other fungi release larger amounts of spores during most of the snow-free period. These microscopic entities, known collectively as the aerospora, have been sampled since 1978 in an aerobiology program concerned with immunological, public health and ecological issues. A central ecological issue is annual pollen and spore dispersal as a function of certain weather variables and an indicator or predictor of vegetation responses to directional changes in those variables, i.e., to climate change.

The aerospora is an important biometeorological phenomenon and a prime candidate for long-term monitoring. This candidacy is enhanced by the need for data to under-

stand and manage the significant public health problems posed by pollen and spores as aeroallergens. It is further enhanced by the relative ease and low cost of sampling. A general objective of this article is to indicate potential value in the continued long-term monitoring of airborne pollen and spores in Alaska and adjacent Canada.

Although the multiyear data set now available represents only a few years and is only partially analyzed, major annual and longer-term variations in the aerospora are becoming evident. Specific objectives of this article are (1) to introduce some features of the annual variations, (2) to show changes in annual variations after 1986, (3) to present a preliminary correlation analysis suggesting specific weather variables influencing pollen dispersal, and (4) to discuss possible implications of observed aerospora changes for short-term climate changes that might be of global change significance.

This work is strictly preliminary and somewhat speculative because the lack of funding and investigator compensation has sorely restricted sample processing and precluded any computerization and efficient analysis of aerospores or accessory weather data.

METHODS

Gravimetric aerial samples were obtained as early as 1978 in Fairbanks [Anderson, 1984], and volumetric sampling with Burkard instruments began there and in Anchorage, Palmer and Juneau in 1982 and Whitehorse in 1984 [Anderson, 1983, 1985, 1986]. This provides minimal representation for the four most populated bioclimatic regions, southeastern, south-central and interior Alaska and southern Yukon. Most of the data used in this article derive from the sampler on the Arctic Health Research Building on the university campus in Fairbanks. Anchorage data are from the sampler on Providence Hospital in 1982–83 and on the nearby university administration building since then. With only one sampler available per region, estimates of within-site variability are lacking. A region's sampler was located to obtain as good a mix of regionally important pollen and spore taxa as it would have been in the author's judgment, at any other location.

Servicing the samplers, processing samples in the laboratory, and microscopy are standard or have been described elsewhere [Ogden et al., 1974; Anderson, 1985]. Basic data generated for each taxon are daily average numbers of pollen grains or spores per cubic meter of air. Sampling begins in April and continues into August or later, and well over 100 daily samples per location per year are obtained.

Pollen onset day and pollen and spore annual production are the primary aerospore variables in this article. Onset for a taxon is defined as the first day of apparently fresh pollen

grains followed by continuing and generally increasing appearances in daily samples. Annual production is the total of a taxon's daily average concentrations for the season. Peak concentration for a taxon is its highest daily average concentration in a season.

No sampling was done in 1979 and 1980. For 1978 and 1981, when gravimetric samplers only were used, and for 1990 for which Burkard samples have not been processed, volumetric productions were estimated. Estimates were extrapolations from gravimetric data based on high correlations between gravimetric and volumetric data in eight other years when both kinds of sampler were used side by side.

The main aerial pollen taxa in Fairbanks and Anchorage are early alder = *Alnus tenuifolia*; willow = *Salix* spp.; poplar/aspen = *Populus balsamifera* and *P. tremuloides*; birch = *Betula papyrifera*, mostly, and *B. glandulosa*; alder = *Alnus crispa*; spruce = *Picea glauca* and *P. mariana*; and grass = Gramineae, mostly *Calamagrostis canadensis*, *Bromus inermis* and *Hordeum jubatum*. Lesser taxa allocated to other pollen are larch = *Larix laricina*, pine = *Pinus contorta*, *Juniperus* spp., *Chenopodium album*, *Plantago major*, *Prunus* spp., *Shepherdia canadensis*, Cyperaceae, *Artemisia* spp. and several others. Some species are identified not by the distinctiveness of their pollen at taxonomic level but by their exclusive or near-exclusive representation in the surrounding vegetation.

VARIATIONS IN POLLEN PRODUCTION

Figure 1 shows the ranges of aerial pollen production in Fairbanks between taxa and over the years within taxa. The left bar for a taxon indicates its highest annual production, read on the logarithmic scale, and the year of that production. With the year is the percentage of that production of the highest of all, birch in 1987. Lower in each highest-production bar is the highest peak concentration, also read on the vertical scale, and its year.

The right bar of each pair indicates the lowest annual production of the taxon and year of occurrence. Here the second figure is the percentage of the highest production of the taxon indicated by the left bar. Within each lowest-production bar is the lowest peak concentration and year.

The following observations concerning Figure 1 are particularly interesting.

(1) Maximum and minimum annual productions range widely between taxa. Birch pollen production has been nearly 100 times the grass maximum, even while grasses are fairly abundant in the area of the sampler. Spruce trees are also plentiful, but spruce pollen, the second most abundant type, has reached only 28 percent of the maximum amount produced by birch. Minimum productions range from only 60 grains in early alder in 1981 to about 1200 in the upland alder in 1984 and about 1400 in birch in 1986. Most notable is the differential variation of pollen production between taxa through time. The outstanding example is birch and alder. While these are botanically close and have nearly identical seasons, their maximum and minimum productions occurred in four different years, as did their highest and lowest peak concentrations. This and other cases of differential variation signify that taxa are responding individually to endogenous and certain external influences, while they probably are also responding to other environmental variables affecting them simultaneously.

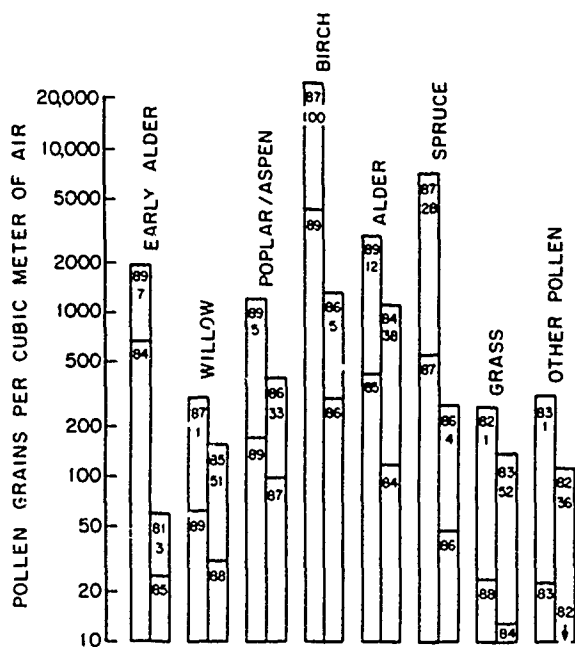


Figure 1. Ranges of annual aerial pollen production and peak daily average concentrations within and between taxa in Fairbanks. See text for explanation.

(2) There is a wide range of within-taxon variation in pollen production over the years. The most conspicuous examples are birch and spruce with maximum productions exceeding minimums by 20 and 26 times respectively. The least variation is in grass where the maximum seen so far has been somewhat less than twice the minimum. Parallel large differences in within-taxon peak concentrations are also seen, even while highest and lowest peak concentrations were in different years from maximum and minimum productions in nine out of the 16 cases.

The complex variability represented in Figure 1 calls for continued monitoring of the aerospora to determine any more or less regular patterns of annual variation. One pattern becoming evident in Fairbanks and seen in other northern countries [Andersen, 1980; Nilsson, 1984; Jäger, 1990] is the biennial cycle of relatively higher and lower pollen production in alder and birch. There is possibly also a pattern in spruce, with high pollen production every fourth or fifth year separated by years of much lower production. Such patterns are presumably under some endogenous control. Endogenous controls will have to be recognized, preferably through statistical time-series analyses, in order conclusively to identify separate environmental controls. Beyond that, the statistical basis for identifying environmental controls will only improve as the data set grows with continued aerospora monitoring.

(3) Minimum annual productions in all taxa occurred in 1986 or earlier (Figure 1). Maximum productions occurred after 1986 except in grass and other pollen. Different behavior by grass from the woody taxa might be expected because its season is later and it is influenced by different environmental conditions. Other pollen comprises several woody and herbaceous taxa flowering from early spring to late summer and controlled by several different preceding- and current-year variables [Solomon, 1979]. The high other pollen in 1983 was due largely to unusual production by larch and pine. That was probably promoted by favorable mid-growing season weather in 1982 which caused the high grass production that year (Figure 1).

CHANGES IN POLLEN ONSET

Observation 3 above suggested a comparative analysis of pre-1986 and post-1986 subsets of the 11-year data set available for Fairbanks. Exclusion of 1986 data gave a prominent time break between the two subsets. Also, poplar/aspen and birch pollen production were very low in 1986, probably abnormally so owing to infestations in 1985 of larvae of the aspen tortrix and spruce marked black moths.

The variable pollen onset and two associated variables will be examined, then attention will return to annual production. Table 1 shows that in all taxa the average day of onset was earlier after 1986 by from four to 12 days. The average was 7.4 days earlier. The change is greatest in the earliest flowering taxa and decreases regularly through later taxa to grass, again behaving independently.

The variable degree-days at onset is an expression of the early growing season heat input necessary for final floral maturation and pollen release [Solomon, 1979]. Positive differences between daily average temperatures and 0°C were summed to the onset day of each taxon in each year. For a taxon, the summation is its degree-days at onset for the year. In general, while onset day has ranged considerably, by from 14 days in spruce to 20 days in early alder and grass,

degree-days at onset have been fairly constant from year to year. This is seen in the low CVs (coefficients of variance) for degree-days at onset listed in Table 1 for pre- and post-1986 periods. Higher CVs are associated with the earlier flowering taxa, but these are statistical consequences of low numbers of degree-days.

There have, however, been some noteworthy changes in the degree-days situation since 1986. In all taxa except birch and poplar/aspen, essentially unchanged, degree-days as three-year averages became lower. In willow, spruce and grass the percentage differences from pre-1986 averages are probably statistically significant. Furthermore, annual variation in degree-days at onset increased after 1986 except in poplar/aspen and grass. The latter two negative changes probably are not significant owing to the very low CVs before and after 1986. In the other taxa the CVs are generally low as well, especially before 1986. But the changes are relatively greater, and all these increases might be significant.

CHANGES IN POLLEN AND SPORE PRODUCTION

Table 2 lists average annual productions for the seven main pollen taxa plus other pollen before and after '86. Except for grass, all productions increased. All of the increases are probably statistically significant, and the big increases in early alder and birch are especially notable considering the roles of these as Alaska's major aeroallergens. Some of the increase in birch pollen might be a function of the increasing size of several trees relatively near the sampler. However, the abrupt change between pre- and post-1986 productions is not consistent with gradual tree growth.

In addition to post-1986 pollen production increases, fungus spore production has increased substantially too. Much work remains to be done with available samples and data, but a comparison for the July 10-31 period was possible. Average production for this period was higher by 113 percent in two years after 1986 compared with three years before.

Table 2 indicates the variation from year to year in pollen production as this is expressed by coefficients of variance. As predicted by Figure 1, the latter are rather high. They reflect the considerable ranges of within-taxon annual productions expressed by percentages in the right-hand bars in Figure 1. Lower percentages indicate wider ranges. Linear regression of the eight post-1986 CVs against the corresponding percentages yielded a respectable negative correlation of $r = -0.90$. Of the post-1986 CVs, five are higher than the corresponding pre-1986 values, and of these the poplar/aspen, birch and spruce CVs might be significantly higher.

The apparent big decrease in willow pollen production variation (Table 2) is not significant in view of the low CVs before and after 1986. Grass has behaved differently again by being the only taxon to produce less pollen after 1986, although not much less, and by exhibiting a substantial decrease in annual production variation. Other pollen, a mixture of taxa, exhibits a mixed change, to somewhat increased production after 1986 with a substantially reduced production variation.

POLLEN DISPERSAL IN ANCHORAGE

To the extent that work with Anchorage samples and data has been possible, changes in pollen production and timing similar to those in Fairbanks are evident. Table 3 reports

Taxon	n	Av. Onset Day	Change Days Earlier	Av. DDs °C	Change	DDs CV %	Change
Early Alder							
pre-1986	3	4/27		5		21	
post-1986	3	4/15	12	4	-5%	27	29%
Willow							
pre-1986	4	5/3		45		14	
post-1986	3	4/24	9	33	-20%	42	200%
Poplar/Aspen							
pre-1986	6	5/3		46		1	
post-1986	3	4/25	8	46	-1%	10	-9%
Birch							
pre-1986	6	5/12		106		7	
post-1986	3	5/7	5	107	0.5%	17	143%
Alder							
pre-1986	6	5/11		118		3	
post-1986	3	5/7	4	112	-4%	19	533%
Spruce							
pre-1986	6	5/24		448		6	
post-1986	3	5/20	4	422	-6%	14	133%
Grass							
pre-1986	6	6/19		561		3	
post-1986	3	6/9	10	477	-15%	2	-33%

Table 1. Pollen onset day characteristics in Fairbanks after 1986 compared with before 1986.

Taxon	n	Pre-1986			Post-1986			
		\bar{X}	CV %	n	\bar{X}	CHNG	CV %	CHNG
Early Alder	5	>172	98	3	886	415%	104	6%
Willow	6	>250	19	4	288	15%	7	-63%
Poplar/Aspen	6	>602	14	4	636	39%	35	15%
Birch	6	5346	42	4	15,357	187%	59	40%
Alder	5	1777	29	4	2227	25%	32	10%
Spruce	6	1843	41	4	3061	66%	97	137%
Grass	3	227	32	3	207	-9%	23	-28%
Other Pollen	4	200	45	3	225	13%	9	-80%

Table 2. Average annual pollen production and its variation in Fairbanks after 1986 compared with before 1986.

post-1986 increases in the four most important aerial pollen taxa and in fungus spores. The increase in poplar/aspen pollen is greater than in Fairbanks, in birch much less, in alder somewhat less, and in spruce virtually the same. The enormous increase in fungus spores is certainly an exaggeration owing to insufficient work with the samples. However, it does indicate conditions in May considerably more conducive to fungus growth than before 1986. Increased

warmth and moisture would be more conducive conditions.

Five taxa in Anchorage (Table 3) exhibit average onset days earlier after 1986 by numbers of days comparable to Fairbanks. Poplar/aspen and grass are earlier by the same amount in both places, while the other three taxa are relatively earlier in Anchorage than Fairbanks. Actual average onset days vary moderately and differentially between both places.

Taxon	Annual Prod'n Increase	Average Onset Day Before	Average Onset Day After	Days Earlier
Poplar/Aspen	69%	4/27	4/19	8
Birch	6%	5/12	5/2	8
Alder	10%	5/15	5/3	12
Spruce	63%	5/25	5/19	6
Grass	na	6/17	6/7	10
Fungi	1705%	na	na	-
(May only)				

Table 3. Some pollen and spore dispersal characteristics in Anchorage after 1986 compared with before 1986.

Average Temp. During	n =	All Years 8	High Years Only 4	Low Years Only 4
July		0.47	0.63	0.69
August		-0.04	-0.03	0.62
Week 1 after E _m ¹		0.54	0.15	0.28
Week 2 after E _m		0.76	0.87	0.54
Weeks 1 and 2 after E _m		0.81	0.76	0.48
Weeks 3 and 4 after E _m		0.44	0.01	-0.33
Month 1 after E _m		0.78	0.66	0.06
Weeks 1 and 2 after E _a ²		0.54	0.75	0.52
Weeks 3 and 4 after E _a		0.52	0.65	0.99
Month 1 after E _a		0.61	0.65	0.82
10 highest-concentration days		-0.15	-0.38	-0.99

Table 4. Annual birch pollen production in Fairbanks as a function of 11 preceding-year temperature variables.

INFLUENTIAL WEATHER VARIABLES

Exactly which temperature and other weather variables influence pollen production and timing is of central interest. Identification of specific variables will require systematic computerized multiple correlation analyses, testing all potential variables, of the kind done for ragweed in New Jersey by Reiss and Kostic [1976].

A preliminary pocket-calculator analysis with pollen data for birch only in Fairbanks yielded clues to specific influential temperature variables. Production data for eight years were used, excluding the estimated productions for 1978, 1981 and 1990. Weather data from the College Observatory on the university campus were used. The eight years' pollen data as a set were correlated by linear regression with 11 preceding-year temperature variables (Table 4) and eight current-year variables (Table 5). The pollen data were then divided into high- and low-year subsets, and similar correlations performed for the subsets. The reason was the possibility that actual productions in high years are more influenced by external conditions than in low years [Andersen, 1980].

Tables 4 and 5 contain a few noteworthy correlation coefficients as preliminary suggestions of the most influential

Average Temp. During	n =	All Years 8	High Years Only 4	Low Years Only 4
March		-0.10	-0.34	0.57
April		0.62	0.85	0.90
May		0.24	0.78	0.80
14 days preceding onset		-0.34	-0.46	0.20
First 10 days of production		-0.66	-0.49	-0.07
First 2 weeks of production		-0.66	-0.57	-0.43
5 highest-concentration days		-0.71	-0.56	0.01
10 highest-concentration days		-0.73	-0.68	-0.26

Table 5. Annual birch pollen production in Fairbanks as a function of eight current-year variables.

temperature variables. There are no correlations where all production data are treated together, but there are two or three in the high- and low-year subset columns. Birch pollen production in high years correlates with average temperature in the second week after the main birch pollen season in the preceding year ($r = 0.87$) and with the average temperature in April of the current year ($r = 0.85$). Production in low years correlates highly with temperatures somewhat later in the previous growing season ($r = 0.99$) and with temperature in April of the current year ($r = 0.90$). Most curious is the high negative correlation between production in low years and the average temperature on ten days of highest pollen concentration in the preceding year.

DISCUSSION

Changes after 1986 in five pollen dispersal variables in two widely separated Alaskan locations are summarized in Table 6. First, average onset day is earlier in all taxa in both locations and much earlier, by more than a week, in most. This reflects probable earlier accumulations of requisite heat sums, which require higher daily average temperatures after February. It indicates an increase in growing season length insofar as the growing season doesn't end sooner. A more usable growing season is one of the more significant effects in the North anticipated with carbon dioxide-induced climate change [Bowling, 1984]. Also, earlier pollen onset means longer periods of trouble for allergy and asthma sufferers.

Regarding average degree-days at onset, these are mostly the same after 1986 as before except for grass. This indicates a constancy of physiological response to one environmental factor and suggests that changes in other pollen dispersal variables are environmentally, not internally, induced.

Table 6 reveals a strong tendency toward increased variation in degree-days at onset after 1986, although it must be noted again (Table 1) that the CVs are based on only three data each, 1987-1989. If continued aerospora monitoring confirms this increase, then the relatively greater influence of some variable(s) other than cumulative air temperature will be indicated. These might be soil temperature, partly a function of snow cover, or soil moisture, largely a function of precipitation the preceding autumn. Thus the much

Taxon	Average Onset Day		Average D-Ds at Onset	Annual Variation In D-Ds	Average Annual Production		Annual Variation In Prod'n
	F	A	F	F	F	A	F
Early Alder	E	-	n	i	I	-	i
Willow	E	-	d	I	i	-	D
Poplar/Aspen	E	E	n	n	i	I	I
Birch	E	E	n	I	I	i	I
Alder	e	E	d	I	i	i	-
Spruce	e	e	d	I	I	I	I
Grass	E	E	D	n	d	-	d
Other Pollen	-	-	-	-	i	-	D

Table 6. Summary of changes in aerial pollen dispersal characteristics in Fairbanks (F) and Anchorage (A) after 1986. E = much earlier; e = somewhat earlier; D = significant decrease; d = minor decrease; I = significant increase; i = minor increase; n = no change; - = not available.

needed work with weather data and additional years' pollen data will look for changes after 1986 in, among others, late winter snow cover and melting and autumn rain.

Probably the most important finding so far from long-term aerospora monitoring is the increased pollen production after 1986 by all taxa in both locations except grass in Fairbanks. The increases probably are responses to higher early through mid-growing season temperatures [Solomon, 1979; Andersen, 1980]. The analysis concerning Tables 4 and 5 implicated average April temperature, and that agrees with earlier heat sums for pollen onset. Also implicated was temperature some time after pollen dispersal. The exact period of greatest preceding-year temperature influence will vary within taxa from year to year and among taxa in any one year. However, all periods will probably occur after early June and before August.

Table 6 reveals a strongly mixed change in annual variation in pollen production after 1986. Again n values are low (3 or 4), but some of the data are compelling, particularly for birch and spruce which exhibited the greatest production CV increases. In birch 1987-1990 productions in thousands were 26.7, 6.0, 18.4 and 10.3 grains per cubic meter of air. Spruce productions were 7.4, 1.0, 1.3 and 2.6. These highly variable data, plus the data for poplar/aspen and possibly early alder, suggest that for these taxa those temperature variables influencing pollen production have become more variable. An additional or alternative possibility is the relatively weaker influence of some other factor, e.g., a moisture variable.

The general increase in allergenic pollen production is, like the earlier onsets, corroborated by the increased frequency of complaints by allergy and asthma victims [Freedman, 1990]. Unfortunately for these persons, but of much biometeorological interest, a very severe pollen season for 1991 must be predicted, even as early as August 1990. This prediction is based partly on the extraordinary warmth of June and July 1990 coupled with adequate, if not abundant rain. For birch and alder, the "ragweeds" of Alaska, this prediction is also based on their biennial cycles. Since 1985 they have been in phase, with odd-numbered years the high ones. Great spruce pollen production is also predicted for 1991 in Fairbanks because it will be the fourth year since

the last very high production (Figure 1). This coordination of environmental and endogenous influences could cause an extraordinary pollen season severity, but low early spring temperatures in 1991 could mitigate the situation.

The weather changes reflected by changes in pollen and spore dispersal after 1986 constitute a short-term climate change. Whether this is of global change significance remains to be proven. It is certain that the rate and magnitude of climate change in these very few years, as reflected by aerospora data, are no greater than in several recorded short-term climate oscillations [Bowling, 1984].

The pollen data are partly congruent with the 11-year sunspot cycle analyzed by Juday [1984] in terms of its apparent influence on Alaskan mean annual temperatures. Indeed, the present data suggest the hypothesis that pollen dispersal variations, mediated by air temperatures, follow the sunspot cycle. While the low sunspot numbers ending cycle 21 would have been in 1985 and 1986 [Juday, 1984], seven of the lowest annual pollen productions or lowest peak concentrations occurred in those years (Figure 1). Poplar/aspen and birch lows in those years were explained earlier by insect larva damage, but the willow low in 1985 and the exceptional spruce low in 1986, at only four percent of the next year's maximum, cannot be so explained. Moreover, 1985 was a relatively low pollen year for early alder and poplar/aspen and the second lowest for birch, and 1986 was the second lowest for willow and other pollen. Only grass sustained relatively high pollen production in 1985-86.

The last sunspot maximum was the moderately high and flat one in 1980, and corresponding mean annual temperature maxima in Fairbanks were 1978 and 1981 [Juday, 1984]. The first pollen data were obtained in 1978 and suggest relatively high productions. Indeed, alder pollen in 1978 was possibly almost twice that graphed in Figure 1 for 1989. No pollen data are available for 1979 or 1980. Pollen production in 1981 was low to intermediate, and that is inconsistent with the hypothesis that pollen dispersal follows the sunspot cycle. However, while the mean temperature for 1981 was fairly high [Juday, 1984], the growing season temperature was one of the lowest on record [Bowling, 1984]. A low growing season temperature the previous year, even with a high mean annual temperature, would also

have had an inhibiting effect on pollen production by birch and the other woody perennials as is suggested by the correlations in Table 4.

If pollen dispersal follows the sunspot cycle, then more or less regular increases and decreases in pollen production and onset day changes should be observed. They are not. Except for the probable internally influenced production patterns in alder, birch and spruce, no regularity is apparent in the data. This seems even more inconsistent with the hypothesis when the pre- and post-1986 data subsets are examined separately. These represent the downswing of one sunspot cycle and the upswing of the next. In neither period is there a hint in any taxon of a regular decrease or increase.

The fact remains, however, that the highly irregular pollen data after 1986 average to earlier onsets and higher productions than before. This means that in the second of two consecutive periods between sunspot maxima and a minimum, when sunspot numbers should have been approximately the same, there was a more vigorous biological response. This is a hint in a temperature influenced vegetation function of "a staircase increase in temperatures" [Juday, 1984] that could be occurring with the global increase of atmospheric greenhouse gases.

It might be that the congruence of low growing season and mean annual temperatures is more probable during sunspot minima. Pollen data for 1985-86 would agree with that. Conversely, high growing season temperatures might be more probable in association with high mean annual tem-

peratures at times of sunspot maxima. Pollen data for 1978 would agree with that, but not for 1981. The latter data thus allow no prediction of growing season temperatures in 1991 and/or 1992, which should see the next sunspot maximum. Continued aerial sampling to determine pollen and spore dispersal characteristics in those years will be valuable. It will test the prediction of pollen season severity made earlier, which is of much public health interest, and the hypothesis that pollen dispersal roughly follows the 11-year sunspot cycle. Beyond that, continued monitoring of the aerospora will have implications for agronomy, beekeeping, forestry, paleoecology and plant pathology.

ACKNOWLEDGMENTS

A grant from the short-lived Alaska Council on Science and Technology enabled the start of volumetric aerial sampling in five locations in 1982. At a later time, assistance from the Susman and Asher Foundation kept the aerobiology program alive. The Anchorage sampler was serviced voluntarily by members of the Providence Hospital and university maintenance staffs, mostly by Sam Burrell, Sam Dunagan and Jeff Tappe. The Fairbanks samplers were serviced a few times by Jeff Conn, Larry Johnson and Heather McIntyre. Numerous physicians, allergic persons, ecologists and others have provided encouragement and moral support. An anonymous reviewer assisted generously with the penultimate draft of this article.

REFERENCES

- Andersen, S. T., Influence of climatic variation on pollen season severity in wind-pollinated trees and herbs, *Grana*, 19, 47-52, 1980.
- Anderson, J. H., Aeropalynology in Juneau, Alaska. Results of the first season's use of a volumetric sampler for allergenic and other airborne pollen and spores, 33 pp., (Photocopy), Institute of Arctic Biology, University of Alaska Fairbanks, 1983.
- Anderson, J. H., A survey of allergenic airborne pollen and spores in the Fairbanks area, Alaska, *Annals of Allergy*, 52, 26-31, 1984.
- Anderson, J. H., Allergenic airborne pollen and spores in Anchorage, Alaska, *Annals of Allergy*, 54, 390-399, 1985.
- Anderson, J. H., Aeropalynology, allergenics, and vegetation in Whitehorse. Report on a study of airborne pollen and spores at Whitehorse General Hospital in 1984, 19 pp. (Photocopy), Institute of Arctic Biology, University of Alaska Fairbanks, 1986.
- Anderson, J. H., A prototype standard pollen calendar for Anchorage, Alaska. An explanatory and interpretive manual. And A prototype standard pollen calendar for Fairbanks, Alaska, etc., 14 pp. each plus charts, (Photocopy), Institute of Arctic Biology, University of Alaska Fairbanks, 1989.
- Bowling, S. A., The variability of the present climate of interior Alaska, in *The Potential Effects of Carbon Dioxide-Induced Climatic Changes in Alaska*, edited by J. H. McBeath, pp. 67-75, School of Agriculture and Land Resources Management, University of Alaska Fairbanks, 1984.
- Freedman, D., Hay fever: Many are suffering this season as the pollen count stays high, *Anchorage Daily News*, July 19: H-1-H-2, 1990.
- Jäger, S., Tageszeitliche Verteilung und langjährige Trends bei allergiekompetenten Pollen, *Allergologie*, 13, 159-182 + Bildteil, 1990.
- Juday, G. P., Temperature trends in the Alaska climate record: Problems, update, and prospects, in *The Potential Effects of Carbon Dioxide-Induced Climatic Changes in Alaska*, edited by J. H. McBeath, pp. 76-91, School of Agriculture and Land Resources Management, University of Alaska Fairbanks, 1984.
- Nilsson, S. (Ed.) *Nordic Aerobiology. Fifth Nordic Symposium on Aerobiology, Abisko, Sweden, August 24-26, 1974*, 97+ pp., Almqvist & Wiksell, Stockholm, 1984.
- Ogden, E. C., et al., *Manual for Sampling Airborne Pollen*, 182 pp., Hafner/Macmillan, New York, 1974.
- Reiss, N. M., and S. R. Kostic, Pollen season severity and meteorologic parameters in central New Jersey, *Journal of Allergy and Clinical Immunology*, 57, 609-614, 1976.
- Solomon, A. M., Pollen, in *Aerobiology: The Ecological Systems Approach*, edited by R. L. Edmonds, pp. 41-54, Dowden, Hutchinson & Ross, Stroudsburg, 1979.

92-17829

AD-P007 325



Potential Effects of Global Warming on Calving Caribou

Warren G. Eastland and Robert G. White

Institute of Arctic Biology, University of Alaska Fairbanks, Fairbanks, Alaska, U.S.A.

ABSTRACT

Calving grounds of barren-ground caribou (*Rangifer tarandus*) are often in the portion of their range that remains covered by snow late into spring. We propose that global warming would alter the duration of snow cover on the calving grounds and the rate of snowmelt, and thus affect caribou population dynamics. The rationale for this hypothesis is based upon the following arguments. For females of the Porcupine Herd, one of the few forages available before and during early calving are the inflorescences of cotton grass (*Eriophorum vaginatum*), which are very digestible, high in nitrogen and phosphorus, and low in phenols and acid-detergent fiber. The nutritional levels of the inflorescences are highest in the early stages of phenology and decline rapidly until they are lowest at seed set, about 2 weeks after being exposed from snow cover. The high nutritional level of cotton grass inflorescences is important to post-paturient caribou attempting to meet nutritional requirements of lactation while minimizing associated weight loss. The pattern of weight regain in summer is important to herd productivity as female body weight at mating influences conception in late summer and calving success in spring. Therefore, temporal changes in snowmelt may have major effects on nutritional regimes of the female.

INTRODUCTION

Plasticity in timing of calving is a possible adaptation to environmental changes such as temporal changes in snowmelt; however, such adaptation may be quite limited, as timing of mating in caribou is temporally controlled. This suggests that small changes in snowmelt because of global warming could have multiplicative effects on the nutritional regime of the caribou, affecting female fecundity, survival of calves and, therefore, herd productivity.

Date of snowmelt across the arctic is earlier than in the past (Figure 1) [Foster, 1989], but it is uncertain whether this is attributable to changes in global climate or natural weather cycles. Timing and duration of snowmelt are of great potential importance to caribou (*Rangifer tarandus granti*) herd productivity because it influences the timing of emergence and abundance of forage plants for pregnant and lactating females.

NUTRITIONAL EFFECTS ON CARIBOU PRODUCTIVITY

Caribou productivity is dependent upon rates of pregnancy and calf survival, both of which are dependent upon female nutritional levels. One of the primary forages of calving caribou is inflorescences of the tussock-forming cotton grass, *Eriophorum vaginatum* (Figures 2,3) [Lent, 1966; Kuropat and Bryant, 1980; Kuropat, 1984]. Immediately after release from snowcover, *Eriophorum* inflorescences begin to elongate (Table 1). Nutritional levels of inflorescences are highest at the onset of elongation and decline steadily until seed set [Kuropat, 1984], which occurs within 10 days. Caribou can take advantage of this high-nutrition forage by calving in areas of extended snowmelt [Fleck and Gunn, 1982; Eastland et al., 1989]. Following snowmelt, early flowering legumes constitute an important dietary protein source which is followed by rapidly expanding willow

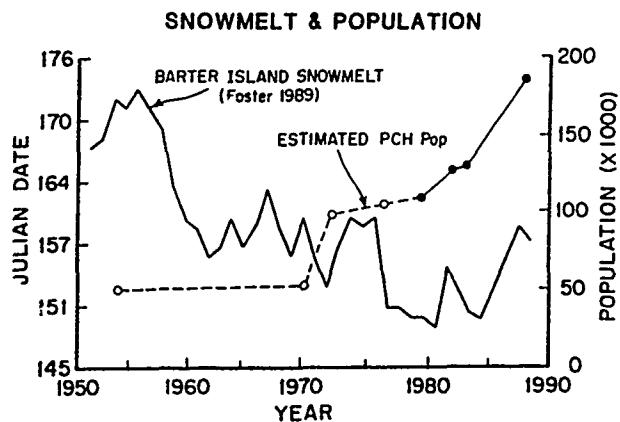


Figure 1. Date of complete snowmelt at Barter Island, Alaska and size of the Porcupine Caribou Herd (PCH). Snowmelt data to 1984 from Foster [1989]. Open circles are questionable data, solid circles represent systematic estimates.

leaves (Figure 2). Plant biomass increases markedly which maximizes food intake [White and Trudell, 1980] and caribou rapidly change their diet throughout summer to take advantage of new growth of other vascular plant foliage as it becomes available. High levels of nutrition result in peak milk production immediately post calving and, as a consequence, calf growth rate is maximized [White and Luick 1976, 1984; Rognmo et al., 1983; Skogland, 1984; White, 1990]. A high body weight of weaned calves entering winter is associated with increased survival to yearling age.

Female caribou are less likely to conceive unless they regain weight, lost during winter and early lactation, in order to meet a minimum threshold for conception [Thomas, 1982; Reimers, 1983; White, 1983; White and Luick, 1984; Skogland, 1985; Tyler, 1987; Lenvik et al., 1988; Cameron et al., 1991]. Therefore the pattern of post-calving maternal weight gain is important. Maximized weight gains throughout the summer by "phenological chasing" by caribou in Arctic Alaska has been suggested frequently [Klein, 1970, 1982; Kuropat and Bryant, 1980; White and Trudell, 1980; White et al., 1981; Kuropat, 1984]; and it involves fol-

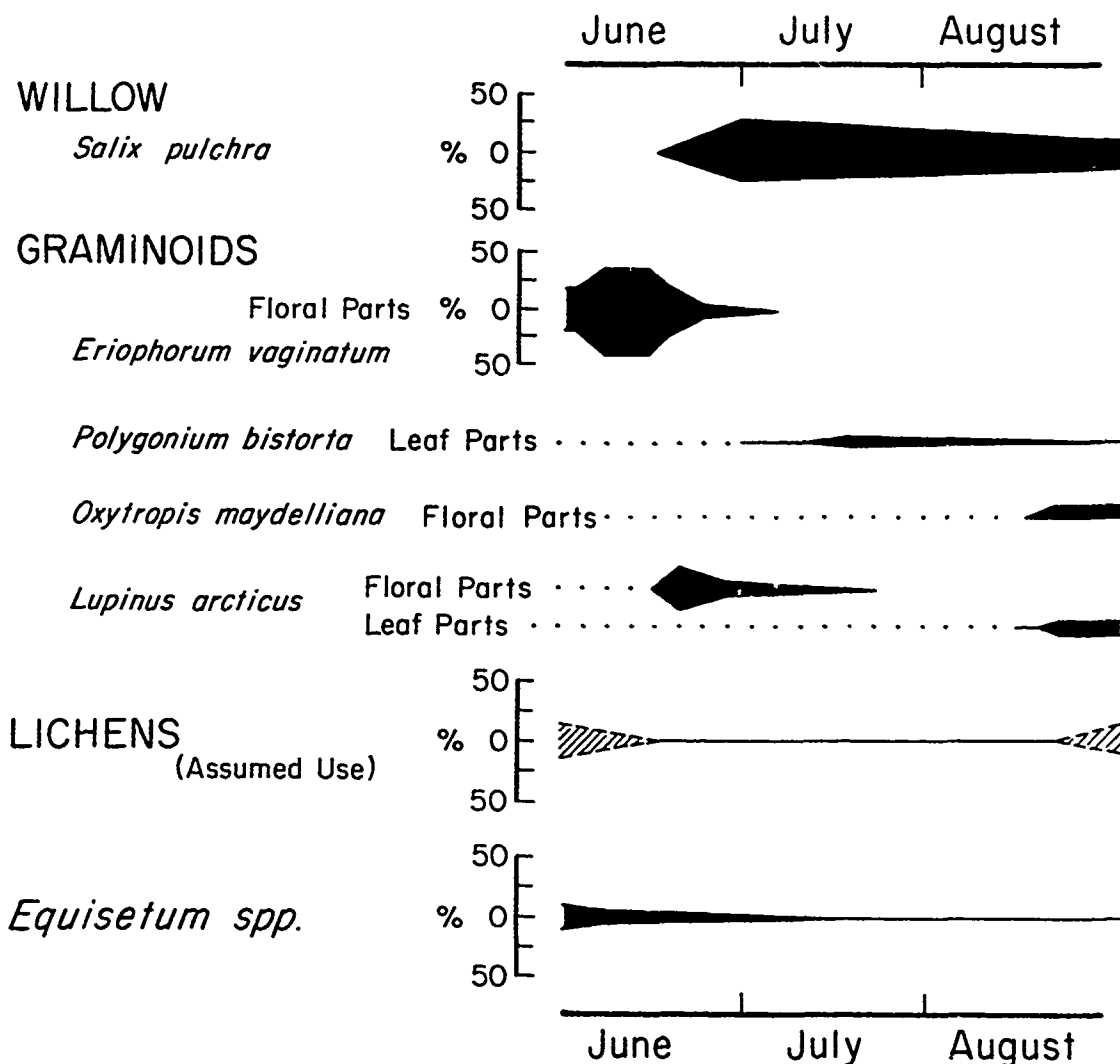


Figure 2. Relative amounts of various forage species used by caribou in spring and summer months. From Kuropat [1984, Figure 3, p. 40].

	Time after removal of snowcover in days		
	0	1	2
N	22	47	11
$\bar{X} \pm SD$ (mm)	60.2 ± 7.8	72.2 ± 11.1	85.6 ± 14.1
range (mm)	44-71	52-94	68-124
95% CI (mm)	59.0-61.4	71.2-73.2	83.4-87.8

Table 1. *Eriophorum vaginatum* inflorescence lengths after removal of snowcover. CI = confidence interval.

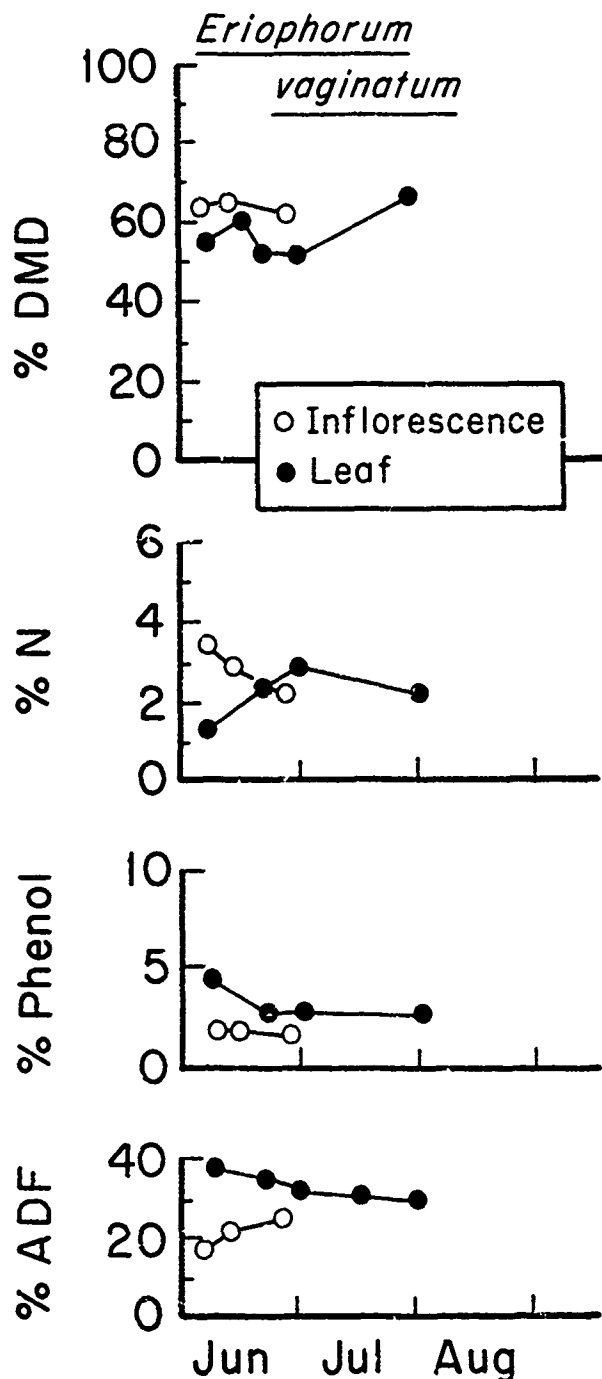


Figure 3. Nutrient levels of *Eriophorum vaginatum* inflorescences and leaves including dry matter digestibility (DMD), nitrogen (N), phenols, and acid detergent fiber (ADF). From Kuropat [1984, Figure 5, p. 52].

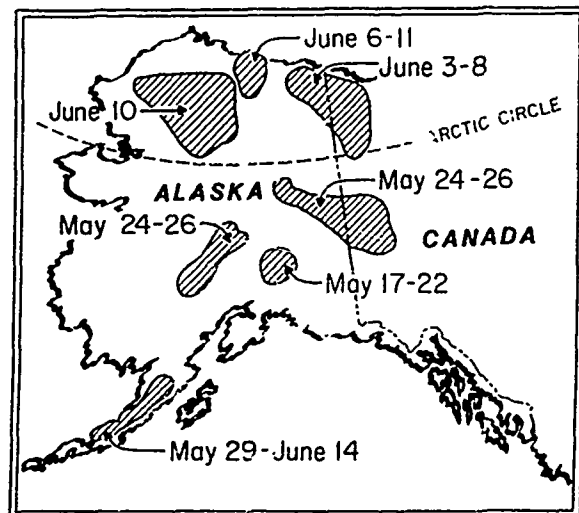


Figure 4. Approximate calving dates of representative Alaskan caribou herds.

lowing the phenological progression of plants, feeding upon each member of the plant community as it reaches its highest level of nutrition and/or biomass. Choice of vegetation type is important to selecting for species diversity, maximizing eating rate and minimizing the intake of chemically defended plant parts [Kuropat and Bryant, 1980; White and Trudell, 1980]. Most plants are at their highest levels of nutrition and lowest levels of antiherbivory compounds when they are in relatively early stages of phenological development. Thus any environmental or climate change that alters plant phenology has implications that could be important for caribou productivity.

IMPLICATIONS OF GLOBAL CLIMATE CHANGE ON SNOWMELT AND CARIBOU NUTRITION

Shortened duration of snowmelt could result from global warming and it may increase emergent vegetation for pregnant caribou, but also it will likely truncate the period of phenological variation in the plant community throughout early summer, thus reducing temporarily the extent of phenological chasing by caribou. Detrimental effects could be minimized if caribou have the ability to respond in their timing of nutritional demands, particularly through temporal changes in reproduction.

Caribou and reindeer (*R. t. tarandus*) calving is synchronized with green-up on the calving grounds [Fleck and Gunn, 1982; Eastland et al., 1989; Skogland, 1989]. Time of calving is separated by as much as 6 weeks between herds in Norway [Skogland, 1989] and in Alaska by as much as 3 weeks (Figure 4). Also, for individual females within a single herd peak calving date varies between years, but the time span between first and last calf-drop is much smaller than between-herd calving times [Skogland, 1989].

If global warming promotes earlier snowmelt, hence earlier green-up, can the timing of calving adapt to match the change? Under experimental conditions, female caribou captured as calves and confined on new ranges with earlier green-up, i.e., that differ from their natal ranges, changed their timing of calving to match local green-up [R. G.

White, unpublished data]; however, Skogland [1989] indicated that this may not be true of all *Rangifer*. Estimates of the timing of peak calving (the time at which 50% of the calves have been born) for the Porcupine Caribou Herd indicate that peak calving now occurs 4 days earlier than a decade ago [S. G. Fancy, unpublished data]. Thus there is strong evidence for the ability of caribou to adapt to local climate change, but the limits of adaptation remain unknown.

GLOBAL CLIMATE CHANGE AND THE TIMING OF CARIBOU MIGRATION

Pregnant caribou frequently winter hundreds of miles from the calving grounds and initiate migration in anticipation of green-up [Kelsall, 1968; Skogland, 1968; Fancy, 1989]. Therefore, timing of arrival on the calving grounds, in order to make maximum use of a progressively earlier snowmelt, probably has a large stochastic component. Those females wintering closest to the calving grounds may be affected by the changing climatic condition and may move accordingly. For instance, during May 1990 an extreme early snowmelt in the northern foothills of the Brooks Range resulted in early *Eriophorum* emergence, throughout May [R. G. White, R. D. Cameron, and K. Gerhart, unpublished observations], this was associated with heavy use by those pregnant females of the Porcupine herd that were in this area, fairly close to the calving grounds. Alternatively, timing of caribou migration may fail to allow pregnant females to meet changes in timing of green-up, even if their migration pattern changes, which could result in an inability

of females to obtain sufficient nutrients and energy for efficient lactation. This would increase the mortality rate of calves. If plant phenology is also truncated then a decrease in pregnancy rate of lactating cows would be predicted in autumn. This would result in a decrease in overall herd productivity and, ultimately, herd size.

ENHANCEMENT OF CARIBOU PRODUCTIVITY BY CLIMATIC EFFECTS

Finally, caribou may adapt to changing climate and increase herd productivity and herd size because of a longer plant growing season. In this scenario, herd size would increase to the full carrying capacity of the range and any further ecological perturbations could then result in a drastic herd decline. Unless herd size were constrained to carrying capacity by factors extrinsic to forage, the population would exceed the capacity of the range and decrease rapidly from nutritional stress.

We have not considered factors such as competition from other herbivores, predation, or insect harassment in our assessment of the potential effects of global warming on calving caribou. All factors would modulate herd responses irrespective of the nutritional effects.

ACKNOWLEDGMENTS

Warren G. Eastland was the recipient of a stipend from the Alaska Cooperative Wildlife Research Unit funded by the USF&WS (RWO #27). The authors thank many colleagues at the Institute of Arctic Biology for discussion and input to this paper.

LITERATURE CITED

- Cameron, R. D., W. T. Smith, and S. G. Fancy, Comparative body weights of pregnant/lactating and non-pregnant female caribou, in *4th North American Caribou Workshop, Proceedings*, edited by C. Butler and S. P. Mahoney, pp. 109-114, Newfoundland and Labrador Wildlife Division, St. John's, Newfoundland, 1991.
- Eastland, W. G., R. T. Bowyer, and S. G. Fancy, Effects of snowcover on calving site selection of caribou, *J. Mammal.*, 70, 824-828, 1989.
- Fancy, S. G., L. F. Pank, K. R. Whitten, and W. L. Regelin, Seasonal movements of caribou in Alaska as determined by satellite, *Can. J. Zool.*, 67, 644-650, 1989.
- Fleck, E. S., and A. Gunn, Characteristics of three barren-ground caribou calving grounds in the Northwest Territories, *N.W.T. Wildl. Serv. Prog. Rept.* 7, 1-158, 1982.
- Foster, J. L., The significance of the date of snow disappearance on the arctic tundra as a possible indicator of climate change, *Arct. Alp. Res.*, 21, 66-70, 1989.
- Kelsall, J. P., The migratory barren-ground caribou of Canada, *Can. Wildl. Serv. Monogr. No.* 3, 1968.
- Klein, D. R., Tundra ranges north of the boreal forest, *J. Range Manage.*, 23, 8-14, 1970.
- Klein, D. R., Factors influencing forage quality for reindeer, in *Wildlife-Livestock Relationships Symposium, Proceedings 10*, edited by J. M. Peek and P. D. Dalke, pp. 383-393, Univ. Idaho, For., Wildl., and Range Exp. Sta., Moscow, ID, 1982.
- Kuopat, P. J., Foraging behavior on a calving ground in northwestern Alaska, M.S. Thesis, 95 pp., Univ. Alaska, Fairbanks, 1984.
- Kuopat, P. J., and J. P. Bryant, Foraging behavior of cow caribou on the Utukok calving grounds in northwestern Alaska, in *Proc. Internat. Reindeer/Caribou Symp., Røros, Norway. 1979*, edited by E. Reimers, E. Gaare, and S. Skjenneberg, pp. 64-70, Direktoratet for vilt og ferskvannsfisk, Trondheim, 1980.
- Lenvik, D., E. Bo, and A. Fjellheim, Relationship between the weight of reindeer calves in autumn and their mother's age and weight in the previous spring, *Rangifer*, 8, 20-24, 1988.
- Reimers, E., Reproduction in wild reindeer in Norway, *Can. J. Zool.*, 61, 211-217, 1983.
- Rognmo, A., K. A. Markussen, E. Jacobsen, H. J. Grav, and A. S. Blix, Effects of improved nutrition in pregnant reindeer on milk quality, calf birth weight, growth, and mortality, *Rangifer*, 3, 10-18, 1983.
- Skogland, T., The effects of food and maternal conditions on fetal growth and size in wild reindeer, *Rangifer*, 4, 39-46, 1984.
- Skogland, T., The effect of density dependent resource limitation on the demography of wild reindeer, *J. Animal Ecol.*, 54, 359-374, 1985.
- Skogland, T., Comparative social organization of wild reindeer in relation to food, mates, and predator avoidance, *Advances in Ethol.* 29, 74 pp., 1989.
- Skoog, R. O., Ecology of caribou (*Rangifer tarandus granti*) in Alaska, Ph.D. Thesis, University of California, Berkeley, 1968.
- Thomas, D. C., The relationship between fertility and fat reserves of Peary caribou, *Can. J. Zool.*, 60, 597-602, 1982.
- Tyler, N. J. C., Fertility in female reindeer: the effects of nutrition and growth, *Rangifer*, 7, 37-41, 1987.
- White, R. G., Foraging patterns and their multiplier effects on productivity of northern ungulates, *Oikos*, 40, 377-384, 1983.
- White, R. G., Nutrition in relation to season, lactation and growth of north temperate deer, in *Biology of Deer*, edited by R. E. Brown, Springer-Verlag, New York, 1990.
- White, R. G., and J. R. Luick, Glucose metabolism in lactating reindeer, *Can. J. Zool.*, 54, 55-64, 1976.
- White, R. G., and J. R. Luick, Plasticity and constraints in the lactational strategy of reindeer and caribou, *J. Zool. Soc. London*, 51, 215-232, 1984.
- White, R. G., and J. Trudell, Patterns of herbivory and nutrient intake of reindeer grazing tundra vegetation, in *Proc. Internat. Reindeer/Caribou Symp., Røros, Norway. 1979*, edited by E. Reimers, E. Gaare, and S. Skjenneberg, pp. 180-195, Direktoratet for vilt og ferskvannsfisk, Trondheim, 1980.
- White, R. G., F. L. Bunnell, E. Gaare, T. Skogland, and B. Hubert, Ungulates on Arctic Ranges, in *Tundra Ecosystems: A Comparative Analysis*, IBP Vol. 25, edited by L. C. Bliss, O. V. Heal, and J. J. Moore, pp. 397-483, Cambridge University Press, Cambridge, 1981.

AD-P007 326



92-17830



Growing Season Length and Climatic Variation in Alaska

B. S. Sharratt

USDA-ARS, University of Alaska Fairbanks, Fairbanks, Alaska, U.S.A.

ABSTRACT

The growing season has lengthened in the contiguous United States since 1900, coinciding with increasing northern hemispheric air temperatures. Information on growing season trends is needed in arctic regions where projected increases in air temperature are to be more pronounced. The lengths of the growing season at four locations in Alaska were evaluated for characteristic trends between 1917 and 1988. Freeze dates were determined using minimum temperature criteria of 0° and -3°C. A shortening of the season was found at Sitka and lengthening of the season at Talkeetna. The growing season shortened at Juneau and Sitka during the period 1940 to 1970, which corresponded with declining northern hemisphere temperature. Change in the growing season length was apparent in the Alaska temperature record, but the regional tendency for shorter or longer season needs further evaluation.

INTRODUCTION

Studies related to the change in the northern hemisphere mean temperature indicated trends for increased temperatures during the last century [Hansen and Lebedeff, 1987]. Similar observations were made in the Alaskan temperature record [Juday, 1984]. Climate simulations project the possibility of the warming trend continuing with a more pronounced increase in temperature at higher latitudes [Manabe and Stouffer, 1980].

The growing season of the midwestern United States has apparently lengthened since 1900 [Changnon, 1984; Skaggs and Baker, 1985] coinciding with warmer northern hemispheric temperatures during this time. Brinkman [1979] found a lengthening of the growing season using a maximum temperature criteria and shortening of the season using a 0°C minimum temperature criteria for determining the season length. The lengthening of the season since 1900 has been largely due to a tendency for earlier last spring freezes [Changnon, 1984; Skaggs and Baker, 1985]. Since the peak of the northern hemisphere temperature in 1940, a shortening of the growing season in the midwestern [Brown, 1976; Moran and Morgan, 1977] and eastern U.S. has been observed [Pielke et al., 1979]. Skaggs and Baker [1985] found no evidence for such a shortening of the growing season since 1940 in Minnesota.

The Alaska temperature record was utilized to determine the characteristic trend of the growing season in a subarctic region. Changes in the season may be more dramatic than studies elsewhere due to the projected latitudinal differences in temperature.

METHODS

The source of data used for this study was Climatological Data, Alaska (U.S. Department of Commerce). Climate station records were searched to ascertain stations having a long, homogeneous and stable history. Four stations were chosen for analysis. The length of record common among the stations was 1917 to 1988.

Characteristics of the climate stations are tabulated in Table 1 and locations within Alaska mapped in Figure 1. All stations have been relocated since 1917. Homogeneity of the growing season length time series was evaluated using data from neighboring stations. Between five and ten years of data prior to and after the station move year were available for two to three neighboring stations. A t test on the difference series formed between the station used in this study and each of the neighboring stations indicated homogeneity for all comparisons.

The length of the growing season was defined as (1) the number of days between the last occurrence in spring and first in fall of a 0°C minimum air temperature and (2) the

Station	Latitude ¹	Longitude ¹	Elevation ¹ (m)	Moves ²			Description
				No.	Range of elevation (m)	Range of distance (m)	
Juneau	58° 18'N	134° 24'W	24	3	0	500	Established 1881. Present population 19,500. Surrounding terrain is steep, heavily wooded and in proximity to ocean.
Sitka	57° 03'N	136° 20'W	20	3	11	1610	Established 1842. Present population 7800. Topography is rolling with mountains and in proximity to ocean.
Talkeetna	62° 18'N	150° 06'W	105	3	3	800	Established 1917. Present population 300. Topography is slightly rolling and forested.
Fairbanks	64° 51'N	147° 52'W	140	2	8	80	Established 1904. Present population 22,600. Terrain is rolling with forest and cropland. Discontinuous permafrost.
¹ Present location ² Since 1917							

Table 1. Characteristics of climate stations used in the analysis of growing season length in Alaska.

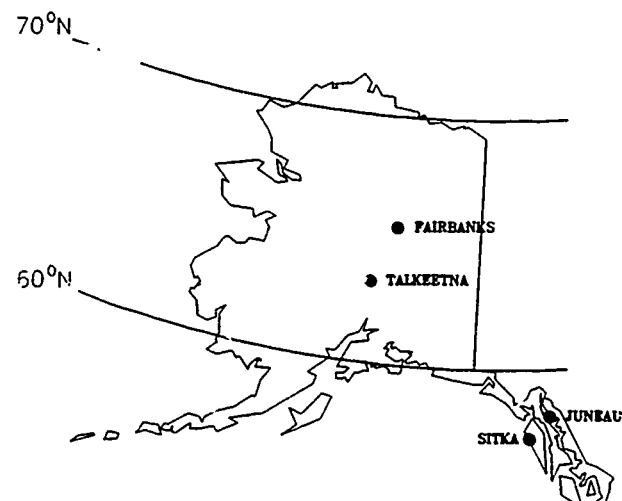


Figure 1. Locations of climate stations in Alaska used to determine trends in the growing season length between 1917 and 1988.

same as the previous definition except for an occurrence of a -3°C minimum temperature. The first definition has been used by others [Moran and Morgan, 1977; Brinkmann, 1979; Skaggs and Baker, 1985] and the last corresponds to the approximate temperature at which plant tissue freezes [Nath and Fisher, 1971]. All months of the growing season were searched for the occurrence of the minimum temperatures. In some years, a minimum temperature occurred

during the summer months (July and August) and the length of the growing season was the greatest number of consecutive days between the occurrence of the minimum temperatures.

The beginning and end of the growing season in years with missing daily temperatures were interpolated using neighboring stations with similar temperature characteristics. Data from neighboring stations having the highest correlation in daily minimum temperature prior to and following the missing records were generally used to assess freeze dates. Data analysis with and without the reconstructed freeze dates indicated identical trends in growing season length. Time trends in growing season length for the full record were evaluated using two methods. The first consisted of a linear regression analysis on the unsmoothed data of growing season length versus year. Second, the data were split in half (1917–1952 and 1953–1988) and the means compared using a small sample *t* test.

RESULTS AND DISCUSSION

The trend in the length of the season is represented in Figure 2 by a 7-year running mean. Trends in the full length of record are apparent at Sitka and Talkeetna. The slope estimates of the growing season length time series at the four stations are reported in Table 2. There was no change in the length of the season at Juneau and Fairbanks; however a change had occurred at Sitka and Talkeetna. The growing season (0°C) had decreased by 15 days at Sitka and lengthened 49 days at Talkeetna over the 70-year period of record. These trends were similar for both methods of defining the growing season (0°C and -3°C minimum temperature criteria).

Station	Slope ¹			
	1917-1988		1940-1970	
	-3°C	0°C	-3°C	0°C
Juneau	-0.13	0.02	-0.63	-1.06*
Sitka	-0.08	-0.21*	-1.10*	-0.37
Talkeetna	0.39**	0.68**	0.30	0.46
Fairbanks	0.05	0.17	0.11	-0.33

¹ **, * indicate significance at a probability level of 0.05 and 0.10, respectively.

Table 2. Slope estimates of time series of growing season length (days yr⁻¹) at four stations in Alaska, 1917-1988 and 1940-1970.

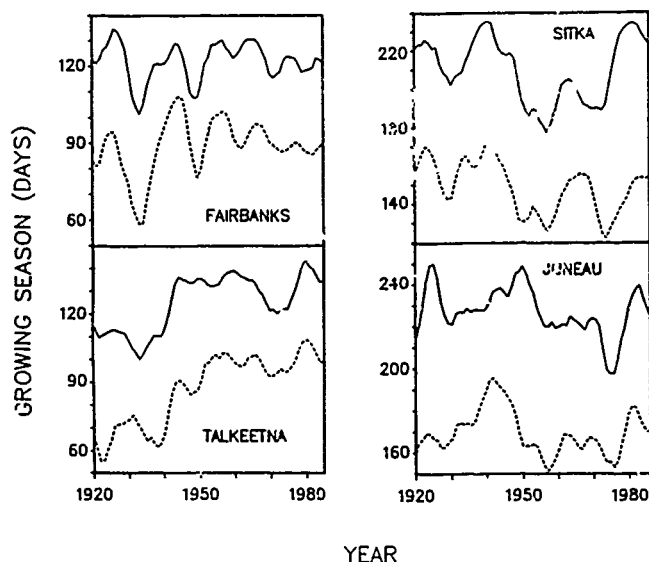


Figure 2. Variation in the length of the growing season (criteria: 0°C lower line, -3°C upper line) at four locations in Alaska, 1917-1988.

Station	Difference ¹	
	-3°C	0°C
Juneau	11.4	6.5
Sitka	10.3	11.4*
Talkeetna	-15.0**	-26.6**
Fairbanks	-5.1	-7.9

¹ **, * indicate probability levels of 0.05 and 0.10, respectively.

Table 3. Difference in the growing season length between the periods 1917-1952 and 1953-1988 at four stations in Alaska.

Differences in the characteristics of the growing season when grouped by first and second halves of the record (1917-1952 and 1953-1988) are summarized in Table 3. The length of the season was shorter for the latter part of the record at Sitka. In contrast, the season was longer for the second half of the record at Talkeetna.

Observations of the northern hemisphere mean temperature have indicated a warming from the 1880s to 1940s and a cooling from the 1940s to the early 1970s [Hansen and Lebedeff, 1987]. Similar temperature characteristics were observed in Alaska with a recent warming since the early 1970s [Juday, 1984]. The period of cooling during 1940-1970 was substantiated by an apparent shortening of the growing season at most climate stations during those years (Figure 1). Slope estimates of the time series analysis on the growing season length was tabulated in Table 2. A shortening of the season from 1940 to 1970 was found at all stations except Talkeetna, and the slope was discernible only at Juneau and Sitka.

CONCLUSIONS

The length of the growing season in Alaska during the last 72 years has shortened at Sitka and lengthened at Talkeetna. More evidence is needed to discern if these trends are associated with a regional grouping pattern.

REFERENCES

- Brinkmann, W. A. R., Growing season length as an indicator of climatic variations?, *Climatic Change*, 2, 127-138, 1979.
- Brown, J. A., Shortening of growing season in the U.S. corn belt, *Nature*, 260, 420-421, 1976.
- Changnon, S. A., Jr., Climate fluctuations in Illinois: 1901-1980, *Bulletin 68*, pp. 34-37, Illinois State Water Survey, 1984.
- Hansen, J., and S. Lebedeff, Global trends of measured surface air temperature, *J. Geophys. Res.*, 92, 13345-13372, 1987.
- Juday, G. P., Temperature trends in the Alaska climate record: Problems, updates, and prospects, in: *The Potential Effects of Carbon Dioxide-Induced Climatic Changes in Alaska*, edited by J. H. McBeath, pp. 76-89, University of Alaska Agricultural Experiment Station Misc. Publ. 83-1, 1984.
- Manabe, S., and R. J. Stouffer, Sensitivity of a global climate model to an increase of CO₂ concentration in the atmosphere, *J. Geophys. Res.*, 85, 5529-5554, 1980.
- Moran, J. M., and M. D. Morgan, Recent trends in hemispheric temperature and growing season indices in Wisconsin, *Agric. Meteorol.*, 18, 1-8, 1977.
- Nath, J., and T. C. Fisher, Anatomical study of freezing injury in hardy and non-hardy alfalfa varieties treated with cytosine and guanine, *Cryobiology*, 8, 420-433, 1971.
- Pielke, R. A., T. Styles, and R. M. Biondini, Changes in growing season, *Weatherwise*, 32, 207-210, 1979.
- Skaggs, R. H., and D. G. Baker, Fluctuations in the length of the growing season in Minnesota, *Climatic Change*, 7, 403-414, 1985.
- U.S. Department of Commerce, *Climatological Data, Alaska*, National Oceanic and Atmospheric Administration, Environmental Data Service, National Climatic Center, Asheville, NC, 1917-1987.

Ecological Aspects in Construction of West Siberian Oil Field Surface Facilities

I. D. Scvortzov and P. N. Crushin

State Scientific Research and Design Institute of Oil and Gas Industry, GIPROTYUMENNEFTEGAS, Tyumen, U.S.S.R.

ABSTRACT

The exploitation of arctic regions, where permanently frozen grounds are widespread, leads to problems concerning the climate and the geo-cryological environment. One of the most urgent tasks is to minimize effects on the environment, otherwise irreversible, catastrophic processes, the deterioration of permafrost into swamps, fouling subsoil waters and rivers, ground surface pollution with petroleum products, and destruction of fish and birds, may occur.

The measures aimed at providing the environmental ecological equilibrium during the exploitation of the northern oil deposits of West Siberia are described in this paper. These measures are worked out during the design stage. Then appropriate engineering decisions and product procedures are chosen, where much prominence is given to reliability of the oil and gas field facilities.

The paper includes information about developing measures for the preventive systematic maintenance of the oil pipelines, maintenance schedule, prediction of accidents and certain procedures for their rectification.

The Effects of Geographical Latitude on the Dynamics of Medical Data

I. V. Naborov

1st Moscow Medical Institute, GTK, Moscow, U.S.S.R.

T. K. Breus

Institute of Space Research, Moscow, U.S.S.R.

ABSTRACT

Polar regions play an increasing social and economic role in human life. It is also known that they are not the most favorable places for human beings to live. There are some examples which show that the frequency and seriousness of different illnesses increases with the increasing geographical latitude. In the northern regions seasonal amplitudes of illnesses are notably increasing. At the same time it was found that the higher the latitude, the higher the degree of solar activity influence on a number of illnesses, such as cardiovascular and nerve diseases, reaching its maximum level at auroral latitudes. Such geographical distributions of sickness rate have a reasonable explanation. In auroral latitudes the influence of corpuscular radiation (solar wind) on the Earth's magnetosphere and its electrodynamics is demonstrated vividly. Investigation of similar influences on biological objects in polar regions within the program "Global Change" is necessary and may also include other physical or social factors. In such cases medical emergency data play a role in the search for biotropic external influences.

AD-P007 327



The Commons Game: A Lesson in Resources Management

Carla A Kirts

School of Agriculture and Land Resources Management, University of Alaska Fairbanks, Fairbanks, Alaska, U.S.A.

Mark A. Tunio

Department of Civil Engineering, University of Alaska Fairbanks, Fairbanks, Alaska, U.S.A.

ABSTRACT

The Commons Game was developed to demonstrate behavioral patterns involved in individual decision-making regarding commons property and it has been used in various psychology courses. In this study the game was used to teach university students the complexities and frustrations of managing commons property natural resources. More specifically the purpose of the study was twofold: to determine the extent to which the game, when used in a natural resources management context, meets the teaching objectives of the game as specified by the game's developer; and to determine whether the game is an effective teaching tool.

The sample population was composed of 36 students enrolled in ALR/EQS 193 during the Spring 1989, Fall 1989, and Spring 1990 semesters. The team-taught course contains three elements: an introductory lecture, the game, and a postgame analysis session. Data were obtained from students' opinions of instruction, content analyses of students' three- to five-page essays, and observations recorded during the postgame analysis/discussion session. A brief description of the game is included in the paper, but details are intentionally omitted because the game is copyrighted.

The game met its teaching objectives when used in a natural resources management context and in combination with an introductory lecture and postgame analysis session. Topics discussed in student essays were the best evidence that the game met the objectives of producing an understanding of social trapping and illustrating trust versus greed. Frustration with the social dilemma was evident according to faculty observations made during the game conferences and throughout the postgame analysis session. From the students' opinions of instruction, the game appears to be an effective teaching tool. Students rated the game as a valuable learning experience. From a faculty perspective, the game provides an accurate, realistic model of natural resources management and is an effective instructional tool.

Further study is warranted to determine the actual decision-making patterns players use in trying to solve the game's dilemma. Associating these patterns of play with real world resource decision-making patterns would be an ultimate goal.

INTRODUCTION

The Commons Game [Powers et al., 1983] was developed to demonstrate behavioral patterns involved in individual decision-making regarding commons property.

Its creators "sought a more experiential approach to teaching about social traps" [Powers, 1985/86, p. 3]. It has been used in psychology classes and analyzed from several perspectives [Powers and Boyle, 1983; Powers, 1987]

92-17831



including its effectiveness in promoting students' understanding of the commons dilemma [Powers, 1985/86; Kirts et al., 1991]. In this study the Commons Game was used to teach university students the complexities and frustrations of managing commons property natural resources.

For purposes of this study, "commons property natural resources" were defined as natural resources which, in theory, are "owned" by everyone but, in reality, "owned" by no one. Examples include air, oceans, sunshine, and public lands such as national parks and national forests. Most often, these resources are exploited due to human greed and lack of incentives to act otherwise [Hardin, 1968; Haefele, 1974; Hardin and Baden, 1977; Cutter et al., 1985]. Effective management of public domain resources, particularly on a global scale, will be a major concern for future generations. This is especially evident in light of recent efforts to enhance public participation in decision-making processes affecting public domain natural resources management.

PURPOSE OF THE STUDY

The purpose of the study was twofold: to determine the extent to which the Commons Game, when used in a natural resources management context, meets the teaching objectives of the game as specified by the game's developer; and to determine whether the game is an effective teaching tool. According to Powers [1985/86], the objectives of the game are:

- to produce an understanding of the social trapping character of a commons, i.e., that short-term, individual gain tends to dominate long-term collective gain;
- to illustrate the importance of trust when one's gains are dependent not only on what one does but also on what others do; and
- to allow students to experience the difficulties and frustrations of attempting to solve the commons dilemma with only a small amount of control over others' actions (p. 5).

METHODOLOGY

The sample population was composed of students enrolled in Agriculture and Land Resources/Environmental Quality Science (ALR/EQS) 193—Commons Property Resource Decision Making—during the Spring 1989, Fall 1989, and Spring 1990 semesters (N=36), at the University of Alaska Fairbanks. ALR/EQS 193 is a freshman-level course designed to acquaint students with concepts and issues associated with management of commons property natural resources. The course is team-taught by an environmental engineer and a natural resources educator, worth one semester credit, and scheduled to permit three-hour class sessions.

The course contains three elements: an introductory lecture, the game, and a postgame discussion session. The three-hour lecture includes:

- definitions (including relationships between and among) of natural resource, management, conservation, and commons;
- fundamental management concepts including the conservation philosophy continuum, the basis of management, natural resources classification, ecosystems and "ecological balances," carrying capacity, sustained yield, the tyranny of geography [Bennett, 1983], the

three E's of natural resources management (ecology, economics, and emotions), and who manages natural resources in the United States; and

- concepts pertaining to the commons such as historical perspectives, the need for management, population effects, the role of technical fixes [Hardin, 1968], individual rights versus responsibilities, and examples of commons resources and issues.

The postgame discussion outline includes topics such as trust, greed, individual versus social decision-making, effects of uncertainty, the role of reward and incentives/motives, goal perception, values, and application of the game to the real world of resources management. To culminate the experience, students are required to prepare a three- to five-page essay explaining their final thoughts and conclusions regarding the commons dilemma.

Data were obtained from students' opinions of instruction, a content analysis of essays, and observations made by faculty during the postgame discussion session. The opinion-of-instruction survey was instructor designed. Students were asked to place an "X" on a continuum labeled at the end-points from 0 to 10 to indicate his/her rating of nine statements related to the course. Essays were graded according to 10 elements, each worth a possible four points: neatness, organization, content documentation, grammar, errors, conciseness, analysis, logic/support, and general effect.

Only descriptive statistics are reported in this paper because the participants were "captive" and not randomly selected [Tuckman, 1978], class sizes varied substantially (from 4 to 19), and trends instead of comparisons were the focus of the study. All data analyses were performed using a Macintosh PC with StatWorks software.

THE GAME—HOW IT IS PLAYED

The Commons Game is copyrighted. This description will not contain details such that the game could be replicated. A copy of the game may be purchased from Dr. Powers (see References).

All rules are given via prepared scripts. Four- to six-person groups make concealed, individual plays of colored cards representing various management options one can impose on the commons (Table 1). Points are awarded to individual players according to the card played and its subsequent value (or penalty) derived from the rules or a payoff matrix developed to represent the current state of the commons (Table 2). As the commons is threatened, the payoff matrix reflects fewer point gains, thus indicating lowered productivity. The more times the exploitation card is played, the faster the payoffs for both exploitation and cooperative use decline. The state of the commons may be improved by playing the resource enhancement card, but rehabilitation occurs more slowly than exploitative decline.

Players are told to accumulate the maximum number of points and that the player with the highest number of points will receive \$5. The words "win" or "winner" are never used by the game directors. Players are also told the game will continue for 60 rounds; however, the game is stopped at 50 rounds to offset possible end-effects such as last-minute hoarding.

Periodic three-minute conferences are allowed during the game. The group may change any rules of the game with the

Card Color	Management Action	Effect
Green	Intensive Use, Exploitation	From payoff matrix (high points), Commons down per green card played
Red	Wise Use, Conservation	From payoff matrix (medium points)
Black	Enforcement, Police Action	-6 divided among black card players; Green card players lose 20 each
Orange	Rehabilitation, Resource Enhancement	-6 divided among orange card players; Red card players gain 10 each; Commons up one hole if no green(s)
Yellow	Non-use, Preservation	+6 to each yellow card player

Table 1. Management Options and Point Structure of The Commons Game.

exception of the point structure. For instance, shields concealing each individual's play could be removed, the \$5 could be divided equally among all players, and/or green cards could be collected. Also, randomly assigned "natural events" may occur during the game that improve or degrade the commons.

RESULTS

Twenty-nine males and seven females participated in the course during the study period. During the Fall 1988, Spring 1989 and Fall 1989 semesters, 19, 13 and 4 students, respectively, were enrolled for a total of 36 students. There was a mix of class standings represented: 12 seniors, 8 juniors, 7 sophomores, 3 freshmen, 2 graduate students, 3 unclassified and 1 professional. Twenty-four of the students had previous or concurrent instruction and/or experience in natural resources management. The mean number of semester credits in which the students were concurrently enrolled was 13.49 (a full-time semester is 12 credits) with a 3.10 semester grade point average (GPA) on a 4-point scale. Their university-career, cumulative GPA up through the semester in which ALR/EQS 193 was taken was 2.98.

All 36 students played the game, 32 prepared a student opinion of instruction form, and 34 submitted essays (two students audited). The means and minimum/maximum scores for each item on the instructor-designed opinion of

instruction survey are given in Table 3. On a 10-point continuum, the lowest mean (3.36) occurred for "How much experience in commons resources decisions I had prior to the course" while the highest mean (8.14) occurred for "How effective the postgame/postlecture analysis reflected the concepts of commons property management." The next highest mean (7.86) was for "How effective the game was in representing commons concepts."

Of 40 possible points, the mean score for the essays was 34.44, with a range from 24 to 40. All means for each of the 10 essay elements were above 3.5 on a 4-point scale except for errors, grammar, and documentation. Final scores tended to be pulled down by the mechanics of essay preparation rather than by content or logic. The papers ranged from 406 to 1668 words with a mean of 975.8 words.

As shown in Table 4, essays contained a variety of topics. The most often discussed topics were social trapping dilemmas, possible solutions, real world examples of commons resources problems, gaming strategy and definition of "commons." Uncertainty and decision-making were seldom discussed.

Because this study is only the beginning of a long-term approach to studying the Commons Game, some generalizations from faculty observations of student behaviors during the game and the postgame analysis session are presented. These should not be interpreted as hard data; instead they provide insight into understanding data presented herein or provide impetus for future studies aimed at determining the game's instructional effectiveness and the decision-making patterns and strategies of the players. These observations are woven, as appropriate, into the discussion section of this paper.

CONCLUSIONS AND DISCUSSION

The student sample in this study appeared to be average given credit load and GPA. The group was diverse with respect to class standing. While the sample was 80% male, the conclusions of this study should not be confounded or skewed. According to Powers and Boyle [1983], males and females do not differ in their approach to the game.

The game met its teaching objectives when used in a natural resources management context and in combination with

Number of Red Cards Played in the Round	Points Received by Red Play	Points Received by Green Play
0	--	100
1	40	102
2	42	104
3	44	106
4	46	108
5	48	110
6	50	---

Table 2. Payoff Matrix with the Commons at a Zero State.
(The state of the commons can range from -8 to +8, including 0.)

Statement	Mean*	Min/Max
How much knowledge of natural resources I had prior to this course	5.64	1.0/9.0
How much experience in natural resources management I had prior to this course	4.25	0.0/10.0
How much knowledge of commons resources I had prior to this course	4.45	0.0/9.0
How much experience in commons resources decisions I had prior to this course	3.36	0.0/9.0
How much effort I put into this course compared to my other courses	5.40	1.0/9.0
How much this course challenged me	6.75	3.0/10.0
How much I learned from this course	7.37	2.0/10.0
How effective the game was in representing commons concepts	7.86	1.5/10.0
How effective the postgame/postlecture analysis reflected the concepts of commons property management	8.14	5.0/10.0

 *Based on a 10-point continuum.

Table 3. Means and minimum/maximum scores for the Student Opinion of Instruction.

an introductory lecture and postgame analysis session. Topics discussed in student essays were the best evidence that the game met the objectives of producing an understanding of social trapping and illustrating trust versus greed. Frustration with the social dilemma, the third teaching objective, was evident according to faculty observations made during the game conferences and throughout the postgame analysis session.

In every postgame discussion session, students made personal reference to the frustration and futility of trying to solve the commons problem without everyone's cooperation. General observations support Powers' [1987] conclusion that communication (i.e., conferencing) tends to improve cooperation for a while; however, this study revealed that communication may break down as the

commons improves and the temptation for defaulting on the agreed cooperative arrangement increases. At this point, players personally experienced the frustration and complexity of managing a commons.

Ending the game at 50 rounds, rather than the 60 players were initially told, provides an excellent means of avoiding an end-effect. Several teams specifically planned for the end of the game and plans tended to reflect a "catch-as-catch-can" or "every-man-for-himself" attitude, regardless of the state of the commons. The next generation was seldom considered. Further studies designed to allow one team to begin where a previous team left off may more realistically simulate long-term management. Long-term vision was not a popular topic in student essays or during the analysis sessions, while on the other hand, the dilemma of managing commons resources revolves around providing for the next generation.

Another method of providing a time perspective is to begin the game at a randomly selected starting point—not always at zero, a somewhat steady state. After all, most commons are in trouble because they are not in a steady state. Therein lies the management problem.

From the student opinions of instruction, the game appears to be an effective teaching tool. Students had little experience or knowledge of commons resources management and decision-making and, on the student opinion of instruction, rated the game as a valuable learning experience.

From a faculty perspective, the game provides an accurate, realistic model of natural resources management and is an effective instructional tool. The original objectives of the game can be met when the game is used in a natural resources management context and in conjunction with an introductory lecture and postgame analysis. Further study is warranted to determine the actual decision-making patterns players use in trying to solve the game's dilemma. Associating these patterns of play with real world resource decision-making patterns would be an ultimate goal.

Topic	Frequency*
Social trapping dilemma (individual versus society)	24
Possible solutions to commons management	24
Real world examples of commons resource problems	21
Strategy used to play The Commons Game	19
Definition of "commons"	17
Overpopulation and carrying capacity	14
Human greed versus trust	14
Individual rights and freedom	14
Goal of resource management	10
Long/short term vision and planning	9
Concept of "winning"	8
Uncertainty	4
Decision making	2

 *N=34; mean number of topics per essay, 5.35 with a range of 2-9.

Table 4. Number of essays containing selected topics.

REFERENCES

- Bennett, C. F., *Conservation and Management of Natural Resources in the United States*, John Wiley & Sons, New York, 1983.
- Cutter, S. L., H. L. Renwick, and W. H. Renwick, *Exploitation, Conservation, Preservation: A Geographic Perspective on Natural Resource Use*, Rowman & Allanheld, Totowa, NJ, 1985.
- Haefele, E. T. (Ed.), *The Governance of Common Property Resources*, Johns Hopkins University Press, Baltimore, 1974.
- Hardin, G. J., The tragedy of the commons, *Science*, 162, 1243-1248, 1968.
- Hardin, G. J., and J. Baden (Eds.), *Managing the Commons*, W. H. Freeman & Co., San Francisco, 1977.
- Kirts, C. A., M. A. Tumeo, and J. M. Sinz, The commons game: Its instructional value when used in a natural resources management context, *Simulation and Gaming: An International Journal of Theory, Design, and Research*, 22, 5-18, 1991.
- Powers, R. B., The commons game: Teaching students about social dilemmas, *Journal of Environmental Education*, 17, 4-10, 1985/86.
- Powers, R. B., Bringing the commons into a large university classroom, *Simulation and Games: An International Journal*, 18, 443-457, 1987.
- Powers, R. B., and W. Boyle, Generalization from a commons-dilemma game: The effects of a fine option, information, and communication on cooperation and defection, *Simulation and Games: An International Journal*, 14, 253-274, 1983.
- Powers, R. B., R. E. Duus, and R. S. Norton, The commons game. Unpublished manuscript (research version), Utah State University, Logan, 1983.
- Tuckman, B. W., *Conducting Educational Research*, New York: Harcourt Brace Jovanovich, 1978.
- Note: A copy of The Commons Game may be purchased from Dr. Richard Powers at P.O. Box 307, Oceanside, OR 97134.*

Section E:
**Ice Sheet, Glacier and Permafrost
Responses and Feedbacks**

Chaired by

M. Meier
University of Colorado
U.S.A.

F. Roots
Environment Canada
Canada

AD-P007 328



92-17832



State and Dynamics of Snow and Ice Resources in the Arctic Region Derived from Data in the World Atlas of Snow and Ice Resources

Vladimir M. Kotlyakov and Natalya N. Dreyer
Institute of Geography, U.S.S.R. Academy of Sciences, Moscow, U.S.S.R.

ABSTRACT

The compilation of the World Atlas of Snow and Ice Resources has been in progress in the Soviet Union for more than 15 years. The effort ranks as one of the most important glaciological projects ever undertaken because of its comprehensiveness and global scope. Several hundred of the most prominent scientists in the U.S.S.R., including 300 specialists from 40 research institutions, participated in the work. The United Nations Educational, Scientific and Cultural Organization (UNESCO) and many other researchers from many nations provided broad scientific assistance to the compilers of the Atlas by compiling various datasets, analyzing maps, and giving advice. The Atlas is a major contribution of the U.S.S.R. to the Hydrological Programme (IHP) and will also be presented by the Soviet Union to the International Geosphere-Biosphere Programme (IGBP), because many parameters associated with change in the cryosphere are included. The Atlas presents, in a systematic arrangement, comprehensive data and information about the global distribution of snow and ice, compiled since the early 1950s. The Atlas includes about 1000 maps, ranging in scale from 1:25,000 (local or individual glaciers) to 1:90,000,000. The maps in the Atlas are distributed throughout the 17 subject sections.

INTRODUCTION

The objective of the World Atlas of Snow and Ice Resources is to show the global occurrence of snow and ice, including all types of glacio-nival phenomena, the variability of these phenomena in the past, their present-day regime, and a means for predicting their future development [Kotlyakov, 1976].

The majority of regions included in the Atlas are located at either high altitudes or in the polar regions, where the distribution of stations is inadequate and field studies are limited. Comprehensive research was conducted throughout the process of compilation, and several new computational methods were developed to determine snow and ice parameters, especially in the characterization of the nature of inadequately studied regions of mountain glaciers. The methods were based on the concept of glacio-nival systems advanced recently in the U.S.S.R. [Kotlyakov and Krenke, 1979].

A glacio-nival system is a natural system in which snow and ice play a dominant role in its composition and

processes, thereby determining the development of the system and its interactions with the environment. Separate components of a glacio-nival system, for example glaciers and snow cover, may form independent systems and may be mapped as such.

Glacio-nival systems, and glacier systems as a specific case, can be characterized by a cartographic representation that includes several fundamental parameters, in which the generalized concept of the distribution of this or that characteristic of the system can be applied to a specific region. The patterns remain continuous despite the discrete nature of the points of occurrence from which they are computed and graphically plotted. The cartographic representation presents a certain abstraction, structured according to objective rules; it emphasizes the regularities of glacier systems caused by the impact of continuously distributed processes, such as climatic factors, but excludes the influence of random, discrete factors, such as orographic setting.

The main peculiarity of glacio-nival objects is the wide range in their spatial dimensions. The prevalence of small,

separately located mountain glaciers and their occurrence in small areas caused us to develop different ways of depicting them on maps of different scales, including the already mentioned cartographic representation of glacier systems.

Quantitative as well as qualitative properties of phenomena are depicted on small-scale maps in the Atlas. Quantitative characteristics make up the basic content of all the maps, plotted with the use of isolines of temperatures, precipitation, snow cover, and runoff. Maps of ice-formation zones, factors associated with avalanche occurrence, former glaciated areas, permafrost, and mudflow activity depict qualitative properties. On some maps qualitative categories are singled out on the basis of numerical features. Examples are: the degree of avalanche activity in relation to the density of an avalanche network and recurrence interval; the nature of glacier fluctuations with respect to the magnitude of glacier terminus fluctuations; and prevailing and accompanying type of glaciers, including reference to the relationship of glaciers of different types, all expressed as percentages.

Rather than discuss maps in all 17 subject sections of the Atlas, we shall address only three representative sections, including maps of snow cover, total runoff and meltwater runoff, and snow and ice storage. This will demonstrate graphically the resource-estimating objectives of the Atlas.

SNOW COVER MAPS

To compensate for the paucity of initial data, methods of grapho-analytical computations of the macroscale fields of the norms of snow storage and geographo-statistical computation methods of the main properties of snow resources have been worked out.

On the basis of joint interpretation of maps of the maximum water equivalent content of snow cover, the properties of its time variability, including duration of and conditions associated with snow cover existence, it became possible to characterize snow systems of the earth [Getker and Ivanovskaya, 1989]. In this paper we would like to analyze the peculiarities of snow systems which exist in polar regions and adjacent regions.

In the permanent snow systems of Antarctica and higher elevations of Greenland, snow accumulation occurs throughout the year, although annual snowfall amounts decrease when moving inland from the coastal areas. Maximum snow storage (expressed in water content equivalent) varies from 20 mm in the interior regions of Antarctica to 700 mm in the coastal mountains of western Antarctica and southwestern Greenland. The annual variability of snow accumulation in the inland areas is not large; the coefficient of variation C_v is 0.2–0.4, with values of norms up to 0.4–0.5, the latter the result of the frequent passage of cyclones.

Snow systems of the northern continental mountains embrace all the mountainous areas of the Arctic and subarctic and mountain ranges in the northern part of the temperate belt, including those situated under conditions of extreme continental climate. Typical snow systems are located in the Brooks and Mackenzie Mountains, on Ellesmere Island, the Verkhoyanskiy Range, Byrranga and Chersky Mountains, and in the polar Ural mountains. Well-pronounced temperature inversions are formed in the lower zones of these mountains; because of the duration of the cold period of 240–330 days varies very little all over the

entire region. The maximum snow storage is mainly determined by the annual amount of frozen precipitation. The values of snow storage exceed 35–40 cm of water equivalent only in the crestal zones, while in the internal valleys, screened by the lateral ranges, where a thin snow cover forms, the snow cover thickness is only 15–20 cm.

The main regularity in the distribution of maximum snow storage is the decrease when moving from the ocean or windward slope within a mountain massif, and insignificant increase with elevation. The altitudinal gradient does not exceed 5–15 mm of water equivalent for 100 m. Snow storage on the windward slopes usually exceeds snow storage on the leeward slopes by 5–15 cm of water equivalent.

The dominating anticyclonic regime of the weather in the winter produces a minimum year-to-year variability of snow storage, when compared with all other systems. The variation coefficient changes within limits of 0.15–0.30, and the mean square deviation of snow storage from the mean long-term values most frequently makes up only 2–6 cm. The duration of the existence of this type of systems is large, on the order of 200–300 days. The variations of the conditions of formation and disappearance of snow cover in mountain regions are insignificant, reaching 1.5 months only in the highest and most humid areas. The latitudinal trend in the change of snow resources' properties is insignificant.

Moving to the south of the polar region proper, it is worth mentioning that snow systems of the northern coastal mountains of western and eastern margins of the continents are widespread within the Alaska Range, and the Wrangell, Chugach, and St. Elias Mountains of Alaska and mountainous regions of Iceland and Scandinavia in northwestern Europe. These mountains are located along paths of intense maritime cyclones; thus the amount of frozen precipitation is much greater here when compared with previously mentioned regions in more continental locations. In the more southern parts of the mountains, combined with the heating effect of the nearby ocean, the range of duration of cold period can vary; therefore the maximum snow storage can vary within wide limits. The greatest amount of annual snowfall—more than 400 cm water content equivalent—accumulates in the mountains of southeastern Alaska, and in this region the areas of extreme snow accumulation are very extensive. The role of the latitudinal factors in the distribution of snow storage over the coastal windward slopes is insignificant. Thus, at latitude 60°N, on the Aleutian Ridge and on the western slopes of mountain ranges on Vancouver Island, at latitude 49°N, the range of altitudinal changes of the maximum snow storage is the same, 100–130 cm. Latitudinal zonation is completely manifested only in the intermontane highlands. The altitudinal gradient of snow accumulation in the near-crestal zone produces an increase in the annual total up to 10–40 cm for each additional 100 m in elevation. The year-to-year variability of the maximum snow storage grows abruptly: C_v changes from 0.2 up to 0.5, decreasing when moving inland away from the coast and with decreasing elevation.

The duration of snow cover also lengthens with increasing elevation, from 150 days to a full year (perennial snow). The minimum values are observed at the lower elevations of the "warmest" western coasts, while the maximum values are located in the accumulation areas of major glacier systems.

Mountain System	Area covered by computations	Total volume of river runoff km ³	The volume of melt runoff	
			km ³	% of total runoff
Mountains of Southeastern Alaska, Alaska Range, Alaska	440	486	340	70
Brooks Range, De Long Mountains, Alaska	220	65	53	82
Rocky Mountains, Canada & U.S.	442	224	109	49
Monashee, Cariboo, Selkirk, Percell Mountains, Canada	356	288	120	42
Coast Ranges, Cascade Range, Canada & U.S.	926	1270	491	39
Caucasus, U.S.S.R.	245	114	41	36
Pamir-Alai, U.S.S.R.	120	58	38	66

Table 1. Runoff Resources of Mountain Systems.

TOTAL RUNOFF AND MELT WATER RUNOFF

When compiling the various maps, the altitudinal relations between the total river runoff and meltwater runoff were widely used. Maps of snow accumulation areas were used to extrapolate meltwater runoff from the higher elevations of drainage basins. The lack of observational data and insufficient hydrological knowledge of the alpine areas forced us to widely use analysis of climatic maps of the glacio-nival zone, to estimate the periods of above-freezing temperatures and annual amount of liquid precipitation, and to prepare maps of annual snow storage and solid precipitation.

The Atlas presents an approximate evaluation of water resources from total river runoff, including its meltwater component, for many mountain systems, including Alaska (Table 1). The upper and lower limits of the meltwater runoff and also the values of altitudinal intervals, from which the computations of the runoff resources were made, were determined from the relationship of runoff to the altitude of the basin. The lower boundary of meltwater runoff depends on the limit of a stable snow cover. The position of the upper limit depends on the height of ranges which form the mountain system, the extent of glacierization, and the presence of heat resources throughout the ablation period. When identifying the upper boundary of meltwater runoff, we referred to glacioclimatic maps which show the areas where above-freezing temperatures are infrequent. Taking into account that even though the mean annual daytime temperature remains below 0°C, and melting may occur when daily summertime temperatures are above freezing, we singled out the areas which lack meltwater runoff within these areas [Ananicheva and Dreyer, 1989].

It is of interest to compare the values of the runoff in the mountain systems of Alaska with other regions. It can be seen from Table 1 that the proportion of meltwater runoff from snowpack and glaciers in the total river runoff increases in conjunction with continentality of the region, that is, increasing distance from influence of moisture-laden maritime airmasses and associated cyclonic activity. In the extremely continental regions of northern Alaska, especially in the Brooks Range and De Long Mountains, meltwater runoff makes up more than 80%; by comparison, in the Coast Ranges of western North America it is less than 40%. The largest share of meltwater runoff in the mountains of southeastern Alaska, about 70%, is related to an extremely high annual snowfall and the high degree of glacierization in this region.

The maximum values of runoff are typical for southeastern Alaska: total runoff in the altitudinal interval of 500–1000 m makes up 245 cm, while meltwater runoff above 1000 m is 193 cm. Maximum values of meltwater runoff are recorded on the northern slopes of the Caucasus, 235 and 229 cm respectively, but only for altitudes above 4000 m (Table 1). The difference in the amount of meltwater runoff in the two regions (southeastern Alaska and Caucasus, U.S.S.R.) is caused by the fact that heat resources during the ablation period, presented as the total degrees of above-freezing temperatures at the altitude of the equilibrium line on the northern slope of the Greater Caucasus (Bolshoi Kavkaz), make up 250–500°C, while in southeastern Alaska they range from 100–650°C. In the Caucasus, melting occurs in all the altitudinal ranges and above-freezing temperatures are recorded on the north slopes for 80 to 150 days annually. In southeastern Alaska the duration of the period with temperatures above 0°C is 55 to 120 days [Davidovich, 1988]; above 3100 m there is virtually no meltwater runoff. Thus the occurrence of meltwater runoff in regions of high snowfall is nearly completely dependent upon heat resources. This relationship is typical of meltwater runoff from glaciers, and the runoff of meltwater from snow depends on the water content and quantity of snowpack.

The total runoff and meltwater runoff, estimated from the altitudinal intervals and expressed in the water content equivalent, increases in conjunction with elevation, but as the areas of these intervals decrease along with increasing elevation, the distribution of the total and meltwater runoff resources is quite different. The maximum values coincide with the belt of 500–1000 m in mountains of southeastern Alaska; in the Coast Ranges they are at altitudes of 1000–2500 m, in the western and central Pamirs at 3000–4000 m, and in the eastern Pamirs at 4000–4500 m. In all cases, the contribution of meltwater runoff increases with elevation, eventually reaching 90% or more of the total.

We hope that the application of these newly developed cartographic methods to the study of predictive regularity in the distribution of meltwater runoff and total runoff resources in mountain systems and on macroslopes of the mountain system is useful. It allows us to identify the areas where the main part of meltwater resources are formed, which is very important for the development of nature- and water-protection measures, the selection of optimum reference sites for monitoring, etc.

SNOW AND ICE STORAGE

Glacio-nival resources are represented most completely on the Atlas maps of glaciological zonation and ice storage. Step-by-step zonation of the entire world, including small-scale zonation of the earth and medium-scale zonation of particular areas is included in the Atlas. It is significant for geography in general and is based on a combination of orographic, hydrological, and glaciological approaches. The zonation approach allows us to better understand glaciological peculiarities of the earth and to organize the computation of snow and ice resources in specific natural regions [Kotlyakov and Dreyer, 1984].

The maps of natural ice storage on scales from 1:1,500,000 to 1:7,500,000, accompanied by summation tables, give the general idea of the total areas and volumes of glaciers, the volumes and specific values of their annual meltwater runoff, and seasonal snow cover and the date of its maximum areal distribution in each of the regions. During compilation of the maps, evaluations of mean thickness of glaciers in various glacierized basins were carried out in conjunction with computations of the time interval (cycle) of ice mass throughout glaciers, an important index of glacier resources.

The area and volume of glaciers and sea ice and specific values of maximum snow storage are depicted on the map of the Arctic in water content equivalent. The areas of

glacierization, volume of glacier ice, specific values of meltwater from glaciers, and maximum snow storage, the mean thickness of glaciers, extent of glacierization, and the time interval for ice mass throughout the mountains, are shown on the map of southeastern Alaska for each region.

The content of the maps presented and several other maps in the World Atlas of Snow and Ice Resources make it possible to describe numerically the role of precipitation in the largest mountain-glacier regions of the Northern Hemisphere. The important role of liquid precipitation in the heat balance of maritime glaciers has been established. Dependence of global changes in snowfall on the processes of atmospheric circulation has also been established: the growth of snowiness in the northern and southern hemispheres is related to the prevailing meridional types of circulation, and its decrease is linked to the zonal type of circulation. Computations have shown that heat losses on the melting of seasonal snow cover make the rate of atmospheric heating three times slower than expected, while orographic conditions play a decisive role in the development of mountain glaciers.

The compilation of the maps of the World Atlas of Snow and Ice Resources has been completed. All maps are now being published in Moscow and in Kiev. Although the volume of maps is large, we hope that the Atlas will be released in 1993 and contribute to a better understanding of global change occurring in glacio-nival phenomena on earth.

REFERENCES

- Ananicheva, M. D., and N. N. Dreyer, Kartograficheskiye metody issledovaniya talogo snegovogo i lednikovogo stoka gornyykh stran [Cartographic methods of studying snow melt and glacier runoff from mountain systems], *Data of Glaciological Studies (DGS)*, 67, 49–55, 1989.
- Davidovich, N. V., Teplivyye resursy perioda ablyatsii v krupneishikh gorno-lednikovyykh stranakh vnepolyarnyykh shirot [Heat resources during the ablation period of the largest mountain-glacier systems in non-polar latitudes], *DGS*, 64, 134–145, 1988.
- Getker, M. I., and T. E. Ivanovskaya, Snezhniy pokrov v gornyykh sistemakh Zemli (opyt klassifikatsii) [Snow cover in the Earth's mountain systems], *DGS*, 67, 30–38, 1989.
- Kotlyakov, V. M., Zadachi sozdaniya Atlasa snezhno-ledovykh resursov mira [The main objectives in creating the World Atlas of Snow and Ice Resources], *Vestnik AN SSSR*, 10, 95–100, 1976.
- Kotlyakov, V. M., and N. N. Dreyer, Glavniye itogi rabot nad Atlasom snezhno-ledovykh resursov mira [The main results from compilation of World Atlas of Snow and Ice Resources], *DGS*, 51, 89–95, 1984.
- Kotlyakov, V. M., and A. N. Krenke, Nivalno-glyarsialnye sistemy Pamira i Gissaro-Alaya [Glacio-nival systems of the Pamirs and Gissar-Alai], *DGS*, 35, 25–33, 1979.

AD-P007 329



92-17833



Mass Balance of Antarctica and Sea Level Change

C. R. Bentley

Geophysical and Polar Research Center, University of Wisconsin-Madison, Madison, Wisconsin, U.S.A.

M. B. Giovinetto

Department of Geography, University of Calgary, Alberta, Canada

ABSTRACT

The overall mass balance of the Antarctic ice sheet has been estimated by comparison of the best available data on input in the form of snowfall with output in the form of ice flux through gates at or near the margin of the ice sheet. Surface melt is a negligible contributor to mass balance and has been ignored. Bottom melt under large ice shelves remains a major source of uncertainty. We conclude that there is probably an excess input of 2–25% of the total input, equivalent to a sea level lowering of 0.1–1.1 mm yr⁻¹. Although errors remain, it becomes increasingly clear that an antarctic contribution to current sea level rise is unlikely. We attribute a reported iceberg flux that is larger than the mass input to a non-equilibrium break-back of the fronts of the ice shelves.

INTRODUCTION

In this paper we have combined all the information we could find about the net mass balance of the Antarctic ice sheet. The approach we have used is to compare mass input values with corresponding mass output values where both are known, and then to extrapolate to the rest of the ice sheet in several ways.

We have used primarily the nomenclature, mass inputs, and areas of drainage systems given by Giovinetto and Bentley [1985], modified in minor ways. Values for mass inputs and areas cited without reference are from this source. Those mass inputs are, we believe, the most accurate (as well as the smallest) estimates available for reasons given by Giovinetto and Bentley [1985], Giovinetto and Bull [1987], and Giovinetto et al. [1989]. However, differences between compilations are not great in most places, and where other authors have estimated net mass balances for particular drainage systems (or parts of systems) we usually have used their estimates without modification. The one major difference from Giovinetto and Bentley [1985] is in the Lambert Glacier drainage basin, for reasons explained below.

BALANCE MEASUREMENTS

In this section the observations are summarized in three groups: systems with input and outflow on the inland

(grounded) ice; systems entirely on an ice shelf, and combined systems that include both inland and ice shelf ice but without measurements at the grounding line. The most desirable measurement in regard to sea level change would include output flux precisely across a grounding line. In actuality, output is usually measured either some distance inland of the grounding line or at or near the front of an ice shelf. In the latter case, some interpretation of the regimen of the ice shelf, particularly the rate of bottom melting, is necessary in order to estimate the net mass balance inland of the grounding line. The ice shelf systems are, of course, irrelevant for the direct determination of sea level change since they are already in the ocean, but they are included because measurements on ice shelves are an aid to interpreting the third type of system wherein the output is known only at the front of an ice shelf.

Many geographic names are cited in this section—too many to show on a small map. All can be approximately located by the drainage systems in which they occur (Figures 1–4).

Inland Ice Only

See Table 1 and Figure 2.

Jutulstraumen (in system K'A). The outflow is from Van Autenboer and Declair [1978]. The input was found by multiplying the total estimated input for the encompassing

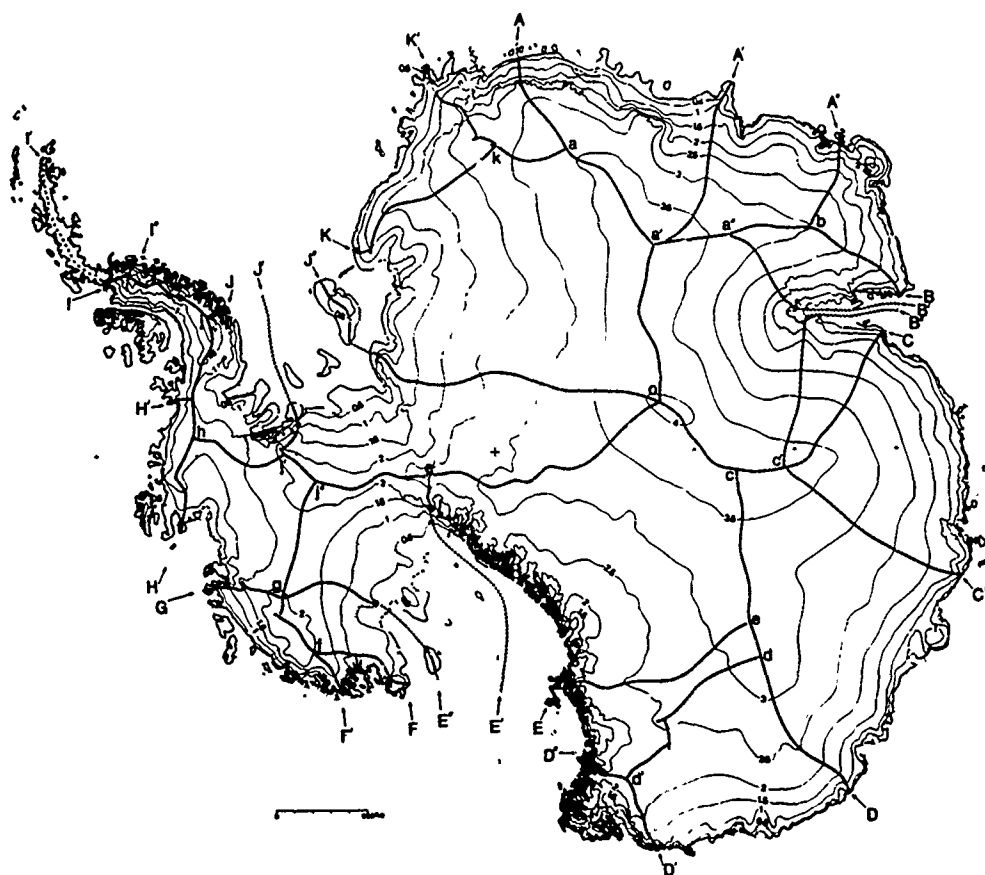


Figure 1. Map of antarctic surface elevation and drainage systems. Contour interval is 0.5 km. Drainage systems are referred to in the text by their coastal limits, marked by capital letters. From Giovinetto and Bentley [1985].

system K'A, 31 Gt yr^{-1} , by the ratio of the areas of the Jutulstraumen drainage system, $124 \times 10^3 \text{ km}^2$ [McIntyre, 1991, quoted by Swithinbank, 1988], and system K'A, $234 \times 10^3 \text{ km}^2$.

Eastern Queen Maud Land (system A'A"). The most important output in this system is through Shirase Glacier: 14 Gt yr^{-1} [Fujii, 1981]. Other measured outputs are 1.5 Gt yr^{-1} across the Soya Coast [Shimizu et al., 1978], 10.4 Gt yr^{-1} through Rayner Glacier [Morgan et al., 1982], and 4.4 Gt yr^{-1} in the Molodezhnaya area [Bogorodsky et al., 1979]. We have completed system A'A" by extrapolating outputs to the Prince Olav and Prince Harald Coasts, using the mean flux across the Soya Coast ($0.012 \text{ Gt km}^{-1} \text{ yr}^{-1}$), to get 6 Gt yr^{-1} .

Eastern Enderby Land (in system A"B). Outflow is through a small gate near the coast [Morgan et al., 1982]. Inputs are from Kotlyakov et al. [1974] and Bull [1971] and from flow across a gate approximately along the 2000-m elevation contour [Morgan and Jacka, 1981].

Lambert Glacier (system B'B"). The outflow from this vast system is through a narrow gate where Lambert Glacier feeds into the Amery Ice Shelf [Allison, 1979]. There has been disagreement as to whether there is net accumulation or net ablation in an extensive region in the interior in which

there are no measurements [Allison, 1979; Allison et al., 1985; McIntyre, 1985a,b]. Recently Seko et al. [1990], from AVHRR imagery, found a striped pattern on the surface that appears to require a positive accumulation rate. Therefore, we prefer the interpretation of Allison [1979]. Nevertheless, we include as an alternative in Table 1 the interpretation of McIntyre [1985a] as quantified for accumulation rates by Giovinetto and Bentley [1985]. Also included is an ablation rate on the Lambert Glacier itself of 7 Gt yr^{-1} [Allison, 1979].

Western Wilkes Land (in system CD). There are three overlapping systems considered here. The first ("interior" in Table 1) is in the deep interior with an outflow measured across a line from Pionerskaya station to Dome C station [Young, 1979; Kotlyakov et al., 1983]. The second system ("flank") is inland of a gate approximately along the 2000-m elevation contour, downstream from the eastern half of the Pionerskaya–Dome C line [Hamley et al., 1985; Jones and Hendy, 1985]. Measurements along the 2000-m contour line actually extend several hundred kilometers farther to the west [Young et al., 1989a], downstream from the western half of the Pionerskaya–Dome C line; analysis is not yet complete, but preliminary results show no significant imbalance there either [W. F. Budd, personal communication,

System	Mass			Imbalance	
	Accumulation Gt yr ⁻¹	Outflow Gt yr ⁻¹	Net Gt yr ⁻¹	Fraction %	Significant?
Jutulstraumen	16	11	+5	+31	no
Eastern Queen Maud Land	35	35	0	0	no
Eastern Enderby Land	13	10	+3	+23	no
Lambert Glacier (Allison/McIntyre)	50/18	11	+39/+7	+78/+39	yes/no
Western Wilkes Land: interior	27	21	+6	+22	no
flank	64	65	-1	-2	no
Totten Glacier	44	40	+4	+9	no
Combined	79	75	+4	+5	no
East Antarctica into Ross Ice Shelf	77	51	+26	+34	yes
West Antarctica into Ross Ice Shelf	91	99	-8	-9	no
Thwaites Glacier	49	44	+5	+10	no
Pine Island Glacier	76	26	+50	+66	yes
Rutford Ice Stream	12	18	-6	-50	no
	—	—	—	—	
TOTALS	498	381	+118	+24%	

Table 1. Measured Mass Balances, Inland Ice Alone

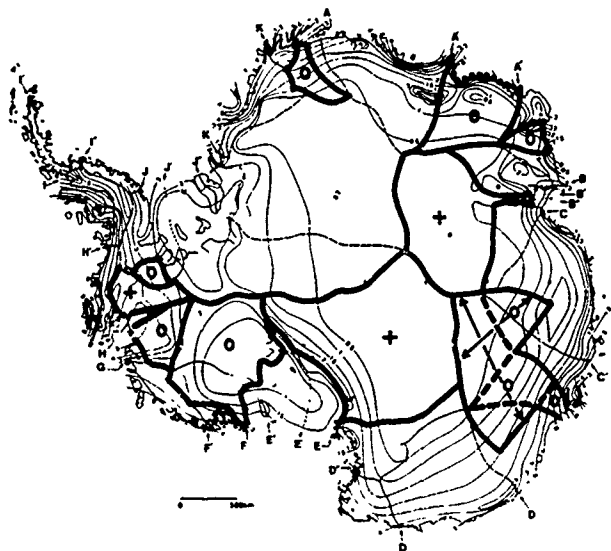


Figure 2. Map of surface mass balance rates [from Giovinetto and Bentley, 1985], upon which the inland-ice systems containing net balance determination have been delineated. O means no significant imbalance, + means a significant positive net balance. See Table 1.

1990). The third system, which encompasses part of the previous two, has its outflow through Totten Glacier [Young et al., 1989b]. We have calculated the input flux in based on data given by Jones and Hendy [1985].

East Antarctica into the Ross Ice Shelf (system EE'). The flux through the Transantarctic Mountains into the Ross Ice Shelf is given by Bentley [1985].

West Antarctica into the Ross Ice Shelf (system E'F). Output is from Shabtaie and Bentley [1987].

Thwaites Glacier (in system GH). Both input and output here are from Lindstrom and Hughes [1984].

Pine Island Glacier (in system GH). The output is from Lindstrom and Hughes [1984]. Two different estimates of input come from Crabtree and Doake [1982] and Lindstrom and Hughes [1984].

Rutford Ice Stream (in system JJ'). Crabtree and Doake [1982] give both input and output across the grounding line.

Summary. The indicated imbalance for each system is shown in Table 1, both in Gt yr⁻¹ and in percentage of input. Also in Table 1 is our interim opinion as to whether each particular imbalance is significant, based on the calculated value and an interim assessment of the accuracy and completeness of the measurements; the systems are marked correspondingly in Figure 2. Generally speaking, the error in an input figure for a single drainage system is around 15% (see Shabtaie and Bentley [1987] for an update on the analysis of Giovinetto [1964] that led to an error estimate of 20–25%). Outputs are accurate to about 5 or 10%, except on Jutulstraumen where ice thickness is measured by gravity rather than by radar. We are currently preparing a more thorough evaluation of input and output errors.

Ice Shelves Only

See Table 2 and Figure 3.

Amery Ice Shelf, Lambert Glacier flow band (system B'B'). We estimated the outflow based on data given by Budd et al. [1982]. They give velocities across a line 50 km south of the ice front, and ice thicknesses across half of the line. We have assumed that the transverse ice thickness profile is symmetric around the center line, as the velocities are. We have also delimited the section of the outflow line that corresponds to the outflow from Lambert Glacier using flow lines shown by Budd et al. [1982]. The excess output

System	Mass				
	Inflow Gt yr ⁻¹	Accumulation Gt yr ⁻¹	Outflow Gt yr ⁻¹	Net Gt yr ⁻¹	Basal melt implied m yr ⁻¹
Amery I.S., Lambert flow band	11	4	20	-5	-0.3
Grid eastern Ross Ice Shelf	51	41	55	+37	+0.15
Grid western Ross Ice Shelf	99	34	97	+36	+0.15
TOTALS	161	79	172	+68	

Table 2. Measured Mass Balances, Ice Shelves Alone

Combined Systems

See Table 3 and Figure 4.

The approach in this section is to compare the output from the ice shelves with the input over the whole system, to calculate the bottom melt rate under the ice shelf that would be required for steady state, and to judge whether that rate is reasonable in light of whatever other information may exist.

Amery Ice Shelf (system BC). The outflow is the total across the gate of Budd et al. [1982]. Bottom accumulation on the ice shelf was calculated from the estimated bottom-freeze rate of 0.7 m yr⁻¹ [Budd et al., 1982]. The huge positive net mass balance indicated for this system could only be reduced to zero by a bottom melt rate under the ice shelf of 1.5 m yr⁻¹, which is not reasonable in view of the observed freezing rather than melting. We conclude that the net positive balance is significant.

George VI Ice Shelf (most of system H'I). Inputs and outputs for this system are from Potter et al. [1984]. The high value of equilibrium melt rate is supported by both strain rate measurements on the ice shelf [Bishop and Walton, 1981] and ocean-water isotope data [Potter et al., 1984].

Ronne and Filchner Ice Shelves (system JK). Outputs here are from observations on the positions of the ice front in different years [Lange, 1987]. From Lange's [1987] tables it is possible to separate the output into systems JJ' (western Ronne Ice Shelf), JJ'' (eastern Ronne Ice Shelf), and J''K (Filchner Ice Shelf). The indicated basal melt rates under the ice shelf average about a third of a meter per year, which is a reasonable rate overall. However, the result for the eastern Ronne Ice Shelf is not reasonable taken alone because of the extensive bottom freeze-on that is known to occur here [Engelhardt and Determann, 1987; Thyssen, 1988].

Brunt and Riiser-Larsen Ice Shelves and Stancomb-Will Ice Tongue (in system KK'). From data given by Orheim [1986] we have estimated 30 Gt yr⁻¹ out from the Riiser-Larsen Ice Shelf and 18 Gt yr⁻¹ out from the Stancomb-Will Ice Tongue. Lange [1987] gives 24 Gt yr⁻¹ out at the front of the Brunt Ice Shelf. Using these output rates and an input to system KK' of 80 Gt yr⁻¹ leads to a melt rate for steady state of 0.16 m yr⁻¹. However, measurements on the ice shelves have indicated melt rates on the order of 1 m yr⁻¹ [Thomas, 1973; Gjessing and Wold, 1986], which are incompatibly larger. The implication then is that this system has an overall negative mass balance. It is impossible to say how much of this should be attributed to the inland ice, which would

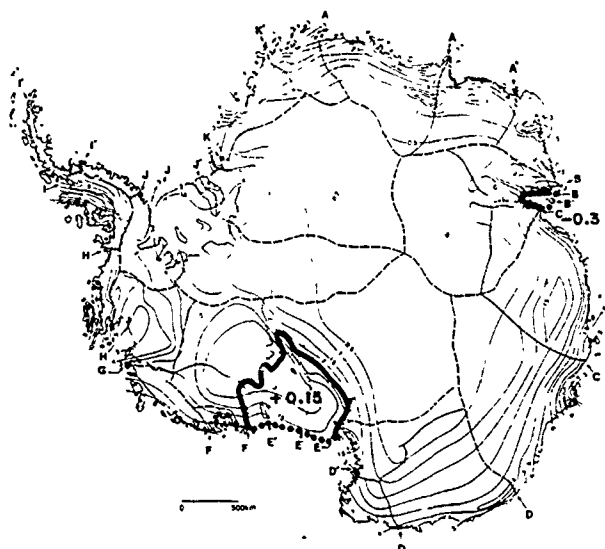


Figure 3. Map of surface mass balance rates [from Giovinetto and Bentley, 1985] upon which the ice shelf systems containing net balance determination have been delineated. Numbers are the bottom melt rates calculated on the assumption of steady state. See Table 2.

implies, for a steady-state ice shelf, a bottom-freeze-on rate of 0.3 m yr⁻¹, which is a reasonable figure in the light of the other indications of bottom freezing [Budd et al., 1982].

Western Ross Ice Shelf (system EE'). Input and output data are from Bentley [1985]; the output is through a gate that is roughly 100 km south of the ice front. The net positive mass balance corresponds to an average bottom melt rate of 0.15 m yr⁻¹ for an assumed steady-state ice shelf. For comparison, the average melt rate estimated for the entire ice shelf by Pillsbury and Jacobs [1985] is 0.28 m yr⁻¹ ± 50%. These estimates are not significantly different, so there is no evidence that the ice shelf is out of steady state.

Eastern Ross Ice Shelf (system EF). Output and input estimates are from Shabtaie and Bentley [1987]; output is again through a gate about 100 km south of the ice front. The net balance leads to an equilibrium bottom melt rate of 0.15 m yr⁻¹, the same as for the western portion of the shelf.

System	Mass					Reasonable?
	Accumulation	Basal melt measured	Outflow	Net	Basal melt for steady state	
	Gt yr ⁻¹	Gt yr ⁻¹	Gt yr ⁻¹	Gt yr ⁻¹	m yr ⁻¹	
Amery Ice Shelf (Allison/McIntyre)	97/65	-11	25	+83/+51	+1.5/+0.9	no
		(-0.7 m yr ⁻¹)				
George VI Ice Shelf	52		4	+48	+2.1	yes
Western Ronne Ice Shelf	91		47	+44	+0.37	yes
Eastern Ronne Ice Shelf	103		44	+79	+0.28	no
Filchner Ice Shelf	107		60	+47	+0.35	yes
Brunt & Riiser-Larsen I.S.'s	80	45	72	-37	+0.16	no
		(1 m yr ⁻¹)				
TOTALS	530	34	252	+244		

Table 3. Measured Mass Balances, Combined Systems

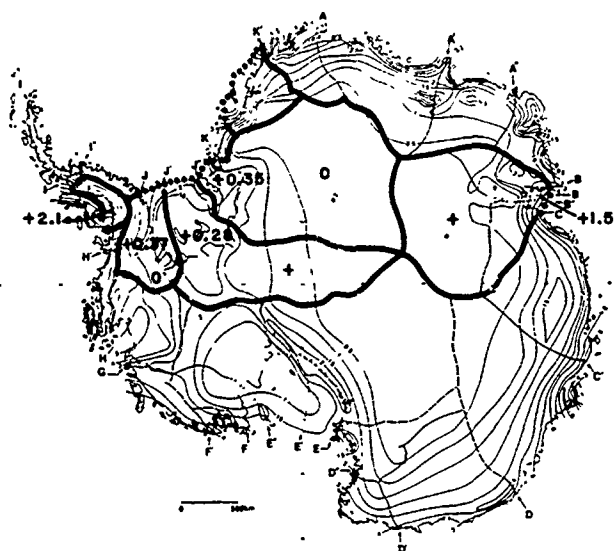


Figure 4. Map of surface mass balance rates [from Giovinetto and Bentley, 1985] upon which the combined systems containing net balance determination have been delineated. O means no significant imbalance, + and - mean significant positive and negative net balance, respectively. Numbers are bottom melt rates calculated on the assumption of steady state. See Table 3.

affect sea level, and how much to the ice shelves, which would not.

CURRENT ANTARCTIC NET MASS BALANCE

There are many ways that one could proceed from the data presented to assess the state of the ice sheet as a whole. Because the uncertainty in extrapolation is substantially larger than the errors of measurement, we have not felt it feasible to calculate a mean imbalance with a standard error estimate. Rather, we have chosen three methods of extrapolation designed to indicate the likely range of overall mass balance. First, to get a low figure, assume that all the systems, both with and without measurements, are in balance

except those that we have indicated as significantly out of balance. Assign the entire negative imbalance of the Brunt/Riiser-Larsen system to the inland ice, assume that the inland portion of the entire Filchner/Ronne system is in balance, and accept the McIntyre interpretation for the Lambert Glacier system. The sum of the net balances for the three unbalanced systems, East Antarctica into the Ross Ice Shelf (+26 Gt yr⁻¹), Pine Island Glacier (+50 Gt yr⁻¹), and Brunt/Riiser-Larsen Ice Shelves (-37 Gt yr⁻¹), is 39 Gt yr⁻¹, which is equivalent to a sea level lowering of 0.11 mm yr⁻¹.

As a second approach, which will give a high figure, take the sum of all the inputs and outputs (including Allison's interpretation for the Lambert Glacier system) for the systems that comprise inland ice only and then assume that these regions are, on the average, typical of the ice sheet as a whole. To extrapolate we have weighted in two ways; by mass input, because the regions without measurements are predominantly in the coastal zones of heavier snowfall, and by area. These two methods of weighting lead to overall positive net mass balances of 400 Gt yr⁻¹ (1.10 mm yr⁻¹ sea level lowering) and 290 Gt yr⁻¹ (0.79 mm yr⁻¹ sea level lowering), respectively (Table 4).

Our third approach is to use all the systems that include inland ice. Again assign all imbalances to the inland ice; also assume that the inland portions of the George VI, Ronne, and Filchner Ice Shelf systems are in balance. Extrapolate to the rest of the ice sheet as before, using both mass input and area as weighting factors. The results then are 140 Gt yr⁻¹ (0.39 mm yr⁻¹) and 110 Gt yr⁻¹ (0.30 mm yr⁻¹), respectively (Table 4).

These different extrapolations together suggest an overall positive mass balance in the range 40–400 Gt yr⁻¹, i.e., a contribution to sea level lowering of 0.1–1.1 mm yr⁻¹.

A different type of approach is to consider what the implication would be, for the regions without measurements (Figure 5), of assuming either that the Antarctic ice sheet is making no contribution to sea level change at all, or that it actually contributes to sea level rise. Assume first that the overall net balance is zero. The negative net mass balance required for the unmeasured regions, into which the input is 870 Gt yr⁻¹, is 40–400 Gt yr⁻¹, or 5–55% of the input. For

	From Grounded Areas Alone		From All Measurements	
	By Mass	By Area	By Mass	By Area
Total mass input (M)	1660 Gt yr ⁻¹		1660 Gt yr ⁻¹	
Total area (A)		12.1 x 10 ⁶ km ²		12.1 x 10 ⁶ km ²
Mass input to measured systems (m)	500 Gt yr ⁻¹		980 Gt yr ⁻¹	
Fraction of total mass input ($f_m=m/M$)	30 %		59 %	
Areas of measured systems (a)		5.1 x 10 ⁶ km ²		8.6 x 10 ⁶ km ²
Fraction of total area ($f_a=a/A$)		42 %		71 %
Mass excess in measured systems (d_m)	120 Gt yr ⁻¹	120 Gt yr ⁻¹	80 Gt yr ⁻¹	80 Gt yr ⁻¹
Mass excess extrapolated to whole ice sheet (δ_m/f_m)	400 Gt yr ⁻¹		140 Gt yr ⁻¹	
(δ_m/f_a)		290 Gt yr ⁻¹		110 Gt yr ⁻¹
Fraction of total input	24 %	17 %	8 %	7 %
Equivalent sea level lowering	1.1 mm yr ⁻¹	0.8 mm yr ⁻¹	0.4 mm yr ⁻¹	0.3 mm yr ⁻¹

Table 4. Contribution to Sea Level

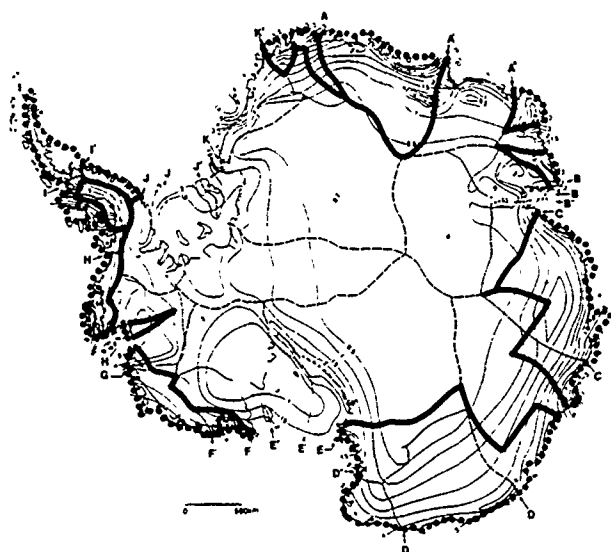


Figure 5. Map of surface mass balance rates [from Giovinetto and Bentley, 1985] upon which the systems without net balance measurement have been delineated. Dotted lines denote the outflow perimeters.

the Antarctic to be contributing 0.5 mm yr⁻¹ to sea level rise, as has sometimes been proposed, an additional 180 Gt yr⁻¹ would have to be supplied, which would imply a negative net balance of 30–80%!

Is there any reason to suspect that the regions without measurements are characterized by strongly negative net

balances? In fact, what evidence there is suggests the contrary. For example, system AA' along the Queen Maud Land coast has in input of 77 Gt yr⁻¹ and a coastline that is 1150 km long. The mass flux for balance would be 0.067 Gt km⁻¹ yr⁻¹, essentially the same as for neighboring system K'A, which contains Jutulstraumen. But satellite images [Swithinbank, 1988] show no outflow systems in section AA' nearly comparable to Jutulstraumen. Extensive mountain ranges in the interior sub-parallel to the coast block ice flow through them—the flux through the entire Sør Rondane is less than 2 Gt yr⁻¹ [Van Autenboer and Decleir, 1978]. The problem in this sector seems to be how the outflow can even equal the input, let alone exceed it.

In Wilkes Land, early work by Lorius [1962] in a small sector along the Adelie Coast (section DD') (not included in our compilation because there were no measurements of ice thickness) suggested a positive net mass balance. The only system whose outflow actually has been measured at the coast, that through Totten Glacier, is in balance. Farther to the west, the small coastal sector in Enderby Land is in balance or slightly positive.

In Graham and eastern Palmer Lands (section IJ) the evidence is mixed and there is no clear trend, as extrapolation of sparse data in this region of rugged terrain is difficult [C. S. M. Doake, personal communication, 1989].

Thus what evidence there is suggests that the coastal areas are no more likely to show large negative net mass balances than the interior. We find nothing to contradict the conclusion of a net positive balance of a few hundred Gt yr⁻¹, i.e., a negative contribution to observed sea level rise of several tenths of a millimeter per year. Note that this conclusion has not changed from that of Budd and Smith [1985], who estimate 0–1 mm yr⁻¹ sea level lowering based on fewer data and a different approach

ICEBERG FLUX

Data from a systematic program of iceberg observation in the waters around Antarctica, in which nearly all ships traveling to and from Antarctica participate, have been analyzed carefully by Orheim [1985, 1988, personal communication, 1989], taking into account multiple sightings, mean residence times, and size distributions. His conclusion is that the total calving rate from the continent, ignoring the recent giant icebergs, is at least as large as the total mass input onto the continent. If melting under the ice shelves is added as an output term, the implication is for a negative net mass balance.

The indicated imbalance is equivalent to an average break-back rate of 1 km yr^{-1} along all the ice-shelf fronts around the continent. There is at least qualitative evidence to indicate that such a break-back is occurring. Zakharov [1988] has compiled information from maps and satellite images on frontal positions of the ice shelves and floating glacier tongues around Antarctica over the last century. He found that through the 1970s a larger proportion of the fronts were advancing than at any other time in his coverage. Unfortunately, his data end in 1980, but it would be reasonable to suppose that after a period of unusual advance a net break-back would occur. In the Antarctic Peninsula region the Wordie (section HT), George VI (section H'I), and Larsen Ice Shelves (section IT") have all been decaying in recent years (even aside from the $11,000\text{-km}^2$ calving event from the Larsen Ice Shelf in 1986) [C. S. M. Doake,

personal communication, 1989]. Shirase Glacier tongue has broken back in the 1980s [Nishio, 1990]. Williams and Ferrigno [1988] and Ferrigno et al. [1990] document large-scale retreat or recession in several areas, although their study is dominated by the super-giant icebergs that are not included in the iceberg flux calculations. Overall, a general retreat of the floating ice margins of the ice sheet is indicated, but whether that retreat is large enough to account for the excess iceberg flux remains problematical.

CONCLUSION

At present the antarctic contribution to sea level change probably is a lowering that lies between $0.1\text{--}1.1 \text{ mm yr}^{-1}$. That amounts to $40\text{--}400 \text{ Gt yr}^{-1}$ total excess mass input, or 2 to 25% of the total yearly input. Our estimate is not significantly different from most of those in the past, but the expanding coverage of the ice sheet makes it increasingly difficult to attribute any contribution to sea level rise to Antarctica. Excess iceberg flux probably reflects a secular breakback of ice shelf fronts.

ACKNOWLEDGMENTS

This work was supported by NSF grant DPP86-14011 to the University of Wisconsin and NSERC grant OGP0036595 to the University of Calgary. This is contribution number 514 of the Geophysical and Polar Research Center of the University of Wisconsin-Madison.

REFERENCES

- Allison, I., The mass budget of the Lambert Glacier drainage basin, Antarctica, *J. Glaciol.*, 22, 223–235, 1979.
- Allison, I., N. W. Young, and T. Medhurst, On reassessment of the mass balance of the Lambert Glacier drainage basin, Antarctica, *J. Glaciol.*, 31, 378–381, 1985.
- Bentley, C. R., Glaciological evidence: The Ross Sea sector, in *Glaciers, Ice Sheets, and Sea Level: Effects of a CO₂-Induced Climatic Change*, Attachment 10, pp. 173–196, National Academy Press, Polar Research Board, Washington, DC, 1985.
- Bishop, J. F., and J. L. W. Walton, Bottom melting under George VI Ice Shelf, Antarctica, *J. Glaciol.*, 27, 429–447, 1981.
- Bogorodsky, V. V., G. V. Trepov, and A. N. Sheremet'ev, Use of radio-echo measurements in determining the thickness and velocity of an Antarctic ice sheet, *Physics of the Solid Earth*, 15, 69–74, 1979.
- Budd, W. F., and I. N. Smith, The state of balance of the Antarctic ice sheet: an updated assessment—1984, in *Glaciers, Ice Sheets, and Sea Level: Effects of a CO₂-Induced Climatic Change*, Attachment 9, pp. 172–177, National Academy Press, Polar Research Board, Washington, DC, 1985.
- Budd, W. F., M. J. Corry, and T. H. Jacka, Results from the Amery Ice Shelf Project, *Ann. Glaciol.*, 3, 36–41, 1982.
- Bull, C. B. B., Snow accumulation in Antarctica, in *Research in the Antarctic*, edited by L. O. Quam, pp. 367–421, American Association for the Advancement of Science Publ. No. 93, Washington, DC, 1971.
- Crabtree, R. D., and C. S. M. Doake, Pine Island Glacier and its drainage basin: results from radio echo sounding, *Ann. Glaciol.*, 3, 65–70, 1982.
- Engelhardt, H. F., and J. Determann, Borehole evidence for a thick layer of basal ice in the central Ronne Ice Shelf, *Nature*, 327, 318–319, 1987.
- Ferrigno, J. G., R. S. Williams, Jr., B. K. Lucchitta, and B. F. Molnia, Recent changes in the coastal regions of Antarctica documented by Landsat images, *this volume*, 1991.
- Fujii, Y., Aerophotographic interpretation of surface features and an estimation of ice discharge at the outlet of the Shirase Drainage Basin, Antarctica, *Antarctic Record*, 72, 1–15, 1981.
- Giovinetto, M. B., and C. R. Bentley, Surface balance in ice drainage system of Antarctica, *Antarctic J. U.S.*, 20, 6–13, 1985.
- Giovinetto, M. B., and C. Bull, Summary and analyses of surface mass balance compilations for Antarctica, 1960–1985, *Byrd Polar Research Center Report No. 1*, The Ohio State University, 1987.
- Giovinetto, M. B., C. R. Bentley, and C. B. B. Bull, Choosing between some incompatible regional surface-mass-balance data sets in Antarctica, *Antarctic J. U.S.*, 24, 7–13, 1989.
- Gjessing, Y., and B. Wold, Absolute movements, mass balance and snow temperatures of the Riiser-Larsenisen Ice Shelf, Antarctica, *Norsk Polarinstitutt Skrifter*, 187, 23–31, 1986.
- Hamley, T. C., I. N. Smith, and N. W. Young, Mass balance and ice flow law parameters for East Antarctica, *J. Glaciol.*, 31, 334–339, 1985.
- Jones, D., and M. Hendy, Glaciological measurements in Eastern Wilkes Land, Antarctica, *ANARE Res. Notes*, 28, 164–173, 1985.

- Kotlyakov, V. M., N. I. Barkov, I. A. Loseva, and B. N. Petrov, Novaia karta pitaniia lednikovogo pokrova Antarktity (New map of the accumulation on the Antarctic Ice Sheet): Institut Geografii, Adadessila Nauk SSSR, *Materialy Glaciologicheskikh Issledovani, Khronika Obsuzhdeniia*, 24, 248-255, 1974.
- Kotlyakov, V. M., M. B. Dyurgerov, P. A. Korolyev, Accumulation and mass balance of the large ice-catchment basin in East Antarctica (In Russian), in *Materials of glaciological chronicles of discussion 47*, pp. 49-61, Academy of Sciences of the U.S.S.R. Soviet Geophysical Committee, 1983.
- Lange, M. A., Quantitative estimates of the mass flux and ice movement along the ice edges in the Eastern and Southern Weddell Sea, in *The Dynamics of the West Antarctic Ice Sheet*, edited by J. Oerlemans and C. J. van der Veen, pp. 57-74, D. Reidel Publishing, Amsterdam, Netherlands, 1987.
- Lindstrom, D., and T. J. Hughes, Drawdown of the Pine Island Bay drainage basins of the West Antarctic ice sheet, *Antarctic J. U.S.*, 19, 56-58, 1984.
- Lorius, C., Contribution to the knowledge of the Antarctic ice sheet: a synthesis of glaciological measurements in Terre Adelie, *J. Glaciol.*, 4, 79-92, 1962.
- McIntyre, N. F., A reassessment of the mass balance of the Lambert Glacier drainage basin, Antarctica, *J. Glaciology*, 31, 34-38, 1985a.
- McIntyre, N. F., Reply to "On reassessment of the mass balance of the Lambert Glacier drainage basin, Antarctica," *J. Glaciol.*, 31, 381-382, 1985b.
- McIntyre, N. F., Ice sheet drainage basins, balance and measured ice velocities and sub-glacial water, in *Antarctica: Glaciological and Geophysical Folio*, sheet 12, edited by Drewry, D. J., Scott Polar Research Institute, University of Cambridge, 1991, In press.
- Morgan, V. I., and T. H. Jacka, Mass balance studies in East Antarctica, in *Sea Level, Ice, and Climatic Change* (Proceedings of the Canberra Symposium, December 1979), IAHS Publ. No. 131, pp. 253-260, 1981.
- Morgan, V. I., T. H. Jacka, G. J. Akerman, and A. L. Clarke, Outlet glacier and mass-budget studies in Enderby, Kemp, and Mac. Robertson Lands, Antarctica, *Ann. Glaciol.*, 3, 204-210, 1982.
- Nishio, F., Ice front fluctuations of the Shirase Glacier, East Antarctica, *this volume*, 1991.
- Orheim, O., Iceberg discharge and the mass balance of Antarctica, in *Glaciers, Ice Sheets, and Sea Level: Effects of a CO₂-Induced Climatic Change*, Attachment 12, pp. 210-215, National Academy Press, Polar Research Board, Washington, DC, 1985.
- Orheim, O., Flow and thickness of Riiser-Larsenisen, Antarctica, *Norsk Polarinstitut Skrifter*, 187, 5-22, 1986.
- Orheim, O., Antarctic icebergs - production, distribution and disintegration, *Ann. Glaciol.*, 11, 205, 1988.
- Pillsbury, R. D., and S. S. Jacobs, Preliminary observations from long-term current meter moorings near the Ross Ice Shelf, Antarctica, in *Oceanology of the Antarctic Continental Shelf*, American Geophysical Union, Antarctic Research Series, Vol. 43, edited by S. S. Jacobs, pp. 87-107, 1985.
- Potter, J. R., J. G. Paren, and J. Loynes, Glaciological and oceanographic calculations of the mass balance and oxygen isotope ratio of a melting ice shelf, *J. Glaciol.*, 30, 161-169, 1984.
- Seko, K., T. Furukawa, and O. Watanabe, The surface condition on the Antarctic ice sheet, *this volume*, 1991.
- Shabtaie, S., and C. R. Bentley, West Antarctic ice streams draining into the Ross Ice Shelf: Configuration and mass balance, *J. Geophys. Res.*, 92, 1311-1336, 1987.
- Shimizu, H., O. Watanabe, S. Kobayashi, T. Tamada, R. Naruse, and Y. Ageta, Glaciological aspects and mass budget of the ice sheet in Mizuho Plateau, in *Glaciological Studies in Mizuho Plateau, East Antarctica, 1969-1975*, Memoirs of National Institute of Polar Research, Special Issue No. 7, pp. 264-274, 1978.
- Swithinbank, C. W. M., *Antarctica: Satellite image atlas of glaciers of the World*, United States Geological Survey Professional Paper 1386-B, 1988.
- Thomas, R. H., The dynamics of the Brunt Ice Shelf, Coats Land, Antarctica, *Scientific Report No. 79*, British Antarctic Survey, 1973.
- Thyssen, F., Special aspects of the central part of the Filchner/Ronne Ice Shelf, *Ann. Glaciol.*, 11, 173-179, 1988.
- van Aulenboer, T., and H. Declair, Glacier discharge in the Sør-Rondane, a contribution to the mass balance of Dronning Maud Land, Antarctica, *Zeitschrift für Gletscherkunde und Glazialgeologie*, 14, 1-16, 1978.
- Williams, Jr., R. S., and J. G. Ferrigno, Documentation on satellite imagery of large cyclical or secular changes in antarctic ice sheet margin, *EOS (Transactions, American Geophysical Union)*, 69, 365, 1988.
- Young, N. W., Measured velocities of interior East Antarctica and the state of mass balance within the I.A.G.P. area, *J. Glaciol.*, 24, 77-87, 1979.
- Young, N. W., I. D. Goodwin, N. W. J. Hazelton, and R. J. Thwaites, Measured velocities and ice flow in Wilkes Land, Antarctica, *Ann. Glaciol.*, 12, 192-197, 1989a.
- Young, N., P. Malcolm, and P. Mantell, Mass flux and dynamics of Totten Glacier, Antarctica (abstract), *Ann. Glaciol.*, 12, 219, 1989b.
- Zakharov, V. G., Fluctuations in ice shelves and outlet glaciers in Antarctica, *Polar Geography and Geology*, 12, 297-311, 1988.

AD-P007 330



92-17834



The Impact of Global Warming on the Antarctic Mass Balance and Global Sea Level

W. F. Budd and Ian Simmonds

Department of Meteorology, University of Melbourne, Parkville, Victoria, Australia

ABSTRACT

The onset of global warming from increasing "greenhouse" gases in the atmosphere can have a number of important different impacts on the Antarctic ice sheet. These include increasing basal melt of ice shelves, faster flow of the grounded ice, increased surface ablation in coastal regions, and increased precipitation over the interior. An analysis of these separate terms by ice sheet modeling indicates that the impact of increasing ice sheet flow rates on sea level does not become a dominant factor until 100–200 years after the realization of the warming. For the time period of the next 100 years the most important impact on sea level from the Antarctic mass balance can be expected to result from increasing precipitation minus evaporation balance over the grounded ice. The present Antarctic net accumulation and coastal ice flux each amount to about $2000 \text{ km}^3 \text{ yr}^{-1}$, both of which on their own would equate to approximately 6 mm yr^{-1} of sea level change. The present rate of sea level rise of about 1.2 mm yr^{-1} is therefore equivalent to about 20% imbalance in the Antarctic mass fluxes.

The magnitude of the changes to the Antarctic precipitation and evaporation have been studied by a series of General Circulation Model experiments, using a model which gives a reasonable simulation of the present Antarctic climate, including precipitation and evaporation. The experiments examine the changes in the Antarctic precipitation (P) and evaporation (E) resulting separately from decreasing incrementally the Antarctic sea ice concentration and from global warming accompanied by decreased sea ice cover.

For total sea ice removal the changes obtained were $P:+23\%$; $E:-8\%$; $(P-E):+48\%$. For global warming with sea ice reduction by about two thirds the changes were $P:+47\%$; $E:+22\%$; $(P-E):+68\%$. This latter increase in mass flux is equivalent to about 4 mm yr^{-1} of sea level lowering which could provide a small but significant offset to the sea level rise expected from ocean thermal expansion and melting of temperate glaciers.

INTRODUCTION

Considerable interest has developed in recent years regarding the role of the Antarctic ice sheet in possible future changes of sea level. It was indicated by Budd et al. [1987] and Budd [1988] that the major response of the Antarctic ice sheet to global warming which could contribute to sea level rise, from increased ice flow, would be delayed for over a century following the warming, while the floating ice

shelves diminished. On the other hand, for the shorter term, the effect of increasing precipitation over the Antarctic would have an immediate impact in contributing to sea level lowering. Table 1 shows the current estimates of Antarctic snow accumulation in relation to sea level change. In spite of the uncertainty in the accumulation estimates the present Antarctic accumulation rate is equivalent to about five times the current rate of sea level rise. An appreciable increase in

Area of Antarctic grounded ice	13 x 10 ⁶ km ²
Mean accumulation rate (water)	160 ± 20% mm yr ⁻¹
Mean total water equivalent influx	2.1 x 10 ³ km ³ yr ⁻¹
Sea level change equivalent	~6 mm yr ⁻¹
Current rate of sea level rise	~1.2 mm yr ⁻¹

Table 1. Antarctic Mass Flux and Sea Level Change.

the Antarctic accumulation rate from global warming could therefore provide a significant offset to the increase in sea level expected from thermal expansion and the melting of temperate glaciers, cf. Robin [1986].

Increasing attention is therefore being directed towards analyses of the present Antarctic precipitation and accumulation rates and their likely changes with global warming. Simple assessments of accumulation rate change, based on temperature changes and the saturation vapor relation alone, are inadequate because other factors, such as atmospheric dynamics, are also involved. For example the present Antarctic winter accumulation is higher than that of summer, in spite of lower temperatures during winter. Another approach is to consider the balance of the atmospheric vapor transport. Bromwich [1990] has shown that the net southward atmospheric water vapor fluxes from coastal radiosonde data, in spite of coarse spacing, provide a reasonable match with the present net mass balance for the Antarctic accumulation.

Reference has been made to increases in Antarctic precipitation from General Circulation Models (GCMs) for the double CO₂ (or total Greenhouse gases) scenarios (2 x CO₂) as an indication of possible Antarctic accumulation changes. Grotch [1988] showed that the results of the four GCMs which he surveyed gave precipitation increases in the Antarctic between 20 and 50% for the 2 x CO₂ simulations relative to the control simulations for the present climate. It is important to recognize that the net accumulation is the difference between precipitation (P) and evaporation (E), and so changes to both need to be considered in relation to climate change.

Since the proportional increase in evaporation in the polar regions for the 2 x CO₂ case is less than that of precipitation it can be expected that the proportional increase in (P-E) would be even greater than that of P alone.

It was found by Simmonds and Budd [1990] that the fraction of open water in the sea ice also greatly influences the Antarctic precipitation. As global warming can be expected to be associated with a decrease of the sea ice cover as well as a temperature increase, it is considered worth exploring the impact of decreasing the sea ice cover, as well as increasing the sea surface temperature (SST), independently, on the changes to Antarctic precipitation and evaporation. A series of GCM experiments have therefore been carried out to provide sensitivity studies of the impact of reduced sea ice cover separately in addition to the impact of global warming combined with reduced sea ice.

DESCRIPTION OF MODEL AND EXPERIMENTS

The GCM used here is the Melbourne University spectral model Version V.3 with wave number 21 (rhomboidal truncation) and 9 levels in the vertical. A basic description of the model physics is given by Simmonds [1985] and a com-

parison of the model climatology with observations is presented in Simmonds et al. [1988]. In particular the model gives a favorable representation of the global surface pressure and precipitation distributions which are relevant to the surface fluxes and the latent heat exchanges addressed here. An evaluation of the global surface fluxes from the model has been given by Simmonds and Dix [1989] and an assessment of model performance in the Antarctic is presented by Simmonds [1990a]. This control version of the model uses 100% sea ice cover with no open water leads in the sea ice region. A parameterization scheme for prescribed sub-grid scale leads, or open water fraction, is described by Simmonds and Budd [1990].

A series of experiments with different open water fractions has been carried out to evaluate the sensitivity of the climate to open water within the sea ice zone. The open water fractions chosen were 0, 5, 20, 50, 80 and 100% and the corresponding experiments are denoted here by W₀, W₅, W₂₀, W₅₀, W₈₀, and W₁₀₀. The simulations have been run for perpetual January and July with prescribed sea surface temperatures (SSTs) and sea ice extent, with the open water fraction replacing sea ice by water at the freezing point (-1.8°C). The control run was for 660 days, and the anomaly runs 390 days, with the climatologies computed for the last 600 and 300 days respectively.

To simulate the impact of global warming, including a decrease of the sea ice cover, reference was made to a number of other GCM simulations of the response to the doubling of atmospheric carbon dioxide content (2 x CO₂ experiments). Grotch [1988] showed that for the July period (June, July, August) the model responses for surface temperature were largest, and most different between models, in the region of the Antarctic sea ice. The large differences between models is partly due to poor control simulations as well as to the differences in simulation of changes in sea ice cover.

The procedure adopted here for the sensitivity study was to take the zonal mean SST range of the four models analyzed by Grotch and add this to the present SST distribution to provide the SSTs for the equivalent 2 x CO₂ experiment. This preserves the longitudinal pattern of the SSTs and is in effect not unlike the prescription of an ocean flux correction to preserve the SST pattern as described by Hansen et al. [1984]. The zonal mean temperature anomalies (for 20° Lat. intervals) are given in Table 2. The Antarctic sea ice for this experiment is reduced by the outer two grid points and replaced by water at freezing point, and the open water fraction within the sea ice zone was prescribed at 20%. Note that there are more grid points in the sea ice zone in this model, compared to the four models referred to above, because of the higher resolution 21-wave model used here. For the July equivalent 2 x CO₂ case treated here the area of the sea ice zone (including the open water fraction) is reduced to 4.6 x 10⁶ km² from 15.7 x 10⁶ km² in the control which is based on the present observed sea ice

Latitude	80	60	40	20	0	-20	-40	-60
ΔT°C	1.6	3.4	3.8	2.9	2.6	2.8	3.4	6.2

Table 2. Zonal Mean SST Increases (ΔT) for WARM Experiment.

Latitude Band °S	Area of Ice 10 ³ km ²	Elevation		P	Model Balance		Observed Accumulation A mm yr ⁻¹
		Obs.	Model		E mm yr ⁻¹	(P-E)	
90-85	997	2.76	2.34	128	113	15	68
85-80	2909	1.95	2.22	325	113	212	82
80-75	4234	1.94	1.88	387	139	248	135
75-70	4273	1.22	1.17	438	270	168	209
70-65	1681	0.22	0.36	712	332	380	424
65-60	94	0.00	-0.03	913	402	511	598

Table 3. Antarctic Accumulation: Simulated and Observed.

climatology given by Zwally et al. [1983]. This simulation experiment for the equivalent $2 \times \text{CO}_2$ global warming scenario is denoted as "WARM." In this experiment the actual amount of CO_2 in the atmosphere was not changed from that of the control.

GCM CONTROL SIMULATION OF THE ANTARCTIC MASS BALANCE

The annual mass balance for the model control simulation has been estimated from the mean of the January and July rates of precipitation minus evaporation, converted to an annual total. Observations show that winter precipitation, and summer evaporation, are generally larger than their annual averages [cf. Rusin, 1961]. Observations of the separate components of precipitation and evaporation are notoriously difficult to obtain so reference is made to the annual net accumulation of snow in water equivalent. It is considered that the mean of the simulated January and July values gives a reasonable estimate of the annual total until the full annual cycle from the model is available.

A summary of the model results for P, E and P-E over the Antarctic as a function of latitude is given in Table 3 along with the mean elevation and area of the latitude bands and the net accumulation from an updated compilation of Budd and Smith [1985]. A map of the distribution of the corresponding mean precipitation rate for January and July is shown in Figure 1, the evaporation rate for January is shown in Figure 2 and the annual mean distribution of (P-E), represented by the January and July means, is shown in Figure 3.

It should be noted that even though the model has better resolution than those analyzed by Grotch [1988] there are still some noticeable discrepancies in the Antarctic topography which can influence the precipitation and evaporation. Nevertheless the general decrease of the net (P-E) with distance towards the pole is quite comparable with that of the net accumulation. The proportion of evaporation to precipitation obtained here is similar to the results from other evaluations, e.g., Loewe [1957], Rusin [1961], Schwerdtfeger [1984].

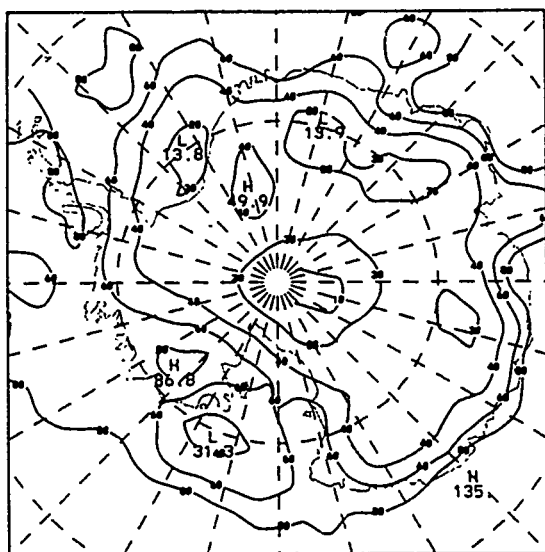


Figure 1. Mean of the precipitation rates in the January and July control simulations. The contour values are 10, 20, 40 and 80 cm yr⁻¹.

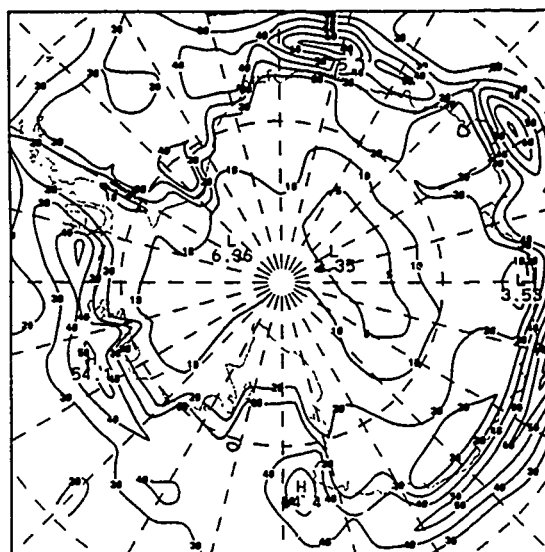


Figure 2. Evaporation rate in the January control simulation. The contour interval is 10 cm yr⁻¹ and the 5 cm yr⁻¹ contour is also shown.

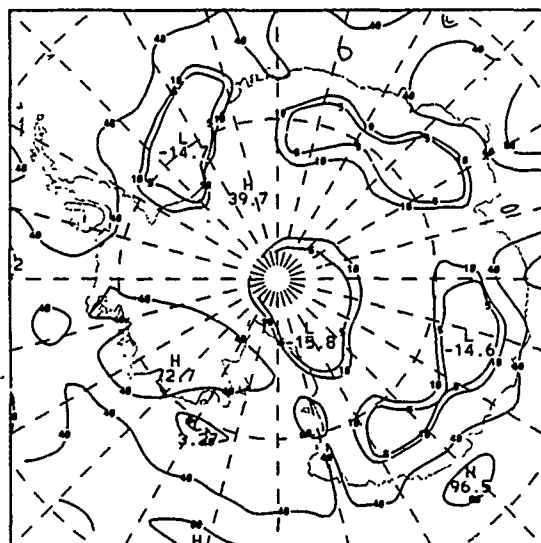


Figure 3. Mean of the precipitation minus evaporation rates in the January and July control simulations. The contour values are 5, 10, 40 and 80 cm yr⁻¹.

Evaporation rates in the Antarctic over snow are particularly difficult to measure. Budd [1967] obtained values of 400 mm yr⁻¹ at 100 m elevation reducing to 200 mm yr⁻¹ at 600 m over blue ice of the ablation zone inland of Mawson. In a recent review of blue ice fields in the Antarctic, Mellor and Swithinbank [1989] report ablation rates at sites above 2000 m in the interior varying from 100 mm yr⁻¹ about latitude 70°S to about 50 mm yr⁻¹ south of 80°S. Recognizing the coarse resolution of the spectral model the totals over the ice sheet obtained for the control simulation may be considered as reasonable viz. average precipitation 372 mm yr⁻¹, evaporation 204 mm yr⁻¹ and P-E 168 mm yr⁻¹, compared with the average accumulation from the Budd and Smith compilation of 160 mm yr⁻¹ over grounded ice. This value of average accumulation is in about the

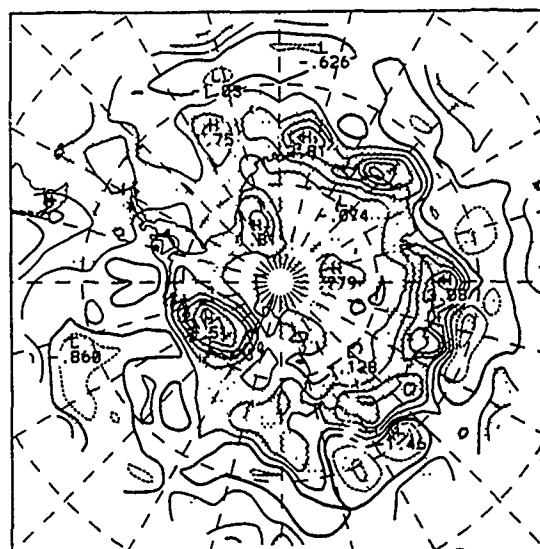


Figure 4. Difference between the precipitation rates of the WARM and the control simulations. The contour interval is 0.5 mm day⁻¹, and zero contour is accentuated and negative contours are dashed. Regions of differences significant at the 95% confidence level are stippled.

middle of the range of estimates reviewed by Giovinetto and Bull [1987].

MODEL RESULTS FROM REDUCED SEA ICE AND GLOBAL WARMING

Only a brief summary can be given here. We therefore consider only the results for the July simulations. A more detailed analysis of the impact of the ice reduction on precipitation is given by Simmonds [1990b]. Tables 4 and 5 summarize the results for the changes in the Antarctic region, including the total and percentage changes of P, E and (P-E) from the model simulations for decreasing sea ice (W_0 to W_{100}) and for the case of global warming (WARM).

Parameter	Over Sea Ice Zone					Over Antarctica			
	P mm day ⁻¹	E W m ⁻²	SH W m ⁻²	T _s °C	T _a °C	E W m ⁻²	SH W m ⁻²	T _s °C	T _a °C
Experiment									
W ₀	2.47	20.3	-46.2	-19.3	-16.8	16.0	-61.8	-40.3	-30.7
W ₅ - W ₀	0.0	3.8	12.1	2.0	1.2	0.29	-1.1	0.9	0.6
W ₅₀ - W ₀	0.15	22.8	75.6	12.5	7.6	-0.86	-2.6	4.2	3.1
W ₈₀ - W ₀	0.05	28.9	94.7	16.0	10.1	-1.71	-2.1	5.8	4.7
W ₁₀₀ - W ₀	-0.06	28.0	102.9	17.6	11.1	-1.42	-3.6	7.2	5.6
WARM- W ₀	0.66	10.0	58.2	13.5	10.7	+2.85	-7.3	9.5	7.9

Table 4. Simulated Changes from Control (W_0) for Experiments W₅, W₅₀, W₈₀, W₁₀₀, and WARM. P=Precipitation; E=Evaporation; SH=Sensible Heat; T_s=Surface Temperature; T_a=Air Temperature.

	P	P/P ₂₀	E	E/E ₂₀	(P-E)	(P-E) ₂₀
	mm day ⁻¹	%	mm day ⁻¹	%	mm day ⁻¹	%
Experiment						
W ₀	1.02	84	0.56	102	0.46	69
W ₅	1.09	89	0.57	104	0.52	78
W ₂₀	(1.22)	(100)	(0.55)	(100)	(0.67)	(100)
W ₅₀	1.30	106	0.53	96	0.77	115
W ₈₀	1.37	112	0.50	91	0.87	130
W ₁₀₀	1.50	123	0.51	93	0.99	148
WARM	1.79	147	0.66	120	1.13	168

Table 5. Simulated Changes to Precipitation P, Evaporation E, and Balance (P-E) Relative to 20% Open Water Case (W₂₀).

The percentage changes have been shown relative to the case of 20% open water to represent the observed situation as given by Zwally et al. [1983]. A tape reading problem has meant we do not have access to all the data for W₂₀, and so the values shown in parentheses in Table 5 have been interpolated.

A monotonic increase in total precipitation over the Antarctic is obtained with increasing fraction of open water. The increases in evaporation over the continent are less, particularly in the interior. For the case of the global warming simulation there is an even larger increase in precipitation and although the evaporation also increased it changed less proportionally than the precipitation over the Antarctic. Consequently the net (P-E) increased more on the continent in percentage terms than did P alone. The pattern of increase in precipitation is shown for the case of (WARM - W₀) in Figure 4, which shows the bulk of the addition is in the high accumulation belt below about 2500 m.

Figure 5 shows the zonal average changes relative to the control (W₀) for the cases W₅, W₅₀, W₁₀₀ and WARM, of the P, E, and P-E results. For the sea ice reduction there is reduced evaporation and precipitation just north of the sea ice and increases over the sea ice area and the Antarctic continent. For the WARM case there is a more general increase in precipitation south of 30°S, except for just north of the sea ice area (55°-60°S) with larger increases further south. The evaporation increase is more in the tropics decreasing towards the pole except the large increase over the area where the sea ice was removed. Note that the zonal averages are strongly influenced by the changes over the Ross and Weddell Seas which extend to 77°S and overlap with the changes over the continent.

Table 5 shows that for both ice removal and warming there is a greater increase of P than E over the continental grounded ice which through the mass balance P-E can affect sea level.

To place the sea level change implications in perspective, if the increase in balance (P-E) from Table 5 of 68% for the WARM July case is taken as representative of the change in the Antarctic annual mass balance then this would contribute to about two thirds of 6 mm yr⁻¹, viz 4 mm yr⁻¹ towards sea level lowering as a consequence of the equivalent 2 x

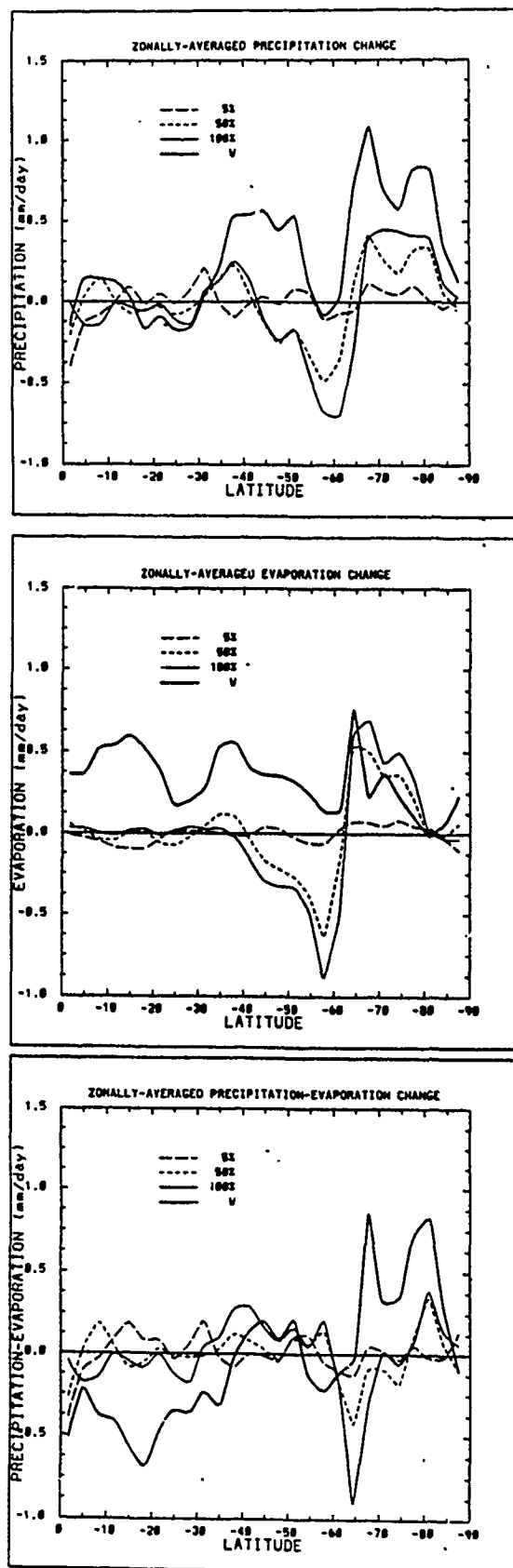


Figure 5. Differences of the four experiments from the July control of the zonal average of the precipitation (a) (top), evaporation (b) (middle), and precipitation minus evaporation (c) (bottom). The experiments are for 5, 50 and 100% open water and the WARM case.

CO₂ global warming. This appears to be about double the impact of earlier estimates where the relatively smaller changes in evaporation were not adequately considered [Houghton et al., 1990].

As an example of the possible impact on future sea level change the following hypothetical scenario is examined.

Suppose an effective doubling of CO₂ with other greenhouse gases occurs by the year 2030. Suppose a 20-year delay occurs before the full oceanic warming responds to the change and assume a linear increase of the changes from 1990 to 2050. The following contributions to sea level change are estimated and, except for the Antarctic contribu-

tion, are broadly in the range of estimates presented in Table 9.9 of the IPCC [Houghton et al., 1990]:

Estimated sea level changes by 2050 are:	
Ocean thermal expansion	+ 300 mm
Temperate glacier melt	+ 90
Greenland ice sheet change	0
Antarctic balance change	- 120
Total net change	+ 270 mm

The increase in Antarctic precipitation and mass balance can therefore be expected to provide a small but significant offset to the increase in sea level resulting from ocean thermal expansion and the melting of glaciers over the next

REFERENCES

- Bromwich, D. H., Estimates of Antarctic precipitation, *Nature*, 343, 627-629, 1990.
- Budd, W. F., Ablation from an Antarctic ice surface, *Proceedings of the International Conference on Low Temperature Science*, Sapporo 1966, pp. 431-446. Institute of Low Temperature Science, Hokkaido University, 1967.
- Budd, W. F., The expected sea level rise from climate warming in the Antarctic, in *Greenhouse: Planning for Climate Change*, edited by G. I. Pearman, pp. 74-82, E. J. Brill, Leiden, 1988.
- Budd, W. F., and I. N. Smith, The state of balance of the Antarctic Ice Sheet, in *Glaciers, Ice Sheets and Sea Level: Effect of a CO₂ induced climatic change*, U.S. Dept. of Energy Report DOE/EV/60235-1, pp. 172-177, 1985.
- Budd, W. F., B. J. McInnes, D. Jenssen, and I. N. Smith, Modelling the response of the West Antarctic Ice Sheet to a climatic warming, in *Dynamics of the West Antarctic Ice Sheet*, edited by C. J. van der Veen, and J. Oerlemans, pp. 321-358, Reidel, Dordrecht, 1987.
- Giovinetto M. B., and C. Bull, Summary and analysis of surface mass balance compilations for Antarctica 1960-85, *Report 1*, Byrd Polar Research Center, Ohio State University, 90 pp., 1987.
- Grotch, S. L., Regional intercomparisons of general circulation model predictions and historical climate data, *DOE/NBB-0084*, 291 pp., 1988.
- Hansen, J., A. Lacis, D. Rind, G. Russell, P. Stone, I. Fung, R. Ruedy, and J. Lerner, Climate sensitivity: Analysis of feedback mechanisms, in *Climate Processes and Climate Sensitivity* (Maurice Ewing Series, No. 5), edited by J. E. Hansen and T. Takashi, pp. 130-163, American Geophysical Union, Washington, DC, 1984.
- Houghton, J. T., G. J. Jenkins, and J. J. Ephraums (Eds.), *Climate Change: The IPCC Assessment*, 365 pp., Cambridge University Press, 1990.
- Loewe, F., Precipitation and evaporation in the Antarctic, in *Meteorology of the Antarctic*, edited by M. P. van Rooy, Weather Bureau, Pretoria, pp. 71-89, 1957.
- Mellor, M., and C. Swithinbank, Airfields on Antarctic glacier ice, *CRREL Report 89-21*, 97 pp., U.S. Army Corps of Engineers, Cold Regions Research and Engineering Laboratory, 1989.
- Robin, G. deQ., Changing the sea level, Chapter 7 in *The Greenhouse Effect, Climatic Change and Ecosystems*, edited by B. Bolin et al., SCOPE, 29, pp. 323-359, J. Wiley, Chichester, 1986.
- Rusin, N. P., Meteorological and Radiational Regime of Antarctica, Translated by Israel Program for Scientific Translation 1964. Office of Technical Services, U.S. Dept. of Commerce, Washington, DC, 1961.
- Schwerdtfeger, W., Weather and climate of the Antarctic, in *Developments in Atmospheric Science 15*, 261 pp., Elsevier, Amsterdam, 1984.
- Simmonds, I., Analysis of the 'spinup' of a general circulation model, *J. Geophys. Res.*, 90, 5637-5660, 1985.
- Simmonds, I., Improvements in General Circulation Model performance in simulating Antarctic climate, *Antarctic Science*, 2, 287-300, 1990a.
- Simmonds, I., Impact of reduced sea ice concentration on the Antarctic mass balance, *Proceedings of the Centre for Mathematical Analysis*, vol. 25, edited by G. A. Latham and J. A. Taylor, pp. 39-48, Australian National University, 1990b.
- Simmonds, I. and W. F. Budd, A simple parameterization of ice leads in a GCM and the sensitivity of climate to a change in Antarctic ice concentration, *Ann. Glaciol.*, 14, 266-269, 1990.
- Simmonds, I., and M. Dix, The use of mean atmospheric parameters in the calculation of modelled mean surface heat fluxes over the world's oceans, *J. Phys. Oceanogr.*, 19, 205-215, 1989.
- Simmonds, I., G. Trigg, and R. Law, *The Climatology of the Melbourne University General Circulation Model*, 67 pp., Publication No. 31, (NTIS PB 88 227491.), Department of Meteorology, University of Melbourne, 1988.
- Zwally, H. J., J. C. Comiso, C. L. Parkinson, W. J. Campbell, F. D. Carsey, and P. Gloersen, *Antarctic sea ice, 1973-1976. Satellite passive-microwave observations*, 206 pp., NASA Scientific and Technical Information Branch, NASA SP-459, 1983.

The Greenland Ice Sheet Contribution to Sea Level Changes During the Last 150,000 Years

A. Letréguilly, N. Reeh, and P. Huybrechts

Alfred Wegener Institute for Polar and Marine Research, Bremerhaven, Germany

ABSTRACT

Because of a possible greenhouse warming, it is expected that the Greenland ice sheet will retreat due to increased melting. By reconstructing the past evolution of the ice sheet, it is possible to obtain some insight as to the type of variations that are possible, as well as the contribution to sea level. The Greenland ice sheet is presently the second largest ice sheet of the world, and its contribution to sea level changes is not negligible.

The evolution of the Greenland ice sheet has been computed by means of a thermo-mechanical ice sheet model (developed by Huybrechts [1989]). The surface accumulation and ablation, which are climate dependent, are driven by the temperature record obtained from the Greenland ice margin studies [Reeh, this volume]. Some sensitivity experiments have shown that the model results are strongly dependent on the mass balance history. The simulation of the Greenland ice sheet provides a continuous volume changes record, which can easily be converted into sea level changes. It shows that at the last glacial maximum, the ice sheet was larger, which created a 1-m lowering of sea level. During the last interglacial, 130,000 years B.P. (Emiliani sub-stage 5e), the ice sheet was substantially more restricted than today, part of Southern Greenland being ice free. This corresponds to a 2-m rise in sea level. However, this is not the only warm episode; around 100,000 years B.P., a warm period about 20,000 years long (sub-stage 5c) also creates a restricted ice sheet, and hence a sea level 2 m higher than today for that period.

During the ice age, the ice sheet, bounded by the steep slopes of the coastline, did not extend much further. The amount of ice stored corresponds then to a sea level decrease of one meter, which is only a small fraction of the 130-m lowering at the end of that period. However, for a moderately warmer climate, such as the climate of the 5e and 5c sub-stages, the Greenland ice sheet will account for a substantial part of the sea level rise; unlike Antarctica, a rise in temperature increases the ablation more than the accumulation, causing a rapid retreat of the ice margin.

AD-P007 331



92-17835



A Post-Cromerian Rise in Sea Level

Eric Olausson

Hultvägen 9, S-440 06 Grdö, Sweden

ABSTRACT

The intensified cooling in the northern hemisphere during the Elsterian-Saalian ice ages (isotopic stages 22-6) resulted in a reduction of the Antarctic ice sheet by $10-15 \times 10^6 \text{ km}^3$, equal to a rise in sea level by about 40 m. This rise in sea level changed the hydrography of the Black Sea during the late Pleistocene warmer times, caused anoxic conditions in the eastern Mediterranean during the corresponding warming-up phases, and enhanced water transport of less saline water from the Pacific into the Arctic Ocean (the present sill depth of the Bering Strait is about 50 m). The increased supply of less saline water strengthened the halocline in the Arctic Ocean, increasing the sea ice there and, by higher albedo, its cooling effect on the adjacent continents.

EVIDENCE FROM THE EASTERN MEDITERRANEAN-BLACK SEA

The eastern Mediterranean was stagnant during the last three interglacials (Holsteinian, Eemian, and Holocene) as well as some intervening interstadials [Olausson 1961, 1965, 1991]. The cause of the anoxic phases of the eastern Mediterranean was mainly increased supply of water from the Black Sea. This water constituted approximately 85% of the total water input responsible for the density stratification in the surface water mass of the eastern Mediterranean. During the last two ice ages, the water connection between the Black Sea and the eastern Mediterranean was cut off because of lower sea level and the Black Sea basin was filled with fresh (glacial) water. During the following warmer period, the eastern Mediterranean water transgressed into the Black Sea and the stored water (ca. $0.5 \times 10^6 \text{ km}^3$ water) poured into the eastern Mediterranean. This flushing of the Mediterranean with fresh water stored in the Black Sea may have been the factor that determined whether stagnation would occur.

During each of the temperate and warmer ages, from the Holsteinian to the early Holocene, sea water transgressed into the Black Sea, in contrast to the situations during the Cromerian and still older Pleistocene interglacials when the Black Sea was a fresh water lake (Figure 1). No sapropelitic muds seem to have been formed in the eastern Mediterranean during the times the Black Sea was a lake (early Pleistocene-Holsteinian). A drop in the sill depth (Bos-

porus), presently at -40 m, and/or an erosion in the channel between the Black Sea and the Mediterranean could explain this change in the Eastern Mediterranean-Black Sea connection, but another, more probable interpretation will be offered here.

EVIDENCE FROM DEEP-SEA CORES AND FROM THE ANTARCTIC

The early Pleistocene, from the Praetiglian up to the end of the Cromerian, was characterized by several, less intense glacial ages with intervening interglacials. The extent of the ice sheets in the northern hemisphere during these early Pleistocene glacial ages is not known, but judging by the $\delta^{18}\text{O}_c$ values (Figure 2) and the absence of their marginal formations (end moraines, etc.), they were much smaller than the area covered during the subsequent three glacial ages (the Elsterian, Saalian and Weichselian). It appears from the $\delta^{18}\text{O}$ -analyses (Figure 2) that the $\delta^{18}\text{O}$ in foraminifers fluctuates with an amplitude of 0.6‰ around the mean value of -1‰ (± 0.3) from the late Pliocene to the late Cromerian (isotope stage 23). The isotopic peak-to-valley amplitude then doubles (from 0.6 to ca 1.2‰). From isotopic stage 12 up to the Holocene the maxima and minima of the $\delta^{18}\text{O}_c$ decrease by 0.5 (-0.7)‰. A decrease by 0.5‰ in planktonic foraminifers means a reduction of the $\delta^{18}\text{O}$ of the ocean water by this amount during these 200,000-300,000 years (a temperature rise by three degrees during this time of falling temperature is not probable). Whence did this water come?

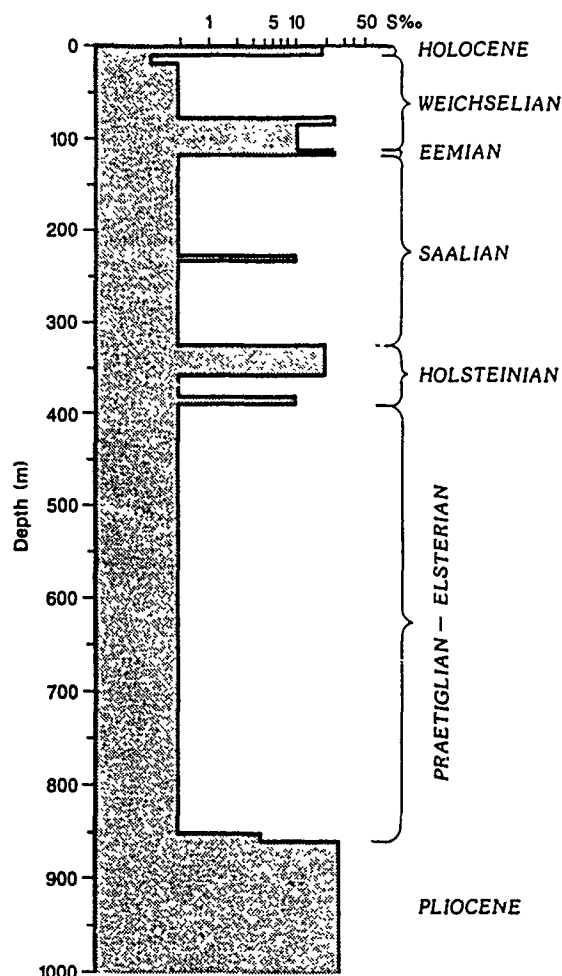


Figure 1. Generalized interpretation of environmental conditions in the Black Sea at diatomaceous intervals and intermediate units in ‰ salinity (according to Schrader [1978], Figure 29) and the tentative Pleistocene stratigraphy given in earlier papers [Olausson, 1965, 1982, 1988].

According to Robin [1987] the ice volume on the Antarctic continent was some $40 \times 10^6 \text{ km}^3$ in late Miocene times. Since then the volume has diminished by about $10\text{--}15 \times 10^6 \text{ km}^3$ due to the Pleistocene global cooling (the reduction of ice is due *inter alia* to the fact that the accumulation rate at the Antarctic is much lower during cool than during warm ages; see further Robin [1987]). If we assume a melting of ice in the Antarctic by about $15 \times 10^6 \text{ km}^3$ with a $\delta^{18}\text{O}$ value therein of -40‰ we arrive at the aforementioned change of $\delta^{18}\text{O}$ of the sea water (0.5‰). Furthermore, a supply of $15 \times 10^6 \text{ km}^3$ of water to the oceans is equal to a 40-m rise in sea level. This is the sill depth at the present Bosphorus (and nearly that of the Bering Strait as well). Thus, the sea level stood at approximately -40 m during the Cromerian interglacial, and reached its lowest level during the intense Elsterian glacial age, being at higher levels during the later glacials and interglacials (Figure 3).

High sea level stands during the Eemian are in evidence [see further, e.g., Flint, 1971, pp. 329–343], but not necessarily from the Holsteinian, which may suggest that the aforementioned melting of the Antarctic ice was finished during the Saalian ice age. Since most of the times from the

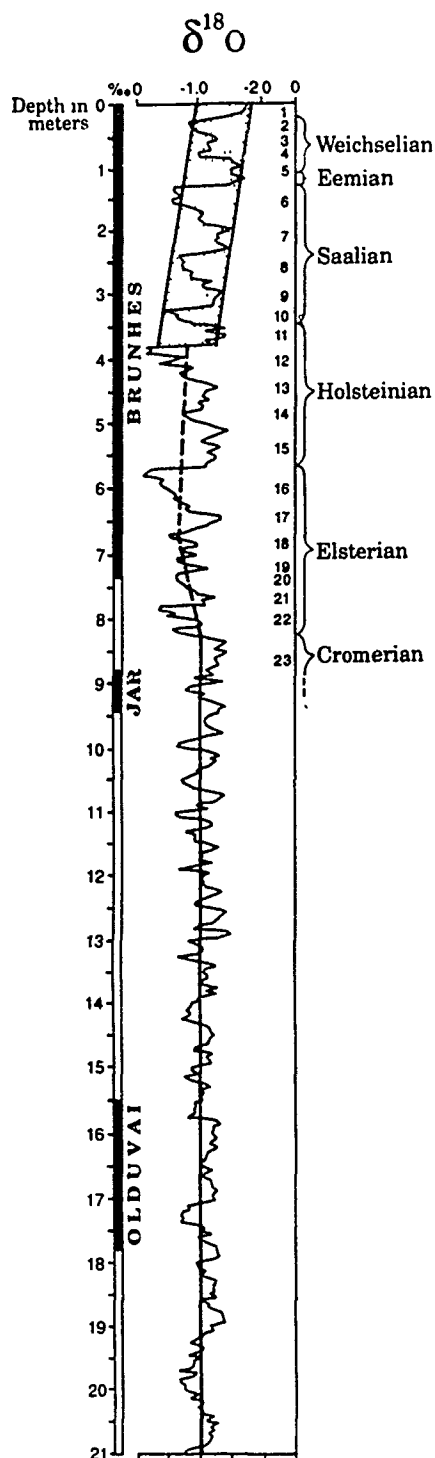


Figure 2. The oxygen-isotopic and paleomagnetic records in core V28-239 from a depth of 3490 m in the equatorial Pacific ($3^{\circ}15'N$, $159^{\circ}11'E$) according to Shackleton and Opdyke [1976]. The correlation with the European Pleistocene stratigraphy is according to Olausson [1982]. Note that the $\delta^{18}\text{O}$ fluctuates around -1 per mil from the late Pliocene to the end of the Cromerian interglacial (isotopic stage 23). Then the minima reach higher $\delta^{18}\text{O}$ values. From the late Holsteinian (isotopic stage 12) there is a more or less continuous decline of the $\delta^{18}\text{O}$ upcore to the Holocene age, which is attributed to a reduction of the Antarctic ice sheet of about 15 milj. km^3 and a sea level rise of about 40 m.

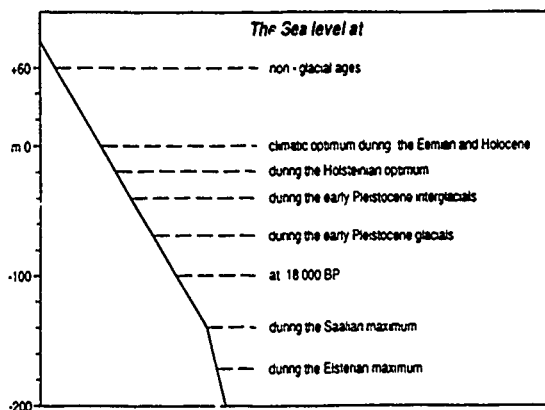


Figure 3. Pleistocene sea level stands.

Elsterian to the end of the Saalian were cool ice ages, there should be a more or less continuous reduction of the Antarctic ice sheet due to the climatic deterioration.

The conclusion is therefore that the very intense cooling and glaciations in the north during late Pleistocene times caused both a partial melt of the Antarctic ice, due to lower accumulation rate, and a rise in the sea level to such an extent that the Black Sea developed euxinic conditions by inflow from the Mediterranean. Therefore the flushing, the key point in the development of the anoxic phases of the eastern Mediterranean discussed above, was a result of this Antarctic melt and the global rise of the sea level.

The sill depth of the Bering Strait is presently ca. 50 m and a rise in the sea level by ca. 40 m would have enhanced the water transport into the Arctic Ocean, increasing the sea ice there and, by higher albedo, its cooling effect [see further Olausson and Jonasson, 1969; Olausson, 1988].

The reason for the severe coolings starting from the Elsterian ice age is not yet known.

The average depth of the shelf break is uniform, averaging about 130 m over most of the world ocean [Kennett, 1982, p. 29]. This may have been developed during the Elsterian-Saalian ice ages (Figure 3).

CONCLUSION

There was evidently a global rise in the sea level during the Elsterian-Saalian (-Weichselian?) ages by about 40 m due to a partial reduction of the Antarctic ice sheet. This reduction resulted from the intensified cooling in the northern hemisphere during the aforementioned late Pleistocene times. This rise in the sea level caused a transgression into the Black Sea which then developed euxinic conditions during the Holsteinian-Holocene interglacials and some intervening interstadials. The Black Sea waters then developed anoxic conditions in the eastern Mediterranean during twelve deglacial-warming-up phases.

ACKNOWLEDGMENTS

Financial support was given by the Swedish Natural Science Research Council. Discussions with professor Gordon de Q. Robin are greatly appreciated.

REFERENCES

- Flint, R. F., *Glacial and Quaternary Geology*, 892 pp., J. Wiley, New York, 1971.
- Kennett, J. P., *Marine Geology*, 752 pp., Prentice-Hall Inc., Englewood Cliffs, NJ, 1982.
- Olausson, E., Studies of deep-sea cores, *Rept. Swedish Deep-Sea exped.*, 8, 337-391, 1961.
- Olausson, E., Evidence of climatic changes in North Atlantic deep-sea cores, with remarks on isotopic paleotemperature analysis, in *Progress in Oceanography*, 3, edited by M. Sears, pp. 221-252, Pergamon, Norwich, 1965.
- Olausson, E., Pleistocene stratigraphy and chronology, *Geol. Förel. Stockholm Förel.*, 104, 255-256, 1982.
- Olausson, E., On the Cenozoic oceans: evidence of the calcium carbonate content, $\delta^{13}\text{C}$ and $\delta^{18}\text{O}$, *Geol. Förel. Stockholm Förel.*, 67, 103-118, 1988.
- Olausson, E., Carbon and oxygen isotope composition of foraminifera in two cores from Bannock Basin area (Eastern Mediterranean), *Marine Geology*, 1991, In press.
- Olausson, E., and U. C. Jonasson, The Arctic Ocean during the Würm and early Flandrian, *Geol. Förel. Stockholm Förel.*, 91, 185-200, 1969.
- Robin, G. de Q., The Antarctic ice sheet, its history and response to sea level and climatic changes over the past 100 million years, *Palaeogeogr., Palaeoclimatol., Palaeoecol.*, 67, 31-50, 1988.
- Schrader, H. J., Quaternary through Neogene history of the Black Sea, deduced from the paleoecology of diatoms, silicoflagellates, ebridians and chrysomonads, in *Initial Rept. Deep Sea Drilling Project*, 42 (2), edited by D. A. Ross, Y. P. Neprochnov, et al., pp. 789-867, U.S. Government Printing Office, Washington, DC, 1978.
- Shackleton, N. J., and N. D. Opdyke, Oxygen-isotope and paleomagnetic stratigraphy of the Pacific core V28-239, late Pliocene to latest Pleistocene, *Geol. Soc. Amer. Memoir* 145, 449-464, 1976.

Meltwater Runoff Lag from Arctic Glaciers and Ice Caps During Global Warming

W. T. Pfeffer, M. F. Meier, and T. H. Illangasekare
University of Colorado, Boulder, Colorado, U.S.A.

ABSTRACT

Predictions of the contribution of glacier wastage to future sea level change in response to global warming must consider refreezing of meltwater in cold snow. Runoff from surface melt generated in cold permeable snow is delayed because the water first percolates locally and refreezes. Calculations to date show that this process may significantly reduce predicted sea level rise from Greenland and Arctic ice caps over the next 50–150 years.

We present an extended analysis of this process for the circumpolar arctic glaciers and ice caps. Calculations are presented which provide estimates of the quantity of water refrozen by this process for the entire Arctic (given simple climate change scenarios) and the consequent effect on predictions of future sea level.

Measurement Error and Climate Change Implications of Glacier Mass Balance Records from Western Canada

Melinda M. Brugman

National Hydrology Research Institute, Environment Canada, Saskatoon, Saskatchewan, Canada

ABSTRACT

Trends in temperature, precipitation, insolation and large-scale atmospheric circulation have been shown to correlate with glacier mass balances measured in western Canada and elsewhere in North America. In order to understand these apparent correlations, a detailed analysis of measurement error is needed. In this paper, the error issue is examined for Sentinel, Place, Helm, Woolsey, Peyto and Ram River glaciers. All these glaciers have experienced a strongly negative cumulative mass balance, except Sentinel, which is located in the western portion of the Coast Ranges. All the glaciers, even Sentinel, have dramatically retreated throughout the measurement period at rates of one to five meters per year. Helm and Sentinel glaciers are only a few kilometers apart, yet they display markedly different mass balance records. We must ask, how reliable are the glacier data?

To answer this question, the effects of measurement bias (i.e., error) due to internal accumulation, basal melt, inadequate or improper pole placement, pole movement, map inaccuracy, surface slope change, wind and avalanche redistribution of snow, albedo change due to changing patterns of crevassing, surface dust and rock coverings are first considered. Then, computed errors in summer, winter and net balance data are compared to that of meteorological parameters obtained for each glacier site. Observer and technique changes are examined. Errors attributable to data manipulation are detailed.

Cumulative balance error is best computed by remapping the surface of the glacier and directly calculating the total volume change since the beginning of the measurement period. Efforts are presently underway to do this by direct mapping or estimation of changes in glacier volume from stake surveys, radar and seismic sounding of glacier depths and earlier glacier surface maps.

Balance error should be further analyzed with new maps, and observation techniques updated to include accurate annual field surveys and remote sensing data. Increased standardization of measurement methods at all the sites (Canadian and non-Canadian) should reduce the possibility of error due to observer bias. In summary, regular remapping of surface contours and glacier cross-sectional profiles is necessary to properly check the accuracy of long-term glacier mass balance data.

Ice Front Fluctuations of the Shirase Glacier, East Antarctica

Fumihiko Nishio

National Institute of Polar Research, Tokyo, Japan

ABSTRACT

The Shirase Glacier drainage basin in the Queen Maud Land ice sheet is drained by a fast-moving ice stream with a flow rate of 2–3 km yr⁻¹ at the mouth of Shirase Glacier. In order to predict likely ice sheet responses to future changes in climate, it is essential to understand the controls on ice stream motion.

In the upstream region of the Shirase Glacier drainage basin, the ice sheet has thinned by approximately 1 m yr⁻¹. The possible cause of thinning is basal melting at the ice–bedrock interface. Since thinning began, the Shirase Glacier has been flowing as a fast-moving ice stream to the mouth of this drainage basin.

At the mouth of the ice stream, the Shirase Glacier crosses the grounding line and a 15-km-wide floating ice tongue extends 80 km to the north. At the grounding line the mean velocity is 2.5 km per year, the ice thickness is about 500 m and gradually decreases towards the front.

The positions of the front of the ice tongue have been determined since 1957 by ground survey and recently by LANDSAT MSS and TM, and MOS-1 MESSR satellite images. Since 1957 the ice tongue has been retreating to the mouth of Shirase Glacier and at present there is no ice tongue evident in MOS-1 MESSR imagery obtained in February 1989 by the Multi-purpose Satellite Receiving System at Syowa Station.

In summer, Lützow-Holm Bay remains covered with thick landfast sea ice, preventing the ice tongue from flowing seaward by ice stream motion. However, since 1957 the floating ice tongue has disintegrated three times, in the middle of the 1960s, 1980 and 1988, due to the retreat of the fast ice in Lützow-Holm Bay.

Annual mean air temperatures at Syowa Station since 1957 have increased by approximately 1°C, and 1980 was 2°C higher than the average annual temperature. This suggests that the fast ice cover in the Lützow-Holm Bay is probably sensitive to climate changes in the Antarctic region and is linked to the existence of the ice tongue of the Shirase Glacier.

Recent rapid shrinkage of the ice tongue is, therefore, associated with the indication of increasing mean annual temperature at Syowa Station, Antarctica.

Changes in Ice Cover Thickness and Lake Level of Lake Hoare, Antarctica

Robert A. Wharton, Jr.

Biological Sciences Center, Desert Research Institute, Reno, Nevada, U.S.A.

Gary D. Clow

Astrogeology Branch, U.S. Geological Survey, Menlo Park, California, U.S.A.

Christopher P. McKay

Space Sciences Division, NASA Ames Research Center, Moffett Field, California, U.S.A.

Dale T. Andersen

Lockheed Engineering and Sciences Co., Washington, D.C., U.S.A.

George M. Simmons, Jr.

Department of Biological Sciences, Virginia Tech, Blacksburg, Virginia, U.S.A.

ABSTRACT

Results from 10 years of ice thickness measurements at perennially ice-covered Lake Hoare in Southern Victoria Land, Antarctica are reported. The ice cover of this lake thinned appreciably during the period 1979 to 1986 at a rate exceeding 20 cm yr⁻¹, from an initial thickness of 5.5 m. Since 1986, the ice cover thickness seems to have leveled off at about 3.5 m. We suggest that the mode of behavior of the ice cover on this lake may have made a transition from (1) a thick "dry" ice cover in which sublimation is the dominant form of mass removal from the ice cover, to (2) a thinner "wet" ice cover in which near-surface melting and subsequent percolation of meltwater through the ice becomes at least as important as sublimation in the removal of mass from the surface of the ice cover. We also discuss a parametric analysis of the response of a model of the thick "dry" ice cover to various environmental factors, including surface temperature, sunlight, wind speed, and the amount of light-obscuring surface sediments. This analysis shows that of the above factors, an increase in mean annual temperature is the most plausible explanation for the thinning of the ice cover. Data concerning lake level and degree days above freezing are presented to show the relationship between peak summer temperature and the volume of glacier-derived meltwater entering Lake Hoare each summer. From these latter data and from previous observations by others that the lakes in the dry valleys are rising, we infer that the peak summer temperatures have been above zero for a progressively longer period of time each year since 1973.

Thermal and Hydrologic Responses of an Arctic Watershed to Climatic Warming

Larry D. Hinzman and Douglas L. Kane

Water Research Center, University of Alaska Fairbanks, Fairbanks, Alaska, U.S.A.

ABSTRACT

The implications of global warming reach beyond warmer air temperatures, milder winters and longer summers. The potential effects of climatic warming on the hydrologic regime of an arctic watershed were explored with respect to physical changes in the active layer and the resultant changes in the components of the annual water balance and the nature of the hydrologic cycle. With the advent of climatic warming, the annual depth of thaw in the permafrost will increase, affecting the amount of soil moisture storage, the depth to the water table, even the shape of the runoff hydrograph. The gradual thawing of the active layer was simulated using TDHC, a heat conduction model which incorporated phase change. The results of four possible scenarios of climatic warming were input into HBV, a hydrologic model, to elucidate the effects on the hydrologic regime. The results indicate an earlier spring melt event, greater evaporation, greater soil moisture storage, and a potential for severe moisture stress on current vegetation types in early summer unless the precipitation pattern changes. The amount of free water in the soil will largely depend upon precipitation patterns and amount.

Contemporary Climate Change in the Mackenzie Valley, N.W.T. and the Impact upon Permafrost

Alan Judge

Terrain Sciences Division, Geological Survey of Canada, Ottawa, Ontario, Canada

Angus Hedley

Canadian Climate Centre, Atmospheric Environment Service, Downsview, Ontario, Canada

Margo Burgess

Terrain Sciences Division, Geological Survey of Canada, Ottawa, Ontario, Canada

Kay MacInnes

Land Resources Division, Indian and Northern Affairs, Yellowknife, Northwest Territories, Canada

ABSTRACT

Many global change scenarios predict a pronounced warming of the Arctic regions over the next several decades. The impacts of a possible warming of several degrees on the permafrost environment have important implications locally and globally.

Although permafrost temperatures may be expected to change in response to an increase in air temperature, the relationship between air and ground temperature is a result of complex and poorly known surface energy exchange processes. The magnitude, extent and rate of permafrost response to climate change are, therefore, not simple to predict. A cooperative project was established in 1986 in order to examine and better understand permafrost and climate relationships along the Mackenzie Valley corridor. Several instrumented sites have been established and gradually equipped with AES automatic weather stations and GSC/INAC deep ground temperature boreholes. Analysis and monitoring of ground temperature and climate data will provide information on both recent surface temperature changes and on the ground thermal response to current local climate trends. Analysis of existing air temperature data from standard meteorological stations yields statistically significant increases of about 1 K in the past 50 years. In contrast the arctic coast shows some evidence of cooling in the same time-frame.

Preliminary examination of ground temperature profiles from the Mackenzie Valley provides evidence of recent surface increases of up to 3 K. The present northward decrease of surface temperature in the western arctic is roughly 0.7 K per degree of latitude and thus the southern margins of permafrost might be expected to retreat northwards by several hundred kilometers over the next century.

AD-P007 332



92-17836



Response of Permafrost to Changes in Paleoclimate

T. E. Osterkamp, J. P. Gosink, T. Fei, and T. Zhang

Geophysical Institute, University of Alaska Fairbanks, Fairbanks, Alaska, U.S.A.

ABSTRACT

Solutions to the Stefan problem for the motion of the base of ice-bearing permafrost in response to changes in paleoclimate were obtained using perturbation, finite difference, and finite element methods. Paleotemperature models were used to investigate the thickness response, compare solution methods, determine the current state of the permafrost, and to determine constraints on the models. The perturbation and finite difference methods used the approximation of linear temperature profiles while the finite element method did not. There was a transient thickness response of about 41 kyr implying that paleotemperature records of greater length are needed for models and that the permafrost loses its "memory" of past conditions for much longer times. Faster thawing rates, slower freezing rates, and greater variations in thickness were found for the perturbation and finite difference solutions compared to the finite element solution. These appear to be caused by the simplifying assumptions in the former solutions. A lag (20 kyr) exists between changes in surface temperature and thickness response and a small thermal offset is apparent in the finite element solution. Small asymmetries exist in the freezing and thawing rates and thickness response. Paleotemperature models based on ice cores predict current permafrost thicknesses that are too large. Models with the long-term mean surface temperature of permafrost within a few degrees of the current value of -11°C and with full glacial temperatures no more than $6-8^{\circ}\text{C}$ lower are compatible with current Prudhoe Bay conditions. These include models developed for East Siberia, from isotopic profiles in deep sea sediments, and for Barrow, Alaska, modified for Prudhoe Bay. These models predict that the permafrost thickness at Prudhoe Bay varied by $\leq 10\%$ (≤ 60 m) over the last glacial cycle. Freezing and thawing rates were less than 6 mm yr^{-1} . At present, this permafrost should be near its long-term equilibrium thickness and should be thawing at $< 1 \text{ mm yr}^{-1}$.

Time scales for the thickness response of deep continuous permafrost are of the same order as the periods of recent glaciations (10^5 years) over the past 10^6 years. Therefore, it is appropriate to consider the permafrost response to the inferred changes in paleotemperatures associated with these glaciations. Three solutions have been obtained to address this question. An approximate analytical (perturbation) method was used to solve the heat balance equation at the phase boundary (base of the ice-bearing permafrost) assuming linear temperature profiles in the permafrost and constant geothermal heat flux (which also yields a linear

temperature profile) under the permafrost. A numerical solution (finite difference method) was constructed using the same assumptions. The third solution, which does not use these assumptions, is a complete numerical scheme using finite elements to numerically integrate the thermal energy equation from the permafrost surface, through the phase boundary, and deep into the underlying unfrozen materials. Applications of the solution methods to paleotemperature models at the surface of the permafrost were used to compare the solutions, to investigate the thickness response of the permafrost, to assess the current state of the permafrost,

and to develop general constraints on paleotemperature models of the surface temperature history, T_s , of the permafrost near Prudhoe Bay, Alaska.

The solution methods were applied to step, linear, sinusoidal, and other potential paleotemperature models of T_s . Except for the sinusoidal model, these models are not generally periodic. Perturbation solutions which are polynomials in time, t , for models consisting of a series of step or linear changes in T_s can be used to approximate any T_s provided each step or linear segment is long compared to the time constant, $t_c = X^2/4D$, where X is the permafrost thickness and D its diffusivity.

There was a transient response in X for all solutions which, for the models and Prudhoe Bay conditions, was nearly nil after about 200 kyr. For the sine model, the perturbation solution yields a transient time constant, $t_a = hX_0/J \approx 41$ kyr, where h is the volumetric latent heat, X_0 the long-term periodic mean permafrost thickness ($X_0 = \bar{X}_e = K_1 (T_e - \bar{T}_s)/J$) and J the deep undisturbed geothermal heat flux. Since the transient response affects the predicted X , then results obtained from calculations extending over one time constant or less will generally be influenced by the transient. When T_s is periodic, the transient can be eliminated by choosing the initial permafrost thickness, X_i , to be the value found at the end of two or more cycles. Permafrost at Prudhoe Bay loses its "memory" of past conditions for times much longer than one time constant. As a result, the effects of possible submergence of some areas at Prudhoe Bay, Alaska by high sea levels >45 kyr B.P. cannot be detected at present, given the uncertainties in the data.

Long-term mean permafrost thickness, \bar{X} , calculated from the time average of X , usually differed slightly between solutions and with \bar{X}_e . This may be partially a result of small computational errors but when the thermal conductivity in the permafrost, K_1 , was set equal to that of the underlying unfrozen material, K_2 , the difference was nearly eliminated, suggesting that it was, at least primarily, a result of thermal offset.

The perturbation and finite difference solutions predicted amplitudes for X ($513.5 \text{ m} \leq X \leq 686.5 \text{ m}$ and $510 \text{ m} \leq X \leq 685 \text{ m}$ respectively for the sine model) which were generally greater than the finite element values ($531.5 \text{ m} \leq X \leq 657.5 \text{ m}$ for the sine model) by about one fourth to one third.

There is a lag between T_s and changes in X . For the sine model, the lag angle, $\beta = \arctan(\omega t_a) \approx 19$ kyr, where ω is the frequency.

Small asymmetries exist in X and \dot{X} for the numerical solutions. These are most apparent in the sine model where, for the finite element solution, values of \dot{X} for thawing are greater than for freezing which results in changes of X for thawing which are greater than for freezing. The curve for X vs. t is also slightly wider (in time) compared to a pure sine function when $X < \bar{X}$ and narrower when $X > \bar{X}$. The curve for \dot{X} is slightly wider during freezing and narrower during thawing.

The finite element solution for a sine model of T_s was used to compare the response of permafrost containing brine and ice to that of permafrost containing pure ice. Temperatures and phase boundary motion are qualitatively similar for the two cases. However, for permafrost containing brine, phase boundary velocities and thickness variations ($-6.0 \text{ mm yr}^{-1} \leq \dot{X} \leq 5.2 \text{ mm yr}^{-1}$ and $345 \text{ m} \leq X \leq 523 \text{ m}$)

were greater compared to permafrost that contained pure ice ($-3.9 \text{ mm yr}^{-1} \leq \dot{X} \leq 3.8 \text{ mm yr}^{-1}$ and $365 \text{ m} \leq X \leq 487 \text{ m}$). These differences are attributed to temperature-dependent thermal properties, distributed latent heat effects, and the conversion of only part of the soil solution to ice near the phase boundary when brine is present in the permafrost.

Temperature profiles in the permafrost are nearly linear for the finite element solution, which supports the linear assumption used in the perturbation and finite difference solutions. The long-term variations in paleotemperatures lead to disturbances in the temperature profiles extending to 2 to 3 km depth for Prudhoe Bay conditions.

Paleotemperature models for the surface temperature of permafrost are constrained in that they must predict the current permafrost conditions at Prudhoe Bay to within the uncertainties. Currently, $X \approx 600 \text{ m}$, $J_1 \approx 55 \text{ mW m}^{-2}$, $T_s = -11^\circ\text{C}$, and X is unmeasured but inferred to be close to zero.

The step model of Brigham and Miller [1983] which was developed for the Barrow area was modified for Prudhoe Bay conditions and has $\bar{T}_s \approx -13.3^\circ\text{C}$ and $\bar{X}_e \approx 739 \text{ m}$ with $-8^\circ\text{C} \geq T_s \geq -15^\circ\text{C}$. It leads to a prediction of current $X \approx 712 \text{ m}$, which is slightly greater than the uncertainty (about $\pm 15\%$), with $712 \text{ m} \leq X \leq 755 \text{ m}$.

A normalized SPECMAP curve [Matteucci, 1989] was modified and linearized to produce a relatively warm model with $\bar{T}_s \approx -11^\circ\text{C}$, $\bar{X}_e \approx 600 \text{ m}$, and $-8^\circ\text{C} \geq T_s \geq -14^\circ\text{C}$. Current $X \approx 602 \text{ m}$ with $562 \text{ m} \leq X \leq 646 \text{ m}$.

A paleotemperature model developed for East Siberia [Maximova and Romanovsky, 1988] yields predictions in excellent agreement with current conditions. This model has $\bar{T}_s \approx -11.3^\circ\text{C}$, $\bar{X}_e \approx 616 \text{ m}$, and T_s ranging from -7°C to slightly colder than -17°C . Values of \bar{T}_s are about 2°C warmer than the modified step model while values for T_s during glacial periods agree with the estimates of Brigham and Miller [1983]. Current $X \approx 601 \text{ m}$ with $557 \text{ m} \leq X \leq 660 \text{ m}$.

Predictions based on the East Siberian model, modified SPECMAP model, and on the modified step model indicate that the permafrost should be near its equilibrium thickness and thawing (less than 1 mm yr^{-1}) in response to the warming since the last glacial period. The predicted current heat flow in the permafrost at X is about $58\text{--}61 \text{ mW m}^{-2}$, slightly larger than observed, and increasing. This indicates that the currently observed value may be slightly greater than the true heat flow at depth.

Computations based on paleotemperature models determined from the isotopic profile in the Vostok ice core predict current values for X which are much too large. Results from the Camp Century ice core are expected to be similar. It does not seem likely that these models will be useful for interpreting permafrost thickness variations in the Alaskan Arctic.

It appears that paleotemperature models for the surface temperature of permafrost in the Prudhoe Bay area will need to have \bar{T}_s within a few degrees of the current T_s (-11°C) and minimum temperatures during the last glacial period within about $6\text{--}8^\circ\text{C}$ of current T_s . These conclusions are based on results from a limited number of models. Except for the step model, these models were developed for other distant regions.

Modeling of the response of the permafrost to changes in the paleoclimate is hampered by the lack of reliable paleo-

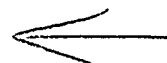
temperature models for the surface temperature of the permafrost and information on the thermal properties and heat flow in the permafrost.

ACKNOWLEDGMENTS

This research was sponsored by the Earth Sciences Section, Division of Polar Programs, National Science Foundation under Grant Nos. DPP86-19382 and DPP-87-21966, and U.S. Geological Survey Award No. 14-08-001-G1305.

REFERENCES

- Brigham, J. K., and G. H. Miller, Paleotemperature estimates of the Alaskan Arctic Coastal Plain during the last 125,000 years, *Proc. Fourth Intl. Conf. Permafrost*, pp. 80-85, National Academy Press, Washington, DC, 1983.
- Matteucci, G., Orbital forcing in a stochastic resonance model of the Late-Pleistocene climate variations, *Climate Dynamics*, 3, 179-190, 1989.
- Maximova, L. N., and V. Y. Romanovsky, A hypothesis for the Holocene permafrost evolution, *Proc. Fifth Intl. Conf. Permafrost*, pp. 102-106, Norwegian Inst. Tech., Trondheim, Norway, 1988.



92-17837



AD-P007 333



The Antarctic Glacial Geologic Record and GCM Modeling: A Test

D. H. Elliot

Byrd Polar Research Center and Department of Geology & Mineralogy, The Ohio State University, Columbus, Ohio, U.S.A.

D. H. Bromwich

Byrd Polar Research Center, The Ohio State University, Columbus, Ohio, U.S.A.

D. M. Harwood

Department of Geology, University of Nebraska, Lincoln, Nebraska, U.S.A.

P.-N. Webb

Byrd Polar Research Center and Department of Geology & Mineralogy, The Ohio State University, Columbus, Ohio, U.S.A.

ABSTRACT

A recent GCM (General Circulation Model) study of Antarctic glaciation by Oglesby concluded that (1) oceanic heat transport is relatively unimportant in the development and maintenance of Antarctic glaciation; (2) height and polar position, not the Antarctic Circumpolar Current, have led to thermal isolation; and (3) surface elevation may be crucial for glaciation. Model results are here evaluated against the Pliocene geologic record for Antarctica.

The Sirius Group, widely distributed in the Transantarctic Mountains, contains diatom floras suggesting open marine conditions in interior East Antarctica as recently as about 3 m.y. ago. The Sirius deposits also contain a sparse fossil flora including *Nothofagus* wood, demonstrating snow-free conditions and elevated summer temperatures within 500 km of the South Pole. Based on fission track data and marine sediments, uplift rates for the Transantarctic Mountains are estimated to average 50–100 m m.y.⁻¹ for the last 10 m.y., although rates may have been higher during the last 3 m.y. The continental interior is also most unlikely to have changed elevation by more than a few hundred meters in the last 3 m.y. If the dating of the Sirius is correct and uplift rates have not been an order of magnitude higher, then polar location and elevation cannot be primary controls on the formation and subsequent fluctuations of the ice sheet.

The cause of this discrepancy between modeling results and observations can be sought in limitations to the model (NCAR CCM1) used by Oglesby. It is known that atmospheric GCMs generally do not simulate the modern Antarctic climate with great realism. This is also true for the NCAR CCM1 as evidenced by deficiencies in simulated cyclone behavior, cloud cover amounts, air temperatures and snowfall rates. Another substantial limitation is that there is no simulation of ocean dynamics. The ocean does not transport heat poleward, and appears in the model only via specified sea surface temperature fields. Recent work with a coupled atmosphere–ocean GCM indicates that the atmosphere and ocean are strongly linked in these latitudes, and that this interaction is a dominant aspect of climatic variation on (at least) the decadal time scale.

Initial results indicate that GCM performance generally needs to be enhanced and, in particular, that realistic interactive atmosphere–ocean models are needed. An improved geologic data base, particularly with respect to age determinations and amounts and rates of uplift, would facilitate model validation.

INTRODUCTION

Concern about the possibility of global climate change resulting from human activities has given rise to renewed interest in records of paleoclimate as measures of the natural variability of the earth's climate system. Present climate is regarded as an interglacial within the coldest part (last 2–3 m.y.) of the present Cenozoic Ice Age that started tens of millions of years ago. Fluctuations of the climate system are evident in, for instance, the terrestrial record of glacial deposits and the oxygen isotope signal derived from ice and deep-sea sediment cores.

Numerical modeling of past climate can be viewed in terms of three different time scales and resolutions. Ice cores, tree rings and other records can give proxy climate data with annual resolution and time scales of several thousand years [Wigley et al., 1981; Bradley, 1983]. Ice cores from the East Antarctic ice sheet give decadal to millennial resolution on time scales of more than 100,000 years, and can be correlated with the high resolution deep sea cores on the basis of oxygen isotope stage chronology [Lorius et al., 1985, 1989]. Longer time scales are obtained from most deep sea cores and from other geologic data but resolution is generally limited. Only the last category provides information on the full range of natural variability and therefore is most important in understanding the framework for any changes in climate.

Interest in modeling past climate is increasing. Results of research on, for instance, Cretaceous (120–65 Ma) and Eocene (~55–40 Ma) climates have been presented by Barron [1983] and Cirbus Sloan and Barron [1990]. The inherent limitations of geologic data, which increase with the age of the record being considered, make evaluation of

results difficult. Here we examine results of modeling Antarctic conditions [Oglesby, 1989] in the light of inferences drawn from terrestrial deposits of Late Pliocene age (~3 Ma) in Antarctica [Webb et al., 1984; McKelvey et al., 1991]. We choose this Pliocene example for comparison of model results with the geologic record because continental positions were no different than today and no major geographic change has occurred in Antarctica except for the size of the ice sheets.

MODELING STUDY OF ANTARCTIC ICE SHEET FORMATION

Oglesby [1989] used an atmospheric general circulation model (GCM) developed by the National Center for Atmospheric Research (NCAR) to evaluate possible mechanisms that could lead to the development of ice sheets in Antarctica. The GCM employed was the Community Climate Model (CCM) which has been used for a wide variety of climate diagnostic and climate change studies [Williamson, 1990]. The model code evolves over time as simulations of additional processes are added and improved numerical schemes are implemented. Version 1 of the CCM (CCM1), unchanged since June 1987, was used in Oglesby's study.

Table 1 summarizes some of the key attributes of the CCM1 simulations carried out by Oglesby [1989]. The CCM1 and equivalent models produce global fields of the main climatic variables by numerical time integration, over an array of grid points, of five non-linear partial differential equations (two for momentum and one each for energy, mass conservation, and moisture) from specified initial conditions [Williamson et al., 1987]. Typical integration times required for the model atmosphere to approach a state of

ASPECT	TREATMENT
Predictive Equations	Conservation of mass, momentum, energy and moisture. Clouds are derived.
Numerical Details	Vertical and time calculations are carried out by finite differences, but horizontal computations involve a spectral-transform method. A sigma vertical (or terrain following) coordinate system is used.
Time Step	30 minutes
Horizontal Resolution	Spectrally truncated at rhomboidal wave 15 (R15), about 7.5° longitude by 4.5° latitude. At 70°S, this corresponds to 280 km x 500 km.
Vertical Resolution	12 unevenly spaced levels, 6 of which are below 300 hPa over terrain near sea level.
Treatment of the Ocean	Represented only by specified interface conditions; sea surface temperatures and sea ice distribution are either assumed or derived from present climatological data. No ocean dynamics (e.g., currents, poleward heat transport, thermohaline convection) is permitted.
Antarctic Topography	Specified from higher resolution data which are spectrally truncated to R15.
Radiation Modes	Perpetual January (austral summer) and July (austral winter). Solar radiation does not change from one simulation day to the next. These constructs are used because of their computational efficiency, and because the results closely approximate those obtainable from seasonal simulations. Seasonal (solar radiation varies with calendar day) - includes a calculation of snow accumulation and ablation.

Table 1. Relevant Characteristics of Oglesby's NCAR CCM1 Simulations (material extracted from Oglesby [1989] and Williamson et al. [1987]).

quasi-equilibrium with the imposed boundary conditions are a few hundred days for perpetual runs and many years for seasonal runs. In the present context, which deals with phenomena manifested over time scales of 10^5 to 10^7 years, it is particularly important to emphasize that only the behavior of the atmosphere is modeled, and that no dynamic interaction with the ocean or the ice sheets is permitted. The ocean surface characteristics and the topography of Antarctica are specified boundary conditions although in reality these can vary significantly over time periods as short as 10^3 to 10^4 years. Another key aspect is that the horizontal and vertical spacing of the grid points is much too coarse to yield adequate simulations of the katabatic wind circulation which probably plays a central role in the dynamics of the modern Antarctic atmosphere [e.g., Parish and Bromwich, 1991].

Oglesby used a set of 16 CCM1 simulations with different boundary conditions to evaluate the impact of two mechanisms upon the development of glaciation on the Antarctic continent over the last twenty million years or so: opening of the seaway (Drake Passage) between South America and Antarctica, and changing the elevation of the continent. Oceanic conditions prior to the opening of the Drake Passage were presumed to be characterized by increased oceanic poleward heat transport in comparison to today because of the disruption of the Antarctic Circumpolar Current. This oceanic change was represented in the model by specifying sea surface temperatures above freezing at the Antarctic coast during winter with the consequent absence of sea ice. The impact of variations in the height of Antarctica was examined by comparing simulations with elevations everywhere less than 200 m with those using the modern high elevation Antarctic topography. Seasonal cycle simulations with an explicit surface budgeting for snow accumulation and ablation were carried out; Antarctic grid points were initialized to be free of snow during the first summer. The goal was to ascertain whether any combination of sea surface temperatures and continental elevations could result in the complete melting of accumulated winter snow during subsequent summers. The prescribed continental snow cover for perpetual runs and the specified atmospheric CO_2 content were also varied.

The following conclusions were obtained by comparing the CCM1 runs:

(1) The presence or absence of oceanic flow through the Drake Passage has little impact on Antarctic glaciation. The small impact on simulated glaciation conditions of the presumed warmer high latitude sea surface temperatures (that accompany a closed Drake Passage) arises because of the small storm transport of heat and water vapor into the interior of the continent. The higher sea surface temperatures may, in fact, promote ice sheet growth through increased winter snowfall.

(2) Antarctica is thermally isolated by its elevation and its polar location (which results in long periods with little or no sunlight) rather than by the Antarctic Circumpolar Current.

(3) The height of the continent may play an essential role in ice sheet formation and maintenance (today, average surface temperatures decrease by about 1°C for each 100-m increase in elevation).

(4) Greatly increased atmospheric CO_2 concentrations have little impact over the changes resulting from removal of sea ice and elevated sea surface temperatures.

(5) Even with low continental elevations and very warm seas (model sea surface temperatures at the Antarctic coast during July = 14°C) the model is only able to produce tundra-like conditions (i.e., treeless, but without a permanent snow cover).

It is clear that the model wants to form an ice sheet with Antarctic geography and bedrock elevations close to those at present. This result does not necessarily imply a steady ice sheet buildup. Fluctuations in size could arise, for example, because of ice flow and varying net mass input from the atmosphere as the ice sheet topography changes. However, glaciological scaling calculations [W. A. Jones, personal communication, 1990] show that it is very difficult to get size fluctuations large enough to produce the open marine conditions in the deep interior of the continent which are implied by the glacial geologic results outlined below. Possible causes for model bias are presented in the Discussion section.

ANTARCTIC GEOLOGIC RECORD

Although the record of glaciation in Antarctica goes back to the early Oligocene (ca. 36 Ma) [Barrett et al., 1989; Hambrey et al., 1989; Wise et al., 1991] or possibly older [Barron et al., 1991; Birkenmajer, 1991], evidence from the Pliocene Sirius Group [Webb et al., 1984; McKelvey et al., 1991] and the correlative Pagodroma Tillite [McKelvey and Stephenson, 1990] provide the most dramatic evidence for substantial contrasts in Antarctic climate and ice sheet configuration through time.

The Sirius comprises scattered glacially related sedimentary deposits throughout the Ross Sea sector of the Transantarctic Mountains. The Sirius consists of compact till deposited directly by ice and interbedded glaciofluvial and glaciolacustrine sediment. Deposits assigned to the Sirius are found in a variety of topographic settings, most of which are related to present-day glacial drainage through the mountains. The most striking aspect of the principal occurrences of the Sirius [Harwood, 1986a] is the presence of rare marine microfossils and "microclasts" of marine biogenic sediment (these microclasts consist of clumps of diatom skeletons that could not have been transported aerially or by traction currents). These originate from marine sediments in subglacial basins of East Antarctica that were eroded and transported by the ice sheet to the Transantarctic Mountains [Webb et al., 1984]. The dominant microfossils are marine diatoms of early Pliocene age, although other fossil groups are present and other, older time intervals are also represented [Harwood, 1986a,b].

The marine sediments and associated microfossils reflect several episodes of extensive deglaciation when marine embayments or seaways covered intracratonic basins. Age dating for these marine incursions is afforded by application of Southern Ocean diatom biostratigraphy (developed over 20 years through deep sea drilling and piston coring in high southern latitudes including McMurdo Sound at 78°S). The diatomaceous sediments indicate a deep water (>75 m) marine depositional setting that was ice-free for several months of the year in order to allow for annual diatom blooms and accumulation of sediment consisting predominantly of diatom skeletons.

This scenario of repeated deglaciation and marine incursion presented by the Sirius data is supported by similar

micropaleontologic records from the Pagodroma Tillite [McKelvey and Stephenson, 1990] which is found adjacent to the eastern margin of the Amery Ice Shelf (Figure 1). These records and that from the Vestfold Hills (Figure 1) reported by Pickard et al. [1988] argue that deglaciation was not a local phenomenon, but involved a massive reduction in ice volume compared to the present-day ice sheet [Harwood, 1986a]. The Pliocene high stand of sea level, noted around the globe, supports this deglacial event [Haq et al., 1987; Dowsett and Cronin, 1990].

The biogenic sediments derived from the marine basins were picked up by basal ice as the ice sheets centered near or on the Gamburtsev Mountains expanded over the basins that were now emergent [Mercer, 1987] through uplift, isostatic rebound effects or Pliocene sediment infilling of the basins. Continued expansion to and through the Transantarctic Mountains resulted in deposition of the Sirius sediments (Figure 2). Climate at the time of Sirius deposition, however, was still relatively mild as indicated by the "temperate" character of Sirius tills, association with water-lain

deposits, and the presence of fossil *Nothofagus* vegetation that was growing in the Transantarctic Mountains at the time of till deposition [Webb and Harwood, 1987; Carlquist, 1987]. The *in situ* and near *in situ* plant remains also include a variety of pollen and spores [Askin and Markgraf, 1986]. Although modern *Nothofagus* may be able to tolerate winter temperatures as low as -22°C [Sakai et al., 1981], its southern limit in South America is near the 5°C mid-summer isotherm [Mercer, 1986, 1987]. Such conditions must have existed in the Dominion Range at an altitude somewhere between sea level and 1800 m, depending on the amount of uplift since that time [Mercer, 1987]. Antarctica went from a largely deglaciated condition in early- to mid-Pliocene time, to one in which a temperate ice sheet occupied most, if not all, of East Antarctica in the late Pliocene, and finally to full polar glaciation similar to today in the latest Pliocene-earliest Pleistocene [Harwood and Webb, 1990].

The occurrence of *Nothofagus* is significant in another way. As a group, *Nothofagus* seeds have very limited potential for dispersal [Van Steenis, 1971]. Thus, once lost from

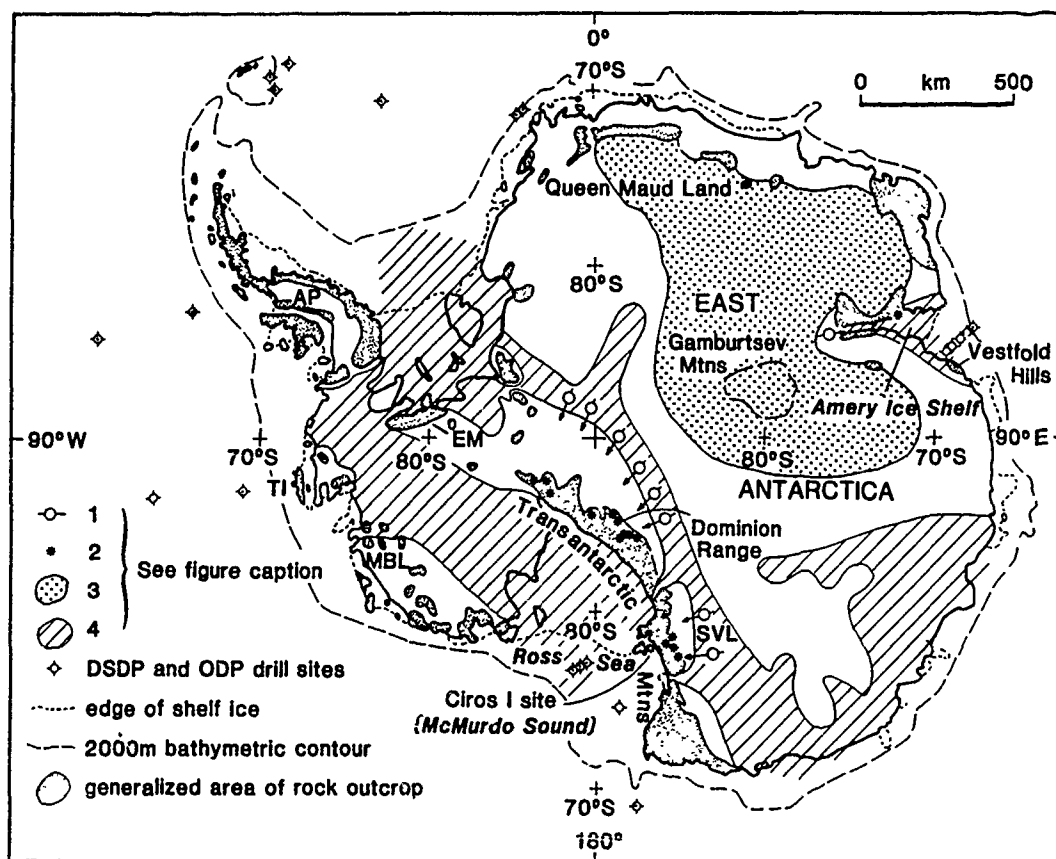


Figure 1. Antarctic paleogeography (superimposed on present-day geography) for the Early Pliocene (3–5 Ma) at the time of deposition of microfossils that were subsequently reworked into the Sirius Group. The Gamburtsev Mountains, enclosed by the long dashed lines, are more than 3000 m high but are entirely subglacial at present. Permanent ice, if present in the Early Pliocene, is inferred to have been confined to the elevated mountainous areas (ice not indicated for these areas) of West Antarctica (Marie Byrd Land, Thurstion Island, Ellsworth Mountains), the Antarctic Peninsula, the Transantarctic Mountains and to a residual ice sheet located on the higher elevations of East Antarctica. DSDP - Deep Sea Drilling Project; ODP - Ocean Drilling Program; AP - Antarctic Peninsula; EM - Ellsworth Mountains; MBL - Marie Byrd Land; SVL - South Victoria Land; TI - Thurstion Island. (1) Inferred source and subsequent transport direction for now-recycled marine microfossils in Sirius and Pagodroma sediments. (2) Outcrops where recycled marine microfossils (Sirius Group sediments and Pagodroma Tillite) are now found. (3) Inferred extent of residual ice sheet during Early Pliocene time. (4) Inferred marine basins during early Pliocene time.

Antarctica, reintroduction is most unlikely. The survival of this group in Antarctica until Sirius time (mid-Pliocene) implies that previous glaciations were never as cold as today. Thus, the present-day climate system may be a poor analog for analysis of pre-Sirius (Tertiary) glacial paleoenvironments.

Support for this period of mild Pliocene conditions in Antarctica is provided by the 2.5 Ma Kap København Formation from north Greenland [Funder et al., 1985; Böcher, 1989] which today has a polar climate. The contained plant remains and invertebrates indicate climatic conditions now found no closer than 2000 km to the south. Other deposits indicating equally mild conditions are found in Arctic Canada (Worth Point Formation; see Vincent [1989]) and northern Alaska (Gubik Formation; see Carter et al. [1986]) and collectively demonstrate that this interval of relative warmth was a bipolar phenomenon.

Elevations across the continent 2–3 m.y. ago are hard to establish. Uplift of the Transantarctic Mountains began at about 60 Ma [Fitzgerald, 1989] and since then they have risen about 5 km [Gleadow and Fitzgerald, 1987] giving average uplift rates of ~ 85 m m.y.⁻¹. The fission track data

suggest, however, that the rates of uplift were greatest in the early stages and this is supported by results from the CIROS I core [Barrett et al., 1989]. The occurrence of granite and metamorphic rock clasts in the basal sediment of the CIROS I core (Figure 1) suggests the Transantarctic Mountains in south Victoria Land (SVL) were no more than 1600 m lower than today during the early Oligocene 35 m.y. ago [Barrett et al., 1989]. This argues for higher average rates of uplift in the early stages and lower average rates in the last 35 m.y., possibly as low as 45 m m.y.⁻¹. Upper Miocene to Pliocene (7–3 Ma) marine sediments in the Dry Valleys (SVL) imply similar rates of uplift, about 40 m m.y.⁻¹ before 3 Ma and 125 m m.y.⁻¹ thereafter [Ishman and Webb, 1988; McKelvey, 1991]. In contrast to these rates of uplift, Mercer [1987] argued that the Sirius was deposited below 500 m elevation and that a minimum uplift of 1300 m in 2–3 m.y. (650–435 m m.y.⁻¹) has occurred at the Dominion Range because otherwise temperatures would have been too high for the existence of an ice sheet during deposition of the Sirius and growth of *Nothofagus*. A 600-m offset of Sirius beds on the Dominion Range demonstrates vertical movements in the last 2–3 m.y. The Transantarctic Mountains are

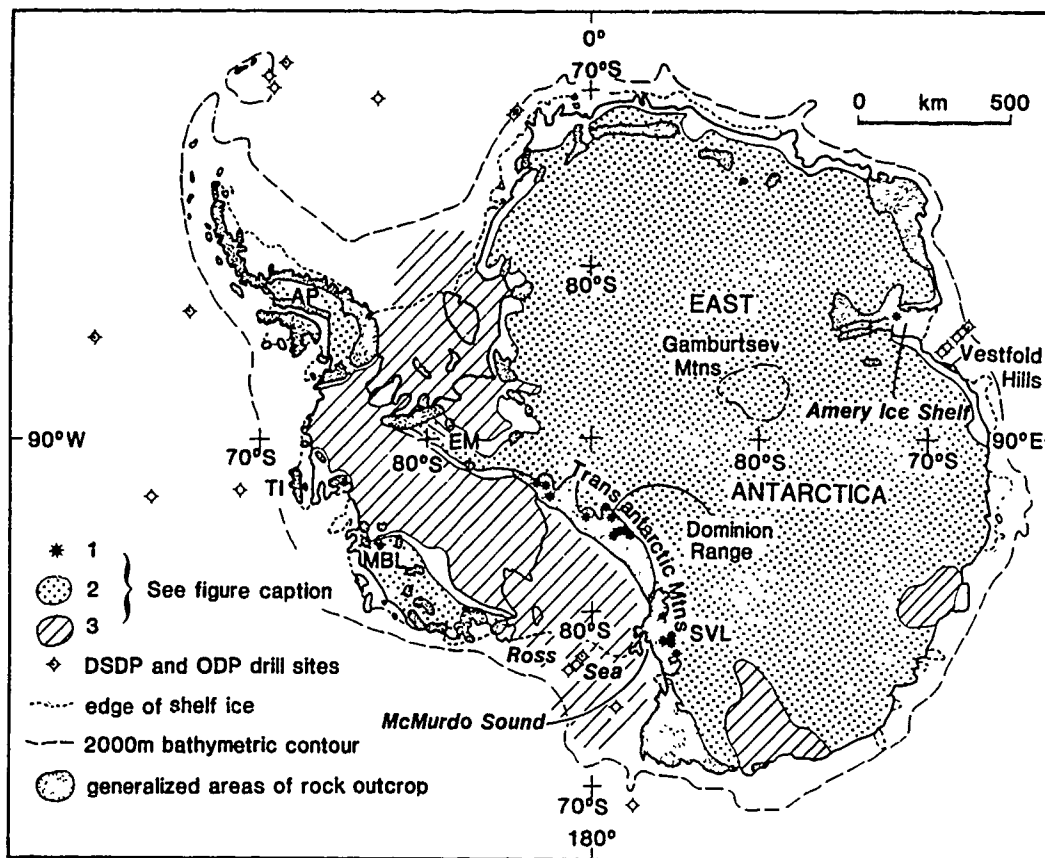


Figure 2. Antarctica in the late Pliocene (2–3 Ma) at the time of deposition of the marine microfossil-bearing Sirius Group and Pagodroma Tillite. The ice sheets are thought to have been temperate (wet-based) and therefore confined to regions above sea level in East Antarctica and elevated regions in West Antarctica; ice shelves would not have existed but tidewater glaciers would have been common. Modern ice divides have uncertain application to deposition of the Sirius Group. (1) Outcrops of Sirius Group sediments and Pagodroma Tillite. (2) Inferred limits of ice sheets during late Pliocene time. (3) Inferred marine basins during late Pliocene time.

thought to be a rift shoulder [Sturm and ten Brink, 1989] and thus may exhibit rapid vertical movements. Most of the available evidence does not support rapid recent movement although high rates (1000 m m.y.^{-1}) are inferred by Behrendt and Cooper [1991] and somewhat lower rates ($\sim 500 \text{ m m.y.}^{-1}$) may be required for the Dominion Range Sirius deposits. Polar climates, in which the freeze-thaw mechanism for rock disintegration is largely inactive, do not lead to rapid denudation of exposed rock in mountain ranges. Thus, for the Transantarctic Mountains, elevations may have been as much as 1500 m lower $3\text{--}5 \text{ m.y.}$ ago than they are today. This is, however, insufficient to alter major circulation patterns, e.g., the Transantarctic Mountains would still have been an effective barrier, more than 1500 m high, to lower tropospheric airflow.

No comparable evaluation can be made for other parts of the continent. An average uplift rate for the last 30 m.y. of 50 m m.y.^{-1} has been argued for the Amery Ice Shelf region [Wellman and Tingey, 1981]. No data exist for Queen Maud Land. Marie Byrd Land, however, is dominated by young alkaline volcanoes with associated hyaloclastites, and significant vertical movements in the Late Cenozoic have been suggested by LeMasurier and Rex [1983].

The bedrock elevation of East Antarctica is the key in terms of ice sheet growth. Cold polar ice sheets are not particularly effective agents of erosion because, where frozen to the bed, movement at the base of the ice sheet is accommodated within the basal ice, not at the contact. Estimates of erosion by the Laurentide ice sheet of North America amount to only a few tens of meters for much of the formerly ice-covered area [Dyke et al., 1989]. Erosion is unlikely to have significantly changed bedrock elevation since the mid Pliocene. Most of the interior of East Antarctica is a craton and can be expected to behave like other cratonic areas such as the Canadian shield, or Africa; vertical movements, other than those associated with isostatic rebound following deglaciation, are likely to be slow ($<100 \text{ m m.y.}^{-1}$). Mercer [1987], however, suggests a rate of uplift as high as 200 m m.y.^{-1} for the central part of the marine basin from which the microfossils in the Sirius were derived. The subglacial Gamburtsev Mountains, possibly a volcanic edifice like the Tibesti Mountains in the Sahara, may be a young geological feature and could play a crucial role as a primary center for ice sheet growth. Broad, high bedrock elevations comparable to the Colorado Plateau region or the Tibetan Plateau, both thought to be significant for northern hemisphere climate [Ruddiman and Raymo, 1988; Ruddiman and Kutzbach, 1989], are not part of the late Cenozoic ($<10 \text{ m.y.}$) history of Antarctica.

The extremes of Pliocene climatic conditions in Antarctica have occurred with essentially today's geology and bedrock topography.

DISCUSSION

The glaciated continent indicated by the model results is in marked contrast to the very dynamic ice sheet conditions revealed by the glacial geologic and paleontologic findings outlined above. For the Pliocene the continental position and (ice-free) topography were essentially those of today.

Some causes for the apparent model shortcomings could include:

(1) The simulations come solely from an atmospheric model. The ocean behavior is specified and limited to a

description of the sea surface conditions. A realistic coupled atmosphere-ocean model (incorporating, for instance, simulations of sea ice and CO_2 variations) may produce very different results (as illustrated for a different context by the work of Stouffer et al. [1989]).

(2) The present location and extent of Antarctica were used for all simulations. For example, no excursions of warm ocean currents into the continental interior were allowed [Oglesby, 1989].

(3) The strong sensitivity of the modeled net snow buildup to the prescribed snow surface albedo [Oglesby, 1991].

(4) The model's inability to reproduce accurately the present-day characteristics of climatic variables that are important for this study (especially the seasonal cycle simulations) is also a significant limitation. These include:

(a) Cyclone behavior near Antarctica is not satisfactorily simulated. The model's circumpolar low pressure trough is located too far north, is not deep enough, and does not have minima at the correct longitudes [see Williamson and Williamson, 1987; Xu et al., 1990]. The model may not, as a result, be able to represent accurately the horizontal heat transport into the continent by storms both for present and altered topographic conditions. Furthermore, the likely inability of the model to resolve satisfactorily the katabatic wind circulation (the dominant component of the mean meridional mass circulation) implies that the entire atmospheric heat budget may not be correctly represented.

(b) Annual precipitation rates over Antarctica produced by the model appear to be two to three times larger than observed, although the simulated seasonal cycle is qualitatively representative [compare Williamson and Williamson, 1987; Bromwich, 1988]. Clearly, the amount of annual snowfall is central to the question of whether a shallow, simulated snowfield can survive through the summer ablation period, and is strongly influenced by the storm transport of water vapor across the coastline [Bromwich, 1988].

(c) Simulated total cloud amounts for July monotonically increase from six tenths at 55°S to eight tenths at 85°S [Oglesby, 1989] rather than being high over the ocean and falling to around four tenths near South Pole [Schwerdtfeger, 1970]. This shortcoming means that the surface conditions over the continent will not be correctly modeled. Another GCM [Shibata and Chiba, 1990] showed a strong sensitivity of the modeled winter Antarctic climate to cloud cover characteristics over the continent.

(d) Simulated surface air temperatures from $70\text{--}85^\circ\text{S}$ are around 8°C warmer than actual during both summer and winter [compare Taljaard et al., 1969; Schwerdtfeger, 1970; Oglesby, 1989]. Such a warm bias is important because summer melting may be simulated to continue much longer and to be more active than is actually the case.

Although, in principle, modeling results cannot be valid if incompatible with observational data, in reality geologic data also have certain limitations. In the geologic argument presented here, six uncertainties need to be recognized.

(1) The age of the Sirius Group is dependent on how well the age of the diatom assemblages can be established and

whether Southern Ocean biostratigraphic ages can be directly applied to the continental interior. Diatom biogeography suggests that a pan-Antarctic biostratigraphic scheme applies to both the surrounding ocean and the continental interior [Harwood, 1991] during the Pliocene and that age assignments for the Sirius could not differ by more than 0.5 m.y. from that in the Southern Ocean. Mercer [1987] provides an analysis of the whole problem of the Sirius deposits.

(2) Other interpretations of Antarctic glacial history derived from a variety of evidence include suggestions of an older (pre-Pliocene) age for Sirius Group deposits [Mercer, 1987], ice sheet overriding of the Transantarctic Mountains [Mayewski, 1975; Denton et al., 1984], and only limited elevation changes of the Transantarctic Mountains during the last several million years [Stern and ten Brink, 1989; McKelvey, 1991]. Other aspects of, and perspectives on, Antarctic glacial history can be found in Denton et al. [1991].

(3) The climate tolerances of extant *Nothofagus* species are well known [Poole, 1987]; however the affinities of the Pliocene Antarctic *Nothofagus* from the Sirius have yet to be established definitively, and in any case it is likely to have tolerances unique to polar environments. Therefore, although qualitative statements can be made, precise temperatures (mean annual temperature, etc.) and elevation limits cannot be drawn directly for the *Nothofagus* in the Sirius sediments.

(4) The geologic argument is critically dependent on knowing the rates and amounts of uplift of the Transantarctic Mountains and the continental interior during the last 5 m.y. Fission-track dating cannot resolve this, at least in part because of the likelihood of episodic uplift. Furthermore, rates established at one site in the Transantarctic

Mountains may not apply to the whole of a cross-range transect at that locality, and even if they did, the rates established in that one sector may not necessarily apply to the range as a whole. Raised marine sequences spanning the last 10 m.y. (dated paleontologically or by radiometric methods) from around the East Antarctic craton could provide significant constraints, as would information on the exposure ages of rock platforms (provided by cosmogenically induced radionuclides).

(5) Bedrock topography is poorly known for large parts of East Antarctica and therefore uncertainties exist in the location of possible centers of ice sheet initiation and growth.

(6) Finally, the rates of erosion are essentially unknown although widely regarded as very slow.

It is clear that an improved geologic database would substantially improve the ability to validate model results. This should be accompanied by improvements in the performance of the models, so that, at least, present-day conditions can be simulated with some confidence [compare Simmonds, 1990]. The most pressing task appears to be the development of realistic coupled atmosphere-ocean models for high southern latitudes accompanied by incorporation of more precise paleogeographic information gained through geologic records.

ACKNOWLEDGMENTS

Preparation of this paper was supported by NSF grants DPP-8716258 to D. H. Elliot and DPP-8916134 to D. H. Bromwich. Fieldwork and subsequent laboratory studies on the Sirius deposits have been supported by NSF grants DPP-8117889, 8315533 and 8420622. We are grateful for the constructive input from reviewers R. Oglesby and E. Barron. Byrd Polar Research Center contribution 727.

REFERENCES

- Askin, R. A., and V. Markgraf, Palynomorphs from the Sirius Formation, Dominion Range, Antarctica, *Antarct. J. U.S.*, 21, 34-35, 1986.
- Barrett, P. J., M. J. Hambrey, D. M. Harwood, A. R. Pyne, and P. N. Webb, Synthesis, in *Antarctic Cenozoic History from the CIROS I drill hole, McMurdo Sound*, edited by P. J. Barrett, *DSIR Bull.*, 245, 241-251, 1989.
- Barron, E. J., A warm, equable Cretaceous: The nature of the problem, *Earth Science Reviews*, 19, 305-338, 1983.
- Barron, J. A., B. Larsen, and J. G. Baldauf, Evidence for late Eocene-early Oligocene Antarctic glaciation: and observations on Late Neogene glacial history of Antarctica: results from ODP Leg 119, in *Proceedings, ODP Scientific Results, 119*, edited by J. A. Barron, B. Larsen, et al., College Station, TX (Ocean Drilling Program), 1991, in press.
- Behrendt, J., and A. K. Cooper, Evidence of rapid Cenozoic uplift of the shoulder escarpment of the Cenozoic West Antarctic rift system and a speculation on possible climate forcing, *Geology*, 19, 315-319, 1991.
- Birkenmajer, K., Tertiary glaciation in the South Shetland Islands, West Antarctica: evaluation of data, in *Geological Evolution of Antarctica*, edited by M. R. A. Thomson, J. A. Cramie, and J. W. Thomson, pp. 629-632, Cambridge University Press, Cambridge, 1991.
- Böcher, J., Boreal insects in northernmost Greenland: palaeo-entomological evidence from the Kap København Formation (Plio-Pleistocene), Peary Land, *Fauna norv.*, Ser. B 36, 37-43, 1989.
- Bradley, R. S., *Quaternary Paleoclimatology*, 472 pp., Allen and Unwin, Boston, 1983.
- Bromwich, D. H., Snowfall in high southern latitudes, *Rev. Geophys.*, 26, 149-168, 1988.
- Carlquist, S., Upper Pliocene-lower Pleistocene *Nothofagus* wood from the Transantarctic Mountains, *Aliso*, 11, 571-583, 1987.
- Carter, D. L., J. Brigham-Grette, L. Marinovich, Jr., V. L. Pease, and J. W. Hillhouse, Late Cenozoic Arctic Ocean sea ice and terrestrial paleoclimate, *Geology*, 14, 675-678, 1986.
- Cirbus Sloan, L., and E. J. Barron, "Equable" climates during Earth History, *Geology*, 18, 489-492, 1990.
- Denton, G. H., M. L. Prentice, D. E. Kellogg, and T. B. Kellogg, Late Tertiary history of the Antarctic ice sheet: Evidence from the Dry Valleys, *Geology*, 12, 263-267, 1984.
- Denton, G. H., M. L. Prentice, and L. H. Burckle, Cenozoic history of the Antarctic ice sheet, in *Geology of Antarctica*, edited by R. J. Tingey, Oxford Univ. Press, 1991, in press.

- Dowsett, H. J., and T. M. Cronin, High eustatic sea level during the middle Pliocene: Evidence from the southeastern U.S. Atlantic Coastal Plain, *Geology*, 18, 435–438, 1990.
- Dyke, A. S., J.-S. Viret, I. T. Anderson, L. A. Dridge, and W. R. Cowan, The Laurentide Ice Sheet and an introduction to the Quaternary Geology of the Canadian Shield, pp. 178–189 in Chapter 3 of *Quaternary Geology of Canada and Greenland*, edited by R. J. Fulton; *The Geology of North America*, Geol. Soc. America, K-1, 837 pp., 1989.
- Fitzgerald, P. G., Uplift and formation of the Transantarctic Mountains: application of apatite fission track analysis to tectonic problems, 28th International Geological Congress, Abstracts vol. 1, p. 491, Washington, DC, 1989.
- Funder, S., N. Abrahamsen, O. Bennike, and R. W. Feyling-Hanssen, Forested Arctic: Evidence from North Greenland, *Geology*, 13, 542–546, 1985.
- Gleadow, A. J. W., and P. G. Fitzgerald, Uplift history and structure of the Transantarctic Mountains – new evidence from fission track dating of basement apatites in the Dry Valleys area, southern Victoria Land, *Earth Planet. Sci. Lett.*, 82, 1–14, 1987.
- Hambrey, M. J., B. Larsen, W. E. Ehmann, and ODP Leg 119 Shipboard Party, Forty million years of Antarctic glacial history yielded by Leg 119 of the Ocean Drilling Program, *Polar Record*, 25, 99–106, 1989.
- Haq, B. U., J. Hardenbol, and P. R. Vail, Chronology of fluctuating sea levels since the Triassic, *Science*, 235, 1156–1167, 1987.
- Harwood, D. M., Recycled siliceous microfossils from the Sirius Formation, *Antarct. J. U.S.*, 21, 101–103, 1986a.
- Harwood, D. M., Diatom biostratigraphy and paleoecology with a Cenozoic history of Antarctic ice sheets, Thesis, 592 pp., Ohio State University, Columbus, OH, 1986b.
- Harwood, D. M., Cenozoic diatom biogeography in the southern high latitudes: inferred biogeographic barriers and progressive endemism, in *Geological Evolution of Antarctica*, edited by M. R. A. Thomson, J. A. Crame, and J. W. Thomson, Cambridge University Press, Cambridge, 1991.
- Harwood, D. M., and P. N. Webb, Early Pliocene deglaciation of the Antarctic ice sheet and late Pliocene onset of bipolar glaciation, *EOS, Transactions of the American Geophysical Union*, 71, 538–539, 1990.
- Ishman, S. E., and P. N. Webb, Late Neogene benthic foraminiferal record from the Victoria Land Basin margin, Antarctica: application to glacio-eustatic and tectonic events, in *Benthos '86, Rev. Paleobiol.*, Vol. Spec. 2, 523–551, 1988.
- LeMasurier, W. E., and D. C. Rex, Rates of uplift and the scale of ice level instabilities recorded by volcanic rocks in Marie Byrd Land, West Antarctica, in *Antarctic Earth Science*, edited by R. L. Oliver, P. R. James, and J. B. Jago, pp. 603–670, Australian Academy of Science, Canberra, 1983.
- Lorius, C., J. Jouzel, C. Ritz, L. Merlivat, N. I. Barkov, Y. S. Korotkevich, and V. M. Kotlyakov, A 150,000-year climatic record from Antarctic ice, *Nature*, 316, 591–596, 1985.
- Lorius, C., G. Raisbeck, J. Jouzel, and D. Raynaud, Long-term environmental records from Antarctic ice cores, in *The Environmental Record in Glaciers and Ice Sheets*, edited by H. Oeschger and C. C. Langway, pp. 343–361, John Wiley and Sons, 1989.
- Mayewski, P. A., Glacial geology and late Cenozoic history of the Transantarctic Mountains, Antarctica, *Report No. 56, Institute of Polar Studies, Ohio State Univ., Columbus*, 168 pp., 1975.
- McKelvey, B. C., The Cainozoic glacial record in South Victoria Land – A geological evaluation of the McMurdo Sound drilling projects, in *Geology of Antarctica*, edited by R. J. Tingey, Oxford Univ. Press, 1991, In press.
- McKelvey, B. C., and N. C. N. Stephenson, A geological reconnaissance of the Radok Lake area, Amery Oasis, Prince Charles Mountains, *Antarctic Science*, 2, 53–66, 1990.
- McKelvey, B. C., P.-N. Webb, D. M. Harwood, and M. C. G. Mabin, The Dominion Range Sirius Group – A record of the late Pliocene–early Pleistocene Beardmore Glacier, in *Geological Evolution of Antarctica*, edited by M. R. A. Thomson, J. A. Crame, and J. W. Thomson, pp. 675–682, Cambridge Univ. Press, Cambridge, 1991.
- Mercer, J. H., Southernmost Chile: A modern analog of the southern shores of the Ross embayment during Pliocene warm intervals, *Antarct. J. U.S.*, 21, 103–105, 1986.
- Mercer, J. H., The Antarctic Ice Sheet during the late Neogene, in *Palaeoecology of Africa and the Surrounding Islands*, vol. 18, edited by J. A. Coetzee and E. M. van Zinderen Bakker, pp. 21–33, A.A. Balkema, Rotterdam, 1987.
- Oglesby, R. J., A GCM study of Antarctic glaciation, *Climate Dynamics*, 3, 135–156, 1989.
- Oglesby, R. J., Sensitivity of glaciation to initial snow cover, CO₂, snow albedo, and oceanic roughness in the NCAR CCM, *Climate Dynamics*, 4, 219–235, 1991.
- Parish, T. R., and D. H. Bromwich, Continental-scale simulation of the Antarctic katabatic wind regime, *J. Climate*, 4, 135–146, 1991.
- Pickard, J., D. A. Adamson, D. M. Harwood, G. H. Miller, P. G. Quilty, and R. K. Dell, Early Pliocene marine sediments, coastline, and climate of East Antarctica, *Geology*, 16, 158–161, 1988.
- Poole, A. L., Southern Beeches, *New Zealand DSIR Information Series*, 162, 148 pp., Science Information Publishing Centre, 1987.
- Ruddiman, W. F., and J. E. Kutzbach, Forcing of Late Cenozoic Northern Hemisphere climate by plateau uplift in Southern Asia and the American West, *J. Geophys. Res.*, 94, 18409–18427, 1989.
- Ruddiman, W. F., and M. E. Raymo, Northern Hemisphere climate regimes during the past 3 Ma: possible tectonic connections, *Phil. Trans. R. Soc. Lond.*, B 318, 411–430, 1988.
- Sakai, A., D. M. Paton, and P. Wardle, Freezing resistance of trees of the south temperate zone, especially subalpine species of Australasia, *Ecology*, 62, 563–570, 1981.
- Schwerdtfeger, W., *The Climate of the Antarctic*, Vol. 14, edited by S. Orvig, pp. 253–355, *World Survey of Climatology*, edited by H. E. Landsberg, Elsevier, 1970.
- Shibata, K., and M. Chiba, Effects of radiation scheme on the surface temperature and wind over the Antarctic and on circumpolar lows, *Proc. NIPR Symp. Polar Meteorol. Glaciol.*, 3, 58–78, 1990.

- Simmonds, I., Improvements in general circulation model performance in simulating Antarctic climate, *Antarct. Science*, 2, 287-300, 1990.
- Stern, T. S., and U. S. ten Brink, Flexural uplift of the Transantarctic Mountains, *J. Geophys. Res.*, 94, 10315-10330, 1989.
- Stouffer, R. J., S. Manabe, and K. Bryan, Interhemispheric asymmetry in climate response to a gradual increase of atmospheric CO₂, *Nature*, 342, 660-662, 1989.
- Taljaard, J. J., H. van Loon, H. L. Crutcher, and R. L. Jenne, *Climate of the Upper Air: Southern Hemisphere*, Vol. 1, Temperatures, dew points and heights at selected pressure levels, *NAVAIR-50-1C-55*, 135 pp., Chief of Naval Operations, Washington, DC, 1969.
- Van Steenis, C. G. G. J., *Nothofagus*, a key genus of plant geography, in time and space, living and fossil, ecology and phylogeny, *Blumea*, 19, 65-98, 1971.
- Vincent, J.-S., Quaternary geology of the northern Canadian Interior Plains, pp. 100-138 in Chapter 2 of *Quaternary Geology of Canada and Greenland*, edited by R. J. Fulton; Geol. Soc. Amer., *The Geology of North America, K-1*, 837 pp., 1989.
- Webb, P.-N., and D. M. Harwood, Terrestrial flora of the Sirius Formation: Its significance for Late Cenozoic glacial history, *Antarct. J. U.S.*, 22, 7-11, 1987.
- Webb, P.-N., D. M. Harwood, B. C. McKelvey, J. H. Mercer, and L. D. Stott, Cenozoic marine sedimentation and ice volume variation on the East Antarctic craton, *Geology*, 12, 287-291, 1984.
- Wellman, P., and R. J. Tingey, Glaciation, erosion and uplift over part of East Antarctica, *Nature*, 291, 142-144, 1981.
- Wigley, T. M. L., M. J. Ingram, and G. Farmer, *Climate and History*, 530 pp., Cambridge University Press, Cambridge, 1981.
- Williamson, D. L., CCM Progress Report - July 1990, *NCAR/TN-351+PPR*, 108 pp., National Center for Atmospheric Research, Boulder, CO, 1990.
- Williamson, D. L., J. T. Kiehl, V. Ramanathan, R. E. Dickinson, and J. J. Hack, Description of NCAR Community Climate Model (CCM1), *NCAR/TN-285+STR*, 112 pp., National Center for Atmospheric Research, Boulder, CO, 1987.
- Williamson, G. S., and D. L. Williamson, Circulation statistics from seasonal and perpetual January and July simulations with the NCAR Community Climate Model (CCM1): R15, *NCAR/TN-302+STR*, 199 pp., National Center for Atmospheric Research, Boulder, CO, 1987.
- Wise, S. W., Jr., J. Breza, D. M. Harwood, and W. Wei, Paleogene glacial history of Antarctica, in *Controversies in Modern Geology*, edited by D. W. Muller, J. A. Mackenzie, and H. Weissert, pp. 155-171, Academic Press, London, 1991.
- Xu, J.-S., H. von Storch, and H. van Loon, The performance of four spectral GCMs in the Southern Hemisphere: the January and July climatology and the semiannual wave, *J. Climate*, 3, 53-70, 1990.

A Search for Short-Term Variations in the Flow of Ice Stream B, Antarctica

W. D. Harrison and K. A. Echelmeyer

Geophysical Institute, University of Alaska Fairbanks, Fairbanks, Alaska, U.S.A.

N. Humphrey

Division of Geological and Planetary Sciences, California Institute of Technology, Pasadena, California, U.S.A.

ABSTRACT

There is good theoretical and geologic evidence that some ice sheets, both past and present, are inherently mechanically unstable to climate or sea level changes, and can disintegrate over short periods of time; examples of this behavior in small tidewater glaciers are well documented. The West Antarctic Ice Sheet, which is grounded below sea level, is thought to be the least stable of the present ice sheets. Recent observations of several investigators have focused attention on the role that the large ice streams draining into the Ross Ice Shelf play in the stability of the ice sheet. These streams, at least in some cases, appear to be transient features, out of balance with their accumulation areas and subject to large changes; one of them, Ice Stream C, appears to have stagnated within the last century or so. Another, Ice Stream B, seems to move largely by the deformation of an underlying till layer.

Given this background of interesting flow behavior, we have been searching for short-term changes in the flow (which are often seen on mountain glaciers) as indicators of flow mechanisms of Ice Stream B. The measurements began in November 1988 and continued to the end of 1989. During the austral field seasons daily motion studies were conducted with EDM and UHF positioning systems. The 1988 data showed the speed near the edge of the ice sheet to be constant at 1.00 m d^{-1} within the sensitivity of a few per cent. During the 1988 field season meters were installed to measure the horizontal and vertical components of ice strain to a resolution of about 1 part in 10^6 . Seismic activity in the ice was also monitored. These data were recorded by data loggers for recovery in late 1989, and will be reported.

The Velocity Field of Antarctic Outlet Glaciers

B. K. Lucchitta

U.S. Geological Survey, Flagstaff, Arizona, U.S.A.

J. G. Ferrigno, T. R. MacDonald, and R. S. Williams, Jr.

U.S. Geological Survey, Reston, Virginia, U.S.A.

ABSTRACT

Climate-induced changes in the area and volume of polar ice sheets may severely impact the Earth's densely populated coastal regions; melting of the West Antarctic ice sheet alone could cause a sea level rise of 3.5 meters. Yet the mass balance (the net gain or loss) of the Antarctic ice sheets is still poorly known, and it is not entirely certain whether the Antarctic ice sheets are growing or shrinking. Moreover, the velocity field of most ice streams and outlet glaciers has not yet been explored.

An extensive set of Landsat images covering Antarctica was acquired in the early to middle 1970s. Recently, a program to re-acquire Landsat images over the coastal regions of Antarctica was initiated by an International Consortium of SCAR (Scientific Committee on Antarctic Research). These later views of the same scenes permit the measurement of outlet-glacier velocities by tracking the translational movement of crevasses in the floating part of the glaciers. This technique is precise enough to establish velocity gradients both along and across glaciers. We applied the technique to 15 outlet glaciers around the coast of Antarctica. Preliminary results indicate a range in average velocities from a low of 0.1 km per annum to a high of 2.2 km per annum. The two highest velocities measured to date are in the Pine Island and Land Glaciers in Maria Byrd Land of West Antarctica. As soon as new image acquisitions permit additional measurements, we will expand our study to include as much of the Antarctic coastline as possible. We anticipate that the study will eventually yield a near-comprehensive view of the outlet-glacier velocity field of Antarctica.

AD-P007 334



92-17838



Glacier Terminus Fluctuations in the Wrangell and Chugach Mountains Resulting from Non-Climatic Controls

Matthew Sturm

U.S.A. CRREL-Alaska, Ft. Wainwright, Alaska, U.S.A.

Dorothy K. Hall

NASA-Goddard Space Flight Center, Greenbelt, Maryland, U.S.A.

Carl S. Benson

Geophysical Institute, University of Alaska Fairbanks, Fairbanks, Alaska, U.S.A.

William O. Field

Box 583, Great Barrington, Massachusetts, U.S.A.

ABSTRACT

Non-climatically controlled fluctuations of glacier termini were studied in two regions in Alaska. In the Wrangell Mountains, eight glaciers on Mt. Wrangell, an active volcano, have been monitored over the past 30 years using terrestrial surveys, aerial photogrammetry and digitally registered satellite images. Results, which are consistent between different methods of measurement, indicate that the termini of most glaciers were stationary or had retreated slightly. However, the termini of the 30-km-long Ahtna Glacier and the smaller Center and South MacKeith glaciers began to advance in the early 1960s and have advanced steadily at rates between 5 and 18 m yr⁻¹ since then. These three glaciers flow from the summit caldera of Mt. Wrangell near the active North Crater, where increased volcanic heating since 1964 has melted over 7×10^7 m³ of ice. We suspect that volcanic meltwater has changed the basal conditions for the glaciers, resulting in their advance.

In College Fjord, Prince William Sound, the terminus fluctuations of two tidewater glaciers have been monitored since 1931 by terrestrial surveying, photogrammetry, and most recently, from satellite imagery. Harvard Glacier, a 40-km-long tidewater glacier, has been advancing steadily at nearly 20 m yr⁻¹ since 1931, while the adjacent Yale Glacier has retreated at approximately 50 m yr⁻¹ during the same period, though for short periods, both rates have been much higher. The striking contrast between the terminus behavior of Yale and Harvard Glaciers, which parallel each other in the same fjord, and are derived from the same snow field, supports the hypothesis that their terminus behavior is the result of dynamic controls rather than changes in climate.

INTRODUCTION

Although the advance or retreat of a glacier may be a good indicator of climate change, particularly when many glaciers in a region are considered, several dynamic processes can result in terminus changes that are independent of

climate. Best known of these is the phenomenon of surging, which has resulted in terminus advances of many kilometers in just a few years [Meier and Post, 1969]. Less well known are the dynamic processes associated with glacier-volcano interactions and tidewater glaciers, both of which can result

in non-climatically controlled terminus changes. We believe examples presented here from the Wrangell and Chugach mountains of Alaska demonstrate the importance of understanding the dynamic setting when interpreting climate change from glacier terminus fluctuations.

METHODS

The following methods were used to map the positions of glacier termini.

(1) Terrestrial surveys: Intersection surveys using a theodolite from a base line of known length, or bearing-distance surveys using a theodolite and distance ranger from a known point have been used to map glacier termini with an accuracy of ± 5 m or better, depending on how well the base line is established.

(2) Photogrammetry: Qualitative changes in the termini positions of glaciers were determined from aerial and terrestrial photographs. The first aerial photographs of Mt. Wrangell were taken by Bradford Washburn in 1937. Subsequent aerial photography was done by the USGS in 1948 and 1957. In addition, we have photographed the summit and flank glaciers from 1961 to the present, including mapping-quality vertical aerial photographs taken annually since 1972. Orthophoto maps (scale=1:25,000) have been made from the photographs taken in 1957, 1977, 1979, 1981 and 1988 [Sturm, 1983; Benson and Follett, 1986]. Comparison of these orthophoto maps allows changes in glacier termini to be measured to ± 10 m.

(3) Satellite imagery: Landsat Multispectral Scanner (MSS; 80 m resolution) and Thematic Mapper (TM; 30 m resolution) images were analyzed to determine terminus changes [Krimmel and Meier, 1975; Hall et al., 1988]. Lower resolution MSS images were registered digitally to the higher resolution TM images using rock outcrops as control points. Once registered, changes in terminus positions could be determined for all the glaciers in the image. For glaciers on Mt. Wrangell, a MSS image taken 18 September 1973 was compared to a TM image taken 16 September 1986; for the glaciers of College Fjord in the Chugach Mountains, a MSS image taken 15 August 1973 was compared to a TM image taken 1 August 1985.

TERMINUS ADVANCE ASSOCIATED WITH VOLCANIC HEATING IN THE WRANGELL MOUNTAINS

Mt. Wrangell (elev. 4317 m) is an active volcano located near the northwestern end of the Wrangell Mountains [Benson and Motyka, 1978]. Its summit caldera is about 6 km across and filled with ice to depths greater than 500 m [Clarke et al., 1989]. Along its rim are three craters, 0.5 to 1.0 km in diameter, and several active fumarole fields. Fifteen glaciers radiate from the summit ice cap (Figure 1). Mt. Wrangell's recent volcanic history includes probable minor phreatic eruptions in 1899, 1902, 1908, 1911, 1912, 1921 and 1930 [Motyka, 1983], though no lava flows younger than several thousand years have been identified nor are they likely to exist [Nye, Alaska Division of Geologic and Geophysical Surveys, personal communication, 1990].

An abrupt increase in the volcanic heat flux centered under the North Crater (Figure 1) took place in 1965 [Benson et al., 1975; Benson and Motyka, 1978; Motyka, 1983; Benson et al., 1985]. We believe this was a result of

the great Alaska earthquake of 27 March 1964 centered in nearby Prince William Sound [National Academy of Sciences, 1968]. The change in heat flux was manifested in increased fumarolic activity along the rim of the crater, and increased melting of the ice in the North Crater. Between 1908 [Dunn, 1909] and 1965 this ice-filled crater was in equilibrium, with accumulation balanced by glacier flow and basal melting due to geothermal heat (there is no surface melting at this elevation). Since 1965, more than 7×10^7 m³ has melted in the crater [Benson and Motyka, 1978; Motyka, 1983; Benson et al., 1985; Benson and Follett, 1986]. Changes in ice surface contours adjacent to, but outside, the North Crater indicate that there has also been increased heating in these locations. Due to the local topography, some of the subglacial meltwater produced by the heating has probably drained down the northeast flank of the mountain.

Between the end of the 19th century and 1957, when aerial mapping photographs were taken, there was a general retreat of all the glaciers on Mt. Wrangell. Comparison of maps made from the 1957 photographs with plane table maps made in 1902 [Mendenhall, 1905] shows that most of the glaciers retreated between 100 and 400 m; the MacKeith glaciers on the northeast flank of the volcano retreated more

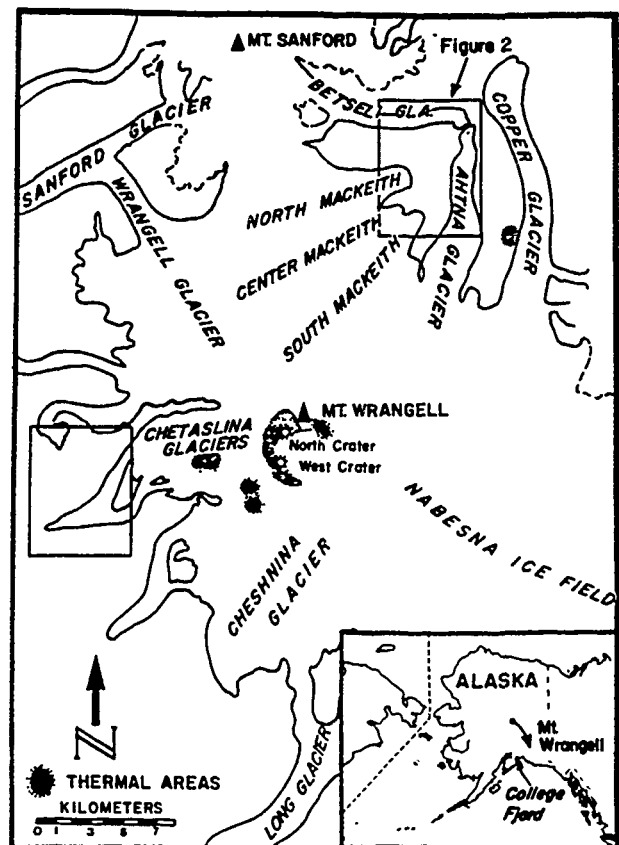


Figure 1. Mt. Wrangell in the Wrangell Mountains of Alaska, showing the fifteen glaciers that radiate from its summit. Inset shows location of Mt. Wrangell and of College Fjord in the Chugach Mountains.

than a kilometer (Figure 2). When first observed in 1902 [Mendenhall, 1905], the MacKeith glaciers were confluent with the Ahtna Glacier, which was connected with the Betseli Glacier. The deglaciated area is now covered by thin, discontinuous ice-cored moraine with sparse vegetation and lichen cover consistent with recent deglaciation. (MacKeith, Ahtna and Betseli are unofficial names.)

In about 1965, four out of the fifteen glaciers radiating from Mt. Wrangell began to advance. They are the South, Center and North MacKeith glaciers, and the 30-km-long Ahtna Glacier (Figures 1 and 2). All are located on the northeast flank of the volcano, adjacent to one another, and all flow directly from the vicinity of the North Crater. Photographs taken by B. Washburn in 1937, the U.S. Navy in 1948, L. Mayo of the USGS in 1965, and the authors since 1965, show that these four glaciers had retreated to a minimum position by 1937, remained stationary between 1937 and 1965, and then began to advance in 1965. The North MacKeith Glacier, which flows from an accumulation area that is only partly on Mt. Wrangell, with about half its accumulation coming from nearby Mt. Sanford [Sturm, 1983] advanced about 300 m between 1957 and 1981, but has been stationary since that time. The other three glaciers have advanced 320 to 480 m in the past 25 years, and continue to advance today. Average rates of advance are:

Ahtna Glacier	10 m yr ⁻¹
S. MacKeith Glacier	18 m yr ⁻¹
C. MacKeith Glacier	16 m yr ⁻¹
N. MacKeith Glacier	6 m yr ⁻¹ (until about 1981).

The start of these advances coincided with the abrupt increase in volcanic heating of the North Crater. Glaciers on nearby Mt. Sanford (4950 m) including the Betseli Glacier (Figures 1 and 2) have been stationary or retreating. All other glaciers on Mt. Wrangell are retreating.

TERMINUS ADVANCE AND RETREAT OF TIDE-WATER GLACIERS IN THE CHUGACH MOUNTAINS

College Fjord, a 40-km-long fjord in Prince William Sound, cuts into the heart of the Chugach Mountains and contains six tidewater glaciers, five large valley glaciers and dozens of smaller glaciers. The glaciers of College Fjord have been described by Gilbert [1903], Tarr and Martin [1914], and Field [1932a,b, 1975]. The two largest tidewater glaciers in the fjord are Harvard and Yale glaciers, which are derived from the same snow fields. Observations show that the Harvard Glacier has advanced while the Yale Glacier has simultaneously retreated, with the retreat rates being more than twice the advance rates.

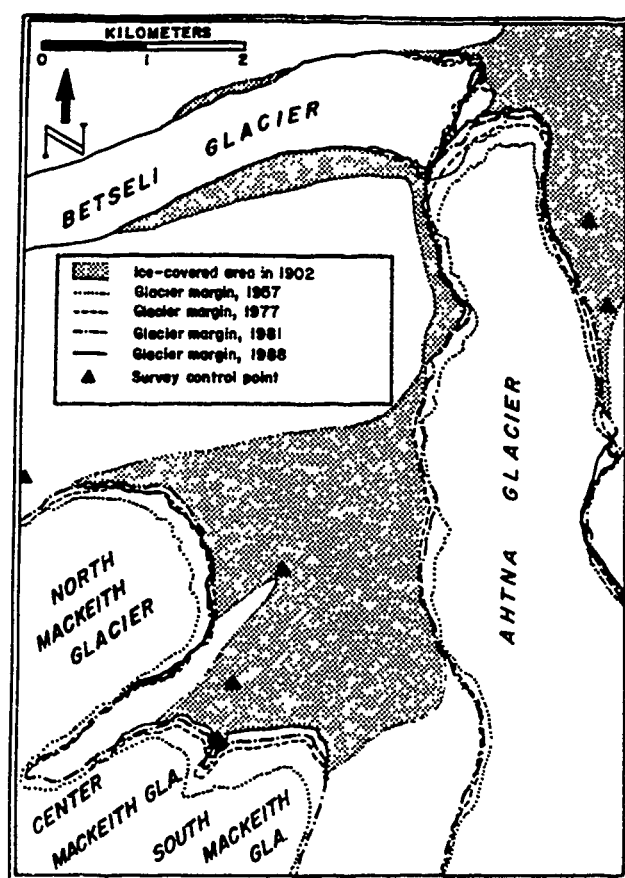


Figure 2. Terminus positions of the glaciers on the northeast flank of Mt. Wrangell mapped on orthophoto maps made from controlled vertical aerial photographs taken in 1957, 1977, 1981 and 1988. Uncontrolled vertical aerial photographs taken in 1965 show negligible change since 1957.

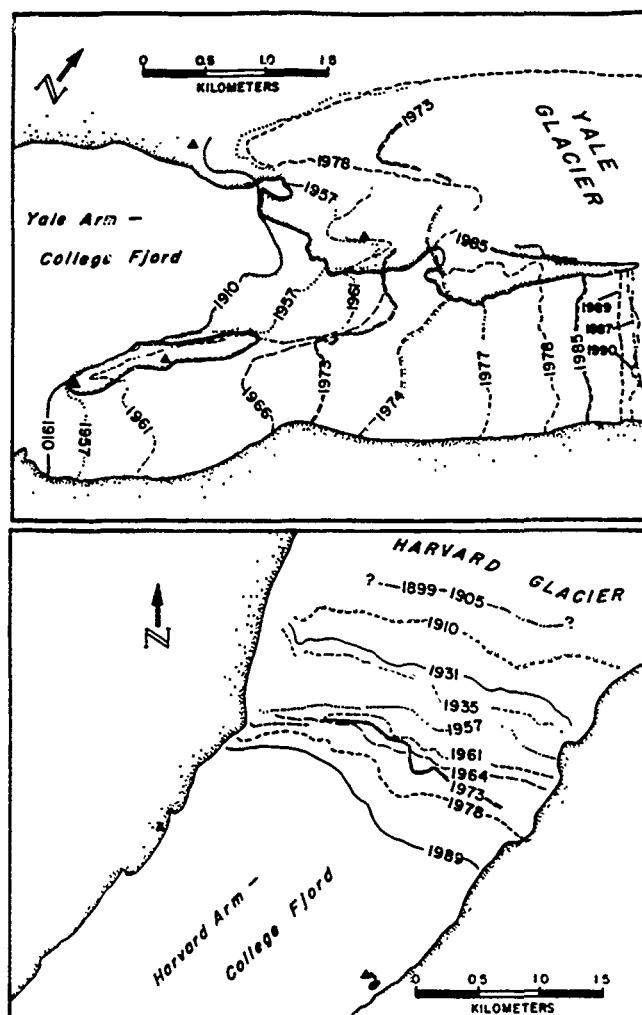


Figure 3. Terminus positions of the Yale and Harvard Glaciers, Prince William Sound, College Fjord, Alaska.

Harvard Glacier has been advancing since 1905, and possibly earlier [Viereck, 1967] (Figure 3). Its position prior to 1887 is unknown, but comparison of maps made in 1887, 1899 and 1905 suggests that the terminus was nearly stationary during these 18 years [Tarr and Martin, 1914]. In 1905, it began to advance. In 1935, it was still advancing and knocking over 250-year-old trees [Cooper, 1942], indicating that it had not been that far advanced since at least 1685. Between 1905 and 1969, it advanced at 12 to 20 m yr⁻¹ [Field, 1975; Brown et al., 1982; Meier and Post, 1987]; since 1969 its advance rate has increased.

Yale Glacier has been retreating since the early 19th century (Figure 3). In 1794, Whidbey of Vancouver's expedition was unable to proceed more than five kilometers up the fjord due to floating ice. Applegate in 1887 got about the same distance into the fjord [Tarr and Martin, 1914; Field, 1975]. From this, we conclude that rapid calving was taking place from a large tidewater glacier, probably Yale Glacier. Botanical evidence [Cooper, 1942; Viereck, 1959] suggests that Yale Glacier reached a maximum position sometime between Whidbey's and Applegate's visits. By 1910, when Tarr and Martin [1914] mapped its terminus, Yale Glacier had retreated 3.5 to 5 km. Thick alder growth in front of the glacier suggested that most of the retreat had occurred prior to 1860. Between 1910 and 1957, Yale Glacier's terminus had a complex history [Field, 1975, p. 385] with a net retreat of about 0.5 km, but after 1957, a rapid retreat began that may have ended around 1987, as no further retreat has taken place since then.

In July, 1989, the terminus of the Yale Glacier had retreated so far that it could not be surveyed from the existing control points. Therefore, the most recent terminus positions of Yale Glacier shown in Figure 3 are based on (a) satellite imagery for 1985; (b) observations and terrestrial photographs taken in 1989; and (c) uncontrolled vertical aerial photographs supplied by Austin Post for 1987 and 1990. These sources indicate that by 1974, Yale Glacier had retreated into a reach of the fjord only half as wide as the reach it occupied prior to 1974; according to Mercer [1961] this suggests that the rate of retreat should have decreased. Nevertheless, Yale Glacier's retreat rate accelerated, reaching a maximum value of 345 m yr⁻¹ between 1974 and 1978. This was apparently due to the greater water depth in the narrow reach of the fjord [Austin Post, personal communication, 1991]. We think it is unlikely that the Yale Glacier will continue to retreat much longer. The active calving terminus is only a few hundred meters down-glacier from a distinct rise in the glacier surface, indicating a step in the subglacial topography. With further retreat, the glacier will probably reach its stable retracted position.

DISCUSSION

The advance of the glaciers on the northeast flank of Mt. Wrangell does not appear to be the result of climate change. We suspect that volcanic meltwater has changed the basal conditions for these glaciers, resulting in their advance. Only glaciers flowing from the northeast side of the North Crater are advancing, and the advance began in 1965 when volcanic activity and meltwater produced by it increased. Most runoff from subglacial melting outside the crater

would flow down the northeast flank. This volcanically produced subglacial runoff is not subject to seasonal variation, as is surface runoff, and the glaciers on the northeast flank show little or no seasonal variation in surface speed. In contrast, the Chetaslina Glacier on the west side of Mt. Wrangell shows a greater than 50% increase in surface speed during the spring and summer [Sturm, 1983]. The Chetaslina Glacier is closer to the "normal" mode of glacier flow, which shows an increase in speed in spring and summer when surface runoff penetrates to the bed of the glacier and increases sliding [Sturm, 1983; Echelmeyer and Harrison, 1990].

The striking contrast between the terminus behavior of Yale and Harvard Glaciers, which parallel each other in the same fjord and are derived from the same snow field, supports the hypothesis that their terminus behavior is the result of dynamic rather than climatic controls. If climate controlled the terminus behavior, we would expect more synchronous behavior between the two glaciers. In general, the terminus positions of tidewater glaciers are thought to be the result of a complex interaction of the fjord depth, ice thickness and calving rate, with climate and mass balance playing a secondary role. Post [1975] and Meier and Post [1987] suggest that tidewater glaciers followed a cycle that consists of three phases:

- (1) A period of slow advance during which the glacier moves down the fjord through deep water by maintaining a submarine moraine shoal in front of the terminus, thereby limiting calving of icebergs and maintaining positive mass balance.

- (2) A period of relative stability during which the terminus is nearly stationary, terminating in shallow water on a submarine moraine.

- (3) A period of rapid "catastrophic" retreat during which the terminus retreats off a submarine moraine shoal, commences calving at a high rate in deep water, and continues to retreat up the fjord.

This cycle may be triggered by climatic change, but at any given time the terminus position of the glacier is primarily controlled by the balance between glacier flow and calving activity. Yale Glacier appears to be near completion of the catastrophic retreat part of the cycle; Harvard Glacier is in the advancing stage.

CONCLUSIONS

Though the advance and retreat of glaciers can be good indicators of climate, the examples presented above show that non-climatic controls can also produce changes in glacier terminus positions. In fact, these non-climatically induced changes are often larger than those produced by climate.

ACKNOWLEDGMENTS

Hundreds of people have been involved in collecting the more than 50 years of field data we have presented here and we thank them all. In the most recent surveys and in preparing this paper we had help from Roman Motyka, Dan Solie, Betsy Sturm, and Carl Tobin. Special thanks to Austin Post for reviewing the manuscript and allowing us to use his data from the Yale Glacier.

REFERENCES

- Benson, C. S., and A. B. Follett, Application of photogrammetry to the study of volcano-glacier interactions on Mt. Wrangell, Alaska, *Photogrammetric Engineering and Remote Sensing*, 52, 813-827, 1986.
- Benson, C. S., and R. Motyka, Glacier-volcano interactions of Mt. Wrangell, Alaska, in *University of Alaska-Geophysical Institute Annual Report 1977-1978*, pp. 1-25, 1978.
- Benson, C. S., D. Bingham, and G. Wharton, Glaciological and volcanological studies at the summit of Mt. Wrangell, Alaska, *Snow and Ice Symposium-Proceedings of the Moscow Symposium, August 1971*, IASH-AISH Publication No. 104, pp. 95-98, 1975.
- Benson, C. S., R. Motyka, D. Bingham, G. Wharton, P. MacKeith, and M. Sturm, Glaciological and volcanological studies on Mt. Wrangell, Alaska, in *Interaction between Volcanism and Glaciology*, edited by Kotlyakov, Vinogradov, and Glazovsky, pp. 114-133, Glaciological Researches No. 27, Soviet Geophysical Committee, Academy of Sciences of the USSR, 1985.
- Brown, C. S., M. F. Meier, and A. Post, Calving speed of Alaska tidewater glaciers, with application to Columbia Glacier, *U.S. Geological Survey Professional Paper 1258-D*, 1982.
- Clarke, G. K. C., G. M. Cross, and C. S. Benson, Radar imaging of glaciovolcanic stratigraphy, Mount Wrangell Caldera, Alaska: interpretation model and results, *J. Geophys. Res.*, 94, 7237-7249, 1989.
- Cooper, W. S., Vegetation of the Prince William Sound Region, Alaska, with a brief excursion into post-Pleistocene climatic history, *Ecological Monographs*, 12, 1-22, 1942.
- Dunn, R., Conquering our greatest volcano, *Harper's Monthly Magazine*, 118(706), 497-509, 1909.
- Echelmeyer, K., and W. D. Harrison, Jakobshavns Isbrae, West Greenland: seasonal variations in velocity—or lack thereof, *J. Glaciol.*, 36, 82-88, 1990.
- Field, W. O., The glaciers of the northern part of Prince William Sound, Alaska, *Geogr. Rev.*, 22, 361-388, 1932a.
- Field, W. O., The mountains and glaciers of Prince William Sound, Alaska, *Am. Alpine J.*, 1, 445-458, 1932b.
- Field, W. O. (Ed.), *Mountain Glaciers of the Northern Hemisphere*, Vol. 2, 932 pp., U.S.A. Cold Regions Research and Engineering Laboratory, 1975.
- Gilbert, G. K., *Alaska Harriman Alaska Expedition*, Vol. 3. *Glaciers and Glaciation*, 231 pp., Doubleday, Page and Co., New York, 1903.
- Hall, D. K., K. Bayr, and W. M. Kovalick, Determination of glacier mass balance change using thematic mapper data, *Proceedings of the Eastern Snow Conference*, pp. 192-196, Lake Placid, New York, 1988.
- Krimmel, R. M., and M. F. Meier, Glacier applications of ERTS Images, *J. Glaciol.*, 15, 391-402, 1975.
- Meier, M. F., and A. Post, What are glacier surges?, *Can. J. Earth Sci.*, 6, 807-817, 1969.
- Meier, M. F., and A. Post, Fast tidewater glaciers, *J. Geophys. Res.*, 92, 9051-9058, 1987.
- Mendenhall, W. C., Geology of the Central Copper River Region, Alaska, *U.S. Geological Survey Professional Paper 41*, 1905.
- Mercer, J. H., The response of fjord glaciers to changes in the firm limit, *J. Glaciol.*, 3, 850-858, 1961.
- Motyka, R., Increases and fluctuations in thermal activity at Mt. Wrangell, Alaska, Ph.D. dissertation, 349 pp., University of Alaska Fairbanks, 1983.
- National Academy of Sciences, The Great Alaska Earthquake of 1964 - Hydrology, *Publication 1603*, Washington, DC, 1968.
- Post, A., Preliminary hydrographic and historic terminal changes of Columbia Glacier, Alaska, *U.S. Geological Survey Hydrological Investigations Atlas 559*, 1975.
- Sturm, M., Comparison of glacier flow of two glacier systems on Mt. Wrangell, Alaska, M.S. Thesis, 186 pp., University of Alaska Fairbanks, 1983.
- Tarr, R. S., and L. Martin, *Alaskan Glacier Studies*, 498 pp., National Geographic Society, Washington, DC, 1914.
- Viereck, L. A., Unpublished Report of the botanical work done during the 1957 expedition of the American Geographical Society as part of the IGY, 1959.
- Viereck, L. A., Botanical dating of recent glacial activity in western North America, in *Arctic and Alpine Environments*, edited by H. E. Wright and W. H. Osburn, pp. 189-204, Indiana University Press, 1967.

Radar Mapping of Malaspina Glacier, Alaska, with Applications for Global Change Investigations

John E. Jones and Bruce F. Molnia
U.S. Geological Survey, Reston, Virginia, U.S.A.

ABSTRACT

An ongoing radar study by the U.S. Geological Survey has used airborne, satellite, and ice-penetration radar to map glacier-surface features and sub-glacier bedrock relief of Malaspina Glacier, Alaska. Preliminary results of this study indicate that it may be possible to develop a model using satellite radar data to estimate the volume of some ice sheets. This model would be used in mass balance studies for global change investigations.

X-band (~3 cm wavelength) airborne radar (1975, 1980, and 1986) and L-band (~24 cm wavelength) Seasat satellite radar (1978) images show complex bright and dark radar backscatter patterns on the surface of Malaspina Glacier. These patterns, 0.5 to 10 km in length, resemble bedrock features in nearby mountains, such as cirques and drainage networks. Plane-table/alidade profiles, ice-penetration radar (~150 m wavelength) soundings, and other field data collected in 1988 and 1989 show that many of the radar backscatter patterns correspond to adjacent topographic highs and lows with a maximum relief of 100 m on the surface of the glacier. Many of the surface features of the glacier mimic the sub-glacier bedrock features at depths greater than 600 m below the ice surface. Preliminary analysis indicates that a relationship exists between the wave amplitude of these ice flow features, the ice flow velocity, and the depth of the ice.

These and other findings resulting from this study indicate that data from the eight international radar satellites planned for launch in the 1990s can be used on some ice sheets to (1) map landing sites and transportation routes by identifying crevassed zones and hummocky surface morphology, and (2) develop a geographic information system model of ice flow dynamics, based on wave amplitude, flow velocity, and areal coverage, to estimate ice volume for global change studies.

AD-P007 335



92-17839



Climate-Related Research in Svalbard

K. Sand

SINTEF Norwegian Hydrotechnical Laboratory, Trondheim, Norway

J. O. Hagen

Norwegian Polar Research Institute, Oslo Lufthavn, Norway

K. Repp

Norwegian Water Resources and Energy Administration, Oslo, Norway

E. Berntsen

Norwegian National Committee for Hydrology, Oslo, Norway

ABSTRACT

The Svalbard archipelago is located in the Norwegian Arctic, 76–81°N. In the Kongsfjord area, 79°N, on northwest Spitsbergen, there has been increasing research activity in several climate-related disciplines over the last few years. This research will contribute to the global efforts on monitoring and detecting possible global changes. An intensified program monitoring hydrological processes was run from 1974 to 1978 and restarted in 1988. One well-equipped station for atmospheric research is also established. Four major glaciers are being thoroughly investigated, a program which includes mass balance studies, drainage patterns and core analyses. Since 1978 a permafrost station has been operated in Svea, south-central Spitsbergen. The trend in glacier mass balance analyses shows fairly stable negative conditions, the net balance is slightly increasing due to a slight increase in the winter precipitation. There is no sign of climatic warming through increased melting. The temperature data show a very slight cooling during the ablation period. A reconstruction of mass balance data for the Brøgger glacier shows that the mass balance has been consistently negative since 1918.

INTRODUCTION

Svalbard is the geographical name of the archipelago situated between latitudes 76°N and 81°N and longitudes 10°E and 35°E in the Norwegian Arctic (Figure 1). The total area is about 63,000 km² of which 60% is covered by glaciers. Ice-free land areas have continuous permafrost with thickness varying from less than 100 m near sea level up to 500 m in the higher mountains [Liestøl, 1977]. Temperatures are high considering the latitude, largely due to the North Atlantic Current (a continuation of the Gulf Stream) of which a branch flows toward the west coast of Spitsbergen. Long-term average temperatures from Isfjord Radio

for the coldest month (March) and the warmest month (July) are 11.7°C and +4.7°C, respectively. Precipitation is less than 400 mm per year on the west coast of Spitsbergen, increasing eastward. Desert areas are found on the north-eastern part of this island.

This paper gives an overview of present climate-related research carried out in Svalbard within different geophysical sciences. Most of this research is being carried out in the Kongsfjord area, 79°N, on northwest Spitsbergen, which over the last few years has become an arctic field laboratory. The scope of this paper is limited to meteorology, permafrost, glaciology, hydrology and chemistry of the atmos-

phere. Finally, some aspects about Svalbard as an arctic field laboratory are presented.

METEOROLOGY

The primary climate controls of the area are light and radiation conditions, ocean currents, sea ice limits and the atmospheric circulation patterns [Steffensen, 1982]. The area experiences 3–4 months of midnight sun in the summer

with a net radiative heat gain, and similarly 3–4 months of continuous darkness in the winter with a net radiative heat loss. The warm North Atlantic current flows partly toward the west coast of Spitsbergen where in winter it creates the northernmost area of open water in the Arctic. A cold south-west-bound current flows along the east side of Svalbard, drawing the ice limit south. The general large scale air currents in the area are determined by the low pressure area near Iceland and high pressures over Greenland and the Arctic Ocean. The prevailing winds are westerly or south-westerly and transport mild air from lower latitudes toward the Svalbard area. At present five synoptic meteorological stations are being operated by the Norwegian Meteorological Institute (DNMI) (Table 1).

There are also meteorological stations in Hornsund and Barentsburg operated by Polish and Soviet authorities,



Figure 1. The Svalbard archipelago.

Station	Start of obs.	End of obs.
Isfjord Radio	1934	1976
Longyearbyen	1916	1977
Svalbard Airport, Longyearbyen	1975	-
Ny-Ålesund	1961	-
Bjørnøya	1920	-
Hopen	1944	-
Svea	1978	-

Table 1. Meteorological stations in Svalbard.

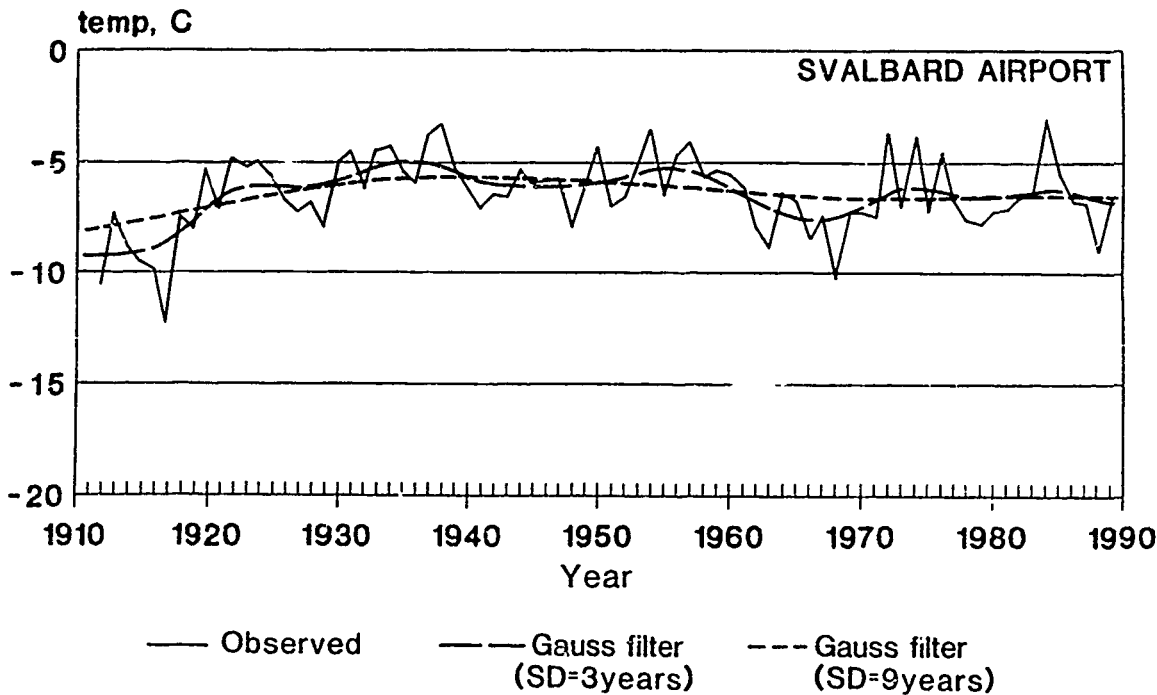


Figure 2. Air temperature at Svalbard Airport 1911–1989. (Reconstruction from correlation analyses, by Inger Hansen-Bauer, DNMI.)

respectively. DNMI also have automatic observations of air temperature, air pressure and wind at Phippsøya, Kong Karls Land, Kvitøya and Grimgfjell.

All the meteorological stations in Svalbard have Polar Tundra climate according to the Köppen system for climate classification [Steffensen, 1982]. Temperature records are available from 1911 on. Figure 2 shows a continuous temperature time series for Svalbard Airport, reconstructed from correlation analyses using data from Longyearbyen and Green Harbour (near Barentsburg). Remarkable is the rapid temperature rise from 1912 to 1920, which corresponds to a temperature rise recorded all over north-western Europe. On the west coast of Spitsbergen the mean temperature for December–February increased by about 8°C from around 1915 to the middle of the 1920s. As would be expected, this temperature rise was linked with a corresponding change in the general air circulation, leading to an intensified transport of mild air from the south. From the end of the 1950s to the end of the 1960s there was a falling trend in the mean temperature, while the start of the 1970s had a corresponding rise. The last years seem to show a falling tendency again. Such short-lived oscillations in temperature are not unusual and are apt to be especially conspicuous for the winter season in high latitudes, where, for instance, small changes in the preferred course of the low-pressure systems may have great consequences in temperature.

Little is known about the areal distribution of precipitation. Measurements of snowdepth indicate that the largest precipitation takes place in eastern areas where annual amounts of more than 1000 mm of water have been estimated. The driest area seems to be the central part of Spitsbergen from Van Mijenfjorden northward, which is sheltered from "precipitation-carrying" air streams [Hisdal, 1985].

PERMAFROST

Few direct measurements of permafrost thickness have been made. Liestøl [1977] quotes several reports of temperature measurement in boreholes and in the coal mines from different parts of Svalbard. Permafrost depth varied from 75 m to 450 m, and temperature gradients between 40 and 50 m °C⁻¹. The results from three borehole measurements shown in Figure 3 show almost vertical temperature curves in the upper 100 m. The explanation might be the warm climate period between 1920 and 1960. Theoretical calculations also show that the depth of this heat wave caused by the climate change is reasonable. The same phenomenon is observed in boreholes in Alaska [Gold and Lachenbruch, 1973]. Gregersen and Eidsmoen [1988] report permafrost investigations in the shore areas near Longyearbyen and Svea carried out in 1987. Reported gradients of 10 and 20 m °C⁻¹ are steep compared to gradients reported by Liestøl [1977]. The shoreline temperatures are generally higher than the temperatures measured in reference boreholes away from the shore, indicating influence from the sea which acts as a heat source. Isotherms for the shore area, based on temperature measurements and theoretical calculations, indicate that the permafrost extends less than 50 m out from the shoreline.

A permanent station for permafrost research was established in Svea in 1978 and is operated by the Norwegian

Geotechnical Institute. The station has an automatic data collection system recording all sensors every hour year round. Data are stored on magnetic tapes. This system records meteorological parameters, radiation, heat flux on the ground surface and ground temperatures. Manual observations are made weekly of thaw depth, groundwater table, thickness of dry crust, soil moisture, snow depth and snow density [Bakkehøi, 1982].

GLACIOLOGY

Increased glacier melting is one of the easiest measurable effects of temperature rise. In Svalbard regular monitoring of glacier mass balance started in 1950 on Finsterwaldbreen by the Norwegian Polar Research Institute (NP). At present NP's monitoring program includes accumulation and ablation measurements of four major glaciers: Finsterwaldbreen southwest of Svea, and Austre Brøggerbreen, Midtre Lovénbreen and Kongsvegen in the Kongsfjord area near Ny-Ålesund.

Soviet glaciologists started systematic annual mass balance measurements in 1966 on Vøringbreen in Grønfjorden. In the years 1973–1976 they extended the mass balance monitoring program to include four more glaciers: Bogerbreen, Bertilbreen, Longyearbreen and Daudbreen. At present the Soviet program includes Vøringbreen and Bertilbreen only.

At Brøggerbreen a series of 22 years of mass balance data are available (Figure 4). The mean annual specific net balance during this period is -0.46 m water equivalent.

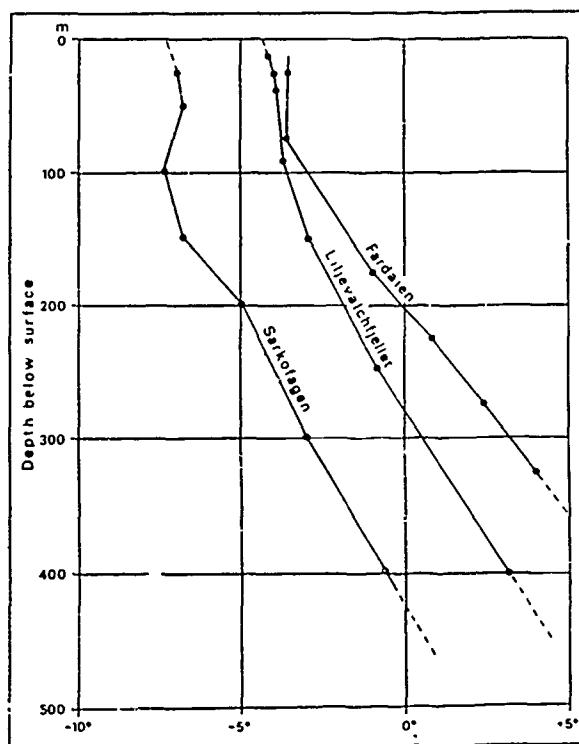


Figure 3. Temperature curves from three different boreholes: in the middle from Liljevalchfjellet near Sveagra, to the right from the Endaten valley, and to the left from the Sarkofagen mountain ridge near Longyearbyen. Note the upper part of the curves perhaps reflecting the milder climate starting about 1920. (After Liestøl [1977].)

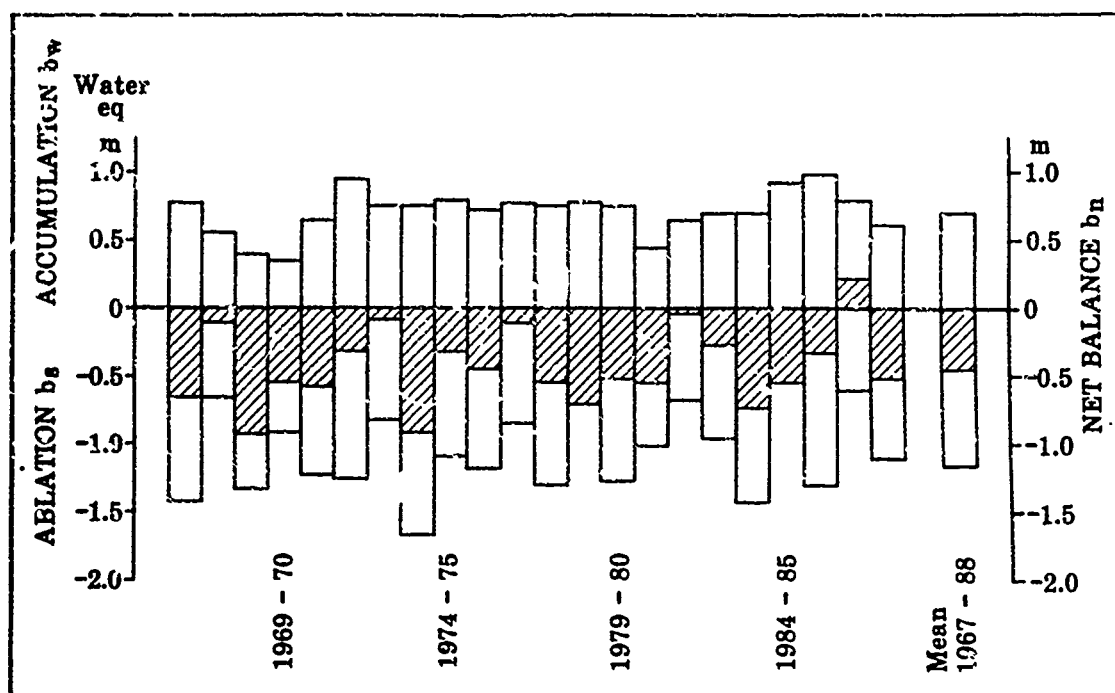


Figure 4. Mass balance of the Brøggerbreen Glacier 1966–1968. (From Hagen and Østøl [1990].)

Hagen and Lefauconnier [1990] found a high correlation between glacier net balance and meteorological parameters. A coefficient of correlation $R=0.90$ was obtained using accumulated positive degree days during summer and fall, and winter precipitation, as independent variables.

They also constructed the net mass balance for Brøggerbreen from 1912 to 1988 (Figure 5). From their calculation the total mass of ice lost from 1912 to 1988 was 34.35 m water equivalent, corresponding to a mean value of -0.45 m per year. The glacier started shrinking in 1918, corresponding to an increase of the mean summer temperature. Glacier front observations from a number of glaciers indicate that the glaciers in Svalbard reached their maximum as late as around the year 1900 (corresponding to the so-called Little Ice Age).

However, most of the glaciers in Svalbard are of the surging type. Thus rapid retreat of the front of these glaciers may be just a result of a quiescent period, and not a result of

a warmer climate with a high melt rate. It is therefore necessary to be aware of this phenomenon and make careful measurements of volume change when the climatic signals from these glaciers are interpreted.

Since 1918 the mass balance of Brøggerbreen has been consistently negative. Between 1921 and 1988 the loss of ice at Brøggerbreen was reduced from -0.63 m to -0.35 m water equivalent per year.

As far as one can see from more than twenty years of continuous mass balance measurements (1967–1988) in northwest Spitsbergen there is no indication of increased mass loss/melting rate on the glaciers. The glaciers have had a steady decrease in volume with negative net balance nearly all years. The only trend of change is a small increase of the winter accumulation, thus a slightly decreasing negative net balance.

HYDROLOGY

A research program monitoring hydrological processes in the Bayelva Basin near Nyl-Ålesund was run from 1974 to 1978 [Repp, 1979]. In this program special emphasis was put on glacier erosion, glacier hydrology and sediment transport. Prior to this program very few hydrological investigations had been made in Svalbard.

The Bayelva Basin has an area of 29 km^2 of which 51% is covered with glaciers. Nearly all runoff from the basin occurs during the summer months June–August and is dominated by snowmelt and glacier melt. The early runoff takes place on the surface; later on the meltwater drainage is englacial and subglacial. Temporary meltwater lakes on the glacier are common phenomena. These lakes usually drain in a few hours when an englacial drainage channel opens.

The supermafrost drainage is very minor. Repp [1979] estimated it to be less than 1% of the total runoff from the

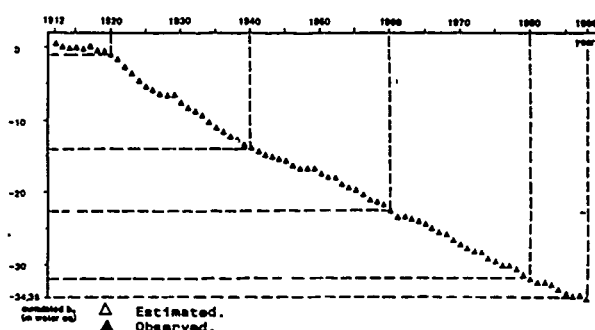


Figure 5. Cumulative net balance of the Brøggerbreen Glacier 1912–1988. (From Lefauconnier and Hagen [1990].)

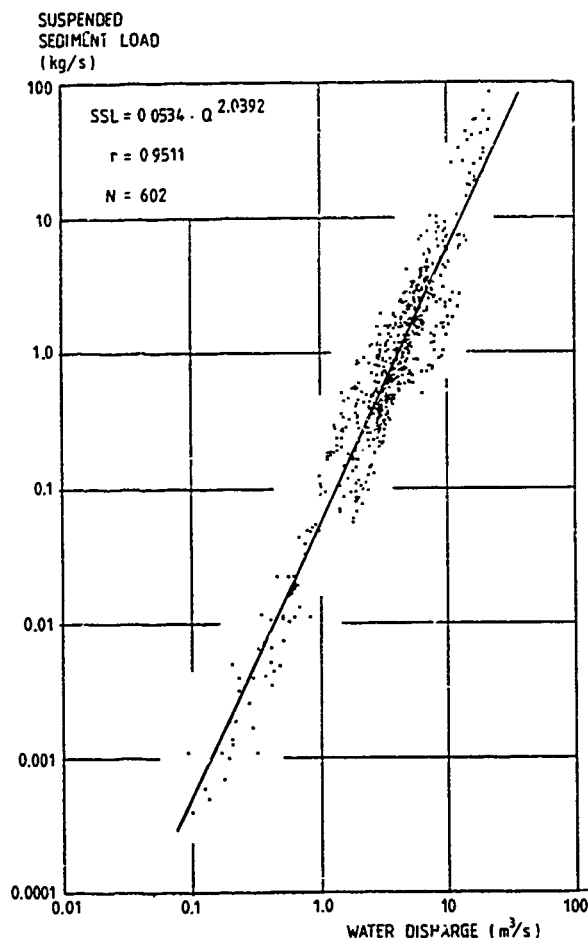


Figure 6. Sediment curve 1973–1978. (From Repp [1979].)

basin. Maximum recorded runoff during the years 1973–1978 was $1100 \text{ l s}^{-1} \text{ km}^{-2}$ while the mean specific runoff during this period was estimated to $32 \text{ l s}^{-1} \text{ km}^{-2}$.

The sediment transport from the basin is quite high; the maximum suspended sediment load measured was 3830 mg l^{-1} . The suspended sediment load is found to be strongly correlated with water discharge:

$$\text{SSL} = 0.0534 \cdot Q^{2.0392} \quad (1)$$

SSL is suspended sediment load and Q is water discharge. Equation (1) yielded a correlation coefficient $R=0.95$ during 602 days of observation 1973–1978 (Figure 6). The bottom load is estimated to be 30% of the total sediment transport as an average. The annual suspended sediment transport varied between 6646 tons and 16,558 tons, i.e., 228 tons km^{-2} to 567 tons km^{-2} . Assuming that sediment transport in Bayelva reflects the glacier erosion, this indicates an erosion intensity of 0.5 mm yr^{-1} , which is significantly more than observed for warmer glaciers in Norway.

The hydrological investigations in the Bayelva Basin were restarted in 1988 by the Norwegian National Committee for Hydrology. A general need for more information and knowledge of hydrological processes in arctic areas was felt by different research communities in Norway [Hagen et al., 1987]. The first phase of this program was the establish-

ment of permanent hydrological observation stations in Svalbard. Three research sites were selected: Bayelva near Ny-Ålesund, DeGeer River north of Longyearbyen, and Endalen Basin/Isdammen Reservoir near Longyearbyen.

Bayelva Basin was chosen in order to continue the extensive work done during the 1970s. In addition hydrological data would increase the value of this area as an arctic field laboratory for several scientific disciplines. Permanent installations for water discharge and sediment transport measurements were put in the main river. Water conductivity sensors will be installed at different sites. A meteorological station is established on Brøggerbreen during the period May–September every year.

In the DeGeer River a hydrometric station has been installed. The drainage area is 78.4 km^2 . The site was selected primarily because only 13% of the basin was glacier covered.

The Endalen Basin/Isdammen Reservoir is located near Longyearbyen. The Endalselva River feeds the Isdammen Reservoir which is the water supply source for Longyearbyen (approximately 1200 inhabitants). The area was selected because hydrological information is very important for proper operation of the water supply reservoir. The monitoring program includes instrumentation for water balance studies of the Isdammen Reservoir, sediment transport in the Endalselva River, groundwater movements and water quality. The stations in the Bayelva Basin and DeGeer River are in operation during 1990, while the program for the Endalen Basin/Isdammen Reservoir has not yet materialized due to economic constraints.

CHEMISTRY OF THE ATMOSPHERE

Toward the end of the 1970s oil exploration on the continental shelves started to move further north. In order to establish a base for evaluation of the concurrent pollution problems, a comprehensive study of the air pollution situation in the Norwegian sector of the Arctic was carried out by the Norwegian Institute for Air Research (NILU) during the 5-year period 1981–1985. Under this program four measuring stations were established in the high Arctic with an extended measurement program in Ny-Ålesund [Ottar et al., 1986].

The wintertime arctic haze, with concentration levels of man-made pollutants which are comparable to average concentrations over the industrialized continents, is due to pollutants emitted from sources within the arctic air mass. In late winter and spring, this cold and stable air mass, characterized by very low deposition rates and absence of photochemical activity, may engulf large parts of northern Eurasia. Aircraft measurements show that the vertical extension of this haze is typically less than 2000 m. The presence of further haze layers at elevations up to 5000 m or more is due to sources outside the arctic air mass. Also natural aerosols are present at high altitudes, in the form of soil dust, which may have originated from the large deserts in Asia or Africa (Figure 7). Local sources in Spitsbergen may also contribute to the haze layers, but this contribution is limited to emissions from sources in major settlements in the Svalbard archipelago. The local contamination of air can be traced as high as 1000 m.

A large-scale multilayer atmospheric dispersion model has been formulated, utilizing the concept of transport along

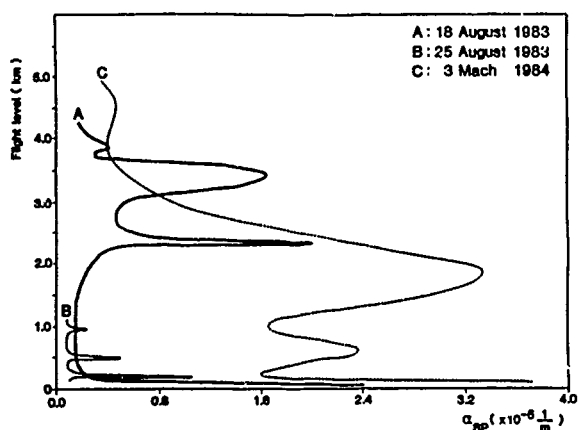


Figure 7. Aerosol concentrations at different levels obtained by aircraft measurements. (From Ottar [1986].)

isentropic surfaces. Calculations using available meteorological data and a spatial emission survey for the northern hemisphere show that the model is capable of simulating the advection of pollutants from different source areas into the Arctic at different elevations. The model calculations show that sources in the USSR contribute most to the high sulfur dioxide and sulfate aerosol concentrations at low altitudes during winter and spring (approximately 80% in March 1983), while other European sources contribute more to the concentrations at higher altitudes (approximately 60% above 2–3 km). At the highest levels there is also contribution from sources in North America. Various statistical techniques, such as principal component analysis and chemical mass balance apportionment, have also been used to prove these results.

Henriksen et al. [1990] report atmospheric ozone measurements in Tromsø that began in 1935. In recent years ozone measurement stations have been established in Longyearbyen and Ny-Ålesund. These stations show very good

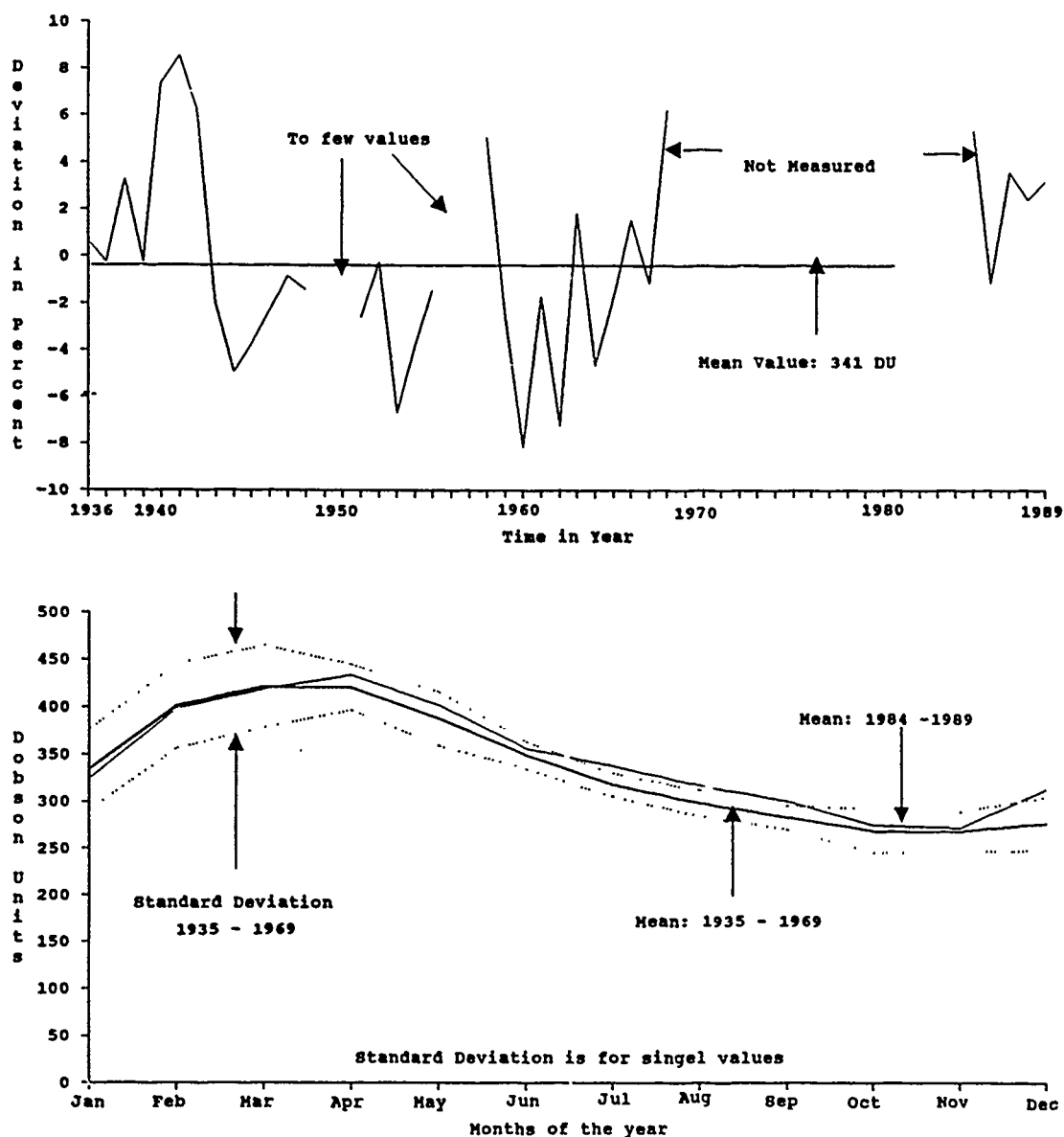


Figure 8. Longterm (upper graph) and annual variation (lower graph) of ozone in Tromsø 1935–1989. (From Henriksen [1990].)

correlation with the Tromsø station. The data from 1935–1969 were used to obtain an annual variation of stratosphere ozone in a period with obviously no influence from CFC release. For the period 1985–1989 the annual variation was obtained separately showing that the ozone layer was thicker during these five years than during 1935–1969 (Figure 8).

NILU's research station for atmospheric chemistry in Ny-Ålesund has been in operation since 1978. In 1989 a new permanent research station was established at the top of Zeppelin Mountain (475 m a.s.l.), 2.1 km from Ny-Ålesund. The station is part of the European Monitoring and Evaluation Program (EMEP) aimed at monitoring large-scale transport mechanisms of air pollutants, and the EUROTRAC (EUREKA) program which focuses on tropospheric ozone research. During 1990 a measurement program initiated by the Norwegian Research Council for Science and Humanity (NAVF) will be implemented. This program includes monitoring of greenhouse gases, tropospheric ozone and CFCs.

SVALBARD—AN ARCTIC FIELD LABORATORY

The present regulations for Svalbard were established in an international treaty of 1920. Sovereignty was awarded to Norway, with a number of restrictions. By the act of 17 July 1925, Svalbard became part of the Kingdom of Norway. The treaty was signed by nine nations in 1920. It has subsequently been signed by 26 more nations. Under the treaty, all nations have equal rights to exploit the islands' resources.

At present Norway, the Soviet Union and Poland have permanent activities in Svalbard. This paper hopefully indicates a high level of research activity within different disciplines concentrated in a limited area in the high arctic. This offers a unique opportunity to carry out interdisciplinary research projects. The permanent research bases in Ny-Ålesund and Svea also offer laboratory facilities and logistics. In addition Poland operates a permanent research station in Hornsund.

The area is easily accessible considering its high latitude. Airlines offer several regular flights a week from the Norwegian mainland and during the summertime ships also get into the settlements in Svalbard. Soviet airlines fly biweekly from Murmansk to Longyearbyen.

According to recommendations from the Norwegian scientific community [NOU, 1989] the future Norwegian effort within arctic research should be focused on environmental research, resource management and operations in the north. The same scientific community also expresses a need for international cooperation.

ACKNOWLEDGMENTS

The authors wish to thank the Norwegian Institute for Air Research, the Norwegian Geotechnical Institute, the Norwegian Meteorological Institute and Dr. Kjell Henriksen (University of Tromsø) for valuable contributions to the paper.

REFERENCES

- Bakkehoi, S., Collection of data at the permafrost station in Svea, Spitsbergen, in *Frost Action in Soils*, no 24. (In Norwegian), pp. 3–8, 1982.
- Gregersen, O., and T. Eidsmoen, Permafrost conditions in the shore area at Svalbard, in *Permafrost*, edited by K. Senneset, pp. 933–936, Fifth International Conference on Permafrost, 2–5 Aug 1988, Trondheim, 1988.
- Hagen, J.O., and O. Liestøl, Longterm glacier mass balance investigations in Svalbard 1950–1988, *Ann. Glaciol.*, 14, 102–106, 1990.
- Hagen, J.O., K. Hegge, M. Kristensen, K. Repp, and K. Sand, Polar hydrologi (Polar hydrology), *Report to the Norwegian National Committee for Hydrology*, 10 pp., Oslo, 1987.
- Henriksen, K., T. Svenøe, and S. Larsen, Longterm ozone measurements in Tromsø, Norway, Personal communication, 1990.
- Hisdal, V., *Geography of Svalbard* (second edition), Norwegian Polar Research Institute, Oslo, 1985.
- Lefauconnier, B., and J. O. Hagen, Glaciers and climate in Svalbard, statistical analysis and reconstruction of the Brøgger glacier mass balance for the last 77 years, *Ann. Glaciol.*, 14, 148–152, 1990.
- Liestøl, O., Pingos, springs and permafrost in Spitsbergen, *Norsk Polarinstitutt Årbok* 1975, pp. 7–29, 1977.
- NOU, Norsk polarforskning (Norwegian Polar Research), *Official Norwegian Report submitted to the Norwegian Department of Environment*, 124 pp., Oslo, ISBN 82-583-0160-8, 1989.
- Ottar, B., Belastung der Arktis durch Emissionen aus anthropogenen Quellen, *VDI Berichte*, 608, 17–46, 1987.
- Ottar, B., Y. Gotaas, Ø. Hov, T. Iversen, E. Joranger, M. Oehme, J. Pacyna, A. Semb, W. Thomas, and V. Vitols, Air pollutant in the Arctic, *NILU OR 30/86, 0-8144*, 80 pp., Norwegian Institute for Air Research, Lillestrøm, 1986.
- Repp, K., Breerosjon, glasio-hydrologi og materialtransport i et høyarktisk miljø, Brøggerbreene, vest-Spitsbergen (Glacier erosion, glacial hydrology and sediment transport in a high arctic environment; the Brøgger Glaciers, West Spitsbergen), Thesis, 136 pp., University of Oslo, 1979.
- Steffensen, E. L., The climate at Norwegian Arctic stations, *Klima, the Norwegian Meteorological Institute*, 5, 44 pp., Oslo, 1982.
- Gold, L. W., and A. H. Lachenbruch, Thermal conditions in permafrost—a review of North American literature, in *Permafrost*, Second International Conference on Permafrost, pp. 3–23, 1973, Yakutsk, USSR. North American Contribution, Washington, DC, National Academy of Sciences, 1973.

Application of Aerial Photographs to Registration of Dynamic Phenomena in Polar Environment

K. Furmanczyk and J. Trzajs

Department of Remote Sensing and Marine Cartography, University of Szczecin, Szczecin, Poland

ABSTRACT

Aerial photographs were taken during the Antarctic expedition of the Polish Academy of Science. A helicopter was used to make an aerial photographic survey of the area surrounding Admiralty Bay, King .George Island in the South Shetland Archipelago. Photographs were taken using a simple, self-constructed, multi-spectral camera. The photographic materials were used to compile a map of the changes of glacier fronts in Admiralty Bay, to compare with the British Admiralty map which was made twenty years ago. This map shows areas not covered by snow and ice during the summer.

Apart from long-term changes of extent of glacier fronts, photographs were used to analyze surface dynamical phenomena in Admiralty Bay. There were many growlers, very small icebergs, on the surface of the bay, and these were used to measure the velocity and the direction of surface mass drift. Simultaneously, the melt-water on the surface, with a strong concentration of suspended materials, was treated as an indicator of the tidal cycle in Admiralty Bay.

Inversion of Borehole Temperature Data for Recent Climatic Changes: Examples from the Alaskan Arctic and Antarctica

G. D. Clow and A. H. Lachenbruch
U.S. Geological Survey, Menlo Park, California, U.S.A.

C. P. McKay
NASA, Ames Research Center, Moffett Field, California, U.S.A.

ABSTRACT

A temperature disturbance at the earth's surface causes a downward-propagating thermal wave which can be sampled at later times in a geophysical borehole. This effect allows the surface temperature history at a given site to be reconstructed from precise temperature measurements at depth within the earth. Continuous permafrost regions are well suited for this type of paleoclimate reconstruction since they lack the disturbing effects of groundwater flow.

Application of Backus-Gilbert theory to this inverse problem indicates the highest temporal resolution that can be obtained for surface disturbances occurring at time $\sim t_0$ before present is $\pm 0.40 \cdot t_0$. This assumes ideal measurement geometry. If temperature measurements are limited to depths less than z_b , temporal resolution is severely degraded for event times to $> z_b^2/(18k)$ where k is the thermal diffusivity. Optimal resolution is retained back to ~ 40 Y.B.P. (160 Y.B.P.) when measurements to depths of 150 m (300 m) are utilized in the inversion. The resolution of events at time $\sim t_0$ is also degraded if the vertical distance between measurements (dz) is $> (kt_0/2)^{0.5}$. This is unlikely to cause a problem in practice, except when temperature data are acquired from a limited number of fixed thermistors.

We are applying formal inversion techniques to the Alaskan Arctic dataset reported earlier by Lachenbruch and Marshall [*Science*, 234, 689-696, 1986]. On the basis of their data and a forward analysis, they concluded much of the permafrost surface in this region has warmed 2-4°C during the last century. Application of inverse methods to this dataset provides improved estimates of the magnitude and timing of the recent arctic warming. Inversion of a recent temperature profile from the 300-m DVDP hole 11 in Taylor Valley, Antarctica, shows clear evidence for a 1°C warming during the last ~ 15 years. Although it is unclear whether the signal from this isolated hole is due to a climatic disturbance, the inferred warming does coincide with the general rise in lake levels throughout the antarctic dry valleys during this period.

Climate Change and Permafrost Distribution in the Soviet Arctic

Oleg A. Anisimov

State Hydrological Institute, Leningrad, U.S.S.R.

Frederick E. Nelson

Department of Geography, Rutgers University, New Brunswick, New Jersey, U.S.A.

ABSTRACT

Anticipated global warming during the next century will produce many environmental changes, including widespread thawing of permafrost in the northern hemisphere. The climate change scenario based on the method of paleoclimatic reconstruction developed at the USSR State Hydrological Institute was used to drive a model of permafrost distribution. Results indicate north- and eastward movement of permafrost boundaries, a substantial lengthening of the growing season, and significant soil warming in permafrost areas. Some implications of these changes for the Soviet Union are discussed.

Permafrozen Temperature Regime Affected by Climate Variability

P. A. Yanitsky

Institute of Northern Development, Tyumen, U.S.S.R.

ABSTRACT

The paper reports on the numerical-analytical solution for the problem of periodically constant heat exchange in permafrost. There are no initial conditions and the task at issue is based upon the soil conductive heat exchange simulation. In addition, at thawing or freezing, the parameters of water/ice transition, geothermal temperature gradient and the snow cover impact upon the soil heat transition to outer ground have also been taken into account. This solution is governed by the following characteristics: annual air temperature change; winter precipitation accumulation; thermo-physical soil properties either in thawed or in frozen state.

Considering the adduced solution the following parameters can be determined: the soil temperature at zero year amplitude level; the frost penetration lower boundary depth; and others. The calculated data are presented and compared with the results of previous field tests. The influence of the quantitative characteristics, such as variable climate and winter precipitation accumulation, upon the soil temperature pattern will be shown; in particular, the frost penetration lower boundary depth is varied by yearly average temperature increase or decrease. The regions where one-two degree yearly average temperature increases result in total permafrost disappearance have been located.

Computer Simulation of the Retrospective and Perspective Geocryological Situations in the Polar Regions

L. S. Garagula, V. E. Romanovsky and N. V. Seregina

Department of Geocryology, Faculty of Geology, Moscow University, Moscow, U.S.S.R.

ABSTRACT

We constructed a mathematical model to study the freezing and thawing processes of soils under temperature fluctuations on the earth's surface. A substantial part of the model is a computer routine for the numerical solution of a one- or two-dimensional, multi-frontal Stefan's problem. The results were adopted for investigation of the unsteady thermal fields and of freezing-thawing of heterogeneous soils under complicated rhythmic changes of the earth's surface temperature. This is an effective method to simulate the past, present and future geocryological conditions and to estimate corresponding landscape, engineering and hydrogeological environments, i.e., to detect evolutionary and technogenic trends in the changes.

The method includes the solution of direct and inverse geocryological problems. It is based on the reconstructions of paleoclimatic and significant geological events during the Quaternary (glaciations, sea transgressions and regressions, denudations and sedimentation velocities), provided by field observations on the structures, compositions, physical properties, thicknesses and thermal field fluctuations of the frozen soils above different geological and hydrogeological structures. All these parameters are used to describe various natural situations and serve as initial data for the computer simulation of the permafrost dynamics.

AD-P007 336



92-17840



Paleotemperature Reconstruction for Freeze-Thaw Processes During the Late Pleistocene Through the Holocene

V. E. Romanovsky, L. N. Maximova, and N. V. Seregina

Department of Geocryology, Faculty of Geology, Moscow State University, Moscow, U.S.S.R.

ABSTRACT

Variations in ground surface temperatures for different regions of the USSR were studied using the basic principles of Milankovitch global climate-change theory and harmonic analysis with cycle periods of 200, 100, 41, 21, and 11 thousand years (ka). The amplitude of these cycles has been calculated based on the following assumptions: (1) Climatic rhythms are represented as sinusoidal variations of temperature with periods of 200 (T'), 100 (T1), 41 (T2), 21 (T3) and 11 (T4) ka. (2) Minima of harmonics T' and T2 occurred between 25 and 26 ka ago, while minima of period T3 occurred between 22 and 23 ka ago; in addition, maxima of periods T1 and T4 were 5 ka ago. (3) Northern hemisphere deviations from present-day temperatures during the last cold epoch were up to 9°C in high latitudes, ice-free areas and 5°C for lower latitudes; during the last warm epoch, these values were 4 and 2°C, respectively.

Harmonics T2, T3 and T4 were combined in an attempt to refine the paleotemperature variations in different regions of the USSR from the late Pleistocene to the present. This long-term model is tested with a series of computer simulations of perennial freezing that show good agreement with reconstructions of paleopermafrost distribution and with its present vertical structure.

A model of surface temperature change is developed for middle- and short-term climate fluctuations. For this, temperature fluctuations with periods of 2000–1500, 300–200, 100–90, 40, 22 and 11 years are assumed. Cycles of 100, 40, 22 and 11 years can be studied from meteorological data.

The middle- and short term cycles are the most important for understanding and predicting permafrost dynamics, especially in the southern extremes of permafrost distribution. However, 300–200 and 2000–1500 year cycles cannot be studied using meteorological data. Fluctuations of mountain glaciers offer a means of studying these long-term cycles.

INTRODUCTION

The difficulty with permafrost paleoreconstructions is a shortage of knowledge about chronological sequences of the climatic events during the late Pleistocene and Holocene. There is not enough data for mathematical modeling of the permafrost dynamics because of the need to discover climatic rhythms and to fully describe such rhythms quantitatively (period, amplitude, phase).

The present-day permafrost structure formed, in general, during the late Pleistocene and Holocene. Therefore, this time period (approximately 100 ka) is the most important for the modeling of the history of the formation of permafrost. The most difficult problem is the reconstruction of the temperature conditions on the ground surface during this time period. However, there presently are some fundamental elaborations about global climatic changes that allow this problem to be solved quantitatively. It is important to

assume the existence of dramatic climate oscillations during the Pleistocene with the background of general climate cooling during the Cenozoic. According to the Milankovitch theory, the long-term changes (with periods of tens and hundreds of years) are associated with fluctuations in the amount of solar energy striking the Earth's surface caused by periodic changes in the earth's orbital drive.

The knowledge of middle- and short-term climate variations is important, especially for applications to engineering predictions. The periods of such variations likely are 2000–1500, 300–200, 100–90, 40, 22, and 11 years. There has been very little study of these rhythms. Currently, there is no conclusive theory of these variations. Such a theory is necessary for an explanation of their derivation and for forecasting of middle- and short-term climate changes. The study of glacier dynamics may be used for this purpose.

THE STUDY OF LONG-TERM CLIMATE VARIATIONS

The study of long-term variations allows the discovery of general trends for climate changes during the late Pleistocene and Holocene for different regions of the permafrost zone in the USSR. The paleotemperature curves (Figures 1 and 2) have been calculated in accordance with established practice [Maximov, 1972; Sergin, 1975; Zubakov, 1986; and others]. Based on the assumptions presented in the abstract, a system of equations was derived yielding the amplitudes of the T2, T3, and T4 harmonics and enabling construction of the summary paleotemperature curves [Maximova and Romanovsky, 1986, 1988]:

$$t(\tau)|_{\tau=\tau_{\min}} - t(\tau)|_{\tau=\tau_0} = A;$$

$$t(\tau)|_{\tau=\tau_{\max}} - t(\tau)|_{\tau=\tau_0} = B;$$

$$\frac{dt(\tau)}{d\tau}|_{\tau=\tau_{\max}} = 0;$$

where $t(\tau)$ is a function of total temperature; τ_{\max} and τ_{\min} are the time periods of the last thermal maximum and minimum; τ_0 is the present time, and "A" and "B" are temperature deviations from the present-day values during the periods of minimum and maximum. The amplitudes of T and T1 harmonics were assumed to equal 1°C.

The climatic variations in the late Pleistocene and Holocene obtained from the curves are in agreement with the consensus opinion of the paleoclimatic peculiarities of that time. The paleotemperature curve (Figure 1) illustrates principal climatic events of the late Pleistocene–Holocene and their time interval corresponding to the isotopic oxygen profile of ice from the boreholes at the Vostok station in Antarctica [Gordienko et al., 1983] and to its paleogeographic interpretation. Figure 1 shows movement of the ice sheet margin between Indiana and Quebec during the last major climatic cycle and the general mean global temperature curve according to Imbrie and Imbrie [1986]. Both examples are in agreement with the theoretical paleotemperature curve (Figure 1a).

From the curve obtained for the highlands of southeastern Siberia over an interval of 160 ka, the following events can be identified [Zubakov, 1986]: the Riss–Wurmian thermo-

chron 130–117 ka ago with a climatic optimum 125–120 ka ago and the Wurmian cryochron 117–15 ka with climatic warming about 100–90 ka (95–80 ka by the isotopic oxygen curve), a dramatic cooling about 75 ka (75–70 ka by the isotopic oxygen curve), an intra-Wurmian rise in temperature with a peak about 48 ka, and late Wurmian cooling 33–15 ka (with a minimum 27–24 ka by the isotopic oxygen curve), and climatic warming in the Holocene 15 ka ago.

The summary curves obtained (Figure 2) confirm the known facts on the rise in the amplitude of climatic changes from southeastern to northwestern USSR, as well as the Holocene thermal maximum lagging behind in the same direction [Khotinsky, 1977]. The earlier terms of the thermal maximum in East Siberia, as compared with the European North and West Siberia, can be explained by the laws governing the changes in individual rhythm amplitudes in these regions. In accordance with the Milankovitch theory of climatic fluctuations, there are significant latitudinal differences in the T2 and T3 rhythms: the former dominates at high latitudes and near 45°N, its amplitude approaching zero, while the amplitude of the T3 rhythm increases toward the south.

According to the solutions obtained, the amplitude of the T2 rhythm decreases from 8–9.5°C in the European North down to 2.5°C in the Far East. The amplitude of the T3 rhythm increases from 1°C in northern West Siberia to 1.5–2°C in the Transbaikal region. The total range of climatic variations and the time of their maximum manifestations varies accordingly. Thus, in northern West Siberia (the Ob' River basin) where the amplitude of the T2, T3 and T4 rhythms equals 7.2, 1.2, and 0.5°C, respectively, the total amplitude of temperature variations reaches 16°C and the Holocene thermal maximum dates around 4.5–6.5 ka ago. In the Transbaikal region, where the least difference between the T2 and T3 rhythms and T4 rhythm is practically lacking, the summary total amplitude of climatic variations is twice as small and the Holocene thermal maximum has the earliest dating from 10–11 to 8 ka ago. Such an early beginning of the maximum is acknowledged by the investigators of the region [Yendrikhinsky, 1982]. One can refine the thermal maximum time in the Holocene by superposing the middle-term rhythm (2–1.5 ka) of Shnitnikov [1957] on the curves obtained.

The process of ground freezing in the late Pleistocene glacial epoch and thawing during the Holocene temperature maximum in the Baikal rift zone depressions was studied in accordance with these temperature variations. This region was chosen for experimental examination of the hypothetical temperature variations because of a number of circumstances. The position of depressions, extending latitudinally, allows the changes in surface temperatures due to the displacement of geographical zones to be ignored. The landscapes of lacustrine-alluvial plains in the depression floors over the investigated period of time (80 ka) changed insignificantly [Belova, 1985]. This permits the supposition that the dynamics of the temperature field in the ground were determined practically by climatic variations. Two permafrost horizons have been identified in the depressions—the late Pleistocene and the Holocene [Zamana, 1980]. They can occur independently, constitute a two-stage section (Upper-Angara and Barguzin depressions), and merge into a single frozen series (Chara depression).

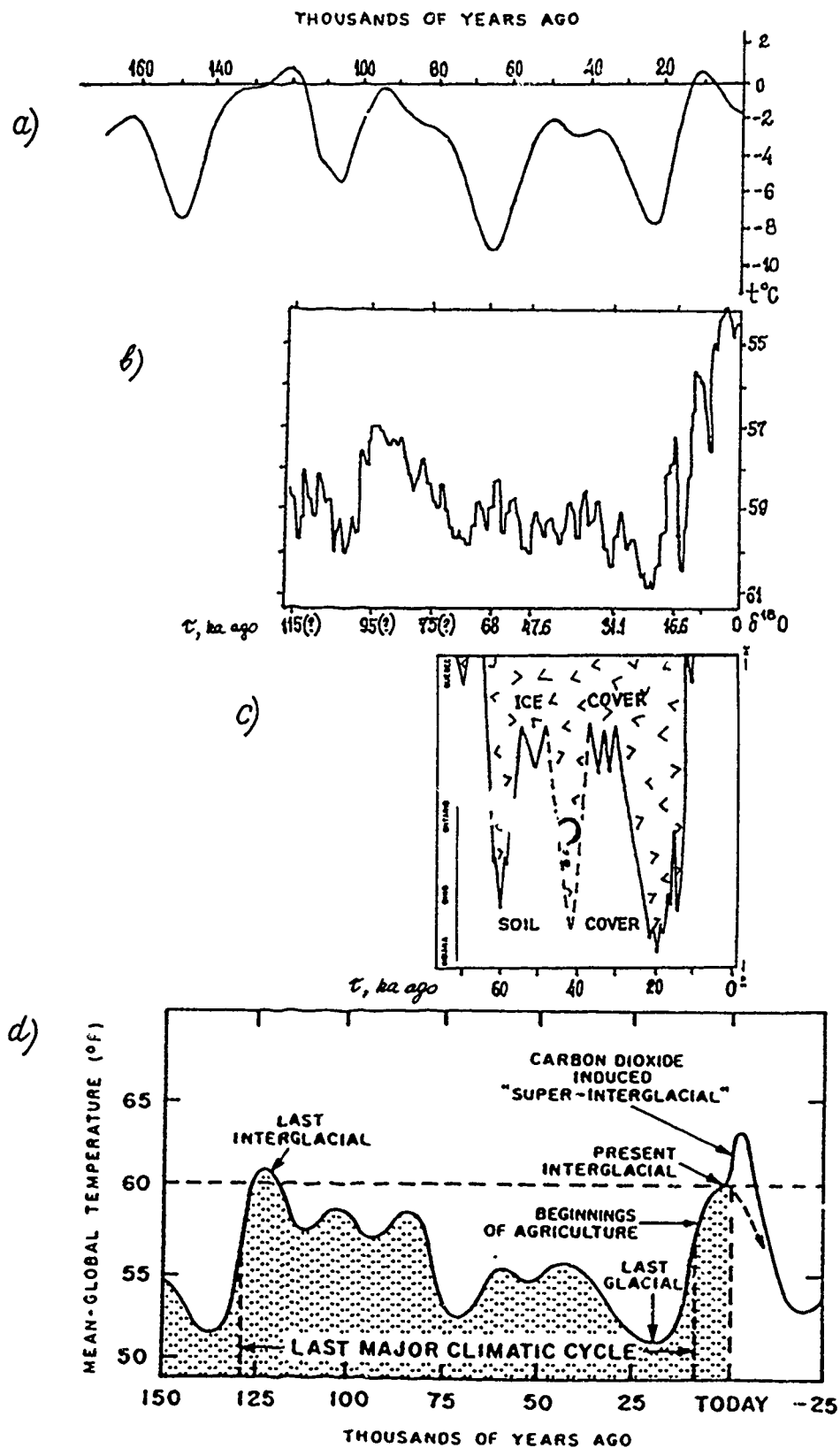


Figure 1. Principal climatic events of the late Pleistocene-Holocene: comparison of the theoretical paleotemperature curve for southern East Siberia (a) with isotopic oxygen profile of ice from the boreholes at the Vostok station in Antarctica (b), with fluctuations of the ice sheet margin between Indiana and Quebec during the last major climatic cycle (adapted from Imbrie and Imbrie [1986]) (c), and with general mean global temperature curve according to Imbrie and Imbrie [1986] (d).

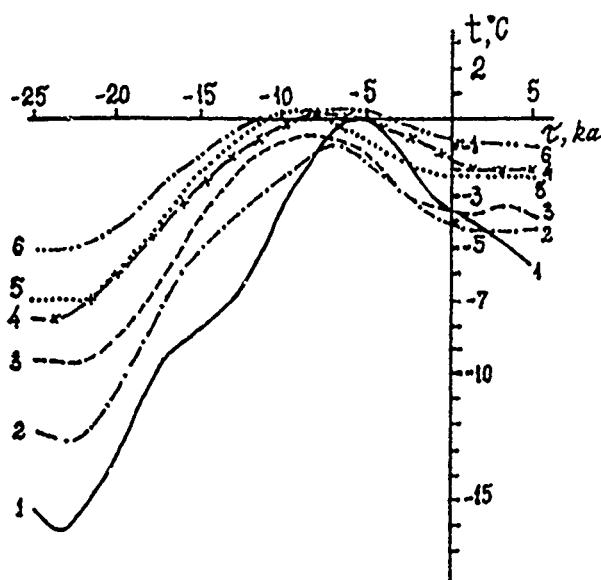


Figure 2. Relative changes of summary ground surface temperatures with time in different regions of the permafrost zone: 1, 2 - West Siberia (1 - Ob' River region; 2 - Yenisei River region); 3, 4 - East Siberia (3 - north of 65°N; 4 - south of 65°N); 5 - Transbaikalian region; 6 - Far East.

The appropriate examples of models are given in Figure 3. The presence of the two-stage section has made it possible to compare the estimated and actual depths of ground freezing and thawing at three levels: the bottom of the Holocene horizon, as well as the top and bottom of the Late Pleistocene frozen ground. The corresponding actual data are for the depths from 30–50 m to 80–110 m, 70–150 m, and 130–300 m; maximum thickness of the relict permafrost horizon amounts to 150–200 m, but in the regions with high present-day temperatures this horizon is intensively degrading and is only several meters thick.

Ground freezing and thawing have been simulated numerically using the programs for solution of Stefan's multifront problem developed at the Department of Geocryology, Moscow State University [Seregina, 1989; Romanovsky et al., 1991].

Comparison of the computed data and factual data yields positive results. This, in the opinion of the authors, justifies the attempt of refining the paleotemperature variations in different regions of the USSR for the late Wurm–Holocene by summing of the harmonics T1, T2, T3, and T4.

STUDY OF THE MIDDLE- AND SHORT- TERM CLIMATE VARIATIONS

The model of long-term cycles describes only a general tendency of the permafrost to form and change its main features in space and time over large regions of the permafrost zone.

For engineering applications, it is more important to establish the dynamics of the permafrost and its temperature field on concrete sites through relatively short time intervals (from ten to one hundred years). The depth of such changes may be relatively small (not more than 50–100 meters). It is possible only if some regularity of middle- and short-term climate changes is known. So the problem is to arrange middle-term (with periods of hundreds and a few thousand years) and short-term (with periods of tens and a few hundred years) climatic cycles.

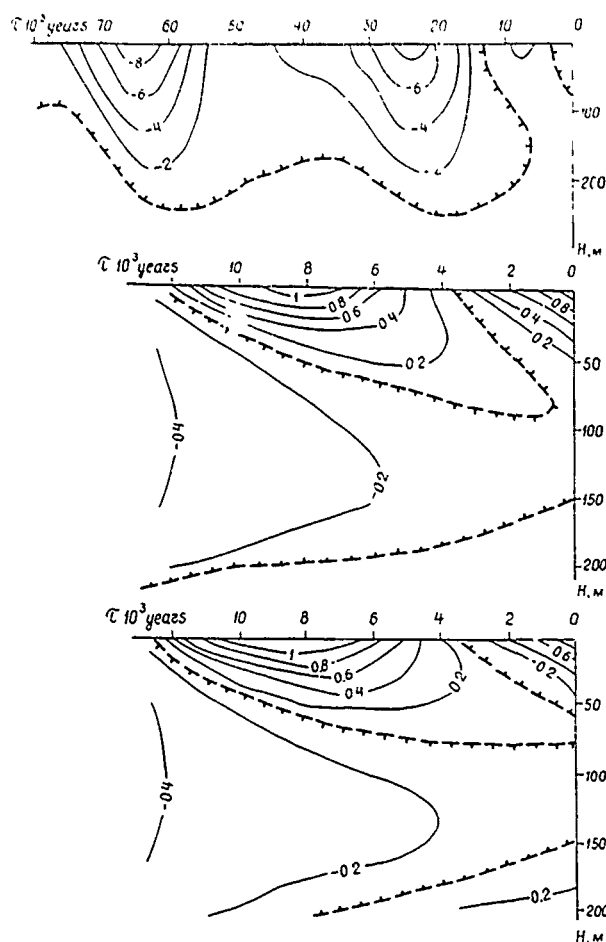


Figure 3. Variation of perennial thawing and freezing of rudaceous deposits in the mountain depressions of the Transbaikalian region in the late Pleistocene and Holocene: (a) complete thawing of the Pleistocene frozen ground strata; in the section: perennially frozen ground of the Holocene; (b) merging of partially thawed Pleistocene and formation of Holocene perennially frozen ground into a single frozen strata; and (c) a two-stage section permafrost strata with the Pleistocene and Holocene horizons.

The long-term meteorological data can be used for identification of the short-term climate changes without understanding their derivations. As an example of such a possibility, Figure 4 shows selected temperature data dating back to 1530 for the north face of the Alps [Huybrechts et al., 1989]. It is possible to recognize from these data several rhythms with periods of 300, 400, 40 and perhaps 22 years. The amplitudes of these rhythms are approximately 0.4°C, 0.4°C, and 0.5°C, respectively. It seems that the amplitudes of the 40- and 22-year rhythms are not constant, but change with time.

Figure 5 shows changes in the average temperature of the northern hemisphere [Imbrie and Imbrie, 1986]. This graph shows that two rhythms with periods of 100 and 40 years can be recognized, and these rhythms have approximately the same phases over the whole northern hemisphere.

The difficulty of the solution of the middle-term climatic change problem is the absence at the present time of some common theory about the derivation of such changes (like the theory of Milankovitch for the long-term cycles). However, there is good knowledge of natural phenomena that are sensitive to climate change. One such phenomenon is mountain glaciers.

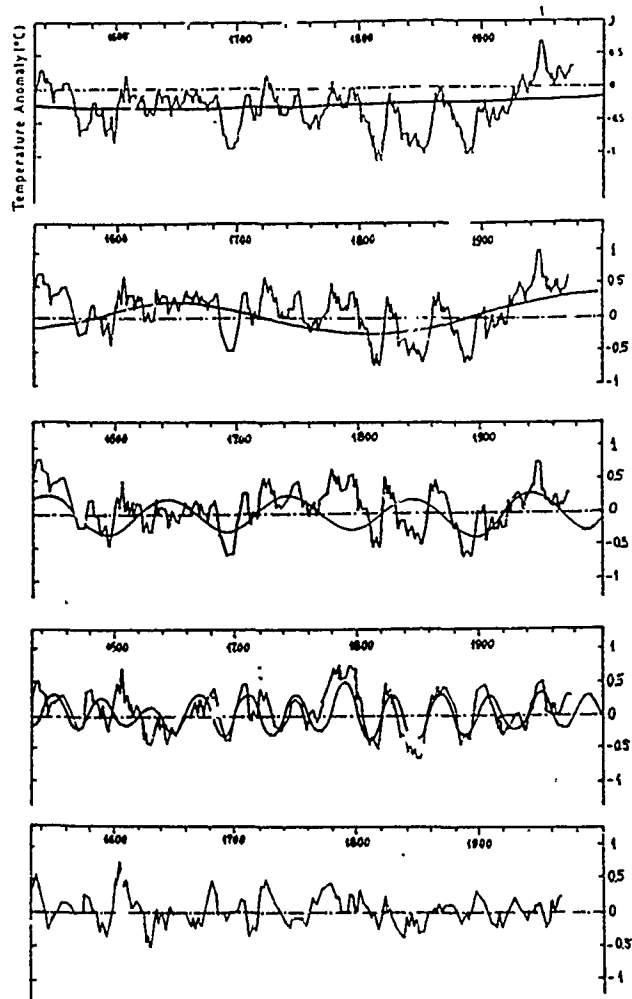


Figure 4. Temperature data dating back to 1530 for the north face of the Alps are given as 10-year running means and expressed as anomalies with respect to the 1901–1960 mean for Basel (from Huybrechts et al. [1989] and 1500-year cycle (a); temperature anomaly data except 1500-year rhythm and 300-year cycle (b); temperature anomaly without 1500-year and 300-year rhythms and 100-year cycle (c); temperature anomaly without 1500-, 300- and 100-year rhythms and 40-year cycle (d); temperature anomaly without 1500-, 300-, 100- and 40-year rhythms; perhaps it includes 22-year cycles (e).

THE POSSIBILITY AND DIFFICULTY OF USING MOUNTAIN GLACIERS FOR CLIMATIC RHYTHMS PREDICTION

It is obvious that mountain glaciers react to global long-term climate changes. However, it is difficult to study long-term changes using glacier data because following the advance of the glaciers, geomorphological and geological features of the previous glacial deposits are destroyed. Therefore, we know glacier dynamics in response to climate change for only the last 20,000 years, i.e., during the last period of deglaciation of mountain glaciers. The last deglaciation is a stable process of common retreat of the mountain glaciers, in general, over at least the whole northern hemisphere. This process has been continuing in Alaska since 12–15,000 years ago [Calkin, 1988]. In Europe and in the USSR, deglaciation of mountain glaciers has continued

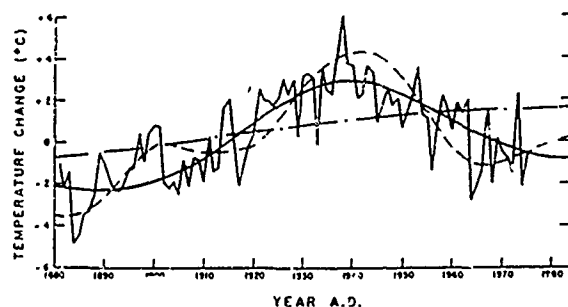


Figure 5. Climate of the past 100 years. This graph shows changes in the average annual temperature of the northern hemisphere. Since 1939, average temperatures have declined about 0.6°C. (From Imbrie and Imbrie [1986].)

for the last 13–14,000 years [Maximov, 1972]. Deglaciation is a complex process. With a background of general retreat of the glaciers, there are the rhythmical retreat-advance movements of the shorter periods. The total number of such cycles for glaciers in Europe and the Soviet Union is 7 over the last 12,000 years, and 5 cycles over the last 8000 years for Alaska. Therefore, there are the rhythmical changes of climate with a period of 1500–2000 years. Sometimes, it is possible to recognize the shorter "inner" rhythms in glacier movement, but there is not sufficient data for final conclusions.

More detailed study of concrete glaciers allows the establishment of the presence of such rhythms. However, it is difficult to generalize such data from several glaciers because the phases of the short-term changes of the positions of the glacier fronts are different. Even over the same region and neighboring glaciers, it is possible that one of them is retreating and another is advancing [Wood, 1988].

The cause of such glacier behavior is the presence of positive and negative feedbacks in the system Glacier–Local Mainland–Atmosphere–Ocean. The result of the feedback effect is the apparently random reaction of glaciers of different size, geometry, stability and location to the same global climate changes. The main problem is the use of mountain glacier movement as an indicator of middle- and short-term climate changes.

CONCLUSION

Climate changes have the character of oscillation. The study shows that surface temperature changes can be described as some superposition of distinct harmonic oscillations with different periods (from tens of years to hundreds of thousands of years and more). The main rhythms are synchronous at least for the whole northern hemisphere. The peculiarity of manifestations of summary surface temperature changes, including different times of thermal maximum and minimum during the late Pleistocene and Holocene over the different regions of the permafrost zone can be explained exclusively through differences in the distinct harmonic amplitudes for these regions. Mountain glacier movement can be used in the analysis of middle- and short-term climate changes, but the presence of the feedback mechanism must be taken into account.

The short-term changes can be studied through long-term meteorological records. At the present time in the field of glaciology, there is a need for a prediction mechanism and a theory of climate change, particularly of middle- and short-term changes.

REFERENCES

- Belova, V. A. *Rastitelnost' i klimat pozdnego kainozoya yuga Vostochnoy Sibiri*, 158 pp., Novosibirsk: Nauka, 1985.
- Gordienko, F. G., V. M. Kotlyakov, Ye. S. Korotkevitch, N. I. Barkov, and S. D. Nikolaev, *Novye rezultaty izotopokislorodnykh issledovaniy ledyanogo kerna iz skvazhiny so stantsii Vostok do glubiny 1412 m.-Materialy glyatsiol. issled. Khronika, obsuzhdeniya*, vyp. 46, 168-170, Moskva, 1983.
- Huybrechts, Ph., P. de Nooze, and H. Declerq, Numerical modeling of glacier d'Argentiere and its historic front variations, in *Glacier Fluctuations and Climatic Change*, edited by J. Oerlemans, pp. 373-389, Kluwer Academic Publishers, 1989.
- Imbrie, J., and K. P. Imbrie, *Ice Ages*, 224 pp., Harvard University Press, Cambridge, Massachusetts and London, England, 1986.
- Khotinsky, N. A., *Golotsen Severnoi Evrazii*, 197 pp., Moskva, 1977.
- Maximov, Ye. V., *Problemy oledneniya zemli i ritmy v prirode*, 296 pp., Leningrad: Nauka, 1972.
- Maximova, L. N., and V. E. Romanovsky, *Kolebaniya klimata i nekotorye osobennosti razvitiya mnogoletnemerzlykh porod v golotsene na territorii SSSR*. V knige: *Geokriologicheskie issledovaniya*, pp. 45-57. Moskva: Izdatelstvo MGU, 1986.
- Maximova, L. N., and V. E. Romanovsky, A hypothesis of the Holocene permafrost evolution, *Proc. Fifth Int. Conf. on Permafrost*, pp. 102-106, Norwegian Inst. Tech., Trondheim, Norway, 1988.
- Romanovsky, V. E., L. S. Garagula, and N. V. Seregina, Freezing and thawing of soils under the influence of 300- and 90-year periods of temperature fluctuations, *this volume*, 1991.
- Seregina, N. V., *Programma resheniya dvukhmernoy mnogofronovoy zadachi Stefana metodom sglazhivaniya entalpii*, 1989.
- Sergin, S. Ya., *Temperatura poverkhnosti zemli v nainolee teplye i cholydnye epokhi pozdnechetvertichnogo vremeni*, *Izvestiya AN SSSR, ser. geogr.*, 3, 37-48, 1975.
- Shnitnikov, A. V., *Izmenchivost' obshchei uvlazhnennosti materikov severnogo polushariya*, 337 pp., *Zapiski BGO*, v. 16. Novaya seriya. Moskva-Leningrad: Izdatelstvo AN SSSR, 1957.
- Yendrikhinsky, A. S., *Posledovatelnost' osnovnykh geologicheskikh sobytii na territorii Yuzhnoi Sibiri v pozdnem pleistotsene i golotsene*. V knige: *Pozdnyy pleitotsen i golotsen yuga Vostochnoy Sibiri*, pp. 6-35. Novosibirsk: Nauka, 1982.
- Zamana, L. V., *Glubokozemnyye mnogoletnemerzlye породы во впадинах Северного Прибайкалья*. V knige: *Geokriologicheskie usloviya zony BAM* pp. 31-37. Yakutsk: Izdatelstvo IM SO AN SSSR, 1980.
- Zubakov, V. A., *Globalnye klimaticheskie sobyitiya pleistotsena*, 286 pp., Leningrad: Gidrometeoizdat, 1986.

AD-P007 337



92-17841



Freezing and Thawing of Soils Under the Influence of 300- and 90-Year Periods of Temperature Fluctuation

V. E. Romanovsky, L. S. Garagula, and N. V. Seregina

Department of Geocryology, Faculty of Geology, Moscow State University, Moscow, U.S.S.R.

ABSTRACT

Mathematical modeling of perennial freeze and thaw is used in geocryology to solve both scientific and engineering problems. The surface temperature of a substrate is given as either a constant (stationary problem) or a function with a fixed period of fluctuation (periodic problem).

In this paper a numerical permafrost model is developed for the southern Siberia region to study the influence of rhythmic climate change on the dynamics of permafrost. The mathematical model is represented as a two-dimensional heat conduction problem for a moist substrate with "the latent heat effect" for complex geological structures. This model takes into account a complex periodic temperature change at the soil surface and a stable heat flow at the lower and lateral boundaries for a steady domain. The enthalpy method to arrive at a numerical solution for this problem is used. It has been realized as a fully implicit local one-dimensional finite-difference scheme on an irregular grid.

The calculations of the dynamics of temperature fields and permafrost boundaries are discussed to evaluate this scheme for the southern permafrost region of Eastern Siberia. The modeled results show that transects of temperature fields along some profiles (particularly at sites with complex geological structures) contain more information about permafrost dynamics than do ground temperature profiles from isolated boreholes. The combined use of both the field temperature data along profiles, and mathematical modeling, will provide a more reasonable explanation of present permafrost structure and more accurately forecast permafrost change in the future.

THE NUMERICAL MODEL

Under natural conditions the formation and dynamics of permafrost take place as the result of temperature change at the earth's surface caused by the superposition of climatic cycles with different periods [Kudryavtsev, 1978; Balobaev and Pavlov, 1983; Maximova and Romanovsky, 1985, 1988; Zubakov, 1986]. The objective of these studies is to construct a mathematical model to simulate natural conditions and to compare the results of modeling with single sinusoidal climatic fluctuations and superimposed fluctuations.

The following notation is used in the analyses:

x, y - spatial coordinates,
 t - time,

U - temperature,
 V^* - freezing temperature,
 Q - latent heat per unit volume,
 C - coefficient of heat capacity,
 λ - coefficient of heat conductivity,
 T - time length of experiment,
 U_0 - initial temperature,
 $p \equiv p(x, y, t)$ - point of the domain D ,
 $\Phi(x, y, t) = 0$ - equation of the freezing front in its implicit form, n - unit normal,
 $p + 0$ - index for a function whose variable trends to the point on the front from the part of the domain with greater enthalpy,
 $p - 0$ - the case opposite to the previous,

$\Delta t_n = t_n - t_{n-1}$ - time step,
 $t_{n+1/2} = t_n + \Delta t_n/2$ - time point,
 $h_{x,i} = x_i - x_{i-1}$ - spatial step in the direction X,
 $h_{y,j} = y_j - y_{j-1}$ - spatial step in the direction Y,
 U_{ij} - discrete solution at the nth time step,
 U_{ij}^1 - discrete function corresponding to the n+1/2 timestep
 U_{ij}^2 - discrete solution at the n+1 time step,
 C_s - smooth coefficient of heat capacity,
 λ_s - smooth coefficient of heat conductivity
 g - geothermal gradient.

The model can be represented in the following form in the domain

$$D = \{0 < x < 1, 0 < y < 1, 0 \leq t \leq T\}$$

in the X,Y,t - space :

$$C(U, x, y) \frac{\partial U}{\partial t} = \text{div}(\lambda(U, x, y) \nabla U) \text{ and } (x, y, t) \in D,$$

$$U \equiv U(x, y, t) \neq V^* \quad (1)$$

$$U(x, y, 0) = U_0(x, y),$$

$$\left. \frac{\partial U}{\partial n} \right|_{x=0} = \left. \frac{\partial U}{\partial n} \right|_{x=1}, \quad \left. \frac{\partial U}{\partial n} \right|_{y=1} = g$$

$$U(x, 0, t) = \varphi(x, t),$$

$$U(x, y, t) = V^* \text{ where } P(x, y, t) \in \Phi(x, y, t),$$

$$Q(x, y) \frac{\partial \Phi}{\partial t} = ((\lambda \nabla U)|_{p=0} - (\lambda \nabla U)|_{p=0}, \nabla \Phi),$$

where $p \in \Phi(x, y, t) = 0$.

In order to solve problem (1) we need the initial temperature $U_0(x, y)$; however, our main problem is periodic in time, so $U_0(x, y)$ is unknown. From Meyermanov [1986], we know the solution of problem (1) with a periodic function $\varphi(x, t)$ and an arbitrary function $U_0(x, y)$ tends to the solution of the periodic equation.

For a numerical solution of the problem (1), we use the enthalpy method. We smooth the enthalpy function with a first-order polynomial. The advantage of this method is that the temperature field can be found without knowing the position of the freezing front at a previous time layer (as, for example, in variational-difference method). This is especially important when we have three or more fronts (as in our case).

To solve the smoothed differential problem in the enthalpy formula we use a fully implicit local one-dimensional finite-difference scheme (always stable):

$$C_s(x_i, Y_j, U_{ij}^1) (U_{ij}^1 - U_{ij}) = \Delta t_{n+1} \Lambda_1 U_{ij}^1,$$

$$C_s(x_i, Y_j, U_{ij}^2) (U_{ij}^2 - U_{ij}^1) = \Delta t_{n+1} \Lambda_2 U_{ij}^2,$$

where

$$\begin{aligned}
 \Lambda_1 U_{ij} &= \frac{2}{h_{x,i} + h_{x,i+1}} [\lambda_s(x_{i+1} - 0.5h_{x,i}, Y_j, \\
 &\quad \frac{U_{i+1,j} + U_{ij}}{2} - \frac{U_{i+1,j} - U_{ij}}{h_{x,i+1}} - \lambda_s(x_i - 0.5h_{x,i}, Y_j, \\
 &\quad \frac{U_{ij} + U_{i-1,j}}{2} - \frac{U_{ij} - U_{i-1,j}}{h_{x,i}}]; \\
 \Lambda_2 U_{ij} &= \frac{2}{h_{y,j} + h_{y,j+1}} [\lambda_s(x_i, Y_{j+1} - 0.5h_{y,j}, \\
 &\quad \frac{U_{i,j+1} + U_{ij}}{2} - \frac{U_{i,j+1} - U_{ij}}{h_{y,j+1}} - \lambda_s(x_i, Y_j - 0.5h_{y,j}, \\
 &\quad \frac{U_{ij} + U_{i,j-1}}{2} - \frac{U_{ij} - U_{i,j-1}}{h_{y,j}}].
 \end{aligned} \quad (2)$$

The boundary conditions for the first equation of system (2) are given as $t=t_{n+1/2}$, and for the second as $t=t_{n+1}$. For the scheme (2), the boundary conditions of the second type are approximated with the second order of h_x, h_y [see, for example, Seregina, 1989] and with the first order of Δt . So the approximation order of the scheme is $O(h_x^2 + h_y^2 + \Delta t)$.

We used a simple iteration method for the solution of the nonlinear discrete system at each time layer. The solution from the previous time layer was considered to be the initial approximation of the iterative process. The program was written in FORTRAN-IV. The program bisects the time step in the case of iterative divergence at each half of the time layer.

The results of the numerical experiments: after the division of the time step, it is more economical not to use the maximum time step; the convergence of the solution of the initial problem to the solution of the periodic problem depends weakly upon the initial temperature function; we reach the periodic regime after 4-5 periods. Calculation time depends greatly upon the upper boundary condition $\varphi(x, t)$; therefore the calculation time in the case of a 300-year period is several times larger than in the case of the 90-year period.

GEOLOGICAL STRUCTURE, PHYSICAL PROPERTIES AND CLIMATE DYNAMICS

This mathematical model was used for the analysis of permafrost dynamics in the southern regions of Eastern Siberia. Paleogeographers determined in these regions the climatic rhythms with periods of about 90 and 300 years and amplitudes with fluctuations about 2°C and a mean temperature of approximately 0°C. These temperature values were used as upper boundary conditions. Lower boundary conditions were given by the geothermal gradient of 0.01°C m⁻¹ at a depth of 400 m.

The geological structure of the study consists of two parts. The first part is a layer of alluvial sands with a 10-m thickness and a sandstone base. The second part is also a layer of alluvial sands, but with a 50-m thickness.

Thermal and physical properties of soils are indicated in Table 1.

Soil Content\Thermal and Physical Properties	$\lambda_{th}/\lambda_{fr}$ W m ⁻¹ K ⁻¹	C_{th}/C_{fr} J m ⁻³ K ⁻¹	Q J m ⁻³
Alluvial Sands	1.5 1.7	2095x10 ³ 1676x10 ³	8380x10 ⁴
Sandstones	3.6 3.6	1048x10 ³ 838x10 ³	1257x10 ⁴

(λ_{th} , λ_{fr} - heat conductivity of thawed and frozen ground,
 C_{th} , C_{fr} - heat capacity of thawed and frozen ground)

Table 1. Thermal and Physical Properties of Soil.

CLIMATE CHANGES AND PERMAFROST DYNAMICS

The freeze-thaw problem was solved with three upper boundary conditions, a 90-year period, a 300-year period and the superposition of these fluctuations. Data analysis shows the following results (Figure 1): the sinusoidal temperature with a period of 90 years forms a layer of permafrost with a thickness of 9.3 m with the front in the alluvial layer (Figure 1C).

The rate of freeze-thaw is near 0.25 m yr⁻¹. The lower boundary of permafrost is located at a depth of approx-

imately 9 m through a period of 30-35 years. At the 90-year time interval, there is no permafrost for 17.5 years.

Fluctuations of temperature with 300-year periods cause perennial freezing at the 29-m depth (the frozen layer includes 10 m of alluvial sands and 19 m of sandstones) in the first part of the domain. In the second part of the domain, these fluctuations of temperature cause perennial freezing at the 15-m depth (Figure 1B).

The freezing rate of alluvial sands is about 0.14 m yr⁻¹. The rate for freezing of sandstones is approximately 0.3 m yr⁻¹. In the first part of the domain, the lower permafrost boundary is located at a depth of 29 m for 50-60 years. In the second part of the domain, the lower permafrost boundary is located at a depth of 15 m for 75-80 years. At the 300-year time interval, permafrost doesn't exist for 75-80 years.

Superposition of the 90- and 300-year period temperature fluctuations results in a new 900-year period of temperature fluctuations at the soil surface (Figure 1). During this 900-year period, the temperature fluctuations cause three cycles of warming (U 0)-cooling (U 0). The durations of these warming-cooling cycles are 277 years, 346 years and 277 years.

During the first cycle (277 years), there is a time of warming at about 137 years, with two temperature maxima of +1.5°C and with one minimum of 0°C in the middle of the warming period. At the cooling interval (140 years), there are two temperature minima, one at the beginning of

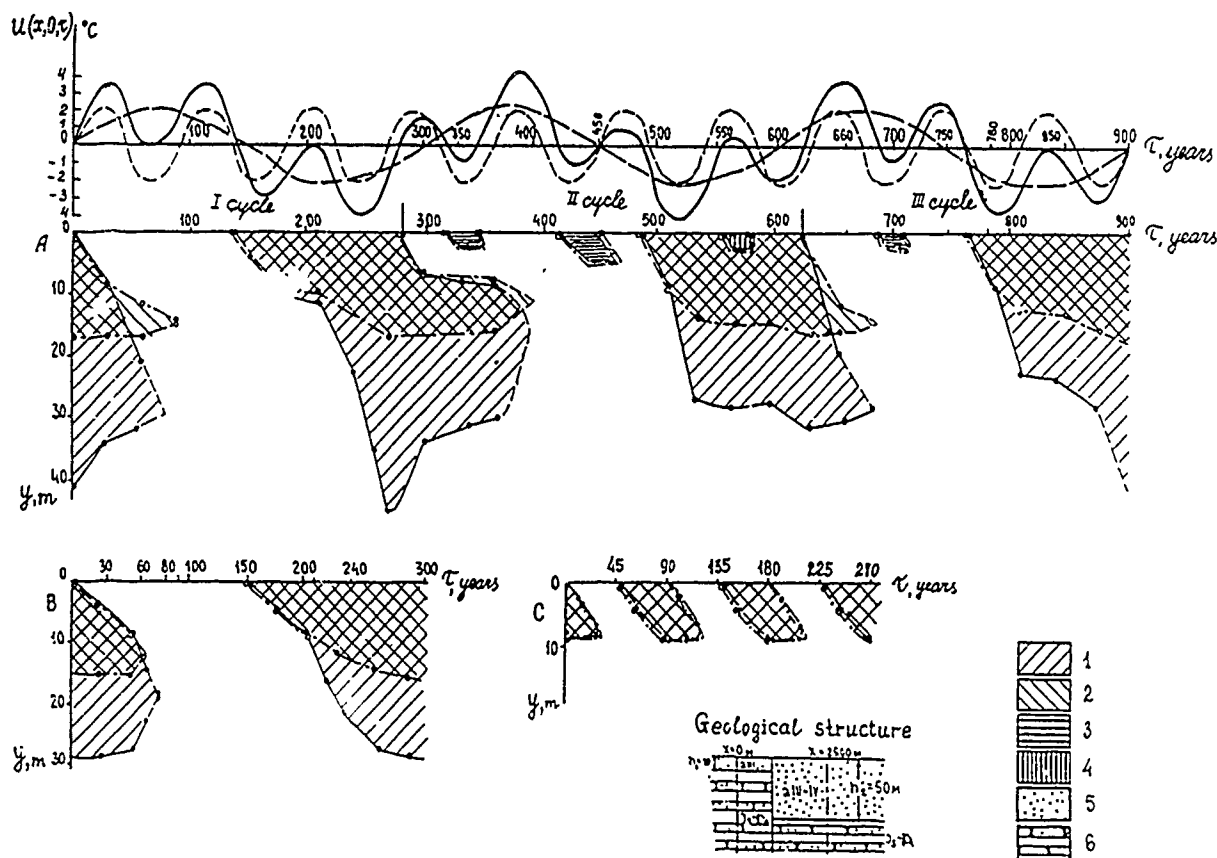


Figure 1. Dynamics of freezing-thawing of soils under the superposition of temperature fluctuations at the earth's surface with 300- and 90-year periods (A); under temperature fluctuations with a 300 year period (B); under fluctuation with 90-year periods (C). The behavior of the surface temperature is shown in the upper graph. The computation results are given for two parts of the domain: (1) permafrost in the first part; (2) permafrost in the second part; (3) short-term permafrost; (4) talik, which gives discontinuous permafrost; (5) sands; (6) sandstones.

the interval (-1.2°C), and the other at the end (-2°C). In the middle of the cooling interval, there is one maximum with a temperature not greater than 0°C .

During the second cycle (364 years), there is a time of warming (208 years) with three temperature maxima of $+0.7^{\circ}\text{C}$, $+2.0^{\circ}\text{C}$ and $+0.5^{\circ}\text{C}$, and two temperature minima (-0.3°C and -0.6°C). At the time of cooling (138 years), there are two temperature minima (-2.0°C and -0.9°C) and one maximum ($+0.3^{\circ}\text{C}$).

During the third cycle, there is a time of warming (137 years), with two maxima ($+1.8^{\circ}\text{C}$ and $+1.5^{\circ}\text{C}$) and one minimum (-0.2°C). At the time following cooling (140 years), there are two minima (-1.9°C and -1.2°C) and one temperature maximum (0°C). The thermal history is opposite that of the first cycle.

Analysis of the summary temperature curve shows that total warming occurs in the middle of the 900-year period, and this warming is caused by temperature fluctuations with a 300-year period. The fluctuations with 90-year periods cause a temporary lowering of the surface temperature below 0°C .

The formation and dynamics of permafrost caused by the temperature fluctuations are different with respect to different cycles of 900 years. As shown in Figure 1, simple stable conditions of freeze-thaw occur during the first cycle. The maximum thickness of permafrost here is near 45 m. The existence of permafrost is near 140 years. During the previous period of warming, thawed soils exist continuously during a 55-year period.

Dynamics of freezing are defined by the positions of the surface temperature minima. The first minimum (connected with temperature fluctuations with a 90-year period) caused the rapid freezing (velocity is near 0.25 m yr^{-1}) of alluvial sands to a depth of 8 m. After that, the rate of freezing reduces and the freezing layer with a thickness of 2 m arises during 30 years. At that time, the surface temperature is near 0°C .

The next 90 years of cooling (coinciding with 300 years of cooling) cause the freezing of the sandstones at a rate of 0.55 m yr^{-1} . The freezing front reaches a depth of 45 m and remains at this depth during the 10 years until a change of temperature sign on the surface.

The warming, connected with temperature maximum of fluctuation with a 90-year period, causes the thawing of soils from the top and bottom. This is the beginning of the second warming-cooling cycle.

During 20 years at the second cycle, the thawing of permafrost from below occurs at a rate near 0.5 m yr^{-1} . The lower boundary of permafrost rises from 45 to 32 m. After 20 years, the rate of thawing sharply slows, and during the next 100 years, the front rises only 4 m.

As indicated in Figure 1, the thawing from above (during 115 years) is complete at a depth of 30 m in the sandstone. The rate of thawing is influenced by the soil properties and temperature fluctuations at the surface. During the first 20 years, the thawing rate of alluvial sands is near 0.3 m yr^{-1} ; the depth of thawing reaches 7.5 m. During the next 60 years, the thawing front actually remains stationary. At the same time, the surface temperature falls to -0.5°C and remains negative for almost 30 years. The short-term permafrost with a thickness of about 1.5 m is forming. The thawing layer with a thickness of 6 m appears. The existence of

short-term permafrost causes an actually invariable location of permafrost cover during 30 years.

After thawing of short-term permafrost, the thawing of soils from above proceeds with a rate of about 0.1 m yr^{-1} during the next 35 years. It ends with the meeting of the upper and lower fronts. The end of thawing occurs when the maxima of the 300- and 90-year periods coincide. Twenty years after the end of thawing the short-term permafrost with 6 m thickness is formed and exists for 60 years.

At the end of the second cycle, the depth of freezing is 27–31 m for 150 years. The duration of freezing to a 27-m depth is equal to 50 years; the rate of freezing is near 0.56 m yr^{-1} . After that, the freezing front is actually invariable. Such a position of lower permafrost boundary is defined by a temperature maximum of fluctuation with a 90-year period. The surface temperature is positive for 20–30 years. Talik with thickness near 1.5 m exists over the cover of permafrost. Ten years after the freezing of the talik, the lower freezing front falls to a 31-m depth (for 30 years).

The third cycle begins with thawing of permafrost from above and from below, conditioned by positive surface temperature. The rate of thawing from below is about 1.5 m during the 70-year period. The rate of thawing from above is about 0.4 m yr^{-1} . After 70 years, the upper and lower fronts meet at a depth of 28 m.

During the next 70 years, the section consists of thawing soils. This is initiated by positive surface temperature. However, at the beginning of this time interval, short-term permafrost is formed with a thickness of about 1 m and remains frozen for about 20 years. This short-term permafrost is initiated by negative surface mean temperature. During the last part of the third cycle, there is permafrost for 140 years, with a maximum depth here of 41 m.

Analysis of the processes in the second part of the domain (with 50 m thickness of alluvial sands) shows that differences in the lower boundary of permafrost during time cycles are insignificant (near 1 m). This is due to the fact that heat for phase changes in alluvial sands is 7 times greater than in sandstones. The first part of the domain (with 10-m thickness of alluvial sands), the lower boundary of permafrost, is stable only for a short time (near 10 years).

The position of the upper permafrost boundary, formation of short-term and discontinuous permafrost is similar in the first and second parts of the domain. Regularity of formation and duration of the permafrost (with respect to the upper front) are common for both geological sections at the 900-year period.

TWO-DIMENSIONAL TEMPERATURE FIELD DYNAMICS

The application of a two-dimensional mathematical model also allows the characterization of the anomalies of temperature dynamics. The typical positions of isotherms correspond to a definite stage within the cycles as indicated in Figure 2. There are four stages: the first, from the beginning of freezing until the time the freezing front reaches the sandstones in the second domain; the second, until completion of perennial freezing; the third, the time of thawing of permafrost; the fourth, the time of warming and cooling without phase changes.

The forming of a one-dimensional temperature field is typical for the first stage (see Figure 2.1). The boundary of

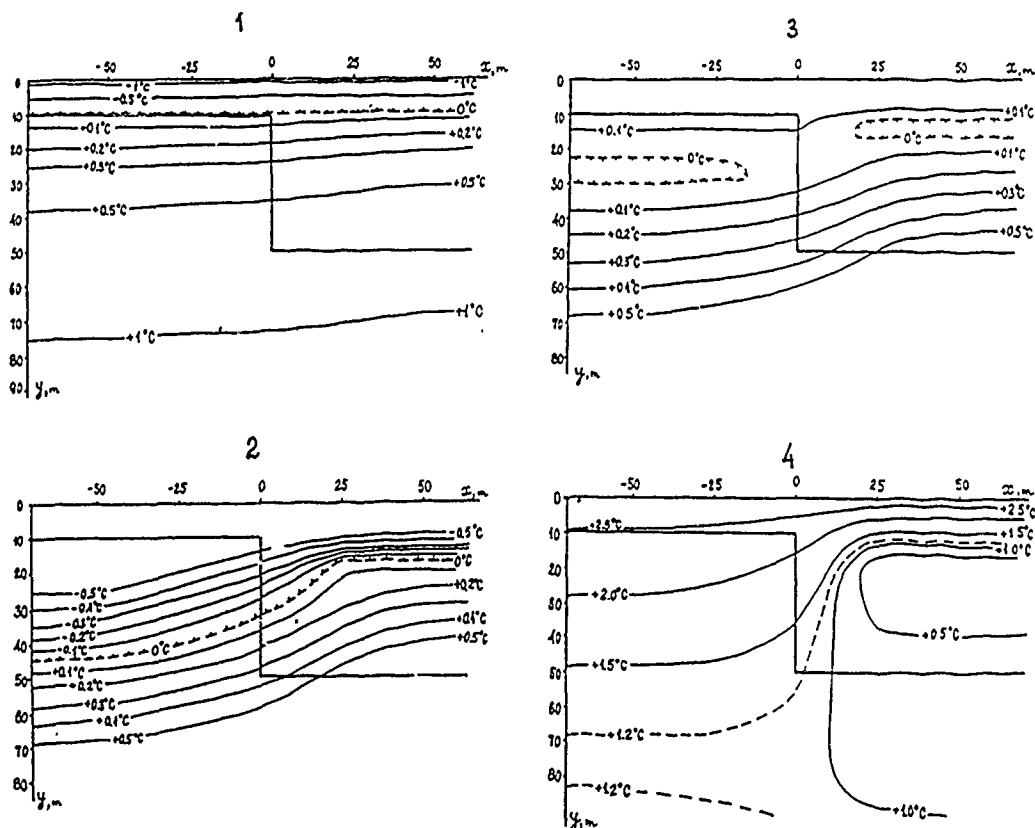


Figure 2. Isotherms in the domain, consisting of two parts: (1) at the beginning of perennial freezing (the front doesn't go out of the sand layer); (2) at the end of freezing, when permafrost has maximum thickness; (3) at the end of thawing; (4) at the moment of complete thawing.

two parts with different geological structures influences isotherms insignificantly. During the second stage, there is a two-dimensional temperature field. Isotherms are forming a "step" near the boundary of the two parts. The "step" is similar to the shape of the freezing front (see Figure 2.2). Configurations of temperature field and freezing front are like "reverse projection" to "geological projection."

During the third stage, permafrost is thawing from above. While the upper front is in alluvial sands, the temperature field in upper thawing soils is one dimensional. Temperature fields in relic permafrost are losing gradient rapidly, while the temperature is going to 0°C . The smoothing of projections in the lower front is the consequence of this fact. During the next thawing, the upper front in the second part of the domain reaches the sandstones. The velocity of the front is increasing. The projection shape of the upper front is forming. This is similar to the projection during freezing.

Thawing leads to partition of relic permafrost in different geological sections. We can explain the formation of an open talik in the zone of geological projection (Figure 2.3) by maximizing the thermal flow. At the fourth stage, all permafrost thaws. At this time, the temperature field is essentially two-dimensional; isotherms have the shape of high "step" near the contact of two geological sections. Here the maximum of the horizontal part of the heat flow exists (Figure 2.4). There are small temperature gradients in alluvial sands at the beginning of permafrost formation and at the end of thawing.

CONCLUSION

Temperature fluctuations with periods of 90 years do not lead to deep freezing of the ground (less than 10 m) and do not penetrate at great depths (less than 40–50 m). Three-hundred-year fluctuations lead to greater depths of freezing of the ground (about 30 m in our case).

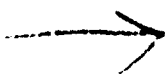
Superposition of both of these fluctuations creates a more complex distribution of the temperature field and of its dynamics. Cooling periods vary in duration when permafrost exists; therefore, the thickness of permafrost during each period is also different. Maximum thickness occurs when the minima of both rhythms coincide. The thickness of permafrost exceeds 43 m, i.e., more than 10 m greater than the maximum depth of freezing by the "pure" 300-year fluctuation. Superposition of the fluctuations also leads to complex alternation of short-term permafrost and of not-transparent taliks near the surface of the ground.

The modeled results show for each stage within the cycles that the surface temperature change is characterized by a distinct feature of temperature field and location of the permafrost boundary in a domain with complex geological structure. This fact allows for the use of such domains to generate temperature field data for more reasonable explanations of the present permafrost structure and a more accurate prediction of temperature field and permafrost dynamics in the future.

All results of this article are important for reconstruction investigations in the southern part of the permafrost zone.

REFERENCES

- Balobaev, V. T., and A. V. Pavlov, *Dinamika kriolitozony v svyazi s izmeneniyami klimata i antropogennym vozdeystviem*, V knige: *Problemy geokriologii*, 184-194, Nauka, Moskva, 1983.
- Kovalenko, V. D., L. D. Kizim, A. M. Pashestjuk, and V. G. Nikolaev, *Issledovanie prizhin izmenzhivosti klimata*, V knige: *Agroklimati-zheskie resursy Sibiri*, 103-113, Izdatelstvo VASCHNIL, Novosibirsk, 1987.
- Kudrjavzhev, V. A., *Obshee merzlotovedenie*, 463 pp., Izdatelstvo MGU, Moskva, 1978.
- Maximova, L. N., and V. Ye. Romanovsky, A hypothesis for the holocene permafrost evolution, *5th International Conference on Permafrost*, edited by K. Senneset, 2-5 August 1988, Trondheim, Norway, Vol. 1, pp. 102-106.
- Metody resheniya kraevykh i obratnykh zadazh teploprovodnosti (pod redakciey A. V. Uspenskogo), 262 pp., Izdatelstvo MGU, Moskva, 1975.
- Maximova, L. N., and V. Ye. Romanovsky, *Kolebanya klimata i nekotorye osobennosti razvitya nogoletnemerzlykh porod v golocene na territorii SSSR*, *Geokriologizheskie issledovanya*, 45-57, Izdatelstvo MGU, Moskva, 1985.
- Meyermanov, A. M., *Zadazha Stephana*, 239 pp., Nauka, Novosibirsk, 1986.
- Moiseenko, B. D., and A. A. Samarsky, *Ekonomizheskaya schema skvoznogo szheta dlya mnogomernoy zadazhi Stephana*, *Zhurnal vyzhisli-tel'noy matematiki i matematizheskoy fiziki*, 5(5), 816-827, 1965.
- Rozanov, M. I., *Parametry godizhnykh kolez derevyev kak informatsionnaya osnova dolgosrozhnogo prognozirovaniya bioekologizheskikh ressursov*, V knige: *Agroklimatizheskie resursy Sibiri*, 80-102, Izdatelstvo VASCHNIL, Novosibirsk, 1987.
- Seregina, N. V., *Nekotorye matematizheskie modeli zadazh geokriologii i metody ich zhislen'nogo resheniya*, V knige: *Geokriologizheskie issledovanya*, 48-54, Izdatelstvo MGU, Moskva, 1989.
- Zubakov, V. A., *Globalnye klimatizheskie sobytya pleystotsena*, 285 pp., Gidrometeoizdat, Leningrad, 1986.



92-17842

AD-P007 338



Microbiological Weathering of Silicates in Permafrost

T. P. Kolchugina and S. P. Fedosova

Department of Geocryology, Faculty of Geology, Moscow State University, Moscow, U.S.S.R.

ABSTRACT

Microorganisms are known to degrade soils in temperate regions. Viable microbes have been found in permafrost-zone soils, and it is of interest to determine if these organisms can participate in silicate weathering in permafrost at low temperatures. The degradation of oligoclase and hornblende when exposed to psychrophilic bacteria *Aeromonas* sp. at low and average temperatures was considered in this study.

A sterile glycerine solution was added to sterilized soil samples to serve as a source of carbon for the bacteria and to prevent the transition of the liquid phase to a solid state. The degradation of the oligoclase at +20, +4, and -1.5°C was examined after 109 days of incubation; the degradation of the hornblende at +20, +4, and -8°C was examined after 360 days.

The bacteria grew in all variants, except the sterile controls. The bacterial number at +20°C was 50 times more than in other non-sterile variants. The bacteria promoted the release of Ca and Na from the oligoclase and did not promote the release of Si from this mineral. The content of the Ca in the media exceeded the content of other elements.

Microbiological weathering of silicates in permafrost is possible even at temperatures below zero, if carbon and a liquid phase are present; moreover, the levels of mineral transformation are comparable with the levels of transformation at moderate temperatures.

INTRODUCTION

Microorganisms are known to be capable of degrading soils in temperate regions [Aristovskaya, 1980]. Because viable microbes have been found in permafrost-zone soils, it is of interest to determine if these organisms can participate in silicate weathering in permafrost at low temperatures. The results of this study may be of interest not only to soil microbiologists, but also to specialists in other areas, for example, civil engineering.

OBJECTIVES

The objective of the study reported herein is to estimate the level of microbiological weathering of silicates at low and average temperatures. Specifically, the degradation of oligoclase and hornblende when exposed to psychrophilic bacteria *Aeromonas* sp. was considered. The bacteria previously were isolated from the Kolym lowland permafrost.

EXPERIMENTAL APPROACH

Mineral samples were placed in glass vessels and sterilized. After the samples were sterilized, 50 ml of a sterile glycerine solution was added to each vessel. The glycerine served as the source of carbon for the growing bacteria and prevented the transition of the liquid phase to a solid state.

The degradation of the oligoclase at +20, +4, and -1.5°C was examined after 109 days of incubation; the degradation of the hornblende at +20, +4, and -8°C was examined after 360 days. The experiments were conducted under static conditions without changing the fluid growth media.

The number of bacteria on the solid starch-ammonia medium were counted after incubation. Also, the pH of the media was determined. The mineral particles from the fluid phase were separated by filtration through filter paper and the media was analyzed. The Si, Ca, and Na contents in the media in the oligoclase were measured, and the Fe, Ca, and

Mg contents in the hornblende were measured. The Si and Fe contents were measured using the spectrophotometric method; the Ca and Mg by titration; and the Na by flame-photometric method.

To discover the production of the complex forms of the elements (the forms of the elements that combine with bacterial metabolites, for example, organic acids) and simple (non-complex) forms, the following procedure was used: Aliquots of the filtrates were placed in platinum plates and evaporated in a waterbath, then calcined at 700°C for four hours. The chemical element content of the calcined portions of the media was measured and was assumed to be the total element content. The content of elements in the initial media was equal to the content of non-complex (simple forms). By deducting the quantity of the simple forms from the quantity of the total content of the elements, the content of the complex forms was obtained.

DISCUSSION OF EXPERIMENTAL DATA

The bacteria grew in all variants, except the sterile controls as shown in Table 1. The bacterial number at +20°C was 50 times more than in other non-sterile variants. The pH of the liquid media was in all cases 6.44–6.95.

Table 1 shows that the bacteria promoted the release of Ca and Na from the oligoclase and did not promote the release of Si from this mineral. Also, we noted that the content of Ca in the media exceeded the content of the other elements.

The concentration of Ca in the non-sterile media was approximately twice that of the same index in the sterile media. The level of Ca release was almost the same at low and average temperatures, despite fewer numbers of microorganisms at low temperatures. The solutions contained more simple Ca forms than complex as shown in Table 2. One can assume that difficulties in the bacterial metabolite production existed at low temperatures; the formation of complex element forms slightly increased with the increase of temperature.

The bacterial development led to the intensive release of Na from the oligoclase (Table 1). The rates were the same at different temperatures. After the procedure of calcining at 700°C, Na was not found in the media (Table 2). This fact may be tied to the high volatility of Na.

Quite different conformities with law were discovered for Si. The bacterial growth led to the decrease of Si release (total) from the oligoclase to the liquid media (Table 1)

The quantity of the chemical elements, which were lost by the mineral samples during the experiment (total, in % from initial content in the minerals)								
Temperature C°	Variants: microbe presence (m) or sterile control (s)	Microbe Content mln/ml	Oligoclase (109 days)			Hornblende (360 days)		
			SiO ₂	CaO	Na ₂ O	Fe ₂ O ₃	CaO	MgO
+20	m	1.1	0.03	5.4	0.7	0.011	0.16	0.30
	s	0.0	0.11	2.7	0.4	0.0	0.16	0.22
+4	m	0.02	0.03	6.0	0.7	0.029	0.08	0.28
	s	0.0	0.06	2.7	0.4	0.011	0.16	0.44
-1.5	m	0.02	0.02	2.7	0.7	---	---	---
	s	0.0	0.05	1.3	0.2	---	---	---
-8	m	0.01	---	---	---	0.029	0.02	0.78
	s	0.0	---	---	---	0.0	0.16	0.45

Table 1. The Microbe Content in the Liquid Phase and Degradation of the Minerals.

Temperature C°	Variants: microbe presence (m) or sterile control (s)	The Content of Elements (mg)						
		SiO ₂			CaO			Na ₂ O
		Total	Simple	Complex	Total	Simple	Complex	Simple
+20	m	0.2	0.4	0.0	2.8	1.7	1.1	0.6
	s	0.7	0.3	0.3	1.4	0.6	0.7	0.3
+4	m	0.2	0.1	0.1	3.1	2.2	0.9	0.6
	s	0.4	0.5	0.0	1.4	1.4	0.0	0.3
-1.5	m	0.1	0.0	0.1	1.4	0.9	0.5	0.6
	s	0.3	0.02	0.3	0.7	0.6	0.1	0.2

Table 2. The Formation of Simple and Complex Forms of Elements During the Experiment (Oligoclase).

independent of the temperature. In sterile controls, the Si content was approximately 2-3 times that in the bacterial variants. An evident dependence between the formation of different Si forms, the number of bacteria, and the temperature does not appear in the data collected (Table 2).

The bacteriological weathering of the hornblende differed from that of the oligoclase. The microorganisms did not promote the release of Ca and Mg from the hornblende to the growth media (Table 1). At the same time, the Ca content in the liquid phase was several times less than in the oligoclase variants. The bacteria influenced the transition of Fe from the hornblende to the media at all temperatures considered in the study.

The levels of the bacterial degradation of these minerals were almost the same at low and average temperatures. The character of microbiological weathering was different: while microorganisms promote the release of Ca in the case of oligoclase, they don't influence the transition of this element from the hornblende to the media. The hornblende was more resistant to the microbiological weathering (as well as to the sterile degradation) compared with the oligoclase. Also, one

may suppose that the decrease of temperature is followed by the mitigation of bacterial metabolite production.

SUMMARY AND CONCLUSION

Microbiological weathering of silicates in permafrost is possible even at temperatures below zero, if carbon and a liquid phase are present; moreover, the levels of mineral transformation are comparable with the levels of transformation at temperate temperatures.

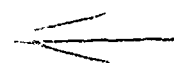
ACKNOWLEDGMENTS

The bacteria were previously isolated by our colleagues A. Siminova, V. Soina and E. Vorobiova, Soil Science Faculty, Moscow State University.

The elemental analyses were performed in the Geological Faculty chemical laboratory by M. Yukina, S. Lebedenko, L. Semko and V. Kulbery.

REFERENCE

Aristovskaya, T. V., *Microorganisms as the component of biogeocenosis*, p. 187, Nauka, Moscow, 1980.



Anthropogenic Structures in the Geosystems (Landscapes) of the Permafrost Zone

V. P. Antonov-Druzhinin

Laboratory of the Geotechnical Systems of the Cold Regions, Monitoring Trust, Novy Urengoy, U.S.S.R.

ABSTRACT

Problems created by oil and gas field development in Arctic regions attract much attention in the discussion of the interaction of civil and industrial buildings and structures with permafrost.

The investigations carried out must permit the evaluation of changes in the natural environment and single out the anthropogenic component of these changes, must ensure accident-free operation of oil and gas transport units, safety of people and environmental control in the mineral resource production regions of the Arctic.

Taking the "pipeline-environment" system example, this report characterizes the spatial-temporal structure of the gas transport geotechnical system as a natural-anthropogenic, physico-geographical object.

The natural subsystem of this object consists of several structures (referred to as areas and zones). These structures are characterized by different dynamics of regeneration processes of anthropogenic disturbances. It is found that the most negative ecological consequences during the development of the regions at the boundary of tundra and forest-tundra are associated with the disturbances of pre-tundra forests.

The least perceptible ecological changes are typical for anthropogenic transformation of bog geo-systems. The anthropogenic structures, which are formed here, are characterized by a state most similar to the initial conditions and, often, by an increase of biomass in the landscapes.

All these data are presented according to the author's investigations in the permafrost zone of Western Siberia.

Engineering-Geological Monitoring Within the Soviet Global Change Program (the Northern Regions of Western Siberia)

G. I. Pushko

Trust of Engineering-Geological Monitoring, Novy Urengoy, U.S.S.R.

ABSTRACT

For the purpose of investigation and control of the changes in the natural environment of the northern regions of Western Siberia, a special service of engineering-geological monitoring (IGM) was created within the system of the USSR State Gas Concern.

The engineering-geological monitoring of geotechnical systems involves tracking, evaluation, analysis and prediction of ongoing changes in their geologic environment and their negative after-effects for interacting technosphere objects. Also, scientific and engineering substantiation of preventive and restorative measures and other management decisions as well as technological provisions for their realization are included.

In addition to observing the state of the geologic environment (settling and displacement of buildings, structures and communications, causes of deformation and forecasting their further development) the main tasks of this service are the elaboration of scientifically grounded recommendations and design concepts for prevention and elimination, recultivation of damaged landscapes, development of repair and restoration work technology and participation in performing responsible operations. Most important of the latter are stabilization of damaged soil bases, consolidation of deformed foundations, curing and recultivation of damaged and polluted areas of the geologic environment, recovery of water-intake wells and industrial effluent-disposal wells.

The leading establishment of this service is the Trust of Engineering-Geological Monitoring and Research (TIGMI) in Novy Urengoy. TIGMI maintains close contacts with the USSR National Global Change Committee through the Geophysical Committee of the USSR Academy of Sciences. The Trust activities are presented in the first part of the Global Change Data Bank Catalogue.

Section F:
Paleoenvironmental Studies

Chaired by

D. Elliot
Ohio State University
U.S.A.

C. Lorius
Laboratoire de Glaciologie et Géophysique
de l'Environnement
France

AD-P007 339



92-17843



Palynological Data as Tools for Interpreting Past Climates: Some Examples from Northern North America

P. M. Anderson

Quaternary Research Center, University of Washington, Seattle, Washington, U.S.A.

ABSTRACT

Documenting past climates and their associated terrestrial ecosystems is one means of predicting how modern landscapes may respond to changing atmospheric composition resulting from the addition of greenhouse gases. Fossil pollen preserved in lake and bog sediments is an especially valuable source of paleoclimatic information. Initially, pollen records were used only as qualitative estimates of climate change, but more recent analyses indicate they can provide accurate quantitative reconstructions. The floristic simplicity of tundra and boreal forest and the coarse taxonomic resolution of northern pollen taxa were believed to seriously limit the use of pollen for interpreting high latitude paleoclimates. However, current studies in Alaska and Canada demonstrate that pollen data are relatively strong and sensitive climate indicators. The status of paleoclimate reconstructions based on pollen records from northern North America is discussed using isopoll maps, response surfaces, analogs, and percentage diagrams.

INTRODUCTION

Change characterizes earth's climate history as evidenced by long-term variation, such as the glacial-interglacial cycles of the latest geological period, or shorter term events like El Niño [Webb et al., 1985; Bartlein, 1988 and references therein]. The current concern over global warming can take advantage of the records of earth's dynamic history to evaluate the significance of projected future conditions on the landscape [Webb and Wigley, 1985]. This task is especially important in the Arctic and Subarctic where the biota is very sensitive to climate fluctuations. . . . where altered atmosphere, ocean, and land interactions at the poles can result in significant changes at lower latitudes [Emanuel et al., 1985; D'Arrigo et al., 1987; Office for Interdisciplinary Earth Studies, 1988].

Two questions are foremost when addressing the issue of global warming: (1) How will future climates differ from today? and (2) What are reasonable expectations for responses of marine and terrestrial systems to the predicted changes? The first question can be answered best through computer modeling of the earth's atmosphere, whereas the second can make use both of computer simulations and historical studies. Since instrumental weather records are short in the North, past temperature and precipitation variations

must be inferred from proxy indicators of past climate. Pollen is one of the most commonly used sources of paleoclimatic information, because it is abundant, closely correlated with certain climate variables, and well preserved in ancient sedimentary records.

Palynologists over the past decade have made great strides toward improving techniques for reconstructing past climates [Webb and Bryson, 1972; Webb and McAndrews, 1976; Webb and Clark, 1977; Howe and Webb, 1983; Bartlein et al., 1984, 1986; Overpeck et al., 1985; Webb et al., 1987; Webb and Bartlein, 1988; COHMAP, 1988]. Their methods rely on careful evaluation of modern pollen-vegetation-climate relationships, the analysis of numerous well-dated fossil records, and qualitative and quantitative comparisons of pollen-based paleoclimatic interpretations to computer simulations. This paper illustrates some of these techniques as applied to data from northern North America and discusses the significance of this work for achieving a better understanding of high latitude climate change.

POLLEN DATA AND PALEOCLIMATE INTERPRETATIONS: AN OVERVIEW

Pollen-based paleoclimate interpretations depend on two equally important components, modern and fossil studies

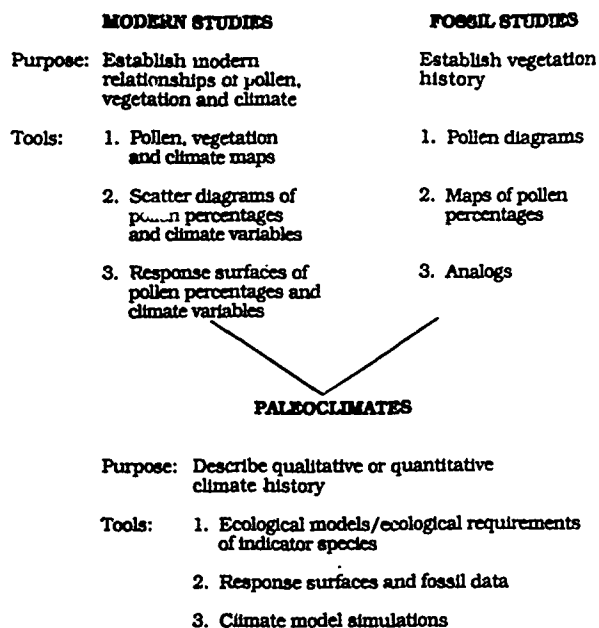


Figure 1. Steps and tools used in deriving pollen-based paleoclimatic interpretations.

(Figure 1). Modern studies establish possible limitations for describing the past by delimiting how well the current pollen rain resolves vegetation patterns as influenced by regional climates, and which pollen taxa are good predictors of climate variables. Evaluation of modern pollen-vegetation-climate relationships is done with maps, scatter diagrams, and response surfaces. Fossil studies that use pollen diagrams or pollen percentage maps provide the historical context for climate reconstructions by examining vegetation change through time.

Combined modern and fossil pollen studies form the basis for either qualitative or quantitative paleoclimate reconstructions. Qualitative climate histories describe broad trends, such as conditions were warmer and wetter than before. These interpretations primarily rely on detailed knowledge of plant ecology and on a general understanding of present vegetation-climate relationships. Quantitative estimates of past climates, on the other hand, are based on statistical relationships between pollen and climate. Fossil and modern pollen assemblages are compared numerically, and specific temperature or precipitation values associated with a modern pollen spectrum are assigned to the fossil assemblage. These climate assignments are strongest when the fossil and modern data are similar, that is, when good analogs exist. Both qualitative and quantitative reconstructions

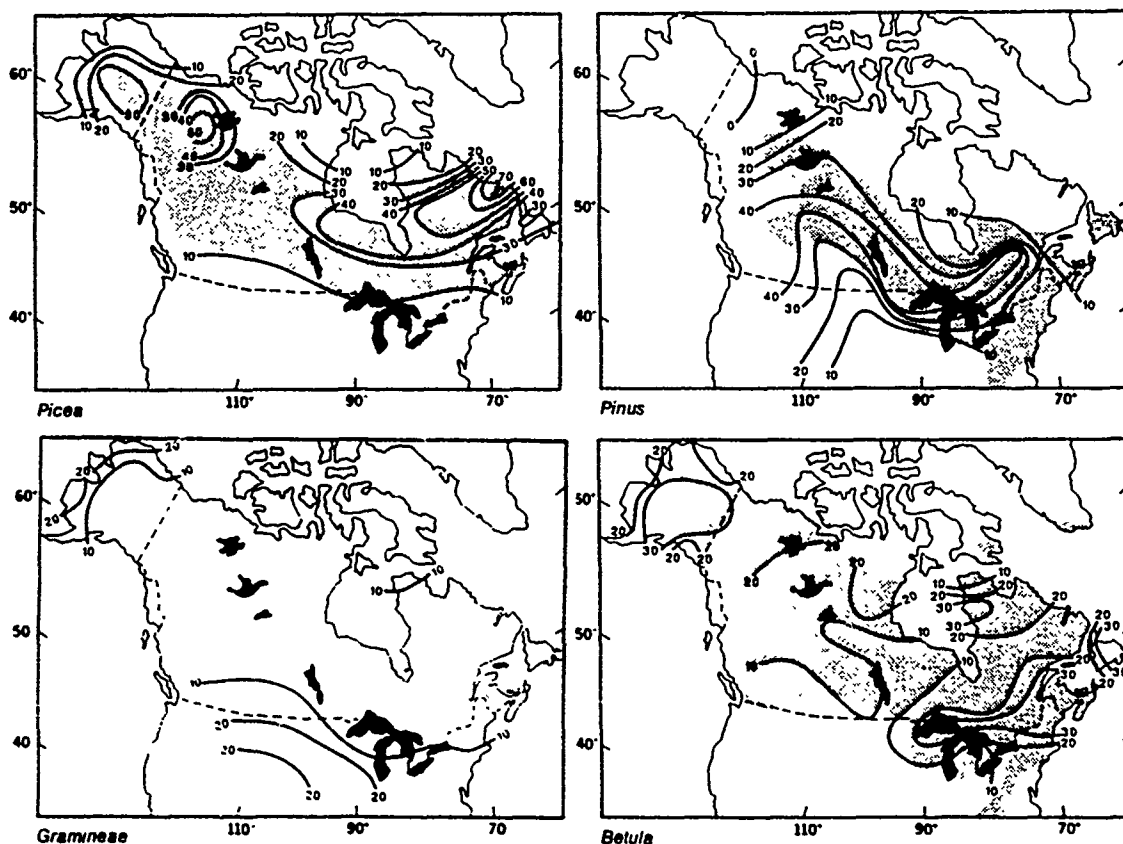


Figure 2. Modern isopoll maps for spruce (*Picea*), pine (*Pinus*), grass (*Gramineae*), and birch (*Betula*). Shaded areas on maps indicate range limits of spruce, pine, and tree birches. Maps from Anderson et al. [1991].

tions can be compared to model simulations to obtain a more complete understanding of the interrelationships of land, ocean, and atmosphere.

MODERN POLLEN STUDIES

The present is the key to the past and for this reason palynologists invest much effort examining modern pollen, vegetation, and climate associations [Webb, 1974, 1985; Birks et al., 1975; Davis and Webb, 1975; Webb and McAndrews, 1976; Webb et al., 1978; Delcourt et al., 1983; Prentice, 1983, 1988]. Boreal forest and tundra are floristically simple, but research in Alaska suggests that significant regional variations characterize both plant communities and pollen data [Anderson and Brubaker, 1986]. For example, the 10% spruce (*Picea*) contour line or isopoll (line of equal pollen percentages) approximates the location of Alaskan treeline, whereas areas with 10–20% spruce pollen are open woodland, and greater than 20% spruce pollen corresponds to closed boreal forest (Figure 2). Similarly important spatial variations are evident in data spanning the North American continent [Anderson et al., 1991]. Pine (*Pinus*), for example, does not grow in northern Alaska but is a typical component of the Canadian forest (Figure 2). This distribution is faithfully represented in the pine isopoll map where pine pollen is virtually absent from Alaska but exceeds 40% in the central Canadian regions. Isopoll patterns also show surprisingly clear representations of the distributions of multi-species genera such as birch (*Betula*, Figure 2). In Alaska, areas with greater than 30% birch pollen indicate the presence of paper birch (*B. papyrifera*), and similar percentages in the mixed conifer-hardwood forests of eastern North America reflect the presence of paper and yellow birch (*B. alleghaniensis*). Intermediate percentages of 10% to 20% indicate the tundra shrub birches (*B. glandulosa*/*B. nana*). Variation within tundra is also evident. The highest grass pollen percentages, for example, occur in the wet graminoid-dominated meadows of the Alaskan coast (Figure 2).

Mapped pollen percentages can also be compared to modern climate maps to evaluate similarities in spatial patterns. For example, the 10% and 20% spruce isopolls, which define the tree's transcontinental range, approximate the July 10°C isotherm (Figure 3). The relationship between spruce and annual precipitation, however, is more difficult to define. Describing pollen-climate relationships based on visual inspection of maps is quite crude. To improve comparisons, palynologists assign climate values to each modern pollen site and plot these data in scatter diagrams showing pollen percentages of a single taxon as a function of a single climate variable [Anderson et al., 1991]. In the case of spruce, the scatter diagrams suggest a good relationship between high spruce pollen percentages and moderate July temperatures, thereby verifying the trends evident in the maps (Figure 3). The ambiguous association of spruce to annual precipitation, however, is not clarified by the scatter diagram.

Maps and scatter diagrams are adequate for examining single climate variables that strongly influence vegetation, but plant distributions are rarely a result of such simple one-to-one interactions. Scatter diagrams, however, can be merged to form response surfaces that illustrate pollen variation as a function of two or more climate variables

[Bartlein et al., 1986]. In such multidimensional scatter diagrams, pollen percentages are plotted as a series of graduated dots with larger sizes indicating higher percentages [Anderson et al., 1991] (Figure 3). These diagrams are difficult to read because many sites have the same or similar climate values, thus blurring the distinction of dot sizes. With the aid of computer averaging, contour lines are added to better illustrate trends in the surface. Returning to the spruce example (Figure 3), its response surface not only confirms the importance of July temperature but also clarifies the role of annual precipitation. The predominance of horizontal contours indicates the dominance of July temperature as a controlling factor of the surface. A bullseye pattern in the right-central portion of the response surface, however, suggests that annual precipitation can affect spruce abundance.

The above examples illustrate the need for using several types of analytical tools to fully evaluate modern pollen-vegetation-climate associations; pollen percentage, vegetation, and climate maps assess spatial relationships, while scatter diagrams and response surfaces examine pollen abundances as a function of one or more climate variables. The modern analyses indicate that in northern North America: (1) modern pollen spectra accurately portray vegetation variation; (2) modern pollen spectra are good predictors of climate; (3) pollen abundances of most major taxa are affected by the interaction of two or more climate factors; and (4) major pollen taxa display unique response surfaces, suggesting that individual species or genera will respond differently to climate change.

FOSSIL POLLEN STUDIES

The percentage diagram is the most traditional and basic means of displaying fossil pollen data. A typical diagram from northern Alaska (Figure 4) shows three vegetation periods corresponding to a three-part stratigraphic sequence: an herb tundra zone dating to the full-glacial (18,000–14,000 B.P.), a late-glacial shrub tundra transition zone (14,000–9000 B.P.), and a Holocene zone (9000–0 B.P.) containing boreal and tundra elements [Livingstone, 1955; Brubaker et al., 1983]. This sequence suggests a simple northward migration of modern vegetation types following gradual post-glacial warming. A careful consideration of multiple Alaskan and Canadian pollen records, however, indicates a more complex vegetation history [Ritchie, 1984, 1987; Anderson, 1988; Anderson et al., 1989; Anderson and Brubaker, 1991].

Spatial variation, so characteristic of today's northern environments, was equally important in the past. Paleo-vegetation patterns are difficult to describe when using pollen percentage diagrams alone, but combining diagrams into maps easily illustrates the distributional changes of taxa through time and space. For example, maps showing patterns of spruce pollen distribution at different times help trace the development of the Alaskan boreal forest (Figure 4). The 10% spruce isopoll approximates the location of modern Alaskan treeline and ancient 10% contours probably also indicate the past presence of significant spruce populations. The maps show the early arrival of spruce in eastern Alaska, its rapid spread to the south-central Brooks Range, a subsequent mid-Holocene population decline, and a final migration westward to its present distribution ca. 4000 B.P.

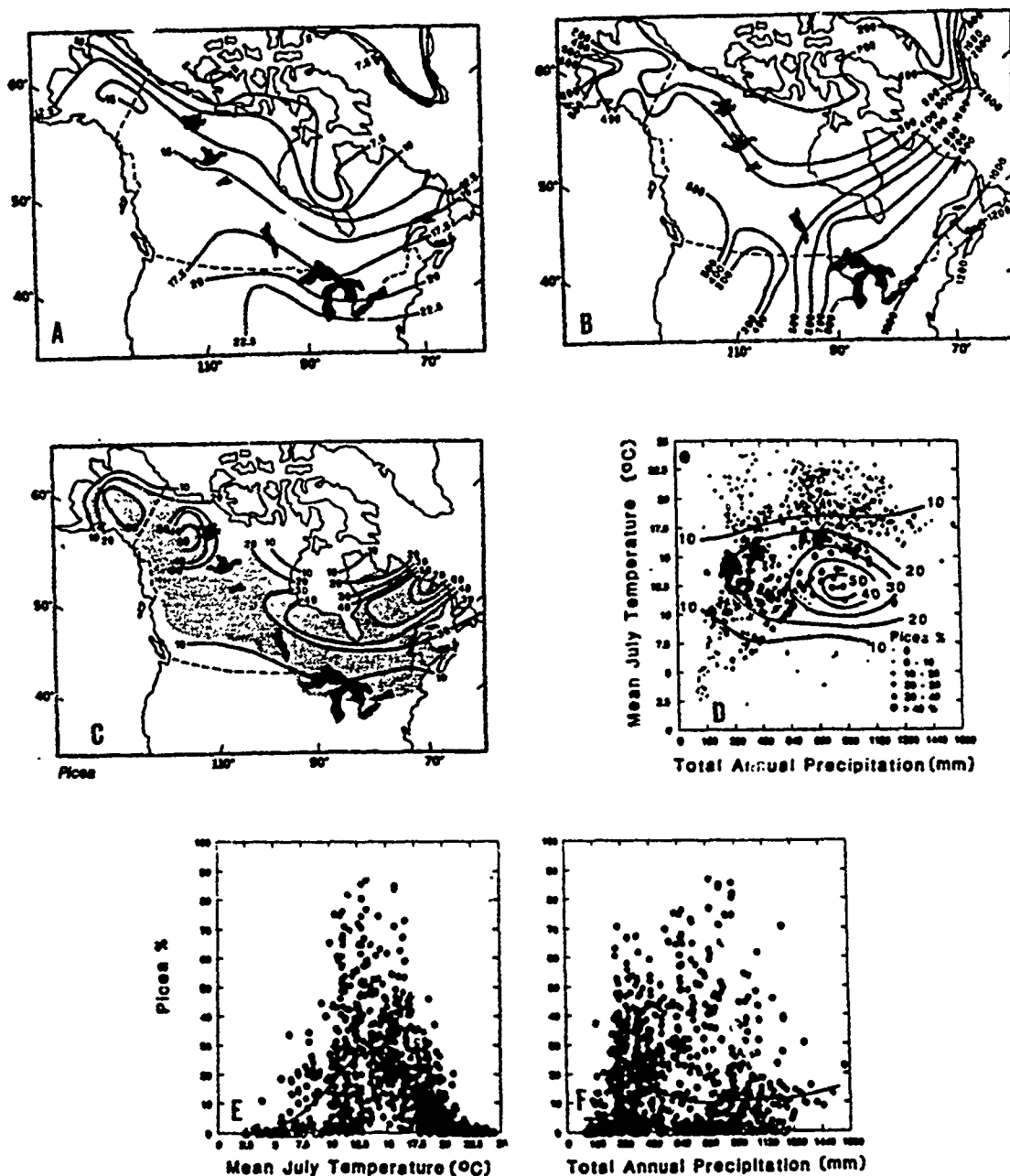


Figure 3. Contour maps of (A) mean July temperature, (B) mean annual precipitation, and (C) modern spruce pollen percentages. Scatter diagrams illustrate the relationship of spruce pollen percentages with (E) July temperature and (F) annual precipitation. Data from both scatter diagrams are combined in (D) the spruce response surface. Figures from Anderson et al. [1991].

[Anderson and Brubaker, 1991]. As with the modern pollen samples, multiple widespread sites are required before spatial or temporal variation can be documented adequately.

Paleovegetational interpretations of pollen diagrams and maps require palynologists to relate past plant communities as represented by fossil pollen assemblages to those seen today; in other words, to attempt to find modern analogs. For many years vegetation histories were built around qualitative assessments of analogs, but quantitative comparisons are now possible in areas with large modern data sets [Prentice, 1980; Overpeck et al., 1985]. Qualitative analyses

commonly assume that the further back in time, the poorer the analog. Quantitative comparisons of fossil sites from northern Alaska and northwestern Canada, however, indicate this assumption is not entirely correct [Anderson et al., 1989]. The best analogs, not surprisingly, are found for Holocene spectra, the poorest analogs characterize the late-glacial, and possible analogs of full-glacial spectra are located in Banks Island and the northern Alaskan coast (Figure 5).

Pollen percentage diagrams, percentage maps, and analog analysis attest to the recent development of modern boreal

RUPPERT LAKE

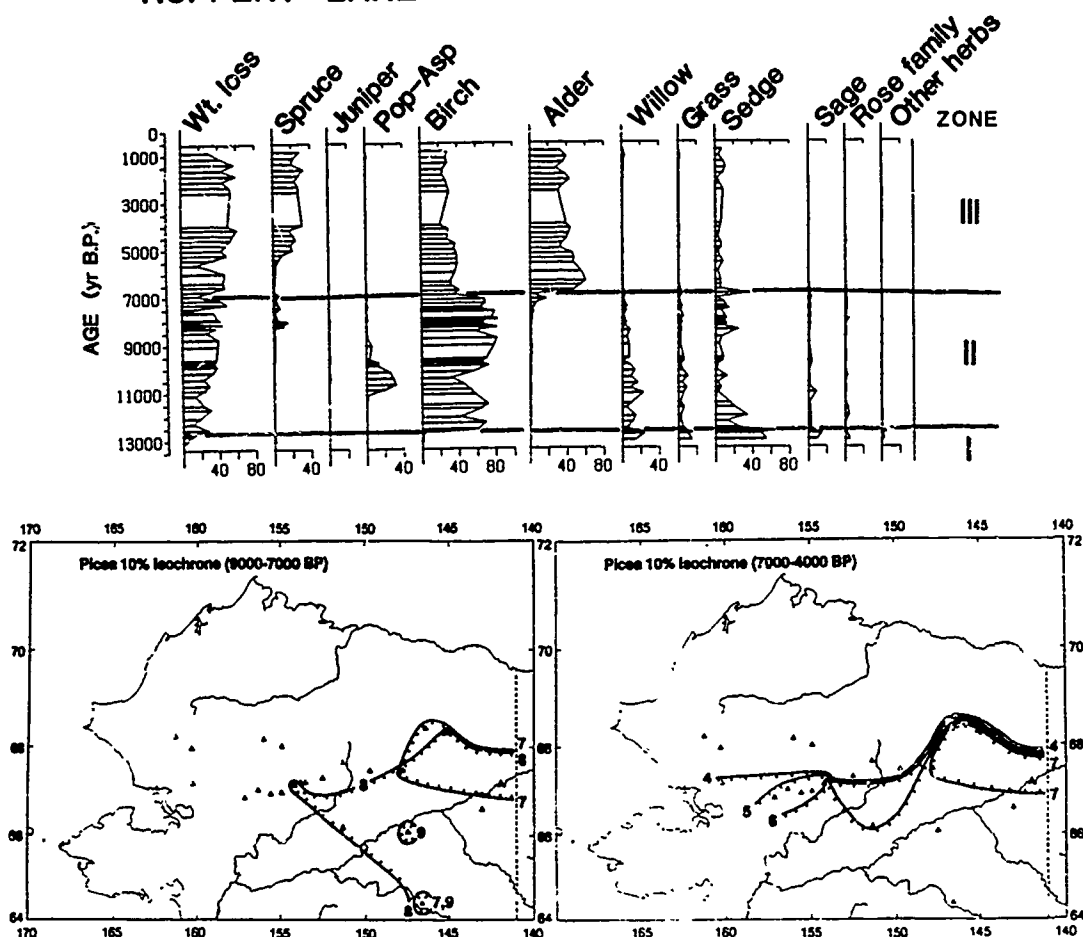


Figure 4. Pollen percentage diagram of Ruppert Lake, northcentral Alaska (adapted from Brubaker et al. [1983]). Data from percentage diagrams can be plotted by time period and the maps summarized with an isochrone map. Here the 10% isopoll has been plotted for 9000 to 4000 B.P. showing the postglacial spread of spruce throughout northern Alaska. Hatchures point in direction of higher pollen percentages. Isochrone maps are from Anderson and Brubaker [1991].

forest and tundra. These communities apparently did not survive intact in glacial refugia but rather are the result of complex migrational histories of individual taxa. Consistent large-scale patterns of change documented in the pollen maps indicate that distributions of taxa through time primarily reflect responses to changing climates and not to more local edaphic factors. Even though the climate signal [*in sensu* Webb et al., 1978] is strong in Northern pollen records, analog analyses suggest the statistical validity of quantitative paleoclimate estimates will vary depending on the time period examined.

PALEOCLIMATIC INTERPRETATIONS

Pollen-based paleoclimate reconstructions can be either qualitative or quantitative. Qualitative interpretations require a detailed understanding of the ecological requirements of indicator species represented in the pollen record. Through the plant's ecology, palynologists can relate changes in vegetation type to general trends in past climate (e.g., period A is warmer and drier than period B but cooler and wetter than present). The arrival of paleoclimate computer simulations, however, permits a new level of sophistication [Kutzbach and Wright, 1985; Kutzbach and Street-

Perrott, 1985; Kutzbach and Guetter, 1986; Barnosky et al., 1987; COHMAP, 1988] because (1) they provide independently derived paleoclimate scenarios that can be evaluated with pollen-based reconstructions; (2) their results can be used to form hypotheses about past climates that then can be tested with fossil data; and (3) when the data and model agree, the model provides mechanistic explanations of climate change not obtainable through analysis of fossil data alone.

Quantitative climate reconstructions are made possible with the availability of large modern data sets [Bartlein et al., 1984, 1986; Webb and Bartlein, 1988]. Simply put, these quantitative techniques first numerically compare modern and fossil pollen assemblages and then assign paleoclimate values to the fossil spectra based on modern pollen-climate relationships [see Webb and Clark, 1977; Howe and Webb, 1983; Bartlein et al., 1984; and Webb et al., 1987 for more details]. Quantitative reconstructions benefit from model simulations for the same reasons outlined for qualitative data-model comparisons.

Although a large modern data set now exists for northern North America, no transcontinental quantitative reconstructions have yet been done. Several qualitative syntheses,

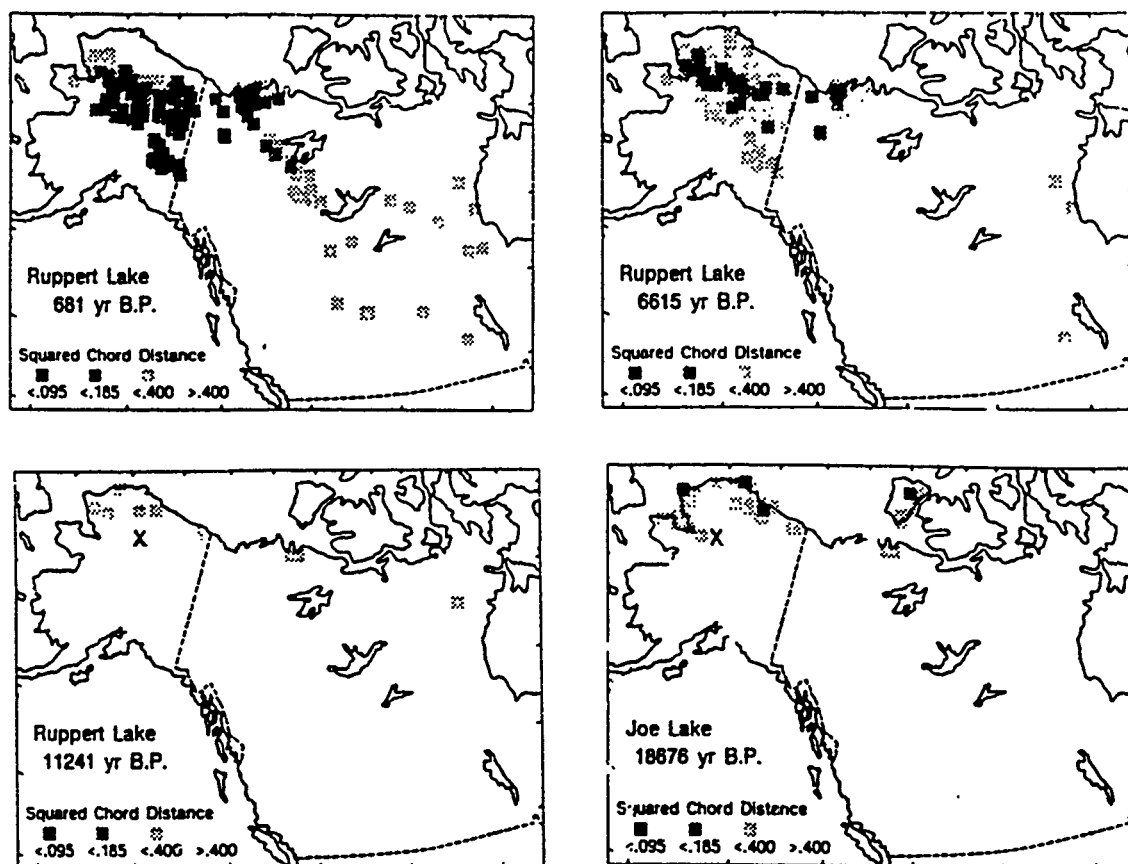


Figure 5. Maps showing the similarity of modern pollen spectra to a fossil pollen assemblage (from Anderson et al. [1989]). Locations of modern samples are indicated by a shaded square and the fossil site is located with an X. The darker the square the more similar are the modern and fossil pollen. The Ruppert Lake 681 B.P. map represents present conditions, Ruppert Lake 6615 B.P. mid-Holocene times, Ruppert Lake 11,241 B.P. the late-glacial, and Joe Lake 18,676 B.P. the full-glacial.

however, are available [see Ritchie, 1987; Barnosky et al., 1987; and Anderson and Brubaker, 1991 for details]. They indicate that strong regional responses to global climate changes occurred over the past 18,000 years. Comparison of pollen-based interpretations with model results suggests that regional climates were in large part controlled by seasonal variation in insolation and extent of glacial ice [Barnosky et al., 1987]. Some of the existing uncertainty in qualitative assessments of high latitude climate histories should be clarified as quantitative reconstructions become available.

DISCUSSION

Quantitative estimates of past temperature and/or precipitation are currently lacking for northern North America, but results of previous palynological research provide important insights into the general nature of high latitude vegetation response to climate change. This work indicates a complex vegetation history for even such simple biomes as the boreal forest and tundra and suggests an equally complex climate history. Modern northern communities did not move intact from glacial refugia to their present locations, but rather boreal and arctic taxa responded individually to climate variations. Thus the composition and distribution of today's communities are relatively recent occurrences and from a geological perspective can be viewed as ephemeral [Watts, 1973]. Isolated transects or

individual fossil pollen records are inadequate to describe such paleoenvironmental changes, and a sample grid of well-dated sites is a necessity before valid paleovegetational or paleoclimatic reconstructions can be done. Qualitative comparisons of paleoclimates inferred from fossil data with computer simulations are in general agreement and suggest that (1) northern high latitudes are particularly sensitive to changes in insolation and extent of glacial ice, and (2) within the North, regions differ in their responses to global climate change.

The few examples presented in this paper illustrate the steps required before quantitative paleoclimatic estimates can be attempted. The collection and analysis of modern and fossil data are time consuming, but thorough analyses of these data provide the needed foundation for interpreting past climate change. This foundation is particularly strong for northern North America because (1) clear modern pollen-climate relationships are now well documented; (2) a vegetation history is well defined based on a sufficient number of carefully analyzed fossil sites; and (3) the presence or absence of good modern analogs, and thus the potential for accurate climate reconstructions, is established for the past 18,000 years. The understanding of land-atmosphere interactions provided by these modern and fossil pollen studies will only improve as quantitative paleoclimate estimates are completed and model simulations improve. Enough infor-

mation, however, is available to suggest that the lessons from the past should be kept in mind when planning for the future.

ACKNOWLEDGMENTS

This paper has benefited from numerous discussions with Pat Bartlein, Linda Brubaker, Konrad Gajewski, and Jim

Ritchie, who have been invaluable colleagues in exploring the late Quaternary history of northern North America. Research presented in this paper was supported by the following grants: National Science Foundation DPP8106806, DPP8403598 and DPP8619214 to Anderson and Brubaker and ATM8713980 to Bartlein; NSERC grants to Gajewski and Ritchie.

REFERENCES

- Anderson, P. M., Late Quaternary pollen records from the Kobuk and Noatak River drainages, northwestern Alaska, *Quat. Res.*, 29, 263-276, 1988.
- Anderson, P. M., and L. B. Brubaker, Modern pollen assemblages from northern Alaska, *Rev. Palaeobot. Palynol.*, 46, 273-291, 1986.
- Anderson, P. M., and L. B. Brubaker, Vegetation history and the development of boreal forest in northcentral Alaska: a mapped summary of late-Quaternary pollen data, *Ecological Monographs*, 1991, In review.
- Anderson, P. M., P. J. Bartlein, L. B. Brubaker, K. Gajewski, and J. C. Ritchie, Modern analogues of late-Quaternary pollen spectra from the western interior of North America, *J. Biogeogr.*, 16, 573-596, 1989.
- Anderson, P. M., P. J. Bartlein, L. B. Brubaker, K. Gajewski, and J. C. Ritchie, Vegetation-pollen-climate relationships for the Arcto-Boreal region of North America and Greenland, *J. Biogeogr.*, 1991, In press.
- Barnosky, C. W., P. M. Anderson, and P. J. Bartlein, The northwestern U.S. during deglaciation; vegetational history and paleoclimatic implications, in *North America and Adjacent Oceans during the Last Deglaciation*, edited by W. F. Ruddiman and H. E. Wright, Jr., pp. 289-322, Geological Society of America, 1987.
- Bartlein, P. J., Late-Tertiary and Quaternary paleoenvironments, in *Vegetation History*, edited by B. Huntley and T. Webb, III, pp. 113-152, Kluwer Academic Publishers, 1988.
- Bartlein, P. J., T. Webb, III, and E. Fleri, Holocene climatic change in the northern Midwest: pollen-derived estimates, *Quat. Res.*, 22, 361-374, 1984.
- Bartlein, P. J., I. C. Prentice, and T. Webb, III, Climatic response surfaces from pollen data for some eastern American taxa, *J. Biogeogr.*, 13, 35-57, 1986.
- Birks, H. J. B., T. Webb, III, and A. A. Berti, Numerical analysis of pollen samples from central Canada: a comparison of methods, *Rev. Palaeobot. Palynol.*, 20, 133-169, 1975.
- Brubaker, L. B., H. L. Garfinkel, and M. E. Edwards, A late-Wisconsin and Holocene vegetation history from the central Brooks Range: implications for Alaskan paleoecology, *Quat. Res.*, 20, 194-214, 1983.
- COHMAP Members, Climatic changes of the last 18,000 years: observations and model simulations, *Science*, 241, 1043-1052, 1988.
- D'Arrigo, R., G. G. Jacoby, and I. Y. Fung, Boreal forest and atmosphere-biosphere exchange of carbon dioxide, *Nature*, 329, 321-323, 1987.
- Davis, R. B., and T. Webb, III, The contemporary distribution of pollen in eastern North America: a comparison with the vegetation, *Quat. Res.*, 5, 395-434, 1975.
- Delcourt, H. R., P. A. Delcourt, and T. Webb, III, Dynamic plant ecology: the spectrum of vegetational change in space and time, *Quat. Sci. Rev.*, 1, 153-175, 1983.
- Emanuel, W. R., H. H. Shugart, and M. P. Stevenson, Climatic change and the broad-scale distribution of terrestrial ecosystem complexes, *Climate Change*, 7, 29-43, 1985.
- Howe, S., and T. Webb, III, Calibrating pollen data in climatic terms: improving the methods, *Quat. Sci. Rev.*, 2, 17-51, 1983.
- Kutzbach, J. E., and P. J. Guetter, The influence of changing orbital parameters and surface boundary conditions on climate simulations for the past 18,000 years, *J. Atmos. Sci.*, 43, 1726-1759, 1986.
- Kutzbach, J. E., and F. A. Street-Perrott, Milankovitch forcing of fluctuations in the level of tropical lakes from 18 to 0 kyr BP, *Nature*, 317, 130-134, 1985.
- Kutzbach, J. E., and H. E. Wright, Jr., Simulation of the climate of 18,000 Years BP: results for the North American/North Atlantic/European sector and comparison with the geologic record of North America, *Quat. Sci. Rev.*, 4, 147-187, 1985.
- Livingstone, D. A., Some pollen profiles from arctic Alaska, *Ecology*, 36, 587-600, 1955.
- Office for Interdisciplinary Earth Studies, *Arctic Interactions Recommendations for an Arctic Component in the International Geosphere-Biosphere Programme*, 41 pp., UCAR, Boulder, CO, 1988.
- Overpeck, J. T., T. Webb, III, and I. C. Prentice, Quantitative interpretation of fossil pollen spectra: dissimilarity coefficients and the method of modern analogs, *Quat. Res.*, 23, 87-108, 1985.
- Prentice, I. C., Multidimensional scaling as a research tool in Quaternary palynology: a review of theory and method, *Rev. Palaeobot. Palynol.*, 31, 71-104, 1980.
- Prentice, I. C., Postglacial climatic change: vegetation dynamics and the pollen record, *Prog. Phys. Geogr.*, 17, 273-286, 1983.
- Prentice, I. C., Records of vegetation in time and space: the principles of pollen analysis, in *Vegetation History*, edited by B. Huntley and T. Webb, III, pp. 17-42, Kluwer Academic Publishers, 1988.
- Ritchie, J. C., *Past and Present Vegetation of the Far Northwest of Canada*, University of Toronto Press, Toronto, 1984.
- Ritchie, J. C., *Postglacial Vegetation of Canada*, University of Cambridge Press, Cambridge, 1987.
- Watts, W. A., Rates of change and stability in vegetation in the perspective of long periods of time, in *Quaternary Plant Ecology*, edited by H. J. B. Birks and R. G. West, pp. 195-206, Blackwell Scientific Publishers, 1973.

- Webb, T., III, Corresponding patterns of pollen and vegetation in lower Michigan: a comparison of quantitative data, *Ecology*, 55, 17-28, 1974.
- Webb, T., III, Holocene palynology and climate, *Paleoclimate Analysis and Modeling*, edited by A. D. Hecht, pp. 163-197, John Wiley and Sons, 1985.
- Webb, T., III, and P. J. Bartlein, Late Quaternary climatic change in eastern North America: the role of modeling experiments and empirical studies, *Bull. Buffalo Soc. Natural Sci.*, 33, 3-13, 1988.
- Webb, T., III, and R. A. Bryson, Late- and postglacial climatic change in the northern Midwest, USA: quantitative estimates derived from fossil spectra by multivariate statistical analysis, *Quat. Res.*, 2, 70-115, 1972.
- Webb, T., III, and D. R. Clark, Calibrating micro-paleontological data in climatic terms: a critical review, *Ann. N.Y. Acad. Sci.*, 288, 93-118, 1977.
- Webb, T., III, and J. H. McAndrews, Corresponding patterns of contemporary pollen and vegetation in central North America, *Geol. Soc. Amer. Memoir 145*, 267-299, 1976.
- Webb, T., III, and T. M. L. Wigley, What past climates can indicate about a warmer world, in *The Potential Climate Effects of Increasing Carbon Dioxide*, edited by M. C. MacCracken and F. M. Luther, pp. 239-257, U.S. Department of Energy, 1985.
- Webb, T., III, R. A. Lasenki, and J. C. Bernabo, Sensing vegetation patterns with pollen data: choosing the data, *Ecology*, 59, 1151-1163, 1978.
- Webb, T., III, J. E. Kutzbach, and F. A. Street-Perrott, 20,000 years of global climatic change: paleoclimatic research plan, in *Global Change*, edited by T. F. Malone and J. G. Roederer, ICSU Press, 1985.
- Webb, T., III, P. J. Bartlein, and J. E. Kutzbach, Postglacial climatic and vegetational changes in eastern North America since 18ka: comparison of the pollen record and climate model simulations, in *North America and Adjacent Oceans during the Last Deglaciation*, edited by W. F. Ruddiman and H. E. Wright, Jr., pp. 447-462, Geological Society of America, 1987.

AD-P007 340



92-17844



High-Latitude Tree-Ring Data: Records of Climatic Change and Ecological Response

Lisa J. Graumlich

Laboratory of Tree-Ring Research, University of Arizona, Tucson, Arizona, U.S.A.

ABSTRACT

Tree-ring data provide critical information regarding two fundamental questions as to the role of the polar regions in global change: (1) what is the nature of climatic variability? and (2) what is the response of vegetation to climatic variability? Tree-ring-based climatic reconstructions document the variability of the climate system on time scales of years to centuries. Dendroclimatic reconstructions indicate that the climatic episodes defined on the basis of documentary evidence in western Europe (i.e., "Medieval Warm Episode," ca. A.D. 1000–1300; "Little Ice Age," ca. A.D. 1550–1850) can be observed at some high-latitude sites (ex., Polar Urals). Spatial variation in long-term temperature trends (ex., northern Fennoscandia vs. Polar Urals) demonstrates the importance of regional-scale climatic controls. When collated into global networks, proxy-based climatic reconstructions can be used to test hypotheses as to the relative importance of external forcing vs. internal variation in governing climatic variation. Specifically, such a global network would allow the quantification of the climatic response to various permutations of factors thought to be important in governing decadal- to centennial-scale climatic variation (i.e., solar insolation, volcanic activity, trace gas concentrations).

Tree populations respond to annual- to centennial-scale climatic variation through changes in rates of growth, establishment, and mortality. Tree-ring studies that document multiple aspects of high-latitude treeline dynamics (i.e., the timing of tree establishment, mortality, and changes from krummholz to upright growth) indicate a complex interaction between growth form, population processes, and environmental variability. Such interactions result in varying sensitivities of high-latitude trees to climatic change.

INTRODUCTION

A number of fundamental questions arise when the scientific community is asked to address the prospects for, and consequences of, major environmental change due to the accumulation of trace gases in the atmosphere [IGBP, 1990]. Questions directed towards identifying the dominant processes governing climatic variability and ecosystem response include: (1) what is the natural variability of the climate system?, (2) what is the relative importance of external forcings vs. internal oscillations of the atmosphere-ocean system in governing climatic variation?, and (3) what is the effect of climatic variation on ecosystem dynamics?

To address these questions, quantitative information on climatic forcing and system response can be extracted from natural archives of many types including tree-rings, ice cores, marine and terrestrial sediments, corals, and paleosols [Bradley, 1990]. On time scales of decades to centuries, tree-ring data are particularly valuable because they provide records of seasonal to annual climatic variation and information regarding the response of vegetation to climatic variation. In high-latitude environments tree-ring-based studies of environmental change are especially critical due to the paucity of long-term climate or vegetation records and the projected sensitivity of high-latitude climates to CO₂-induced warming.

RECONSTRUCTED NORTHERN HEMISPHERE TEMPERATURE DEPARTURES

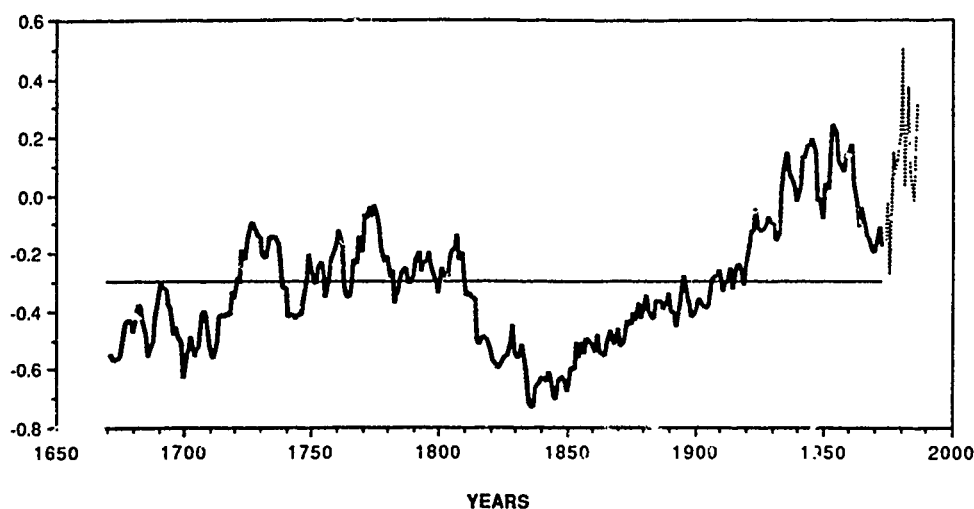


Figure 1. Northern Hemisphere annual temperature reconstruction (solid line) for 1671–1973 based on tree-ring data from North American treeline sites. Instrumental temperature data for 1974–1989 shown as dashed line. Temperatures departures are from the 1951–1980 mean. Figure modified from Jacoby and D'Arrigo [1989].

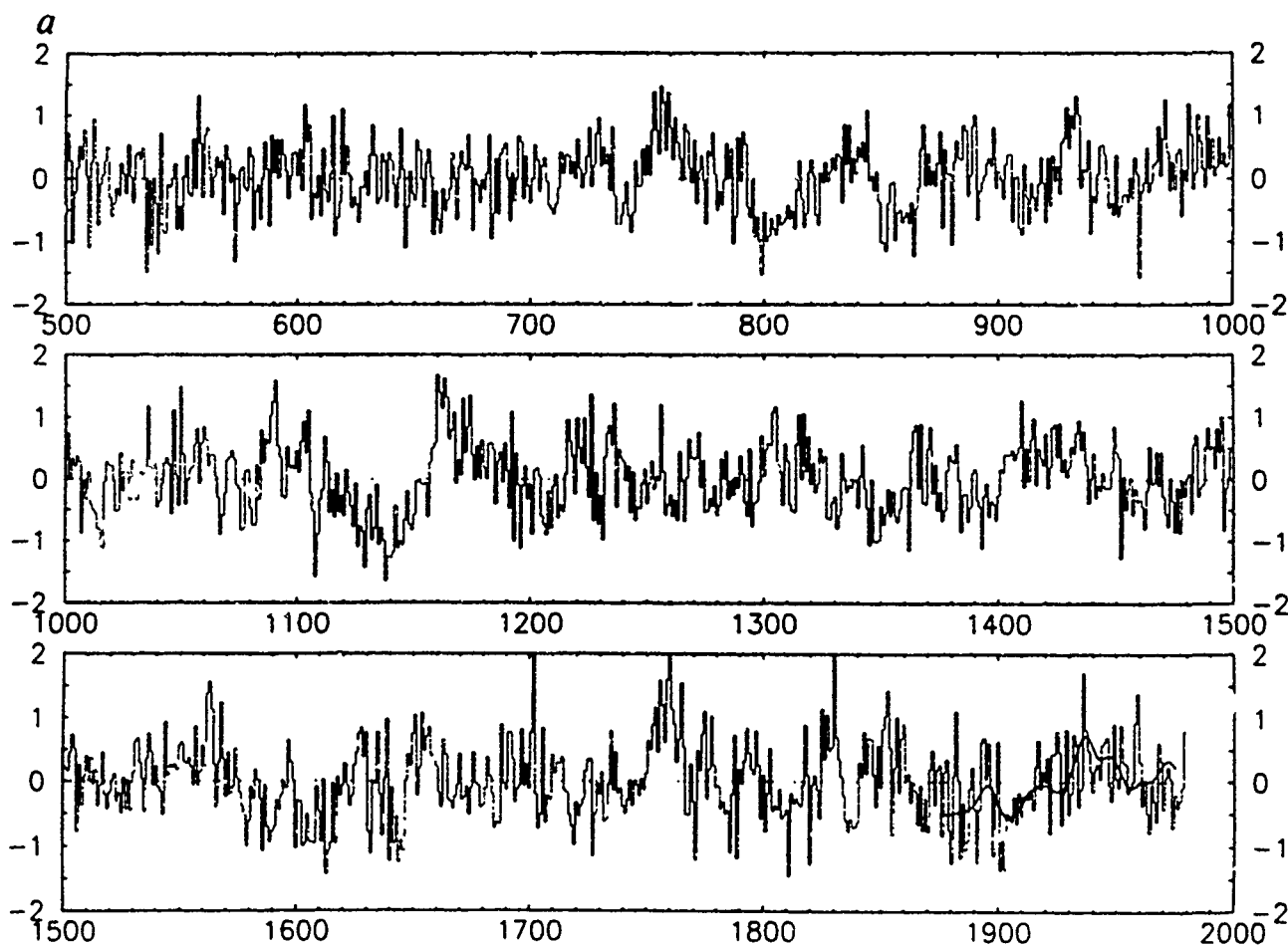


Figure 2. Reconstructed northern Fennoscandian temperature anomalies for summer (April–August mean) based on ring width and maximum density data from Scots pine. Temperature departures are from the 1951–1970 mean. Observed temperatures, smoothed with a 10-year low pass filter, are also shown after 1876. Figure from Briffa et al. [1990].

In this paper I review selected tree-ring-based studies that explore the ramifications of past environmental variability for our understanding of global change in high latitudes. The papers reviewed here represent diverse approaches to two fundamental questions: (1) What is the nature of climatic variability at high latitudes? and (2) What is the response of high-latitude trees to climatic variability?

WHAT IS THE NATURE OF CLIMATIC VARIABILITY AT HIGH LATITUDES?

In general, summer temperature is the climatic variable most limiting to tree growth at high latitudes and thus has been the variable most frequently reconstructed from tree-rings. Reconstructions of summer temperatures based on tree-ring data are available for central Alaska and northwestern Canada [Garfinkel and Brubaker, 1980; Jacoby et al., 1985], northern Fennoscandia [Briffa et al., 1988, 1990], the polar Urals [Graybill and Shiyatov, 1992], and the Northern Hemisphere annual temperature series [Jacoby and D'Arrigo, 1989].

The reconstruction of Northern Hemisphere annual temperature by Jacoby and D'Arrigo [1989] is particularly relevant to characterizing climatic variability because it represents a reconstruction of a hemispheric-scale temperature series. Jacoby and D'Arrigo reconstructed Northern Hemisphere surface temperatures based on ring-width data collected at 11 high-latitude sites spanning over 90 degrees of longitude from Alaska to eastern Canada. The resulting temperature reconstruction (Figure 1) allows qualitative inferences about the importance of external forcings (i.e., volcanic activity, changes in solar insolation, and increasing atmospheric CO₂) in governing Northern Hemisphere surface temperature variation. Jacoby and D'Arrigo conclude that the warming trend of the 20th century has exceeded the natural variability of the climate system over the past 300+ years. This observation lends support to the contention that recent trends in the Northern Hemisphere temperature series reflect forcing by increasing trace gas concentrations. Jacoby and D'Arrigo also note the coincidence of a cool episode from 1671 to the early 1700s with the later part of the Maunder "sunspot" minimum. Similarly, a pronounced cool period in the early 1800s corresponds to the timing of the major volcanic eruption of Tambora in 1815 and a period of lowered sunspot activity from 1795–1825. The qualitative comparison of the timing of specific forcing functions and the temperature series represents a mode of analysis that offers great potential for unraveling the relative importance of different climatic forcings. The integration of their results with other climatic proxy data for specific times in the past when external climatic forcing is particularly strong should yield new insights into the response of the climate system to such external perturbations.

While the reconstruction of Northern Hemisphere annual temperature is important because it represents a spatially integrated measure of global climatic change, regional reconstructions are also valuable for their information on the spatial variability of long-term climatic trends. Two recently published reconstructions of high-latitude summer temperature illustrate the spatial variability seen in long-term temperature trends. Briffa et al. [1990] used ring-widths and maximum latewood densities of living and remnant Scots pine (*Pinus sylvestris*) from a single site in northern Sweden

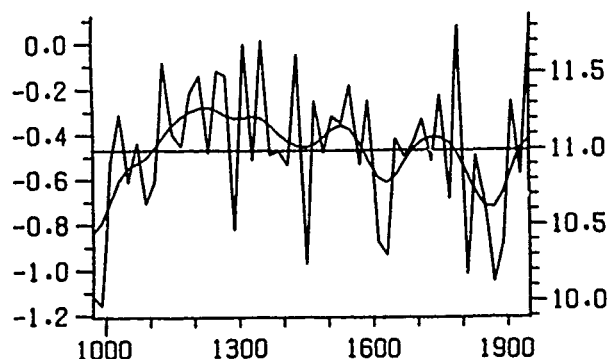


Figure 3. Twenty-year averages of reconstructed June–July temperatures in the Polar Urals based on ring-width data from Siberian larch (modified from Graybill and Shiyatov [1992]).

to reconstruct "summer" (April–August) temperature for northern Fennoscandia back to A.D. 443 (Figure 2). Similarly, Graybill and Shiyatov [1992] used ring widths of living and remnant Siberian larch (*Larix sibirica*) collected in the Polar Urals to reconstruct "summer" (June–July) temperature back to A.D. 961 (Figure 3).

The summer temperature reconstructions for Fennoscandia and the Polar Urals exhibit two distinct patterns of long-term temperature variation. The reconstruction of summer temperatures for Fennoscandia exhibits alternating periods of warm and cool conditions that persist for several decades at time. No evidence is found for the climatic episodes defined in Europe on the basis of documentary historical evidence. Specifically, their reconstruction does not indicate a period of warmth from A.D. 1000–1300 ("Medieval Warm Epoch") or a period of cold conditions from A.D. 1550–1850 ("Little Ice Age"). In contrast, the reconstruction of summer temperatures for the Polar Urals shows low frequency variation coincident with the European historical records with temperatures equalling or exceeding modern values from A.D. 1100–1300 and temperatures declining to low values during the early 1600s and late 1800s. The temperature patterns are corroborated by evidence that treeline rose by 100–120 m during the Medieval Warm Epoch and declined to modern levels during the mid-1600s.

Several factors explain the discrepancy between these two reconstructions. Regional-scale climatic controls are quite different between the two regions with the climate of Fennoscandia heavily influenced by oceanic heat transport from lower latitudes while the climate of the Polar Urals reflects a more continental location. Such factors may be responsible for regional differences in century-scale climatic fluctuations. Additionally, the different frequency characteristics of the two series may be attributed to the varying approaches taken to remove the low-frequency variation in the ring-width data thought to represent non-climatic influences (i.e., tree ageing, forest stand dynamics). The raw tree-ring data underlying the Fennoscandia reconstruction were standardized by methods that remove a large portion of the variance at periods of 200 years or greater and therefore low frequency trends would be removed in this process. The data used in reconstructing Polar Urals temperature were standardized using methods that conserve more low fre-

quency variation and the resulting reconstruction reflects this more conservative approach. Standardization methods heavily influence the frequency domain characteristics of the resulting reconstructions and further attention needs to be directed towards maintaining the low frequency fidelity of tree-ring and other proxy-based reconstructions.

WHAT IS THE RESPONSE OF HIGH LATITUDE TREES TO CLIMATIC VARIABILITY?

High-latitude trees respond to climatic variation on annual time scales through variation in radial growth rates and on decadal and longer time scales through phenotypic changes (i.e., krummholz vs. normal growth) and population expansions and contractions. Such changes can be quantified using dendrochronologic techniques and these data provide a critical long-term perspective on the nature of ecosystem response to climatic variation as well as quantitative information that can be used to develop and test models of forest response to global change [Graumlich, 1989].

The effects of climate on annual variation in radial growth of white spruce (*Picea glauca*) growing at or near treeline in the Brooks Range of Alaska were analyzed using 14 tree-ring chronologies [Garfinkel and Brubaker, 1980]. White spruce responds positively to current summer and previous autumn temperatures, a finding that is consistent with other studies at northern treeline sites [Jacoby, 1982]. In addition, at many of the sites, growth is positively correlated with summer precipitation, implying that internal water stress may limit photosynthesis when temperatures are high. Ecophysiological studies conducted on trees at the study site indicated that stomatal conductance decreases sharply at vapor pressure deficits similar to those commonly experienced in the field during the growing season [Goldstein, 1981]. Precipitation during the growing season thus favors growth by reducing vapor pressure deficits and ensuring ample soil moisture. These findings imply that any predictions of increasing white spruce growth rates due to rising temperatures associated with global warming must take into account local moisture conditions.

In addition to changes in radial growth rates, climatic change at high latitudes can result in changes in the growth form of trees from krummholz to monopodial trees with normal stems. Such phenotypic plasticity has important implications for population dynamics at treeline: while sexual reproduction can occur regularly in trees, krummholz are often unable to produce a large number of cones and viable seeds. Payette et al. [1989] demonstrated that the ability of black spruce populations to respond to climatic change may depend on growth form at time of climatic change. Payette and coworkers dated changes in growth form and elevation of the snow-air interface recorded by subfossil black spruce at a treeline site in northern Quebec. Three periods of contrasting growth forms were interpreted in terms of climatic forcing: high krummholz (<2 m high) reflected cool conditions from A.D. 1305–1435, trees and high krummholz reflected warm conditions from A.D. 1435–1570, and low krummholz (<50 cm high) reflected cold conditions from A.D. 1570 to the present. The strong interaction between phenotype, population processes, and environmental change is well illustrated by these results. The sensitivity of black spruce populations to climatic change is strongly affected by positive feedbacks mediated through vegetative control of

snow accumulation. At protected sites, upright trees catch drifting snow and accumulated snow protects buds and foliage from abrasion and desiccation during severe winter conditions. In such environments sexual reproduction is more likely to be successful providing a regular supply of propagules to accelerate population expansion in times of relative warmth. In contrast, at exposed sites prostrate low krummholz are unable to control the snow drift environment, suffer damage when stems are exposed above the snow-air interface, and rarely reproduce sexually. At such sites, population responses lag behind climatic forcing and the vegetation is resilient to climatic change. Ecological factors thus complicate the interpretation of the history of tree morphologic changes in climate terms.

On longer time scales trees respond to changing climate through population expansions and contractions resulting in changes in altitudinal or latitudinal treeline and/or changes in tree density. Dendrochronologically determined age structures (i.e., dates of tree establishment) and mortality patterns allow the reconstruction of population dynamics back in time. Many investigators have found vigorous tree regeneration at arctic treeline sites during the 20th century that has been attributed to recent warming trends [Kullman 1983; Payette and Fillion, 1985]. Population responses to climatic variation exhibit complex spatial and temporal variability that has been related to such factors as snow accumulation [Payette and Fillion, 1985], fire [Payette and Gagnon 1979; Payette and Fillion, 1985], sexual vs. vegetative modes of reproduction [Payette and Gagnon, 1979; Kullman, 1983], and other life history traits [Kullman, 1983]. These factors can interact to cause a wide variation in the nature of and rates of population response to climatic change.

Finally, while most tree-ring studies of vegetation response to climate are concerned with effects on individuals or populations, tree-ring data can potentially provide important data on rates of CO₂ uptake at the biome level. D'Arrigo et al. [1987] demonstrated that annual variation in tree growth in the North American boreal forest is correlated with CO₂ drawdown at Point Barrow, AK for the period 1971–1982. D'Arrigo and coworkers speculate that the recent increases in the amplitude of the seasonal CO₂ cycle may be caused, in part, by seasonally enhanced growth of the boreal forest. Thus climatically induced changes in composition, structure and productivity of high-latitude northern forests have important implications for the atmosphere-biosphere exchange of CO₂ [Gammon et al., 1985]. Continued research efforts directed towards understanding the interaction of climate and vegetation processes at scales ranging from individuals to entire ecosystems will be enhanced by the long-term perspective afforded by tree-ring-based studies.

CONCLUSIONS

Dendroclimatic data will continue to be an important source of information on global environmental change by elucidating the nature of past climatic variation as well as vegetation response. In order to unravel the separate effects of various external forcings on global climate, the development of networks of multiple proxy climatic data need to be developed [IGBP, 1990]. Towards that end, the global coverage of climatically sensitive tree-ring chronologies should

be extended especially in areas where observational data are of short duration or where the climatic system is thought to be particularly sensitive to external forcing. High-latitude regions fit both criteria and should thus be given high priority in future dendroclimatic research. Similarly, given the long life spans of trees, our knowledge of the complex interaction of climate and arboreal vegetation at high latitudes

must be inferred from indirect sources such as tree-ring-based records of growth variation and population dynamics. In particular, further study of the factors that govern the sensitivity or relative resilience of vegetation to climatic change needs to be given high priority if we are to adequately anticipate the ecological consequences of CO₂-induced climatic change.

REFERENCES

- Bradley, R. S. (Ed.), Global Changes of the Past (Proceedings of the 1989 Global Change Institute at Snowmass), *Publication OIES-6*, Office for Interdisciplinary Earth Studies, UCAR, Boulder, CO, 1990.
- Briffa, K. R., T. M. L. Wigley, P. D. Jones, J. R. Pilcher, and M. K. Hughes, Reconstructing summer temperatures in northern Fennoscandia back to A.D. 1700 using tree-ring data from Scots Pine, *Arctic and Alpine Research*, 20, 385-394, 1988.
- Briffa, K. R., T. S. Bartholin, D. Eckstein, P. D. Jones, W. Karlen, F. H. Schweingruber, and P. Zetterberg, A 1,400-year tree-ring record of summer temperatures in Fennoscandia, *Nature*, 346, 434-439, 1990.
- D'Arrigo, R., and G. C. Jacoby, Jr., Boreal forests and atmosphere-biosphere exchange of carbon dioxide, *Nature*, 329, 321-323, 1987.
- Gammon, R. H., E. T. Sundquist, and P. J. Fraser, History of carbon dioxide in the atmosphere, in *Atmospheric Carbon Dioxide and the Global Carbon Cycle*, edited by J. R. Trabalka, U.S. Department of Energy, DOE/ER-0238, Washington, DC, 1985.
- Garfinkel, H. L., and L. B. Brubaker, Modern climate-tree growth relationships and climatic reconstruction in sub-arctic Alaska, *Nature*, 286, 872-874, 1980.
- Graumlich, L. J., The utility of long-term records of tree growth for improving forest stand simulation models, in *Natural Areas Facing Climatic Change*, edited by G. P. Malanson, pp. 39-49, SPB Academic, The Hague, 1989.
- Graybill, D. A., and S. G. Shiyatov, Dendroclimatic evidence from the northern Soviet Union, in *Climate Since A.D. 1500*, edited by R. S. Bradley and P. D. Jones, Routledge, London, 1992, In press.
- Goldstein, G. H., Ecophysiological and demographic studies of white spruce (*Picea glauca* [Moench] Voss) at treeline in the central Brooks Range of Alaska, Ph.D. Thesis, University of Washington, Seattle, 1981.
- IGBP, The International Geosphere-Biosphere Programme: A Study of Global Change. The Initial Core Projects, *IGBP Report 12*, Stockholm, 1990.
- Jacoby, G. C., Jr., Tree arctic, in *Climate from Tree Rings*, edited by M. K. Hughes, P. M. Kelly, J. R. Pilcher, and V. C. LaMarche, Jr., Cambridge University Press, Cambridge, 1982.
- Jacoby, G. C., Jr., and R. D'Arrigo, Reconstructed Northern Hemisphere temperature since 1671 based on high-latitude tree-ring data from North America, *Climatic Change*, 14, 39-59, 1989.
- Jacoby, G. C., Jr., E. R. Cook, and L. D. Ulan, Reconstructed summer degree days in central Alaska and northwestern Canada since 1524, *Quat. Res.*, 23, 18-26, 1985.
- Kullman, L., Past and present tree-lines of the Handölan Valley, central Sweden, in *Tree-Line Ecology*, edited by P. Morisset and S. Payette, pp. 25-45, Centre d'études nordiques, Université Laval, Québec, 1983.
- Payette, S., and L. Fillion, White spruce expansion at the tree line and recent climatic change, *Can. J. Forest Res.*, 15, 241-251, 1985.
- Payette, S., and R. Gagnon, Tree-line dynamics in Ungava peninsula, northern Quebec, *Holarct. Ecol.*, 2, 239-248, 1979.
- Payette, S., L. Fillion, A. Delwaide, and C. Begin, Reconstruction of tree-line vegetation response to long-term climate change, *Nature*, 341, 429-432, 1989.



92-17845

Polar Ice Cores: Climatic and Environmental Records

C. Lorius

Laboratoire de Glaciologie et Géophysique de l'Environnement, St Martin d'Hères, France

ABSTRACT

Ice cores from Greenland and Antarctica provide multiple proxy records of climatic and environmental parameters. They reveal the anthropogenic impact on aerosol concentrations in Greenland snow (i.e., SO_4 and NO_3) and on atmospheric greenhouse gases. For example, increases over the last 200 years are about 25% for CO_2 , 8% for N_2O and about 200% for CH_4 . Over the last climatic cycle (i.e., ~150 Kyr) the glacial-interglacial surface temperature change may be ~10°C, with glacial stages generally associated with lower snow accumulation and higher concentrations of marine and continental aerosols reflecting enlarged source areas and increased atmospheric transport. Greenland ice has recorded rapid changes of climate during the last ice age and deglaciation. The $\delta^{18}\text{O}$ or δD records from the Vostok ice core (Antarctica) strongly suggest the role of insolation orbital forcing, as well as a close relation between temperature and greenhouse gas concentrations. CO_2 and CH_4 concentrations increase by about 40% and 100% during glacial-interglacial transitions, respectively. It appears likely that fluctuating greenhouse gas concentrations have had a significant role in the glacial-interglacial climate changes by amplifying, together with the growth and decay of the Northern Hemisphere ice sheets, the orbital forcing. Climate sensitivity to greenhouse forcing estimated from paleo-ice core data is consistent with GCM simulations giving a 3-4°C warming for a future doubled atmospheric CO_2 .

THE ICE CORE RECORD

Paleo reconstructions are now recognized as an important element in climatic and environmental studies because they (a) allow assessment of the degree of natural variability and place current observed changes in a broader perspective; (b) assist in understanding causes and mechanisms of change; and (c) contribute to validating models by the comparison of output with empirical data sets.

Although we cannot expect to find in nature an ideal record, ice is a rather close approximation, as summarized in Table 1.

Paleotemperature reconstruction is based on the present correlations between the ratios of ^2H (D) and ^1H and of ^{18}O and ^{16}O in the snow and the temperature conditions both above the inversion layer, where the precipitation is formed, and at the surface. These are correlated via the fractionation processes that occur in the atmospheric water cycle and, although these processes depend on several parameters, a

linear isotope-temperature relationship is generally considered valid for both polar ice sheets [Lorius and Merlivat, 1977; Johnsen et al., 1989]. The validity of using the present observed relationship for paleotemperature reconstruction is supported by various evidence including atmospheric isotope models. Although there is no doubt that the concentration of aerosol species in the air is reflected in snow deposits at the site, quantitative estimations of their atmospheric concentration suffers from an incomplete understanding of the deposition processes, such as the relative contribution of "wet" and "dry" processes. In contrast, relating gas concentrations obtained from ice-core bubbles to the atmospheric value is quite straightforward in samples which do not contain melt layers.

TIME SCALES

For the upper part of the ice sheets the accuracy of the chronology can be very high. Annual layers can be counted

Atmosphere	Ice core
Temperature	D/H, $^{18}\text{O}/^{16}\text{O}$
Precipitation	D/H, $^{18}\text{O}/^{16}\text{O}$, ^{10}Be
Humidity	D/H, $^{18}\text{O}/^{16}\text{O}$
Aerosols	
•natural (continents, sea, volcanoes, biosphere)	Chemicals (Al, Ca, Na, H, SO_4^{--} , NO_3^-)
•man-made	SO_4^{--} , NO_3^- , Pb, radioactive fallout
Circulation	Particles
Gases: natural and man-made	O_2 , N_2 , CO_2 , CH_4 , N_2O

Table 1. Climatic and Environmental Information and Corresponding Ice Core Signal. [Lorius, 1989]

from seasonal variations of parameters such as visual stratigraphy, physical properties, isotopic composition, electrical conductivity, chemicals, etc. The age range over which such variations can be identified varies with factors such as accumulation rate, ice thickness and ice flow, but at great depth they become indiscernible.

Prominent features found in ice cores can be used as reference horizons providing ages when causal events can be documented, i.e., radioactive fallout from nuclear tests over the last three decades, ash or aerosol deposits from volcanoes [Hammer et al., 1985; Legrand and Delmas, 1987]. More generally, large-scale atmospheric events can be used for relative intercomparison between ice cores [Jouzel et al., 1989] or with other paleodata such as those from sea sediments [Petit et al., 1990]. Many of these other records have been independently dated, in particular through the use of radioactive isotopes. Although there are promising possibilities for obtaining absolute ages for ice core records from radioactive and other dating techniques, long time scales have been based so far on numerical modeling of the age distribution through ice sheets by ice dynamics [Reeh, 1989]. The characteristics of the present ice sheet (surface and bedrock topography, accumulation, temperature, ice velocity and viscosity) can be used to compute such an age distribution using steady state models [Budd and Young, 1983]. The accuracy of the method depends on a number of factors. For the upper part of the ice sheets the accuracy can be very high, but for regions near the bed rock complica-

tions of the ice flow can make the derived chronology, as well as the site of origin of the ice, unreliable. In general, inland regions of the thick ice sheets have the best prospects for reliable long-term chronologies in particular when accumulation changes with time can be taken into account.

CURRENT CHANGES: THE ANTHROPOGENIC IMPACT

Possibly because of the unfavorable signal to noise ratio, no clear indication of possible current climatic warming trend has been obtained from shallow ice cores. However, besides providing a reconstruction of significant volcanic events [Hammer et al., 1985; Legrand and Delmas, 1987] over the last centuries and of radioactive fallout from nuclear tests over the last decades, snow and ice layers have recorded atmospheric changes which are of importance for climatic changes.

With regard to aerosols, enhancement in nitrates and sulfates in the Arctic during the past 200 years broadly follows the known inventory of anthropogenic emissions. Changes in NO_3^- were not clearly detectable before the 1950s whereas SO_4^{--} has increased progressively during the last century. Qualitatively this agrees with the known shift of fuel usage from coal to oil and to the rapid growth of automobile emissions of NO_3^- since the 1950s.

Particularly important are findings from Greenland ice cores of a marked enhancement in SO_4^{--} and NO_3^- depositions [Nefel et al., 1985a; Mayewski et al., 1990; and Figure 1] by factors of 3-4 and almost 2 respectively, that have been detected since the beginning of the industrial era. Such trends do not appear in antarctic records in agreement with the concentration of industrial activities in Northern continental areas and the limitation of interhemispheric atmospheric transport for those species with relatively small atmospheric residence times. Recent secular changes of the key greenhouse gases CO_2 , CH_4 and N_2O have been precisely documented from polar ice cores. The increases are schematically shown in Figure 2. Ice core analysis shows that the preindustrial concentration of atmospheric CO_2 was about 280 ppmv in the 18th century and increased to 300 (around 1920) and then to about 320 ppmv in early 1960 [Nefel et al., 1985b] mainly as a result of fossil fuel use and deforestation. At sites whose pore close-off occurs rapidly, the ice core data may be linked with current monitored values which now exceed 350 ppmv. Ice core information has been of crucial importance in documenting current changes before direct atmospheric measurements, which started only about 30 years ago regarding CO_2 and about 10 years ago regarding the other gases, by providing natural reference base lines and variabilities.

For instance, measurements made on ice cores suggest fluctuations of around 10 ppmv in preindustrial periods [Raynaud and Barnola, 1985; Siegenthaler and Oeschger, 1987]. A detailed assessment of such variations is potentially of great value for a better understanding of the CO_2 cycle and its sensitivity to minor climatic changes. At present ice core measurements are the exclusive source of information on the concentrations and trends of methane before the middle of this century [Stauffer et al., 1985; Pearman et al., 1986; Khalil and Rasmussen, 1987]. The ice record is quite complete up to around 1000 years B.P., indicating that methane concentrations were about 700 ppbv

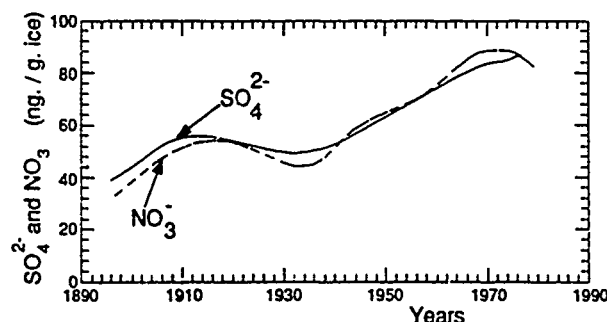


Figure 1. Sulfate and nitrate concentrations (in ng g^{-1}) in Greenland snow over the last century [from Nefel et al., 1985a].

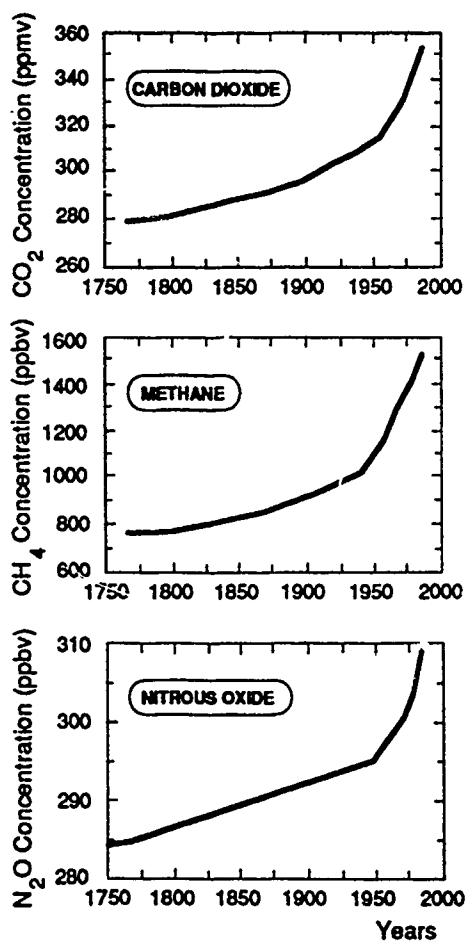


Figure 2. Concentrations of CO_2 [from Siegenthaler and Oeschger, 1987], CH_4 [from Khalil and Rasmussen, 1987] and N_2O [from Khalil and Rasmussen, 1988] over the last two centuries, based on ice core and instrumental data.

200 years ago while current atmospheric values are above 1600 ppbv. There has been considerable discussion as to the probable cause of this increase which may possibly be explained by more or less equivalent contributions from human and natural origins.

Although to a smaller extent, the anthropogenic impact is also affecting N_2O concentrations. Ice core data indicate that the preindustrial concentrations were around 285 ppbv compared to present levels of about 310 ppbv [Khalil and Rasmussen, 1988].

THE LAST ICE AGE

Three deep ice cores reaching back to the Last Glacial Maximum (LGM, 18 Kyr B.P.) have been drilled in Antarctica (Byrd, Dome C and Vostok) and two in Greenland (Camp Century and Dye 3).

The antarctic isotopic records [Johnsen et al., 1972; Lorius et al., 1979; Jouzel et al., 1987] are well correlated over the last 65 Kyr [Jouzel et al., 1989] with a surface temperature change of about 9°C associated with the last deglaciation; the slightly cooler event observed during this transition may eventually correspond to the Younger Dryas episode recorded in the Greenland ice. Ice deposited during the LGM contains much more impurities than Holocene ice; the LGM/Holocene ratios may be as high as 30 for continental dust and around 5 for marine salts [Thompson and

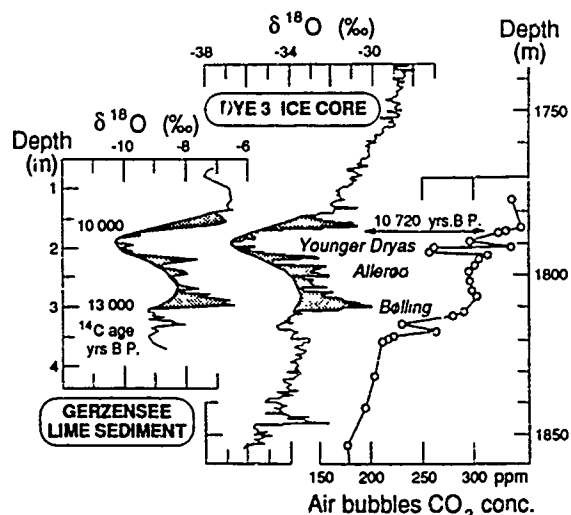


Figure 3. Middle: Detailed $\delta^{18}\text{O}$ profile along a 120 m increment of the Dye 3 Greenland ice core containing ice deposited during the Pleistocene to Holocene transition. Right: CO_2 concentration in air bubbles Left: $\delta^{18}\text{O}$ in lime sediments in the Swiss Lake Gerzensee [from Dansgaard and Oeschger, 1989].

Mosley-Thompson, 1981; Palais and Legrand, 1985; De Angelis et al., 1987]. Although part of the observed variations may be connected with a lower snow accumulation (by $\sim 50\%$) during the LGM, they have been interpreted as mainly resulting from global environmental changes: strengthened sources and meridional transport linked to higher wind speeds (likely induced by stronger temperature gradients with latitude), more extensive arid areas over the surrounding continents, and greater exposure of continental shelves due to a lower sea level [Petit et al., 1981].

In Greenland the $\delta^{18}\text{O}$ isotopic shift associated with deglaciation is larger in the Camp century [Johnsen et al., 1972] record than in Dye 3 [Dansgaard et al., 1982], suggesting temperature changes of respectively 16 and 11°C . Possible explanations for such a discrepancy refer to a latitude or ice thickening effect. LGM ice is also characterized by higher impurities content [Hammer et al., 1985].

A striking feature of the Greenland records is the evidence of rapid climatic changes. During deglaciation the so-called Bolling-Allerød-Younger Dryas oscillation (Figure 3) which is reasonably well dated in the Dye 3 ice core depicts a mean temperature increase in Greenland of about 7°C over a time period on the order of only 50 years, around 10,700 years B.P. [Dansgaard and Oeschger, 1989]. The accumulation rate increased approximately 60%, judging from the rapid increase in annual layer thickness, and concentrations of chemical components in the ice changed drastically, including CO_2 concentrations. This event is believed to have originated in the North Atlantic area. The type of rapid climatic change illustrated by the Bolling-Allerød-Younger Dryas oscillation is not unique. It appears to be the last of a series of events observed throughout the glaciation. During periods around 30 and 40 ky B.P., $\delta^{18}\text{O}$ variations suggest temperature changes of about 5 – 6°C within about a century or less [Dansgaard and Oeschger, 1989].

Over these time intervals the δ temperatures are in phase with dust concentration [Hammer et al., 1985] with higher values during cold conditions. These changes also correspond to CO_2 variations [Stauffer et al., 1984] with low val-

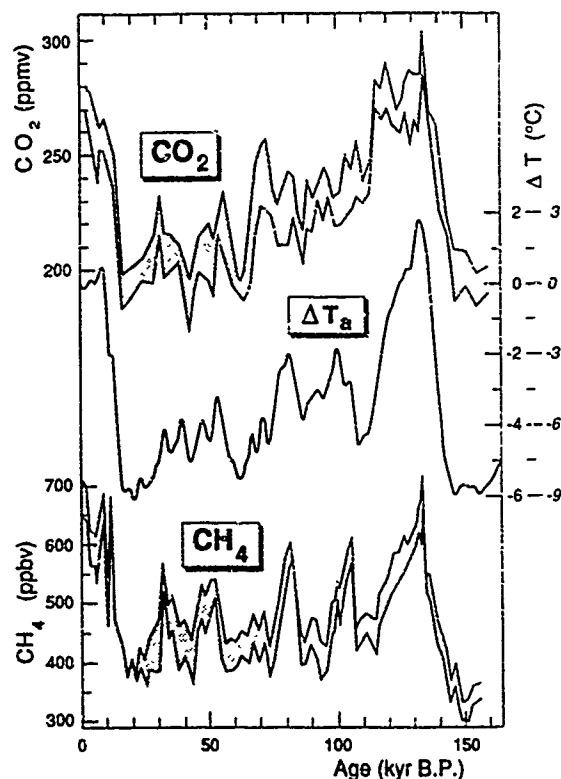


Figure 4. Variation over the last interglacial-glacial climatic cycle as derived from measurements along the 2083-m Vostok ice core of (a) the atmospheric CO_2 concentration [from Barnola et al., 1987]; (b) the atmospheric temperature change over Antarctica [from Jouzel et al., 1987]; and (c) the CH_4 atmospheric concentration [from Chappellaz et al., 1990]. For CO_2 and CH_4 the envelope shown has been plotted by taking into account the different uncertainty sources whereas the temperature record is a smoothed curve. The temperature scale is given for the surface (right and tilted) and above the atmospheric inversion layer (left).

ues in the range of 180–200 ppmv for periods of cold climate and higher values in the range of 240–260 ppmv for mild climatic conditions. So far these abrupt environmental events have not been depicted in the records from Antarctica.

THE LAST CLIMATIC CYCLE

The Vostok ice core from Antarctica provides an environmental record, essentially undisturbed by ice flow conditions, which covers the entire last glacial–interglacial cycle. The surface temperature record [Jouzel et al., 1987] and Figures 4 and 5 show the existence of two interglacials and extend back to the previous ice age. The peak of the previous interglacial is significantly warmer (about 2°C) than the Holocene period. Conditions equivalent to those prevailing during the LGM were encountered only at the end of the penultimate glacial, around 150 ky B.P. The last deglaciation is clearly a two-step process with two warming periods interrupted by a 2°C temperature reversal lasting about 1 ky. The last glacial period is characterized by three well-marked temperature minima (with the one occurring around 110 ky B.P. about 2°C warmer than full glacial conditions) separated by two interstadials respectively 4 and 6°C above

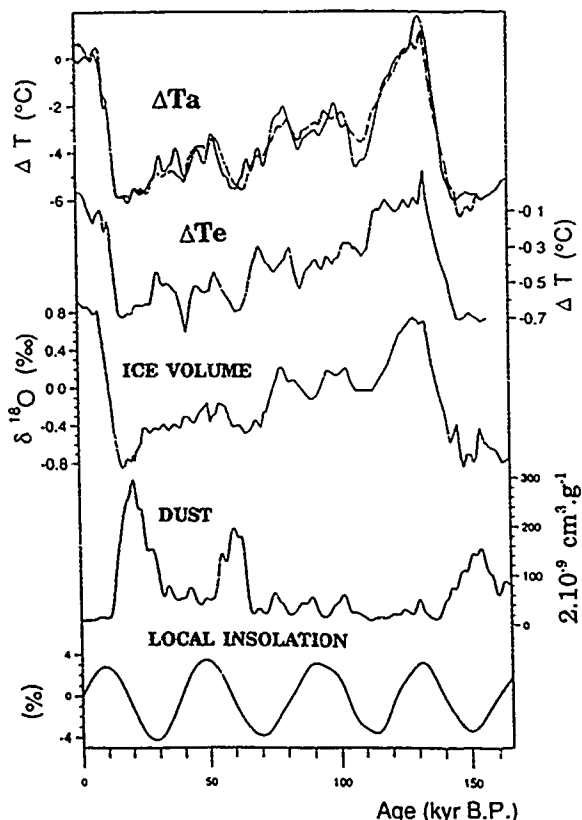


Figure 5. Time series of the Vostok ice core record along with the climatic forcings used in the multivariate analysis: (a) atmospheric temperature change, T_a , in $^\circ\text{C}$, observed and reconstructed (dotted line) from forcing factors; (b) direct greenhouse radiative forcing accounting for CO_2 and CH_4 variations, T_e , in $^\circ\text{C}$; (c) $\delta^{18}\text{O}$ SPECTRA-MAP record taken as a proxy of ice volume change [normalized value from Martinson et al., 1987]. The lowest part of the record has been redated to be in phase with the Vostok temperature record; (d) dust concentration expressed in volume [from Petit et al., 1990]; and (e) percentage change in yearly mean insolation at the Vostok latitude (78°S) [from Berger, 1978].

the minima. A spectral analysis shows that besides the ~ 100 kyr oscillation there are periodicities of 40 and 20 kyr which confirm the astronomical (Milankovitch) theory of ice ages. The accumulation, estimated both from the isotopic composition of the ice and ^{10}Be concentrations [Raisbeck et al., 1987] is clearly related to temperature changes with values reduced to about 50% during full glacials. Glacial stage conditions are also characterized by larger continental and marine aerosols [Legrand et al., 1988]. In contrast there is no relationship between acidity and the temperature record, indicating that there is no long-term correlation between volcanism and climate. Initial studies of the air trapped in polar ice cores revealed that atmospheric concentrations in CO_2 and CH_4 were lower during the LGM than during the Holocene [Delmas et al., 1980; Neftel et al., 1982; Stauffer et al., 1988]. The Vostok record shows that CO_2 concentrations [Barnola et al., 1987 and Figure 4] exhibit two very large changes between levels centered around 190–200 and 270–280 ppmv. They correspond to the transition between full-glacial conditions (low CO_2) of the last and penultimate glaciations and the two major warm periods (high CO_2) of the record, the Holocene and the previous interglacial. The

high level is comparable with preindustrial CO₂ concentration. The CH₄ profile [Chapellaz et al., 1990 and Figure 4] shows strong variations of past concentrations in the 350–650 ppbv range. These variations are well correlated with climate change, the low and high values being characteristic of full glacial and interglacial conditions, respectively.

ICE CORES AND THE GREENHOUSE EFFECT

Ice core data are unique as they provide access to both climatic histories and clues regarding climatic forcings; in particular they have suggested a close association of temperature changes with astronomical forcing and with greenhouse gas concentrations. However the orbital forcing is relatively weak when considered on an annual globally averaged basis; the amplification of this forcing, the observed dominant 100 kyr cycle in the paleo records, the synchronized termination of the main glaciations, and their similar amplitude in the Northern and Southern Hemispheres are not easily explained despite developments including the non-linear response of ice sheets to seasonal orbital forcings. It has been recently proposed [Lorius et al., 1988] that the observed changes in CO₂ and CH₄ have played a significant part in the glacial–interglacial climate changes by amplifying, together with the growth and decay of the Northern Hemisphere ice sheets, the orbital forcing. A multivariate analysis [Genthon et al., 1987; Lorius et al., 1990; and Figure 5] shows that 90% of the variance of the Vostok temperature record can be explained by five climate inputs. The aerosol loading and non sea-salt sulfates which may affect the albedo of clouds through the number of Cloud Condensation Nuclei and the local insolation change have

been found to play a minor role. Only both the Northern Hemisphere orbital forcing represented by the $\delta^{18}\text{O}$ marine record, a proxy of the Northern Hemisphere ice volume, and the greenhouse forcing, represented by the radiative forcing linked with CO₂ and CH₄ concentration change, appear to have had a similar and major contribution. From these results $\sim 50 \pm 10\%$ is a reasonable estimate for the contribution of greenhouse gases to glacial–interglacial climatic change [Lorius et al., 1990]. This is in agreement with General Circulation Model simulations for the LGM [Broccoli and Manabe, 1987; Rind et al., 1989] which indicate that greenhouse gases could have contributed to about 2°C of the 4–5°C change on a global average. These orbital and greenhouse contributions are expected to include slow and fast feedback respectively. The radiative greenhouse forcing associated with glacial–interglacial changes is $\sim 2 \text{ W m}^{-2}$ which implies a temperature change of 0.7°C without feedback; the total effect of 2°C leads to an amplification factor of ~ 3 which represents fast feedback effects [Lorius et al., 1990]. The sensitivity of climate to future greenhouse forcing is of current concern and GCM experiments for temperature changes resulting from a doubled CO₂, corresponding to a radiative forcing of 4 W m^{-2} , yield equilibrium warmings between 1.9 and 5.2°C and amplification factors ranging from 1.6 to 3.5 [Mitchell, 1989].

Ice core results suggest then that changing concentrations of greenhouse gases have had a significant role in explaining the magnitude of past global temperature changes and are consistent with a climate sensitivity of 3 to 4°C for a future doubled atmospheric CO₂.

REFERENCES

- Barnola, J. M., D. Raynaud, Y. S. Korotkevich, and C. Lorius, Vostok ice core provides 160,000 year record of atmospheric CO₂, *Nature*, 329, 408–414, 1987.
- Berger, A., Milankovitch theory and climate, *Rev. Geophys.*, 26, 624–657, 1988.
- Broccoli, A. J., and S. Manabe, The influence of continental ice, atmospheric CO₂, land albedo on the climate of the Last Glacial Maximum, *Climate Dynamics*, 1, 87–99, 1987.
- Budd, W. F., and N. W. Young, Application of modelling techniques to measured profiles of temperature and isotopes, in *The Climatic Record in Polar Ice Sheets*, edited by G. de Q. Robin, pp. 150–179, Cambridge University Press, 1983.
- Chappellaz, J., J. M. Barnola, D. Raynaud, Y. S. Korotkevich, and C. Lorius, Ice core record of atmospheric methane over the past 160,000 years, *Nature*, 345, 127–131, 1990.
- Dansgaard, W., H. B. Clausen, N. Gundestrup, C. U. Hammer, S. J. Johnsen, P. M. Kristinsdottir and N. Reeh, A new Greenland deep ice core, *Science*, 218, 1273–1277, 1982.
- Dansgaard, W., and H. Oeschger, Past environmental long-term records from the Arctic, in *The Environmental Record in Glaciers and Ice Sheets*, edited by H. Oeschger and C. C. Langway, Jr., pp. 287–318, John Wiley Sons Ltd., 1989.
- De Angelis, M., N. I. Barkov, and V. N. Petrov, Aerosol concentrations over the last climatic cycle (1660 ky) from an Antarctic ice core, *Nature*, 325, 318–321, 1987.
- Delmas, R. J., J. M. Ascencio, and M. Legrand, Polar ice evidence that atmospheric CO₂ 20,000 yr B.P. was 50% of present, *Nature*, 284, 155–157, 1980.
- Genthon, C., J. M. Barnola, D. Raynaud, C. Lorius, J. Jouzel, N. I. Barkov, Y. S. Korotkevich, and V. M. Kotlyakov, Vostok ice core: climatic response to CO₂ and orbital forcing changes over the last climatic cycle, *Nature*, 329, 414–418, 1987.
- Hammer, C. U., H. B. Clausen, W. Dansgaard, A. Neftel, P. Kristinsdottir and E. Johnson, Continuous impurity analysis along the Dye 3 deep core, in *Greenland ice cores: geophysics, geochemistry and the environment*, edited by C. C. Langway, H. Oeschger and W. Dansgaard, pp. 90–94, *Geophysical Monograph* 33, American Geophysical Union, Washington, DC, 1985.
- Johnsen, S. J., W. Dansgaard, H. B. Clausen, and C. C. Langway, Oxygen isotope profiles through the Antarctic and Greenland ice sheets, *Nature*, 235, 429–434, 1972.
- Johnsen, S. J., W. Dansgaard, and J. White, The origin of Arctic precipitation under glacial and interglacial conditions, *Tellus*, 41B, 452–468, 1989.
- Jouzel, J., C. Lorius, J. R. Petit, C. Genthon, N. I. Barkov, V. M. Kotlyakov, and V. N. Petrov, Vostok ice core: a continuous isotope temperature record over the last climatic cycle (160,000 years), *Nature*, 329, 403–409, 1987.
- Jouzel, J., R. Russel, R. J. Suozzo, R. J. Koster, J. W. C. White, and W. S. Broecker, Simulations of the HDO and H₂O atmospheric cycles using the NASA GISS General Circulation Model: the seasonal cycle for present day conditions, *J. Geophys. Res.*, 92, 14739–14760, 1987.

- Jouzel, J., G. Raisbeck, J. P. Benoist, F. Yiou, C. Lorius, D. Raynaud, J. R. Petit, N. I. Barkov, Y. S. Korotkevitch, and V. M. Kotlyakov, The Antarctic climate over the late glacial period, *Quat. Res.*, 31, 135-150, 1989.
- Khalil, M. A. K., and R. A. Rasmussen, Atmospheric methane: Trends over the last 10,000 years, *Atmos. Envir.*, 21, 2445-2452, 1987.
- Khalil, M. A. K., and R. A. Rasmussen, Nitrous oxide: Trends and global mass balance over the last 3,000 years, *Ann. Glaciol.*, 10, 73-79, 1988.
- Legrand, M. R., and R. J. Delmas, Volcanic H₂SO₄ in the antarctic ice sheet: a 220 yr continuous record, *Nature*, 327, 671-676, 1987.
- Legrand, M., C. Lorius, N. I. Barkov, and V. N. Petrov, Vostok (Antarctica) ice core: atmospheric chemistry changes over the last climatic cycle (160,000 yr), *Atmos. Envir.*, 22, 317-331, 1988.
- Lorius C., Polar ice cores and climate, in *Climate and Geo-Sciences*, Edited by A. Berger et al., pp. 77-103, Kluwer Academic Publishers, 1989.
- Lorius, C., and Merlivat, L., Distribution of mean surface stable isotope values in East Antarctica: observed changes with depth in a coastal area, in *Isotopes and Impurities in Snow and Ice*, Proc. Grenoble Symp. August-September 1975, *IAHS*, 118, 127-137, 1977.
- Lorius, C., L. Merlivat, J. Jouzel, and M. Pourchet, A 30 000 y isotope climatic record from Antarctic ice, *Nature*, 280, 644-648, 1979.
- Lorius, C., N. I. Barkov, J. Jouzel, Y. S. Korotkevich, V. M. Kotlyakov and D. Raynaud, Antarctic ice core: CO₂ and climatic change over the last climatic cycle, *EOS*, 69, 26, 681, 683-684, 1988.
- Lorius, C., J. Jouzel, D. Raynaud, J. Hansen, and H. Le Treut, The ice core record: climate sensitivity and future greenhouse warming, *Nature*, 347, 139-145, 1990.
- Martinson D. G., N. G. Pisias, J. D. Hays, J. Imbrie, T. C. Moore, and N. J. Shackleton, Age dating and the orbital theory of the ice ages: Development of a high-resolution 0 to 300,000 year chronostratigraphy, *Quat. Res.*, 27, 477-482, 1987.
- Mayewski, P. A., W. B. Lyons, M. J. Spencer, M. Twickler, C. F. Buck, and S. Whitlow, An ice core record of atmospheric response to anthropogenic sulphate and nitrate, *Nature*, 346, 554-556, 1990.
- Mitchell, J. F. B., The greenhouse effect and climatic change, *Rev. Geophys.*, 27, 115-139, 1989.
- Neftel, A., H. Oeschger, J. Schwander, B. Stauffer, and R. Zumbunn, Ice core sample measurements give atmospheric CO₂ content during the past 40,000 yr, *Nature*, 295, 220-223, 1982.
- Neftel, A., J. Beer, H. Oeschger, F. Zurcher, and R. C. Finkel, Sulphate and nitrate concentrations in snow from South Greenland 1895-1978, *Nature*, 314, (6012), 611-613, 1985a.
- Neftel, A., E. Moor, H. Oeschger, and B. Stauffer, Evidence from polar ice cores for the increase in atmospheric CO₂ in the past two centuries, *Nature*, 45-47, 1985b.
- Palais, J., and M. R. Legrand, Soluble impurities in the Byrd station ice core, Antarctica their origin and sources, *J. Geophys. Res.*, 90, 1143-1154, 1985.
- Pearman, G. I., F. Etridge, F. de Silva, and P. J. Fraser, Evidence of changing concentrations of CO₂, N₂O and CH₄ from air bubbles in antarctic ice, *Nature*, 320, 248-250, 1986.
- Petit, J. R., M. Briat, and A. Royer, Ice age aerosol content from East Antarctic ice core samples and past wind strength, *Nature*, 293, 391-394, 1981.
- Petit, J. R., L. Mounier, J. Jouzel, Y. S. Korotkevich, V. M. Kotlyakov, and C. Lorius, Paleoclimatic and chronological implications of the Vostok dust record, *Nature*, 343, 56-58, 1990.
- Raisbeck, G. M., F. Yiou, D. Bourles, C. Lorius, J. Jouzel, and N. I. Barkov, Evidence for two intervals of enhanced ¹⁰Be deposition in Antarctic ice during the last glacial period, *Nature*, 326, 273-277, 1987.
- Raynaud, D., and J. M. Barnola, CO₂ and climate: information from Antarctic ice core studies, in *Current Issues in Climate Research*, edited by A. Ghazi and R. Fantechi, pp. 240-246, D. Reidel, Dordrecht, Holland, 1985.
- Reeh, N., Dating by ice-flow modelling: a useful tool or an exercise in applied mathematics, in *The Environmental Record in Glaciers and Ice Sheets*, edited by H. Oeschger and C. C. Langway, Jr., pp. 141-160, John Wiley Sons Ltd., 1989.
- Rind, D., D. Peteet, and G. Kukla, Can Milankovitch orbital variations initiate the growth of ice sheets in a General Circulation Model, *J. Geophys. Res.*, 94, 12851-12871, 1989.
- Siegenthaler, U., and H. Oeschger, Biospheric CO₂ emissions during the past 200 years reconstructed by deconvolution of ice core data, *Tellus*, 39B, 140-154, 1987.
- Stauffer, B., H. Hofer, H. Oeschger, J. Schwander, and U. Siegenthaler, Atmospheric CO₂ concentration during the last glaciation, *Ann. Glaciol.*, 5, 160-164, 1984.
- Stauffer, B., G. Fischer, A. Neftel, and H. Oeschger, Increase of atmospheric methane recorded in antarctic ice, *Science*, 229, 1386-1388, 1985.
- Stauffer, B., E. Lochbrunner, H. Oeschger, and J. Schwander, Methane concentration in the glacial atmosphere was only half that of the preindustrial Holocene, *Nature*, 332, 812-814, 1988.
- Thompson, L. G., and E. Mosley-Thompson, Microparticle concentration variations linked with climatic change: evidence from polar ice cores, *Science*, 212, 812-815, 1981.

AD-P007 342



Canadian Ice Caps as Sources of Environmental Data

R. M. Koerner, B. T. Alt, J. C. Bourgeois, and D. A. Fisher
Terrain Sciences Division, Geological Survey of Canada, Ottawa, Ontario, Canada

ABSTRACT

Seven surface-to-bedrock ice cores, varying from 129 to 337 m in length, have been recovered from Canadian high Arctic ice caps since 1964 (Table 1 and Figure 1). While one (Meighen Island) consists entirely of Holocene ice, the others (Devon and Agassiz ice caps) cover time spans of 100,000 years, similar to those from Greenland. Our relatively thin ice caps provide simple drilling conditions but give records of various parameters from several holes down a flow line. Comparison of these records continues to provide information on signal-to-noise ratios and ice cap rheology. The major disadvantage of thin ice caps is poor resolution in ice more than 5000 to 10,000 years old. This is offset, however, by the relative ease of retrieval of significant numbers of pollen grains from all levels in the ice. Thus we have been able to use pollen as a paleoenvironmental tool leading, for example, to identification of basal ice layers as Sangamonian in age. Similarly, although annual melting of snow at the surface precludes the possibility of using ice cores for gas analysis, the persistence of variable melt layer concentrations through the Holocene ice has given a continuous melt layer record showing gradual deterioration of summer climate from a warm peak 8000 to 9000 years ago, to a cold minimum 200 years ago.

INTRODUCTION

Over the past 25 years ice cores have given valuable information on the way climate has changed over the last glacial cycle (ca. 100,000 years). Changes in the oxygen isotope ratios in the ice serve as proxy temperature indicators, gas bubbles yield records of changes in important greenhouse gases, dust particles, ionic concentrations and bio-constituents give information on atmospheric processes and air mass trajectories and the part they played in past environmental change, and changes of ice texture constitute a summer temperature indicator.

However, no single ice core can cover all these parameters. Antarctica is too remote from land to use pollen as an atmospheric tracer. It is also too cold for summer melting to form ice layers that serve as summer climate proxies. Conversely summer melting seriously disturbs the gas record [Stauffer et al., 1985] so that Canadian ice cores are of no use in this respect whereas Antarctica is ideal [Barnola et al., 1987].

The snow accumulation rate at a drill site also affects the ice core record. In areas with low accumulation rates, ice

cores give long records from relatively shallow depth intervals. Thus at Vostok in Antarctica (4 cm ice yr⁻¹), the ice core record revealed so far covers >150,000 years in 2 km of ice; yet this record ends 2 km above bedrock [Lorius et al., 1985]. At Dye-3 (54 cm ice yr⁻¹) the record covers about 120,000 years over a similar core length but ends on bedrock [Dansgaard et al., 1982]. The accumulation rate also affects the temporal resolution of an ice core record. A low accumulation rate such as that at Vostok means about 1 year in 8 is missing from the record [Koerner, 1971] and gives at best a resolution of a few years. In the last glacial period, where the accumulation rate may have been as low as 1 cm ice yr⁻¹ [Lorius et al., 1985] the resolution is even poorer. Dye-3, on the other hand, has seasonal resolution in the Holocene and annual resolution for some depth below that. This has allowed for direct calibration of the ¹⁴C time scale over the past 10,000 years [Hammer et al., 1986].

The Canadian high Arctic ice caps, with an accumulation rate of 10–25 cm ice yr⁻¹, lie somewhere between the Antarctic and Greenland ice cores in terms of temporal resolution (Table 1). However, because the ice cap thicknesses are

92-17846



substantially less, annual layers can only be detected down to a depth equivalent of 6000 years. Only major changes in climate can be detected below this. However, shallow ice depths do not seriously limit the total time span covered in any single surface-to-bedrock ice core (Figure 2). Despite quite different lengths, the Canadian, Dye-3 and Camp Century ice cores cover similar time periods: about 120,000 years from the last interglacial period to the present day. In this case shallow ice depth can prove to be an advantage as it makes bulk sampling of ancient ice much easier. This advantage has been used to provide the large samples necessary for pollen analysis.

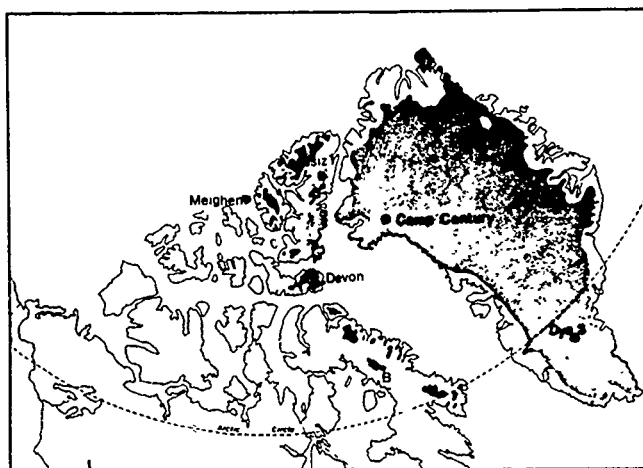


Figure 1. Location map.

Shallow ice depths have also permitted evaluation of signal-to-noise ratios in ice core records [Fisher et al., 1985], and also the variation of different parameters with depth along a flow line [Fisher and Koerner, 1986].

RESULTS

Our ice core program has been attuned to accommodate the advantages and disadvantages of shallow ice cores with intermediate snow accumulation rates and annual summer melting. We now give some of the results of this work.

Pollen

Pollen spectra display counts of different types of pollen grains. Study of the spectra should lead to identification of air mass trajectories affecting general aerosol transport. However, to simplify the discussion we divide the spectrum into two categories: (1) *exotic pollen*, i.e., from south of the

Site (Figure 1)	Surface elevation (m)	Core length (m)	Year drilled
Meighen Ice Cap	268	121	1965
Devon Ice Cap	1800	300	1972
Devon Ice Cap	1800	300	1973
Agassiz Ice Cap	1700	340	1977
Agassiz Ice Cap	1710	137	1979
Agassiz Ice Cap	1715	127	1984
Agassiz Ice Cap	1715	127	1987

Table 1. Surface-to-bedrock ice cores.

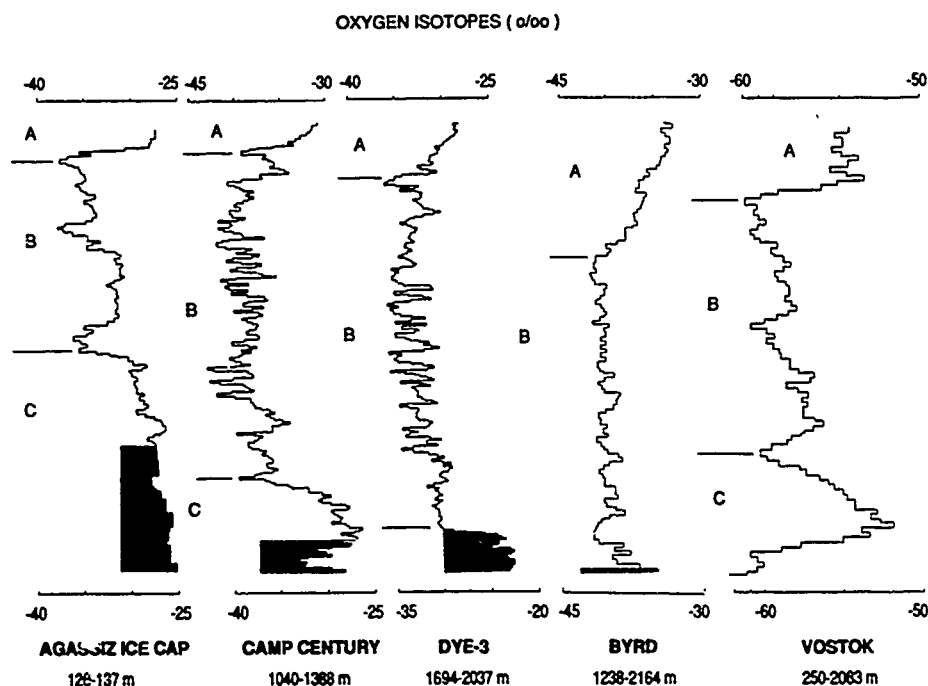


Figure 2. Oxygen Isotope ($\delta^{18}\text{O}$) profiles. The vertical depth scales differ between profiles; all are plotted on linear depth scales with total depth shown under each profile title. The o-scale is expanded from the Vostok profile. All profiles, with the exception of that for Vostok, end at the ice/bed interface. (A) Holocene ice, (B) main part of the last glacial period, (C) glacial/interglacial transition and Sangamon ice. The shaded zones are ice with visible dirt inclusions.

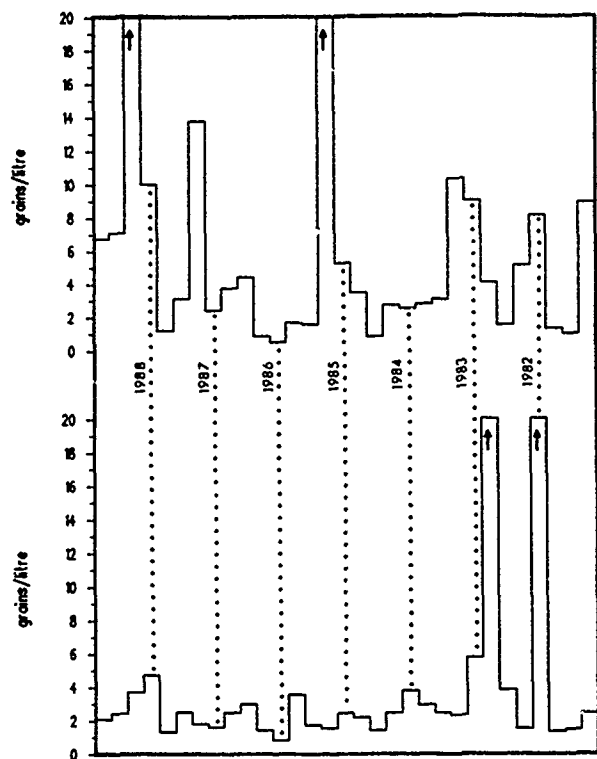


Figure 3. Concentration of pollen grains in surface snows, Agassiz Ice Cap. The dotted lines separate the annual layers where the end of each year is defined as the end of the melt season (July, August). Melting leaves a distinct surface layer each year in the snow pack. The vertical scale is not marked as the samples were taken each year from the surface annual layer. The total depth increment is approximately 4 m. Exotic pollen are shown on the left hand side and regional on the right.

tree line, (2) *regional pollen*, i.e., from the tundra north of the tree line. Transport of exotic pollen involves straight-line distances of 1000 to 25,000 km; trajectory distances must be substantially greater than this. To develop climate/pollen transport functions demands a knowledge of, first, present day spatial variations, and second, of seasonal and interannual variations of the concentrations in the snow.

Pollen concentrations in polar snows are very low: 1 to 15 pollen grains per liter of melted snow; this gives deposition rates of 80–2200 grains $m^{-2} yr^{-1}$. Surprisingly, the higher deposition rates occur on sea ice in the middle of the Arctic Ocean. Overall low deposition rates may be compared to rates of 137,000 grains $m^{-2} yr^{-1}$ on a glacier close to the tree line in northern Labrador [Bourgeois et al., 1985, Tables II and III]. It is, therefore, not possible at present to identify specific source areas; the background sources could include Eurasia as well as North America.

Seasonal pollen concentrations in a snow pit are shown in Figure 3. They are irregular and unusable for detection of annual layers. However, the exotic and regional variations form two distinct data sets which are not always related to each other. High (low) influxes of *regional pollen* to the ice cap site show a relationship to warm (cold) summers as represented by the July temperatures at the nearby weather station of Eureka [Bourgeois, 1990]. A few more years of data (attainable from deeper snow pits on the ice cap) are needed to develop a workable transfer function.

The exotic pollen concentrations are poorly related to

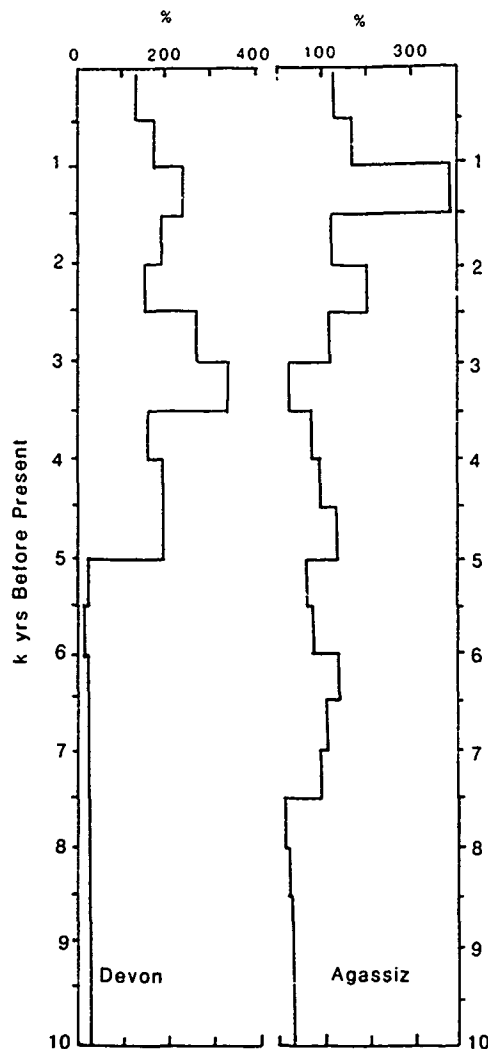


Figure 4. Profiles of total pollen concentrations (exotic plus regional) from Devon Ice Cap and Agassiz Ice Cap expressed as a percentage of the average concentration for the past 10,000 years.

summer temperatures. Instead, concentrations in any one year appear to be related to individual synoptic situations. The position, or absence, of the 500 mb trough seems to be important in this respect. High concentrations of exotic pollen in the 1982 and 1983 spring and summer snow layers (Figure 3) occurred when synoptic conditions promoted a strong and direct flow of air from the south into the Arctic Islands. Conversely, a strong northwesterly flow over the islands in the spring of 1986 resulted in very low exotic pollen concentrations in snow deposited at that time [Bourgeois, 1990].

Despite some progress in our study of pollen concentrations in modern snows it is still difficult to interpret their distribution in ice cores (Figure 4). Pollen concentrations began to increase early in the Holocene on Agassiz Ice Cap [Bourgeois, 1986] but much later on Devon Ice Cap [McAndrews, 1984]. The 3000-year-before-present (B.P.) peak in the Devon core is absent in the Agassiz core but both show peaks at 1000 years B.P. However, neither profile shows a relationship to either the $\delta^{18}O$ or melt layer profiles from the same cores (Figure 5). This is because pollen concentrations are related to different climatic variables such as pol-

len productivity at source and the snow accumulation rate between pollen source and drill site. Low concentrations of pollen in early Holocene ice may be due to persistence of parts of the Laurentide ice sheet to the south.

So far, pollen has proved valuable in defining the major climatic zones in the ice cores. High pollen concentrations (including maple, elm and oak) in the basal ice of both the Devon and Agassiz cores suggest that this ice was formed in a warmer period than today [Koerner et al., 1988]. The position under isotopically very negative ice denoting ice formed during the last glacial period, indicates the basal ice is interglacial. The drill site must, therefore, have been ice-free during the same interglacial period. Examination of the Greenland ice cores in terms of ice texture, dirt content and oxygen isotopes (Figure 2) led to a similar conclusion about the time of origin of the Greenland ice sheet in the location of the drill sites [Koerner, 1989].

Melt Layers

Melt layers in ice sheets are formed by melting of the snow pack surface. Surface melt percolates in to the snow pack where it refreezes as relatively bubble-free ice. Because more ice forms in this way in the snow pack the warmer the summer, the changing concentration with depth of these ice layers serves as an indicator of past summer climate. A study of this nature in the Devon ice cores [Koer-

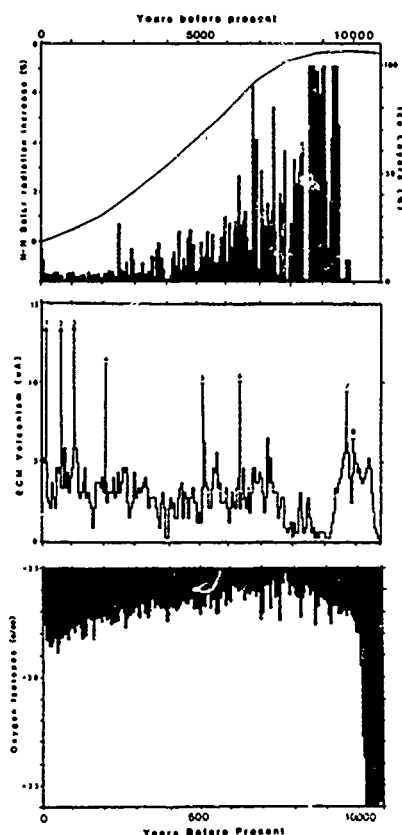


Figure 5. Melt layer concentration, volcanism and oxygen isotopes ($\delta^{18}\text{O}$), Agassiz Ice Cap. Increased solar radiation is for June, July and August for the northern hemisphere and is due to changing orbital parameters [Kutzbach, 1987]. The electrolytic conductivity measurement in the middle profile is made on the solid ice core using a technique developed by Hammer [1980].

ner, 1977] showed that ice layer concentrations also serve as a proxy for mass balance. While the Devon study extended back for only 700 years due to micro-fractures in the core, the shallower, unfractured core from the top of Agassiz Ice Cap extended this record back to the beginning of the Holocene period 10,000 years B.P. [Koerner and Fisher, 1990]. There are three main features of this record (Figure 5): (1) a strong trend of decreasing summer melt layers between 9500 and 2500 years B.P. with (2) maximum melting occurring at the beginning of the Holocene and, (3) a plateau of very low melt within the past 2000 years. We estimate that at the most, 40% of the cooling trend could arise from uplift over the same time interval. There is a significant increase in numbers of melt layers during the past 100 years. This recent increase is also evident on Devon Ice Cap [Koerner, 1977], Muller Ice Cap [Muller, 1962] and a northern Ellesmere ice cap 120 km to the north of Agassiz Ice Cap [Hattersley-Smith, 1963]. However, the modern increase is to levels much lower than those in the early Holocene even when the effect of possible uplift is considered.

The Agassiz melt record (Figure 5) is the first continuous record of summer climate for the high Arctic and can be compared to the discontinuous glacial geology record for the same area. The higher melt layer concentrations for the last 100 years overlap with slightly negative glacier balances measured over the last 30 years.

The melt record (Figure 5) therefore suggests that massive glacier retreat occurred during the first half of the Holocene. This is in general agreement with the geological record for the high Arctic [Blake, 1975; Bednarski, 1986; Hodgson, 1989]. Lower melt concentrations in ice cores representing the last 2500 years, suggesting positive balance over that period, compare to evidence of glacier growth during this period in nearby parts of Greenland [Kelly, 1980], northern Ellesmere Island [Hattersley-Smith, 1966] and Axel Heiberg Island [Muller, 1966].

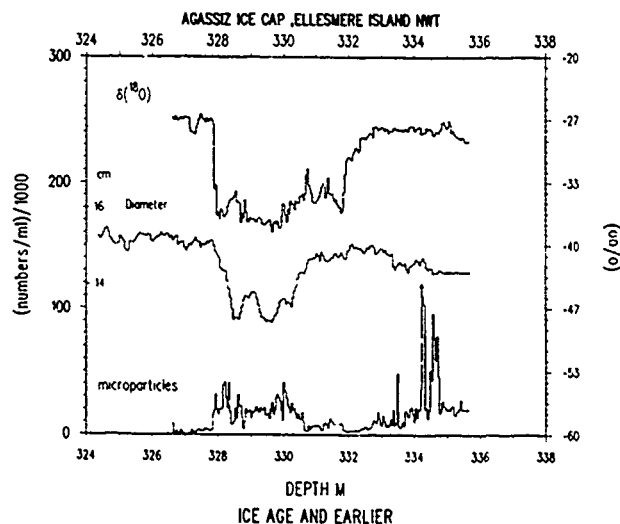


Figure 6. Oxygen isotopes ($\delta^{18}\text{O}$), dust and borehole closure rates for the 1977 core from Agassiz Ice Cap. The initial borehole diameter after drilling was 160 mm. Note the correlation between borehole closure rates and microparticle concentrations. The lower than expected closure rates near the bed are due to the uneven nature of the particle distribution. Most of the dust particles in this section are separated into discrete pear-shaped pockets which are visible to the naked eye.

Rheology

Because they are relatively thin (100–500 m of ice), Canadian ice caps are suited to the study of ice dynamics and ice rheology. For example, four surface-to-bedrock cores drilled from the top of Agassiz ice cap and down the flowline, required only 728 m of drilling. Yet each core covers a complete glacial cycle, including soft glacial-period ice, stiff Holocene ice and sections with unique micro-particle and ionic signatures. Studies on Devon Ice Cap [Paterson, 1977] showed differences between the rheological properties of Holocene and glacial period ice; more

rapid borehole closure rates occur in the latter ice. The boreholes and cores from Agassiz Ice Cap have shown the same characteristics [Fisher and Koerner, 1986]. The different rheological and, hence, dynamic properties of the ice have been partly attributed to differences in the concentrations of microparticles in each type of ice [Koerner and Fisher, 1979; Fisher and Koerner, 1986] although this has been contested by Duval and Lorius [1980]. Further work on this, and other problems of ice dynamics is continuing [Waddington et al., 1985].

REFERENCES

- Barnola, J. M., D. Raynaud, Y. S. Korotkevitch, and C. Lorius, Vostok ice core provides 160,000 year record of atmospheric CO₂, *Nature*, 329, 408-414, 1987.
- Bednarski, J., Late Quaternary glacial and sea-level events, Clements Markham Inlet, northern Ellesmere Island, *Can. J. Earth Sci.*, 23, 1343-1355, 1986.
- Blake, W., Jr., Radiocarbon age determinations and post-glacial emergence at Cape Storm, southern Ellesmere Island, Arctic Canada, *Geografiska Annaler*, 57A, 1-71, 1975.
- Bourgeois, J. C., A pollen record from the Agassiz Ice Cap, northern Ellesmere Island, Canada, *Boreas*, 15, 345-354, 1986.
- Bourgeois, J. C., Seasonal and annual variation of pollen content in the snow of a Canadian high Arctic ice cap, *Boreas*, 19, 313-322, 1990.
- Bourgeois, J. C., R. M. Koerner, and B. T. Alt, Airborne pollen: a unique air mass tracer, its influx to the Canadian high Arctic, *Ann. Glaciol.*, 7, 109-116, 1985.
- Dansgaard, W., and 6 others, A new Greenland deep ice core, *Science*, 218, 1273-1277, 1982.
- Duval, P., and C. Lorius, Crystal size and climatic record down to the last ice age from Antarctic ice, *Earth Planet. Sci. Lett.*, 48, 59-64, 1980.
- Fisher, D. A., and R. M. Koerner, On the special rheological properties of ancient microparticle laden northern hemisphere ice as derived from borehole and core measurements, *J. Glaciol.*, 32, 501-510, 1986.
- Fisher, D. A., N. Reeh, and H. B. Clausen, Stratigraphic noise in time series derived from ice cores, *Ann. Glaciol.*, 7, 76-84, 1985.
- Hammer, C. U., Acidity of polar ice cores in relation to absolute dating, past volcanism, and radioechoes, *J. Glaciol.*, 25, 359-372, 1980.
- Hammer, C. U., H. B. Clausen, and H. Tauber, Ice core dating of the Pleistocene/Holocene boundary applied to calibration of the ¹⁴C time scale, *Radiocarbon*, 28, 284-291, 1986.
- Hattersley-Smith, G., Climatic inferences from firn studies in northern Ellesmere Island, *Geografiska Annaler*, 45, 139-151, 1963.
- Hattersley-Smith, G., Climatic change and related problems in northern Ellesmere Island, N.W.T., Canada, in *Climatic Changes in Arctic Areas During the Last Ten Thousand Years*, edited by Y. Vasari, H. Hyvarinen, and S. Hicks, pp. 137-148, Oulu University, Finland, 1966.
- Hodgson, D. A., Quaternary stratigraphy and chronology, in *Quaternary Geology of Canada and Greenland*, edited by R. J. Fulton, pp. 452-459, Geological Survey of Canada, Ottawa, 1989.
- Kc'ly, M., The status of the neoglaciation in western Greenland, *Rapport Gronlands Geologiske Undersogelske*, 96, 33-38, 1980.
- Koerner, R. M., A stratigraphic method of determining the snow accumulation rate at Plateau Station, Antarctica, and application to South Pole-Queen Maud Land Traverse 2, 1965-6, *Antarctic Research Series II*, edited by A. P. Crary, pp. 225-238, A.G.U., Washington, 1971.
- Koerner, R. M., Devon Island Ice Cap: core stratigraphy and paleoclimate, *Science*, 196, 15-18, 1977.
- Koerner, R. M., Ice core evidence of extensive melting of the Greenland Ice Sheet in the last interglacial, *Science*, 196, 15-18, 1989.
- Koerner, R. M., and D. A. Fisher, Discontinuous flow, ice texture and dirt content in the basal layers of the Devon Island Ice Cap, *J. Glaciol.*, 23, 209-222, 1979.
- Koerner, R. M., and D. A. Fisher, A record of Holocene summer climate from a Canadian high Arctic ice core, *Nature*, 343, 630-631, 1990.
- Koerner, R. M., J. C. Bourgeois, and D. A. Fisher, Pollen analysis and discussion of time scales in Canadian ice cores, *Ann. Glaciol.*, 10, 85-91, 1988.
- Lorius, C., and 6 others, A 150,000 year climatic record from Antarctic ice, *Nature*, 316, 591-596, 1985.
- McAndrews, J. H., Pollen analysis of the 1973 ice core from Devon Island Ice Cap, Canada, *Quat. Res.*, 22, 68-76, 1984.
- Muller, F., Investigations in an ice shaft in the accumulation area of the McGill Ice Cap, in *Preliminary Report 1961-62*, pp. 27-36, Axel Heiberg Research Reports, McGill University, Montreal, 1962.
- Muller, F., Evidence of climatic fluctuations on Axel Heiberg Island, Canadian Arctic Archipelago, in *Proceedings of the Symposium on the Arctic Heat Budget and Atmospheric Circulation*, edited by J. O. Fletcher, pp. 136-156, Rand Corp., Santa Monica, California, 1966.
- Paterson, W. S. B., Secondary and tertiary creep of glacier ice as measured by borehole closure rates, *Rev. Geophys. Space Physics*, 15, 47-55, 1977.
- Paterson, W. S. B., and 7 others, An oxygen-isotope climatic record from the Devon Island Ice Cap, Arctic Canada, *Nature*, 266, 508-511, 1977.
- Stauffer, B., A. Neftel, H. Oeschger, and J. Schwander, CO₂ concentration in air extracted from Greenland ice samples, in *Greenland ice core: Geophysics, Geochemistry and the Environment*, edited by C. C. Langway, H. Oeschger, and W. Dansgaard, *Monograph 33*, pp. 85-89, American Geophysical Union, Washington, DC, 1985.
- Waddington, E. D., D. A. Fisher, and R. M. Koerner, Flow near an ice divide: analysis, problems and data requirements, *Ann. Glaciol.*, 8, 171-174, 1985.



A Two-Million-Year-Old Insect Fauna from North Greenland Indicating Boreal Conditions at the Plio-Pleistocene Boundary

J. Böcher

Zoological Museum, University of Copenhagen, Copenhagen, Denmark

ABSTRACT

The Kap København Formation in NE Peary Land, Greenland, is assumed to be 2.0–2.5 Ma old, i.e., from the Plio-Pleistocene transition. Layers of organic detritus contain a wealth of well-preserved remains of land and fresh water organisms, almost all extant species.

In striking contrast to the present harsh, high arctic conditions at Kap København, the fossil plants and insects show that immediately prior to the Quaternary glaciations a subarctic climate existed in this northernmost land on earth. A rich forest-tundra bordered the Arctic Ocean, and the plant communities were populated with a diverse, predominantly boreal insect fauna.

These discoveries may have significance for the current discussion of the "greenhouse effect." What we find imbedded in the sands at Kap København may present a vision of a future climatic development.

INTRODUCTION

The Kap København Formation in northeastern Peary Land, latitude 82°25' (Figure 1), was discovered in 1979 by the Greenlandic Geological Survey [Funder and Hjort, 1980].

Detailed studies were carried out there in 1983 under the leadership of Svend Funder [Funder et al., 1984, 1985] and were continued in 1986 by the paleobotanist Ole Bennike and me [Bennike, 1987; Böcher, 1989; Bennike, 1990; Bennike and Böcher, 1990].

The Kap København Formation, consisting of more than 100 m of coastal and shallow marine sands, silts and clays, has an areal extent of more than 300 km². Biostratigraphy using mammals (*Hypolagus/Lepus*), molluscs, ostracods, and Foraminifera, paleomagnetic stratigraphy and amino acid stratigraphy suggests that the formation is 2.0–2.5 million years old (Pliocene-Pleistocene transition).

PALEOBOTANY

Paleobotanical investigations have shown that this area, the northernmost land on earth, immediately before the Pleistocene glaciations was covered with a forest-tundra rich in boreal plant species. Many of the existing common and widespread arctic-alpine plant species were present, as

were a few extinct species [Funder et al., 1985; Bennike, 1990; Bennike and Böcher, 1990].

The dominant tree was an extinct species of larch (*Larix groenlandii*; Bennike [1990]). Furthermore black spruce (*Picea mariana*), *Thuja occidentalis* and *Taxus* sp. were present. None of these conifers occur in Greenland today.

The landscape was a mosaic of forest patches interspersed with heath dominated by present arctic-alpine species such as *Dryas octopetala*, *Betula nana*, *Cassiope tetragona*, *Vaccinium uliginosum*, *Ledum palustre*. Of these only *Dryas* is present at Kap København today.

The ancient flora was mainly made up by species with a modern circumpolar distribution, but another prominent element, chiefly made up by trees and shrubs (*Thuja occidentalis*, *Picea mariana*, *Cornus stolonifera*), is now confined to North America. A few are today mainly palaearctic (*Dryas octopetala*, *Betula nana*).

The boreal species of *Thuja*, *Taxus*, *Cornus*, *Viburnum* and a number of fresh water herbs such as *Potamogeton natans* indicate a climate with a mean July temperature about 10°C. The present mean July temperature at Kap København is 3°C. This means that the paleoclimate at the Pliocene to Pleistocene boundary must have been similar to the present climate of interior southernmost Greenland,



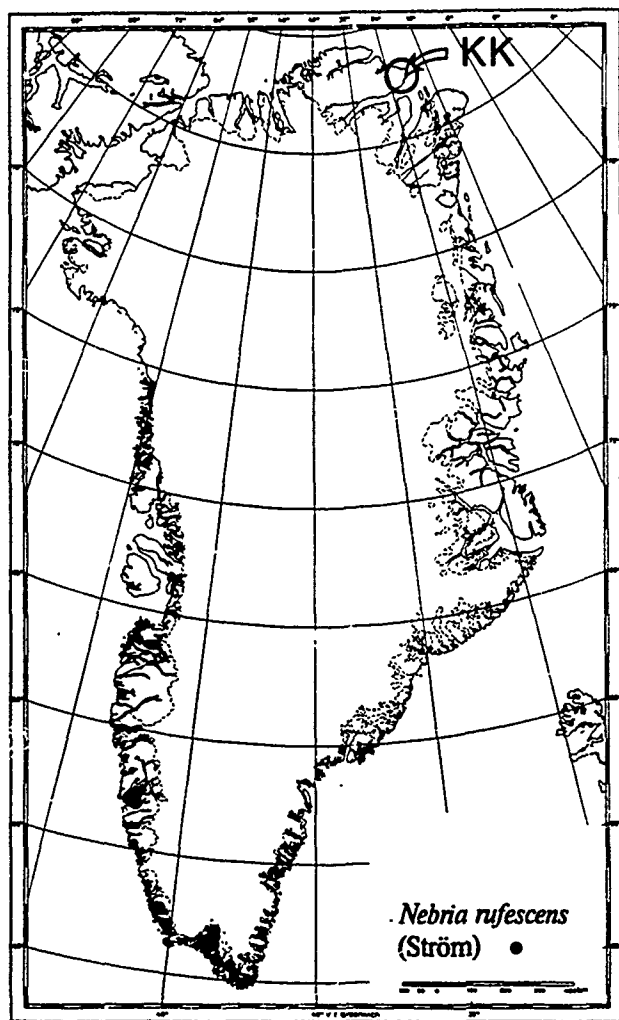


Figure 1. Present distribution in Greenland of *Nebria rufescens* (Ström) (Carabidae) and the position of the Kap København (KK).

2500 km south of Kap København, where, e.g., small birch trees (*Betula pubescens*) are able to grow. A significant difference between the two regions, however, is the length of photoperiod. Kap København has four months without sun whereas there are no months without sun in southern Greenland.

PALEOENTOMOLOGY

So far it has been possible to identify about 40 species and 60 genera (25 families, 6 orders) of insects from the Kap København fossil assemblages (Table 1). All of the identified species are extant species.

Beetles preserve better than other insects because of their hard and resistant exoskeletons, so their higher representation in the Kap København fossil assemblages is not surprising. Only part of the fossils have been identified. It is estimated that the fauna will consist of at least 120 beetle species.

The species diversity of the Kap København fossil beetle assemblage is amazing compared to the present beetle fauna of Greenland. Presently, 33 indigenous species of Coleoptera are known from Greenland [Böcher, 1988]. Most are confined to the climatically favored subarctic and low arctic

	Number of genera	Number of species
COLEOPTERA		
Carabidae	15	24
Dytiscidae	4	1
Gyrinidae	1	-
Hydrophilidae	1	2
Catopidae	1	-
Liodidae	1	-
Silphidae	1	1
Staphylinidae	11	5
Scarabaeidae	1	1
Elateridae	1	-
Buprestidae	-	-
Byrrhidae	1	-
Anobiidae	1	1
Lathridiidae	1	-
Cerambycidae	-	-
Chrysomelidae	4	-
Apionidae	1	-
Curculionidae	7	1
Scolytidae	2	-
HYMENOPTERA		
Siricidae	1	1
Tenthredinidae	-	-
Ichneumonidae	-	-
Chalcididae	-	-
Diapriidae	-	-
Torymidae	1	-
Formicidae	2	1
DIPTERA		
Chironomidae	7	1
Brachycera	-	-
Cyclorrhapha	-	-
LEPIDOPTERA		
	-	-
TRICHOPTERA		
	-	-
HEMIPTERA		
Cicadellidae	-	-

Table 1. Identified insect taxa from the Kap København Formation.

southwestern part of the country; only a few species inhabit the High Arctic. In the relatively warm interior Peary Land two species have been collected, but no living beetles have been found at Kap København.

Only one existing Greenland species, the carabid *Nebria rufescens* (Ström) (Figure 1), has been identified in the fossil material.

The insect fauna also contained three species of ants (Formicoidea) which are totally absent from Greenland today.

Some of the species are now found far away from Greenland. The carabid *Elaphrus sibiricus* Motschulsky, for example, is distributed from central Siberia eastward to China and Japan; and the carabid *Asaphidion alaskanum* Wickham is restricted to Alaska and Northwest and Yukon Territories.

The majority (90%) of the identified species are boreal. The boreal component includes temperate-boreal species such as the weevil *Grypus equiseti* Fabricius and the carabid *Notiophilus biguttatus* (Fabricius).

Many species are associated with fresh water biotopes, living in damp, luxuriant places close to the water (e.g., the carabid genera *Nebria* and *Patrobus*). Others, however, live on open, sandy or gravelly shores and banks of lakes and streams. These are generally thermophilous, diurnal and highly active predators, hunting by means of vision and, accordingly, dependent on a high incidence of sunshine during the active season (species of the carabid genera *Cicindela*, *Elaphrus*, *Asaphidion*, *Bembidion*, *Notiophilus* and the staphylinid genus *Stenus*).

Few limnic species have been identified, but the large number of unidentified water beetles (more than 20 species) plus many larval fragments of caddis flies (Trichoptera) and midges (Chironomidae) indicate the presence of an abundance of different freshwater biotopes in the ancient landscape. The occurrence of the dytiscid beetle *Agabus bifarius* (Kirby) is especially interesting because its present habitat is stated to be shaded, temporary ponds in rough fescue (*Poa*) prairie in North America [Larson, 1975].

Other species indicate dune areas (*Aegialia*), open tundra and fairly xeric heathland.

A number of species and genera such as the carabid genus *Dromius*, the "death watch beetle" (*Hadrobregmus pertinax* (L.)), woodliving weevils (*Pissodes*), bark beetles (*Scolytus*, *Pityophthorus*) and the carpenter ant (*Camponotus herculeanus* (L.)) are intimately connected with trees and thus represent further evidence of the existence of *in situ* forest when the Kap København sediments were deposited. Fly holes and galleries in fossil wood reveal the existence of still more arboricolous forms such as Buprestidae, Cerambycidae (longhorn beetles) and the giant tree wasp, *Urocerus gigas* (L.).

Similar to the biogeography of the fossil flora, the majority (55%) of the identified insect species are circumpolar or

holarctic while the remainder are nearctic (30%) and palaearctic (15%).

The paleontological and paleobotanical interpretations based on Kap København Formation fossils are in agreement. The environment 2 million years ago was biologically highly varied, in contrast to the present desert-like, high arctic conditions.

CONCLUSIONS

Studies during the last three decades, primarily in the U.K. and North America, have shown that subfossil insect assemblages, especially beetles, are a highly effective tool for the reconstruction of ancient environments [e.g., Coope, 1975, 1979, 1986; Matthews, 1977, 1988]. A method for quantifying paleoclimatic information from the present geographic ranges of beetles has been utilized to produce paleotemperature curves in the United Kingdom [Atkinson et al., 1987].

The Kap København Formation is well dated at 2 million years ago. During its deposition the position of the continents and oceans, the orientation of the earth's axis, and the position of the North Pole were all similar as today.

The fossils from the Kap København Formation at the Plio-Pleistocene boundary imply a climate, 800 km from the North Pole, that was significantly warmer, allowing trees to grow on the beaches of the Arctic Ocean.

The Kap København Formation thus presents—to cite Russell Coope (in litt.)—"a scenario that may indicate the possible consequences of global warming on a world whose geography is much as we see it today, but a scenario that has no equivalent at the present day or in later Pleistocene interglacials."

REFERENCES

- Atkinson, T. C., K. R. Briffa, and G. R. Coope, Seasonal temperatures in Britain during the past 22,000 years, reconstructed using beetle remains, *Nature*, 325, 587–592, 1987.
- Bennike, O., News from the Kap København Formation, Plio-Pleistocene, North Greenland, *Polar Research*, 5, 339–340, 1987.
- Bennike, O., The Kap København Formation: stratigraphy and palaeobotany of a Plio-Pleistocene sequence in Peary Land, North Greenland, *Meddelelser om Grønland, Geoscience* 23, 85 pp., 1990.
- Bennike, O., and J. Böcher, Forest-tundra neighbouring the North Pole: Plant and insect remains from the Plio-Pleistocene Kap København Formation, North Greenland, *Arctic*, 43, 331–338, 1990.
- Böcher, J., The Coleoptera of Greenland, *Meddelelser om Grønland, Bioscience* 26, 100 pp., 1988.
- Böcher, J., 1989, Boreal insects in northernmost Greenland: palaeo-entomological evidence from the Kap København Formation (Plio-Pleistocene), Peary Land, *Fauna norvegica, Ser. B*, 36, 37–43, 1989.
- Coope, G. R., Climatic fluctuations in Northwest Europe since the last interglacial, indicated by fossil assemblages of Coleoptera, in *Ice Ages, Ancient and Modern*, edited by A. E. Wright and F. Mosely, pp. 153–168, *Geological Journal, Special Issue* 6, 1975.
- Coope, G. R., Coleoptera analysis, in *Handbook of Holocene Palaeoecology and Palaeohydrology*, edited by B. E. Berglund, pp. 703–713, John Wiley & Sons, Chichester, 1986.
- Funder, S., and C. Hjort, A reconnaissance of the Quaternary geology of Eastern North Greenland, *Grønlands Geologiske Undersøgelse, Rapport*, 99, 99–105, 1980.
- Funder, S., O. Bennike, G. S. Mogensen, B. Noe-Nygaard, S. A. S. Pedersen, and K. S. Petersen, The Kap København Formation, a late Cainozoic sedimentary sequence in North Greenland, *Grønlands Geologiske Undersøgelse, Rapport*, 120, 9–18, 1984.
- Funder, S., N. Abrahamsen, O. Bennike, and R. W. Feyling-Hansen, Forested Arctic: Evidence from North Greenland, *Geology*, 13, 542–546, 1985.
- Larson, D. J., The predacious water beetles (Coleoptera: Dytiscidae) of Alberta: Systematics, natural history and distribution, *Quaestiones Entomologicae*, 11, 245–498, 1975.
- Matthews, J. V., Coleoptera fossils: their potential value for dating and correlation of late Cenozoic sediments, *Can. J. Earth Sci.*, 14, 2339–2347, 1977.
- Matthews, J. V., Late Tertiary arctic environments: A vision of the future?, *Geos*, 18, 14–18, 1989.

Late Quaternary Paleoceanography and Paleoclimatology from Sediment Cores of the Eastern Arctic Ocean

U. Pagels and S. Köhler

GEOMAR, Research Center for Marine Geosciences, Kiel, Germany

ABSTRACT

Box cores recovered along a N-S transect in the Eurasian Basin allow the establishment of a time scale for the Late Quaternary history of the Arctic Ocean, based on stable oxygen isotope stratigraphy and AMS ^{14}C dating of planktonic foraminifers (*N. pachyderma* l.c.). This high resolution stratigraphy, in combination with sedimentological investigations (e.g., coarse fraction analysis, carbonate content, productivity of foraminifers), was carried out to reconstruct the glacial and inter-glacial Arctic Ocean paleoenvironment.

The sediment cores, which can be correlated throughout the sampling area in the Eastern Arctic Ocean, were dated as representing oxygen isotope stages 1 to 4/5. The sedimentation rates varied between a few mm ka^{-1} in glacials and approximately one cm ka^{-1} during the Holocene. The sediments allow a detailed sedimentological description of the depositional regime and the paleoceanography of the Eastern Arctic Ocean.

Changing ratios of biogenic and lithogenic components in the sediments reflect variations in the oceanographic circulation pattern in the Eurasian Basin during the Late Quaternary. Carbonate content (1–9wt.%), productivity of foraminifers (high in interglacial, low in glacial stages) and the terrigenous components are in good correlation with glacial and interglacial climatic fluctuations.



The Record of Global Change in Circum-Antarctic Marine Sediments

P. F. Barker, C. J. Pudsey, and P. D. Larter

British Antarctic Survey (Natural Environment Research Council), Cambridge, England

ABSTRACT

Sediment drilling, using rigs located on sea ice inshore, and Ocean Drilling Program facilities farther offshore, have described the stepwise cooling of Antarctica through the Cenozoic, setting the scene for more detailed studies of short-period, recent change. Such studies will not be easy. The virtual absence of carbonate sediments and the strength of bottom currents in some regions are fundamental limitations. Nevertheless, Antarctic ocean sediments contain a record of global change which complements the record of the ice sheet, and extends it back in time. Pelagic and hemipelagic sediments of the ocean basins record changes in primary productivity, dissolution, sea ice extent and the strength of deep ocean circulation, and in the volume of the main circum-Antarctic water masses. Prograded sediments of the Antarctic continental shelf and slope contain a record of glacial/interglacial changes in ice sheet volume. Modern piston-coring techniques are capable of revealing changes over the last glacial cycle in some detail, in suitably expanded sections. At lower sediment accumulation rates, a less detailed but longer record can be obtained. It can already be shown that, at and around glacial maximum, (a) grounded ice sheets extended to the Antarctic continental shelf edge, (b) the marginal sea ice zone lay up to 5° farther north, and (c) Weddell Sea Bottom Water flow was far slower than at present. These have implications for the carbon cycle in the oceans, which is of considerable importance in global change.

INTRODUCTION

The principal elements of the circum-Antarctic climatic regime are the continental ice sheet and its fringing ice shelves, sea ice and the two main components of Southern Ocean circulation, Antarctic Bottom Water (AABW) and, bounding the Antarctic region in the north, the Antarctic Circumpolar Current (ACC). These are all potentially important to any assessment of global climate change, not only as sensitive indicators of change but also as parts of powerful climatic feedback mechanisms. For example, ice sheet melt, sea level rise, ice sheet/shelf flotation and break-out (with shelf encroachment of warmer water), loss of ice sheet support and enhanced flow form a potent positive feedback loop [Bentley, 1984; Fastook, 1984; Potter and Paren, 1985]. Another such is ice sheet/shelf and sea ice melting and global albedo reduction [e.g., Shine et al., 1984]. Other loops, affecting biogenic productivity and CO₂

transport, involve ice shelves, sea ice and bottom water formation and the vigor and axial position of the ACC.

The circum-Antarctic marine sedimentary record, sampled principally by DSDP and ODP drilling, contains evidence of the long-term development of the present regime, which sets the scene for the study of short-term (glacial/interglacial) change. For example, although paleomagnetic measurements show Antarctica to have lain over the south pole for more than 90 Ma [e.g., Norton and Sclater, 1979], a continental ice sheet appears to have extended to sea level (as demonstrated by glacial diamictites and by ice-rafted debris in marine sediments of Oligocene and younger age [see Schlich, Wise et al., 1989; Kennett and Barker, 1990 for example]) only during the last 40 Ma. The details of waxing and waning of the ice sheet since then are disputed [e.g., Miller et al., 1987; Shackleton, 1987; Prentice and Matthews, 1988], but oxygen isotopic measurements on



lower-latitude sediments imply major cooling at 37 Ma, at 16 to 12 Ma (late middle Miocene), and at about 2.4 Ma (mid-Pliocene time: see Shackleton and Kennett [1975] for example).

Deep waters also cooled significantly 37 Ma ago and deep circulation increased worldwide, causing widespread erosion [e.g., Benson, 1975; Johnson, 1985]. These changes have been attributed to high-latitude events, including the earliest production of bottom water at the Antarctic margin. Present-day AABW is renewed mainly in the southern Weddell Sea, by the production of brine beneath forming sea ice, coupled with supercooling at the base of the floating ice shelves [Gill, 1973; Foldvik and Gammelsrod, 1988]. It is uncertain whether Oligocene bottom water could have formed in exactly the same way.

At present the Polar Front, closely coincident with and probably causally related to the ACC [Gill and Bryan, 1971], isolates the Antarctic continent. It limits the southward flow of warm surface waters, and Antarctic Intermediate Water, diving northward from it, seals the base of the thermocline, maintaining the low temperature of deep waters in lower latitudes. The ACC developed in the early Miocene, following the completion of a deep-water path around the continent, with the opening of Drake Passage and separation of the continental fragments surrounding the juvenile Scotia Sea [Barker and Burrell, 1977; 1982].

The ACC is extremely vigorous, being wind-driven throughout its path. Fluctuations of the Polar Front position of several degrees of latitude are a feature of modern circulation, and eddies are common [e.g., Bryden, 1979; Cheney et al., 1983]. The ACC extends to the seabed: it erodes and redeposits abyssal sediments near its axis [e.g., Kennett and Watkins, 1976; Barker and Burrell, 1977], making a complete sedimentary record of its history difficult to obtain. There is evidence that, south of Australia at least, it has migrated northward with time [Kemp et al., 1975].

Along with the progressive separation and cooling of the Antarctic water masses over the past 40 Ma came an increase in the solubility of CaCO_3 . The calcite compensation depth (CCD) now lies at about 500 m around Antarctica south of the Polar Front, so that with rare exceptions [see Grobe et al., 1990] biogenic carbonate is not preserved in the marine sedimentary record. Antarctic deep marine sediments are siliceous biogenic (largely diatomaceous) and terrigenous in origin. The transition from a calcareous to a siliceous biofacies began in the Oligocene, and was complete in some areas by the middle Miocene (before 15 Ma at ODP Site 696, S. Orkney microcontinent), in others much later (ca. 7 Ma on Maud Rise [Barker, Kennett et al., 1988]).

The lack of biogenic carbonate precludes the easy determination of oxygen isotope paleotemperatures and ^{13}C values: oxygen isotopic measurements on diatoms have yielded plausible paleotemperatures [Labeyrie and Juillet, 1982; Leclerc and Labeyrie, 1987] but the method is difficult and slow, and has not come into common use.

A valuable contribution to an understanding of global change in the polar regions would be to establish the glacial/interglacial variability of the volume of the grounded ice sheet, the extent of ice shelves and sea ice, the volume of bottom water production and vigor of the ACC, and the intensity and extent of biogenic productivity. This would

serve to establish the sensitivity of these elements to climate change, and the polarity and strength of feedback loops. The task must be accomplished within the constraints of a vigorous ACC and pervasive carbonate (and some silica) dissolution. This paper reviews progress in two such investigations (Figure 1), and suggests ways in which they might be developed in the future.

CONTINENTAL SHELF PROGRADATION AND GROUNDING ICE SHEETS

Grounded ice sheets transport unsorted sediment (glacial till) in a sheared layer up to 10 m thick at the base of fast-flowing ice streams [Bentley, 1987; Alley et al., 1989]. Elsewhere the ice base is not lubricated in this way and ice flow (and thus sediment transport) is considerably less. There is strong evidence from drill sites in the Ross Sea and Prydz Bay [Barrett, 1989; Barron, Larsen et al., 1989] and from piston cores [e.g., Kellogg et al., 1984; Anderson et al., 1980; 1984] that glacial till occurs widely on the continental shelves of Antarctica. Off west side of the Antarctic Peninsula, an area of moderately low temperatures, high relief and precipitation (and thus of fast glacier flow), piston core and sidescan sonar data (BAS unpublished) suggest that debris

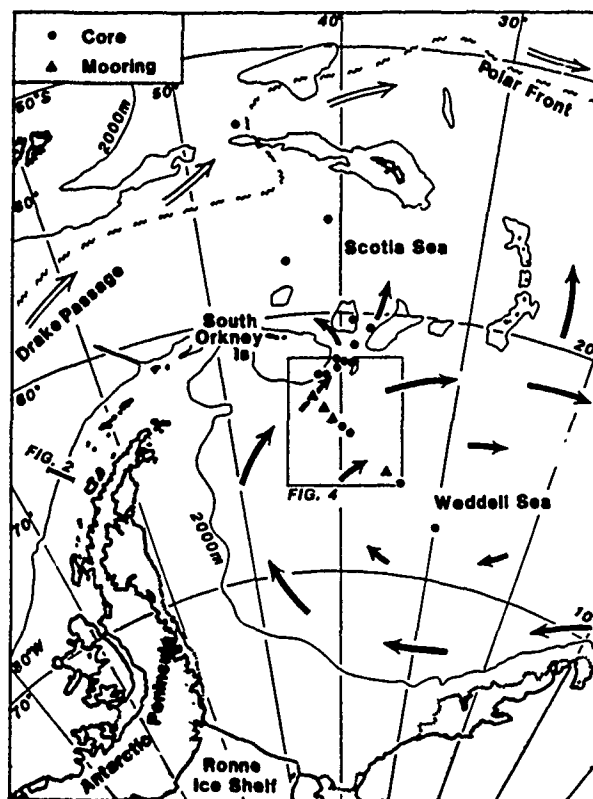


Figure 1. Locations of seismic reflection profile (Figure 2) on Antarctic Peninsula margin [Larter and Barker, 1989, 1991], and of piston core and mooring transect in northern Weddell Sea [Pudsey et al., 1988; Pudsey, in prep.] (Figure 4). Weddell Sea Bottom Water is formed on the southern shelf and slope of the Weddell Sea, beneath and in front of the Filchner and Ronne Ice Shelves, and flows clockwise around the gyre (black arrows), across the transect. Farther downstream, some escapes northward into the South Atlantic beneath the Antarctic Circumpolar Current (double arrows), and westward into the Scotia Sea and Southeast Pacific.

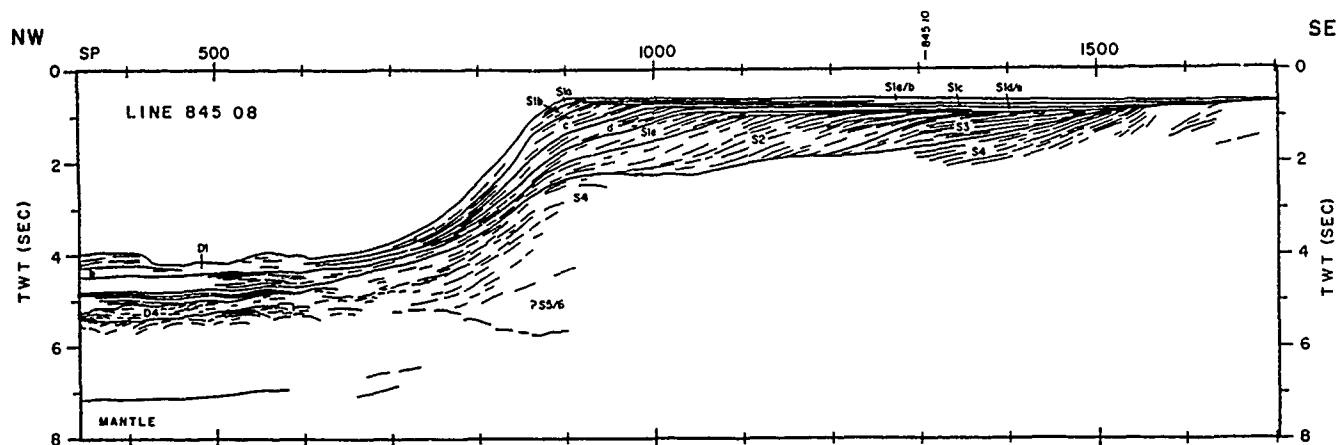


Figure 2. Line drawing of seismic reflection profile across the Antarctic Peninsula Pacific margin (located in Figure 1), showing prograded sediment wedge (Sequences S1, S2) built from basal till transported beneath ice sheets grounded to the shelf edge during glacial maxima [from Larter and Barker, 1989, 1991]. Note inward-sloping shelf profile and steep slope (up to 17°). Similar wedges occur elsewhere around Antarctica off ice sheet drainage outlets. See Figure 3 for model.

was transported to the continental shelf edge by a grounded ice sheet during the last glacial maximum. A thick wedge of prograded sediment has built out the continental shelf [Larter and Barker, 1989, 1991] (Figure 2), and the great depth of the shelf, inward-sloping shelf profile, high seabed acoustic velocity and steep continental slope suggest that the wedge is largely derived from glacial till. A seismic sequence stratigraphic model of glacial/interglacial sedimentation on shelf and slope has been developed [Larter and Barker, 1989, 1991] (Figure 3) which infers an extreme glacial/interglacial cyclicity in both the amount and nature of terrigenous sediment supply to the shelf edge and upper slope. Deposition on the slope is continuous, with varying lithology, but on the shelf deposition is sporadic and re-erosion common. Along the western Antarctic Peninsula shelf at least, the wedge has prograded evenly along strike. Thus it seems likely that, whatever topographic heterogeneity controlled ice stream location inshore during glacial maxima, on the outer shelf the unresisting tills allowed ice streams to diverge and coalesce into broad low-profile ice sheets, so that at the continental shelf edge they became essentially a line source of sediment.

Similar prograded sediments are found off the major ice drainage outlets around the continent, in Prydz Bay [Stagg, 1985; Barron, Larsen et al., 1989], the southern Weddell Sea [Haugland et al., 1985] and Ross Sea [Hinz and Block, 1984] and, less well-developed, on the Wilkes Land margin [Eitrem and Smith, 1987]. In all these places, the outer shelf is smooth with high seabed acoustic velocities, the shelf is deeper inshore and the slope is smooth. In these places also, the topset beds of the prograded wedge parallel the present-day shelf profile. In general, topset beds at these other ice sheet drainage locations are poorly developed compared with the Antarctic Peninsula, where steady but rapid thermal subsidence following mid- to late Cenozoic ridge-crest subduction has helped preserve them (Figure 1).

Elsewhere around Antarctica, away from major ice stream outlets, those margins which have been examined show rougher and slightly shallower continental shelves (though still overdeepened inshore) and very dissected slopes. Ice sheets were probably grounded to the shelf edge here, as elsewhere, but were much slower-moving, and

transported much less sediment. These margins are comparatively sediment starved.

The prograded wedges and deep shelves are strong evidence that, around most of Antarctica during the last glacial maximum, ice sheets were grounded out to the continental shelf edge, and that similar extensive grounding occurred at earlier glacial maxima, for an unknown period back in time. In consequence, the prograded wedges contain a record (continuous in the foreset beds) of the extent of grounded ice sheets through time. In the north of the Antarctic Peninsula, where tectonic events can be precisely dated, the glacial sedimentary record offshore is limited to about the last 5 Ma [Larter and Barker, 1989, 1991]. There are indications that 5 Ma may be the full extent in this region of the mode of glaciation that involves ice sheet grounding to the shelf edge: drilling at ODP Site 694 [Barker, Kennett et al., 1988] recorded a pulse of massive turbidites of latest Miocene age. A smaller, similar feature was sampled at Site 696. These were considered to reflect the deep erosion of a previously weathered and better-sorted sedimentary succession on the Antarctic Peninsula and South Orkney continental shelf, at the onset of the shelf-edge grounding mode. Older glaciations along the Antarctic Peninsula [e.g., Birkenmajer and Zastawniak, 1989] may have been more local events.

Elsewhere around Antarctica, there is undoubtedly an older record of grounded ice sheets extending to the shelf edge, than exists along the Antarctic Peninsula. CIROS-1 drilling in the Ross Sea for example [Barrett, 1989], sampled what appears to be a similarly produced topset/foreset succession of Oligocene age.

Recognition of this common glacial/interglacial mode of deposition around Antarctica opens the door to a complete assessment of the history of continental glaciation (beyond the threshold level of ice stream extension to sea level), to a comparison of the severity of East and West Antarctic glaciation and even, with the aid of realistic numerical models, to estimates of the amount of sediment removed from the continent by glaciation through time, and changes in the volume of grounded ice. To do all this would need careful description of the sediment masses by high resolution seismic stratigraphy, and drilling (in several areas) for chronostratigraphic control. The older, inshore part of the

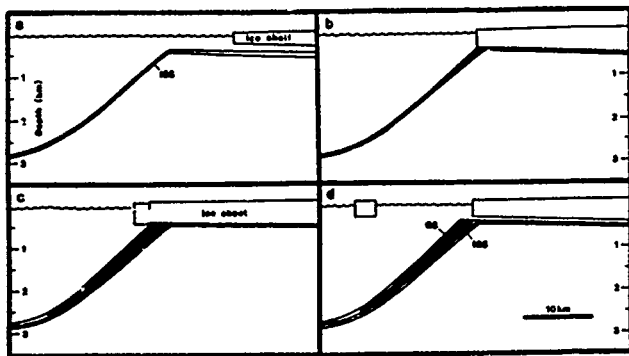


Figure 3. Model for development of a single glacial seismic sequence on outer shelf and slope, during one glacial cycle: (a) interglacial and early stage of ice sheet advance; intergrounding subsequence (IGS) of hemipelagic biogenic mud with ice-rafted detritus is being deposited on shelf and slope, seaward of ice shelf (as today); (b) initial grounding; erosion and compaction of IGS start beneath grounded ice, with basal debris transport to (shelf edge) grounding line; (c) glacial maximum; erosion, compaction, basal transport and upper slope deposition of grounding subsequence GS (reworked IGS from shelf and till from farther inland) continue; (d) early stage of glacial retreat; sequence boundary, as deposition of IGS recommences on continental shelf. Note that deep glacial erosion on continental shelf during (b) and (c) will merge single sequences together: only 8 sequences in ca. 5 Ma have been identified so far in S1 and S2 of Figure 2; however, a complete and detailed record exists within the slope deposits.

succession will be accessible by drill rigs located on sea ice, like CIROS-1, but the younger, outer shelf and slope provinces can only be drilled by a dynamically positioned vessel like JOIDES Resolution. Community efforts are underway [Cooper and Webb, 1990] to define the sediment distribution and coordinate a drilling proposal. The considerable added benefit of such work lies in testing the grounded ice sheet origin of global eustatic sea level changes [e.g., Haq et al., 1987]. This is still controversial, in detail for pre-Pleistocene times and in principle for pre-Oligocene times.

Some environments, notably the present-day inshore fjords and ice shelf fronts, contain a high-resolution sedimentary record of later post-glacial evolution [e.g., Domack, 1990], but the earlier record will tend to have been eroded during the last glacial maximum. It is preserved in the alternating lithologies of till and diatomaceous mud in the expanded sections of the foreset beds on the continental slope, but these are difficult to sample without a drill ship. To obtain a detailed record of the last glacial cycle, it will be necessary to look elsewhere. One option, not seriously attempted as yet, is to see if the intense cyclicity of shelf sediment transport is preserved in any way in the turbidite and other deposits of the continental rise, which have been produced by mass wasting and redeposition of the continental slope deposits. Turbidites are not widely used to provide paleoenvironmental information, for obvious reasons, but the particular environment of the Antarctic continental margin, where upper slope sediments are unsorted and were deposited essentially from a line source at the shelf break, may be more propitious. Long piston cores would provide suitably expanded sections.

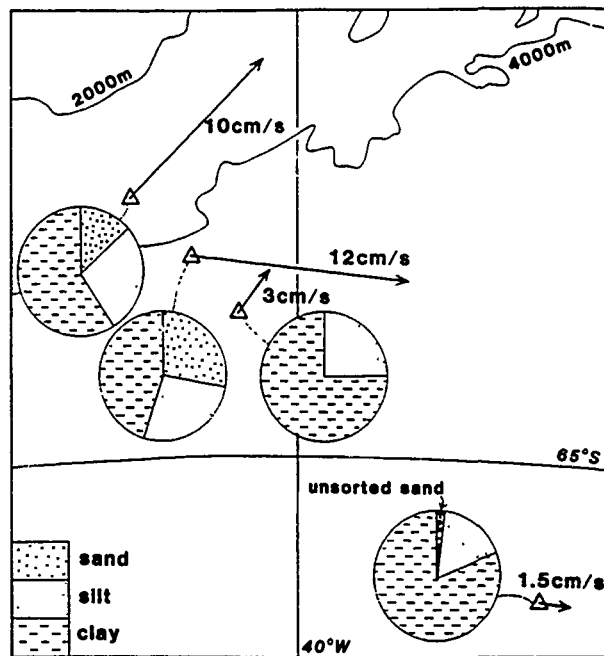


Figure 4. Current velocity and surface sediment grain size at the Weddell Sea mooring sites (located in Figure 1), showing the strong correlation between them. Where average currents are fastest, the proportion of silt and well-sorted fine sand is highest. Where average currents are slowest, there is as much as 80% clay, and the only sand is unsorted, ice-rafted. Glacial age sediments are finer-grained at all sites, reflecting a much slower WSBW transport.

BOTTOM WATER FORMATION

Antarctic Bottom Water today is formed mainly as Weddell Sea Bottom Water (WSBW), by mixing of the ambient Warm Deep Water with waters that have been made more salty by the repeated extraction of fresh water as newly formed sea ice, and cooled beneath the floating ice shelves of the Weddell Sea [Gill, 1973; Foldvik and Gammelsrod, 1988]. WSBW forms the basal layer of the clockwise Weddell Gyre, and some escapes northward beneath the ACC, through deep topographic gaps into the Atlantic and Indian Oceans [Georgi, 1981], and westward along the Antarctic margin into the Pacific. It is a principal supplier of oxygen to the world's deep waters, yet is corrosive to both calcareous and siliceous skeletons of marine organisms.

Investigation of the glacial/interglacial variability of Antarctic Bottom Water makes use of hemipelagic sediments, transferred from the upper continental slope by mass wasting and entrained as a nepheloid layer within the Weddell gyre. A core transect in the northern Weddell Sea (Figure 3) has been used to examine the variations in sediment grain size, spatially away from the gyre margin and temporally down each core [Pudsey et al., 1988]. An array of moored current meters, transmissometers and sediment traps is presently deployed along the line of the transect, and is intended to provide an understanding of the relation between modern sedimentation and bottom water circulation.

Preliminary analysis of the current meter data [Pudsey, in prep.] shows that WSBW in the northern Weddell Sea flows E to NE along the margin of the basin at speeds up to 15 cm sec⁻¹, decreasing towards the gyre center. Sparse older measurements [Foster and Middleton, 1979] are in accord.

The sediments cored are mainly fine-grained terrigenous (hemipelagic) mud, with minor biogenic silica (diatoms) and sparse ice-rafted debris. Sediment grain size and diatom content vary systematically: in cores from 3500 to 4600 m water depth, between 59° and 64°S, the proportion of silt and well-sorted sand in surface sediments increases with average bottom current speed (Figure 4), and the diatom content increases northward as the time extent of seasonal sea ice cover decreases.

Down-core, there is an alternation of diatom-rich and diatom-poor sediment, on a 1–2 m scale, and intervals with more diatoms contain a higher proportion of silt to clay. Stratigraphic control is imperfect, but a preliminary stratigraphy based on magnetic remanence, radiolaria and the relative abundance of certain diatom species strongly suggests that the observed cyclicity in texture and composition corresponds to the main 100 Ka glacial/interglacial cycle [Pudsey et al., 1988; Jordan and Pudsey, in prep.].

Antarctic sea ice cover prevents diatom productivity, and dissolution also reduces the diatom content of abyssal sediments: diatoms are preserved in sea bed sediments today in the northern Weddell Sea where the ice-free period exceeds 3 months. Changes in diatom content down-core are considered to show several long-term N–S (or NE–SW) movements of the summer sea ice edge, similar to others previously detected [Hays et al., 1976; DeFelice and Wise, 1981], and reflecting glacial cycles.

In theory, grain size change in hemipelagic sediment reflects change in either the sediment source or sediment transport. We have already described (Figure 2) a model of glacial shelf-slope sediment transport that includes striking glacial/interglacial contrast in sediment supply to the shelf edge and upper slope, the source region for the hemipelagics. However, several factors argue against the survival of a glacial/interglacial "source signal," as far downstream as the core transect (Figure 3): the considerable sediment catchment range (from 30°E around the entire Weddell Sea margin) of bottom waters crossing the core/mooring transect, the lack of a local (South Orkney) source [King and Barker, 1988], the unsorted nature of glacial tills and evidence from older reworked diatoms of deep sampling of the continental slope by the mass wasting processes which supply the nepheloid layer, are all important. Also of course, the unsorted till presented to the upper slope during glacials has a much coarser grain size distribution than the suspended fine fraction reaching the same site during interglacials: a direct glacial–interglacial source signal would thus be opposite to that observed. Thus, the finer grain size of glacial sediments is almost certainly a true transport signal, reflecting a weaker bottom water circulation. Sites

where modern bottom currents exceed 10 cm sec⁻¹ have a glacial grain size distribution more appropriate to a bottom current an order of magnitude less [Pudsey, in prep.].

This is a preliminary result only, at present, and more work is needed to achieve precise estimates of paleo-current strength and volume transport. However, the clear conclusion that WSBW transport was significantly slower during glacials has implications for global climate, that can be considered now.

(1) The reduction in WSBW transport during glacial maxima is compatible with its conjectured mode of origin: ice sheets grounded to the shelf edge do not expose the deep, cold lower surface that presently causes supercooling, and a more extensive pack ice zone would probably reduce the incidence of coastal polynyas where repeated local sea ice formation creates a concentrated brine.

(2) Reduced WSBW production during glacial periods means reduced oxygen transport to the deep sea, so that less is available to fuel planktonic decay and benthonic respiration (and production of deep CO₂), and a reduced contribution to deep circulation in low latitudes. On both counts this means an effective increase in deep water "age," that may contribute to the ¹⁴C result reported by Shackleton et al. [1988]. It is even possible (though this has not been reported) that anoxic bottom waters could have been created in places, increasing the carbon flux to the sediments. Models of oceanic regulation of atmospheric CO₂, that make use of data on glacial/interglacial variability, will need to take these effects into account.

(3) Increased sea ice cover during glacials reduced biogenic productivity (and thus carbon drawdown into deep water) within the Antarctic zone. In global terms, however, the total effect is indeterminate, since the ACC axis (Polar Front) and other oceanic boundaries would have shifted also. ACC behavior affects climate both directly (it hinders the southward migration of warm waters at most depths) and indirectly (it is the boundary between largely siliceous and largely calcareous primary production, and site of a huge step in the depth of the CCD, a key indicator of dissolved CO₂). Clearly it is important to extend studies of glacial/interglacial variation to the ACC, to describe changes in its velocity and axial position.

ACKNOWLEDGMENTS

We are grateful to Marion Barber, whose analysis of the Weddell Sea current meter data provided the vector averages displayed in Figure 4.

REFERENCES

- Alley, R. B., D. D. Blankenship, S. T. Rooney, and C. R. Bentley, Sedimentation beneath ice shelves: the view from Ice Stream B, *Mar. Geol.*, **85**, 101–120, 1989.
- Anderson, J. B., D. D. Kurtz, E. W. Domack, and K. M. Balshaw, Glacial and glacial marine sediments of the Antarctic continental shelf, *J. Geol.*, **88**, 399–414, 1980.
- Anderson, J. B., C. F. Brake, and N. C. Myers, Sedimentation on the Ross Sea continental shelf, Antarctica, *Mar. Geol.*, **57**, 295–333, 1984.
- Barker, P. F., and J. Burrell, The opening of Drake Passage, *Mar. Geol.*, **25**, 15–34, 1977.
- Barker, P. F., and J. Burrell, The influence on Southern Ocean circulation, sedimentation and climate of the opening of Drake Passage, in *Antarctic Geoscience*, edited by C. Craddock, pp. 377–385, Univ. Wisconsin Press, Madison, 1982.
- Barker, P. F., J. P. Kennett et al., *Proc. ODP, Init. Repts.*, **113**, Ocean Drilling Program, College Station, TX, 1988.
- Barrett, P. J., Antarctic Cenozoic history from the CIROS-I drillhole, McMurdo Sound, *DSIR Bulletin*, **245**, 251 pp., Wellington, New Zealand, 1989.
- Barron, J., B. Larsen et al., *Proc. ODP, Init. Repts.*, **119**, Ocean Drilling Program, College Station, TX, 1989.
- Benson, R. H., The origin of the psychrosphere as recorded in changes in deep-sea ostracod assemblages, *Lethaia*, **8**, 69–83, 1975.
- Bentley, C. R., Some aspects of the cryosphere and its role in climatic change, *AGU Geophysical Monograph* **29**, 207–220, 1984.
- Bentley, C. R., Antarctic ice streams: a review, *J. Geophys. Res.*, **92**, 8843–8858, 1987.
- Birkenmajer, K., and E. Zastawniak, Late Cretaceous–early Tertiary floras of King George Island, West Antarctica: their stratigraphic distribution and palaeoclimatic significance, in *Origins and Evolution of the Antarctic Biota*, edited by J. A. Crame, *Geol. Soc. Sp. Publ.*, **47**, 227–240, 1989.
- Bryden, H. L., Poleward heat flux and conversion of available potential energy in Drake Passage, *J. Mar. Res.*, **37**, 1–22, 1979.
- Cheney, R., J. G. Marsh, and B. D. Beckley, Global meso-scale variability from colinear tracks of SEASAT altimeter data, *J. Geophys. Res.*, **88**, 4343–4354, 1983.
- Cooper, A. K., and P. N. Webb, International Workshop on Antarctic Offshore Seismic Stratigraphy (ANTOSTRAT): Overview and Extended Abstracts, *U.S. Geol. Surv. Open-File Report* 90-309, 130-4, 1990.
- DeFelice, D. R., and S. W. Wise, Jr., Surface lithofacies, biofacies and diatom diversity patterns as models for delineation of climatic change in the southeast Atlantic Ocean, *Mar. Micropal.*, **6**, 29–70, 1981.
- Domack, E. W., Late Quaternary and pre-glacial stratigraphic sequences along the East Antarctic margin: the record from inner shelf basins, in International Workshop on Antarctic Offshore Seismic Stratigraphy (ANTOSTRAT): Overview and Extended Abstracts, A. K. Cooper and P. N. Webb, conveners, *U.S. Geol. Surv. Open-File Report* 90-309, 130-4, 1990.
- Eittrheim, S. L., and G. L. Smith, Seismic sequences and their distribution on the Wilkes Land margin, in *The Antarctic continental margin: geology and geophysics of offshore Wilkes Land*, edited by S. L. Eittrheim and M. A. Hampton, Circum-Pacific Council for Energy and Mineral Resources Earth Science Series, **5A**, 15–43, Houston, Texas, 1987.
- Fastook, J. L., West Antarctica, the sea-level-controlled marine instability: past and future, *AGU Geophysical Monograph* **29**, 275–287, 1984.
- Foldvik, A., and T. Gammelsrod, Notes on Southern Ocean hydrography, sea-ice and bottom-water formation, *Palaeogeogr., Palaeoclim., Palaeoecol.*, **67**, 3–17, 1988.
- Foster, T. D., and J. H. Middleton, Variability in the bottom water of the Weddell Sea, *Deep-Sea Res.*, **26**, 743–762, 1979.
- Georgi, D. T., Circulation of bottom waters in the southwestern South Atlantic, *Deep-Sea Res.*, **28**, 959–79, 1981.
- Gill, A. E., Circulation and bottom water production in the Weddell Sea, *Deep-Sea Res.*, **20**, 111–140, 1973.
- Gill, A. E., and K. Bryan, Effects of geometry on the circulation of a three-dimensional southern-hemisphere ocean model, *Deep-Sea Res.*, **18**, 685–721, 1971.
- Grobe, H., A. Mackensen, H.-W. Hubberten, V. Spiess, and D. K. Fuetterer, Stable isotope and Late Quaternary sedimentation rates at the Antarctic continental margin, in *Geological History of the Polar Regions: Arctic versus Antarctic*, edited by U. Bleil and J. Thiede, pp. 539–572, Kluwer Acad. Publ., Dordrecht, 1990.
- Haq, B. U., J. Hardenbol, and P. R. Vail, Chronology of fluctuating sea levels since the Triassic, *Science*, **235**, 1156–1167, 1987.
- Haugland, K., Y. Kristoffersen, and A. Velde, Seismic Investigations in the Weddell Sea Embayment, *Tectonophysics*, **114**, 293–313, 1985.
- Hays, J. D., J. A. Lozano, N. J. Shackleton, and G. Irving, Reconstruction of the Atlantic and eastern Indian Ocean sectors of the 18,000 B.P. Antarctic Ocean, *Geol. Soc. Amer. Mem.* **145**, 337–372, 1976.
- Hinz, K., and M. Block, Results of geophysical investigations in the Weddell Sea and in the Ross Sea, Antarctica. Exploration in New Regions, *Eleventh World Petroleum Congress, London. PD 2(1)*, pp. 1–13, 1983.
- Johnson, D. A., Abyssal teleconnections II. Initiation of Antarctic Bottom Water flow in the southwestern Atlantic, in *South Atlantic Paleooceanography*, K. J. Hsu and H. J. Weissert, pp. 243–281, Cambridge Univ Press, 1985.
- Kellogg, T. B., R. S. Truesdale, and L. E. Osterman, Late Quaternary extent of the West Antarctic ice sheet, new evidence from Ross Sea cores, *Geology*, **7**, 249–253, 1979.
- Kemp, E. M., L. A. Frakes, and D. E. Hayes, Paleoclimatic significance of diachronous biogenic facies, Leg 28, Deep Sea Drilling Project, in *Init. Repts., DSDP*, **28**, D. E. Hayes, L. A. Frakes, and others, pp. 909–918, U.S. Govt. Printing Office, Washington, DC, 1975.
- Kennett, J. P., and P. F. Barker, Latest Cretaceous to Cenozoic climate and oceanographic developments in the Weddell Sea, Antarctica: an Ocean-Drilling perspective, in *Proc ODP, Sci. Results*, **113**, P. F. Barker, J. P. Kennett, and others, pp. 937–960, Ocean Drilling Program, College Station, TX, 1990.

- Kennett, J. P., and N. D. Watkins, Regional deep-sea dynamic processes recorded by late Cenozoic sediments of the southeastern Indian Ocean, *Geol. Soc. Amer. Bull.*, 87, 321-339, 1976.
- King, E. C., and P. F. Barker, The margins of the South Orkney microcontinent, *J. Geol. Soc.*, 145, 317-331, 1988.
- Larter, R. D., and P. F. Barker, Seismic stratigraphy of the Antarctic Peninsula Pacific margin: a record of Pliocene-Pleistocene ice volume and paleoclimate, *Geology*, 17, 731-734, 1989.
- Larter, R. D., and P. F. Barker, Neogene interaction of tectonic and glacial processes at the Pacific margin of the Antarctic Peninsula, in *Sea Level Change at Active Plate Margins*, edited by D. I. M. Macdonald, Oxford University Press, 1991, In press.
- Labeyrie, L. D., and A. Juillet, Oxygen isotope exchangeability of diatom valve silica; interpretation and consequences for paleoclimatic studies, *Geochim. Cosmochim. Acta*, 46, 967-975, 1982.
- Leclerc, A. J., and L. Labeyrie, Temperature dependence of the oxygen isotopic fractionation between diatom silica and water, *Earth Planet. Sci. Lett.*, 84, 69-74, 1987.
- Miller, K. G., R. G. Fairbanks, and G. S. Mountain, Tertiary oxygen isotope synthesis, sea-level history and continental margin erosion, *Paleoceanography*, 2, 1-19, 1987.
- Norton, I. O., and J. G. Sclater, A model for the evolution of the Indian Ocean and the breakup of Gondwanaland, *J. Geophys. Res.*, 84, 6803-6830, 1979.
- Potter, J. R., and J. G. Paren, Interaction between ice shelf and ocean in George VI Sound, Antarctica, in *Oceanology of the Antarctic Continental Shelf*, edited by S. S. Jacobs, *Antarct. Res. Ser.* 43, pp. 35-58, Amer. Geophys. Union, Washington, DC, 1985.
- Prentice, M. L., and R. K. Matthews, Cenozoic ice volume history: development of a composite oxygen isotope record, *Geology*, 16, 963-966, 1988.
- Pudsey, C. J., P. F. Barker, and N. Hamilton, Weddell Sea abyssal sediments: a record of Antarctic Bottom Water flow, *Mar. Geol.*, 81, 289-314, 1988.
- Schlich, R., S. W. Wise, Jr., et al., *Proc. ODP, Init. Repts.*, 120, Ocean Drilling Program, College Station, TX, 1989.
- Shackleton, N. J., Oxygen isotopes, ice volume and sea-level, *Quaternary Science Reviews*, 6, 183-190, 1987.
- Shackleton, N. J., and J. P. Kennett, Palaeotemperature history of the Cenozoic and the initiation of Antarctic glaciation: oxygen and carbon isotope analyses in DSDP sites 277, 279 and 281, in *Init. Repts, DSDP*, 29, J. P. Kennett, R. E. Houtz, et al., pp. 743-755, U.S. Govt. Printing Office, Washington, DC, 1975.
- Shackleton, N. J., J.-C. Duplessy, M. Arnold, P. Maurice, M. A. Hall, and J. Cartlidge, Radiocarbon age of last glacial Pacific deep water, *Nature*, 335, 708-711, 1988.
- Shine, K. P., A. Henderson-Sellers, and R. G. Barry, Albedo-climate feedback: the importance of cloud and cryospheric variability, in *New Perspectives in Climate Modelling*, edited by A. Berger and C. Nicolis, pp. 135-155, Elsevier, 1984.
- Stagg, H. M. J., The structure and origin of Prydz Bay and MacRobertson Shelf, East Antarctica, *Tectonophysics*, 114, 315-340, 1985.

Eolian Sediments in Arctic Alaska as Sources of Paleoenvironmental Data

L. David Carter

U.S. Geological Survey, Anchorage, Alaska, U.S.A.

ABSTRACT

Eolian sand, silt, and associated fluvial and lacustrine sediments are widespread in Alaska north of the Brooks Range. These sediments and intercalated paleosols record late Quaternary episodes of widespread eolian sediment transport separated by periods of relative landscape stability and the growth of organic soils. The eolian sediments represent paleoenvironments much different from the modern one, in which eolian sediment transport is principally limited to areas adjacent to sediment sources, such as flood plains. Information about these paleoenvironments and their contemporary climates can be obtained by studying the morphology, distribution, and sedimentology of the sediments, and the fossil fauna and flora they contain. For example, eolian sedimentary structures and facies relations can provide information about past wind directions, snow cover, and summer surface moisture conditions and gradients. Fossils such as beetles and ostracods contained in the fluvial and lacustrine sediments can yield information regarding summer temperature and changes in evaporation/precipitation ratios. Furthermore, the sediments and paleosols can be dated by thermoluminescence and radiocarbon to provide a chronology of paleoclimatic and pale-environmental change. Present data suggest three major episodes of widespread eolian sediment movement during the latest glacial/inter-glacial cycle: (1) a long period coincident with the Wisconsin glaciation during which climate was cooler and drier than today and much of the North Slope was a polar desert; (2) an interval during the latest Pleistocene and early Holocene in which climate was warmer and surface moisture conditions were drier than today; and; (3) one or more brief late Holocene intervals during which climate was probably cooler and drier than today. These eolian sediments and intercalated paleosols are being studied in detail as part of the USGS Climate Change Program in order to understand how past environments in arctic Alaska have responded to climatic change. In particular, the paleoenvironment of the latest Pleistocene-early Holocene warm period is being examined as a possible analog for the environment that could result from future climatic warming.



92-17849



Paleoclimatic Significance of High Latitude Loess Deposits

James E. Begét

Dept. Geology and Geophysics, University of Alaska Fairbanks, Fairbanks, Alaska, U.S.A.

ABSTRACT

Loess deposits reflect changing environmental conditions in terrestrial regions, and contain long paleoclimatic records analogous to those found in marine sediments, lacustrine sediments, and ice sheets. Alaskan loess was deposited at rates of *ca.* 0.05–0.5 mm yr⁻¹ during the last 2–3 × 10⁶ years; loess deposits contain some of the longest and most complete proxy climate records yet found. New analytical methods are used to reconstruct changes in climate and atmospheric regime including wind intensity, storminess, temperature, and precipitation. Loess also contains a history of permafrost and paleosol formation, volcanic eruptions, and paleoecologic changes in high latitude regions, as well as Quaternary fossils and early man sites and artifacts. Time series analysis of proxy climate data from loess supports the astronomic model of climate change, although some transient climate events recorded in loess records are too short to be explained by orbital insolation forcing, and may instead correlate with rapid, short-term changes in atmospheric CO₂ and CH₄ content.

INTRODUCTION

Much of our understanding of the pattern and timing of climate changes during the Pleistocene comes from studies of drillcore taken from marine sediments, lacustrine sediments, and ice sheets [Martinson et al., 1987; Kashiwaya et al., 1988; Lorius et al., 1989]. Sedimentation in these environments is continuous or semi-continuous, and in some cases remarkably complete geologic records of sedimentation spanning the last 10⁵–10⁶ years have been obtained (Figure 1). Variations in the nature and character of such sediments through time has been linked with the effects of global climate forcing on local environments.

Similar long proxy records of climate change are extremely rare in terrestrial settings. Thick loess deposits, formed by the incremental accumulation of wind-blown dust, are the closest terrestrial analogue to marine, lacustrine, and ice sheet deposits. Loess in Alaska and other high latitude regions generally accumulates seasonally, as dust entrained by wind from river floodplains is deposited mainly in the late spring, summer, and early fall. Thick loess deposits integrate the results of many successive episodes of deposition, and provide a smoothed record of environmental changes.

The examination of loess deposits provides a new means of reconstructing long-term global changes of climate. Comparison of proxy climate records from loess deposits with those from ice sheets, and marine and lacustrine deposits found in other areas of the world reveals additional information on the character, rate, magnitude, distribution, and forcing mechanisms of global climate changes, particularly as they affected sensitive terrestrial high latitude regions.

PROXY CLIMATIC RECORDS FROM HIGH LATITUDE LOESS DEPOSITS

Thin eolian dust deposits may cover as much as 10% of the earth's surface [Pye, 1987], but thick accumulations of loess are rare. Recently, it has been shown that 200-m-thick loess in China contains a record of at least the last 2.4 Myr [Heller and Liu, 1982], while 30- to 70-m-thick loess in unglaciated central Alaska is as old as 2.5–3.0 Myr [Westgate et al., 1990]. Thick loess deposits are also present in unglaciated Siberia and eastern Europe, although their age is not well known. This discussion of paleoclimatic records from high latitude loess deposits will emphasize recent studies of Alaskan sections, although much of the discussion may be pertinent to the understanding of thick loess sections in Siberia and other high latitude areas.

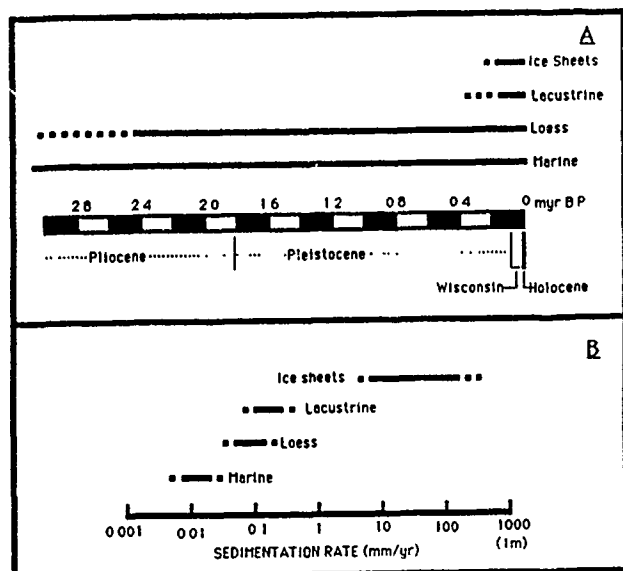


Figure 1. (A). Comparative duration of Quaternary proxy climate records obtained from marine sediments, loess, lacustrine sediments, and ice cores. (B). Comparison of characteristic average sedimentation rates for long marine, loess, lacustrine, and ice sheet proxy climatic sequences.

Alaskan loess is primarily derived from comminuted glacial silt. Large glacial rivers transport the silt for tens or even hundreds of kilometers downstream, where wind episodically remobilizes the silt from river bars [Péwé, 1955]. The thickest Alaskan loess has accumulated in low-lying vegetated and protected areas downwind but near major rivers in unglaciated central Alaska [Begét, 1988].

Loess deposition in most mid-latitude areas of the world was interrupted during major breaks lasting 10^3 – 10^4 years, corresponding to warm interglacial and interstadial intervals when continental ice sheets disappeared and loess deposition stopped. In contrast, some Alaskan loess deposits covering at least 2 – 3×10^5 years appear to be essentially continuous [Begét and Hawkins, 1990]. Radiocarbon dating clearly shows that loess deposition has continued through the Holocene in some areas of Alaska, and older loess deposits also appear to record sedimentation during both glacial and some interglacial periods [Péwé et al., 1988; Begét et al., 1990], perhaps because glaciers have rarely disappeared from the mountains of Alaska during the Pleistocene. Consequently, Alaskan loess can be used to reconstruct changes in Arctic environments during both glacial and interglacial periods of the past, and contains an unusually comprehensive record of prehistoric global climate changes in high latitude regions.

The processes which produce loess are responsive to climate change. Loess is mobilized in suspension during large windstorms, and so is subject to efficient density fractionation during eolian transport. The maximum and modal grain size, mineral content, deposition rate, magnetic susceptibility, and other characteristics of loess deposits change with distance away from a dust source, and vary through time at a single site in response to changes in the intensity or direction of predominant winds [Begét et al., 1990]. By combining magnetic susceptibility and grain size data

reflecting wind intensity with geologic evidence of permafrost or paleosol formation and paleoecologic data it is possible to reconstruct many aspects of ancient climate and environment in high latitude regions.

Sedimentation rates of Alaskan loess vary from about 0.05 – 0.5 mm yr $^{-1}$, with the highest rates occurring nearest rivers which are loess sources, and lower rates at increasingly distal and higher sites [Begét, 1990]. The wide range in sedimentation rate is important in loess paleoclimatic studies, as the thickest, longest loess records generally occur in areas of low sedimentation rate, while shorter records with higher resolution can be found on younger geologic surfaces nearer to loess sources.

Fossils are common in high latitude loess. In some cases entire large Pleistocene mammals such as mammoths and bison have been frozen and preserved in excellent condition in permafrost in reworked loess, providing important information on the paleoecology and paleoenvironments of high latitude areas [Guthrie, 1990]. Not as well known are the numerous examples of frozen soil and wood layers, including perfectly preserved logs, plants, and leaves more than 100,000 years old, which provide an unparalleled direct record of ancient high latitude environments during previous interglacials [Edwards and McDowell, 1990; Begét et al., 1991]. Many early man sites and artifacts have also been found in loess, particularly in Siberia, Alaska, and China.

DATING PALEOCLIMATIC RECORDS IN LOESS

Numerous geochronologic techniques are available to date loess or materials commonly found in Alaskan loess (Table 1). Techniques which have been applied to loess in the past include isotopic and radiogenic methods such as conventional and accelerator mass spectrometry (AMS) ^{14}C , K–Ar, Uranium-series, fission-track and isothermal plateau fission-track, and thermoluminescence dating. In some cases it may also be possible to utilize the ^{39}Ar – ^{40}Ar method, and uranium-trend dating, electron-spin resonance, and calibrated influx measurements of cosmogenic isotopes to date loess sections. A calibrated influx of tropospheric dust rich in magnetic particles has been used to date loess in China [Kukla, 1987; Kukla et al., 1988].

Correlation dating methods, including soil stratigraphy [Colman et al., 1987], have proven to be very useful, especially when coupled with independently obtained numerical ages. Paleomagnetism and tephrochronology are particularly important in Arctic loess studies. Some chemical and biologic dating methods, including amino acid racemization studies of wood and mollusc shells, may also be applicable (Table 1).

TESTING CLIMATIC CHANGE MECHANISMS: ASTRONOMIC MODELS AND ATMOSPHERIC CO_2 AND CH_4 CHANGES

The astronomic model of climate change links the small fluctuations in insolation caused by the orbital geometry of the earth with the major glacial/interglacial fluctuations of the Pleistocene ice ages [Hays et al., 1976]. The discovery of periodic forcing at frequencies characteristic of orbital influences in paleoclimatic time series obtained from marine sediments constitutes strong evidence in favor of this hypothesis [Imbrie and Imbrie, 1980].

The sedimentologic characteristics of loess deposits are

Dating Methods	Material Dated	Other Applications
Radiocarbon	wood, charcoal, soil, bone	m,l
K-Ar, ^{39}Ar - ^{40}Ar	tephra	m,l
U-series	bone, wood	m,l
Fission-track (conventional, thermal plateau)	tephra	m,l
Thermoluminescence	loess	m,l
Electron-spin resonance	loess	m,l
Cosmogenic isotope influx*	loess	g
Magnetic susceptibility	loess	m,l
Paleomagnetism	loess	m,l
Tephrochronology	tephra	m,l,g
Amino-acid racemization	shells, wood	m,l
Soil stratigraphy	paleosols	l
Paleoecologic	forest layers, pollen	m,l,g
Sedimentation rate	loess	m,l
Orbital tuning	loess	m,l

Table 1. Dating techniques applicable to loess sequences.

*dating technique has not yet been tested on loess.

m=marine, l=lacustrine, g=ice sheet.

very different from those of marine sediments, and reflect a very different set of physical processes. The proxy climate record obtained from loess constitutes a set of data obtained and dated independently from the marine record which can be evaluated for periodic forcing using time series analysis (Figure 2).

The ages of recent loess deposits in central Alaska were estimated using several different methods. The radiocarbon method was utilized back to its limit at *ca.* 35,000 years B.P. [Begét, 1990]. A strong buried paleosol formed at a time when spruce was present in interior Alaska during the last interglaciation is assigned an age of 0.125 Myr based on correlations with last interglacial forest beds and pollen sequences [Edwards and McDowell, 1990; Begét et al., 1990, 1991]. The age of older and younger loess is determined by linear interpolation between the surface and radiocarbon-controlled datums, and the major buried paleosol. The Old Crow tephra, recently dated to 0.14 ± 0.01 Myr by the isothermal plateau fission-track method [Westgate, 1988, 1989; Westgate et al., 1990] occurs below the last interglacial paleosol at several sites across central Alaska [Begét et al., 1991], consistent with the general chronology developed for the upper parts of Alaskan loess sequences.

Analysis of loess time series data has revealed forcing at periods of *ca.* 100 Kyr, 41 Kyr, and 23 Kyr, values close to those characteristic of earth's orbital geometry [Begét and Hawkins, 1989]. Although the 100 Kyr periodicity may not be significant because of the brevity of the record, the 41 Kyr and 23 Kyr periodicities are statistically robust and appear to record the effects of orbital obliquity and precession on loess deposition in Alaska. Proxy climatic data from Alaskan loess therefore provides independent support for the astronomic model of climate change. These results are particularly interesting because Alaskan loess sections lie at 64°N , very near the latitude where insolation changes show the strongest correlation with global changes during the last two million years. The new dates on the Old Crow tephra by Westgate and others [1990] provide an opportunity to calibrate and extend the loess chronology and re-evaluate the orbital forcing mechanism.

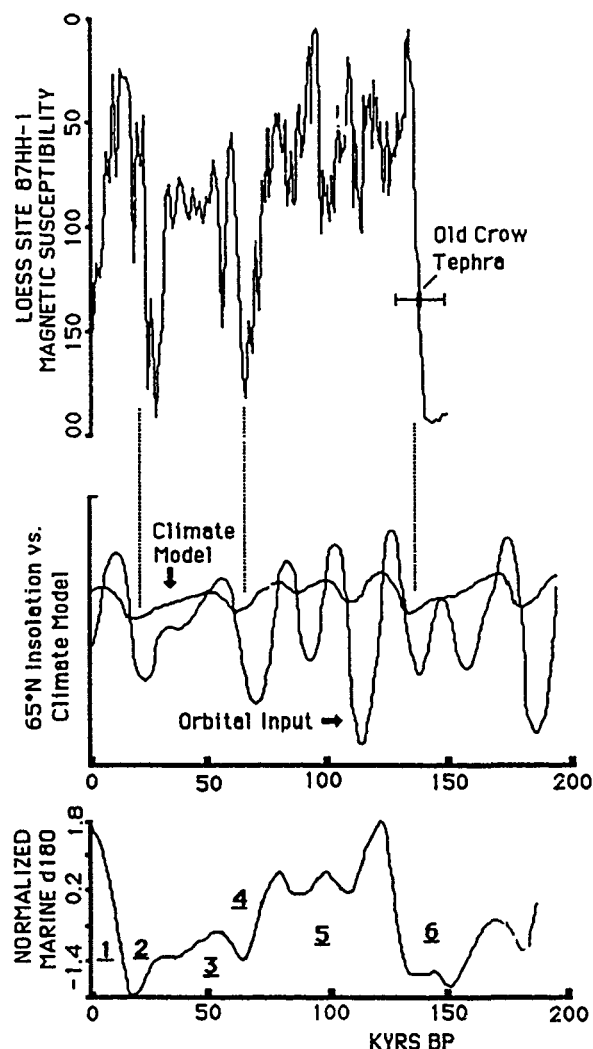


Figure 2. Typical proxy climate record from Alaskan loess, compared with summer insolation at 65°N and normalized marine isotopic record. Correlation based on radiocarbon dating of loess sequences to *ca.* 35 kyr B.P., and position of Old Crow tephra (140 ± 10 kyr B.P.) below last interglacial paleosol complex.

There are also several brief (10^2 – 10^3 years) climate events recorded in Alaskan loess which occurred too rapidly to be explained by the earth's orbital elements, which can only produce slow, regular variations in insolation with periods of 10^4 – 10^5 years [Berger, 1978]. Some of the transient climate events recorded in Alaskan loess may correlate with rapid changes in global atmospheric CO_2 and CH_4 content documented by recent studies of atmospheric gas bubbles in ice cores.

During latest Pleistocene time rapid increases in atmospheric CO_2 occurred about 13,000 years B.P. [Barnola et al., 1987]. In Alaska, an interval of pronounced warming named the "Birch Period" is recorded in palynological records at about this time [Ager, 1982], as well as the initiation of loess deposition in some upland areas where erosion or coversand deposition had predominated [Bigelow et al., 1990]. Subsequent rapid decreases in global atmospheric CO_2 from *ca.* 300 to 250 p.p.m.v. [Dansgaard and Oeschger, 1989] and CH_4 from *ca.* 0.65 to 0.48 p.p.m.v. [Chappellaz et al., 1990] occurred at about 11,000–10,500 years B.P., at the

time of the dramatic "Younger Dryas" cooling in northern Europe. However, the atmosphere is chemically well mixed, and global climate models show that decreases in the "Greenhouse Effect" due to reductions in atmospheric CO₂ and CH₄ concentrations, such as occurred during the latest Pleistocene, cannot be restricted to one region of the planet.

Some evidence suggests widespread climate changes occurred at this time, particularly in high latitude regions of the southern hemisphere [Heusser and Rabassa, 1987; Heusser, 1989; Chappellaz et al., 1990]. Microfaunal and isotopic marine data from the northwest Pacific Ocean also show clear evidence for latest Pleistocene cooling [Kallel et al., 1988]. Loess data from Alaska suggest wind intensity briefly increased at this time, together with transient decreases in regional pollen influx rates [Bigelow et al., 1990], perhaps due to the cooling of the northwest Pacific Ocean or perhaps in response to changes in atmospheric CO₂ and CH₄ content.

During the mid-Wisconsin a similar relationship seems to exist between intervals of high and low wind intensity and transient atmospheric CO₂ and CH₄ changes as delineated by ice core studies. A significant interval of climatic warming and permafrost degradation at ca. 30,000 years is recorded in several areas of Alaska [Hamilton et al., 1988]. This episode, named the "Fox Thermal Event," is also recorded as an interval of low wind intensity in multiple loess sections [Begét, 1990], and correlates well with a transient interval of high atmospheric CO₂ and CH₄ content [Chappellaz et al., 1990]. The mid-Wisconsin, ca. 33–45 Kyr, is an interval of relatively high insolation values, when orbital parameters would produce summer insolation close

to those of modern values. However, dramatic growth of permafrost and high wind intensities recorded in central Alaskan loess of mid-Wisconsin age suggests a particularly cold climatic interval [Hamilton et al., 1988; Begét, 1990]. The transient high latitude cooling may reflect an interval centered at 42 Kyr when atmospheric CO₂ composition decreased to ca. 180–200 p.p.m.v. and CH₄ dropped to ca. 0.40 p.p.m.v., values similar to those reached during the peak of full glacial conditions [Barnola et al., 1987; Chappellaz et al., 1990].

The apparent links between transient intervals of atmospheric CO₂ increase, and episodes of significant warming, permafrost degradation, and generally lower wind intensities recorded in Alaskan loess during the Birch Period at ca. 13 Kyr and the Fox Thermal Event at ca. 30 Kyr, are significant for our understanding of the effects of the modern anthropogenic increase in global atmospheric CO₂. The discovery that brief, natural fluctuations in atmospheric CO₂ in the past have been associated with intervals of climate change in high latitude areas provides support for Greenhouse models of climate change. These data support global climate models which suggest atmospheric CO₂ and CH₄ content plays a very important role in modulating global climate.

If natural short-term changes in atmospheric CO₂ have produced significant climate changes in high latitude regions, as is suggested by recent studies of paleoclimatologic records in Alaskan loess, then it seems likely that the large increase in atmospheric CO₂ occurring during this century due to modern use of fossil fuels may also have a significant effect on climate in high latitude regions.

REFERENCES

- Ager, T., Vegetational history of western Alaska during the Wisconsin glacial interval and the Holocene, in *Paleoecology of Beringia*, edited by D. Hopkins, J. Mathews, C. Schweger, and S. Young, pp. 75–93, Academic Press, New York, 1982.
- Barnola, J., D. Raynaud, Y. Korotkevich, and C. Lorius, Vostok ice core provides 160,000 year record of atmospheric CO₂, *Nature*, 329, 408–414, 1987.
- Begét, J., Tephra and sedimentology of frozen loess, *Fifth International Permafrost Conference Proc.*, Vol. 1., edited by K. Senneset, pp. 672–677, Tapir, Trondheim, 1988.
- Begét, J., Mid-Wisconsinan climate fluctuations recorded in central Alaskan loess, *Geographie Physique et Quaternaire*, 44, 3–13, 1990.
- Begét, J., and D. Hawkins, Influence of orbital parameters on Pleistocene loess deposition in central Alaska, *Nature*, 337, 151–153, 1989.
- Begét, J., D. Stone, and D. Hawkins, Paleoclimate forcing of magnetic susceptibility variations in Alaskan loess, *Geology*, 18, 40–43, 1990.
- Begét, J., M. Edwards, D. Hopkins, M. Keskinen, and G. Kukla, Old Crow tephra found at the Palisades of the Yukon, *Quat. Res.*, 34, 291–297, 1991.
- Berg, A., Long-term variations of caloric insolation resulting from the earth's orbital elements, *Quat. Res.*, 9, 139–167, 1978.
- Bigelow, N., J. Begét, and R. Powers, R., Increase in latest Pleistocene wind intensity recorded in eolian sediments from central Alaska, *Quat. Res.*, 34, 160–168, 1990.
- Chappellaz, J., J. Barnola, D. Raynaud, Y. Korotkevich, and C. Lorius, Ice-core record of atmospheric methane over the past 160,000 years, *Nature*, 345, 127–131, 1990.
- Colman, S. M., K. L. Pierce, and P. W. Birkeland, Suggested terminology for Quaternary dating methods, *Quat. Res.*, 28, 314–319, 1987.
- Dansgaard, W., and H. Oeschger, Past environmental long-term records from the Arctic, in *The Environmental Record in Glaciers and Ice Sheets*, edited by H. Oeschger and C. Langway, pp. 287–319, Wiley, New York, 1989.
- Edwards, M., and P. McDowell, Interglacial deposits at Birch Creek, northeast interior Alaska, *Quat. Res.*, 35, 41–52, 1990.
- Guthrie, R. D., *Frozen Fauna of the Mammoth Steppe: The story of Blue Babe*, 323 pp., University of Chicago, Chicago, IL, 1990.
- Hamilton, T., J. Craig, and P. Sellman, The Fox permafrost tunnel: A late Quaternary geologic record in central Alaska, *Geol. Soc. Am. Bull.*, 100, 948–969, 1988.
- Hays, J., J. Imbrie, and N. Shackleton, Variations in the earth's orbit: pacemaker of the ice ages, *Science*, 194, 1121–1122, 1976.
- Heller, F., and T. S. Liu, Magnetostratigraphical dating of loess deposits in China, *Nature*, 300, 431–433, 1982.
- Heusser, C., Late Quaternary vegetation and climate of southern Tierra del Fuego, *Quat. Res.*, 31, 396–406, 1989.
- Heusser, C., and J. Rabassa, Cold climatic episode of Younger Dryas age in Tierra del Fuego, *Nature*, 328, 609–611, 1987.

- Imbrie, J., and J. Z. Imbrie, Modelling the climatic response to orbital variations, *Science*, 207, 942-953, 1980.
- Kallel, N., L. Labeyrie, M. Arnold, H. Okada, W. Dudley, and J.-C. Duplessy, Evidence of cooling during the younger Dryas in the western North Pacific, *Oceanologica Acta*, 11, 369-375, 1988.
- Kashiwaya, K., A. Yamamoto, and K. Fukuyama, Statistical analysis of grain size distribution in Pleistocene sediments from Lake Biwa, Japan, *Quat. Res.*, 30, 12-18, 1988.
- Kukla, G., Loess stratigraphy in central China, *Quat. Sci. Rev.*, 6, 191-219, 1987.
- Kukla, G., F. Heller, X. M. Liu, F. C. Xu, J. S. Liu, and Z. A. An, Pleistocene climates in China dated by magnetic susceptibility, *Geology*, 16, 811-814, 1988.
- Lorius, C., J. Jouzel, C. Ritz, L. Merlivat, N. Barkov, Y. Korotkevich, and V. Kotlyakov, A 150,000 year climatic record from Antarctic ice, *Nature*, 316, 591-596, 1989.
- Martinson, D., N. Pisias, J. Hays, J. Imbrie, T. Moore, and N. Shackleton, Age dating and the orbital theory of the ice ages: development of a high resolution 1 to 300,000 year chronostratigraphy, *Quat. Res.*, 27, 1-30, 1987.
- Péwé, T., Origin of the upland silt near Fairbanks, Alaska, *Geol. Soc. Am. Bull.*, 66, 699-724, 1955.
- Péwé, T., Quaternary Geology of Alaska, 145 pp., *U.S. Geol. Survey Prof. Paper* 835, 1975.
- Pye, K., *Aeolian Dust and Dust Deposits*, 334 pp., Academic Press, London, 1987.
- Westgate, J., Isothermal plateau fission-track age of the late Pleistocene Old Crow tephra, Alaska, *Geophys. Res. Lett.*, 15, 376-379, 1988.
- Westgate, J., Isothermal plateau fission-track ages of hydrated glass shards from silicic tephra beds, *Earth Planet. Sci. Lett.*, 95, 226-234, 1989.
- Westgate, J., B. Stemper, and T. Péwé, A 3 m.y. record of Pliocene-Pleistocene loess in interior Alaska, *Geology*, 18, 858-861, 1990.



AD-P007 346



92-17850



Global Change and Thermal History as Recorded by Northern North American Tree-Ring Data

G. C. Jacoby and R. D. D'Arrigo

Tree-Ring Laboratory, Lamont-Doherty Geological Observatory, Palisades, New York, U.S.A.

ABSTRACT

Thermal regimes and heat exchange of the polar and subpolar regions play a key role in global climatic change. Principal components analysis of instrumental data for the globe indicate that northern high latitude temperatures are a very strong component of global temperature variations. Tree-ring data from thermally responsive sites in Canada and Alaska yield records of polar and subpolar temperature changes for centuries prior to the relatively short period of instrumental measurements. Tree-ring width based reconstructions of Arctic and northern North American temperatures through 1973 reflect the general positive trend in large-scale instrumental data over the past century. These reconstructions, as well as the raw tree-ring measurements, show that this recent period of warming is unusual relative to the prior few centuries. More recently developed data from Canada confirm previous reconstructions. A maximum latewood density chronology from the Northwest Territories shows a stronger climatic response to warm-season temperatures than ring width data from the same trees. The density information also shows a response to several other temperature-related parameters, including ground-level solar radiation measurements.

In detecting and quantifying global climatic change, tree-ring analysis of high latitude trees provides evidence of recent wide-scale warming in northern North America. This warming will affect boreal forests, northern waters, and human activities. However, more studies are needed to better determine the extent of recent and possible future climatic change and the resulting environmental consequences.

INTRODUCTION

As concern increases about possible anthropogenic influences on climate, much attention is being focused on where the changes of greatest magnitude will take place. Modeling studies using General Circulation Models, or GCMs, as well as compilations of hemispheric temperature data, indicate that the northern polar and subpolar regions are key areas of modeled or recorded change [e.g., Jones et al., 1986; Hansen and Lebedeff, 1987, 1988; Hansen et al., 1988; Mitchell, 1989; Schneider, 1989]. The larger response is due to various climatic feedback effects [Hansen et al., 1988; Mitchell, 1989; Schneider, 1989]. Based on principal components analysis or PCA (Figure 1) much of the variance in the zonally averaged instrumental temperatures for the globe is

attributable to the time series of annual temperature departures for the Arctic zonal band (64–90°N) [S. Lebedeff, personal communication]. Although the high northern latitudes are important climatically [e.g., Kelly et al., 1982; Walsh and Chapman, 1990], temperature records from this region are scarce and relatively short. This impedes characterization of natural long-term climatic variations as well as evaluation of the significance of recent warmer temperatures.

In this paper we review some recent studies which we have made of tree growth in the North American boreal forests and the growth relationships to northern high latitude climatic changes over the last several centuries. The northern limit of tree growth in North America is largely situated south of the 64–90°N Arctic zone. This is especially true in

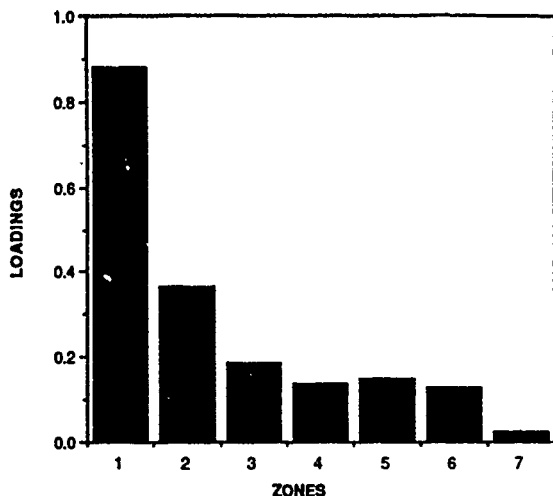


Figure 1. First eigenvector loadings based on principal components analysis (PCA) for 7 temperature zones for the globe from Hansen and Lebedeff [1987]. The eighth zone, representing Antarctica, was not included due to less complete data coverage [S. Lebedeff, personal communication].

eastern Canada where the treeline dips southward. However, the position of the forest-tundra ecotone in North America tends to follow the mean position of the polar front in summer [Bryson, 1966] and the northern forests are strongly influenced by polar air masses and related changes in atmospheric circulation and temperature.

NORTHERN TREE GROWTH AND TEMPERATURE

The dominant factor limiting tree growth in the extreme northern forests is temperature [for a review see Jacoby et al., 1985], allowing the growth characteristics of some of these trees to be used as proxy series of temperature variations. Early observers realized that tree-ring widths from high latitude trees correlated with summer surface air temperatures [e. g., Giddings, 1943; Hustich, 1956]. However, more recent studies indicate that this is really an oversimplification [Garfinkel and Brubaker, 1980; Jacoby and Cook, 1981; Jacoby and Ulan, 1982]. One reason why the tree growth-summer temperature relationship is oversimplified is that the trees used in northern tree-ring studies are primarily evergreen conifers, in which photosynthesis can take place over a much longer season than the relatively short summer period of actual cambial-cell division. In the Subarctic photosynthesis continues down to temperatures near freezing [Kramer and Kozlowski, 1979]. The photosynthates are stored and used in the summer radial growth season. The combined influences of fall and spring photosynthesis and milder winters can impart a temperature response beyond the summer season of cambial-cell division and radial growth [e.g., Fritts, 1976; Kramer and Kozlowski, 1979; Garfinkel and Brubaker, 1980; Jacoby and Cook, 1981; Jacoby and Ulan, 1982; and from correlations between certain treeline chronologies and monthly temperatures for the cooler seasons].

Another complication is that moisture stress can be a major limiting factor at drier sites where there are permeable soils with little moisture retention. At wetter sites, low soil temperatures can inhibit water uptake and also cause moisture stress [Goldstein, 1981].

Although air temperature is indeed important, soil temperature and direct insolation also play a significant role in, respectively, root and needle biochemical processes [Kramer and Kozlowski, 1979]. Variations in borehole temperatures in northern Alaska show an increase at shallow depths indicating actual warming of the near surficial zone in recent times [Lachenbruch and Marshall, 1986]. Such warming should increase the duration and depth of melting of the active layer, which is also the root zone for trees in permafrost areas. A potentially deeper root zone and enhanced nutrient recycling due to warmer temperatures should both benefit tree growth.

TREE-RING CHRONOLOGIES AND RECORDED TEMPERATURE DATA

Using tree-ring series from sites selected for their thermal ecophysiological characteristics, a data set has been assembled which represents tree growth over 90 degrees of longitude in North America (Figure 2, Table 1). The geographical extent of the sites used in our modeling of Arctic zone temperatures covers about one wave length of the Rossby waves over North America [Chang, 1972] and may be considered to represent approximately 25 percent of a circumpolar linear transect.

The compiled tree-ring records, primarily of the species white spruce (*Picea glauca* [Moench] Voss), extend over three hundred years and some trees have survived over five hundred years (Table 1). The tree-ring information was used to develop quantitative reconstructions of annual temperature variations (see below). These estimates indicate that we are in an unusually warm period relative to the prior few centuries.

Several of our dendroclimatic analyses have been made using the temperature data set compiled by Hansen and Lebedeff [1987, 1988], consisting of 80 equal area boxes for the globe. This data set was developed using a spatial averaging technique, in which temperature information is incorporated which may be outside of the actual zone or box but is still relevant to temperature within these areas. The temperature data from individual stations are weighted by the distance from the subboxes used to assemble a particular box [Hansen and Lebedeff, 1987, 1988]. Data are included up to 1200 km from the center of the subboxes. Temperature data extending south to about 55°N are thus included in the temperatures for the Arctic zone or Zone 1. The distant temperatures, in this case extreme southern data, are weighted much less than those within the boxes. This process is very important in developing the data for the Arctic zone where there are few long-term stations. The predictor time series of the box itself is described as the "...temperature trend or temperature change..." and it is this temperature change that is reconstructed. The zonally averaged band of Zone 1 temperatures thus overlaps with the geographical regions where our tree-ring sites are located, some of which are to the south of 64–90°N (Figure 2). Temperature analyses were also made using temperature box data to the south of this zone, as well as with local station data.

METHODS AND ANALYSES

Ring Width Data

A reconstruction of Arctic (Zone 1) temperatures was previously presented in Jacoby and D'Arrigo [1989] (Figure

Site	Location	Lat. (N)	Long. (W)	Species	Years
1. 412	Alaska	67 56	162 18	PIGL	1515-1977*
2. Arrigetch	Alaska	67 27	154 03	PIGL	1586-1975*
3. Sheenjek	Alaska	68 38	143 43	PIGL	1580-1979*
4. TTHH	Yukon	65 00	138 20	PIGL	1459-1975*
5. Mack Mt.	NWT	65 00	127 50	PIGL	1626-1983
6. Coppermine	NWT	67 14	115 55	PIGL	1428-1977*
7. Hornby	NWT	64 02	103 52	PIGL	1491-1983*
8. Churchill	MB	58 43	094 04	PIGL	1650-1988
9. Cape	QB	56 10	076 33	PIGL	1663-1982
10. Ft. Chirao	QB	58 22	068 23	LRL	1650-1974
11. Gaspe	QB	48 35	065 55	THO	1404-1982*
12. S.W. Pond	LB	56 31	061 55	PIGL	1602-1988

Table 1. Site information of northern tree-ring chronologies used to reconstruct Arctic temperatures. Starred sites are those used to reconstruct temperatures for northern North America. PIGL = *Picea glauca*, LRL = *Larix laricina*, THO = *Thuja occidentalis*. NWT = Northwest Territories, MB = Manitoba, QB = Quebec, LB = Labrador.

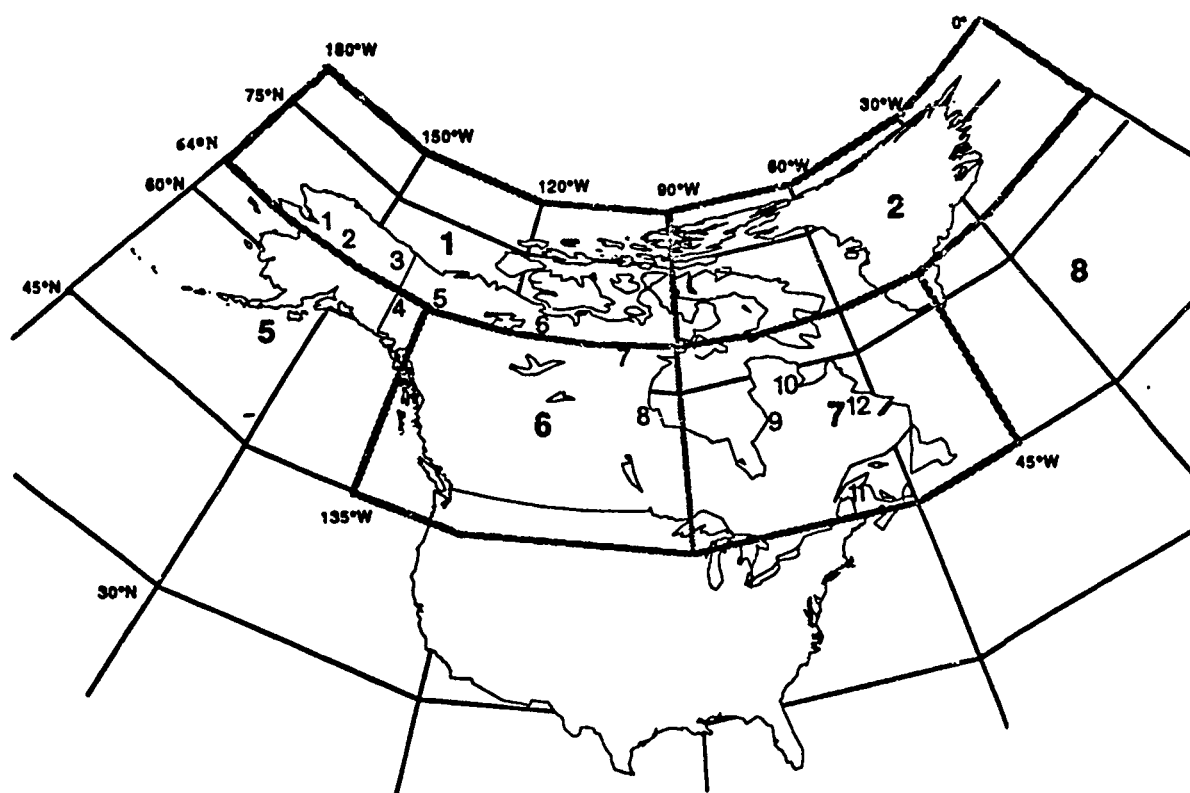


Figure 2. Map of northern North America. Large numbers are the boxes from the global temperature data set of Hansen and Lebedeff [1987]. Outlined are the boxes 1, 2, 6 and 7 used in the reconstruction shown in Figure 3b. Box 5 has a large Pacific maritime area not covered by the tree sites. The Arctic reconstruction (Figure 3a) uses the temperature data from boxes 1 and 2 and the two Arctic boxes over Europe and the USSR. Small numbers are the sites of the tree-ring chronologies used in this study.

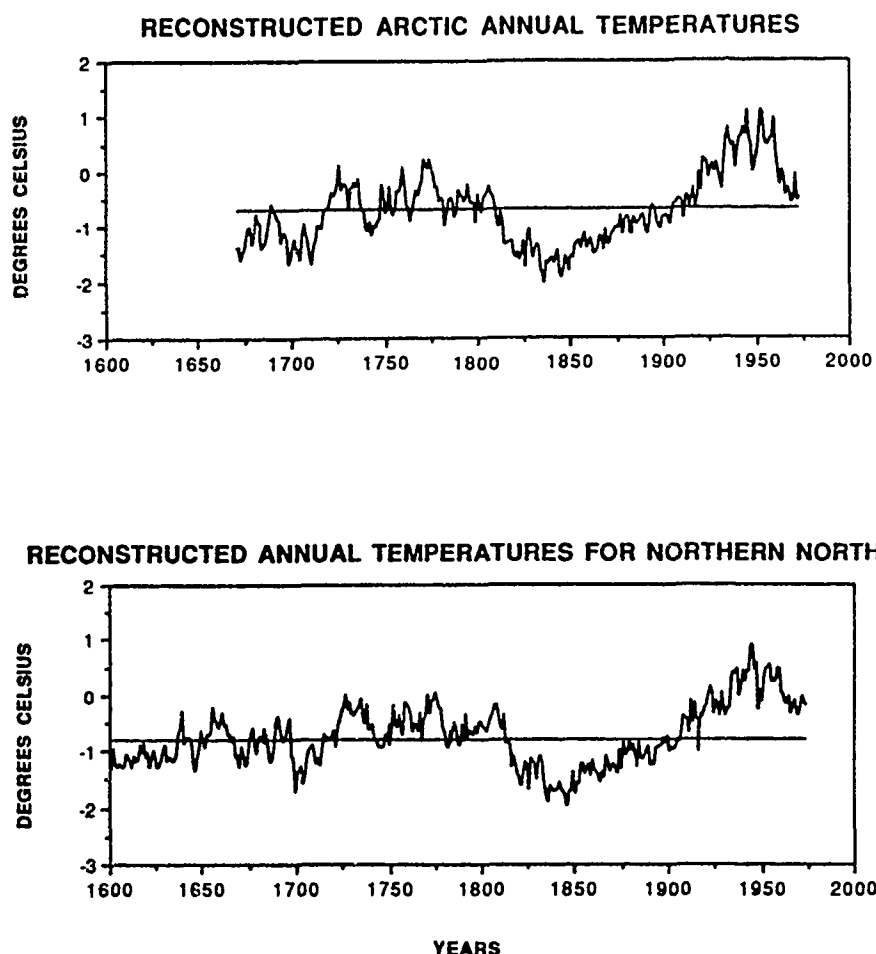


Figure 3. Annual temperature reconstructions for northern latitudes. a: Reconstructed annual Arctic or Zone 1 temperatures [as in Jacoby and D'Arrigo, 1989]. b: Reconstructed annual temperatures for northern North America from boxes 1, 2, 6 and 7 from Hansen and Lebedeff [1987]; as in D'Arrigo and Jacoby [1992].

3a). The reconstruction shows a cooler period around the time of the Maunder Minimum, a relative warming in the 1700s, an abrupt cooling in the early 1800s and a gradual warming trend over the past century (Figure 3a). In more recent modeling we improved the spatial coverage and data by adding a chronology from northern Labrador, an area of relatively weak coverage (Figure 2, Table 1). Also, the chronology from Churchill, Manitoba (Figure 2, Table 1) was modified to include data with more low-frequency climatic information (Scott, P. A., personal communication). The standardization of the raw tree-ring widths for the two new chronologies was done to preserve both high and low frequency variance in the resulting chronologies [Jacoby and D'Arrigo, 1989]. The reconstruction using the two new chronologies is essentially the same as the previous one shown in Figure 3a [Jacoby and D'Arrigo, 1989] but the calibration and verification for different time periods are improved.

In addition to the reconstruction for the Arctic we also selected a subset of seven of the longest chronologies in order to reconstruct annual temperatures for northern North America [D'Arrigo and Jacoby, 1992]. This region is shown

in Figure 2. It encompasses four temperature boxes (1, 2, 6 and 7) as delimited by Hansen and Lebedeff [1987, 1988] which cover much of northern North America. The locations of the seven tree sampling sites used are contained within this four-box area (these sites are starred in Table 1). The longer tree-ring data set enables us to produce a reconstruction back to A.D. 1600 and is very similar to the Arctic reconstruction. The trends for the common period are generally the same. For the earlier period of 1600 to 1671, this reconstruction shows an extended cool interval for the early 1600s and some moderation in the mid-1600s.

Density Studies

An important method which is only now being used extensively in dendroclimatology is densitometric analysis of tree-ring samples [Schweingruber et al., 1978; Hughes et al., 1984; Conkey, 1986; Yanosky and Robinove, 1986; Briffa et al., 1988; Jacoby et al., 1988; Schweingruber, 1988; Thetford et al., 1991]. Briefly, the densitometric data from trees can provide a much better indicator of inter-annual climatic change, with the season of strong direct

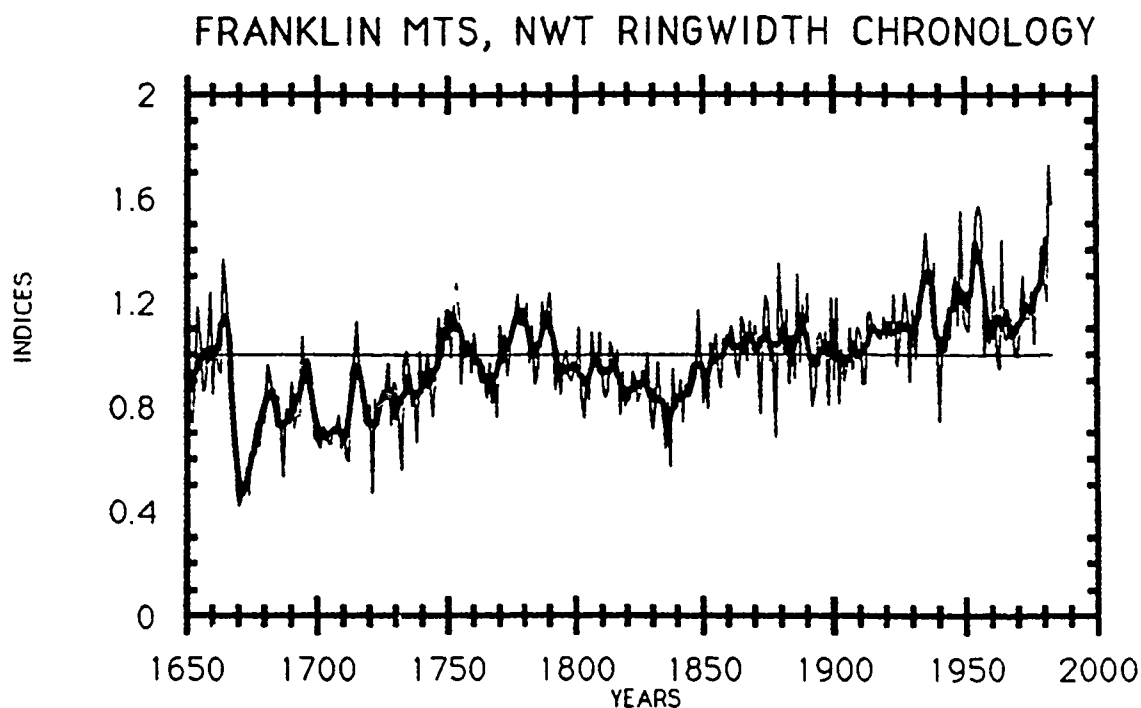
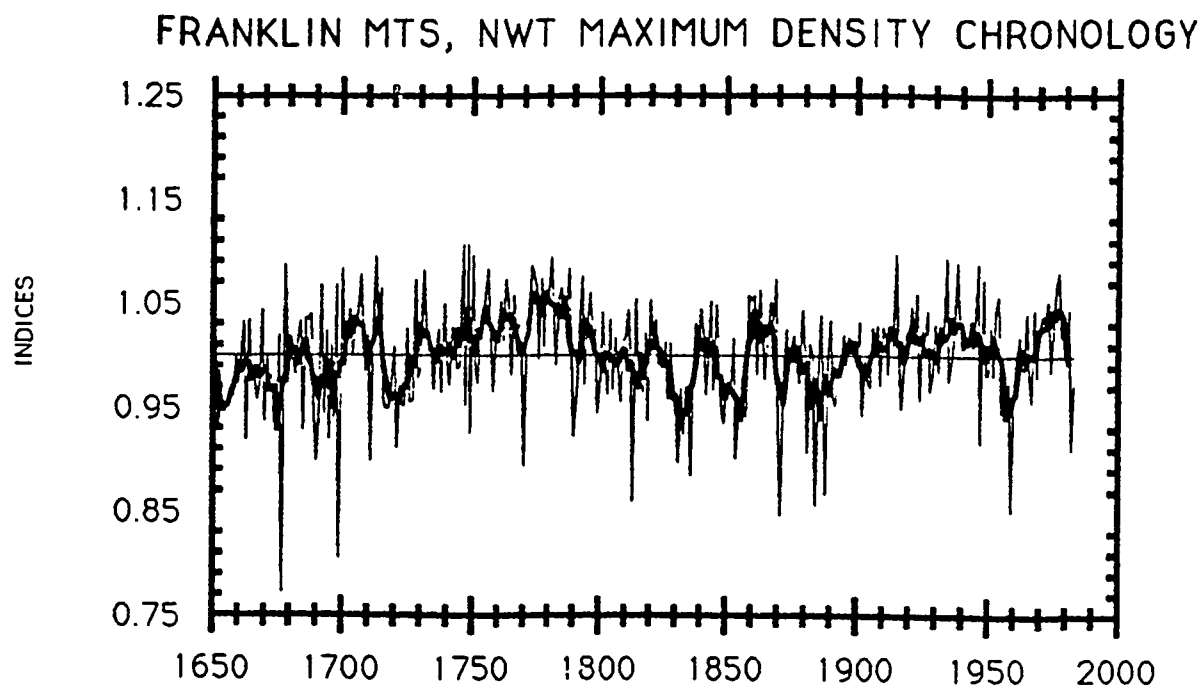


Figure 4. Tree-ring time series of white spruce for Franklin Mountains, N.W.T., Canada obtained using an image analysis system [Thetford et al., 1990]. a: Maximum latewood density chronology. b: Ring width chronology.

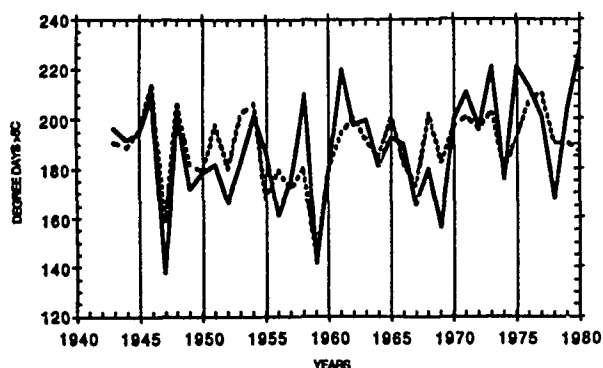


Figure 5. Actual (solid line) and estimated (dashed line) April to August degree days $>5^{\circ}\text{C}$ for Norman Wells, N.W.T., Canada. Estimates (using regression analysis) are based on Franklin Mountains, N.W.T. maximum latewood chronology data.

response to temperature often being much longer than for ring widths.

For a site in the Franklin Mountains, N.W.T., maximum latewood density and ring width chronologies have been developed (Figure 4a,b) using an image analysis technique and software [Thetford et al., 1991]. Significant correlations between the density data and degree day data ($>5^{\circ}\text{C}$) from nearby Norman Wells, N.W.T. extend over five warm-season months rather than only two months for the ring widths. Actual and estimated degree days for April to August are shown in Figure 5. In addition to correlations with monthly summer temperatures, the year-to-year maximum latewood density variations also correlate with ground-level solar radiation measurements. As more density chronologies are developed for high latitude trees in North America, the temperature reconstructions will substantially improve and we will gain more insight into annual and seasonal temperature variations in time and in space.

DISCUSSION AND SUMMARY

The analyses described above are based on tree-ring data from sites carefully selected for minimal moisture stress, openness and exposure to lower-angle insolation. The selection is an attempt to reduce the effects of stand dynamics, paludal effects due to melting of permafrost or drainage changes, fire, animal (including human) disturbance, and other nonclimatic factors. Within each site the ring widths have common low-frequency variations as well as common year-to-year variations. Tree physiology considerations, as noted above, and regression analyses indicate the ring-width variations at the selected sites are responses to, and thus recorders of, thermal information beyond merely air temperature during the summer season of radial growth. Regression analyses show the ring width data to be good predictors of large-scale annual temperature variations. The resulting reconstructions of annual temperature changes for the Arctic and the four North American boxes (Figure 3) follow very closely the variations in the first amplitude of the tree-ring

chronologies. As noted above the temperatures of the high latitude regions contain much of the variance of the northern hemisphere if not global temperature. The two reconstructions indicate that we are in an unusual warming period. Part of this warming, shown by compilations of temperature records which only extend to about 1880, can be considered a recovery from the unusual cold of the Little Ice Age. However the warming since the beginning of this century and the return to warming after the brief mid-century cooling are unusual in the context of the past three and possibly four centuries.

Much attention has been given to the possible growth enhancement in trees and other vegetation by the increased levels of carbon dioxide. In each of these and other reconstructions we have made using high latitude trees we have examined the residual error after the climatic modeling. If there were any nonclimatic increase in growth following a relatively monotonic cause like increased carbon dioxide, there should be a similar trend in the residual error. In the particular high latitude tree species analyzed (through 1973) we do not see such a trend.

The selection to maximize climatic, i.e., temperature, response does not necessarily result in representative curves of typical growth for other boreal trees. Thus recent trends in these trees and sites may not reflect the general growth trends of boreal forests as a whole. To a large degree many trees of the boreal forests do have their growth limited by temperature effects. However, at dry sites or where permafrost melting could lead to paludal conditions, trees could show reduced growth. Warmer conditions could also lead to changes in tree species, diseases and insects present, fire frequency, and other changes in the forests. Other representative growth sites and trees need to be selected to study changes in forest response to climatic change.

Changes in climate, sea ice distributions, potential agricultural environments, and forests may produce dynamic effects in the polar and subpolar regions. Therefore it is crucial to improve and extend the temperature reconstructions back through the major warm period of the last thousand years (i.e., the Medieval Warm Epoch), and to evaluate the present climate relative to that period when presumably there was no anthropogenic carbon dioxide effect. This information about natural variation in long-term climate must be understood for evaluation of any possible anthropogenically altered global climate change.

ACKNOWLEDGMENTS

We acknowledge helpful reviews from E. R. Cook, J. T. Overpeck and P. Anderson. This research was supported by Grants ATM89-15353, ATM87-16630, ATM85-15290 and ATM83-13789 from the Climate Dynamics Program of the National Science Foundation, and Grant No. NAGW-1851 of NASA. We thank J. Hansen and S. Lebedeff for use of their temperature data. We also thank the Government of Canada for logistical assistance. This paper is Lamont-Doherty Geological Observatory Contribution No. 4796.

REFERENCES

- Briffa, K. R., P. D. Jones, J. R. Pilcher, and M. K. Hughes, Reconstructing summer temperatures in northern Fennoscandia back to AD 1700 using tree-ring data from Scots pine, *Arctic Alpine Research*, 20, 385-394, 1988.
- Bryson, R. A., Air masses, streamlines, and the boreal forest, *Geographical Bull.*, 8, 228-269, 1966.
- Chang, J. H., *Atmospheric Circulation Systems and Climates*, Oriental Publ. Co., Honolulu, 326 pp., 1972.
- Conkey, L. E., Red spruce tree-ring widths and densities in eastern North America as indicators of past climate, *Quat. Res.*, 26, 232-243, 1986.
- D'Arrigo, R. D., and G. C. Jacoby, Dendroclimatic evidence from northern North America, in *Climate since AD 1500*, edited by R. S. Bradley and P. D. Jones, Routledge, London, 1992, In press.
- Fritts, H. C., *Tree-Rings and Climate*, Academic Press, New York, 1976.
- Garfinkel, H. L., and L. B. Brubaker, Modern climate-tree growth relationships and climatic reconstruction in sub-Arctic Alaska, *Nature*, 286, 872-874, 1980.
- Giddings, J. L., Some climatic aspects of tree growth in Alaska, *Tree-Ring Bulletin*, 4, 26-32, 1943.
- Goldstein, G. A., Ecophysiological and demographic studies of white spruce (*Picea glauca* [Moench] Voss) at treeline in the central Brooks Range of Alaska, Ph.D. thesis, 193 pp., University of Washington, Seattle, 1981.
- Hansen, J., and S. Lebedeff, Global trends of measured surface air temperature, *J. Geophys. Res.*, 92, 13345-13372, 1987.
- Hansen, J., and S. Lebedeff, Global surface air temperatures: update through 1987, *Geophys. Res. Lett.*, 15, 323-326, 1988.
- Hansen, J., I. Fung, A. Lacis, S. Lebedeff, D. Rind, R. Ruedy, G. Russell, and P. Stone, Global climate changes as forecast by the GISS 3-D model, *J. Geophys. Res.*, 93, 9341-9364, 1988.
- Hughes, M. K., F. H. Schweingruber, D. Cartwright, and P. M. Kelly, July-August temperature at Edinburgh between 1721 and 1975 from tree-ring density and width data, *Nature*, 308, 341-344, 1984.
- Hustich, I., Correlation of tree-ring chronologies of Alaska, Labrador and Northern Europe, *Acta Geographica*, 15, 3-26, 1956.
- Jacoby, G. C., and E. R. Cook, Past temperature variations as inferred from a 400-year tree-ring chronology from Yukon Territory, Canada, *Arctic Alpine Res.*, 13, 409-418, 1981.
- Jacoby, G. C., and R. D. D'Arrigo, Reconstructed Northern Hemisphere annual temperature since 1671 based on high-latitude tree-ring data from North America, *Clim. Change*, 14, 39-59, 1989.
- Jacoby, G. C., and L. D. Ulan, Reconstruction of past ice conditions in a Hudson Bay estuary using tree-rings, *Nature*, 298, 637-639, 1982.
- Jacoby, G. C., E. R. Cook, and L. D. Ulan, Reconstructed summer degree days in central Alaska and northwestern Canada since 1524, *Quat. Res.*, 23, 18-26, 1985.
- Jacoby, G. C., I. S. Ivanciu, and L. D. Ulan, A 263-year record of summer temperature for northern Quebec reconstructed from tree-ring data and evidence of a major climatic shift in the early 1800's, *Palaeogeogr., Palaeoclimatol., Palaeoecol.*, 64, 69-78, 1988.
- Jones, P. D., S. C. B. Raper, R. S. Bradley, H. F. Diaz, P. M. Kelly, and T. M. L. Wigley, Northern Hemisphere surface air temperature variations, 1851-1984, *J. Clim. Appl. Meteorol.*, 25, 161-179, 1986.
- Kelly, P. M., P. D. Jones, C. B. Sear, B. S. G. Cherry, and R. K. Tavakol, Variations in surface air temperatures: Part 2: Arctic regions, 1881-1980, *Mon. Wea. Rev.*, 110, 71-83, 1982.
- Kramer, P. J., and T. T. Kozlowski, *Physiology of Woody Plants*, 811 pp., Academic Press, Orlando, FL, 1979.
- Lachenbruch, A. H., and B. V. Marshall, Changing climate: geothermal evidence from permafrost in the Alaskan Arctic, *Science*, 234, 689-696, 1986.
- Mitchell, J. F. B., The "greenhouse" effect and climate change, *Rev. Geophys.*, 27, 115-139, 1989.
- Schneider, S. H., The greenhouse effect: science and policy, *Science*, 243, 771-781, 1989.
- Schweingruber, F. H., *Tree Rings. Basics and Applications of Dendrochronology*, 276 pp., Reidel, Dordrecht, 1988.
- Schweingruber, F. H., H. C. Fritts, O. U. Braker, L. G. Drew, and E. Schar, The x-ray technique as applied to dendroclimatology, *Tree-Ring Bulletin*, 38, 61-91, 1978.
- Thetford, R. D., R. D. D'Arrigo, and G. C. Jacoby, An image analysis system for generating densitometric and ring width time series, *Can. J. Forest Res.*, 1991, In press.
- Walsh, J. E., and W. L. Chapman, Short-term climatic variability in the Arctic, *J. Clim.*, 3, 237-250, 1990.
- Yanosky, T. M., and C. J. Robinove, Digital image measurement of the area and anatomical structure of tree-rings, *Can. J. Bot.*, 64, 2896-2902, 1986.



Spatial and Temporal Characteristics of the Little Ice Age: The Antarctic Ice Core Record

Ellen Mosley-Thompson and Lonnie G. Thompson

Byrd Polar Research Center, The Ohio State University, Columbus, Ohio, U.S.A.

ABSTRACT

Recently, ice core records from both hemispheres, in conjunction with other proxy records (e.g., tree rings, speleothems and corals), have shown that the Little Ice Age (LIA) was spatially extensive, extending to the Antarctic. This paper examines the temporal and spatial characteristics of the dust and $\delta^{18}\text{O}$ information from Antarctic ice cores. Substantial differences exist in the records. For example, a 550-year record of $\delta^{18}\text{O}$ and dust concentrations from Siple Station, Antarctica suggests that warmer, less dusty conditions prevailed from A.D. 1600 to 1830. Alternately, dust and $\delta^{18}\text{O}$ data from South Pole Station indicate that opposite conditions (e.g., cooler and more dusty) were prevalent during the LIA. Three additional Antarctic $\delta^{18}\text{O}$ records are integrated with the Siple and South Pole histories for a more comprehensive picture of LIA conditions. The records provide additional support for the LIA temperature opposition between the Antarctic Peninsula region and East Antarctica. In addition, periods of strongest LIA cooling are not temporally synchronous over East Antarctica. These strong regional differences demonstrate that a suite of spatially distributed, high resolution ice core records will be necessary to characterize the LIA in Antarctica.

INTRODUCTION

The broad spectrum of chemical and physical data preserved within ice sheets and ice caps provide a multifaceted record of both the climatic and environmental history of the earth. Over the last three decades, ice cores have provided new details about the magnitude, direction, and rate of climatic change during the last 160,000 years. These histories serve as comprehensive case studies that can improve our understanding of future changes in the global environment.

Clarification of the course of future climatic changes requires understanding the origin of the natural variability within the environmental system on time scales ranging from decades to centuries [IGBP, 1989]. The Holocene record (~last 10,000 years) offers the temporal and spatial detail necessary to characterize that variability. The last several thousand years of the Holocene provide the best opportunity to study decadal- and centennial-scale processes as it is the period (1) most relevant to human activities, both present and future; (2) of extremes within the Holocene warm period including the "Little Ice Age" period from

A.D. 1450–1880; (3) of maximum data coverage; (4) for which multi-proxy reconstructions are possible; (5) when annual and decadal resolution is possible so that leads and lags in the system can be studied; and (6) when causes of these changes remain undetermined. In the last decade ice cores have been recognized increasingly as sources of very highly resolved paleoenvironmental time series. Here we examine the characteristics of the most recent neoglacial period or Little Ice Age as it is preserved in Antarctic ice cores.

ANTARCTIC ICE CORE RECORDS

The histories discussed below originated from different areas of the Antarctic (Figure 1) which are characterized by quite disparate net balances, mean annual temperatures, surface climatologies, and ice flow regimes. Dating of ice core records is the first, critical step in paleoclimatic reconstruction and dating precision varies widely among these records. The net annual accumulation and temperature of a site, as well as the sample sizes selected for individual analyses,

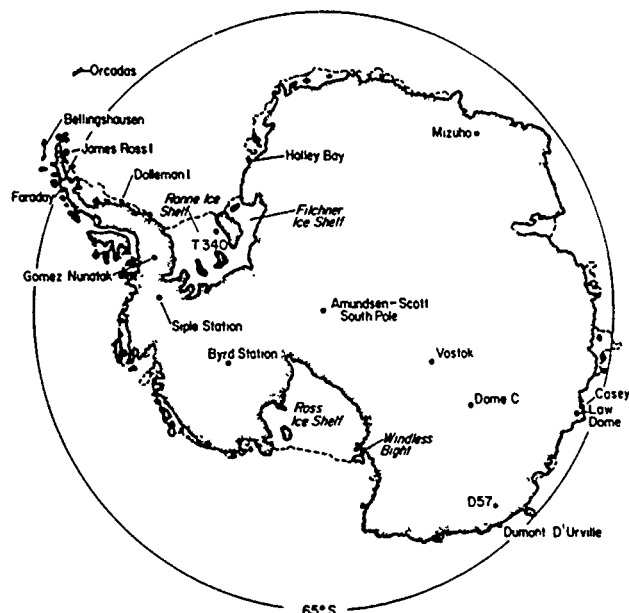


Figure 1. Core sites and meteorological stations discussed in the text.

limit the time resolution possible. To examine the last 500 years as recorded in Antarctic ice cores, annual- to decadal-time resolution is essential and the precision of the time scale is a major consideration. Data drawn from other authors are presented as faithfully as possible with respect to time, and any annual or decadal averages presented were calculated from the time series as originally published. The reader is encouraged to review the original records if more specific information is desired.

Siple Station (75°55'S; 84°15'W; 1054 masl). A 550-year record of the concentrations of dust, $\delta^{18}\text{O}$, and SO_4^{2-} was obtained from a 302-meter core drilled in 1985/86 at Siple Station (Figure 1). This core was cut into 5757 samples each for microparticle concentrations and $\delta^{18}\text{O}$ and into 3492 samples for SO_4^{2-} analyses. The small sample size (and thus large number of samples) was necessary to isolate seasonal signals for establishing the best possible time scale. Both $\delta^{18}\text{O}$ and SO_4^{2-} records exhibit excellent seasonality throughout the entire 302 meters [Mosley-Thompson et al., 1990] and were used to produce the time scale which has an estimated error of 10 years at A.D. 1417 (2%).

South Pole Station (90°S; 2835 masl). A 101-meter core drilled at South Pole in 1974 was cut into 5218 samples for the analysis of microparticle concentrations [Mosley-Thompson and Thompson, 1982] which were used to establish a 911-year record. The core was also cut into 1024 samples for $\delta^{18}\text{O}$ analyses at the University of Copenhagen. The $\delta^{18}\text{O}$ samples were cut to approximate a single year as defined by the current accumulation rate coupled with a steady state calculation of layer thinning with depth. Therefore, the $\delta^{18}\text{O}$ record does not contribute to the refinement of the time scale. The $\delta^{18}\text{O}$ data have been converted into a time series using the time-depth relationship derived from the particulate record. The $\delta^{18}\text{O}$ data from 1974 to 1982 were obtained from a pit 4 km from the station [Mosley-Thompson et al., 1985].

A second isotopic record available from South Pole consists of a very detailed (~900 samples), continuous deuterium (δD) record for the last 100 years with an estimated accuracy of ± 5 years. The annual averages for A.D. 1887–1977 and the smoothed curves used in this paper are reproduced from Jouzel et al. [1983].

Dome C (74°39'S; 124°10'E; 3240 masl). The low net annual accumulation (~37 mm H_2O eq.) at Dome C (Figure 1) precludes establishing an annually resolved record. The most detailed $\delta^{18}\text{O}$ records of the last 1000 years for Dome C are from the upper 100 m of two cores drilled in 1978 and 1979 [Benoist et al., 1982]. Due to the large variability in net accumulation, a high level of smoothing was required to reduce the noise. Smoothing with filter band widths of 512 and 170 years precluded extraction of a detailed record.

T340: Filchner-Ronne Ice Shelf (78°60'S; 55°W). A 100-meter core was drilled in 1984 at site T340 on the Filchner-Ronne Ice Shelf (Figure 1) by the German Antarctic Research Program [Graf et al., 1988]. Net annual accumulation at T340 is ~155 mm H_2O equivalent. The core was dated using the seasonal variations in $\delta^{18}\text{O}$ preserved in much of the core. The quality of the $\delta^{18}\text{O}$ record, and thus the time scale, was compromised by partial melting in the upper part of the core. Essentially, 479 annual layers were identified by $\delta^{18}\text{O}$ and of these, 80 were expressed as small maxima or shoulders on larger peaks. In addition, 5 m of core were unavailable. Extrapolating from surrounding sections led to the addition of 41 years, representing this section. Thus, a total of 520 years was estimated for the core which gives an age of A.D. 1460 for the bottom. No estimate of accuracy was given for the dating of T340.

Law Dome (66°44'S; 112°50'E; 1390 masl). The Australian National Antarctic Research Expedition recovered a 473-meter ice core (BHD) in 1977 from the summit of the Law Dome. The net annual accumulation at the site of core BHD is ~800 mm H_2O and the annual layers thin to approximately 110 mm H_2O eq. at 450 m. Pit studies and total Beta radioactivity profiles confirm the annual character of the well-preserved $\delta^{18}\text{O}$ signal. The upper 28 m (1950–1977) were cut into roughly 10 samples per year to verify the seasonality of the $\delta^{18}\text{O}$ record. Below 28 m, $\delta^{18}\text{O}$ was measured in selected sections and the results were extrapolated over intervening core sections. Recognizing that this introduces some uncertainty in the dating, Morgan [1985] suggests a dating accuracy of $\pm 10\%$.

Mizuho Core (70°41.9'S; 44°19.9'E; 2230 masl). A 150-meter core was drilled at Mizuho Station by Japanese Antarctic Research Expeditions between 1970 and 1976 [Watanabe et al., 1978]. Mizuho is situated in the Antarctic coastal zone (Figure 1) in a region dominated by katabatic winds. The mean annual accumulation is ~450 mm H_2O equivalent, but removal of material by wind produces hiatuses in the annual record making reconstruction of a continuous $\delta^{18}\text{O}$ record from the 150-m core impossible. No obvious seasonal cycles in $\delta^{18}\text{O}$ were found. Principally, the core was dated by matching prominent isotope features to similar features in the upper part of the Camp Century, Greenland core which were assumed to be correlative. Thus, it is impossible to assess the quality of the time scale, but the error is likely to be higher than for other cores considered here.

SURFACE TEMPERATURE AND $\delta^{18}\text{O}$: A.D. 1945-1985

Annual $\delta^{18}\text{O}$ averages, like surface temperatures, exhibit interannual variability in response to large-scale circulation changes which control the frequency, duration, intensity, and seasonality of precipitation from cyclonic storms. In addition, ice core records contain glaciological noise superimposed upon the input signal by both surface and post-depositional processes. The climatological utility of an ice core record as an environmental proxy depends upon whether or not it reflects larger- or regional-scale climatic trends. This assessment for Antarctic ice core records is hindered by the poor availability of long meteorological observations [DOE, 1987].

Comparison of $\delta^{18}\text{O}$ and surface temperatures provides a crude estimate of the larger-scale representativity of the ice core record although there are weaknesses in this approach [see Peel et al., 1988 for discussion]. Mosley-Thompson [1992] provides a more extensive discussion of the comparison of $\delta^{18}\text{O}$ annual averages and meteorological observations for the period of overlap: A.D. 1945-1985. Essentially, conditions at Siple Station reflect those prevailing in the Peninsula more frequently than those prevailing over the polar plateau. In general trends in surface temperatures in the Peninsula are "out of phase" with those in East Antarctica. Likewise, the annual $\delta^{18}\text{O}$ records from Siple and South Pole are out of phase suggesting that trends in the $\delta^{18}\text{O}$ records are consistent with trends in surface temperatures.

THE RECORDS SINCE A.D. 1500

The most recent widespread Neoglacial episode (approximately A.D. 1500-1880), evident in reconstructed Northern Hemisphere temperatures [Grove and Landsberg, 1979] and proxy records [Lamb, 1977; Grove, 1988], is commonly referred to as the Little Ice Age (LIA). Figure 2 illustrates the five Antarctic ice core $\delta^{18}\text{O}$ histories with sufficient time resolution and precision to examine environmental conditions over continental Antarctica during the last 480 years. A record from the Quelccaya ice cap [Thompson et al., 1986], located at 14°S at 5670 meters on the Altiplano of the southern Peruvian Andes, is included as it closely resembles Northern Hemisphere temperatures reconstructed by Grove and Landsberg [1979].

For the records in Figure 2, the Mizuho time scale is the least precise while that for Siple is the most precise. Partial melting makes assessing the Filchner-Ronne T340 time scale difficult; however, if approximately 20 years were missing from the upper part of T340, the major warm and cool events would correspond fairly well with those at Siple. Such errors are possible as the upper part of the core was affected by melting and contained most of the missing core sections for which extrapolations were used. In addition, the T340 $\delta^{18}\text{O}$ record was adjusted for increasing continentality (^{18}O depletion) with depth in the core due to northward ice shelf movement and was finally smoothed with an unspecified filtering function [Graf et al., 1988].

Only selected sections of the Mizuho and Law Dome cores were analyzed. This discontinuous sampling results in a smoothed appearance. By contrast, the South Pole, Siple, and Quelccaya records were continuously analyzed, are annually resolved, and thus exhibit a higher degree of var-

ANTARCTIC ISOTOPE RECORDS SINCE A.D. 1500

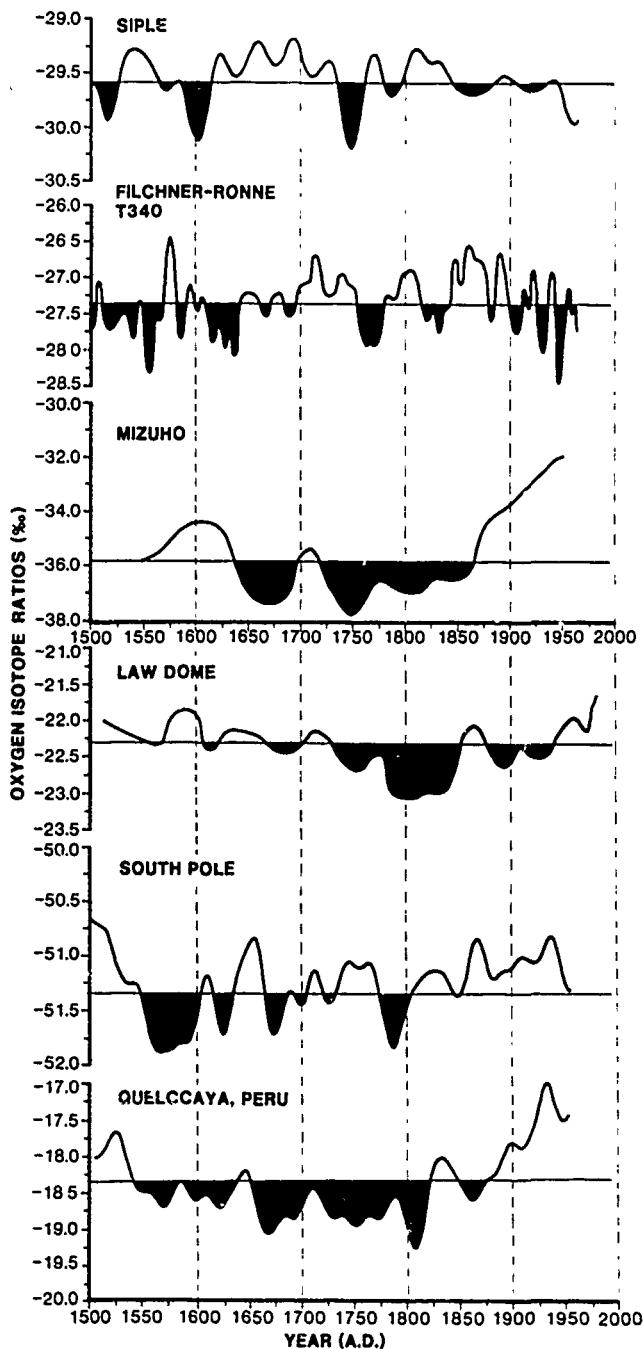


Figure 2. Isotope records for A.D. 1500 to the present for these locations: Siple, T340, Mizuho, Law Dome, and South Pole. A comparable record for Quelccaya Ice Cap, Peru is included. Each time series mean is illustrated by the horizontal line. Isotopic values below the mean suggest cooler than normal temperatures and are shaded.

iability. To facilitate comparison, a 48-point (or 48 year) Gaussian filter was used to smooth the annual data for presentation in Figure 2. The horizontal line is the time series average for each core and values below the mean, interpreted as cooler than average temperatures, are shaded.

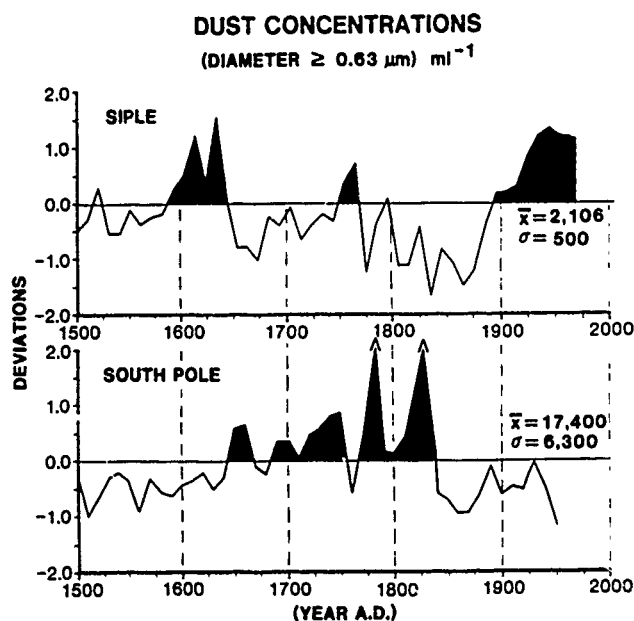


Figure 3. The 10-year unweighted averages of dust content for Siple and South Pole ice core are compared. Microparticle (diameter $\geq 0.63 \mu\text{m}$) concentrations per mL are shown as standardized deviations from their respective time series means.

The records from East Antarctica suggest cooler conditions during much of the LIA while the Siple record indicates warmer conditions for much of that period. Core T340 also suggests warmer conditions from A.D. 1650 to 1830 with a brief cool event at ~A.D. 1760. Clearly, in the last 300 years the T340 record most closely resembles that from Siple, particularly the downward trend in the last century.

Figure 2 reveals several spatial differences. First, Mizuho and Law Dome show the strongest similarity, with coldest conditions between A.D. 1750 and 1850. Although conditions were cooler than average at South Pole from A.D. 1550 to 1800, this period is punctuated by warmer and cooler events with the coldest period in the mid- to late 1500s. Using the empirical $\delta^{18}\text{O}$ -temperature relationship of Aldaz and Deutsch [1967], the "isotopically inferred" temperature depression in the late 1500s may have been $\sim 0.5^\circ\text{C}$. A smoothed δD history from Dome C (not shown) also suggests cooler conditions from A.D. 1200 to 1800; however, because significant noise necessitated high-level smoothing, further time resolution is impossible [Benoist et al., 1982].

These records indicate that a warming trend has prevailed in East Antarctica since A.D. 1850 while cooling has clearly dominated at Siple and T340. The T340 record supports the suggestion that the longer-term trends in the Siple $\delta^{18}\text{O}$ history may reflect similar conditions for much of the Peninsula region. The opposition between the $\delta^{18}\text{O}$ records at Siple and those in East Antarctica is consistent with the currently observed opposition in surface temperatures [Mosley-Thompson, 1992]. Since A.D. 1975 these trends appear to have reversed, with cooling dominating over the Plateau and warming over the Peninsula.

The dust concentrations in cores from Siple and South Pole suggest further differences. Figure 3 illustrates the 10-year unweighted averages of particulate concentrations (diameters $\geq 0.63 \mu\text{m}$) per milliliter sample for both cores. Concentrations above the time series mean for each core are shaded. From A.D. 1630 to 1880 dust concentrations at Siple are below average. A brief dust event around A.D. 1750 is associated with a negative (cooler) excursion in $\delta^{18}\text{O}$ (Figure 2). From A.D. 1880 to the present dust concentrations at Siple have increased while a cooling trend has prevailed (Figure 2). In contrast, at South Pole dust deposition was higher from A.D. 1650–1850. Note that the coldest temperatures at South Pole preceded the increase in dust by 100 years.

CONCLUSIONS

The records of $\delta^{18}\text{O}$ and dust concentrations from Siple Station suggest warmer and less dusty atmospheric conditions from A.D. 1600 to 1830 which encompasses much of the Northern Hemisphere Neoglacial period, the Little Ice Age. Dust and $\delta^{18}\text{O}$ data from South Pole, supported by the $\delta^{18}\text{O}$ results from Law Dome and Mizuho, indicate that opposite conditions (e.g., cooler and more dusty) were prevalent over the East Antarctica Plateau.

The similarity between the $\delta^{18}\text{O}$ records from South Pole and Quelccaya is intriguing. The excellent correspondence between the Quelccaya $\delta^{18}\text{O}$ record and Northern Hemisphere reconstructed temperatures has been demonstrated [Thompson et al., 1986]. The similarity between the South Pole and Quelccaya $\delta^{18}\text{O}$ records, as well as the elevated dust concentrations, suggests the possibility of large-scale upper atmospheric teleconnections between the South American Andes and the high East Antarctica Plateau which warrant investigation beyond the scope of this paper.

Meteorological data from 1945 to 1985 show that the Peninsula–East Antarctica Plateau temperature opposition prevailing during much of the last five centuries is consistent with the present spatial distribution of surface temperature trends. There is some observational evidence suggesting that under present conditions stronger zonal westerlies are associated with cooler conditions on the polar plateau and warmer conditions in the Peninsula region [Rogers, 1983]. The physical processes controlling these spatial relationships must be identified and better understood; however, the observational data base necessary for this assessment is lacking. These regional differences demonstrate that a suite of spatially distributed, higher resolution ice core records will be necessary to characterize more fully paleoenvironmental conditions since A.D. 1500 in Antarctica.

ACKNOWLEDGMENTS

We acknowledge all those who participated in both the field and laboratory aspects of this program. We especially thank Drs. C. C. Langway, Jr. and Willi Dansgaard for making available their unpublished $\delta^{18}\text{O}$ data from the 1974 South Pole ice core. This work was supported by NSF grant DPP-841032A04 to The Ohio State University. This is contribution 725 of the Byrd Polar Research Center.

REFERENCES

- Aldaz, L., and S. Deutsch, On a relationship between air temperature and oxygen isotope ratio of snow and firn in the South Pole region, *Earth Planet. Sci. Lett.*, 3, 2667-2674, 1967.
- Benoist, J. P., J. Jouzel, C. Lorius, L. Merlivat, and M. Pourchet, Isotope climatic record over the last 2.5 KA from Dome C, Antarctica, *Ann. Glaciol.*, 3, 17-22, 1982.
- Department of Energy, A data bank of Antarctic surface temperature and pressure data, *DOS Technical Report 038*, 1987.
- Graf, W., H. Moser, H. Oerter, O. Reinwarth, and W. Stichler, Accumulation and ice-core studies on the Filchner-Ronne Ice Shelf, Antarctica, *Ann. Glaciol.*, 11, 23-31, 1988.
- Grove, J. M., *The Little Ice Age*, 498 pp., Methuen, London, 1988.
- Groverman, B. S., and H. E. Landsberg, Simulated Northern Hemisphere temperature departures: 1579-1880, *Geophys. Res. Lett.*, 6, 767-769, 1979.
- IGBP, Global changes of the past, *Global Change Report No. 6*, 39 pp., 1989.
- Jouzel, J., L. Merlivat, J. R. Petit, and C. Lorius, Climatic information over the last century deduced from a detailed isotopic record in the South Pole snow, *J. Geophys. Res.*, 88, 2693-2703, 1983.
- Lamb, H. H., *Climate: Present, Past and Future, Volume 2: Climatic History and the Future*, 835 pp., Methuen, London, 1977.
- Morgan, V. I., An oxygen isotope-climatic record from Law Dome, Antarctica, *Climatic Change*, 7, 415-426, 1985.
- Mosley-Thompson, Paleoenviromental conditions in Antarctica since A.D. 1500: ice core evidence, in *Climate Since A.D. 1500*, edited by R. S. Bradley and P. D. Jones, Routledge, London, 1992, In press.
- Mosley-Thompson, E., and L. G. Thompson, Nine centuries of microparticle deposition at the South Pole, *Quat. Res.*, 17, 1-13, 1982.
- Mosley-Thompson, E., P. D. Kruss, L. G. Thompson, M. Pourchet, and P. Grootes, Snow stratigraphic record at South Pole: potential for paleoclimatic reconstruction, *Ann. Glaciol.*, 7, 26-33, 1985.
- Mosley-Thompson, E., L. G. Thompson, P. M. Grootes, and N. Gundestrup, Little Ice Age (Neoglacial) paleo-environmental conditions at Siple Station, Antarctica, *Ann. Glaciol.*, 14, 199-204, 1990.
- Peel, D. A., R. Mulvaney, and B. M. Davison, Stable isotope/air-temperature relationships in ice cores from Dolleman Island and the Palmer Land Plateau, Antarctic Peninsula, *Ann. Glaciol.*, 10, 130-136, 1988.
- Rogers, J. C., Spatial variability of Antarctic temperature anomalies and their association with the southern hemispheric circulation, *Ann. Assoc. Am. Geog.*, 73, 502-518, 1983.
- Thompson, L. G., E. Mosley-Thompson, W. Dansgaard, and P. M. Grootes, The Little Ice Age as recorded in the stratigraphy of the tropical Quelccaya ice cap, *Science*, 234, 361-364, 1986.
- Watanabe, O., K. Kato, K. Satow, and F. Okuhira, Stratigraphic analyses of firn and ice at Mizuho Station, *Memoirs of the National Institute of Polar Research, Special Issue 10*, 25-47, 1978.

AD-P007 348



92-17852



Paleoenvironmental Data from Less-Investigated Polar Regions

Rein Vaikm e

Institute of Geology, Estonian Academy of Sciences, Tallinn, Estonia

ABSTRACT

The Arctic holds extensive records of past climatic and environmental changes. Stable isotope variations in polar ice are in many cases important records of paleoclimatic information. Deep ice cores from Antarctica and Greenland, reaching back through the last glaciation, have provided valuable information about the Earth's climate in the past.

This paper discusses the oxygen-18 variations in intermediate-depth ice cores from smaller ice caps of Svalbard, Severnaya Zemlya (North Land) and from the marginal area of the Antarctic ice sheet, covering the time span from 1000 to 8000 years B.P. All profiles studied clearly reflect the main climatic events during this time interval. However, small shifts in time exist between details on different curves. Most probably this is due to certain asynchrony in climatic changes in the various regions.

There are extensive areas in the Arctic, especially in its eastern sector, where no glaciers currently exist and, possibly, in some areas never existed in the past either. These are the areas of permafrost where several forms of ice occur within the ground. The source water for most types of ground ice originates from precipitation, but unlike glacier ice, the range of mechanisms for the formation of ground ice is very large, which considerably complicates the interpretation of their isotopic characteristics.

For paleoclimatic and paleopermafrost reconstructions, the isotopic content of polygonal wedge ice seems to be most promising. The attempts to use isotopic records from segregated ice for paleoenvironmental research will also be discussed.

INTRODUCTION

The Arctic and Antarctic are the key regions for solving several problems identified by the Global Change program. The ecosystems there are extremely sensitive and react quickly to all changes in environmental conditions. Especially sensitive to climatic changes are the glaciers. It is important to note that climatic changes alter not only the balance of the glaciers but also the chemical and isotopic composition of the precipitation feeding them. That is why the isotopic profiles of glaciers have now become one of the main sources of paleoclimatic information [Oeschger and Langway, 1989]. Up to now most of the attention has been focused on the two major centers of current glaciation, Antarctica and Greenland, where the information preserved in

very thick ice sheets covers the climatic changes which occurred during hundreds of thousands of years. However, it has been discovered that in addition to global climatic changes which are reflected to a larger or smaller extent in all glacier profiles, there also exist regional and local changes, which may influence the picture considerably. In order to obtain more exact information it is necessary to study isotopic profiles of glaciers in as many different areas as possible. These include, for instance, the majority of the Arctic archipelagos, mountain glaciers on the continents, as well as the marginal areas of the Antarctic ice sheet, which are considerably more sensitive to climatic changes than the central part of the ice sheet. At the same time, it should be remembered that many of the glaciers of the Arctic archi-

pelagos, especially in the Eurasian Arctic, are temperate. In interpreting the isotopic profiles of such glaciers one has to consider the possible influence of rain and meltwater on the primary isotopic composition [Vaikmäe, 1990].

Besides the isotopic profiles of glaciers, the isotopic variations in permafrost have also found use as sources of paleoclimatic information in recent years. This is an important step forward, providing the opportunity to compare the extent of climatic changes in time and space in various regions of the Arctic. The information used is based on similar source material, i.e., on the isotopic composition of paleoprecipitation.

SVALBARD ICE CORES

High accumulation rates and a wide spectrum of various glacier types make the Svalbard archipelago favorable for the detailed reconstruction of glacioclimatic conditions. Although the average thickness of the glaciers does not exceed 200 m, some glaciers on the archipelago are over 500 m thick [Kotlyakov, 1985]. Their isotopic profiles might, theoretically, contain paleoclimatic information for the entire Holocene.

Table 1 presents the more important data on the Svalbard ice cores studied by us [Punning et al., 1987]. Drill-hole locations on the archipelago are indicated in Figure 1.

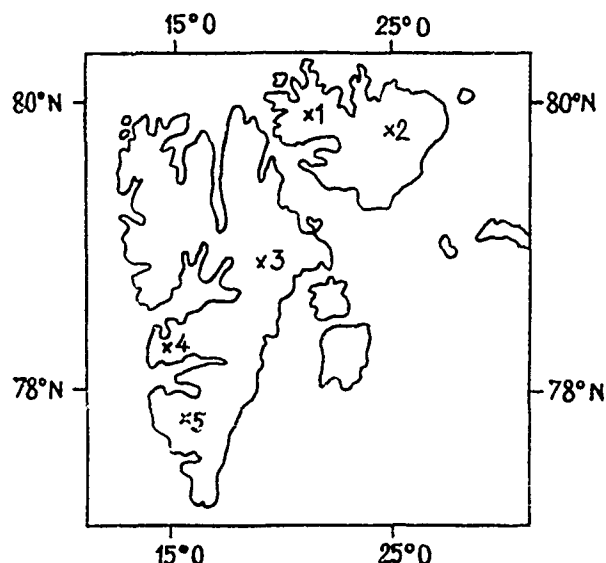


Figure 1. Location of studied glaciers (see Table 1).

The data in Table 1 indicate a decrease in the $\delta^{18}\text{O}$ values with increased accumulation rates for the glaciers. The $\delta^{18}\text{O}$ values also decrease in a north and northeast direction. This reveals a positive correlation between $\delta^{18}\text{O}$ and the temperature, as well as a decrease in the moisture content of the air masses that feed the glaciers when moving northeast from the seasonally ice-free sea.

Figure 2 presents the isotopic profiles of the four studied ice cores reflecting the changes in glacioclimatic conditions on the archipelago during the last thousand years. The Nye model was used to relate the isotope profiles of the ice cores to the time scale. Reference horizons with raised β -activity resulting from nuclear bomb tests serve as a basis for determining the mean accumulation rate [Vaikmäe, 1990]. Relatively negative $\delta^{18}\text{O}$ values in the ice layers which formed between the first half of the 17th century and the beginning of the present century reflect severe climatic conditions during the Little Ice Age. The shift to less negative $\delta^{18}\text{O}$ values starting at the beginning of this century is also characteristic of all the cores and indicates the warming of annual temperatures. The lower parts of the isotopic curves are harder to compare. However, the shift to more negative $\delta^{18}\text{O}$ values in the 12th–13th centuries is observable on three profiles and also relates to a more severe climate. At the same time a certain temporal asynchrony can clearly be noticed between the dynamics of glacioclimatic conditions for glaciers situated in various regions under different geographical conditions. The analysis of the isotopic profiles of the Svalbard glaciers, together with the studies of the structure and texture of the ice cores, has shown that in the case of some glaciers (e.g., the Grønfjord–Fridtjof ice divide) the climatic changes during the period under consideration also caused changes in the feeding type of the glacier [Vaikmäe et al., 1977; Kotlyakov, 1985].

SEVERNAYA ZEMLYA (NORTH LAND) ICE CORE

The $\delta^{18}\text{O}$ variations and Cl^- concentrations in this 556-m-long ice core from the Vavilov ice dome (Severnaya Zemlya) were studied in order to reconstruct long-term climatic changes in the central part of the Arctic [Vaikmäe and Punning, 1984]. Different methods were used to compile the time scale. ^3H from the glacier surface to the depth of 7.5 m and changes in the total β -activity were determined in order to calculate the mean annual accumulation rate which is 10–15 cm of ice [Vaikmäe et al., 1980]. The Nye–Johnson model [Dansgaard et al., 1973] was used to reconstruct the time scale for the remainder of the isotopic profile. After considering the deformation of annual layers due to ice flow

No. in Fig. 1	Glacier	Elevation (m.a.s.l.)	Mean accumulation of ice (cm yr ⁻¹)	Mean $\delta^{18}\text{O}$ (‰)	Mean Cl^- concentration (mg l ⁻¹)
1	Amundsen	700	68	-11.0	0.5
2	Grønfjord-Fridtjof ice divide	450	62	-10.8	35
3	Lomonosov plateau	1000	85	-14.2	4
4	Westfonna (Nordaustlandet)	580	88	-15.5	1.5
5	Austfonna (Nordaustlandet)	700	97	-17.9	1.0

Table 1. Mean $\delta^{18}\text{O}$ and Cl^- values in the studied Svalbard ice cores.

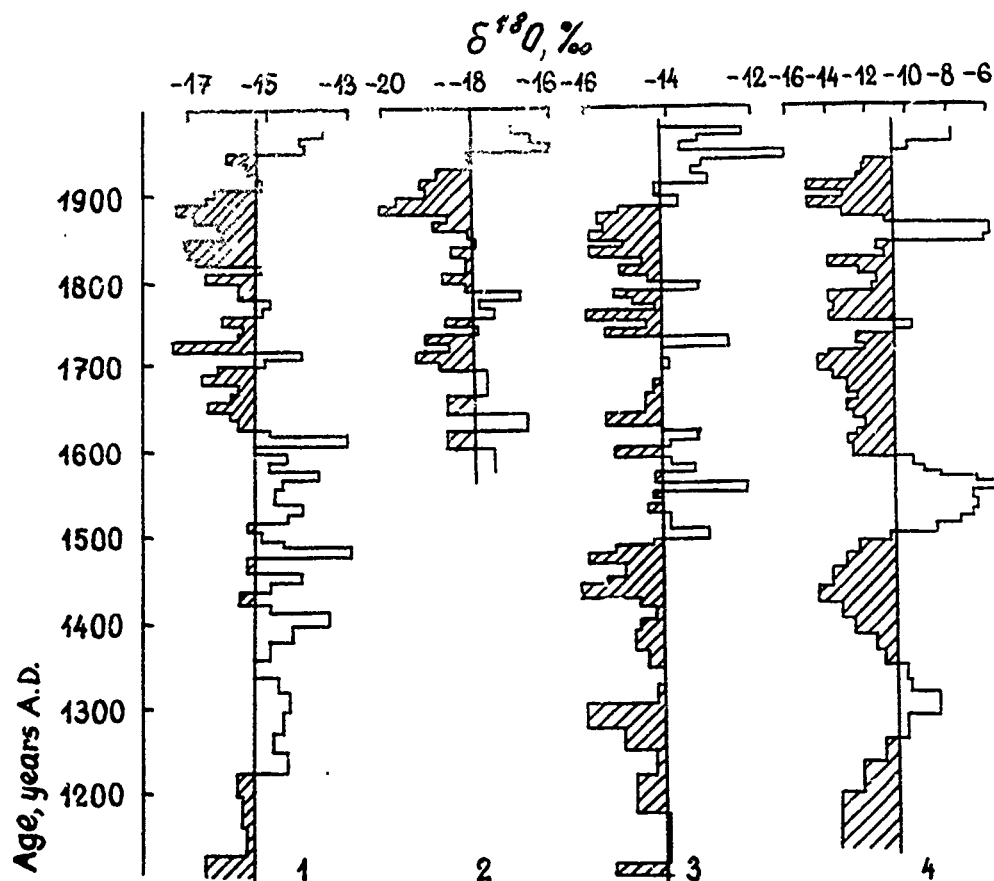


Figure 2. Variations in $\delta^{18}\text{O}$ for the Svalbard ice cores: (1) Westfonna, (2) Austfonna, (3) Lomonosov plateau, (4) Grønfjord-Fridtjof ice divide.

and the possibility that due to only minor accumulation some annual layers may have melted entirely during the summer, it may be assumed that the vertical profile of the studied ice core covers almost the entire Holocene. To check the correctness of time scale calculations we determined $\delta^{18}\text{O}$ and Cl^- variations in detailed samples from various depths of the glacier profile in order to estimate the preservation of seasonal information in the deeper parts of the glacier and possible changes of accumulation rate through time. It appears that seasonal variations are observable up to a depth of 400 m and there are no detectable differences in the mean accumulation rates over longer periods of time. There is still some uncertainty about the time scale for the last part of the core. No sharp changes in the $\delta^{18}\text{O}$ values can be seen in Figure 3, even though such a shift is characteristic of the majority of isotopic profiles determined from glaciers straddling the Pleistocene-Holocene boundary [Dansgaard et al., 1973; Robin, 1981]. It is possible that essential changes in the mean accumulation rate have taken place during the Holocene such that the studied core actually does not cover the entire Holocene and the time scale for the last 100–150 m is incorrect. It is important to note that the lower part of the Vavilov dome isotopic curve reflects climatic conditions similar to the present or even milder. Studies on the archipelago have shown the wide distribution of herbs and shrubs there 15–10 thousands years ago [Makeyev et al., 1979]. Present climatic conditions are

too severe for this kind of flora. Therefore, it is possible that the last part of the isotopic curve actually reflects the milder climatic conditions in this part of the Arctic during the transition from Pleistocene to Holocene. The trend of the curve indicates slow cooling at the beginning of the Holocene. This was followed by rapid warming about 7000 years ago, followed by 2000 years of very unstable climate. The $\delta^{18}\text{O}$, as well as the Cl^- values have varied over a rather wide range around the mean value. This part of the curve evidently reflects the Holocene Climatic Optimum which was followed by relatively stable and cooler climatic conditions about 3000 years ago.

From Figure 3 it would appear that the climate has been comparatively inconsistent in this region during the last 2000 years. During this time, various changes have taken place against the background of a generally milder climate, which on the $\delta^{18}\text{O}$ curve is expressed by a change in the mean $\delta^{18}\text{O}$ toward more positive values and by a simultaneous increase in the concentration of the Cl^- .

NOVOLAZAREVSKAYA (THE ANTARCTIC) ICE CORE

In the Southern Hemisphere we based our investigations of climatic changes on the ice core from a firm glacier situated in a subglacial depression between the Wohlthat massive and the "Institute of Geology of the Arctic" nuntaks south of the Novolazarevskaya Station ($71^{\circ}05'\text{S}$, $11^{\circ}40'\text{E}$),

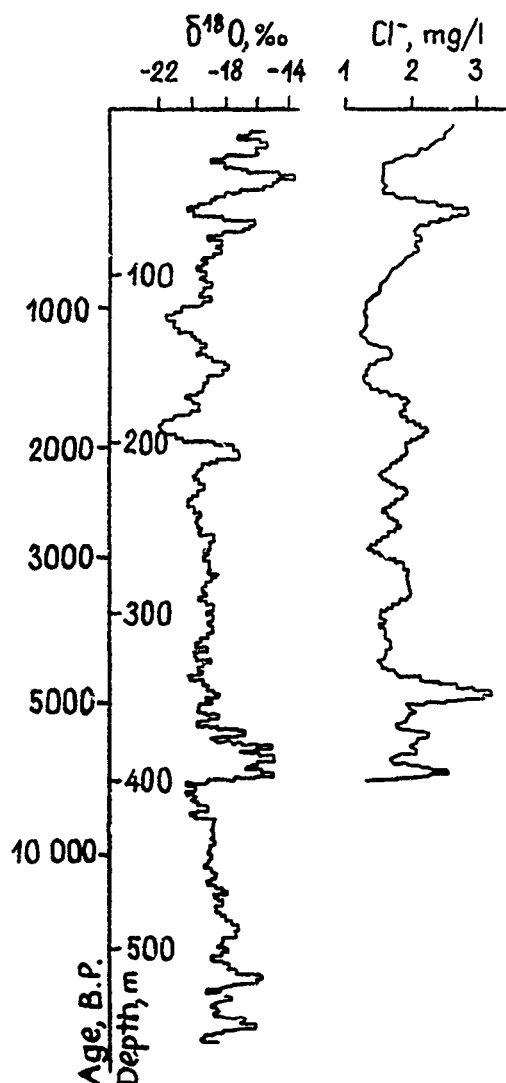


Figure 3. Variations in $\delta^{18}\text{O}$ and Cl^- concentrations for the Severnaya Zemlya ice core.

East Antarctica. The Soviet Antarctic Expedition of 1977 drilled an 809-meter ice core almost through the whole glacier. Integral samples for $\delta^{18}\text{O}$ analysis were taken from the entire core at a step of 20 m. Detailed samples (3 cm each) were taken over a 1-m section of core every 100 m to determine the mean accumulation rate and to study the preservation of isotopic variations. Isotopic analysis of the samples taken from the upper part of the core and from the walls of pits dug in the glacier surface indicates the current mean annual accumulation at the drilling site to be about 0.2 m of ice. This value was confirmed by a visual examination of the stratigraphy in the pit walls. Such an accumulation rate is comparatively high for the Antarctic and allows us to assume that seasonal $\delta^{18}\text{O}$ variations have been preserved to a great depth in the investigated glacier. Considering the bottom relief of the area, the ice flow rate is insignificant at the drilling site and it may thus be presumed that the glacier has mainly formed from precipitation accumulated in this area during the Holocene. Isotopic analysis of detailed samples from various depths of the ice core indicates that sea-

sonal variations of $\delta^{18}\text{O}$ have also been well preserved in the deeper layer of the glacier. The amplitude of $\delta^{18}\text{O}$ variations starts to decrease only below a depth of 600 m.

To compile the time scale we used, as in the case of the Vavilov ice dome, the Nye-Johnson model [Dansgaard et al., 1973], which should work well in the case of the given glacier. According to the model, the $\delta^{18}\text{O}$ profile of the core should reflect climatic changes in the study area over the last 7000–8000 years (Figure 4). The time scale may be considered to be reasonably accurate to a depth of 700 m (i.e., an age of about 5000 years) as the accumulation rates determined by isotopic analysis of detailed samples are in good correlation with those calculated by the model.

Despite the high degree of integration (100 years per sample) the $\delta^{18}\text{O}$ profile in Figure 4 is quite informative. The considerable shift towards less negative values of $\delta^{18}\text{O}$ in the lower part of the profile may be interpreted as a change of the climate towards mildness corresponding to the Holocene Climatic Optimum. Above this the $\delta^{18}\text{O}$ values remain near the mean value of the profile, -25.2‰ , until approximately 3000 years ago when a warming of the climate took place again followed by a moderately cool climate at about 1500 years ago. The $\delta^{18}\text{O}$ profile indicates that the coldest climate during the whole period recorded was during the interval of 1000 to 1500 years ago. This was followed by a slow but constant warming, culminating about 700 years ago. Afterwards, the isotopic data again suggest a rather sharp cooling succeeded by slow but constant warming during a period of about 400 years. This is followed by another cooler period, equal to the previous one in its intensity, which is in good time correlation with the Little Ice Age. At the beginning of the present century a new shift towards warmer climate takes place, but this shift is considerably smaller than the isotopic curves of the Northern Hemisphere. Finally, it is important to mention that the isotopic composition of modern precipitation is about 0.5‰ more negative than the mean value of the whole isotopic profile of the studied ice core.

ISOTOPIC RECORDS FROM PERMAFROST AREAS

In the Arctic, especially in its eastern sector, there are extensive areas where no glaciers currently exist and, possibly, in some areas have never existed in the past either. These are the areas of permafrost where several forms of ice occur within the ground. The source water for most ground ice types originates from infiltrating precipitation. As the isotopic composition of precipitation is dependent upon the condensation temperature of the vapor mass from which the precipitation formed, the ground ice developing directly from the accumulation of unaltered precipitation can reflect climatic changes through time. However, unlike glacier ice, the range of formation mechanisms for ground ice is very large. Hence, the formation conditions of the isotopic composition of ice differs, which can complicate the interpretation of their isotopic characteristics considerably as compared to glacier ice. The possibilities of applying the oxygen-isotope method and the character of the obtained information depend strongly on the type of ice studied. For this reason it is expedient to discuss separately the possibilities and limitations of the method as applied to the main genetic types of ground ice.

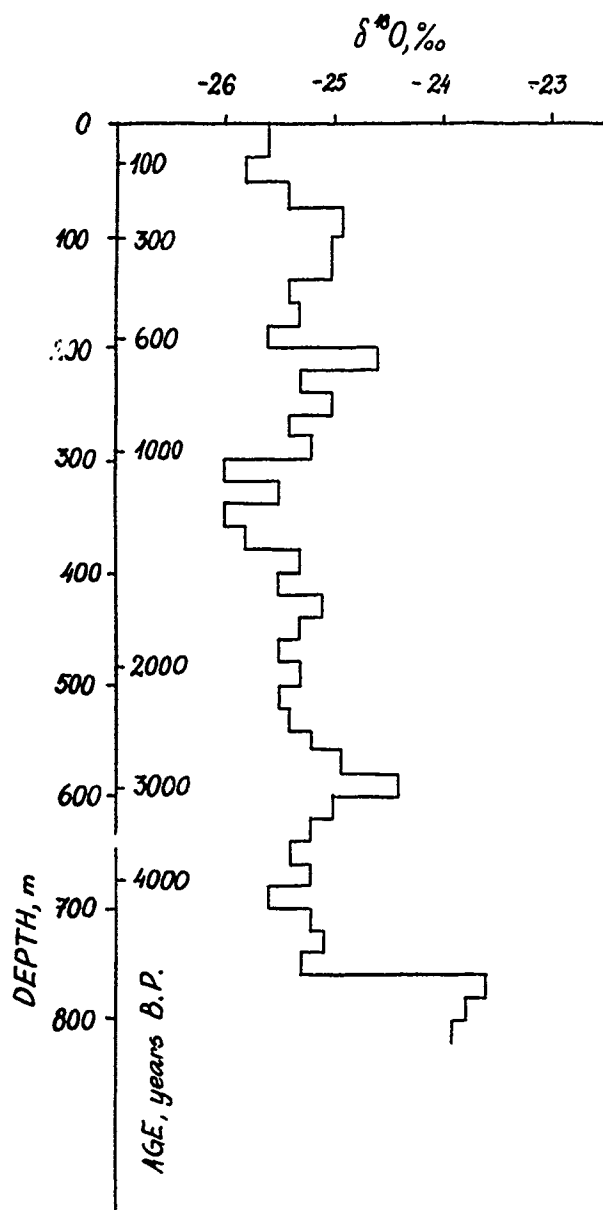


Figure 4. Variations in $\delta^{18}\text{O}$ for the Novolazarevskaya ice core.

Polygonal Wedge Ice

The main formation mechanism of polygonal wedge ice (PWI) is the frost-caused cracking of the ground. In the winter period, the fissures are filled with snow and in the spring-summer period with water which later freezes to form elementary wedges. PWI is formed by the repeated occurrence of this process. Depending on facial conditions the frost-caused fissures may also be filled by river water during floods. In both cases the water is of atmospheric origin and its isotopic composition reflects climatic conditions at the time of precipitation. This serves as the basis for the paleoclimatic interpretation of isotopic variations in PWI. There exists a close correlation between the oxygen-isotopic composition of PWI and the mean winter temperature [Vaikmäe and Konyakhin, 1988]. This conclusion is of great importance for paleoclimatic studies as it provides the basis

for the application of isotopic analysis to ancient PWI for reconstructing records of climate in the past. We are of the opinion that the best PWI to study are those of small and medium size. It is considerably more difficult to interpret $\delta^{18}\text{O}$ variations in huge syngenetic PWI. As the formation process of PWI is rather slow, the evolution of an elementary ice wedge into a huge wedge takes thousands of years. Therefore, the isotopic composition of huge PWI integrates information on climatic changes over too long a time interval.

It has been ascertained that PWI of various ages considerably differs as to $\delta^{18}\text{O}$. The sharpest changes in $\delta^{18}\text{O}$ values of PWI can be found at the transition from late Pleistocene to Holocene. Thus, according to our data, the difference in $\delta^{18}\text{O}$ values between the Pleistocene PWI and the Holocene PWI in the Lower Kolyma is about 6‰ [Arkhangelov et al., 1988]. Similar differences have been seen in the Canadian Arctic by Michel [1990]. It should be mentioned that variations with the same amplitude in the isotopic composition have been detected in glacier ice of the Arctic and the Antarctic for the transition from Pleistocene to Holocene [Dansgaard et al., 1973]. $\delta^{18}\text{O}$ values of the Holocene PWI are close to those of modern ones.

Segregated Ice

Several types of surface water and ground moisture take part in the formation of segregated ice. Their isotopic composition may vary over a wide range. During the migration and crystallization of this water, isotopic fractionation takes place which considerably complicates the interpretation of oxygen isotope data. Marked differences occur between epigenetic and syngenetic ice formations. As indicated by our own investigations, and also judging from the literature, the oxygen-isotope method appears rather uninformative when applied to epigenetic ice.

The water accumulated in the seasonally thawed layer (STL), in cases of syngenetic freezing, may be of many different origins (atmospheric precipitation, surface water, melt water from last winter's ice) and thus also of different isotopic compositions. However, mixing of water and homogenization of the isotopic composition takes place in the STL. As a result of this, the oxygen-isotopic composition of the current STL ice is governed by approximately the same regularities as the presently forming ice wedges. For example, our studies in the Kolyma Lowland showed that periods of warming and cooling can be clearly distinguished according to the oxygen-isotope composition of texture ice from the Yedomia sections [Arkhangelov et al., 1987]. The elucidated property of syngenetic texture ice to react to climatic changes with changes in the isotopic composition is the basis for the suggestion to use $\delta^{18}\text{O}$ variations in such ice for the stratigraphic division of perennial ice.

CONCLUSIONS

The isotopic profiles of glacier ice in the Arctic archipelagos and the Antarctic marginal areas are, despite their comparative shortness, important sources of paleoclimatic information. Their detailed analysis enables us to obtain information not only on global climatic changes but also to estimate the local peculiarities.

An essential but presently still not much used source of paleoclimatic information are the isotopic variations in per-

mafrost. Comparative analysis of the isotopic profiles of glaciers with the latter gives a good opportunity to estimate the distribution of the isotopic composition of paleo-

precipitation on a circumpolar as well as global scale.

This work is a contribution to the IGCP Project 253 "Termination of the Pleistocene."

REFERENCES

- Arkhangelov, A. A., R. A. Vaikmäe, M. A. Konjakhin, and D. V. Mikhajlov, Oxygen isotopic composition of ground ice and surface waters in Kolyma Lowland (in Russian), 16 pp., VINITI, Moscow, 1988.
- Arkhangelov, A. A., R. A. Vaikmäe, D. V. Mikhajlov, J.-M. K. Punning, and V. I. Solomatin, Stratigraphic division of permafrost in Kolyma Lowland using the oxygen isotope method (in Russian), in *New Data in Quaternary Geochronology*, pp. 143-149, Nauka Publ., Moscow, 1987.
- Dansgaard, W., S. J. Johnsen, H. B. Clausen, and N. Gundestrup, Stable isotope glaciology, *Medd. Grønland*, 197, 6-53, 1973.
- Kotlyakov, V. M. (Ed.), *Glaciology of Spitsbergen* (in Russian), 199 pp., Nauka, Moscow, 1985.
- Makeyev, V. M., H. A. Arslanov, and V. E. Garutt, The age of mammoths of Severnaya Zemlya and some problems of the paleogeography of the Late Pleistocene (in Russian), *Proc. USSR Acad. Sci.*, 245, 173-177, 1979.
- Michel, F. A., Isotopic composition of ice-wedge ice in Northwestern Canada, in *Permafrost Canada. Proc. of the Fifth Canadian Permafrost Conference*, pp. 5-9, NRCC, 1990.
- Oeschger, H., and C. C. Langway, Jr. (Eds.), *The Environmental Record in Glacier and Ice Sheets*, Dahlem Workshop on the Environmental Record in Glaciers and Ice Sheets, Berlin, 1988, 393 pp., Wiley Interscience 1989.
- Punning, J.-M., R. Vaikmäe, and K. Tõugu, Variations of $\delta^{18}\text{O}$ and Cl^- in the ice cores of Spitsbergen, *J. Phys. Colloq.*, C148, 619-624, 1987.
- Robin, G. de Q., *The Climatic Record in Polar Ice Sheets*, 212 pp., Cambridge University Press, Cambridge, 1981.
- Vaikmäe, R. A., and M. A. Konyakhin, *Formation of Oxygen Isotope Composition of Current Polygonal Ice Wedges* (in Russian), 21 pp., VINITI, Moscow, 1988.
- Vaikmäe, R., Isotope variations in the temperate glaciers of the Eurasian Arctic, *Int. J. Radiat. Appl. Instrum. Part E, Nucl. Geophys.*, 4, 45-55, 1990.
- Vaikmäe, R. A., F. G. Gordijenko, V. S. Zagorodnov, V. I. Mikhajlov, J.-M. K. Punning, and R. A. Rajamäe, Isotope geochemical and stratigraphic studies on the ice-divide of Grønfjord and Fridtjof glaciers (West Spitsbergen) (in Russian), *Data of Glaciological Stud. No. 30*, 77-87, 1977.
- Vaikmäe, R., and J.-M. Punning, Isotope-geochemical investigations on glaciers in the Eurasian Arctic, in *Correlation of Quaternary Chronologies*, edited by W. C. Mahaney, pp. 385-393, Norwich, 1984.
- Vaikmäe, R. A., J.-M. K. Punning, V. V. Romanov, and N. I. Barkov, Stratigraphy of the Vavilov Ice Dome, Severnaya Zemlya, with the help of isotope-geochemical methods (in Russian), *Data of Glaciological Studies*, 40, 82-87, 1980.

AD-P007 349



92-17853



Little Ice Age Glaciation in Alaska: A Record of Recent Global Climatic Change

Parker E. Calkin and Gregory C. Wiles

Department of Geology, University at Buffalo, Buffalo, New York, U.S.A.

ABSTRACT

General global cooling and temperature fluctuation accompanied by expansion of mountain glaciers characterized the Little Ice Age of about A.D. 1200 through A.D. 1900. The effects of such temperature changes appear first and are strongest at high latitudes. Therefore the Little Ice Age record of glacial fluctuation in Alaska may provide a good proxy for these events and a test for models of future climatic change. Holocene expansions began here as early as 7000 B.P. and locally show a periodicity of 350 years after about 4500 years B.P.

The Little Ice Age followed a late Holocene interval of minor ice advance and a subsequent period of ice margin recession lasting one to seven centuries. The timing of expansions since about A.D. 1200 have often varied between glaciers, but these are the most pervasive glacial events of the Holocene in Alaska and frequently represent ice marginal maxima for this interval. At least two major expansions are apparent in forefields of both land-terminating and fjord-calving glaciers, but the former display the most reliable and detailed climatic record. Major maxima occurred by the 16th century and into the mid-18th century. Culmination of advances occurred throughout Alaska during the 19th century followed within a few decades by general glacial retreat. Concurrently, equilibrium line altitudes have been raised 100–400 m, representing a rise of 2–3°C in mean summer temperature.

INTRODUCTION

An interval of generally cooler climate spanning the 13th through the 19th centuries called the "Little Ice Age" [Grove, 1988] may provide one of the best opportunities to test and refine models that may discriminate between natural and human-induced global climatic changes. For no other interval of global climatic change are baseline conditions so well known, nor is resolution so readily available for the timescales of decades to centuries that are demanded for the study of key climatic interactions [International Geosphere-Biosphere Program (IGBP), 1988].

Historical and recent instrumental records strongly suggest that studies of climate proxy data in the northern hemisphere, and particularly in the Arctic, are critical. It is here where global climatic changes have first appeared (by a century to decades) and where the range, amplitude, and effect of changes has been in the past, and is expected to be in the future, the greatest [Lamb, 1977].

The Little Ice Age occurred in late Holocene time following a brief interval of temperate climate called the "Medieval Optimum" or "Medieval Warm Period" preceded by an interval of Early Medieval glacial advances [Lamb, 1977; Williams and Wigley, 1983]. It was a time of drastic increase in weather variability as well as cooler climate [Lamb, 1977]. The name is appropriate because during this Little Ice Age interval, the world-wide extent of ice in mountain glaciers and in other forms attained a maximum as great as, or in some cases greater than, that at any time since the end of the Pleistocene [Grove, 1988].

The objective of this paper is to summarize the Little Ice Age record as displayed by mountain glacier fluctuations in Alaska since about A.D. 1200. Alaska's mountain glaciers display marginal advance or retreat within a few years to decades of climatic changes. Therefore they may be good indicators of any man-induced warming [e.g., Oerlemans, 1986]. In addition these mountain glaciers are a major component of contemporary sea level rise [Meier, 1984].

The climatic record is inferred largely from moraines or similar deposits whose apparent age is assumed to be a function of the response of the glacier to climate. Major exceptions to this assumption are considered.

Analyses of mass balances (snow accumulation vs. wastage) on mountain glaciers show that annual to decadal variations are comparable between areas within about 500 km [Letreguilly and Reynaud, 1989]. Therefore the glacial chronologies are considered for 11 regions within this span (Figure 1) where some organized study of the total Holocene record of glaciation has been previously undertaken [see Calkin, 1988]. A good deal of scattered data on Little Ice Age glaciation has not been included here because of space limitations. Furthermore, no assumption of equal weight can be placed on these chronologies since they cover widely varying areas, use variable dating methods, and sample anywhere from only a few to nearly 100 glacier forefields. The research sites fall rather naturally into three north-south regions corresponding with Arctic, Continental and Maritime climatic zones (Figure 1). Taken from north to south, these display increasing glacier size, temperature, moisture, and opportunity for dating precision.

Radiocarbon ages presented below have been converted to mean calibrated ages, and for the last one to two millennia, to dates A.D. using the method of Stuiver and Reimer [1986]. Calibration had little effect on lichenometric curves and their derived ages were therefore converted directly to calendar years.

INDIVIDUAL GLACIAL CHRONOLOGIES

Arctic. These high latitude glaciers are dispersed and very small subpolar glaciers that occur within the zone of continuous permafrost. They are sluggish relative to warm-based glaciers to the south; however, they have shorter reaction times because of their size. Precipitation is derived mostly from the distant Bering Sea on the west and ranges between *ca.* 500 to 1000 mm yr⁻¹ with half as snow. The arctic glaciers occur beyond the tree line; therefore chronologies depend heavily on lichenometry, which provides minimum ages for glacier retreat.

Brooks Range. Forefields of 89 glaciers confined mostly to north-trending cirques were mapped along 500 km of the central and eastern Brooks Range at altitudes from 1300 to 2100 m. An additional eight forefields of larger valley glaciers were sampled in the eastern area. A Holocene chronology of at least 11 episodes of glacial advance or stand was initiated as early as 7600 lichen years B.P. and displays a crude periodicity of 350 years after about 4500 years B.P. [Ellis and Calkin, 1984; Haworth, 1988; Calkin, 1988].

A lichenometric curve from the central Brooks Range [Calkin and Ellis, 1980] allows the definition of two, and at least part of a third, clusters of advances with dates of A.D. 1200, 1570, and 1860 (Figures 2,3). These followed an earlier cluster of advances centered about A.D. 854 and which is confirmed locally by a direct radiocarbon date of A.D. 897 [Calkin and Ellis, 1981]. The three Little Ice Age events are displayed at, respectively, 45, 85 and 42 glaciers across the area.

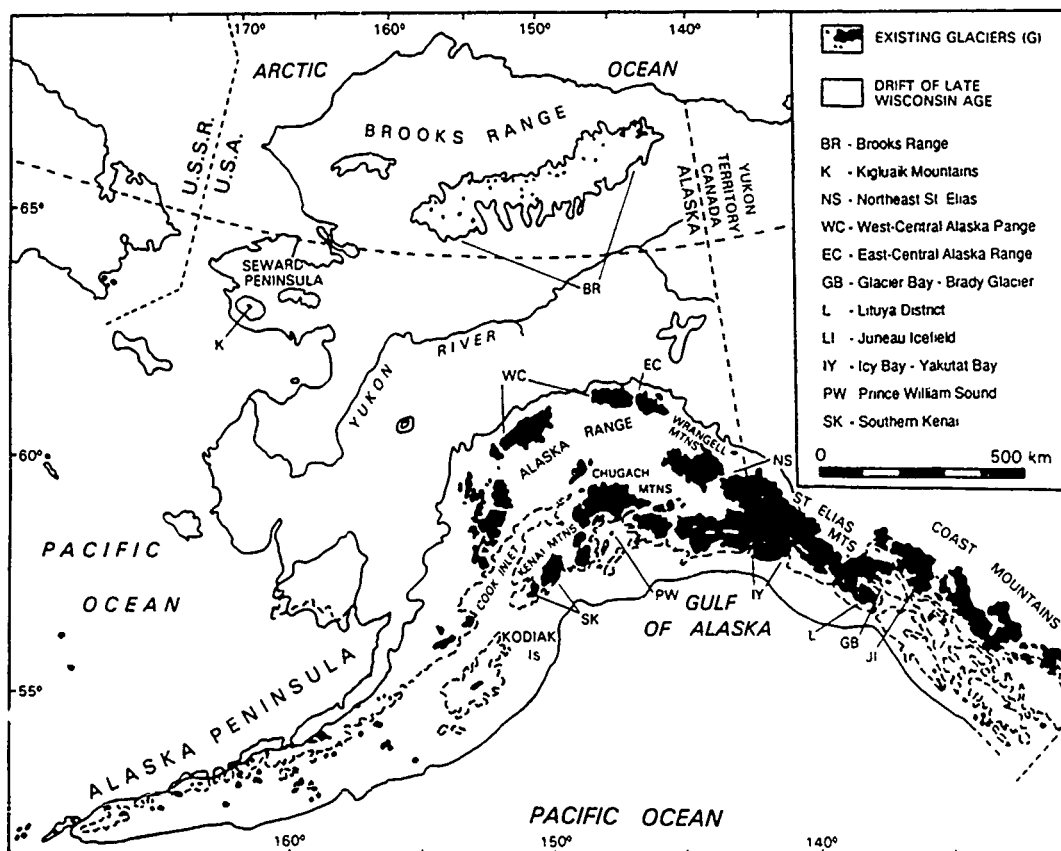


Figure 1. Map of Alaska showing existing glaciers, limits of late Wisconsinan drift and locations of the 11 study areas of late Holocene glaciation (modified from Porter et al. [1983]).

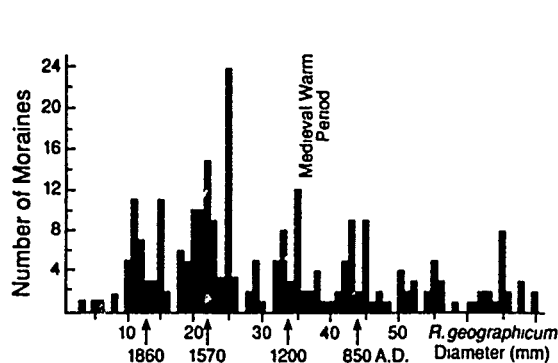


Figure 2. Frequency histogram of *Rhizocarpon geographicum* maximum diameters from late Holocene moraines of the Brooks Range with corresponding dates (modified from Haworth [1988]).

The A.D. 1570 advance, by far the most pervasive, is confirmed locally by radiocarbon dates of A.D. 1566 and A.D. 1637 from glacially overrun moss and wood, respectively. Some evidence suggests that ice margins remained close to these positions until ca. A.D. 1780. In the eastern Brooks Range, moraines of ca. 1860 to 1890 are more prominent than to the west and formed immediately behind those of the preceding advance.

Recession from these advances has reached several hundred meters and is still occurring. Determination of mass budgets of three glaciers and reconstructions at 58 cirque glaciers suggests that maxima were associated with equilibrium line altitudes (ELAs) 100 to 200 m lower and July mean temperatures 2 to 3°C lower than mean values of 1978–1983 [Calkin et al., 1985].

Kigluaik Mountains, Seward Peninsula. Only three tiny cirque glaciers remain today on the Seward Peninsula (Figure 1) southwest of the Brooks Range where peaks are below 1500 m altitude and the climate is more humid and warmer [Calkin et al., 1987; Kaufman et al., 1989]. These glaciers, the Phalarope, Thrush, and Grand Union (unofficial names), occur on a south to north transect at about 800 to 650 m altitude, respectively.

A preliminary lichen curve suggests that the earliest advance probably occurred at Grand Union and Thrush glaciers as early as the early to middle 17th century (Figure 3). Moraine building at Phalarope Glacier may have taken place at the same time or as late as the middle 1700s. Grand Union Glacier also shows an inner moraine that may date from a middle to late 19th century stand [Przybyl, 1988; Calkin, 1988]. The ELAs, now just above the glaciers, may have been less than 100 m lower during these Little Ice Age events.

CONTINENTAL INTERIOR

The sequences obtained here are derived mostly from medium to large valley glaciers and long, temperate tongues of high level icefields that descend to between 2400 to 1500 m altitude on the dry, northern flanks of the Wrangell and St. Elias Mountains as well as the Alaska Range (Figure 1). Moisture for these glaciers moves northward from the Gulf of Alaska bringing 500 to 300 mm of precipitation to the mountains.

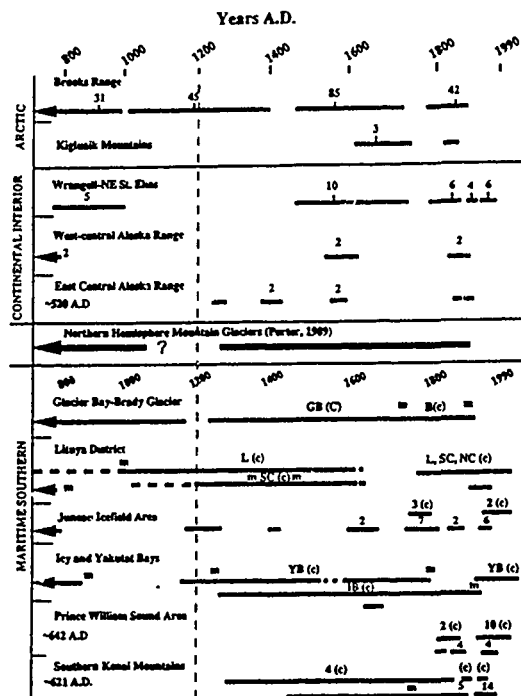


Figure 3. Generalized intervals of glacial advance and moraine formation during late Holocene time across 11 study areas of Alaska. Intervals of advance for noncalving mountain glaciers of the Northern Hemisphere (from Porter [1986, 1989]) are shown for comparison. Explanations: For Prince William Sound and southern Kenai Mountains, advances preceding the LIA culminated ca. A.D. 642 and 621 respectively. Numerals indicate number of glacier-moraines that display the advance and vertical bars are means of lichenometric age clusters. For maritime areas, (c) = fjord-calving glacier, m = time of end moraine formation, GB = Glacier Bay, B = Brady Glacier, L = Lituya Glacier, SC = South Crillon Glacier, NC = North Crillon Glacier, YB = Yakutat Bay glacier complex, IB = Icy Bay glacier complex.

About 22 glaciers, including 14 known to have surged [Post, 1969], were used to develop the chronologies. Surges, involving anomalously high movement rates, are not directly related to climate. Therefore, the typical chaotic or thin moraines considered to result from this type of movement have been avoided by workers who developed the sequences in continental and maritime areas.

Wrangell-Northeastern St. Elias Mountains. Glacier-incorporated tephra, overrun forests, and particularly lichenometry (Figure 4), provide important controls for a late Holocene chronology based on 11 valley glaciers [Denton and Karlén, 1977]. The glacier advances began following an interval of high spruce tree line 3600 to 3000 years B.P.

The Little Ice Age was ushered in following a short-lived Neoglacial expansion between 1169 and 959 B.P. [Denton and Karlén, 1977], and a subsequent ice margin retraction ending ca. A.D. 1440. Denton and Karlén [1977] differentiated four general ages of Little Ice Age moraines on the basis of lichenometry (Figure 4) and position. The oldest advance began at least by ca. A.D. 1500; three subsequent expansions may have been centered on the late 18th to mid-19th, late 19th, and early 20th centuries (Figures 3,4). The relative importance of each of these events is uncertain since

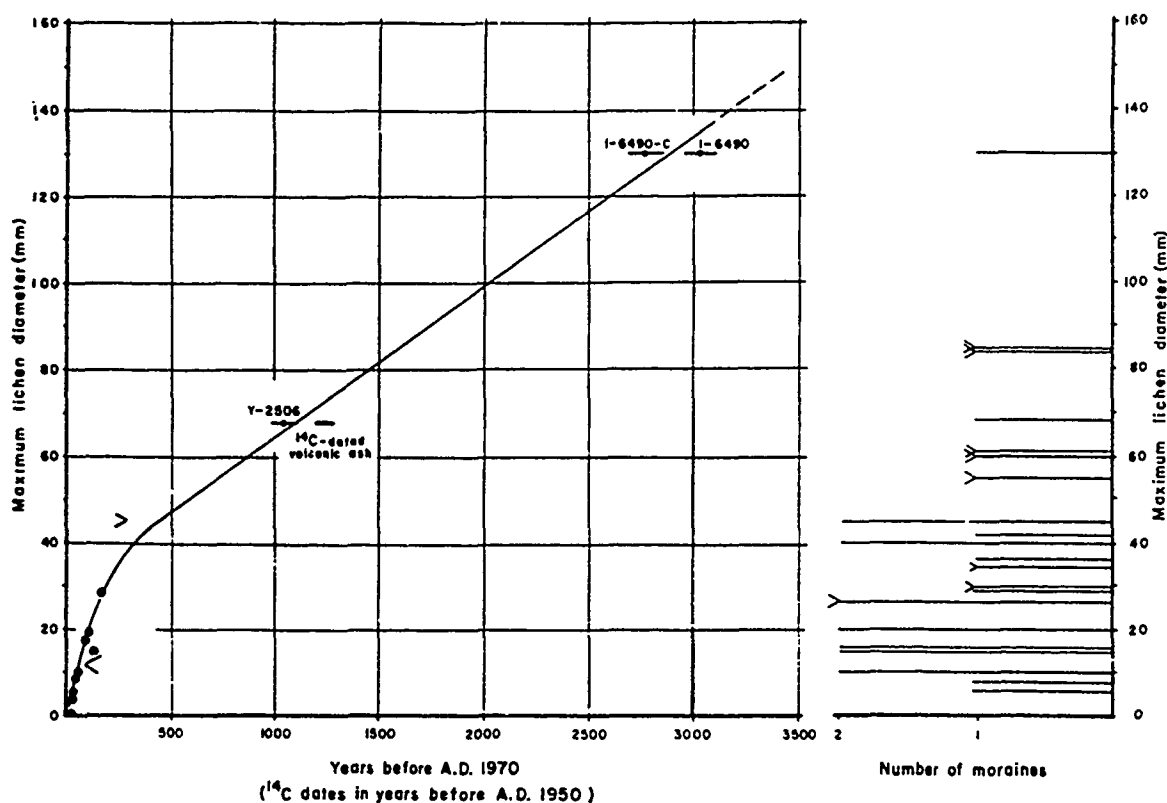


Figure 4. Frequency histogram of *Rhizocarpon geographicum* maximum diameters from late Holocene moraines of the Wrangell-northeastern St. Elias Mountains, with lichen growth curve. Dots show control points. From Denton and Karlén [1977, Figure 4].

the earlier Holocene moraines physically limited Little Ice Age expansions. However, to the south in the Yukon Territory, many maxima occurred in the mid- to late 19th century as shown by limiting radiocarbon ages [Borns and Goldthwait, 1965; Rampton, 1970, 1978; Denton and Karlén, 1977]. Little Ice Age expansions extended the glacier margins by 12–60% of the present glacier lengths or about 1–6 km.

West-Central Alaska Range. Four large glacier tongues that descend northward from the high massif of Mt. McKinley and a lower, nearby peak (Figure 1), variously display evidence of advances between 5850 years BP and ca. 1200 B.P. [Waythomas and Ten Brink, 1982; Ten Brink, 1983]. The earliest of the succeeding Little Ice Age events were readvances of 1–3 km beyond recent ice margins of Yanert Glacier before A.D. 1540 and of the Foraker Glacier before ca. A.D. 1590. A succeeding minor readvance at ca. A.D. 1850 is based on lichen from moraines fronting Peters and Foraker glaciers. This sequence (Figure 3) is built principally on applications of the lichen curve of Denton and Karlén [1977] supported by additional local radiocarbon ages [Ten Brink, 1983; personal communication, 1987].

East-Central Alaska Range. Multiple advances of four valley glaciers at the head of the Delta River, east-central Alaska Range (Figures 1,3), have been recorded by Reger and Péwé [1969] and Péwé and Reger [1983] after ca. 5700 radiocarbon years B.P. Like that of the west-central area (above), the chronology is based on the lichen curve of Denton and Karlén [1977] and several local radiocarbon ages.

One or possibly two minor Little Ice Age "pulses" were

recorded by deposition of outwash at Gulkana Glacier that was associated with a radiocarbon date of A.D. 1245. This followed an advance of the Black Rapids Glacier ca. A.D. 520. More important Little Ice Age expansions occurred at the Canwell, College and possibly the Gulkana glaciers about A.D. 1390 and at the Black Rapids and Gulkana glaciers at A.D. 1560. Historic evidence and lichen data substantiate advances of Gulkana and College glaciers within 25 years beginning soon after A.D. 1875 and 1900, respectively. Rise in the firm limit of Gulkana Glacier may have been as great as 380 m since the Little Ice Age maximum according to map and aerial photograph studies of Mercer [1961].

MARITIME SOUTHERN ALASKA

Climate in this region is dominated by a strong Aleutian low pressure system. Summers are cool, winters mild and precipitation is very heavy; glaciers are temperate. Forests rapidly invade deglaciated areas resulting in chronologies that are supported by abundant radiocarbon and tree ring data. Historical records beginning with the expedition of LaPerouse [1794] in 1786 are available.

Data from grounded tidewater glaciers are an important component of chronologies here. Iceberg-calving fjord glaciers often undergo anomalous, slow advances that depend on end moraine construction at their termini to maintain stability. They also disintegrate and retreat rapidly. These movements are often asynchronous with those of adjoining land-terminating glaciers and with climatic fluctuations on the shorter scale of decades. However, their general regional

pattern of advances and retreats appears to display sensitivity to long-term climatic trends [Goldthwait, 1966; Mann, 1986; Meier and Post, 1987; Porter, 1989] as noted below.

Glacier Bay and Brady Glacier Area. Glacier Bay (Figure 1) was dominated during the Holocene by periodic southeastward flow down the main 100-km-long fjord arm [Goldthwait, 1966]. Flow reached far enough to dam the eastern Muir Inlet arm of the Bay at two times between 2500 B.P. and 900 B.P. followed by major recession [Derksen, 1976; Goodwin, 1988]. A radiocarbon date of A.D. 1209 provides a maximum for the Little Ice Age readvance down the main arm of Glacier Bay. This culminated with moraine building *ca.* A.D. 1700 to 1750 at its probable Holocene maximum near the mouth of the Bay (Figure 3) [Goldthwait, 1966; Goodwin, 1988]. The very large, southern Brady Fjord tongue, adjacent to Glacier Bay, reached its Little Ice Age maximum later at *ca.* A.D. 1886 [Derksen, 1976]. Recession of 75 to 100 km in the main arm of Glacier Bay may have ended by 1929 [McKenzie, 1979], but recession dominates elsewhere.

The late Holocene ELA of the Brady Glacier was about 120 m below that of the present [Derksen, 1976]. However, Goldthwait [1966] reported that the "firm limit" in Muir Inlet may have been at least 300 m lower in 1892 than in 1965.

Lituya District. The Holocene sequence in the Lituya Bay area, west of the Brady Glacier (Figure 3), appears to differ from that at Glacier Bay with respect to the Little Ice Age [Mann and Ugolini, 1985]. No recession corresponding to the Medieval Warm Period may be recorded. Instead, this part of the iceberg-calving Lituya complex filled Lituya Bay soon after 943 B.P. [Goldthwait et al., 1963].

Ice margins persisted at or near their outermost Holocene limits until A.D. 1600, when a variety of data, including historical evidence, suggests that most glaciers in the area began to retreat. Since 1786, glaciers of the Lituya Bay complex have advanced again, some moving down-fjord up to 20–30 m yr⁻¹ [Meier and Post, 1987]. Mann [1986] considered the Lituya System to be in the midst of a climatically insensitive compensatory advance. Nevertheless, comparison of recent dates of retreat of fjord-calving glaciers with land-terminating ones across southern Alaska (Figure 5) suggests that both result from major climatic change [Mann, 1986].

The Finger and LaPerouse glaciers, which terminate on land, directly on the Gulf of Alaska, advanced by the 1890s to near their maximum of perhaps several centuries [Mann and Ugolini, 1985]. These two glaciers have continued oscillating near these termini perhaps because of abundant moisture supply.

Juneau Icefield Area. East of Glacier Bay, outermost Little Ice Age moraines of approximately 12 Alaskan tongues of the Juneau Icefield (Figure 1) and other nearby glaciers have been dated by tree rings, lichen and historic data (Figure 3) [Lawrence, 1950; Miller, 1977]. A brief warm interval was indicated in this area by forest growth between A.D. 838 and 1300. Ice-sheared stumps signal renewed cooling and fluctuation of the Davidson Glacier at A.D. 1265 and 1401 [Egan, 1971]. Moraines of Bucher Glacier are dated at A.D. 1600 [Beschel and Egan, 1965], but are somewhat younger at the Antler Glacier. The Little Ice Age maximum at Davidson Glacier, which occurred by A.D. 1752, destroyed trees over 200 years old [Field, 1975]. Nine other

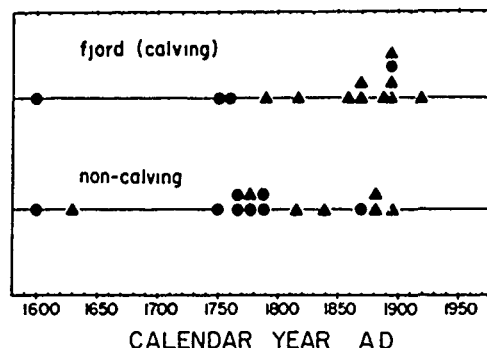


Figure 5. Comparison of timing of the last major retreat of calving and noncalving fjord glaciers in southeast (●) and south-central coastal Alaska (▲) (after Mann [1986, Figure 7]). These preliminary data suggest timing is similar for both sets and reflect the major retreats in the mid 1700s and late 1800s.

glaciers [Lawrence, 1950] have also reached recent maxima in the middle to late 18th century.

All these glaciers receded within a few decades but several paused or slightly readvanced to form end moraines during the early to late 19th century (e.g., Norris Glacier in 1917). Two fjord-calving glaciers, the Taku and Hole in the Wall Glaciers, have readvanced since *ca.* A.D. 1890 [Miller, 1964].

Icy and Yakutat Bays. The largest glaciers of North America, including the Bering and the Malaspina Piedmonts, which are grounded below sea level, together with adjacent long fjord glacier complexes of Yakutat and Icy Bays, extend from the icefields of the St. Elias and Chugach Mountains to the Gulf of Alaska (Figure 1). All of these glaciers are known to surge.

Evidence of early Holocene advance comes from Yakutat Bay [G. Plafker, personal communication, 1987; Calkin, 1988], but major glacier extension from the head of Icy Bay may not have occurred until as late as 1855 B.P. [Porter, 1989]. Two advances to outer Icy Bay, the latter culminating by A.D. 850, occurred before a 35-km recession during a relatively mild climate to the head of Icy Bay by A.D. 1230 [Porter, 1989] (Figure 3).

Renewed advance of the Icy Bay complex began before A.D. 1275 and reached mid-fjord position by the 14th–16th century. It is inferred from historical data to have arrived at its innermost terminal moraine near the mouth of Icy Bay by about the middle of the 19th century [Porter, 1989]. Retreat, which began from its terminal shoal by the 1880s, has totaled about 50 km. Ages from outer Yakutat Bay and the adjacent Russell Fjord tributary [Molnia, 1986] suggest that the Yakutat Bay complex attained its Holocene maximum about A.D. 1250 to 1500 [Plafker and Miller, 1958a,b]. Subsequent recession in Yakutat Bay was succeeded by a second Little Ice Age pulse inducing a stand or readvance to the mid-fjord by the late 17th or early 18th century. The adjacent Malaspina advanced over a forest to near its present position at about the same time [Sharp, 1958].

Middle to late 19th century marginal stagnation has occurred at the Malaspina. The Hubbard Glacier, the main tributary of the Yakutat Bay complex, has been advancing slowly since 1890 when retreat brought it to the head of Yakutat Bay [Plafker and Miller, 1958a,b; see also Mayo,

1987]. Porter's [1989] documentation of the glacier fluctuations in Icy Bay indicates that major episodes of advance encompassed 300 to 500 years, while retreats of that fjord system took less than 150 years.

To the north of the Malaspina Glacier, the Bering Glacier may have reached a recent maximum in the late 19th century before intermittent retreat of 3–5 km [Field, 1975; B. F. Molnia, personal communication, 1987]. The adjacent land-terminating Martin River Glacier, nourished by the same ice field, however, reached its Holocene maximum *ca.* A.D. 1650 [Reid, 1970].

Prince William Sound. Prince William Sound is bordered by an extensive radiating fjord system cut deeply into the tectonically active Chugach and Northern Kenai Mountains (Figure 1). Radiocarbon ages from the mouths of the Barry Arm–Harriman Fjord complex and College Fjord on the west, suggest that trunk glaciers here and perhaps in adjacent fjords reached terminal Holocene positions at fjord mouths *ca.* 3200 to 2500 B.P. [Heusser, 1983].

The earliest evidence of Little Ice Age advance comes from the Nellie Juan Glacier of the nearby Sargent Ice Field where wood of A.D. 1285 is incorporated in its end moraine [Field, 1975]. Little more is known of ice-margin fluctuations in Prince William Sound itself except for the last few centuries (Figure 3). For this period, records ranging from field observations of Vancouver [1798], to more comprehensive measurements and photography of Field [1937], Mercer [1961], Post [1975] or tree ring analyses by Viereck [1967], among others, have yielded a varied history when examined fjord by fjord. Nevertheless, some similarities are evident as indicated below.

Early 19th century extensions were recorded for the land-terminating Amherst, Crescent, Portage, and Toboggan Glaciers as well as the larger tidewater tongues of the Harriman, Yale and Serpentine Glaciers [Field, 1975]. The large Columbia Glacier, terminating farther to the east, was near its maximum late Holocene position in 1850 as well as in 1910, 1920 and 1935 [Post, 1975]. The 1870s, 1880s and possibly the early 1890s [Field, 1975, p. 423] were the most important intervals during which both land- and tidal-terminating glaciers reached more advanced positions than they had for several preceding centuries.

The rise in the firm limit since the Little Ice Age maxima in the east margin of Prince William Sound may be on the order of 230 m. On the far southwestern margin, the rise may have been only about 76 m, as estimated by studies of Mercer [1961].

SOUTHERN KENAI MOUNTAINS

The Little Ice Age record here is based on fluctuations of 15 outlet glaciers of the Harding and Grewingk–Yalik Ice fields (Figure 1). Two land-terminating and two calving glaciers show advance close to present ice margins *ca.* 1340 B.P. (Figure 3) [Post, 1980a,b,c; Wiles and Calkin, 1990] before a succeeding recession that is represented by forest growth centered at A.D. 968.

Little Ice Age activity began after A.D. 1281 based on an age of organics below drift. By A.D. 1442, the land-terminating Grewingk Glacier had extended several kilometers beyond its present position and by A.D. 1460 Tustumena Glacier was approaching its Little Ice Age maximum. Grewingk and Exit Glaciers were at their prob-

able Holocene maximum by A.D. 1650 according to dated wood in lateral moraines.

Tree-ring and lichen ages of 31 moraines from 10 land-based glaciers show renewed glacier activity at about A.D. 1735, 1820, 1850 and 1910. These data suggest ice margins were expanded 1–5 km beyond present margins and also near their maxima in the early 19th century. The four principle fjord-calving glaciers in the area reached their Holocene limits tens of kilometers beyond the present margins in the 1800s. Recession of McCarty and Northwestern fjord glaciers began *ca.* 1850 and 1910 respectively [Post, 1980b,c].

Glaciological reconstructions indicate that Little Ice Age ice tongue volumes of the Grewingk–Yalik Ice field may have been as much as 30% greater than now. ELAs were 260–320 m below those of the present. This may represent a rise of about 2°C in mean summer temperature or perhaps mean annual temperature [Padginton et al., 1990].

SUMMARY AND CONCLUSIONS

This review illustrates some of the variabilities and similarities of Little Ice Age fluctuation in Alaska. Only a very small percentage of Alaska's more than 100,000 individual glaciers have been studied and much of the work in southern Alaska has been focused on fjord-calving glaciers whose movements may not always directly reflect climatic change.

As a group, the Holocene records of mountain glaciation in Alaska display strong Little Ice Age glaciation separated from prior glacial expansions by an interval of recession. The prior glacial expansions, particularly those corresponding with Early Medieval time, were generally less extensive than those of the Little Ice Age. In areas such as the Seward Peninsula, cirque altitudes were too low to allow Holocene glaciers to exist at all prior to the late Little Ice Age.

The interval of glacial recession is correlative with the Medieval Warm Period. This occurred in Alaska prior to *ca.* A.D. 1200 and spanned one to seven centuries. Ice margins were at, or behind, present positions. Brooks Range lichen data suggest that at least one or more glaciers may have been extended during some part of the period. In addition, large fjord glaciers of the Lituya District and perhaps elsewhere in southern Alaska may have been extended during much of this time.

Little Ice Age advances of both land-terminating and fjord-calving glaciers occurred in the 13th century, but prior glacier activity in the more continental areas may have been retarded until the 15th century. Through much of Alaska, mountain glaciers were reaching Holocene and/or Little Ice Age maxima by the 16th century and as late as the early to middle 18th century. The early and middle 1700s were times of culmination of advances in southern maritime areas. However, moraine-building may have been at a minimum in Arctic and Continental Interior areas of Alaska during part of the 18th century.

The 19th century was a time of glacier expansion throughout Alaska. Many of the glaciers which were not blocked by older massive moraines, extended farther than they had during the preceding several centuries, and some advanced to their Holocene maximum positions.

During the very late 19th and early 20th centuries, ice margin recession dominated. Only a small percentage of

glacier ice margins have remained at their 19th century maxima and these were in areas of high precipitation. Recession from Little Ice Age maxima has been on the order of 0.2 km for many cirque glaciers, but up to several tens of kilometers for the fjord glaciers.

Glacier equilibrium lines are presently 100–200 m higher in the Arctic and up to 400 m higher in the Maritime areas than they were through much of the Little Ice Age. This may reflect a late 19th or early 20th century rise in mean summer temperature on the order of 2–3°C (about 1–2°C mean annual change) and/or changes in the precipitation regime [e.g., Lamb, 1977; Williams and Wigley, 1983; Mayo and March, 1990].

ACKNOWLEDGMENTS

This material is based upon work supported by the National Science Foundation under Grants DPP 7619575, 7819982, 8412897 and 8922696. Logistic support has been provided by several groups including ALASCOM, the U.S. Geological Survey, Alaska Division of Geological and Geophysical Surveys, the National Park Service, Alaska State Parks, and the Pratt Museum of Homer. T. D. Hamilton, A. S. Post, Bud Rice, and R. P. Goldthwait provided help in diverse ways, as did fellow researchers J. M. Ellis, L. A. Haworth, and B. J. Przybyl.

REFERENCES

- Beschel, R., and C. P. Egan, Geobotanical investigations of a 16th century moraine on the Bucher Glacier, Juneau Icefield, Alaska, *Proceedings 16th Alaska Science Conference*, pp. 114–115, American Association for the Advancement of Science, 1965.
- Borns, H. W., Jr., and R. P. Goldthwait, Late-Pleistocene fluctuations of Kaskawulsh Glacier, southwestern Yukon Territory, Canada, *Am. J. Sci.*, 264, 600–619, 1966.
- Calkin, P. E., Holocene glaciation of Alaska (and adjoining Yukon Territory, Canada), *Quat. Sci. Rev.*, 7, 159–184, 1988.
- Calkin, P. E., and J. M. Ellis, A lichenometric dating curve and its application to Holocene glacial studies in the central Brooks Range, Alaska, *Arctic Alpine Res.*, 12, 245–264, 1980.
- Calkin, P. E., and J. M. Ellis, A cirque glacier chronology based on emergent lichens and mosses, *J. Glaciol.*, 27, 512–515, 1981.
- Calkin, P. E., J. M. Ellis, L. A. Haworth, and P. E. Burns, Cirque glacier regime and Neoglaciation, Brooks Range, Alaska, *Zeitschrift für Gletscherkunde und Glazialgeologie*, 21, 371–378, 1985.
- Calkin, P. E., B. J. Przybyl, and D. S. Kaufman, Latest Quaternary glaciation, Kigluaik Mountains, northwestern Alaska, *Geol. Soc. America Abstracts with Programs*, 19 (1), 8, 1987.
- Denton, G. H., and W. Karlén, Holocene glacial and tree-line variations in the White River Valley and Skolai Pass, Alaska and Yukon Territory, *Quat. Res.*, 7, 63–111, 1977.
- Derksen, S. J., Glacial geology of the Brady Glacier region, Alaska, *Ohio State University, Institute of Polar Studies Report*, 60, 97 pp., 1976.
- Egan, C. P., Contribution to the late Neoglaciation history of the Lynn Canal and Taku Valley sections of the Alaska Boundary Range, Ph.D. Dissertation, 200 pp., State University, East Lansing, Michigan, 1971.
- Ellis, J. M., and P. E. Calkin, Chronology of Holocene glaciation, central Brooks Range, Alaska, *Geol. Soc. Am. Bull.*, 95, 897–912, 1984.
- Field, W. O., Observations on Alaskan coastal glaciers in 1935, *Geographical Rev.*, 27, 63–81, 1937.
- Field, W. O., *Mountain Glaciers of the Northern Hemisphere*, Cold Regions Research and Engineering Laboratory, Hanover, NH, 1975.
- Goldthwait, R. P., Glacial history, in Soil development and ecological succession in a deglaciated area of Muir Inlet, southeast Alaska, Part 1, edited by A. Mirsky, pp. 1–18, *The Ohio State University, Institute of Polar Studies Report*, 20, 1966.
- Goldthwait, R. P., I. C. McKeller, and C. Cronk, Fluctuations of Crillon Glacier system, southeast Alaska, *Bull. Int. Assoc. Scientific Hydrol.*, 8, 62–74, 1963.
- Goodwin, R. G., Holocene glaciolacustrine sedimentation in Muir Inlet and ice advance in Glacier Bay, Alaska, U.S.A., *Arctic and Alpine Research*, 20, 55–69, 1988.
- Grove, J. M., *The Little Ice Age*, 498 pp., Methuen, London, 1988.
- Haworth, L. H., Holocene glacial chronologies of the Brooks Range, Alaska and their relationship to climate change, Ph.D. Dissertation, 260 pp., State University of New York at Buffalo, Buffalo, NY, 1988.
- Heusser, C. J., Holocene vegetation history of the Prince William Sound region, south-central Alaska, *Quat. Res.*, 19, 337–355, 1983.
- IGBP, Global change, a plan of action, in *Global Change Report 4*, IGBP Secretariat, Stockholm, Sweden, 1988.
- Kaufman, D. S., P. E. Calkin, W. B. Whitford, B. J. Przybyl, D. M. Hopkins, B. J. Peck, and R. E. Nelson, Surficial geologic map of the Kigluaik Mountains area, Seward Peninsula, Alaska, U.S. Geological Survey, *Miscellaneous Field Studies Map MF-2674*, Scale 1:3,360, 1989.
- Lamb, H. H., *Climate: Present, Past and Future*, Vol. 2, 835 pp., Methuen, London, 1977.
- LaPerouse, J. F. G. De, *Voyage Round the World, Performed in the Years 1785, 1786, 1787, and 1788 by the Boussole and Strolabe*, Vol. I, pp. 364–416, and Atlas (Translation from French), A. Hamilton, London, 1799.
- Lawrence, D. B., Glacier fluctuation for six centuries in southeastern Alaska and its relation to solar activity, *Geographical Rev.*, 40, 191–223, 1950.
- Letreguilly, A., and L. Reynaud, Spatial patterns of mass-balance fluctuations North American glaciers, *J. Glaciol.*, 35, 163–168, 1989.
- Luckman, B. H., Global change and the record of the past, *Geos*, 18, 1–8, 1989.
- Mann, D. H., Reliability of a fjord glacier's fluctuations for paleoclimatic reconstructions, *Quat. Res.*, 25, 10–24, 1986.
- Mann, D. H., and F. C. Ugolini, Holocene glacial history of the Lituya district, southeast Alaska, *Can. J. Earth Sci.*, 22, 913–928, 1985.
- Mayo, L., Advance of Hubbard Glacier and closure of Russell Fjord, Alaska: Environmental effects and hazards in the Yakutat area, *U.S. Geological Circular 1016*, pp. 4–16, 1987.
- Mayo, L. R., and R. S. March, Air temperature and precipitation at Wolverine Glacier, Alaska; Glacier growth in a warmer, wetter climate, *Ann. Glaciol.*, 14, 191–194, 1990.
- McKenzie, G. D., Glacier fluctuations in Glacier Bay, Alaska, in the past 11,000 years, *Proceedings of the First Conference on Scientific Research in the National Parks*, Vol. 2, New Orleans, 1976, edited by R. M. Linn, pp. 809–813, 1979.
- Meier, M. F., Contribution of small glaciers to global sea level, *Science*, 226, 1418–1421, 1984.
- Meier, M. F., and A. S. Post, Fast tidewater glaciers, *J. Geophys. Res.*, 92, 9051–9058, 1987.
- Meier, M. F., W. V. Tangborn, L. R. March, and A. S. Post, Combined ice and water balances of Gulkana and Wolverine glaciers, Alaska, and South Cascade Glacier, Washington, 1965 and 1967 hydrologic years, *U.S. Geological Survey Professional Paper 715-A*, 23 pp., 1971.
- Mercer, J. H., The estimation of the regimes and former firm limit of a glacier, *J. Glaciol.*, 3, 850–858, 1961.
- Miller, M. M., Inventory of terminal position changes in Alaskan coastal glaciers since the 1750's, *Proc. Am. Philosophical Soc.*, 108, 257–273, 1964.
- Miller, M. M., Quaternary erosional and stratigraphic sequences in the Alaska–Canada Boundary Range, in *Quaternary Stratigraphy of North America*, edited by

- W. C. Mahaney, pp. 463-492, Halstead Press, Wiley and Sons, New York, 1977.
- Molnia, B. F., Glacial history of the northeastern Gulf of Alaska - A synthesis, in *Glaciation in Alaska - The geologic record*, edited by T. D. Hamilton, K. M. Reed, and R. M. Thorson, pp. 219-236, Alaska Geological Society, Anchorage, 1986.
- Oerlemans, J., Glaciers as indicators of carbon dioxide warming, *Nature*, 320, 607-609, 1986.
- Padginton, C. H., P. E. Calkin, and G. C. Wiles, and V. E. Romanovsky, Reconstruction of icefield glaciers and Little Ice Age climatic change, southern Kenai Mountains, Alaska, *Geol. Soc. Am., Abstracts with Programs*, 22(4), Abstr. No. 177, p. 20, 1990.
- Péwé, T. L., and R. D. Reger, Delta River area, Alaska Range, in *Guidebook to permafrost and Quaternary geology along the Richardson and Glenn Highways between Fairbanks and Anchorage, Alaska*, edited by T. L. Péwé and R. D. Reger, pp. 47-135, Alaska Division of Geological and Geophysical Surveys, Guidebook 1, 1983.
- Plafker, G., and D. J. Miller, Recent history of glaciation in the Malaspina district and adjoining bays, Alaska, *Science in Alaska, 1957, Proceedings 8th Alaskan Science Conference*, pp. 132-133, 1958a.
- Plafker, G., and D. J. Miller, Glacial features and surficial deposits of the Malaspina district, Alaska, *U.S. Geological Survey Miscellaneous Geological Investigations Map 1-271*, scale 1:125,000, 1958b.
- Porter, S. C., Pattern and forcing of Northern Hemisphere glacier variations during the last millennium, *Quat. Res.*, 26, 27-48, 1986.
- Porter, S. C., Late Holocene cycles of advance and retreat of the fjord glacier system in Icy Bay, Alaska, *Arctic Alpine Res.*, 21, 364-379, 1989.
- Porter, S. C., K. L. Pierce, and T. D. Hamilton, Late Wisconsin mountain glaciation in the western United States, in *Late Quaternary Environments of the United States, Vol. 1, The Late Pleistocene*, edited by S. C. Porter, pp. 71-111, Univ. of Minnesota, Minneapolis, MN, 1983.
- Post, A. S., Distribution of surging glaciers in western North America, *J. Glaciol.*, 8, 229-240, 1969.
- Post, A. S., Preliminary hydrography and historic terminal changes of Columbia Glacier, Alaska, *U.S. Geological Survey Hydrographic Investigations Atlas*, 559, 1975.
- Post, A. S., Preliminary bathymetry of McCarty Glacier, Alaska, *U.S. Geological Survey Open-File Report 80-424*, 4 sheets, 1980a.
- Post, A. S., Preliminary bathymetry of Northwestern Fjord and Neoglacial changes of Northwestern Glacier, Alaska, *U.S. Geological Survey Open-File Report, 80-414*, 2 sheets, 1980b.
- Post, A. S., Preliminary bathymetry of Aialik Bay and Neoglacial changes of Aialik and Pederson Glaciers, Alaska, *U.S. Geological Survey Open-File Report, 80-423*, 1980c.
- Przybyl, B. J., The regimen of Grand Union Glacier and the glacial geology of the northeastern Kigluaik Mountains, Seward Peninsula, Alaska, Master's Thesis, 106 pp., State University of New York at Buffalo, Buffalo, New York, 1988.
- Rampton, V. N., Neoglacial fluctuation of the Natzhat and Klutlan Glaciers, Yukon Territory, Canada, *Can. J. Earth Sci.*, 7, 1236-1263, 1970.
- Rampton, V. N., Holocene glacial and tree-line variations in the White River valley and Skolai Pass, Alaska and Yukon Territory: A discussion, *Quat. Res.*, 10, 130-134, 1978.
- Reger, R. D., and T. L. Péwé, Lichenometric dating in the central Alaska Range, in *The Periglacial Environment: Past and Present*, edited by T. L. Péwé, pp. 223-247, McGill-Queens Univ. Press, Montreal, Canada, 1969.
- Reid, J. H., Late Wisconsin and Neoglacial history of the Martin River Glacier, Alaska, *Geol. Soc. Am. Bull.*, 81, 3593-3604, 1970.
- Sharp, R. P., The latest major advance of Malaspina Glacier, Alaska, *Geographical Rev.*, 48, 16-26, 1958.
- Stuiver, R., and P. J. Reimer, A computer program for radiocarbon age calibration, *Radiocarbon*, 28, 1022-1030, 1986.
- Ten Brink, N. W., Glaciation of the northern Alaska Range, in *Glaciation in Alaska - Extended Abstracts from a Workshop*, edited by R. M. Thorson, and T. D. Hamilton, pp. 82-90, University of Alaska Museum Occasional Paper, 2, Fairbanks, Alaska, 1983.
- Vancouver, G., *Voyage of Discovery to the North Pacific Ocean in the Years 1790-1795, Vol 3*, Printed for G. G. Robinson, J. Robinson, and J. Edwards, London, 1798.
- Viereck, L. A., Botanical dating of recent glacial activity in western North America, in *Arctic and Alpine Environments*, edited by H. E. Wright, Jr. and W. H. Osburn, pp. 189-204, Indiana Univ. Press, Bloomington, IN, 1967.
- Waythomas, C. F. and N. W. Ten Brink, Glacial geology of the Swift Fork, Herron and Foraker River Valleys, Alaska, Unpubl. report submitted to the National Park Service and National Geographic Society, 76 pp., 1982.
- Wiles, G. C., and P. E. Calkin, Neoglaciation in the southern Kenai Mountains, Alaska, *Ann. Glaciol.*, 14, 319-322, 1990.
- Williams, L. D., and T. M. L. Wigley, A comparison of evidence for late Holocene summer temperature variations in the Northern Hemisphere, *Quat. Res.*, 20, 286-307, 1983.

The Greenland Ice Sheet Margin as a Source of Paleoenvironmental Data

N. Reeh, H. Oerter, A. Letréguilly, and H. Miller

Alfred Wegener Institute for Polar and Marine Research, Bremerhaven, Germany

ABSTRACT

Oxygen-18 records measured on surface ice samples from Greenland ice sheet margins show that ice of pre-Holocene age is present at many locations along the ice margin. Several records have been obtained from West, North, and Northeast Greenland. At all locations where pre-Holocene ice is found, it constitutes a band running parallel to the ice edge. However, the width of the band varies greatly from one location to another, ranging between 30 m and 1500 m.

So far, the most detailed oxygen-18 record has been obtained from a West Greenland ice margin location. It spans the last glacial (the Wisconsinan), the last interglacial (Sangamon, Eem), and part of the previous glacial (the Illinoian). A correlation with the oxygen-18 records from the Greenland deep ice cores from Camp Century and Dye-3 indicates that neither of these records reach back to the previous glacial, probably due to substantial thinning and retreat of the ice sheet in North and South Greenland in the Eemian interglacial.

The oxygen-18 record has been translated into a Greenland temperature record covering the past 150,000 years. The isotopic temperatures indicate large temperature variations in marine isotopic stage 5, with a climate warmer than at present not only in sub-stage 5e, but also in sub-stage 5c and in a short period of sub-stage 5a.

The ice margin studies indicate that Greenland ice sheet margins have a large potential as sources of paleoenvironmental information. Large volumes of ice can easily be mined, e.g., for Carbon-14 dating and other measurements that require large amounts of ice. Therefore, ice margin studies are an important supplement to deep drilling programs in the interior regions of the ice sheet.

The History of the Climate of the Northern Polar Region in the Holocene and Recent Millennia from Proxy and Historical Data

E. P. Borisenkov and V. M. Pasetsky
Main Geophysical Observatory, Leningrad, U.S.S.R.

ABSTRACT

All data available on the reconstruction of the climate of the northern polar region in different Holocene periods are presented. Primary attention is given to the data on the polar region climate on the USSR European and Asian territory. The possible natural causes responsible for creating the climatic conditions of the Holocene warm and cold epochs in polar regions are analyzed, as well as circulation features of these epochs. The historical data available on the polar region climate are generalized for the past two thousand years and in particular the recent millennium.

It is shown that during the recent millennium the climatic conditions of the northern polar region were very different, which influenced ice conditions and polar navigation. It is also shown that most of the above periods of climate warming and cooling were related to climatic changes in other regions of Europe and Asia. It is inferred that these changes depend to a considerable extent on circulation processes. In this connection an analogy is given between the Arctic warming in the 1930s and 1940s and similar climate warming in other epochs, in particular in the early sixteenth century. Their similarity in circulation processes is shown.



Two Late Quaternary Pollen Records from the Upper Kolyma Region, Soviet Northeast: A Preliminary Report

P. M. Anderson and L. B. Brubaker

Quaternary Research Center, University of Washington, Seattle, Washington, U.S.A.

A. A. Andreev

Laboratory of Paleogeography, Institute of Geography, Moscow, U.S.S.R.

B. I. Chernenky, I. N. Federova, L. N. Kotova, A. V. Lozhkin, A. I. Polujan, and L. G. Rovako

North East Interdisciplinary Research Institute, Magadan, U.S.S.R.

P. A. Colinvaux and W. R. Eisner

Byrd Polar Research Center, The Ohio State University, Columbus, Ohio, U.S.A.

D. M. Hopkins

Alaska Quaternary Center, University of Alaska Fairbanks, Fairbanks, Alaska, U.S.A.

M. C. Miller

Department of Biological Sciences, University of Cincinnati, Cincinnati, Ohio, U.S.A.

ABSTRACT

Pollen records from Sosednee and Elikchan Lakes provide the first continuous late Quaternary vegetation history for the upper Kolyma drainage of the Soviet Northeast. Full-glacial spectra at these sites are similar to those from Eastern Beringia, with high percentages of grass, sedge, and wormwood pollen indicative of herb tundra. In the Elikchan area at approximately 12,500 B.P., herb tundra was replaced by a stone pine-larch forest, perhaps similar to modern forests in the region. In contrast, the herb tundra near Sosednee Lake was succeeded by a birch-alder shrub tundra followed by a larch woodland. Stone pine increased in the region after larch and prior to 8600 B.P. A Holocene decline in stone pine, which is evident at Elikchan Lake, is less marked or absent at Sosednee Lake. The differences in these pollen records is somewhat surprising given the proximity of the two sites. Such differences indicate that numerous well-dated sites will be needed to describe the vegetation and climate histories of Western Beringia.

INTRODUCTION

Lacustrine pollen records provide much of the data for interpreting late Quaternary climatic and vegetational changes for the eastern side of the Bering Land Bridge [e.g., Livingstone, 1955; Colinvaux, 1964; Ager and Brubaker, 1985; Ritchie, 1987; Barnosky et al., 1987]. Researchers in Western Beringia, who rely more on pollen preserved in nonlacustrine settings, have also been concerned with such paleoenvironmental histories as that of the Pleistocene flora

[Giterman et al., 1982; Giterman, 1984; Lozhkin, 1984; Savvinova, 1984], trans-Beringian plant migrations [Yurtsev, 1982, 1984] and paleoclimates [Lozhkin, 1984]. Although using slightly different data bases and analytical techniques, both sets of scientists have noted that Beringia is a key area for understanding the role of climate in shaping the modern arctic and subarctic flora. Today's Beringian biomes will be particularly susceptible to future climatic warming resulting from increased concentration of

92-17854



greenhouse gases [Emanuel et al., 1985; D'Arrigo et al., 1987; Office for Interdisciplinary Earth Studies, 1988]. Although predictions of vegetation response to proposed future climatic scenarios are difficult, an increased understanding of past atmospheric-terrestrial interactions should improve our ability to build more sophisticated models and to make better management decisions.

Building on three decades of work in Beringia, a cooperative U.S.-U.S.S.R. project was initiated to investigate late Quaternary climatic and vegetational histories on both sides of Bering Strait. Two tasks must be successfully accomplished to achieve this goal. The first involves the recovery and palynological and geochemical analyses of lake sediments from poorly known regions of Beringia. The second and more challenging task is finding a common ground between Soviet and American workers for the interpretation of their results. As an example of differences between these approaches, Soviet scientists look first to groups of pollen taxa, such as the sum of trees and shrubs, for their reconstructions of past environments, whereas Americans examine variations among the individual taxa. These different approaches are clearly reflected in the two pollen diagrams presented in this paper. Such conceptual differences, although likely resulting in similar paleovegetational interpretations, can lead to vastly different approaches to paleoclimatic reconstructions. Achieving a better understanding of past climates and their potential as analogs for postulated future climate trends, not only in Beringia but throughout the arctic, will require common methods of data analysis and data management. This note represents the first step towards that goal and describes our

initial findings for the upper Kolyma River region of the Soviet Northeast.

STUDY AREA

The vegetation of the upper Kolyma drainage is a mosaic of taiga and shrub tundra in the valley bottoms and lower mountain slopes. Higher elevations and scree support little or no vegetation. Taiga communities are characterized by two conifer species, larch and dwarf stone pine (see Table 1 for Latin names). The understory consists of shrub birch, willow species, heaths, and, occasionally, alder. Fruticose lichens are abundant throughout the region.

Six lakes from two different regions of the upper Kolyma drainage were cored in August, 1990. We present preliminary pollen results from two of these sites, Sosednee and Elikchan Lakes (Figure 1). Sosednee Lake was formed behind a morainal dam that subsequently was breached permitting an outflow into Jack London Lake. The Jack London Lake district was repeatedly glaciated, most extensively during the middle Pleistocene [Shilo, 1961], with the most recent moraines dating to either isotope stage 2 or 4. Elikchan Lake is one of four interconnected basins and is tectonic in origin. Although lowlands of this region probably remained unglaciated since the mid-Pleistocene, higher elevations in nearby mountains were likely modified by cirque glaciers. The fault that creates the valley of the Elikchan Lakes may have been active as recently as the early late Pleistocene.

RESULTS

Two percentage diagrams represent the first lacustrine pollen records from the Kolyma drainage (Figures 2 and 3; see also Lozhkin and Federova [1989]). Both pollen diagrams include features similar to Alaskan pollen records: an early herb assemblage, followed by an increase in shrub (typically birch followed by alder) and conifer pollen. The Kolyma cores, however, display properties that distinguish them from their Alaskan counterparts.

The Sosednee Lake record currently lacks radiocarbon dates and the Elikchan core is poorly dated. The pollen data, however, suggest the Sosednee record is younger with a basal zone corresponding to zone EL-II at Elikchan Lake. Although precise temporal discussion of these records is not possible until radiocarbon analyses are completed, we

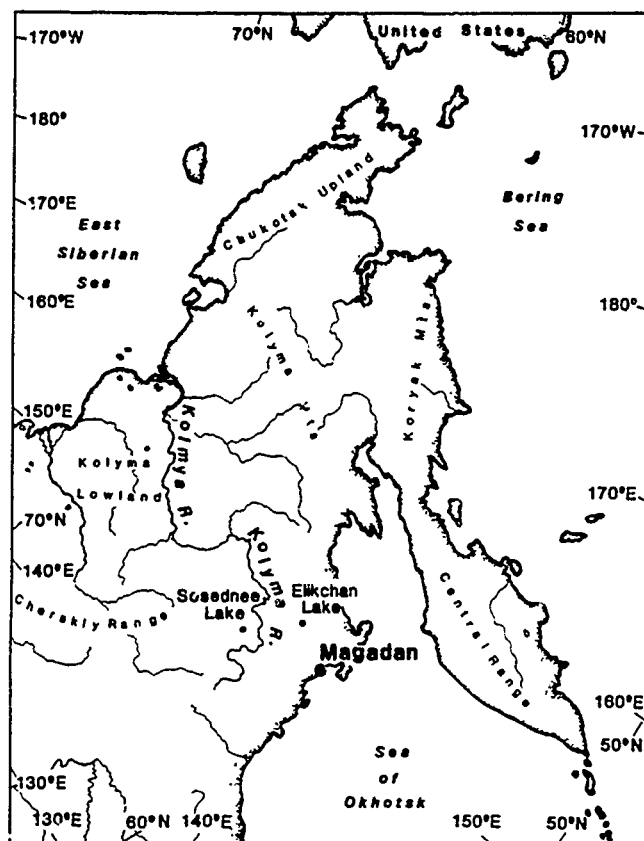
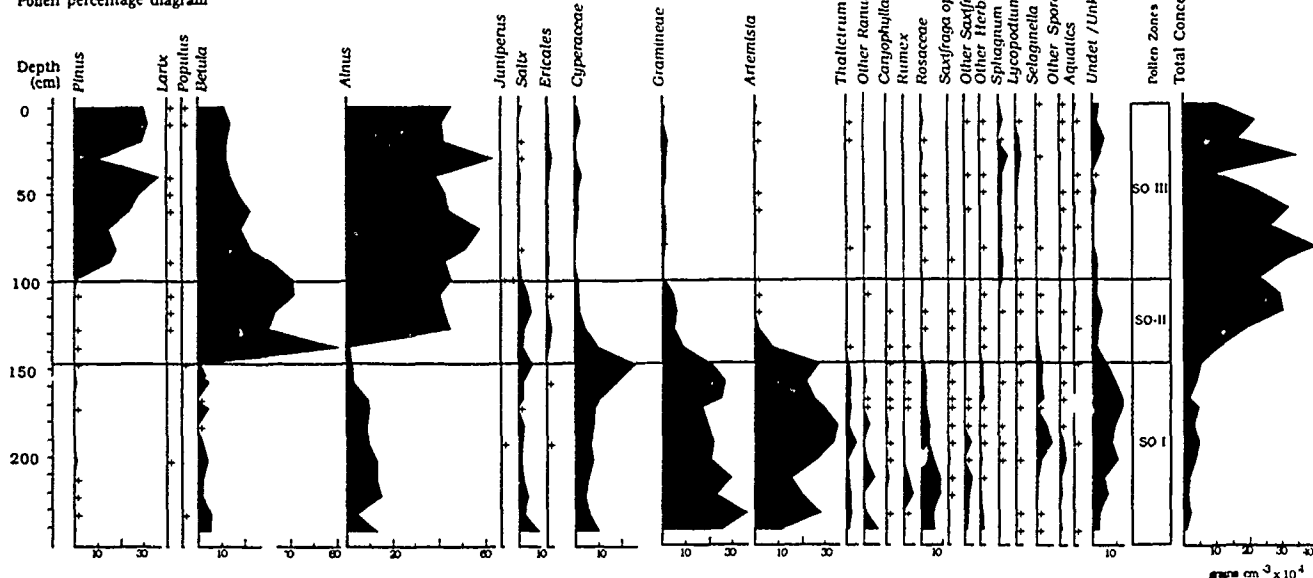


Figure 1. Map of study area showing locations of Sosednee and Elikchan Lakes.

Common Name	Latin Name
stone pine	<i>Pinus pumila</i>
larch	<i>Larix dahurica</i>
birch	<i>Betula exilis</i>
alder	<i>Alnus sinuata</i>
heaths	<i>Ericales</i>
willow	<i>Salix</i>
grass	Gramineae, Poaceae
sedge	Cyperaceae
wormwood	<i>Artemisia</i>
spikemoss	<i>Selaginella sibirica</i>

Table 1. Common and Latin Names of Major Pollen Taxa. [After Hultén, 1968.]

Pollen percentage diagram



The category Other Herbs includes the following. Compositae, Cruciferae, Polyganaceae, Chenopodiaceae, Umbelliferae, and Papaveraceae. The pollen sum includes all identified, unknown, and unidentifiable pollen taxa. Spores and aquatics are expressed as a percentage of the pollen sum.

Figure 2. Pollen percentage diagram from Sosednee Lake, Jack London region. The pollen sum includes all identified, unidentified, and unknown pollen grains. Spores and aquatics are expressed as percent of pollen sum.

believe that the pollen data are sufficient to warrant the following preliminary discussion.

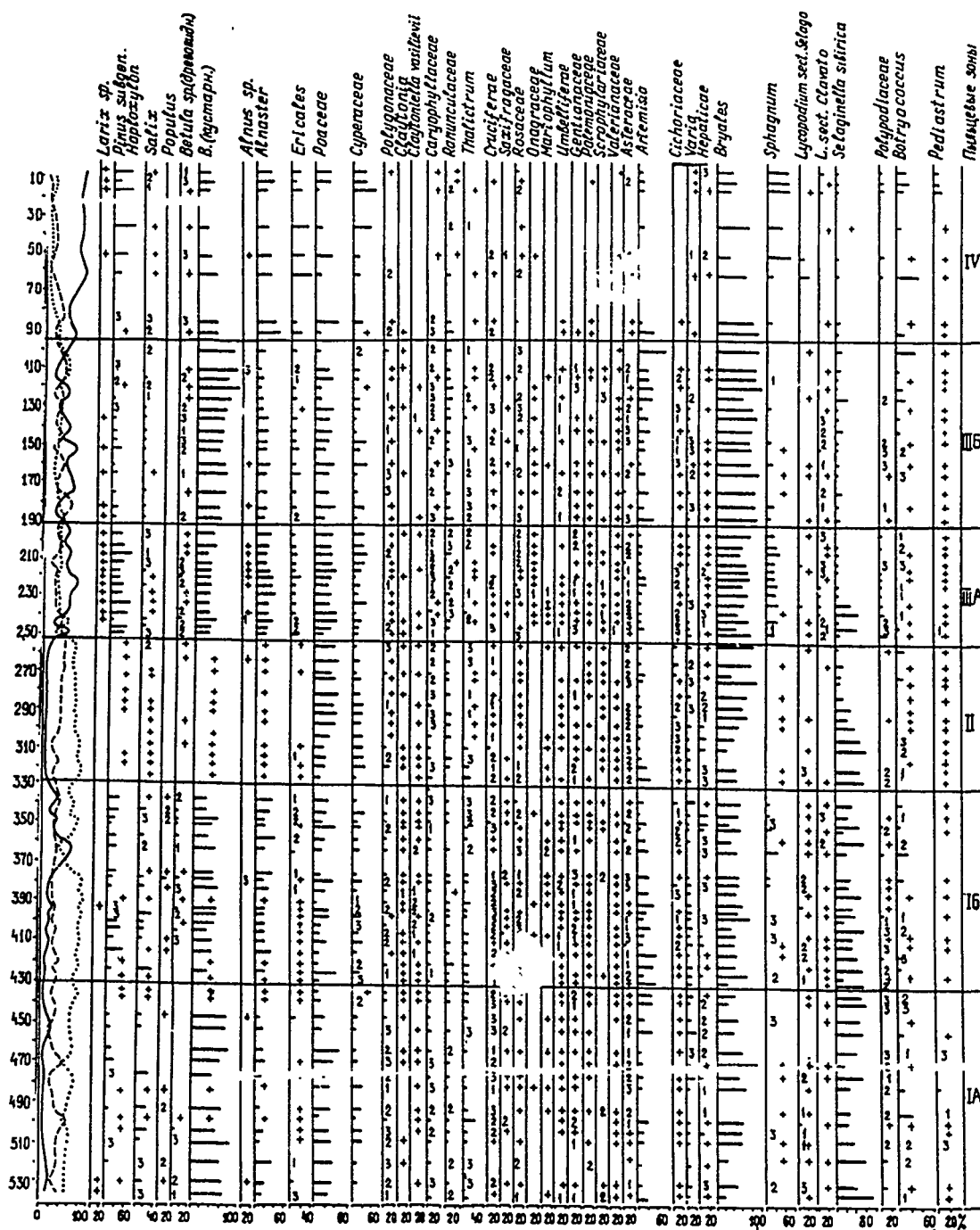
SO-I and EL-II, the herb zones, are characterized by high percentages of wormwood, grass, and sedge and are similar to full-glacial herb zone spectra in Eastern Beringia [e.g., Colinvaux, 1964; Cwynar, 1982; Anderson, 1985]. The Soviet cores display higher percentages of the spikemoss, *Selaginella sibirica*, a phenomenon noted previously in Western Beringia by Soviet palynologists and recorded from the Pribilof Islands [Colinvaux, 1981]. The Sosednee core shows unusually high alder percentages. The Kolyma assemblages are interpreted as herb tundra [Lozhkin and Federova, 1989], but more detailed vegetational interpretations await calculation of pollen accumulation rates.

Sosednee Lake indicates a rapid transition from herb to shrub tundra, estimated to occur ca. 12,500 B.P., with populations of both birch and alder expanding at nearly the same time. This pattern differs from Eastern Beringia where birch shrubs preceded alder by as much as 6000 years [Anderson, 1985; Anderson et al., 1988]. Perhaps the nearly simultaneous appearances of birch and alder result from the expansion of nearby small populations of these taxa. Shrub tundra apparently was of short duration in the Sosednee area, with larch populating the area some time prior to 8600 B.P. Because of the under-representation of larch in pollen records, it is difficult to interpret the extent of trees on the landscape. Given the abundance of shrub pollen, however, it is likely larch had a limited distribution, probably on well-drained soils and/or south-facing slopes. Modern vegetation probably was established during the early Holocene with the arrival of dwarf stone pine (SO-II').

The full-glacial to late-glacial transition at Elikchan Lake (EL-III, EL-IV) differs from that at Sosednee or in Alaska. The Elikchan core lacks a shrub tundra zone with an apparent rapid change from herb tundra to a stone pine-larch woodland approximately 12,500 years ago. Possibly stone pine preceded larch into the Elikchan region, but again the problems of pollen representation and the lack of dates make any interpretation uncertain. The Elikchan (EL-IIIb) record suggests a Holocene decline in stone pine and possibly larch. A decrease in stone pine pollen at Sosednee Lake, marked by only a single sample, may represent a similar trend in the Jack London region, but more pollen samples and radiocarbon dates are needed before the Holocene vegetation histories can be carefully compared.

DISCUSSION

The apparent earlier migration of stone pine into the Elikchan area, as compared to Sosednee Lake, suggests an easterly glacial refugium for this species. Changing paleogeography might also have played an important role in determining regional vegetational variation. Today the Elikchan Lakes, lying 150 km from the Ohkotsk Sea, experience a maritime climate, whereas the Sosednee Lake region 250 km further in the interior has greater seasonal temperature and precipitation fluctuations. With rising sea levels during the late glacial, the Elikchan region would have experienced increasingly maritime climates. Increased snow cover would favor the establishment of stone pine. The dependency of this species on winter precipitation might also account for the mid-Holocene decline in pine as winter precipitation regimes decreased.



Previous interpretations by Lozhkin [1984] and Lozhkin and Federova [1989] suggested that cool dry conditions characterized Western Beringia during the last glacial maximum, with post-glacial warming beginning ca. 13,000–12,500 B.P. and a thermal maximum 8000–4500 B.P. The initial results from the Sosednee and Elikchan cores are in general agreement with such a paleoclimate scenario except that consistent evidence for a post-glacial thermal maximum

Although far from conclusive, these results underscore the need for more work in Western Beringia, especially the analysis of continuous primary sediments such as lake deposits. Careful radiocarbon dating of the Sosednee and Elikchan cores will resolve some of the interpretive ques-

tions posed above. The differences in the pollen records from these two nearby regions strongly argue that the late Quaternary vegetation history of Western Beringia is complex and that a grid sampling design, similar to that used in north-central Alaska [Anderson et al., 1988], is required. The long-term goal of this project is the collection and analysis of such a suite of sites in order to provide a fuller understanding of the late Quaternary climatic history of Beringia.

ACKNOWLEDGMENTS

This project is funded by the North East Interdisciplinary Research Institute, Far Eastern Branch, Academy of Science and the National Science Foundation (ATMS 8915415 to Ohio State University and University of Washington). The authors would like to thank Tom Ager and Tom Hamilton for helpful reviews of the manuscript.

REFERENCES

- Ager, T. A., and L. B. Brubaker, Quaternary palynology and vegetational history of Alaska, in *Pollen Records of Late-Quaternary North American Sediments*, edited by V. Bryant, Jr. and R. G. Holloway, pp. 353–384, American Association of Stratigraphic Palynologists Foundation, Dallas, TX, 1985.
- Anderson, P. M., Late Quaternary vegetational change in the Kotzebue Sound area, northwestern Alaska, *Quat. Res.*, 24, 307–321, 1985.
- Anderson, P. M., R. E. Reanier, and L. B. Brubaker, Late Quaternary vegetational history of the Black River region in northeastern Alaska, *Can. J. Earth Sci.*, 25, 84–94, 1988.
- Barnosky, C. W., P. M. Anderson, and P. J. Bartlein, The northwestern U.S. during deglaciation: vegetational history and paleoclimatic implications, in *North America and Adjacent Oceans during the Last Deglaciation*, edited by W. F. Ruddiman and H. E. Wright, Jr., pp. 289–321, Geological Society of America, Boulder, CO, 1987.
- Colinvaux, P. A., The environment of the Bering Land Bridge, *Ecological Monographs*, 34, 297–325, 1964.
- Colinvaux, P. A., Historical ecology in Beringia: The south land bridge coast at St. Paul Island, *Quat. Res.*, 16, 18–36, 1981.
- Cwynar, L. C., A late-Quaternary vegetation history from Hanging Lake, northern Yukon, *Ecological Monographs*, 52, 1–24, 1982.
- D'Arrigo, R., G. C. Jacoby, and I. Y. Fung, Boreal forests and atmosphere–biosphere exchange of carbon dioxide, *Nature*, 329, 321–323, 1987.
- Emanuel, W. R., H. H. Shugart, and M. P. Stevenson, Climatic change and the broad-scale distribution of terrestrial ecosystem complexes, *Climatic Change*, 7, 29–43, 1985.
- Gitterman, R. E., Kolyma lowland vegetation in the Pleistocene cold epochs and the problem of polar Beringia landscapes, in *Beringia in the Cenozoic Era*, edited by V. L. Kontrimavichus, pp. 214–221, Amerind Publishing Co. Pvt. Ltd., New Delhi, (Translated from Russian), 1984.
- Gitterman, R. E., A. V. Sher, and J. V. Matthews, Jr., Comparison of the development of steppe–tundra environments in west and east Beringia: pollen and macrofossil evidence from key sections, in *The Paleocology of Beringia*, edited by D. M. Hopkins, J. V. Matthews, Jr., C. E. Schweger, and S. B. Young, pp. 43–74, Academic Press, New York, 1982.
- Grichuk, V. P., Changes in species composition of flora of northeastern Eurasia in the late Cenozoic, in *Beringia in the Cenozoic Era*, edited by V. L. Kontrimavichus, pp. 188–200, Amerind Publishing Co. Pvt. Ltd., New Delhi, (Translated from Russian), 1984.
- Hulten, E., *Flora of Alaska and Neighboring Territories*, Stanford University Press, Stanford, CA, 1968.
- Livingstone, D. A., Some pollen profiles from arctic Alaska, *Ecology*, 36, 587–600, 1955.
- Lozhkin, A. V., Late Pleistocene and Holocene vegetation in western Bering land, in *Beringia in the Cenozoic Era*, edited by V. L. Kontrimavichus, pp. 88–95, Amerind Publishing Co. Pvt. Ltd., New Delhi, (Translated from Russian), 1984.
- Lozhkin, A. V., and I. N. Federova, Late Pleistocene and Holocene Vegetation and Climate of Northeastern U.S.S.R. Based on Data from Lake Sediments. Topography and Corresponding Deposits, Northeastern U.S.S.R., pp. 3–9, Paper of the North East Interdisciplinary Research Institute, Far East Branch Academy of Science, 1989.
- Ritchie, J. C., *Postglacial Vegetation of Canada*, University of Toronto Press, Toronto, Canada, 1987.
- Savvinova, G. M., Pleistocene and Holocene vegetation on the upper reaches of the Indigirka and Kolyma Rivers, in *Beringia in the Cenozoic Era*, edited by V. L. Kontrimavichus, pp. 211–213, Amerind Publishing Co. Pvt. Ltd., New Delhi, (Translated from Russian), 1984.
- Shilo, N. A., *Quaternary Deposits of the Yano–Kolyma Gold Belt of Northeast Asia*, Publication of the North East Interdisciplinary Research Institute, Far East Branch Academy of Sciences, Magadan, 1961.
- Yurtsev, B. A., Relicts of the xerophyte vegetation of Beringia in northeastern Asia, in *The Paleocology of Beringia*, edited by D. M. Hopkins, J. V. Matthews, Jr., C. E. Schweger, and S. B. Young, pp. 157–178, Academic Press, New York, 1982.
- Yurtsev, B. A., Beringia and its biota in the late Cenozoic: a synthesis, in *Beringia in the Cenozoic Era*, edited by V. L. Kontrimavichus, pp. 261–279, Amerind Publishing Co. Pvt. Ltd., New Delhi, (Translated from Russian), 1984.

Vegetation, Climate, and Lake Formation During Interglacial Periods in Northeast Interior Alaska

M. E. Edwards

Department of Geology and Geophysics, University of Alaska, Fairbanks, Alaska, U.S.A.

ABSTRACT

In sediment records from the loess-covered southern Yukon lowland (northeast interior Alaska), the onset of interglacial conditions ca. 10,000 years ago is correlated with the development of lakes, probably by deep thawing of ice-rich silt. At Birch Creek, a river cut exposes 12 m of lacustrine sediments and peat with loess above and below. The underlying loess contains the 150,000-year old Old Crow Tephra. By analogy with Holocene records, the lacustrine sequence probably represents a thaw-lake that formed in the previous interglaciation (isotope sub-stage 5e, ca. 125,000 years B.P.).

Sub-stage 5e was probably warmer than any part of the present interglacial and is an important analog for possible future greenhouse climates. *Picea* (spruce) pollen is more abundant in the interglacial sediments than in comparable Holocene sediments, and values of other pollen types also differ between interglacial and Holocene. This suggests that vegetation and climate were unlike those of today. Comparison of the interglacial pollen with modern pollen spectra may allow estimation of vegetation and climate in northeast Alaska during isotope stage 5e.

As future climatic warming may be expected to affect permafrost, further information is needed on the vegetational and climatic conditions that favor ice-melting and the formation of thaw lakes in loess.



Deglaciation and Latest Pleistocene and Early Holocene Glacier Readvances on the Alaska Peninsula: Records of Rapid Climate Change Due to Transient Changes in Solar Intensity and Atmospheric CO₂ Content?

DeAnne S. Pinney and James E. Begét

Dept. of Geology and Geophysics, University of Alaska Fairbanks, Fairbanks, Alaska, U.S.A.

ABSTRACT

Geologic mapping near Windy Creek, Katmai National Park, identified two sets of glacial deposits postdating late-Wisconsin Iliuk moraines and separated from them by volcanoclastic deposits laid down under ice-free conditions. Radiocarbon dating of organic material incorporated in the younger Katolinat till and in adjacent peat and lake sediments suggests that alpine glaciers on the northern Alaska Peninsula briefly expanded between *ca.* 8500 and 10,000 years B.P. Stratigraphic relationships and radiocarbon dates suggest an age for the older Ukak drift near the Pleistocene-Holocene boundary between *ca.* 10,000 and 12,000 years B.P.

We suggest that rapid deglaciation following deposition of the Iliuk drift occurred *ca.* 13,000–12,000 years B.P. in response to large increases in global atmospheric "greenhouse gas" content, including CO₂. Short-term decreases in these concentrations, as recorded in polar ice cores, may be linked with brief periods of glacier expansion during the latest Pleistocene and early Holocene. A transient episode of low solar intensity may also have occurred during parts of the early Holocene. Rapid environmental changes and glacial fluctuations on the Alaska Peninsula may have been in response to transient changes in the concentration of atmospheric greenhouse gases and solar intensity.

INTRODUCTION

Prior to the Quaternary the southwestern end of the Alaska Peninsula consisted of a string of volcanic islands [Detterman, 1986]. The Pleistocene saw these islands connected first by ice, then by the deposits the glaciers left behind. Immediately adjacent to moisture sources in the northwest Pacific Ocean and Gulf of Alaska, the Alaska Peninsula was ideally situated to produce large glaciers [Péwé, 1975; Detterman, 1986]. Pleistocene glacial deposits recognized on the Alaska Peninsula include an unnamed pre-Wisconsin drift; pre-Wisconsin Johnston Hill drift; early-Wisconsin Mak Hill drift, and late-Wisconsin Brooks Lake drift, subdivided into the Kvichak, Iliamna, Newhalen, and Iliuk Stades [Muller, 1952, 1953; Muller et al., 1954; Detterman and Reed, 1973; Detterman, 1986] (Table 1).

The Windy Creek study area is located on the northern Alaska Peninsula immediately west of the Valley of Ten

Thousand Smokes, site of one of the largest volcanic eruptions of historic times (Figure 1). Detailed geologic mapping near lower Windy Creek (Figure 2) has yielded a record of late Quaternary glacial events on the Alaska Peninsula, including periods of latest Wisconsin and early Holocene ice expansion recorded by two previously unrecognized sets of glacial drift deposits.

LATE QUATERNARY GLACIAL AND VOLCANIC DEPOSITS

Three sets of glacial deposits preserved in the Windy Creek study area are of significance to the question of late Quaternary climate of the Alaska Peninsula: the Iliuk, Ukak and Katolinat drifts. The late-Wisconsin Iliuk deposits are stratigraphically separated from the two younger deposits by an extensive suite of volcanogenic deposits known collectively as the "Letha volcanoclastics."



Name		Age
(Unnamed Glaciation)*	Katolinat Stade*	Early Holocene
Brooks Lake Glaciation	Ukak Stade*	Latest Wisconsin
	Iliuk Stade	
	Newhalen Stade	
	Iliamna Stade	
	Kvichak Stade	Late Wisconsin
Mak Hill Glaciation		Early Wisconsin
Johnston Hill Glaciation		Pre-Wisconsin
(Unnamed Glaciation,)		Pre-Wisconsin

*Previously unrecognized

(after Dettlerman and Reed, 1973)

Table 1. Late Quaternary Glacial Chronology of the Alaska Peninsula.

Iliuk Drift. Iliuk-age glacial deposits are the youngest in the standard Alaska Peninsula glacial sequence (Table 1) and, until now, have represented the last recognized advance of Pleistocene glaciers prior to final deglaciation. Surficial morphology of Iliuk moraines in the study area is only slightly modified, having been only somewhat subdued by thin coverings of loess and tephra in protected areas. Ventifacts are locally common on the surface. Till in the moraines is unsorted and boulder- and gravel-rich with a generally coarse silt/sand matrix. Thickness of overlying soil-forming deposits ranges from nonexistent to several tens of centimeters. Iliuk-age ice dammed a lake in Windy Creek valley, generating a thick sequence of glacio-lacustrine deposits. Airfall and redeposited airfall pumice and at least one pyroclastic flow deposit of the Letne volcanoclastic suite immediately overlie Iliuk drift.

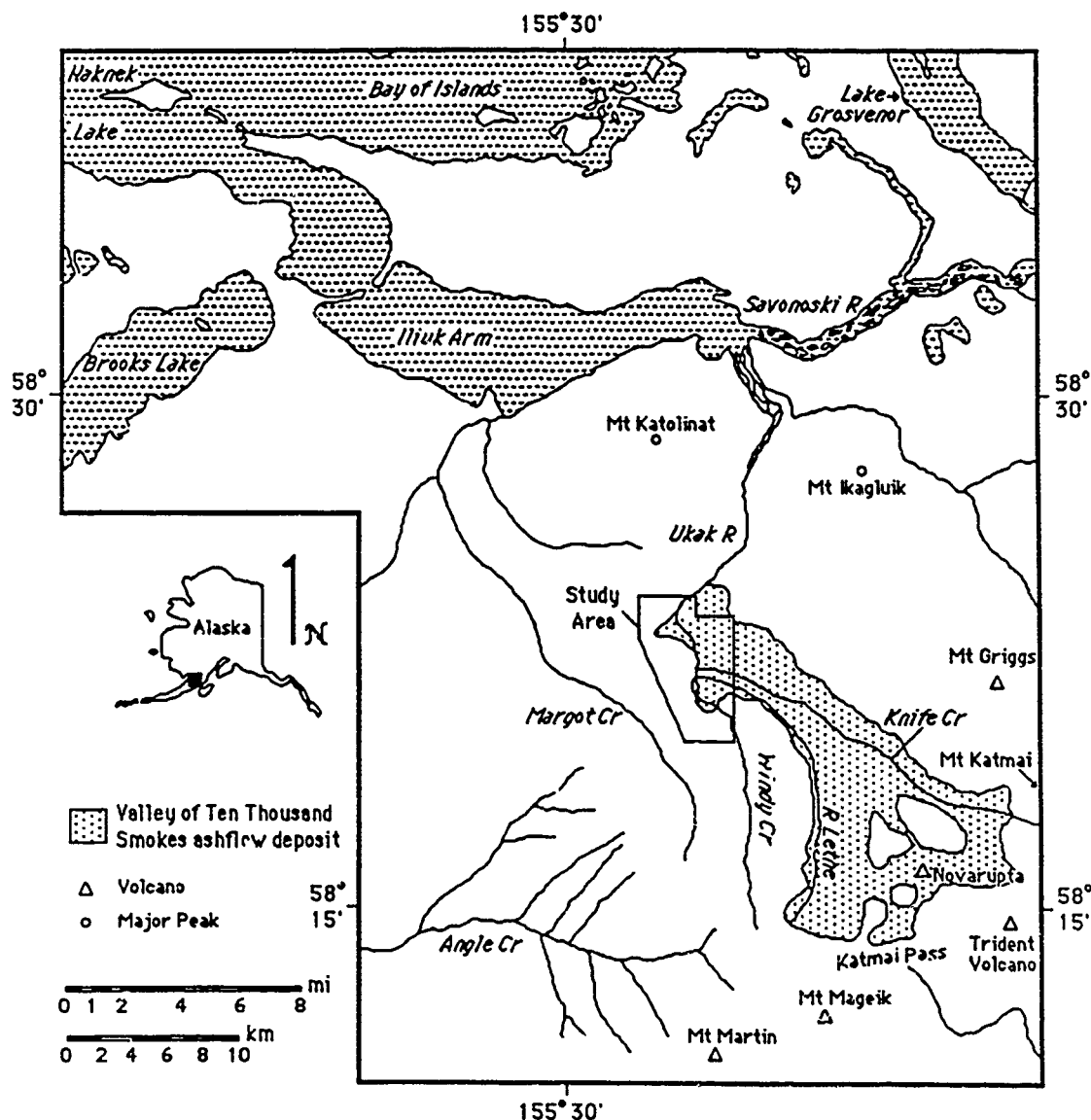


Figure 1. Location of Windy Creek study area.

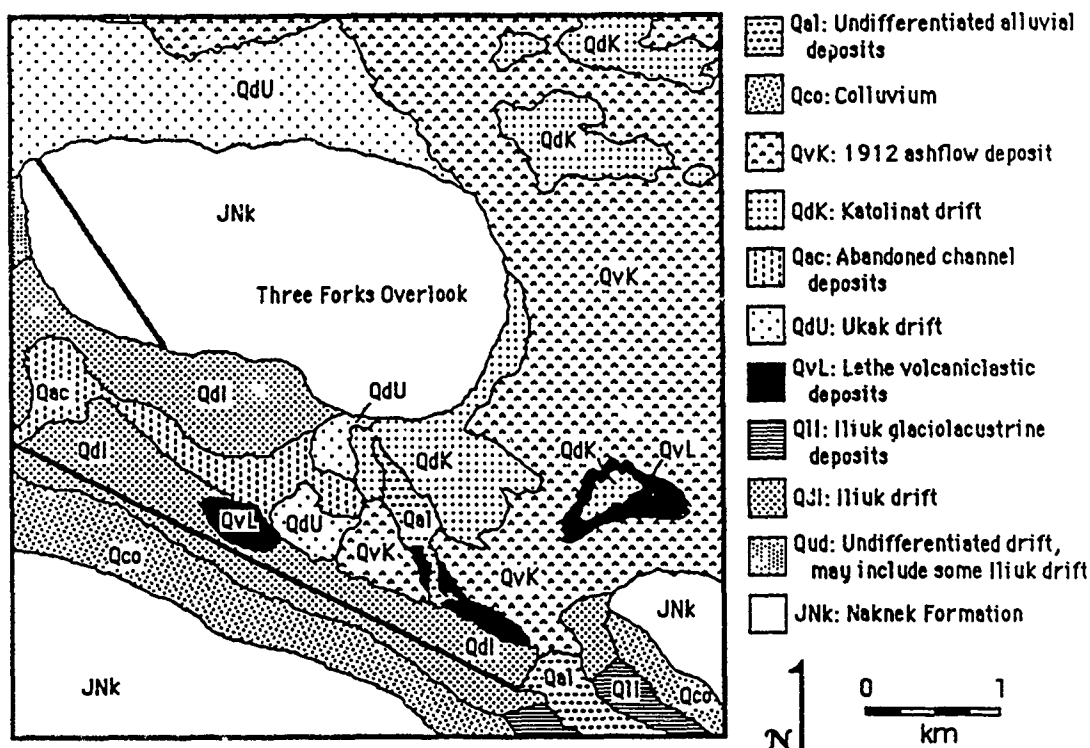


Figure 2. Surficial geology near lower Windy Creek.

Lethe Volcaniclastics. The informally named "Lethe volcaniclastics" comprise an extensive suite of deposits that includes dacitic pyroclastic flows, lahars and lahar-runout flows, and primary and reworked airfall tephra, which were all laid down under ice-free conditions after retreat of Iliukage glaciers. Lethe volcaniclastic deposits overlie Iliuk drift and are overlain by and incorporated into Ukak and Katoliat drifts, making the tephra a potentially important latest Pleistocene marker horizon for the Alaska Peninsula.

Ukak Drift. Extensive dead-ice terrain in the valley bottom between Mt. Katolinat and Three Forks Overlook is the type locality for the Ukak drift. Morphology is that of typical kettle-and-kame topography, being irregular, pitted, and studded with ponds and low-lying marsh between high mounds and ridges of till. The surface is generally well vegetated. The deposit is locally associated with glaciolacustrine sediments. Ukak drift overlies and incorporates Lethe volcanoclastic material, and represents a glacial readvance of at least 3 km from post-Iliuk retreat positions.

Katolinat Drift. The youngest glacial deposit in lower Windy Creek is the Katolinat drift, which is preserved as a nested pair of 10- to 20-m-high, well-developed terminal moraines that were largely buried by the 1912 ashflow of the Valley of Ten Thousand Smokes. Katolinat drift tends to be clay-rich with variable concentrations of clasts, and is composed in part of glacially retransported volcanic rockfall debris. Katolinat moraines are associated with up to 20 m of glaciolacustrine silts and clays rich in dropstones and reworked Letha pumice, and are directly overlain by extensive thick peats and organic-rich silts.

DATING OF DEPOSITS

Dating of Windy Creek deposits (Figure 3) was accomplished by radiocarbon dating, stratigraphy, and tephrochronology. Radiocarbon dating (Table 2) constrains the age of the Katolinat drift between 8680 ± 170 years B.P. and 9850 ± 90 years B.P. The older Ukak drift postdates the Lethe volcanoclastics, which were deposited after retreat of late-Wisconsin Iliuk glaciers. Organic silts underlying Katolinat till, believed to be glaciolacustrine deposits associated with Ukak drift, further corroborate a latest-Wisconsin age with dates of $10,200 \pm 140$ years B.P. and $12,640 \pm 100$ years B.P. at the upper and lower contacts, respectively (Table 2). The latter date also provides a new upper limiting age for the Iliuk, Newhalen, and Iliamna Stades of the Brooks Lake Glaciation that is some 2000 years older than previously reported limiting dates [Detterman and Reed, 1973; Henn, 1978].

CLIMATE VARIABILITY AND GLACIAL FLUCTUATIONS

Geologic records of ice sheet growth around the world constitute one of the fundamental data sets documenting climate change during the Quaternary Ice Ages. In some cases glaciers can respond rapidly to short-term climate forcing, with most glaciers in Alaska and around the world having retreated rapidly in response to mean annual warming of 0.5–1.0° since A.D. 1750 [Grove, 1988]. Supporting evidence is needed, however, before rapid glacial fluctuations such as those documented during the Pleistocene/Holocene transition of the Alaska Peninsula can be attributed to cli-

Table 2. Radiocarbon Dates

Sample No	^{14}C Age	Comments
Beta-25632	3,600 \pm 120 yr BP	woody peat directly overlying Three Forks tephra
Beta-24782	4,300 \pm 70 yr BP	peaty silt directly underlying Three Forks tephra
Beta-33668	8,530 \pm 100 yr BP	peat directly overlying Katolinnat till
Beta-25631	8,680 \pm 170 yr BP	organic silt/clay directly overlying Katolinnat till
Beta-33667	9,850 \pm 90 yr BP	organic-rich soil pod in Katolinnat till
Beta-33665	10,200 \pm 140 yr BP	organic silt directly underlying Katolinnat till
Beta-33666	12,640 \pm 100 yr BP	organic silt underlying Katolinnat till

Table 2. Radiocarbon Dates.

mate change. First, it is desirable that other proxy climate records show evidence of broadly synchronous climate variability. Second, it is desirable to establish an *a priori* link with a plausible climatic forcing mechanism operating on a sufficiently small time scale. The Milankovitch model of climate change links climate variability to orbitally derived insolation curves, but can account only for steady uninterrupted warming or cooling over periods of 10^4 – 10^5 years.

Proxy Climate Records

Proxy climate records are derived when a given parameter varies through time in response to changing climatic conditions. A review of an array of such records shows broad similarities to the late Pleistocene/Holocene glacial geologic record from the Alaska Peninsula (Figure 4). Good agreement exists between deglaciation at ca. 13,000–12,000 years B.P. and rapid warming in ice and marine records. Ice core deuterium records and oxygen-isotope ratios in sediment cores subsequently show temperature minima ca. 11,500 years B.P., and foraminiferal coiling ratios in the northwest Pacific Ocean also record a distinct cold period centered ca. 10,500 years B.P. Transient early Holocene cold intervals of lesser magnitude ca. 8000–9500 years B.P. are suggested by oxygen-isotope ratios in sediment and polar ice cores, and by the micropaleontological records. The ice core deuterium record shows a brief cold period at roughly 7000 years B.P. Allowing for differences in age control, the evidence seems to support the hypothesized transient periods of low temperatures at ca. 10,500–11,500 years B.P. and ca. 7000–9000 years B.P.

Some Possible Mechanisms of Transient Climate Change

We suggest two possible mechanisms which may account for the high degree of climate variability recorded by glacial deposits on the Alaska Peninsula during the Pleistocene/Holocene transition. These include: (1) short-term changes in the atmospheric concentration of greenhouse gases, including CO_2 and CH_4 , and (2) changes in solar intensity.

Atmospheric CO_2 content and, to a lesser extent, CH_4 content are recognized as major instruments of climate change via the "greenhouse" effect. The influence of changing CO_2 is so pronounced that doubling preindustrial concentrations has the potential to increase global temperatures by 1.5–4.5°C, and two to three times that in high latitudes [Hansen et al., 1981; Paterson and Hammer, 1987]. Similarly, decreasing atmospheric CO_2 content will result in cli-

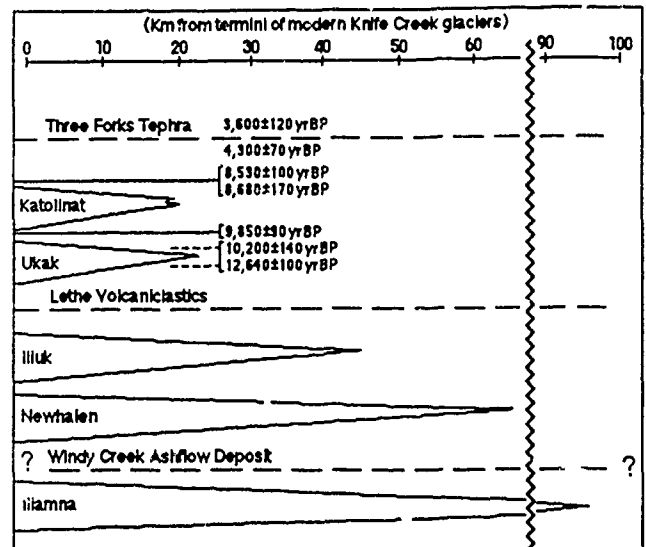


Figure 3. Time-distance plot of glacier advances with radiocarbon dates and major volcanic marker horizons.

matic deterioration. A reduction in CO_2 from ca. 280 p.p.m.v. to 180–200 p.p.m.v. during the last ice age probably accounted for global temperature decreases of 3.0–4.0°C [Genthon et al., 1987].

The role of changing solar intensity in climate change is also important. The rate of ^{14}C production in the earth's atmosphere is inversely related to solar activity; variations in the radiocarbon content of annual tree rings therefore yield a record of solar activity [Denton and Karlén, 1973; Fisher, 1982; Stuiver and Braziunas, 1989]. Fisher [1982] found radiocarbon and ice core oxygen-isotope records highly coherent, indicating that colder temperatures are associated with low solar activity. Changes of about 1% in the solar constant have occurred in historic time and may have accounted for a 1.0–1.5°C temperature drop during the "Little Ice Age" [Eddy, 1977]. Solar intensity variation, operating over much shorter time periods than earth-sun orbital geometries, may thus be important as a potential source of rapid climate change.

Figure 5 shows two late-Quaternary ice core CO_2 records and a solar activity record extending to the beginning of the Holocene. The CO_2 records show large increases in CO_2 content in progress at ca. 13,000–12,000 years B.P., broadly correlative with deglaciation in Southwest Alaska following the Iliuk Stade. Subsequent brief drops in CO_2 concentration, probably corresponding to colder temperatures, occur ca. 8000–9000 years B.P. and during the latest Pleistocene ca. 11,000 years B.P. Proxy records [Stuiver and Braziunas, 1989] suggest that there were multiple comparatively long-lived sunspot minima between about 8000 and 10,000 years ago. Thus, although calculations based upon orbital perturbations alone would suggest that solar insolation was higher than today during summers of the early Holocene, the sun may have undergone several periods when its average intensity was about 1% lower.

We suggest that low atmospheric CO_2 concentrations coupled with, and perhaps in part triggered by, low solar intensity may have been instrumental in creating conditions favorable for rapid transitions between CO_2 "icehouse" effects and CO_2 "greenhouse" effects during the latest Wis-

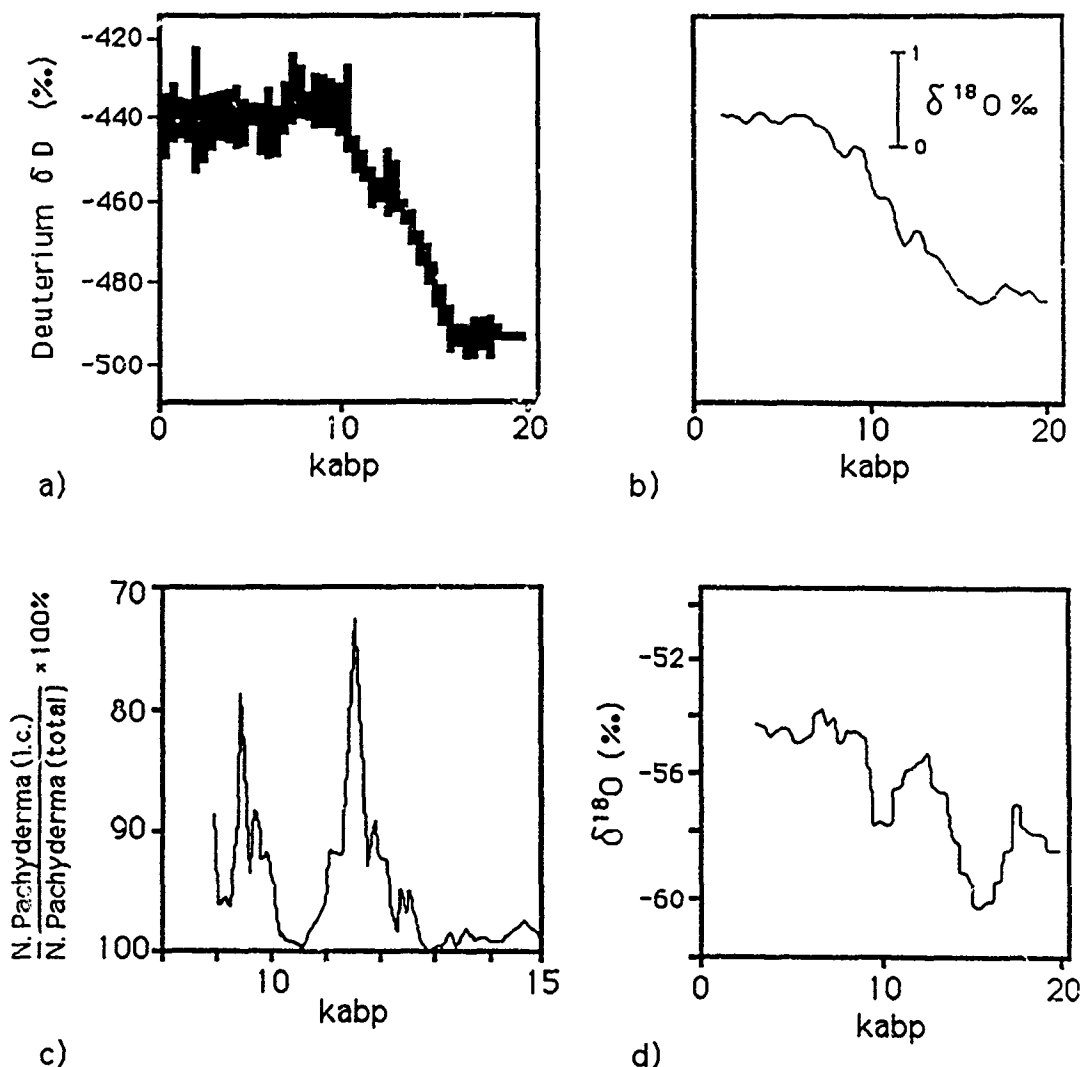


Figure 4. Proxy climate records spanning the last 20,000 years: (a) deuterium concentrations in the Vostok ice core [after Barnola et al., 1987]; (b) stacked oxygen isotope ratios from ocean sediment cores [after Mix and Ruddiman, 1985]; (c) foraminiferal coiling ratios in Pacific sediment core CH84-14 [after Kallel et al., 1984]; (d) oxygen isotope ratios in the Vostok ice core [after Dansgaard et al., 1984]. Time expressed as kiloannum before present (kbp).

consin and the early Holocene. The resulting brief, rapid periods of environmental change could affect glaciers, particularly in certain sensitive, high-latitude areas. Mountainous and close to its Pacific Ocean moisture source, the Alaska Peninsula is ideally suited to record such events.

SUMMARY

(1) Detailed geologic mapping near Windy Creek on the Alaska Peninsula has identified two previously unrecognized sets of post-late-Wisconsin, pre-Neoglacial glacial deposits that reflect episodes of ice expansion.

(2) Radiocarbon dating, stratigraphy and tephrochronology have generated ages of *ca.* 11,000 years B.P. for the Ukak drift and *ca.* 9000 years B.P. for Katolinat drift.

(3) Several independent proxy climate records, including marine data from the Northwest Pacific Ocean, record rapid warming *ca.* 13,000–12,000 years B.P., followed by cold periods within the intervals of *ca.* 10,500–11,500 years B.P. and *ca.* 7500–9000 years B.P.

(4) Variations in atmospheric CO₂ concentration and solar intensity are two possible mechanisms for rapid, transient climate change.

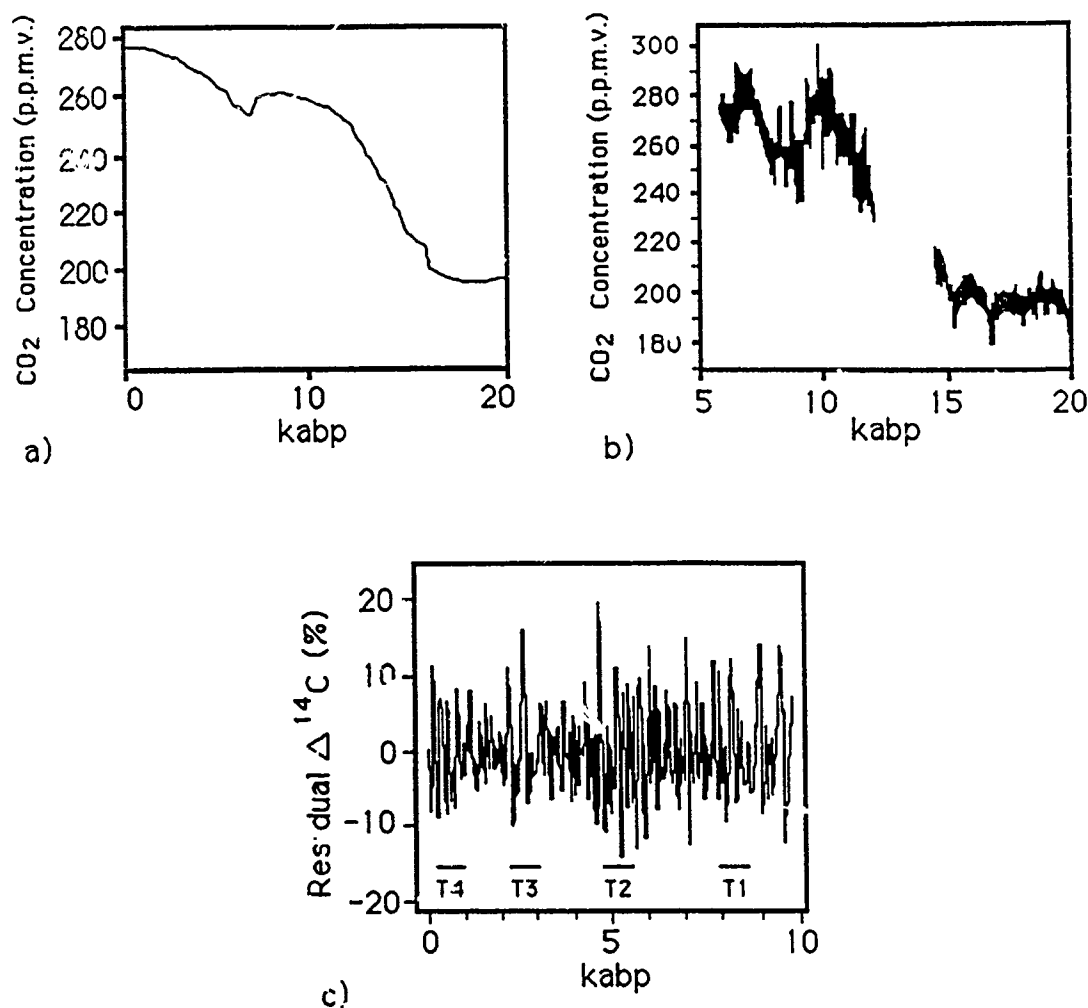


Figure 5. Records of variation in possible climate change mechanisms: (a) CO₂ concentrations in the Vostok ice core [after Barnola et al., 1987]; (b) calculated back of CO₂ concentration in the Byrd ice core [after Neftel et al., 1988]; and (c) solar intensity as expressed by carbon isotope variations in annual tree rings [after Stuiver and Braziunas, 1989]. T1-T4 are episodes of triple oscillations containing at least two of the Maunder- and Spörer-type minima. Time expressed as kiloyear before present (kbp).

REFERENCES CITED

- Barnola, J. M., D. Raynaud, Y. S. Korotkevich, and C. Lorius, Vostok ice core provides 160,000-year record of atmospheric CO₂, *Nature*, 329, 408-414, 1987.
- Dansgaard, W., S. J. Johnsen, H. B. Clausen, D. Dahl-Jensen, N. Gundestrup, and C. U. Hammer, North Atlantic climatic oscillations revealed by deep Greenland ice cores, in *AGU Monograph 29*, edited by J. E. Hansen and T. Takahashi, pp. 288-298, 1984.
- Denton, G. H., and W. Karlén, Holocene climatic variations—their pattern and possible cause, *Quat. Res.*, 3, 155-205, 1973.
- Detterman, R. L., Glaciation of the Alaska Peninsula, in *Glaciation in Alaska: The Geologic Record*, edited by T. D. Hamilton, K. M. Reed, and R. M. Thorson, pp. 151-170, Alaska Geol. Soc., 1986.
- Detterman, R. L., and B. L. Reed, Surficial deposits of the Iliamna quadrangle, Alaska, *United States Geol. Surv. Bull.* 1368-A, 64 pp., 1973.
- Eddy, J. A., Climate and the changing sun, *Climatic Change*, 1, 173-190, 1977.
- Fisher, D. A., Carbon-14 production compared to oxygen isotope records from Camp Century, Greenland and Devon Island, Canada, *Climatic Change*, 4, 419-426, 1982.
- Genthon, C., J. M. Barnola, D. Raynaud, C. Lorius, J. Jouzel, N. I. Barkov, Y. S. Korotkevich, and V. M. Kotlyarov, Vostok ice core: Climatic response to CO₂ and orbital forcing over the last climatic cycle, *Nature*, 329, 414-418, 1987.
- Grove, J. M., *The Little Ice Age*, 498 pp., Methuen Pub., London, 1988.
- Hansen, J., D. Johnson, A. Lacis, S. Lebedeff, P. Lee, D. Rind, and G. Russell, Climate impact of increasing atmospheric carbon dioxide, *Science*, 213, 957-966, 1981.
- Henn, W., Archaeology on the Alaska Peninsula: The Ugashik drainage, 1973-1975, *University of Oregon Anthropological Papers*, 14, 183 pp., 1978.
- Kallel, N., L. D. Labeyrie, M. Arnold, H. Okada, W. C. Dudley, and J.-C. Duplessy, Evidence of cooling during the Younger Dryas in the western North Pacific, *Oceanol. Acta*, 11, 369-375, 1988.
- Mix, A. C., and W. F. Ruddiman, Structure and timing of the last deglaciation: oxygen-isotope evidence, *Quat. Sci. Rev.*, 4, 59-108, 1985.
- Muller, E. H., Glacial history of the Naknek District, Alaska Peninsula, Alaska (abs), *Geol. Soc. Am. Bull.*, 63, 1284, 1952.
- Muller, E. H., Northern Alaska Peninsula and eastern Kilbuck Mountains, Alaska, *United States Geol. Surv. Circ.*, 289, 2-3, 1953.
- Muller, E. H., W. Juhle, and H. W. Coulter, Current volcanic activity in Katmai National Monument, *Science*, 119, 310-321, 1954.
- Neftel, A., H. Oeschger, T. Staffelbach, and P. Stauffer, CO₂ record in the Byrd ice core 50,000-5,000 years B.P., *Nature*, 331, 609-611, 1988.
- Paterson, W., and C. Hammer, Ice core and other glaciological data, in *North America and Adjacent Oceans during the Last Deglaciation, The Geology of North America*, K-3, edited by W. Ruddiman, and H. Wright, pp. 91-109, Geol. Soc. America, Boulder, CO, 1987.
- Péwé, T. L., Quaternary geology of Alaska, *United States Geol. Surv. Prof. Paper* 835, 145 pp., 1975.
- Stuiver, M., and T. F. Braziunas, Atmospheric ¹⁴C and century-scale solar oscillations, *Nature*, 338, 405-408, 1989.

An Algorithm of Approximate Paleotemperature Calculation of the Earth Surface by Temperature Measurements in Deep Boreholes

N. A. Baranova and S. F. Khroutsky

Department of Geocryology, Geological Faculty, Moscow University, Moscow, U.S.S.R.

ABSTRACT

The proposed algorithm of paleotemperature calculation is an independent analytical method of global climatic change in the Upper Pleistocene and Holocene. It is based on construction of determined and non-determined heat exchange models in rocks, i.e., a system approach to the problem.

The determined model of the process is expressed by a mixed marginal problem for the heat conductivity equation. Unknown paleotemperatures of the earth surface as piecemeal-continuous time functions are determined in order to reach the conclusion of a mixed marginal problem of paleotemperature close (in the sense of minimum mean quadratic errors) to modern temperature profiles in deep boreholes. The temperature algorithm is also used to calculate geothermal gradients and the time homogeneity intervals of these quantities. Input data are the heat physical parameters of rocks and the number of discontinuity points of sought-for functions.

A numerical experiment was carried out for a period of about 20,000 years according to real temperature measurements in deep boreholes for a 400-m-thick stratum. As a result, eight "steps" of the group-average of marginal temperature and geothermal gradient were restored. The algorithm is presented as a FORTRAN-IV language program. The transformation of two measured masses into one measured mass is the key feature of the program.

Arctic Environments and Global Change: Evidence in Deep Permafrost Temperatures, Canadian Arctic Archipelago

Alan Taylor

Terrain Sciences Division, Geological Survey of Canada, Ottawa, Ontario, Canada

ABSTRACT

In considering the role of the polar regions in future global change, one may look toward these regions for evidence of past environmental change. Deep ground temperatures provide one window on past surface temperatures, which may be interpreted in terms not only of past climate but also of past environmental conditions.

Across the Canadian Arctic Archipelago, there is no consistent curvature in deep ground temperature profiles that can be modeled in terms of warming of the past century. This contrasts with the result reported by Lachenbruch et al. [1986] for the Prudhoe Bay area of Alaska and may be a consequence of the much larger region and wider well spacing considered in the Canadian case. Any curvature present varies from well to well and may be interpreted in terms of surface temperature changes of the order of 1–3 K on the scale of decades to centuries.

However, there is some evidence that these surface temperature histories may arise from long-term changes in paleoenvironmental factors as well as climate. For instance, the paleoclimate derived from oxygen isotope data at the Agassiz Ice Cap has been compared with the geothermal signature at a well some 180 km to the west. For the Little Ice Age (LIA), the Agassiz paleoclimate explains only half the measured variation in ground temperatures at the geothermal site; the remaining variation may be due to other environmental effects, such as an increase in snow cover following the LIA. This is consistent with extrapolated surface temperatures 7 K higher than other Arctic sites and the unusually deep snow cover observed today.

92-17856



AD-P007 352



**Project CELIA:
Climate and Environment of the Last Interglacial
(Isotope Stage 5) in Arctic and Subarctic North America**

Julie Brigham-Grette

Department of Geology & Geography, University of Massachusetts, Amherst, Massachusetts, U.S.A.

CELIA Board Members

(In alphabetical order; see after References for full addresses:

Mary Edwards, Svend Funder, John Kutzbach, Lou Maher, John V. Matthews, Jr.,
Gifford H. Miller, Alan Morgan, Nat W. Rutter (co-chairman), Charles Schweger (co-chairman),
Charles Tarnocai, Jean-Serge Vincent, Anne de Vernal)

ABSTRACT

Stage 5e of the marine oxygen isotope record is the last time when world ice volume was lower, sea level was higher, and world climate warmer than during any part of the Holocene. To develop more accurate proxy data for natural climate change during the last interglacial, a multidisciplinary group of scientists working as regional teams has developed Project CELIA to generate and synthesize knowledge for this period from high latitude terrestrial and nearshore marine environments. We have cited 13 terrestrial sequences distributed across the Arctic and Subarctic for detailed study based upon well-exposed stratigraphy, abundance of organic remains, and geochronological potential. In addition, information from select marine cores bearing terrestrial pollen and ice cores from Devon and Agassiz Ice Caps will also be incorporated. These data will highlight regional changes in vegetation patterns, tree line position, permafrost distribution, and sea ice conditions from which ocean/atmospheric changes can be inferred. This information will be of value for testing hypotheses generated by GCMs and other simulations of interglacial conditions, refining such models and providing insight to future environments resulting from global warming. CELIA will be carried out over the next 5 years and will be directed by an international board of experts under the auspices of the University of Alberta's Canadian Circumpolar Institute. (CELIA Publication No. 004).

INTRODUCTION

Project CELIA (Climate and Environment of the Last Interglacial in Arctic and Subarctic North America) is an international cooperative research program developed to: (1) generate and synthesize data on Isotope Stage 5 high latitude terrestrial and nearshore marine environments; (2) test hypotheses generated by general circulation models and other warm earth or interglacial simulations; and (3) by documenting the past, provide insight into future environment as a result of global change.

Man's activities during the present interglaciation include the beginnings of forest clearance as early as 10,000 years ago and continuing to the present, and more recently, the rapid modification of the composition of the atmosphere. These have been characterized as a "grand experiment" with an unpredictable outcome. All of mankind is part of that "experiment" and while we cannot simply step out of the ongoing changes because the outcome appears unfavorable, we can prepare for the different world of the near future by gaining precise knowledge on past intervals of warmer

Glacial Marine Sediments from the Antarctic Peninsula: A Record of Climate Change and Glacial Fluctuations During the Late Holocene

E. W. Domack and L. Burkley

Geology Department, Hamilton College, Clinton, New York, U.S.A.

ABSTRACT

Present climate conditions along the western side of the Antarctic Peninsula vary from subpolar, in the north, to polar in the south. Thus, the region provides an ideal setting in which to study the relationship between climate and glacial marine processes in Antarctica. Physical oceanographic measurements (211 CTD casts) and bottom sediment samples (>104) provide the data base for the following conclusions. Subpolar glacial regimes in the South Shetland Islands are dominated by extensive surface melting, elevated equilibrium lines (ELA) and efficient conduction of surface meltwater to the terminus of tidewater and terrestrial glaciers. These conditions control sedimentary processes in the marine realm by the efficient and widespread dispersal of suspended sediment by overflow plumes. Terrigenous facies, therefore, dominate throughout the fjord system.

The transition to polar conditions within glaciers along the Danco Coast and Palmer Archipelago is characterized by lower ELA (near sea level), limited surface melting and dynamic sea ice conditions. Basal melt processes appear to dominate, especially where subglacial marine cavities exist beneath glacial termini. Most terrigenous sediment is transported by ice-rafting or by cold, mid-water plumes, which spread horizontally until restricted by bathymetric features. Biogenic (diatom) muds and ice-rafted debris dominate sedimentation in outer bay settings; the former is enhanced by warmer temperatures, increased sunlight, and minimal disturbance of surface layers within the fjords.

These facies transitions are well constrained statistically by regression analyses of textural and compositional variations with respect to distance from sediment sources (glacial termini). Correlation trends within individual ice drainage systems can be applied to marine sediment cores which contain a record spanning approximately the last 3000 years (based upon accelerator ^{14}C and ^{210}Pb chronologies). A period of enhanced terrigenous (surface meltwater) input following more extensive glacier ice is documented in Hughes Bay on the northern Danco Coast. By analogy with modern conditions it is presumed that mean summer temperatures around 700 to 1000 years B.P. were at least 2°C warmer than at present. A number of depositional cycles are recognized from fjords further south but these require additional study before interpretations are forthcoming.

climate. In order to achieve this, a "control situation" free of human influences is required. A reconstruction of the paleoclimate and paleoenvironment during Stage 5, and particularly Stage 5e, provides such an opportunity.

STAGE 5e, THE LAST INTERGLACIAL

Stage 5e of the marine oxygen isotope record, 126,000 years ago, was the last period of time of lower world ice volume, higher sea level and warmer world climate than during any part of the Holocene. It is the most recent period of time with a climate as warm as that anticipated for the near future as a result of anthropogenic changes to the atmosphere [Dickinson and Cicerone, 1986; Hansen et al., 1987]. In addition, it is now known that CO₂ levels during Stage 5e increased, with the greatest buildup prior to the sharp decline in world ice volumes [Genthon et al., 1987; Bartlein and Prentice, 1989]. Several Stage 5 sites across high latitude North America give indications that tree lines and other species' ranges advanced beyond their Holocene limits and that the permafrost table was either as shallow as now, or that permafrost was absent over much of the subarctic [Schweger and Matthews, 1985; Matthews et al., 1990; Hughes et al., 1991].

In total, Stage 5e is an ideal time period for investigating climate change, especially warming, and the attending environmental responses. This conclusion was also reached by the International Council of Scientific Unions' (ICSU) Scientific Steering Committee on Global Changes of the Past, which identified study of the last interglacial as an international research priority.

PROJECT CELIA: OBJECTIVES

A prime objective of project CELIA is the recovery and synthesis of qualitative and quantitative information on the climate and environment during the last interglacial. This will be accomplished through field and laboratory research on selected high latitude sites where a variety of paleoecological and proxy climate methods (e.g., fossil pollen, insects, seeds, soils properties, stable isotopes) will be employed. Qualitative information should be important in supplementing and enriching the quantitative data sets. As a result of these qualitative and multidisciplinary inputs, CELIA will provide a broader and more complete view of the paleoenvironment of the last interglacial than has heretofore been possible.

Project CELIA will deal only with the arctic and subarctic regions of North America and Greenland. This is appropriate, as northern regions are to be the first to experience future warming and it is here that warming is expected to be greatest. As well, the cold climate of the arctic/subarctic ensures optimal fossil preservation, frequently enabling identification of fossil insects or seeds to the species level. It is in the arctic/subarctic that many species including trees meet their present-day climatic limits, and permafrost, or sporadic permafrost, is widespread. These important environmental discontinuities and thresholds ensure that sensitive and accurate paleoenvironmental records can be established.

The objectives of CELIA may be framed in terms of the following major questions:

(1) What was the distribution of continuous and discontinuous permafrost during Stage 5e? How did permafrost

degradation resulting from warmer temperatures influence the northern landscape? Were there qualitative and quantitative differences between the thermokarst terrain of Stage 5e and that of the early Holocene? What does stratigraphic evidence of deeper than present thawing imply about former mean annual temperatures?

(2) What were the ranges of various plant and animal taxa, and what do these imply about 5e climate? Can we identify particular species that are readily recognized as fossils and whose present distribution is sensitive to various climatic parameters? Are there species which are well represented as fossils but for which autecological information is lacking?

(3) When Stage 5e pollen spectra are compared with modern climate-pollen calibration sets, what numerical estimates are obtained? How useful are pollen data from the high arctic with low pollen production and the possibility of contamination from late Tertiary pollen?

(4) What was the speed and nature of the onset of interglacial conditions at the beginning of Stage 5e? (This is a very important question with respect to "greenhouse warming" and identification of forcing factors.) How much climatic variability characterized the whole of Stage 5, is it possible to easily distinguish 5e, and what is the nature of the stage 5e termination?

(5) What is the nature of the nearshore marine record for Stage 5e and can it be used to correlate terrestrial and deep sea marine records? What has been the extent of coastal erosion and inundation during Stage 5e? Is it possible to determine anything of Stage 5e sea ice conditions?

(6) Finally, to what degree do climatic reconstructions of Stage 5e agree with model simulations for that time period? Do the model simulations provide the type of estimates that can be tested by reference to climate proxy data?

PALEOCLIMATIC MODELS AND HYPOTHESES TESTING

Computer-based climate models are the most effective means of simulating the dynamics of global climate and climate change given orbital perturbations, new forcing functions and boundary conditions. This potential is being widely explored as a means of predicting future global climate under a CO₂-enriched atmosphere. Such models have already been used, not without controversy, to predict marked warming particularly at high latitudes by the turn of the century [Hansen et al., 1988]. Further development and refinement of computer models will be undertaken; however, they will require rigorous testing of model predictions with actual climate or paleoclimatic data sets. It is best, therefore, if climate modelers work closely with other scientist in developing research programs that will facilitate the testing of model simulations. The COHMAP [1988] project designed to test climate simulations based on orbital perturbations over the last 18 ka is an excellent example of such an approach.

Project CELIA is working closely with John Kutzbach, Center for Climatic Research, University of Wisconsin, in developing model runs that can be treated as hypotheses. Preliminary GCM model results for the climate of the last interglacial (126 ka) are now available to CELIA as a first step in this research program. These results indicate that Northern Hemisphere summer radiation was more than 10%

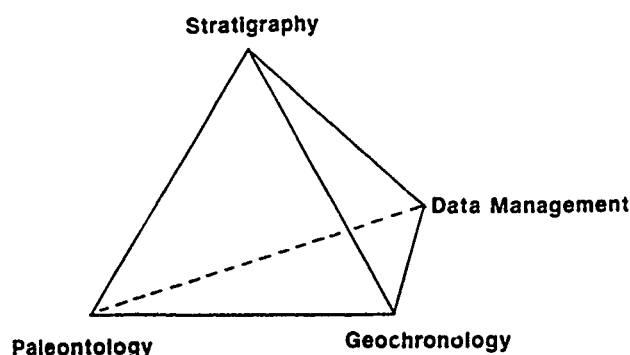


Figure 1. Conceptual framework for research at CELIA sites illustrating how different aspects of studies at individual sites will be coordinated.

greater at 126 ka than at 9 ka [Prell and Kutzbach, 1987]; that July temperatures increased over present-day model values from 4–6°C for large areas of the high latitudes; that January temperatures increased to a maximum of 4°C over northern European Russia (elsewhere, 0–2°C) with a notable exception over the eastern Canadian Arctic where January temperatures declined by 4–6°C; and that there was little change in high latitude precipitation 125,000 years ago.

QUANTITATIVE METHODS

Because project CELIA will involve many researchers and will be making continent-wide comparisons between study sites and resulting data sets, it is important that standardized methods be developed and employed wherever possible. This includes field and laboratory methods as well as data storage protocols (Figure 1). Some computer software has already been developed and a standardized spreadsheet will soon be available [Maher, 1991]. Computer storage facilities are to be established at the Canadian Circumpolar Institute (formerly Boreal Institute for Northern Studies), University of Alberta, and the Department of Geology, University of Wisconsin, to ensure easy access to the CELIA data sets.

Excellent progress has been made in the use of climate-pollen calibration for paleoclimatic reconstructions during the Holocene utilizing various multivariate methods [e.g., Bartlein et al., 1986; MacDonald and Reid, 1989]. The use of such methods will figure prominently in project CELIA as fossil pollen data for the last interglacial become available from the network of study sites; and the project requires that CELIA work closely with a variety of researchers (i.e., L. Brubaker and P. Anderson, Univ. of Washington; P. Bartlein, Univ. of Oregon) in developing modern pollen data sets and the appropriate numerical methods for estimating paleoclimatic parameters.

Certain assumptions must be made, however, regarding analogous conditions of climate, vegetation, and soil development when applying modern climate-pollen data to reconstruct the paleoclimate of the last interglacial. In this regard, the numerical methods employed are not without fault [Maher, 1989]. To meet this problem, project CELIA anticipates that progress will be made in establishing other proxy indicator data sets that can serve as a check on conclusions reached through pollen studies and at the same time provide additional paleoclimatic estimates. Such data sets

might include fossil insects and seeds, hematite production in soils, ground ice history or marine molluscs, to name a few.

GEOCHRONOLOGY

Dating at 80–130 ka isotope Stage 5 (including stages 5a,b,c,d,e) is well beyond the range of radiocarbon dating, necessitating reliance on other dating methods to identify the warmest Stage 5e. There is controversy over the age of the last interglacial and the possibility exists that in some areas the warmest period may not have been during Stage 5e [Funder, 1989]. In Alaska and Yukon Stage 5e is recognized in relationship to the Old Crow tephra [Edwards and McDowell, 1990; Matthews et al., 1990], although even this is not without other points of view [Begét et al., 1990].

Stage 5e must be distinguished on a geochronological basis in order to avoid circular arguments as to what is the last interglacial. It is also important that its duration is known so that rates of change within the period can be established (see objective 4). Application of multiple geochronological methods for each study site will be an important part of CELIA's research activities and will require coordination and close cooperation between a variety of workers and laboratories. The multiple dating method approach has precedence. The literature contains numerous examples of "classic last interglacial" deposits that on subsequent study have been found to greatly pre-date the last interglacial. Such deposits were initially considered last interglacial because they were the uppermost buried deposit with a warmer-than-present fauna or flora. Although the assumption that such horizons ought to represent the last time that the plant was in an interglacial mode, the demonstrated incompleteness of the terrestrial record underscores the fallacy of this interpretation. Because there is some possibility of confusing interstadial and interglacial horizons, even radiocarbon can play an important role.

IMPLEMENTATION AND ADMINISTRATION

CELIA is made up of an active board of thirteen researchers that have study site and methodological expertise, and is administered through the Canadian Circumpolar Institute, University of Alberta. Other researchers will participate in project CELIA through cooperative liaison with the Board or Board members.

Fourteen study sites have been identified on the basis of their potential for future CELIA research, and they range from western Alaska to Greenland, and from terrestrial, coastal, and near-shore marine environments to marine cores that record terrestrial conditions (Figure 2). Research at each site will be the responsibility of a site manager (Figure 3), who is also a Board member, in consultation with the CELIA co-chairmen (Schweger and Rutter) who will serve as geochronology and paleoecology coordinators. The site manager and coordinators, together with other Board members who represent various methodological specializations, will identify the most appropriate methods and personnel to employ for each site, the maintaining of a timetable, and data protocols. A data base manager will be responsible for maintenance of the CELIA data sets and their availability to those undertaking paleoclimatic syntheses.

Regular Board meetings will be scheduled to assure a high level of communication and participation and col-

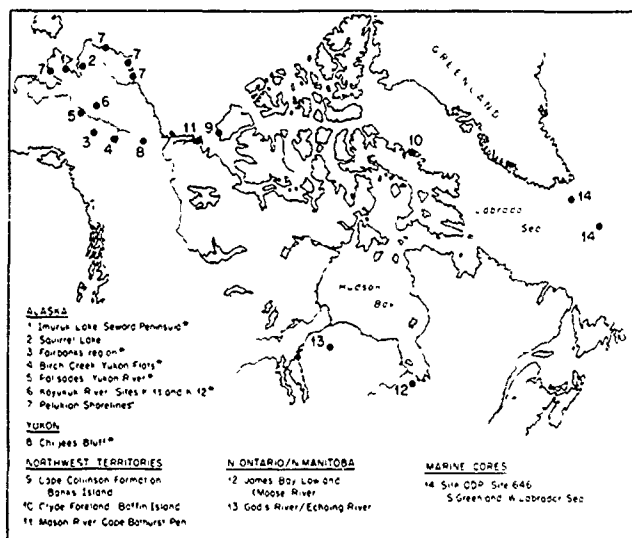


Figure 2. Distribution of selected CELIA sites across Arctic and Subarctic North America and Greenland. These sites are not exclusive of other known and potential 5e sites not listed here for future consideration.

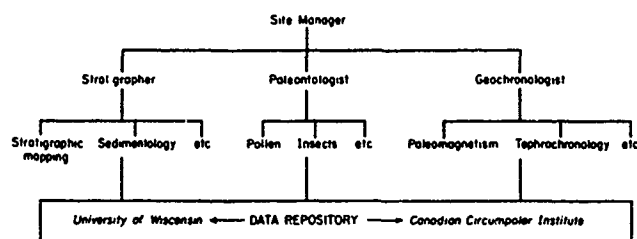


Figure 3. Organizational framework for the collection of samples and processing of data from each CELIA site.

lective decision-making. Project CELIA's first full Board meeting was held January 5-6, 1990, at the then Boreal Institute, University of Alberta; the next was held in the fall of 1990 in Denmark (see below). Project CELIA's progress will be regularly published as single and collected papers under individual or, when appropriate, group authorship. *Quaternary International* Pergamon Press has already offered to publish a journal issue devoted to project CELIA research results. Final results and synthesis will most likely be published as a book or monograph (see timetable).

INTERNATIONAL RELATIONS

Project CELIA presently maintains a close relationship with international global change research groups through the activities of individual Board members. Notable are N. Rutter's participation in ICSU's Scientific Steering Committee for Global Changes of the Past and his role as President of INQUA.

As presently conceived, project CELIA is to reconstruct the climate and environment of Stage 5e for northern North America, including Greenland. Its ultimate success, however, may rest in its international relationships and ability to coordinate hemispheric data sets for climate model testing. Global change is, after all, "global." Therefore, CELIA will seek to establish close ties with Nordic and Soviet researchers as well as with other groups actively researching the last interglacial in terrestrial and marine environments. The

PONAM project (Polar North Atlantic Margins—Late Cenozoic Evolution) designed, in part, to document the last glacial cycle in the North Atlantic is a good example; CELIA Board member G. Miller attended the last PONAM (1989) meeting as an observer.

On October 16-19, 1990, the first workshop funded by NATO's Global Change Program was held in Denmark to interface CELIA with similar projects in Europe and the Soviet Union. The results of this workshop will be published in *Quaternary International*.

SOCIOECONOMIC IMPORTANCE OF CELIA

The region dealt with by project CELIA includes the northern tree line, geographical limits for hundreds of plant and animal species and continuous and discontinuous permafrost. It is also home to native peoples who continue to engage in traditional subsistence activities that are dependent on the timing of spring river breakup, cold and snow, winters, persistence of seasonal ice packs and adequate forage for game species. Because important prehistoric adaptations were made to the nearshore marine environments, much of the archaeological heritage is at or only slightly above the present sea level. Northern oil and mineral exploration has intensified greatly in recent decades, adding to the growing infrastructure provided by governments and native groups, transportation links and construction projects. If future warming occurs, the north will be the first region to sense the change and experience the socioeconomic impacts.

Many studies and publications have noted the "fragile" nature of the arctic/subarctic regions, and call for more baseline information in order to assess environmental and social impacts of human activities in the north. The modification of the atmosphere and the attending climate changes expected over the next decades represent the greatest threat of human intervention in the north. It will have great impacts in all geographic areas and on all aspects of northern life, including changes to plant and animal distributions, pest plants and insects, thawing of permafrost, increasing erosion and slope failure, increasing peatland degradation, destruction of archaeological sites and a host of new problems for northern communities, native peoples and industry.

Through project CELIA site-specific paleoenvironmental data will be synthesized and utilized in developing predictive capabilities regarding global warming at high latitudes. This is an application of great importance to the environment and development of all northern lands.

CELIA TIMETABLE

Although a startup grant provided by the then Boreal Institute led to a draft proposal distributed in 1989, project CELIA must be thought of as beginning with its first full Board meeting in January, 1990. CELIA's five-year timetable will be as follows:

- April, 1990. Release of CELIA proposal to Board members for development of grant proposals.
- Summer, 1990. Limited field investigations using existing funding within CELIA framework; development of data base protocols; submission of major grant proposals (NSERC, NSF, etc.).
- October, 1990. NATO Advanced Studies Workshop held in Hanzhtholm, Denmark, on CELIA to interface with similar European and Asian projects. This was the first workshop

to be funded under NATO's new Global Change initiative.
 April, 1991. Release of data base protocols; planning for summer field work at designated CELIA sites.
 Summer, 1991. Field and laboratory research; CELIA participation at INQUA meetings.
 November, 1991. CELIA Board meeting to report on progress and results and publications.
 Winter, 1991/1992. Laboratory research, planning for summer field work and publication of results.
 Summer, 1992. Field and laboratory research.
 November, 1992. CELIA Board meeting with paleoclimate

researchers to begin process of synthesis and testing.
 Winter, 1992/1993. Laboratory research and synthesis of results.
 Summer, 1993. Limited field work, otherwise laboratory research and synthesis of results.
 November, 1993. CELIA Board meeting to begin final synthesis and preparation for publication of final results.
 Winter, 1993/1994. Final laboratory results and completion of final synthesis.
 June, 1994. Final CELIA Board meeting to edit final publication.

REFERENCES

- Bartlein, P. J., and I. C. Prentice, Orbital variations, climate and paleoecology, *Trends in Ecology (TREE)*, 4, 195-199, 1989.
- Bartlein, P. J., I. C. Prentice, and T. Webb, III, Climate response surfaces from pollen data for some eastern North American taxa, *J. Biogeogr.*, 13, 35-57, 1986.
- COHMAP members, Climatic changes of the last 18,000 years: observations and model simulations, *Science*, 241, 1043-1052, 1988.
- Dickinson, R. E., and R. J. Cicerone, Future global warming from atmospheric trace gases, *Nature*, 319, 109-115, 1986.
- Edwards, M. E., and P. F. McDowell, Interglacial deposits at Birch Creek, northeast interior Alaska, *Quat. Res.*, 35, 41-52, 1990.
- Funder, S. (Ed.), Late Quaternary stratigraphy and glaciology in the Thule area, Northwest Greenland, *Meddelelser om Gronland, Geoscience*, 22, 3-63, 1990.
- Genthon, C., J. M. Barnola, D. Raynaud, C. Lorius, J. Jouzel, N. I. Barkov, Y. S. Korotkevich, and V. M. Kolyakov, Vostok ice core: climate response to CO₂ and orbital forcing changes over the last climatic cycle, *Nature*, 329, 414-418, 1987.
- Begét, J. E., D. B. Stone, and D. B. Hawkins, Paleoclimatic forcing of magnetic susceptibility variations in Alaskan loess during the late Quaternary, *Geology*, 18, 40-43, 1990.
- Hansen, J., I. Fung, A. Lacis, D. Rind, S. Lebedeff, R. Ruedy, and G. Russell, Global climate changes as forecast by Goddard Institute for Space Studies Three-dimensional Model, *J. Geophys. Res.*, 93, 9341-9364, 1988.
- Hughes, O. L., C. Tarnocai, and C. E. Schweger, Testing interglacial climate: Pleistocene stratigraphy, paleopedology, and paleoecology, Little Bear River section, western Mackenzie District, *Can. J. Earth Sci.*, 1991, In review.
- MacDonald, G. M., and R. T. Reid, Pollen-climate distant surfaces and the interpretation of fossil pollen assemblages from western interior of Canada, *J. Biogeogr.*, 16, 403-412, 1989.
- Maher, L. J., Quaternary palynology: Key to the past or the emperor's new suit?, *Geol. Soc. Am. Abstracts with Programs*, 21(6), A211, 1989.
- Maher, L. J., Pollen software. Geology Department, University of Wisconsin, Madison, 1991, In preparation.
- Mathews, J. V., Jr., C. E. Schweger, and J. E. Janssens, The last (Koy-Yukon) interglaciation in the northern Yukon Territory: evidence from Unit 4 at Ch'jee's Bluff exposure, Bluefish Basin, *Géographie physique et Quaternaire*, 44, 341-362, 1990.
- PONAM members, European program on Polar North Atlantic margins—late Cenozoic evolution. European Science Foundation Proposal, 1989.
- Prell, W. L., and J. E. Kutzbach, Monsoon variability over the past 150,000 years, *J. Geophys. Res.*, 92, 8411-8425, 1987.
- Schweger, C. E., and J. V. Mathews, Jr., Early and middle Wisconsinan environments of eastern Beringia: stratigraphic and paleoecological implications of the Old Crow tephra, *Géographie physique et quaternaire*, 39, 275-290, 1985.

CELIA Board Members:

JULIE BRIGHAM-GRETTE, Department of Geology & Geography, University of Massachusetts, Amherst, MA 01003 USA
 MARY EDWARDS, Department of Geology & Geophysics, University of Alaska, Fairbanks, AK 99775 USA
 SVEND FUNDER, Geological Museum, University of Copenhagen, Oster Voldgade 5-7, DK-1350, Copenhagen, Denmark
 JOHN KUTZBACH, Center for Climatic Research, University of Wisconsin, Madison, WI 53706 USA
 LOU MAHER, Department of Geology & Geophysics, University of Wisconsin, Madison, WI 53706 USA
 JOHN V. MATTHEWS, JR., Geological Survey of Canada, Terrain Sciences Division, 601 Booth Street, Ottawa, Ontario K1A 0E8 Canada
 GIFFORD H. MILLER, INSTAAR & Department of Geological Sciences, University of Colorado Boulder, CO 80309 USA
 ALAN MORGAN, Department of Earth Sciences, University of Waterloo, Waterloo, Ontario N 3L 1 Canada
 NAT W. RUTTER, Board Co-Chairman, Department of Geology, University of Alberta, Edmonton, Alberta T6G 2E3 Canada
 CHARLES SCHWEGER, Board Co-Chairman, Department of Anthropology, University of Alberta, Edmonton, Alberta T6G 2H4 Canada
 CHARLES TARNOCAL, Agriculture Canada, Land Resources Research Institute, K.W. Neatby Building, Ottawa, Ontario K1A 0C6 Canada
 JEAN-SERGE VINCENT, Geological Survey of Canada, Terrain Sciences Division, 601 Booth Street, Ottawa, Ontario K1A 0E8 Canada
 ANNE DE VERNAL, University of Quebec at Montreal, Laboratory GEOTOP, 1200 Alexander Street, P.O. 8888, Succ. "A", Montreal, Quebec H3C 3P8 Canada

AD-P007 353



92-17857



A Proxy Late Holocene Climatic Record Deduced from Northwest Alaska Beach Ridges

Owen K. Mason and James W. Jordan

Alaska Quaternary Center, University of Alaska Fairbanks, Fairbanks, Alaska, U.S.A.

ABSTRACT

A climatically sensitive, oscillating pattern of progradation and erosion is revealed in late Holocene accretionary sand ridge and barrier island complexes of Seward Peninsula, northwest Alaska. Archaeological and geological radiocarbon dates constrain our chronology for the Cape Espenberg beach ridge plain and the Shishmaref barrier islands, 50 km to the southwest. Cape Espenberg, the depositional sink for the northeastward longshore transport system, contains the oldest sedimentary deposits: 3700 ± 90 B.P. (β -23170) old grass from a paleosol in a low dune. The oldest date on the Shishmaref barrier islands is 1550 ± 70 B.P. (β -23183) and implies that the modern barrier is a comparatively recent phenomenon. Late Holocene sedimentation along the Seward Peninsula varied between intervals of rapid progradation and erosion. Rapid progradation predominated from 4000–3300 B.P. and from 2000–1200 B.P., with the generation of low beach ridges without dunes, separated by wide swales. During erosional periods higher dunes built atop beach ridges: as between 3300–2000 B.P. and intermittently from 1000 B.P. to the present. Dune formation correlates with the Neoglacial and Little Ice Age glacial advances and increased alluviation in northern and central Alaska, while rapid progradation is contemporaneous with warmer intervals of soil and/or peat formation atop alluvial terraces, dated to 4000–3500 and 2000–1000 B.P. In the last 1000 years, dune building is linked with heightened storminess, as reflected in weather anomalies such as spring dust storms and winter thunderstorms in East Asia and European glacial expansions.

INTRODUCTION

Beach Ridge Archaeology originated as an archaeological survey stratagem to assist in deciphering the tempo of prehistoric technological changes [Giddings and Anderson, 1986]. J. Louis Giddings [1966; Giddings and Anderson, 1986] outlined over 4000 years of prehistory in northwest Alaska using relative beach ridge position as a chronological marker, but he did not correlate deposits from more than one beach ridge complex or examine the internal patterning of individual beach ridge sets to obtain paleoenvironmental data. However, paleoclimatic conditions may be inferred by combining archaeological radiocarbon dates with geological evidence.

Our recent (1986–1989) geoarchaeological studies suggest the following sequence of late Holocene paleoclimate

in northwest Alaska. Warm conditions prevailed about 4000 to about 3300 ^{14}C years B.P. and from 2000–1200 ^{14}C years B.P., resulting in the progradation of the shoreline. Transgressive dunes built between 3300–2000 ^{14}C years B.P. and during the last 1200 years, as a consequence of heightened storminess and coastal erosion during climatic conditions producing world-wide glacial expansion. To place our paleoclimatic record in context, we examine the boundary conditions influencing beach ridge deposition in northwest Alaska.

OCEANOGRAPHIC AND GEOLOGIC SETTING OF THE SOUTHEAST CHUKCHI SEA

The Chukchi Sea is an arm of the Arctic ocean formed by the shores of northwest Alaska and northeast Siberia (Figure

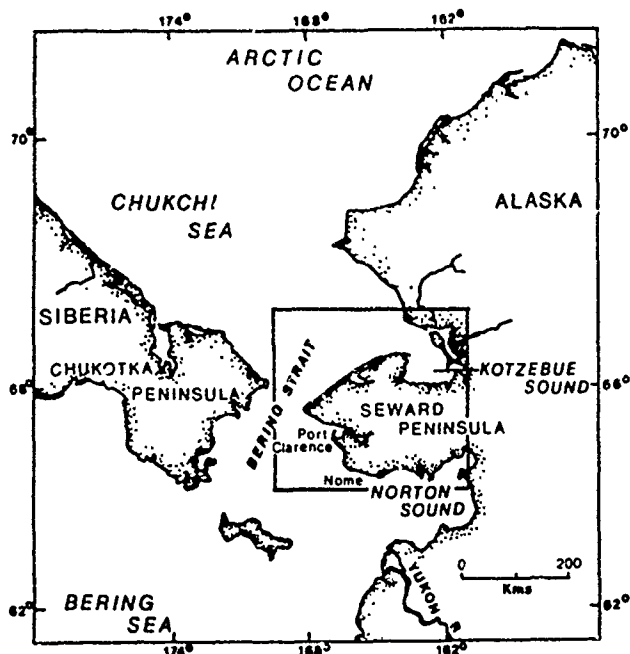


Figure 1. Map of western Alaska.

1), extending north of Bering Strait, 65°N, to the fluctuating summer extent of Arctic pack ice at 71–75°N. Ice covers the entire Chukchi Sea during winter, leaving its shores subject to storm and wave processes for only 4 months in the open water season from July to October [LaBelle et al., 1983]. The Chukchi Sea is microtidal with a range of less than a meter, though meteorological events can cause sea levels to rise as much as 1 m [Hume and Schalk, 1967]. Coastal currents flow northeastward from the Bering Strait, decelerating near the entrance to Kotzebue Sound at Cape Espenberg, a circumstance favoring the deposition of sediment [Sharma, 1979:404].

Five major beach ridge complexes are located at alignments in sediment transport direction along the southeast coast of the Chukchi Sea, at Cape Prince of Wales, Cape Espenberg, Sisualik, Cape Krusenstern and Pt. Hope (Figures 1 and 2). Since longshore sediment movement is tied to the effects of onshore winds [Moore, 1966; Komar, 1976], Moore and Giddings [1961] proposed that the depositional history of each beach ridge complex varied in relation to shifts in the prevailing wind direction in the late Holocene. Net progradation over time also requires a combination of low or moderate tidal levels and a constant source of sediment [Hayes, 1979; Kraft and Chrzastowski, 1985]. Progradation can occur if sea levels are rising only if the supply of sediment is high [Curry, 1964]. To consider these restrictions on progradation, we must consider the tectonic setting and sea level history of the Chukchi Sea.

Tectonic Setting

Kotzebue Sound has not undergone appreciable tectonic effects during the Holocene, based on offshore seismic-reflection studies [Eitrem et al., 1977]. Further, the coastal lowlands of northern Seward Peninsula were not glaciated in the Pleistocene [Péwé, 1975], so we can exclude isostatic factors from our consideration of shoreline processes. For

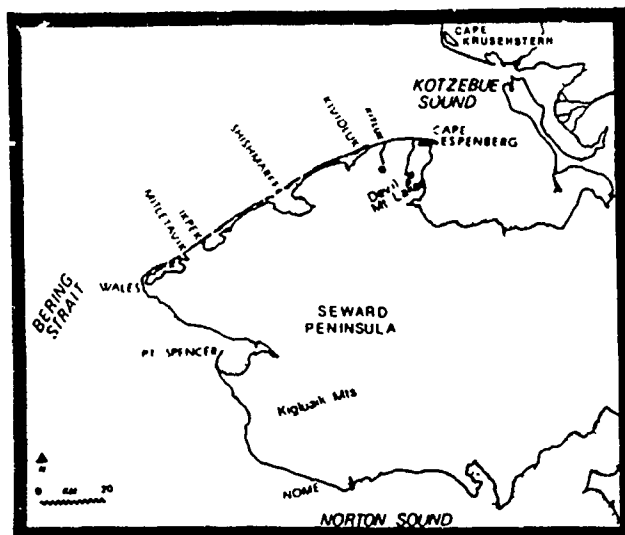


Figure 2. Map of Seward Peninsula and Kotzebue Sound indicating location of beach ridge complexes and other locations mentioned in text.

these reasons, the record of Chukchi Sea shoreline change is principally a reflection of climate-induced changes.

Sea Level History

The shallow (less than 80 m deep) continental shelf of the Chukchi Sea was sub-aerially exposed as part of Beringia during the late Pleistocene, due to the eustatic effects imposed by widespread continental glaciation. The transgression of the Chukchi shelf began before 15,500 B.P. when Bering Strait flooded and continued until the modern sea level was approached at ca. 5000 years ago [McManus et al., 1983]. The evidence for sea level change is from offshore cores and the interpretation of benthic foraminiferal faunas [McManus et al., 1983]. Coring in waters 30–70 m deep with only low annual accumulations of sediment, oceanographers do not record finer scale sea level changes after 5000 B.P. To document late Holocene sea level history we rely on the terrestrial record and its superimposed archaeological remains. Beach ridge deposition in Kotzebue Sound dates from only after 4000 B.P. and provides an upper limiting age on the establishment of near modern sea level, as suggested by Moore [1961] and Hopkins [1967].

Short-term eustatic sea level fluctuations may have produced the higher ridges at Pt. Hope 2000–1500 B.P. [Moore, 1960] and at Pt. Barrow, where Hume [1965] recorded transgressive gravel ridges (0.6–1.0 m above sea level (asl)) dated between 1750–1500 B.P. and 1000–900 B.P. Péwé and Church [1962] also propose that beach ridges 1–2 m asl at Pt. Barrow resulted from high eustatic sea levels prevailing from 1200–1000 B.P. Mason [1990] suggests that sea levels were only temporarily elevated due to low barometric pressure associated with storms which deposited higher gravel ridges. These temporary sea surface elevations are evidence for climatically driven phenomena and not eustatic sea level changes.

In summary, then, the rapid eustatic sea level rise in the Chukchi Sea during the early Holocene precludes the preservation of terrestrial deposits until sea levels comparatively

stabilized ca. 4000 B.P. We assume that sea level has been nearly constant, within 1–2 m of present, during the late Holocene because beach ridge complexes have prograded at nearly all the critical headlands of the Chukchi Sea. Hence higher ridges are evidence of climatic variability and not eustatic effects.

Sediment Sources

Two abundant sediment sources are involved in building barrier and beach ridge deposits around the margins of the southern Chukchi Sea: (a) offshore marine sands on the continental shelf, and (b) sands within terrestrial bluffs. Mason [1990] estimates that about 90% of the sand deposited at Cape Espenberg is offshore sand transported toward the shore under the influence of long-period swell associated with fairweather conditions. The process of onshore transport is temporarily reversed during storms which erode mainland bluffs and transport sediment offshore and subsequently downdrift.

STUDY AREA:

THE NORTHERN SEWARD PENINSULA COAST

The 250-km-long northwest Seward Peninsula coast alternates between extensive stretches of accretional beach and dune ridge topography formed in the Holocene and eroded cliffs of silty sand and tephra of Pleistocene age. Five principal zones (Figure 2) may be defined on the basis

of erosional characteristics [Jordan, 1988], moving south to north: (1) the 30-km-long Wales beach ridge plain; (2) a 20-km stretch of late Holocene dunes overtopping the Pleistocene silt bluffs between Miletavik and Ikpek; (3) the 150-km-long Shishmaref barrier islands; (4) 30 km of tundra-covered bluffs in the Kitluk River region; and (5) the 30-km-long Cape Espenberg beach and dune ridge complex, at the northern extreme of the Peninsula, which serves as the depositional sink for the entire coast. In this paper, we will highlight the record from the Shishmaref Inlet barrier islands and the Cape Espenberg sand spit, which serves as a "type section" for the entire coast. The Wales beach ridge plain is largely unstudied and will not be discussed here [cf. Mason, 1990].

METHODOLOGY

Mason [1937 1990] used geoarchaeological evidence to distinguish depositional units at Cape Espenberg. Jordan [1990] employed similar methods at Kividluk on the Shishmaref barrier islands. The most reliable chronological data are ^{14}C dates on charcoal and temporally diagnostic artifacts from archaeological sites. The cultural chronology of north-west Alaska plays a substantial role in interpreting chronostratigraphic units and is reviewed by Mason [1990] who modifies Giddings and Anderson [1986]. Extensive linear clusters of house depressions are common in the youngest ridges while sites on older ridges are surficial scatters

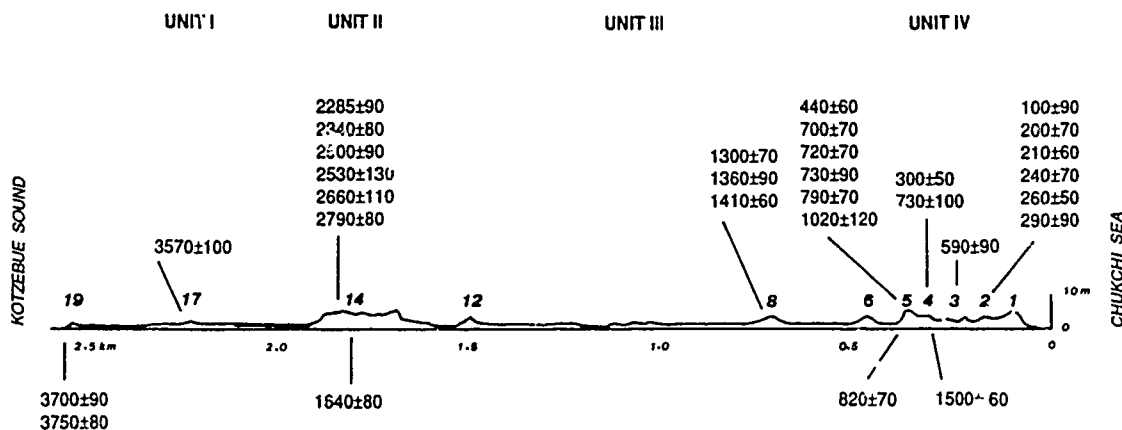
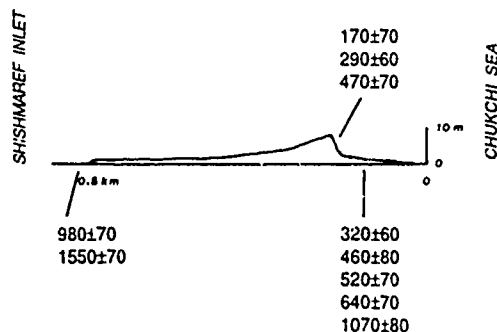


Figure 3(a). Schematic cross-section of Cape Espenberg beach ridge plain. Radiocarbon dates are plotted in relation to distance from modern shore with depositional units shown above. Archaeological dates are plotted above; geological dates below. Two geologic dates from ridges E-4 and E-5 are on marine shell and require a correction of 500 years [cf. Mason and Ludwig, 1991]. Laboratory numbers in Mason [1990]. (b). Schematic Cross-section of Kividluk Island, Shishmaref barrier islands. Laboratory numbers in Jordan [1990].



exposed within the basins of deflation hollows (blowouts) which contain ceramics, lithic artifacts, manufacture debitage and, occasionally, bone or charred sea mammal oil-impregnated sand. Though archaeological charcoal provides most of the radiometric (^{14}C) age assignments, samples have also been obtained from purely geological contexts such as airfall tephra and ^{14}C dates on grasses within paleosols and marine shells (Figure 3). At Espenberg, the cultural ($n=32$) and non-cultural ($n=5$) data sets form a concordant chronology with over 37 radiometric dates [Schaaf, 1988; Harritt, 1989, 1990]. For Kividluk, on the Shishmaref barrier islands, ten dates are available, from both archaeological ($n=3$) and geological contexts ($n=7$) [Jordan, 1990].

Depositional units are also defined on the basis of several other criteria, including pedologic and granulometric data, vegetational differences, and the development of blowouts and frost features. Aerial photo interpretation plays an instrumental role in delineating depositional units on the basis of erosional scarps, vegetational and drainage differences. Three series of photos were used: the coastal NOAA series (1:30,000), the standard U-2 false color imagery (1:60,000) and a National Park Service fixed-wing overflight (1:8000).

Soil formation in the youngest dune ridges consists of thin silty laminae deposited at moisture thresholds, with little or no chemical alteration of grains [Soil Survey, 1975]. In older dune ridges, iron-rich sand particles are oxidized and transported down the soil column, forming mottled weathering zones and, in many places, indurated (ferricrete) horizons. The soil chronosequence at Espenberg is well constrained by archaeological ^{14}C dates and provides a supplemental source of paleoclimatic information (see below). In terms of grain size, older, longer stabilized ridges show finer grain populations whereas younger dune ridges are coarser [Mason, 1987, 1990]. With increasing age, peculiarly arctic phenomena appear: frost-cracks form rectangular patterns across ridges over 500 m from the coast and swale ponds are increasingly large in size and polygonal in shape with increasing distance from the sea.

Two types of shore-parallel sand ridges form along the coasts of the Seward Peninsula, each related to a different depositional agency. Low elevation (seldom >2 m asl), flat beach ridges are marine in origin, deposited during fair-weather, post-storm recovery periods [cf. Carter, 1988]. Dunes, up to 20 m high, form as sand from the beach is carried landward by strong winds and is captured by lyme grass (*Elymus* spp.). Dunes are a signature of fall or winter storm conditions. These contrasting depositional landforms occur in discrete locations at Cape Espenberg and the Shishmaref Islands and provide a dichotomy for the following climatic interpretations.

CAPE ESPENBERG BEACH RIDGE PLAIN

Located at the north extreme of Seward Peninsula, the Espenberg beach ridge plain is attached to the mainland at its western limit and extends eastward into Kotzebue Sound as a series of islands and a spit at its eastern extreme. The Espenberg sand ridges are increasingly differentiated to the east, divisible into 20 laterally continuous ridges at its widest, eastern extent. Few individual ridges continue across the entire system—ridges tend to bifurcate or disarticulate into closely related clusters, as expected on a prograding spit.

The horizontal stratigraphy of Cape Espenberg is divided into four depositional units (Figure 3a). Units alternate between low beach ridges and higher dune ridges, corresponding to differences in the degree of storm-related erosion and deposition in post-storm recovery periods. Unit I formed between 3900–3300 B.P., Unit II from 3300–2000 B.P., Unit III between 2000–1200 B.P. and Unit IV from 1200 B.P. to the present.

The onset of Unit I at Cape Espenberg may be estimated by tephra contained within a buried paleosol on the oldest sand ridge. This thinly bedded (<1 cm) distal tephra is provisionally linked [J. Riehle, written communication, 1988] to the Alaska Peninsula Aniakchak eruption, dated to 4000–3000 B.P. [Miller and Smith, 1987; Riehle et al., 1987]. Another independent date from a buried grass layer from the same (E-20) ridge set yielded a date of 3700 ± 90 B.P. (B-23170), provides an additional upper age estimate of 3880–3580 B.P. (using a two sigma range) for the beginning of beach ridge formation at Espenberg. Therefore, the first beach ridges at Espenberg must date from about 4000 years ago.

Low beach ridges of Unit I were welded onto the Pleistocene mainland in the west and atop an emergent shoal between 4000 and 3300 B.P. Sand in Unit I ridges (E-20 to E-15) is intensely oxidized, forming spodosols (i.e., Bw soil horizon) [Soil Survey, 1975]; evidence of a warmer climate [Mason, 1990]. Ephemeral encampments of Arctic Small Tool tradition-related cultures dated to 3570 ± 100 B.P. (B-19643) [Schaaf, 1988:165] and 3750 ± 80 B.P. (B-33758) [Harritt, 1990].

Massive storms about 3300–3000 B.P. scaped and truncated Unit I ridges and led to the formation of Unit II. In the third millennium, 3000–2000 B.P., the net erosional regime associated with large, frequent storms led to the landward translation of dunes over the older beach ridges. Throughout Unit II times, a 1-km-wide tidal inlet remained open between the two islands of the Espenberg system, an indication of the extent of the intensity of storm activity. Numerous settlements of the Choris and Norton cultures allow an upper age assignment for the construction of the prominent dune ridge (E-14)—Unit II—before 2790 ± 80 (B-33759) to 2285 ± 90 (B-17968) B.P. (Figure 3a) [Schaaf, 1988; Harritt, 1990]. Though site loci are common on the ridge, most archaeological manifestations consist of sparse lithic or ceramic scatters often accompanied by charred, sea mammal oil-bound sands. The association of cultural remains with a buried A soil horizon implies that a brief period of warmer and/or wetter conditions occurred in the middle of the third millennium B.P. (see below).

Extensive progradation and inlet closing started at Espenberg after 2000 B.P. with the addition of low, smooth ridges (E-13 to E-6) separated by swales of over 100 m width in Unit III. Few archaeological remains are encountered in these ridges, which account for nearly half of the horizontal accretion at Cape Espenberg. The permafrost table is less than 70 cm from the top of these ridges, a circumstance leading to the development of frost crack and string bogs. Archaeological traces of several Ipiutak culture houses, dating to ca. 1400–1300 B.P. [Harritt, 1989], occur on E-8, a low ridge only 2 m above sea level. Considering the low elevation and the evidence for human occupation, we gain an

appreciation of the infrequency and lessened intensity of massive storms during the period between 2000–1000 B.P.

In Unit IV, high dunes built up to 20 m above sea level during an erosional regime beginning about 1200 B.P. The high dunes of this period choke off several of the cross-cutting channels in the low-lying Unit III ridges. Radiometric determinations from buried archaeological horizons associated with the western Thule and old Kotzebue cultures reveal that dune-building occurred before 800–600 and 300–200 B.P. [Harritt, 1989] or A.D. 1000–1100 and A.D. 1500–1600, in calibrated ages [Mason, 1990]. The seaward aspect of the dunes is eroding, as indicated by a prominent scarp and photogrammetric measurements that 8 to 13 m of retreat occurred from 1949–1976 [Jordan, 1988].

In summary, dune-building activity is concentrated in three periods at Espenberg: (a) 3300–2000 B.P., (b) from 1200–600 B.P., and (c) with lessened intensity from 250 B.P. to the present. Assuming that dune building is correlative with increased storminess, as in the North Sea [Jelgersma et al., 1970; Lamb, 1988] and Australia [Thom, 1978], then the ridges at Espenberg are a proxy climatic indicator. Planar or beach ridge progradation presumably occurred during "fairweather" post-storm recovery conditions dominated by high pressure conditions as in July/August [cf. Carter, 1986]. During the time periods with less intense and longer storm recurrence intervals, beach ridges would be low (0.7–1.0 m asl) and more likely to be preserved. In times with intense storms, beach ridges formed higher in elevation above sea level (1.0–1.7 m asl). During the winter, these higher storm-elevated beach ridges were more susceptible to eolian deflation, forming low dunes and susceptible to further incorporation by growing beach grass during summer [cf. Carter, 1986; Hesp, 1983].

SHISHMAREF BARRIER ISLANDS

The Shishmaref barrier islands, located 50 km updrift from Cape Espenberg, extend for over 125 km and separate Shishmaref Inlet from the Chukchi Sea. The islands are low in elevation and consist of a single, scarped high dune ridge backed by 13–20 low beach ridges or washover flats separated by numerous abandoned surge channels. Descriptions of the sedimentary environments on the Shishmaref barriers can be found in Jordan [1990]. Geological and archaeological radiocarbon dates provide constraints on the history of barrier island development. Morphologic comparison with well-dated deposits at Cape Espenberg allows a relative age estimate to be made for barrier formation.

Chronostratigraphy

Prior to the progradational phase which began at some time after 2000 B.P., the Shishmaref barriers probably were frequently flooded, consisting of washover flats, numerous surge or tide channels, with only limited or episodic sub-aerial exposure. A geologic date of 1550 ± 70 B.P. (β -28183) was obtained from a basal organic peat horizon exposed in a lagoon-margin trench at Kividluk. This date indicates that marsh vegetation had stabilized the local tidal flat or barrier platform surface, and provides a minimum date for the beginning of beach ridge progradation at Kividluk and the barrier islands to the west. A basal date of 1070 ± 80 B.P. (β -28181) on exhumed shoreface peat on the modern beach at Kividluk reveals that nearly 1 km of horizontal

progradation followed in the 500 years after the stabilization of the barrier platform. Thus, slow vertical accretion accompanied relatively rapid horizontal progradation, forming a thin, seaward-thickening wedge of overwash and eolian sand deposited between 1600 and 1000 B.P.

Shoreface erosion, landward migration of transgressive dunes and the transfer of marine sediments through inlets and surge channels characterizes barrier dynamics for the past 1000 years (Figure 3b). Landward retreat of extensive transgressive dune deposits has provided sediments to both offshore and backshore environments. Backbarrier marsh has expanded onto washthrough flats built above the intertidal zone at Kividluk island [cf. Godfrey et al., 1979].

The barrier island archaeological record is abundant for the period from about 500 B.P. to present and is preserved in eolian settings, particularly in transgressive backbeach dunes which provide sufficient topographic relief above the water table. Prehistoric houses are found atop or in the lee of high transgressive dunes, while low-elevation beach ridges contain only prehistoric and historic cache features. Archaeological loci exposed in dune scarps at Kividluk are dated at 470 ± 70 B.P. (β -34772), 290 ± 70 B.P. (β -17958), and 170 ± 70 B.P. (β -17973) [Schaaf, 1988; Jordan, 1990].

The situation on the Shishmaref barrier islands parallels that of Espenberg during the last 2000 years; however, deposits earlier than 2000 B.P. are not known from the barrier islands. Rapid progradation characterizes the barrier island sedimentary regime during the period 1700–1100 B.P. However, at about 1100 B.P. a high dune ridge began to build on the barrier islands and subsequently has migrated landward under the influence of shoreface erosion. The Shishmaref barriers and Espenberg spit contain varying portions of the late Holocene sedimentary record, but both contain similar deposits from the last 2000 years. Differences between the two areas from 4000 to 2000 B.P. reflect variation in sediment sources, current strength and location in the longshore transport system. The Shishmaref barriers may yet provide similar evidence for the transgressive, stormy interval 3300–2000 B.P. in subsurface deposits or evidence of older barrier island deposits may exist as palimpsests offshore.

DISCUSSION: CROSS-CORRELATIONS WITH OTHER NORTH AMERICAN ARCTIC LOCALITIES

The sequence of storm cycles recorded at Cape Espenberg and the Shishmaref barriers correlates with other beach ridge complexes in western Alaska (i.e., Cape Krusenstern, Wales, St. Lawrence Island and Sisualik) and with other proxy climatic records from northwest Alaska (Figure 4). Temporal parallels in erosion and progradation at other northwest Alaska beach ridge complexes are related to the particular trajectories of North Pacific weather systems and the resultant effects on waves and longshore transport on the nearshore zone of western Alaska [Mason, 1990; Mason and Ludwig, 1991]. Ultimately, the patterns of precipitation leading to glacial expansion and alluvial floods are also linked to the same synoptic patterns.

Progradational regimes at northwest Alaska beach ridge complexes reflect warmer mid-summer climatic conditions from 4000–3000 and 2000–1200 B.P. In the former case, paleosols or stable surfaces dated to 4000–3750 B.P. are reported from isolated localities across northern Alaska and

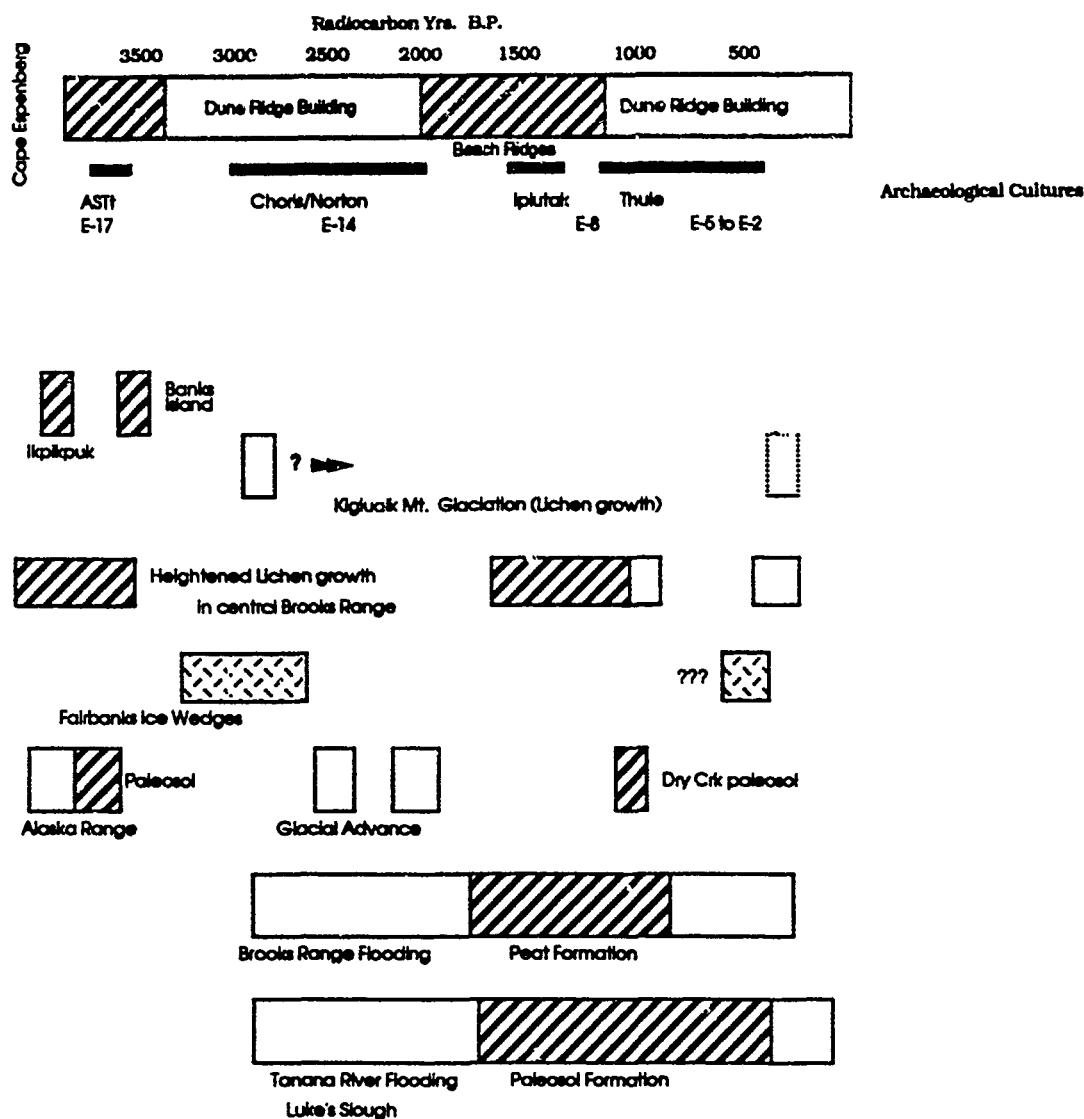


Figure 4. Cross-correlations between Alaskan beach ridges and other proxy climatic records from Alaska and Canada. References in text. Radiocarbon dates from Bering Sea box cores and Yukon Delta cheniers are not discussed in text, cf. discussion in Mason [1990].

northwest Canada, including the Ikpiupuk River southeast of Barrow [Rickert and Tedrow, 1967], on Banks Island [Pissart et al., 1977], at Cape Denbigh in Norton Sound [Giddings, 1964] and in the Nenana River valley south of Fairbanks [Thorson and Hamilton, 1977; Powers and Hoffecker, 1989]. Heightened pollen production ca. 4000 B.P. also indicate the occurrence of warmer summer and/or autumn temperatures in northern Alaska [Brubaker et al., 1983]. At the Alaskan North Slope locality of Kuparuk River section, pollen production peaks after 3500 B.P. but declines 2700 to 2500 B.P. [Walker et al., 1981:165].

Dune growth occurs from 3300–2000 B.P. and episodically during the last 1000 years, during a net erosional regime along the shoreline of Seward Peninsula. Other beach ridge complexes (Cape Krusenstern, Wales, Sisualik) in northwest Alaska also undergo net erosional conditions 3300–2000 years ago and 1200 years to the present [Mason, 1990]. Stormy, erosional regimes on the coasts are tied to increased precipitation and, hence, glacial expansion in the

Kigluak Mountains on the south Seward Peninsula [Calkin, 1988, written communication] and across Alaska [Calkin, 1988]. Eolian sand deposition along the Kuparuk River (near Prudhoe Bay) is due to a colder climatic interval [Walker et al., 1981]. Widespread alluviation associated with glacial expansion occurred in the Brooks Range during 3000–2000 B.P. [Hamilton, 1981] and along the Tanana River [Mason and Begét, 1990] in concert with glacial expansion in the Alaska Range [Ten Brink, 1983]. In addition, Hamilton et al. [1983] report that ice wedges formed in central Alaska about 3500 to 3000 years ago, reflecting cooler temperatures.

The stormier conditions of the third millennium B.P. at Espenberg correlate with the Neoglacial event, as defined by world-wide glacial expansions [Porter and Denton, 1967; Porter, 1986; Röthlisberger, 1988] and the 2500-year B.P. cold climatic event in the Camp Century ice core [Dansgaard et al., 1984]. The width of Unit II is about 75% less than the younger dune ridges in Unit IV and may provide a

relative measure of storm recurrence intervals in the third millennium B.P., i.e., larger storms probably occurred in more rapid succession, as compared to the last 1000 years.

The buried soil dated at 2800–2500 B.P. on the Unit II ridges is evidence of increased precipitation or of a temporary pause in the general trend of climatic cooling. Quite significantly, the record of Espenberg paleosols correlates well with Sorenson and Knox's [1974] reconstruction for the late Holocene displacement of the forest/tundra boundary in north-central Canada, which shows northern advances of treeline (and paleosols) at 3500 and 1600–1100 B.P., with a slight advance at 2600–2200 B.P. and a southward retreat at 2900, 1800 and 800 B.P.

The Espenberg paleosol record reflects a particular combination of climatic and ecological factors. The primary signal is one of stabilized, shrub vegetation and the absence of grasses and appreciable eolian deposition, which indicates the prevalence of increased precipitation coupled with weaker winds. The stabilized surfaces occur during the stormy, cold intervals of Units II and IV, implying that short-term decreases in wind and/or storm intensity punctuated these otherwise stormy periods.

The period between 2000–1000 B.P. contains almost half of the progradation at Espenberg and correlates with a similar progradational regime on the Shishmaref barrier islands 1500–1000 years ago [Jordan, 1989, 1990]. Peat formation atop alluvial terraces is widespread between 2000–1000 B.P. in north-central Alaska [Hamilton, 1981] and Seward Peninsula [Kaufman et al., 1989]. In the White Mountains, near the Yukon Territory, Denton and Karlén [1977] report

that treeline expanded to higher altitudes during a warmer period between 2200–1200 B.P.

For the last 1000 years the sedimentary record of the Seward Peninsula coast may be compared with historic records from China because similar weather phenomena affect both east Asia and Bering Strait. Mason [1990] proposes that dune formation at Cape Espenberg is linked to synoptic phenomena in Siberia which produce anomalous winter thunderstorms and dust storms in Beijing, both of which indicate colder conditions. The onset of cold conditions at Espenberg around 1200–1000 B.P. parallels the evidence presented by Porter [1986] for glacial expansions throughout the northern hemisphere. Thus, the proxy climatic record from Alaskan beach ridges corresponds closely with historic records from both east Asia and Europe, providing a means with which to reconstruct paleoclimate in a region lacking meteorological records prior to A.D. 1800.

ACKNOWLEDGMENTS

We thank the National Park Service and the University of Alaska Geist Fund for monies to field our studies, radio-carbon date samples and obtain aerial photographs. In addition, we both benefited from participation in archaeological surveys conducted by the NPS. The unstinting support of Dr. D. M. Hopkins was instrumental in completing our research. Jeanne Schaaf and Dr. Roger Harritt of the NPS played a critical role in furthering our research. Field and lab assistance by Stefanie Ludwig, Dale Vinson and Mark Moore are also greatly appreciated.

LITERATURE CITED

- Brubaker, L. B., H. L. Garfinkel, and M. E. Edwards, Late Wisconsin and Holocene vegetation change in the Walker Lake/Alatna valley region of the Brooks Range, *Quat. Res.*, 20, 194–214, 1983.
- Calkin, P., Holocene glaciation of Alaska (and adjoining Yukon Territory, Canada), *Quat. Sci. Rev.*, 7, 159–184, 1988.
- Carter, R. W. G., The morphodynamics of beach-ridge formation: Magilligan, northern Ireland, *Marine Geol.*, 73, 191–213, 1986.
- Carter, R. W. G., *Coastal Environments*, Academic Press, New York, 1988.
- Curray, J. R., Transgressions and regressions, in *Papers in Marine Geology*, edited by R. L. Miller, pp. 175–203, MacMillan, New York, 1964.
- Dansgaard, W., S. J. Johnsen, H. B. Clausen, D. Dahl-Jensen, N. Gundestrup, and C. U. Hammer, North Atlantic climatic oscillations revealed by deep Greenland ice cores, *Am. Geophys. Union Monogr.* 29, 288–298, 1984.
- Denton, G. H. and W. Karlén, Holocene glacial and tree-line variations in White River and Skolai Pass, Alaska and Yukon Territory, *Quat. Res.*, 7, 61–111, 1977.
- Eitrem, S., A. Grantz, and O. T. Whitney, Tectonic imprints on sedimentary deposits in Hope basin, in *The U.S. Geological Survey in Alaska: Accomplishments during 1976*, edited by K. M. Blean, pp. 100–103, *United States Geological Survey Circular 751-B*, 1977.
- Giddings, J. L., *The Archaeology of Cape Denbigh*, Brown University Press, Providence, 1964.
- Giddings, J. L., Cross-dating the archeology of northwestern Alaska, *Science*, 153, 127–135, 1966.
- Giddings, J. L., and D. D. Andersen, Beach Ridge Archaeology of Cape Krusenstern: Eskimo and pre-Eskimo settlements around Kotzebue Sound, *Publications in Archaeology No. 20*, National Park Service, Washington, 1986.
- Godfrey, P. J., S. F. Leatherman, and R. Zaremba, A geobotanical approach to classification of barrier beach systems, in *Barrier Islands from the Gulf of St. Lawrence to the Gulf of Mexico*, edited by S. P. Leatherman, pp. 99–126, Academic Press, New York, 1979.
- Hamilton, T. D., Episodic Holocene alluviation in the central Brooks Range: chronology, correlations and climatic implications, In *U.S. Geological Survey in Alaska, Accomplishments during 1979*, edited by N. R. D. Albert and T. Hudson, pp. 21–24, *U.S. Geological Survey Circ. 823-b*, 1981.
- Hamilton, T. D., T. A. Ager, and S. W. Robinson, Late Holocene ice wedges near Fairbanks, Alaska, U.S.A.: Environmental setting and history of growth, *Arctic and Alpine Research*, 15, 157–168, 1983.
- Harritt, R. K., Recent archaeology in Bering Land Bridge National Preserve: the 1988 Field season at Cape Espenberg, paper presented at 16th annual meeting, Alaska Anthropological Assoc., Anchorage, March 3–4, 1989.
- Harritt, R. K., Recent archaeology in Bering Land Bridge National Preserve: the 1989 Field season at Cape Espenberg and in the Ikpek area, paper presented at 17th annual meeting, Alaska Anthropological Association, Fairbanks, March 9–10, 1990.

- Hayes, M. O., Barrier island morphology as a function of tidal and wave regime, in *Barrier Islands from the Gulf of St. Lawrence to the Gulf of Mexico*, edited by S. P. Leatherman, pp. 1-29, Academic Press, New York, 1979.
- Hesp, P. A., Morphology, dynamics and internal stratification of some established foredunes in southeast Australia, *Sedimentary Geol.*, 55, 17-41, 1988.
- Hopkins, D. M., Quaternary marine transgressions in Alaska, in *The Bering Land Bridge*, edited by D. M. Hopkins, pp. 47-90, Stanford University Press, Stanford, CA, 1967.
- Hume, J. D., Sea level changes during the last 2000 years at Point Barrow, Alaska, *Science*, 150, 1165-1166, 1965.
- Hume, J. D., and M. Schalk, Shoreline processes near Barrow, Alaska: A comparison of the normal and the catastrophic, *Arctic*, 20, 86-103, 1967.
- Jelgersma, S., J. de Jong, W. H. Zagwijn, and J. F. van Regteren Altena, The coastal dunes of western Netherlands: geology, vegetational history and archeology, *Mededelingen Rijks Geologische Dienst. Nieuwe Ser.*, 21, 93-167, 1970.
- Jordan, J. W., Erosion characteristics and retreat rates along the north coast of Seward Peninsula, in *Bering Land Bridge National Preserve: An Archaeological Survey*, edited by J. Schaaf, pp. 322-362, National Park Service, Alaska Region, *Res. Management Rep. No. 14*, 1988.
- Jordan, J. W., Late Holocene evolution of barrier islands in the southern Chukchi Sea, Alaska, Unpublished Master's Thesis, Quaternary Studies, University of Alaska, Fairbanks, 1990.
- Kaufman, D. S., P. E. Calkin, W. B. Whitford, B. J. Przybyl, D. M. Hopkins, B. J. Peck, and R. E. Nelson, Surficial geologic map of the Kigluaik Mountains Area, Seward Peninsula, Alaska, *United States Geological Survey Miscellaneous Field Studies Map MF-2074*, 1989.
- Komar, P. D., *Beach Processes and Sedimentation*, Prentice-Hall, Englewood Cliffs, NJ, 1976.
- Kraft, J. C., and M. J. Chrastowski, Coastal stratigraphic sequences, in *Coastal Sedimentary Environments*, edited by R. A. Davis, pp. 625-664, Springer Verlag, New York, 1985.
- La Belle, J. C., J. L. Wise, R. P. Voelker, R. H. Schulze, and G. M. Wohl, *Alaska Marine Ice Atlas*, Arctic Environmental Information and Data Center, Univ. of Alaska, Anchorage, 1983.
- Lamb, H. H., Climate in historical times and transgressions of the sea, storm floods and other coastal changes, in *Weather, Climate and Human Affairs*, edited by H. H. Lamb, pp. 78-103, Routledge, London, 1988.
- Mason, O. K., The Sedimentology and Relative Dating of the Sand Ridge Complexes of the northern Seward Peninsula, Bering Land Bridge National Preserve, *Final Report to National Park Service*, Alaska Regional Office, Anchorage, 1987.
- Mason, O. K., Beach ridge geomorphology of Kotzebue Sound: Implications for paleoclimatology and archaeology, Unpublished Ph.D. Dissertation, Quaternary Science, University of Alaska Fairbanks, 1990.
- Mason, O. K., and J. E. Begét, Late Holocene changes in flood frequency at the Tanana River, Alaska, paper presented at the 17th annual meeting of the Alaska Anthropological Association, 1990.
- Mason, O. K., and S. L. Ludwig, Resurrecting Beach Ridge Archaeology: Parallel Depositional Histories from St. Lawrence Island and Cape Krusenstern, Alaska, *Geoarchaeology*, 1991, In press.
- McManus, D. A., J. S. Creager, R. J. Echols, and M. L. Holmes, The Holocene transgression on the Arctic flank of Beringia: Chukchi valley to Chukchi estuary to Chukchi Sea, in *Quaternary Coastlines and Marine Archaeology: Towards a Prehistory of Landbridges and Continents*, edited by P. M. Masters and N. C. Fleming, pp. 365-388, Academic Press, New York, 1983.
- Miller, T. P., and R. L. Smith, Late Quaternary caldera-forming eruptions in the eastern Aleutian arc, Alaska, *Geology*, 15, 434-438, 1987.
- Moore, G. W., Recent eustatic sea-level fluctuations recorded by Arctic beach ridges. Geological Survey Research 1960, *U.S. Geological Survey Professional Paper 400 B335-7*, 1960.
- Moore, G. W., Arctic beach sedimentation, in *Environment of the Cape Thompson Region, Alaska*, edited by N. Wilimovsky and J. N. Wolfe, pp. 587-608, Atomic Energy Commission, Oak Ridge, TN, 1966.
- Moore, G. W., and J. L. Giddings, Record of 5000 years of Arctic wind direction recorded by Alaskan beach ridges. Abstract. *Special U.S. Geological Soc. Papers*, 68, 1961.
- Peratrovich & Nottingham, Inc., *Shishmaref Erosion Control Engineering Studies*, State of Alaska, Dept. of Transportation and Public Facilities, Anchorage, 1982.
- Péwé, T. L., Quaternary geology of Alaska, *United States Geological Survey Professional Paper 835*, 1975.
- Péwé, T. L., and R. E. Church, Age of the spit at Barrow, Alaska, *Bull. Geol. Soc. Am.*, 73, 1287-1291, 1962.
- Pissart, A., J. S. Vincent, and S. A. Edlund, Dépôts et phénomènes éoliens sur l'île de Banks, Territoires du Nord-Ouest, Canada, *Can. J. Earth Sci.*, 14, 2462-2480, 1977.
- Porter, S. C., Pattern and forcing of Northern Hemisphere glacier variations during the Last Millennium, *Quat. Res.*, 26, 27-48, 1986.
- Porter, S. C., and G. H. Denton, Chronology of Neoglaciation in the North American Cordillera, *Am. J. Sci.*, 255, 177-210, 1967.
- Powers, W. R., and J. F. Hoffecker, Late Pleistocene settlement in the Nenana valley, central Alaska, *American Antiquity*, 54, 263-287, 1989.
- Pye, K., Models of transgressive coastal dune building episodes and their relationship to Quaternary sea level changes: a discussion with reference to evidence from eastern Australia, in *Coastal Research: UK Perspectives*, edited by M. W. Clark, pp. 81-104, Geo-Books, Cambridge, 1984.
- Rickert, D. A., and J. C. F. Tedrow, Pedologic investigations on some aeolian deposits of northern Alaska, *Soil Science*, 104, 250-262, 1967.
- Riehle, J. R., C. E. Meyer, T. A. Ager, D. S. Kaufman, and R. E. Ackerman, The Aniakchak tephra deposit, a late Holocene marker horizon in Alaska, in *Geologic Studies in Alaska 1986*, edited by T. D. Hamilton and J. P. Galloway, pp. 19-24, *U.S. Geological Survey Circular 998*, 1987.
- Röthlisberger, F., *10 000 Jahre Gletschergeschichte der Erde*, Verlag Sauerländer, Aarau, 1986.

- Schaaf, J., The Bering land bridge: An archaeological survey, National Park Service, Alaska Region, *Resources Management Report No. 14*, Anchorage, Alaska, 1988.
- Sharma, G. D., *The Alaskan Shelf*, Springer-Verlag, New York, 1979.
- Soil Survey Staff, Soil taxonomy, *Agriculture Handbook No. 436*, U.S. Dept. of Agriculture, Washington, DC, 1975.
- Sorenson, C. S., and J. C. Knox, Paleosols and paleoclimates related to late Holocene forest/tundra border migrations: Mackenzie and Keewatin, N.W.T., Canada, in *International conference on Prehistory and Paleoecology of western North American Arctic and Subarctic*, pp. 187-203, Archaeological Association, Univ. of Calgary, Calgary, 1974.
- Ten Brink, N. W., Glaciation of the northern Alaska Range, in *Glaciation in Alaska*, R. M. Thorson and T. D. Hamilton, pp. 82-91, Alaska Quaternary Center, *Univ. of Alaska Museum Occasional Paper No. 2*, 1983.
- Thom, B. G., Coastal sand deposition in southeast Australia during the Holocene, in *Landform Evolution in Australasia*, edited by J. L. Davies and M. A. J. Williams, pp. 197-214, Australian National University Press, Canberra, 1978.
- Thorson, R. M., and T. D. Hamilton, Geology of the Dry Creek Site: a stratified early Man site in interior Alaska, *Quat. Res.*, 7, 149-176, 1977.
- Walker, D. A., S. K. Short, J. T. Andrews, and P. J. Weber, Late Holocene pollen and present day vegetation, Prudhoe Bay and Atigun River, Alaskan North Slope, *Arctic and Alpine Research*, 13, 153-172, 1981.



92-17858



Holocene Loess and Paleosols in Central Alaska: A Proxy Record of Holocene Climate Change

N. H. Bigelow

Dept. of Anthropology, University of Alaska Fairbanks, Fairbanks Alaska, U.S.A.

J. E. Begét

Dept. of Geology and Geophysics, University of Alaska Fairbanks, Fairbanks, Alaska, U.S.A.

ABSTRACT

Episodic Holocene loess deposition and soil formation in the sediments of the Nenana valley of Central Alaska may reflect Holocene climate change. Periods of loess deposition seem to correlate with times of alpine glacier activity, while paleosols correspond to times of glacial retreat. These variations may reflect changes in solar activity [Stuiver and Braziunas, 1989]. Other mechanisms, such as orbitally forced changes in seasonality, volcanism, and atmospheric CO₂ variability may also have affected Holocene climates and loess deposition.

INTRODUCTION

Eolian sediments can be sensitive records of climate change [Kukla et al., 1988; Bigelow et al., 1990]. In the Nenana valley, approximately 150–180 km south of Fairbanks, Alaska, a 2-m-thick deposit of sandy loess and loess is present on Pleistocene glacial outwash terraces. Several paleosols in the loess have been radiocarbon dated at the Dry Creek archaeological site (Figure 1). The repeated episodes of paleosol formation and the broad similarity of the Dry Creek stratigraphy to other localities in the Nenana valley indicate that these deposits reflect regional changes in depositional environment. As a result, we suggest the chronology of the loess and its paleosols provides clues to Holocene climates in the Nenana valley.

DRY CREEK EOLIAN STRATIGRAPHY AND CHRONOLOGY

The Dry Creek archaeological site is located at the bluff edge of an early Wisconsin or late Illinoian glacial outwash terrace. The stratigraphy at this site is broadly similar to other archaeological sites in the Nenana and Teklanika valleys, such as Walker Road [Powers and Hoffecker, 1989], Panguingue Creek [Maxwell, 1987], and Owl Ridge [Phippen, 1988] (Figure 1). At Dry Creek, unweathered loess directly overlies outwash gravel; a radiocarbon date of $11,120 \pm 85$ was obtained on hearth charcoal in Loess 2 about 30 cm above the gravel (Table 1 and Figure 2). A

second radiocarbon date of $10,690 \pm 250$, also on cultural charcoal, was collected about 60 cm above the gravel, near the base of Loess 3. A weakly developed paleosol (Paleosol 1), consisting of several discontinuous organic stringers, is located within Loess 3. A sandy loess (Sand 1) separates Loess 2 and Loess 3 and thus was deposited between about 11,100 and 10,700 radiocarbon years ago (Figure 2).

At the contact between Loess 3 and Loess 4 lies a thick, organic, contorted paleosol (Paleosol 2). Four dates on this soil range between $23,930 \pm 9300$ and 7985 ± 105 (Table 1, Figure 2). Two dates (12,080 years and 23,930 years) have large standard deviations (>1000 years), and have possibly been contaminated by older material. The large standard deviation is due to small sample sizes, and pretreatment may have concentrated any lignitic contaminants present in the sample. Lignite is not present at the site, although extensive coal-bearing formations outcrop along the east side of the Nenana river, less than 7 km away [Thorson and Hamilton, 1977]. The two younger dates (9340 ± 195 and 7985 ± 105) are probably closer to the true age of the paleosol. The paleosol may have formed during the entire interval, although the 7985-year date came from a nearby test pit, and the exact correlation with the main section is not certain [Thorson and Hamilton, 1977].

Loess 4 is an unweathered deposit covering Paleosol 2. Loess 5 directly overlies Loess 4 and includes a paleosol with numerous organic stringers (Paleosol 3). This paleosol

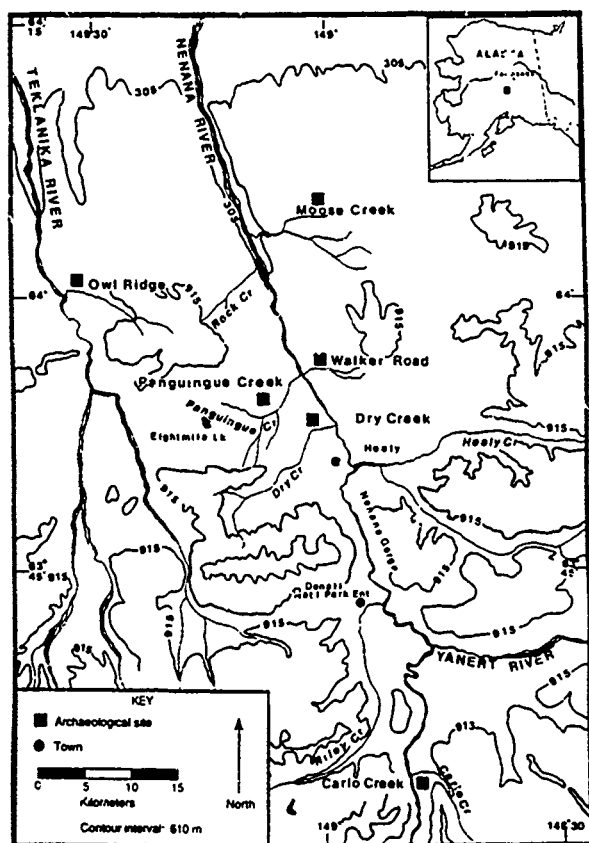


Figure 1. Location of the Dry Creek site and other archaeological sites in the Nenana and Teklanika valleys, north-central Alaska Range.

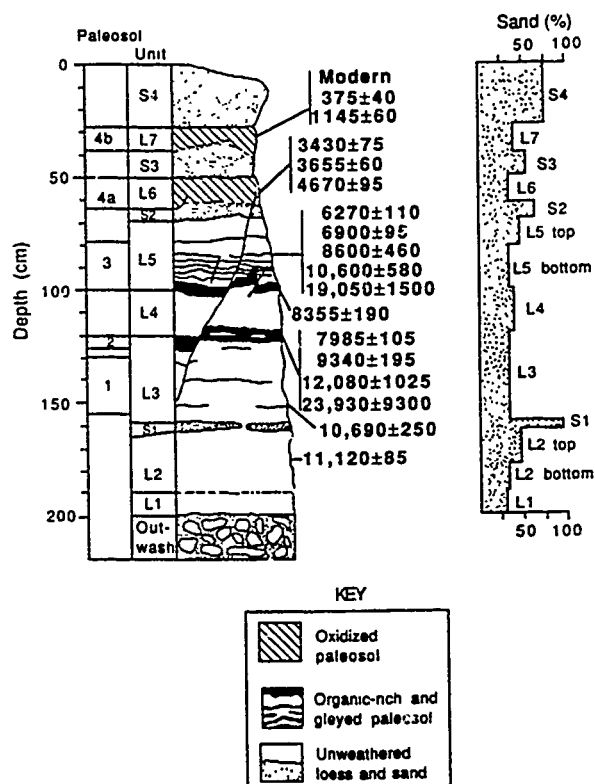


Figure 2. Generalized stratigraphy of the Dry Creek site and provenience of ^{14}C dates (after Thorson and Hamilton [1977]).

Lab No.	^{14}C Age	Material	Provenience	Comments
SI-1933B	Modern	Charcoal	Paleosol 4b	Buried A horizon
SI-2333	375 ± 40	Peat and roots	Paleosol 4b	Buried A horizon
SI-2332	1145 ± 60	Charcoal	Paleosol 4b	Buried A horizon
SI-1934	3430 ± 75	Charcoal	Paleosol 4a	Predates soil formation
SI-1937	3655 ± 60	Charcoal	Paleosol 4a	Predates soil formation
SI-2331	4670 ± 95	Charcoal	Paleosol 4a	Predates soil formation
SI-1935C	6270 ± 110	Charcoal	Paleosol 3	
SI-1935B	6900 ± 95	Charcoal	Paleosol 3	
SI-2115	8355 ± 190	Charcoal	Paleosol 3	
SI-1935A	8600 ± 460	Charcoal	Paleosol 3	
SI-1544	$10,600 \pm 580$	Charcoal	Paleosol 3	Coal contamination?
SI-2328	$19,050 \pm 1500$	Charcoal	Paleosol 3	Coal contamination?
SI-2329	7985 ± 105	Charcoal	Paleosol 2?	Correlation not clear
SI-1936	9340 ± 195	Charcoal	Paleosol 2	
SI-1938	$12,080 \pm 1025$	Charcoal	Paleosol 2	Coal contamination?
SI-1561	$23,930 \pm 9300$	Charcoal	Paleosol 2	Coal contamination?
SI-2880	$10,690 \pm 250$	Charcoal	Paleosol 1	
	$11,120 \pm 85$	Charcoal	Loess 2	

Table 1. Complete radiocarbon date list from the Dry Creek site (after Thorson and Hamilton [1977], Table 4).

consists of a 5-cm-thick organic band at the bottom, and several superposed thin organic bands. The total thickness of Paleosol 3 is almost 20 cm. A single radiocarbon date of 8355 ± 190 was obtained from the lower organic band and a series of five dates were collected from the upper organic bands. These dates range between $19,050 \pm 1500$ and 6270 ± 110 . Two dates ($19,050$ years and $10,600$ years) have large standard deviations (>580 years) and may be affected by the same problems as the anomalous dates for Paleosol 2. The remainder of the dates lie between 8600 and 6270 years ago, and appear to define the general time period of soil formation [Thorson and Hamilton, 1977].

Two additional paleosols (Paleosols 4a and 4b) occur near the top of the section. Both are oxidized horizons, and are separated and capped by unweathered sandy loess (Sands 3 and 4). The dates from the lower paleosol (4a) range between 4670 and 3430 years ago (Table 1). Dates on the upper paleosol (4b) range between 1125 years ago and modern times. The dates from both paleosols are on charcoal from forest fire events, but those from the upper paleosol are on charcoal from the top of the soil horizon while those from the lower paleosol come from within the oxidized horizon.

DOES LOESS CONTAIN A PROXY RECORD OF HOLOCENE CLIMATE CHANGES?

The sequence of loess horizons and paleosols at sites along the Nenana River may reflect changes in regional environments due to climate variability, with paleosols forming during mild, warm intervals while loess was deposited during windier, cold intervals [Bigelow et al., 1990]. The late Pleistocene loess lacks paleosols, while the thick organic Paleosol 2 and Paleosol 3 were developed during the early Holocene, an interval thought to be warmer than today. No sandy loess is found in the early Holocene sediments, but the upper parts of the loess section may record a return to windier and colder conditions associated with the

Neoglacial and the Little Ice Age, as shown by the deposition of Sands 2, 3, and 4 at the top of the eolian section.

The loess and paleosol sequence at Dry Creek can be compared with other Holocene proxy climatic records. Figure 3 suggests similarities between the Dry Creek eolian stratigraphy and Holocene glacial records. The Holocene glacial records are based on the generalized curves of Denton and Karlén [1973] and Røthlisberger [1986], derived from a global synthesis of alpine glacier histories. Also shown is a stable isotope record of high latitude northern hemisphere changes from Greenland Camp Century ice core, which has previously been suggested to resemble the Denton and Karlén record. The Camp Century ^{18}O curve is presented in raw and filtered versions [Dansgaard, 1984]. Also shown is a proxy record of solar intensity based on variations in radiocarbon production [Stuiver and Braziunas, 1989]. Times of paleosol formation in the Nenana River valley appear to be broadly similar to intervals of climatic amelioration approximately 8000 to 6000 calendar years ago, 5000 to 3500 calendar years ago, and 2000 to 1000 calendar years ago. In addition, the periods of loess deposition in the Nenana Valley are similar to those of glacier expansion and cooling as recorded in the other proxy climate records.

A coherence between the solar activity record, alpine glacial histories, and stable isotope changes has previously been suggested [Fisher, 1982; Wigley, 1988; Berger, 1990; Wigley and Kelly, 1990]. Similarities between the loess and paleosol sequence in the Nenana River valley and other proxy climate records suggest that, in some cases, loess can preserve a useful record of climate change.

Although the broad features of the loess sequence appear to be influenced by climate, it is premature to attempt precise correlations of the fine structure of loess sequences with other climate records. Many problems affect interpretations of proxy climate reconstructions, which require caution in making correlations. For instance, Wigley [1988] and Wigley and Kelly [1990] compared the global glacial record constructed by Røthlisberger [1986] with the solar intensity record derived from the ^{14}C data of Stuiver et al. [1986] and noted that the correspondence of a proxy solar record and climatic minima is significant at the 5% level. However, Stuiver et al. [1991] compared the Røthlisberger glacial records with the production rate of ^{14}C and concluded that correlation coefficients between ^{14}C production and the glacial records "do not support a statistically significant relationship between the regional climate and the ^{14}C time series" [Stuiver et al., 1991, p. 20].

HOLOCENE CLIMATE FORCING MECHANISMS

The broad similarities between the loess record in Alaska and Holocene proxy climate records from other areas suggest that some climate changes have been global in extent. There are several possible mechanisms which can produce a widespread terrestrial response. These include processes like orbitally forced insolation changes, short-term solar variability, changes in atmospheric Greenhouse gas concentrations, and volcanic eruptions which produced widespread aerosols, among others. The recognition of coherence between proxy climate records and the history of climatic forcing for any particular mechanism is a necessary, if not sufficient, requirement for demonstrating the importance of

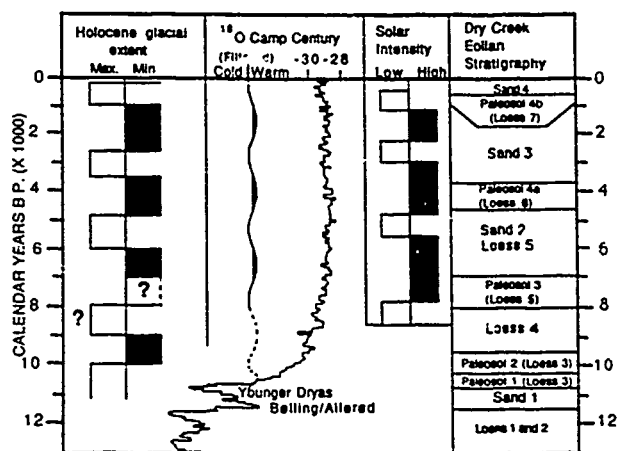


Figure 3. Comparison of global Holocene glacial extent (after Denton and Karlén [1977]; Røthlisberger [1986]), the Camp Century ^{18}O record (after Dansgaard et al. [1984]), variations in solar intensity (after Stuiver and Braziunas [1989]), and the Dry Creek eolian stratigraphy (after Thorson and Hamilton [1977]). Note: radiocarbon dates beyond about 9000 years B.P. can only be estimated in calendar years. Recent work in Barbados suggests $11,000$ years B.P. equals $13,000$ cal. B.P. [Fairbanks, 1990].

any mechanism to climate change. We only discuss several possible climate forcing mechanisms in the light of the proxy record of climate change contained in Alaskan loess.

Orbitally forced changes in seasonality can explain climatic change on the scale of 10^3 – 10^6 years, but cannot explain the short-term changes recognized in the different proxy climatic records. The well-developed early Holocene paleosols preserved in the Nenana valley loess record may reflect an early Holocene warm interval produced by the orbitally controlled maximum of summer temperatures. However, other features of this record, i.e., repeated transitions between loess and paleosols, and changes in sediment texture occur too rapidly to be explained by this mechanism alone.

Berger [1990] has suggested that the short-term solar fluctuations are responsible for global Holocene climate changes. Cosmogenic ^{14}C has varied during the Holocene, probably due to changes in the solar constant [Stuiver and Quay, 1980; Stuiver and Braziunas, 1989]. Relatively high amounts of atmospheric ^{14}C are correlated with the Maunder and Spörer minima, times of low sunspot frequency and low solar intensity [Eddy, 1976, 1977]. The Maunder and Spörer minima (A.D. 1645–1715 and A.D. 1460–1550, respectively) coincide with the Little Ice Age [Eddy, 1976, 1977; Fisher, 1982], suggesting a quiet sun results in lower insolation and, in some cases, glacial advance.

Stuiver and Braziunas [1989] have identified four periods during the Holocene where residence time was anomalously high, suggesting solar activity was low. These oscillations often occurred as triplets of at least two Maunder and Spörer anomalies. These triplets (T1–T4, respectively) are dated 6480–5800 B.C., 3420–2740 B.C., 880–200 B.C., and A.D. 920–1600 (the Little Ice Age). For the purposes of this paper, the ages of the triplets were changed to calendar year B.P. (cal. B.P., years before 1950), so the triple oscillations occurred 8430–7750 cal. B.P., 5370–4690 cal. B.P., 2830–2150 cal. B.P., and 1030–350 cal. B.P. At the Dry Creek site, these periods generally correlate with the deposition of unweathered loess (Figures 3 and 4).

In order to compare times of soil formation at Dry Creek

with the proxy solar record, the Dry Creek radiocarbon dates were calibrated using the computer calibration program from the University of Washington Quaternary Isotope Lab [Stuiver and Reimer, 1986]. Only those dates regarded as accurate (discussed above) were included in the calibration. In instances where one paleosol has several radiocarbon dates, the dates were averaged prior to the calibration. The range of radiocarbon dates on a paleosol could reflect the actual soil-forming interval, although factors such as mean residence time and contamination complicate the interpretation. The 2-sigma range of the calibrated radiocarbon dates are presented in Table 2. Paleosol 3 apparently formed during 7900–7600 cal. B.P., Paleosol 4a between 4400–4000 cal. B.P., and Paleosol 4b about 670–540 cal. B.P.

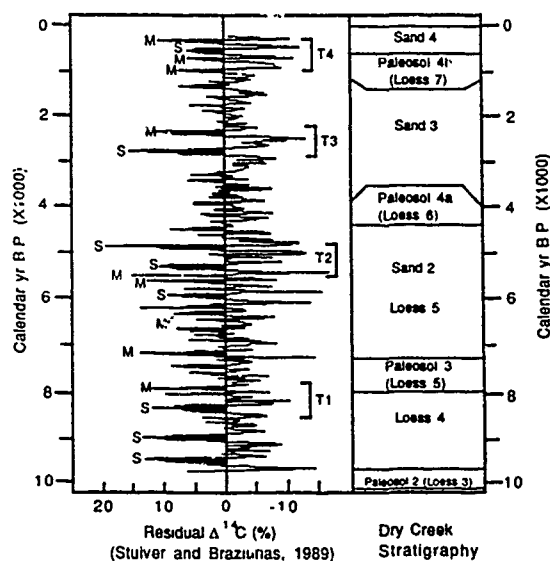


Figure 4. Residual $\Delta^{14}\text{C}$ (after Stuiver and Braziunas [1989]) and the Dry Creek depositional and weathering sequence. M and S are Maunder and Spörer-type anomalies; T1–T4 are periods of triple oscillations.

Lab No.	^{14}C Age	Average*	No. Intercepts	Calibrated* Range B.P. (2 sigma)	Provenience
SI-1933B	375 ± 40				Paleosol 4b
SI-2333	1145 ± 60	612 ± 30	3	667–544	Paleosol 4b
SI-2332	3430 ± 75				Paleosol 4a
SI-1934	3655 ± 60				Paleosol 4a
SI-1937	4670 ± 95	3783 ± 40	1	4400–3995	Paleosol 4a
SI-2331	6270 ± 110				Paleosol 3
SI-1935C	6900 ± 95				Paleosol 3
SI-1935B	8355 ± 190				Paleosol 3
SI-2115	8600 ± 460	6884 ± 70	1	7902–7579	Paleosol 3

Table 2. Dry Creek radiocarbon dates calibrated [Stuiver and Reimer, 1986] to calendar years before 1950. *Calibrated and averaged using University of Washington Quaternary Isotope Lab's computer calibration program 1987, rev. 1.3 [Stuiver and Reimer, 1986].

After calibrating the available radiocarbon dates on the Dry Creek paleosols, the apparent soil-forming intervals seem to broadly fall between the times of triple oscillations (Figure 4), although Paleosols 3 and 4b overlap with Triplets 1 and 4.

Although the proxy climate record from loess and the proxy solar record of Stuiver and Braziunas [1989] show some agreement, there are important differences in the timing and duration of events. Although Berger [1990] has argued that the short-term solar intensity variations of Stuiver and Braziunas must have strongly influenced Holocene climates, it is likely that other mechanisms modulated its effects. Other important sources of climatic forcing during the Holocene may have been changes in the concentra-

tion of atmospheric Greenhouse gases [Hansen and Lacis, 1990], and large volcanic eruptions [Vogel et al., 1990; Begét et al., 1991], although detailed Holocene records of these forcing mechanisms are not well known. It is also possible that there are other important mechanisms not considered here.

ACKNOWLEDGMENTS

We acknowledge discussions about the Nenana Valley sequence with Dr. Roger Powers, Dr. David Hopkins, Dr. Robert Thorson, and Dr. Thomas Hamilton. We are also grateful for careful reviews of this manuscript by Dr. George Kukla and Dr. Richard Reger.

REFERENCES

- Begét, J., O. Mason, and P. Anderson, Age and extent of the ca. 3400 BP Aniakchak tephra, western Alaska, *The Holocene*, 1, 1991, In press.
- Berger, R., Relevance of medieval, Egyptian and American dates to the study of climatic and radiocarbon variability, *Phil. Trans. R. Soc. Lond. A*, 330, 517-527, 1990.
- Bigelow, N. H., J. Begét, and W. R. Powers, Latest Pleistocene increase in wind intensity recorded in eolian sediments from central Alaska, *Quat. Res.*, 34, 160-168, 1990.
- Dansgaard, W., S. J. Johnsen, J. B. Clausen, and C. C. Langway, Jr., North Atlantic climatic oscillations revealed by deep Greenland ice cores, in *Climate Processes and Climate Sensitivity*, edited by J. E. Hansen and T. Takahashi, pp. 288-298, Geophysical Monograph 29, American Geophysical Union, Washington, DC, 1984.
- Denton, G. H., and W. Karlén, Holocene climatic variations—their pattern and possible cause, *Quat. Res.*, 3, 155-205, 1973.
- Eddy, J. A., The Maunder minimum, *Science*, 192, 1189-1202, 1976.
- Eddy, J. A., Climate and the changing sun, *Climatic Change*, 1, 173-190, 1977.
- Fairbanks, R. G., The age and origin of the "Younger Dryas Climate Event" in Greenland ice cores, *Paleoceanography*, 5, 937-948, 1990.
- Fisher, D. A., Carbon-14 production compared to oxygen isotope records from Camp Century, Greenland and Devon Island, Canada, *Climatic Change*, 4, 419-426, 1982.
- Hansen, J. E., and A. A. Lacis, Sun and dust versus greenhouse gases: an assessment of their relative roles in global climate change, *Nature*, 346, 713-719, 1990.
- Kukla, G., F. Heller, X. M. Liu, T. C. Xu, T. S. Liu, and Z. A. An, Pleistocene climates in China dated by magnetic susceptibility, *Geology*, 16, 811-814, 1988.
- Maxwell, H. E., Archeology and Panguingue Creek: a Late Pleistocene/Early Holocene-aged site in central Alaska, Unpublished Master's Thesis, University of Alaska Fairbanks, Fairbanks, AK, 1987.
- Phippen, F. G., Archaeology at Owl Ridge: a Pleistocene-Holocene boundary age site in central Alaska, Unpublished Master's Thesis, University of Alaska Fairbanks, Fairbanks, AK, 1988.
- Powers, W. R., and J. F. Hoffecker, Late Pleistocene settlement in the Nenana valley, central Alaska, *American Antiquity*, 54, 263-287, 1989.
- Röthlisberger, F., *10 000 Jahre Gletschergeschichte der Erde*, Verlag Sauerländer, Aarau, 1986.
- Stuiver, M., and T. F. Braziunas, Atmospheric ^{14}C and century-scale solar oscillations, *Nature*, 338, 405-408, 1989.
- Stuiver, M., and P. D. Quay, Changes in atmospheric Carbon-14 attributed to a variable sun, *Science*, 207, 11-19, 1980.
- Stuiver, M., and P. J. Reimer, A computer program for radiocarbon age calibration, *Radiocarbon*, 28, 1022-1030, 1986.
- Stuiver, M., G. W. Pearson, and T. F. Braziunas, Radiocarbon age calibration of marine samples back to 9000 cal yr B.P., *Radiocarbon*, 28, 980-1021, 1986.
- Stuiver, M., T. F. Braziunas, and B. Becker, Climatic, solar, oceanic, and geomagnetic influences on Late-Glacial and Holocene atmospheric $^{14}\text{C}/^{12}\text{C}$ change, *Quat. Res.*, 35, 1-24, 1991.
- Thorson, R. M., and T. D. Hamilton, Geology of the Dry Creek site: a stratified early man site in interior Alaska, *Quat. Res.*, 7, 149-176, 1977.
- Vogel, J. S., W. Cornell, D. E. Nelson, and J. R. Southon, Vesuvius/Avellino, one possible source of seventeenth century B.C. climatic disturbances, *Nature*, 334, 534-537, 1990.
- Wigley, T. M. L., The climate of the past 10,000 years and the role of the sun, in *Secular Solar and Geomagnetic Variations in the Last 10,000 Years*, edited by F. R. Stephenson and A. W. Wolfendale, pp. 209-224, Kluwer, 1988.
- Wigley, T. M. L., and P. M. Kelly, Holocene climatic change, ^{14}C wiggles and variations in solar irradiance, *Phil. Trans. R. Soc. London A*, 330, 547-560, 1990.

Comparisons of Late Quaternary Climatic Development Between the Arctic and Antarctic Through Calcareous Nannofossils

G. Gard

Department of Geology, University of Stockholm, Stockholm, Sweden, U.S.A.

J. A. Crux

BP Exploration Inc., Houston, Texas, U.S.A.

ABSTRACT

The content of calcareous nannofossils (remnants of microscopic planktonic algae) have been documented in numerous sediment cores from the Norwegian and Greenland Seas and in ODP Hole 704A from the subantarctic South Atlantic. Worldwide species extinctions, inceptions and distinct abundance variations have been used to correlate and date the studied cores, which comprise the last 500,000 years. The biostratigraphy has been correlated to oxygen isotope stratigraphy which shows that intervals rich in nannofossils represent interglacial time periods.

The calcareous nannofossils indicate that during the time period studied, climatic fluctuations were similar in character and timing in both the subarctic and the subantarctic South Atlantic. Abundance patterns of warm water species suggest that surface waters were warmer than today only during oxygen isotope substage 5e (the last interglacial). The environment was interglacial also during isotope stages 9, 11, and 13, while stages 3 and 8 may have been characterized by intermediate glacial conditions. A significantly colder environment than at present prevailed in isotope stages 2, 4, 6, 10 and 12. Isotope stage 7 appears to have been fully interglacial in the subantarctic South Atlantic, but intermediate glacial in the Norwegian sea.

Japanese Ice Core Studies in the Polar Regions

O. Watanabe, Y. Fujii, and F. Nishio

National Institute of Polar Research, Tokyo, Japan

H. Narita

Institute of Low Temperature Science, Hokkaido University, Sapporo, Japan

M. Nakawo

*Nagaoka Institute of Snow and Ice Studies, National Research Center for Disaster Prevention,
Science and Technology Agency, Nagaoka, Japan*

H. Shoji

Faculty of Science, Toyama University, Toyama, Japan

ABSTRACT

A 2500-m-deep ice core drilling project is planned by Japanese glaciologists at the top of the ice sheet in Queen Maud Land, the second highest dome of the Antarctic ice sheet. The deep drilling will be carried out during 1993–1995 at a new inland base (77°22'S, 39°37'E, 3807 m a.s.l.), 1000 km away from Syowa Station (69°00'S, 30°35'E).

The purpose of this project is to reconstruct climatic and environmental records during the past 15–20K years and also to obtain glaciological data relating to the ice sheet formation and the mass balance processes.

This deep drilling is a project developed from a series of drilling projects started at Mizuho Station in 1971. In August 1984, drilling at Mizuho Station reached a depth of 700.6 m. This core is estimated to cover the last 9400 years.

Ice core drilling in the Arctic and also in the third polar region, i.e., the Himalayas and Kunlun Mountains, was also carried out in recent years. In 1983, glacier drilling to a depth of 70 m at 5400-m elevation in the Himalayas, and 86-m-deep drilling to the bottom in Svalbard were accomplished in 1987. A 205-m-deep drilling was carried out in southern Greenland in 1989.

In this paper, the results obtained by these drilling projects will be reviewed and the prospect of our new drilling projects will be introduced.

On the Development in Elaboration of Polar Ice Core Gas Content Analysis

J. P. Semiletov

Pacific Oceanological Institute, Far Eastern Branch of the U.S.S.R. Academy of Sciences, Vladivostok, U.S.S.R.

ABSTRACT

Differences between CO₂ concentrations in ice cores measured by "dry" or "wet" methods are attributed to carbonate contamination of the ice core surfaces [Raynaud et al., 1982]. However, the contribution of natural carbonates in CO₂ content may amount to ~20 Mg kg⁻¹ of ice [Neftel et al., 1982] which corresponds to ~100 ppm CO₂. TIC values differ from the CO₂ concentration in the case of slow wet extraction (~1 h). These differences may be partly connected with fractionation in the system gas-ice+gas hydrate when an ice core sample is crushed imperfectly [Barnola et al., 1983]. In the estimation of CO₂ presence in the CO₂-ice matrix, the contribution of total gas content (VG) is also needed. It depends on the level of transformation, waterdrop-snowflake.

For the Antarctic coastal regions these levels correspond to atmospheric pressures of about 700–800 mbar and for continental sites, for example Vostok, ~600–650 mbar. There, precipitation is connected with the entry of snow by stratospheric genesis in the central Antarctic. In this case, snow CO₂ content is about zero and more "rich" coastal snow contains about 70–80% from equilibrium concentration near sea level. In consequence, the maximal contribution in VG values is about 15–20%. The detailed investigation of this question may be effective for obtaining more precise data on VG stratifications in ice cores.

A new head-space technique of CO₂ and other gas content investigations in ice core is elaborated. Data obtained in 34 Soviet Antarctic Expeditions and in laboratory experiments are discussed.

Evolution of Southern Indian Ocean Surface and Deep Waters During the Paleogene as Inferred From Foraminiferal Stable Isotope Ratios

E. Barrera

Department of Geological Sciences, The University of Michigan, Ann Arbor, Michigan, U.S.A.

B. T. Huber

Department of Paleobiology, Smithsonian Institution, Washington, D.C., U.S.A.

ABSTRACT

During ODP Leg 119, the southernmost pelagic record of carbonate sedimentation of Neogene–Paleogene age in the southern Indian Ocean was recovered at Site 744 (61°34.6'S, 80°35.46'E; water depth 2307 m) and Site 738 (62°42.54'S, 82°47.25'E; water depth 2252 m) in the southern part of the Kerguelen–Heard Plateau. Site 744 late Eocene–Miocene sequence and Site 738 Late Cretaceous–early Oligocene sequences contain continuous records of climatic events in East Antarctica during this time.

Oxygen isotopic ratios of planktonic and benthic foraminifera suggest the following climatic changes: (1) a cool Paleocene, although with higher temperatures than those inferred from published Pacific and southern South Atlantic $\delta^{18}\text{O}$ records; (2) the early Eocene was characterized by the warmest deep and surface waters of the Cenozoic, which were similar in temperature to those from low latitude areas; (3) cooling began in the early- middle Eocene and continued through the remainder of the Eocene (Eocene *Cibicidoides* $\delta^{18}\text{O}$ values are not very different from those of low-latitude sites); (4) a rapid increase in *Cibicidoides* $\delta^{18}\text{O}$ values (1–1.5‰) occurred in the early Oligocene of Site 744. Ice-rafted debris, first recorded in sediments just below the $\delta^{18}\text{O}$ maximum, are also found in the early Oligocene sequence. Oligocene–early Miocene *Cibicidoides* $\delta^{18}\text{O}$ values of about 2‰ and the presence of ice-rafted debris are considered evidence for glacial conditions in Antarctica.

Planktonic foraminiferal assemblages indicate a similar climatic trend. Species diversity was highest during the latest Paleocene and earliest Eocene. It declined during the middle–late Eocene and the low diversity Oligocene faunas were dominated by a few globigerine taxa that are long-ranging and morphologically conservative.

Surface Currents in the Arctic Ocean During the Last 250 ka: Composition of Ice-Rafted Detritus (IRD) as a Key for Ice Drift Directions

M. Kubisch and R. F. Spielhagen

Geomar, Forschungszentrum für Marine Geowissenschaften, Kiel, Germany

ABSTRACT

Eleven long sediment cores from the Arctic Ocean and Fram Strait (78°–86°N) documenting more than 250,000 years of sedimentation history show distinct variations in the composition of coarse sand (500 μm).

Ice-rafted coal fragments deposited during glacial oxygen isotope stages 6 (186–128ka) and 8 (303–245ka) are evidence for ice drift from the Eastern Arctic Ocean through Fram Strait to the Norwegian Sea.

The dominating lithologies, with a high amount of sedimentary rock fragments in the IRD from interglacial stages (7, 5, 1), indicate a similar current pattern as today.

Crystalline rock fragments in glacial sediments decrease from the Barents Shelf margin to the Nansen–Gakkel Ridge where they are replaced by quartzites and cherts.

Sediment-Laden Sea Ice in the Arctic Ocean: Implications for Climate, Environment and Sedimentation

I. R. Wollenburg

GEOMAR, Research Center for Marine Geosciences, Kiel, Germany

S. L. Pfirman

Lamont-Doherty Geological Observatory, Palisades, New York, U.S.A.

M. A. Lange

Alfred Wegener Institut for Polar- and Marine Research, Bremerhaven, Germany

ABSTRACT

Sediments in sea ice were first described by F. Nansen during his famous "Fram expedition (1893–1896). Many researchers observed and recorded sediment-laden or "dirty" sea ice in the Central Arctic, but the origin and incorporation mechanisms are poorly understood and were never the object of detailed studies. Sea ice-rafted sediments are important factors for the albedo and for the ecology and productivity of marine organisms, because of the absorption of solar radiation and lowered light transmission.

Beginning in 1987 in the Eastern Arctic Basin and continuing in 1988, 1989 and 1990 in Fram Strait, Barents Sea and Greenland Sea we conducted a multi-disciplinary sea ice project "on the role and importance of sea ice-rafted sediments for sedimentation in the Arctic Ocean." During the field work very high sediment accumulations were observed and sampled (up to 560 g sediment/kg ice). Most of the material was concentrated in small patches of 1–10 m in diameter, but in some areas, especially in the Eastern Arctic, they covered up to 80% of the ice surface and formed layers of pure mud, 2–3 cm thick.

First estimations of the observed concentrations, the annual ice flow through Fram Strait, and the average sedimentation rate in this area show that the necessary sediment flux can be obtained only by sea ice. Thus, sea ice-rafting seems to be the most important input mechanism of fine grained terrigenous (biogenic and terrigenous) sediment into the ice-covered deep sea regions.

Environmental Marine Geology of the Arctic Ocean

P. J. Mudie

Geological Survey Canada, Atlantic Geoscience Centre, Dartmouth, Nova Scotia, Canada

ABSTRACT

The Arctic Ocean and its ice cover are major regulators of Northern Hemisphere climate, ocean circulation and marine productivity. The Arctic is also very sensitive to changes in the global environment because sea ice magnifies small changes in temperature, and because polar regions are sinks for air pollutants. Marine geology studies are being carried out to determine the nature and rate of these environmental changes by study of modern ice and sea bed environments, and by interpretation of geological records imprinted in the sea floor sediments. Sea ice camps, an ice island, and polar icebreakers have been used to study both western and eastern Arctic Ocean basins. Possible early warning signals of environmental changes in the Canadian Arctic are die-back in Arctic sponge reefs, outbreaks of toxic dinoflagellates, and pesticides in the marine food chain. Eastern Arctic ice and surface waters are contaminated by freon and radioactive fallout from Chernobyl. At present, different sedimentary processes operate in the pack ice-covered Canadian polar margin than in summer open waters off Alaska and Eurasia. The geological records, however, suggest that a temperature increase of 1–4°C would result in summer open water throughout the Arctic, with major changes in ocean circulation and productivity of waters off Eastern North America, and more widespread transport of pollutants from eastern to western Arctic basins. More studies of longer sediment cores are needed to confirm these interpretations, but it is now clear that the Arctic Ocean has been the pacemaker of climate change during the past 1 million years.

Section G:
Aerosols/Trace Gases

Chaired by

L. Barrie
Atmospheric Environment Service
Canada

G. Shaw
University of Alaska Fairbanks
U.S.A.

Chemical Changes in the Arctic Troposphere at Polar Sunrise

L. A. Barrie

Atmospheric Environment Service, Ontario, Canada

ABSTRACT

At polar sunrise, the Arctic troposphere (0 to ~8 km) is a unique chemical reactor influenced by human activity and the Arctic Ocean. It is surrounded by industrialized continents that in winter contribute gaseous and particulate pollution (Arctic haze). It is underlain by the flat Arctic Ocean from which it is separated by a crack-ridden ice membrane 3 to 4 m thick. Ocean to atmosphere exchange of heat, water vapor and marine biogenic gases influence the composition of the reactor. From 21 September to 21 December to 21 March, the region north of the Arctic circle goes from a completely sunlit situation to a completely dark one and then back to light. At the same time the lower troposphere is stably stratified. This hinders vertical mixing.

In this environment, chemical reactions involving sunlight are much slower than further south. Thus, it would not be surprising to find a high abundance of photochemically reactive compounds in the atmosphere at polar sunrise. Between complete dark in February and complete light in April, a number of chemical changes in the lower troposphere are observed. Perhaps the most sensational is the destruction of lower tropospheric ozone accompanied by production of filterable bromine and iodine. The latter are likely of marine origin, although their production may involve anthropogenic compounds. Another change is the shift in the fraction of total sulfur in its end oxidation state (VI) from 50% to 90%. Several gaseous hydrocarbons disappear from the atmosphere at this time. Preliminary observations also indicate a maximum in total non-black carbon on particulate matter. This is consistent with the formation of non-volatile organics from photochemically induced reactions of gas phase organics. Results of the Canadian Polar Sunrise Experiment 1988 are presented.



92-17859



Arctic Haze and Air Pollution

Jozef M. Pacyna

Norwegian Institute for Air Research, Lillestrøm, Norway

G. E. Shaw

Geophysical Institute, University of Alaska Fairbanks, Fairbanks, Alaska, U.S.A.

ABSTRACT

Arctic haze is the phenomenon of large-scale industrial air pollution found all through the arctic air mass. Vertical profiles of air concentrations, obtained during several aircraft measurement programs in the Arctic, have offered the following explanation of arctic haze origin. Very long range, episodic transport of air masses over several thousand kilometers clearly affects the quality of arctic air during both summer and winter. Polluted air masses, carrying a mixture of anthropogenic and natural pollutants from a variety of sources in different geographical areas have been identified in the arctic atmosphere at altitudes from 2 to 4 or 5 km. The layers of polluted air at altitudes below 2.5 km can be traced to episodic transport of air masses from anthropogenic sources situated closer to the Arctic. Pollution material in arctic haze is of submicron size and contains a substantial fraction of black carbon: it interacts strongly with solar radiation. In addition, sulfate and a wide range of heavy metals appear, affecting their natural geochemical cycles. They also serve as indicators of major source regions of emissions in the world. This paper discusses what happens to the haze-related pollutants in the Arctic, what is the contribution of natural sources to the arctic haze and what are local and global effects of arctic haze. Some indications are given of the research to be undertaken in a view to assess the role of the Arctic in global change of the environment.

INTRODUCTION

The origin of arctic air pollution has been an intriguing question for several decades. About 100 years ago Nansen observed a dark stain on the snow in the Polar Basin and suggested that these airborne contaminants may affect the melting snow [Nansen, 1924]. In the 1950s Mitchell and his colleagues observed bands of particles in the air over Alaska [Mitchell, 1956]. However, the origin of this phenomenon was not studied until the 1970s. In the 1970s the increasing acidification of precipitation in Europe [Oden, 1968] had resulted in the first international study of the long-range transport of air pollutants [e.g., OECD, 1977]. A major conclusion drawn from this research was that emissions from major source regions can be measured at receptors a few thousand kilometers away. The Arctic came to be con-

sidered as one large receptor of this pollution. Unexpectedly high values of total atmospheric turbidity measured in the Alaskan Arctic were used to conclude that the arctic atmosphere was polluted by blowing dust and probably the emissions from nearby sources [e.g., Shaw and Wendler, 1972]. Rahn et al. [1977] concluded that although particulate matter in air between distinct haze layers over Alaska was pollution derived, the haze layers themselves were of crustal composition, originating presumably from Asian deserts between 40 and 50°N. The measurements in the Norwegian Arctic [e.g., Larssen and Hanssen, 1979] indicated that polluted air masses traveled over Central Europe and across the Siberian Arctic border, i.e., over heavily industrialized regions.

Major progress in studying arctic haze and its effects on the environment was made during the measurement pro-

grams of the 1980s. Of special importance were ground measurements in Greenland [e.g., Heidam, 1981], the Norwegian Arctic [e.g., Ottar et al., 1986; Heintzenberg et al., 1986], northern Canada [e.g., Barrie and Hoff, 1985] and Alaska [e.g., Shaw, 1982; Li and Winchester, 1990a]. Vertical profiles of air concentrations were obtained during several aircraft measurements in the Arctic, particularly the three Arctic Gas and Aerosol Sampling Program (AGASP) campaigns in 1983 [e.g., Schnell, 1984], 1986 [e.g., Herbert et al., 1989] and 1989, and the BP program in the Norwegian Arctic from 1982 to 1984 [e.g., Ottar et al., 1986].

The overall goal of this paper is to summarize the results from the above-mentioned measurement campaigns, and to conclude on what is known about arctic haze and its effect on the environment. Arctic haze is shown as an example of global change of the environment due to human activity. The paper discusses what we need to know in order to explain the impact of man-made emissions on the quality of the arctic air. Some suggestions are given on the research needed to assess the role of the Arctic in global change.

WHAT IS KNOWN ABOUT ARCTIC HAZE?

The research outlined very briefly in the previous paragraph has contributed to the explanation of the origin of arctic haze, a complex mixture of particles and gases in the polar atmosphere. The main areas of current research can be divided into three topics: the physical and chemical characteristics of arctic haze, the pathways along which air pollutants are transported to the Arctic, and the methods used to assess the origin of arctic haze.

Physical and Chemical Characteristics of the Arctic Haze

Vertical profiles of the winter arctic aerosol indicate that the haze is spatially uniform on scales larger than hundreds of kilometers. In the lower 2–3 km of the atmosphere haze is frequently strongly banded [Ottar and Pacyna, 1986]. The temperature and wind profiles measured through the arctic haze layers suggest that the thermal stability of the lower

arctic troposphere is sufficient to maintain these laminar structures, despite differential advection of the layers by "jets" of wind as concluded by Radke et al. [1989].

Aerosol concentrations in a lower haze layer show significant variations, depending on the meteorological conditions, and most notably the presence of temperature inversions. The greater thickness of the arctic haze layers in the Norwegian Arctic in 1984 (Figure 1a) as compared with 1983 (Figure 1b) was explained by atmospheric stability variations. Temperature inversions aloft were often observed above 2.5 km in 1984, while they were lower in 1983 [Pacyna and Ottar, 1988]. Strong temperature inversions in the Arctic due to a strongly negative heat balance in winter [e.g., Benson, 1986] may even prevent the buildup of haze. The haze is seldom found over Greenland, where there is the highest frequency of inversion gradients, stronger than those measured in other parts of the Arctic.

The measurements of vertical profiles revealed layers of particles in the arctic troposphere between 3 and 5 km (Figure 1a,b), with particle concentrations much lower than those in the lower troposphere.

Aerosol size measurements show significant variations for particles in lower and upper layers. Particle sizes of up to 3 km during winter indicate a dominant fraction of 0.15–0.5- μm -diameter particles, with only a small contribution of >1.0- μm -diameter particles, as presented in Figure 2. In contrast, the coarser particles are predominant in the upper haze bands. The larger concentrations of small particles in the lower layer seem to be associated with air masses transported directly from a given pollution region. They may also be a result of an enhanced gas-to-particle conversion, as suggested by Bodhaine [1989].

Vertical profiles of the summer arctic aerosol indicate that enhanced concentrations of particles are very seldom measured below 2 km. However, the measurements in the Norwegian Arctic sporadically indicated layers of polluted air with a well-defined lower boundary at about 2 km [Pacyna and Ottar, 1988]. The upper boundaries >ca. 3.5 km were more variable. This layer seems to be similar, in terms

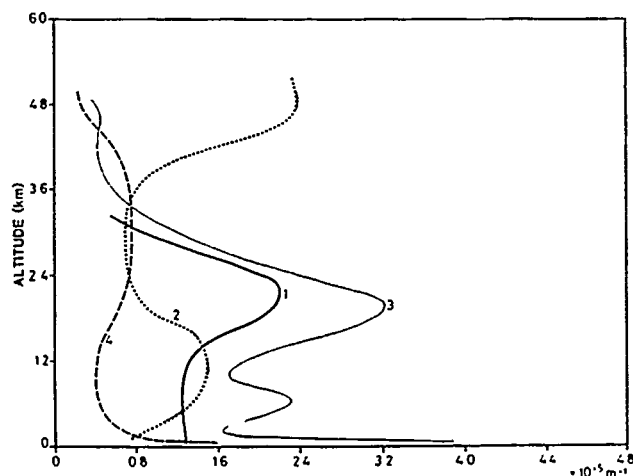


Figure 1a. The aerosol light scattering coefficient (σ_{sp}) values vs. flight altitude during flights on 1 March 1984 (1), 2 March 1984 (2), 3 March 1984 (3) and 7 March 1984 (4).

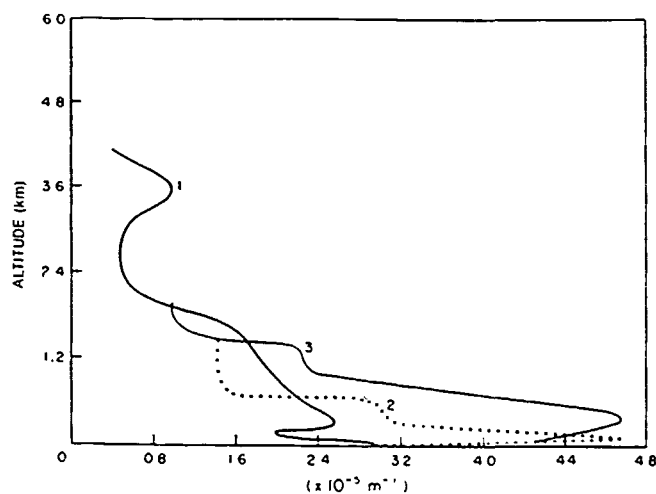


Figure 1b. The aerosol light scattering coefficient (σ_{sp}) values vs. flight altitude during flights on 21 March 1983-I (1), 21 March 1983-II (2) and 22 March 1983 (3).

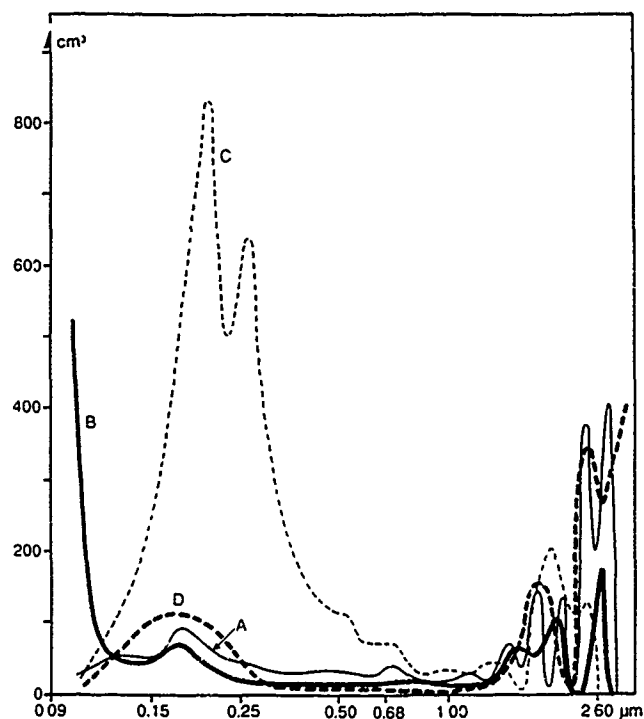


Figure 2. Concentration of particles (N) vs. particle size (Dp): (A) at 3300 m on 18 August 1983; (B) at 900 m on 25 August 1983; (C) at 1800 m on 3 March 1984; (D) at 3500 m on 3 March 1984.

of origin, to the upper layer of polluted air observed during the winter half-year.

The chemical description of arctic haze during winter can be as follows: sulfate concentrations of ca. $2 \mu\text{g m}^{-3}$, organic carbon concentrations of $1 \mu\text{g m}^{-3}$, black carbon (soot) plus associated water concentrations of $0.3\text{--}0.5 \mu\text{g m}^{-3}$, a few tenths of a $\mu\text{g m}^{-3}$ of other substances and a few $\mu\text{g m}^{-3}$ of

water. Concentrations of nitrates are low. The chemical composition of the aerosols measured in the Norwegian Arctic during the winter flight is shown in Figure 3. It can be suggested that high concentrations of several anthropogenic trace metals and natural compounds are measured in the lower layer of the arctic haze (up to 2–3 km). The upper layer (up to 4–5 km) contains a mixture of natural and anthropogenic trace metals with the latter group in small concentrations.

The size-differentiated chemical composition of particles can be characterized as follows. The accumulation mode aerosols ($0.1\text{--}1.0 \mu\text{m}$ dia.) which are haze related, are generally composed of anthropogenic pollutants with the sulfuric acid being the dominant winter aerosol [e.g., Barrie, 1985]. Coarse particles (larger than $2 \mu\text{m}$ dia.) consist of clay minerals, other soil constituents and, to a lesser extent, sea salt compounds [e.g., Radke et al., 1984]. These particles, as well as giant particles (larger than $10 \mu\text{m}$) are not, however, well correlated with haze. The cation-anion budgets for arctic aerosol prove that the haze-related mode of aerosols is acidic. The measured acidity and pH of aerosol particles from the Arctic was reported by Lazrus and Ferek [1984].

SO_2 is of greatest significance among the gases that may directly affect the arctic haze aerosol because some SO_2 converts to particulate sulfate. This conversion may take place near the source regions, along the transport pathways or in the Arctic when springtime brings sunshine to the region. According to Barrie and Hoff [1984], the strong seasonal variation of sulfates is mainly due to seasonal variations in the oxidation rate of SO_2 in the atmosphere.

Nitrogen oxides were also measured in the Arctic, showing significantly higher concentrations in spring than in summer [e.g., Jaffe et al., 1991].

Transport of Polluted Air into the Arctic

Our understanding of the meteorological conditions leading to the arctic haze phenomenon has been improved by the

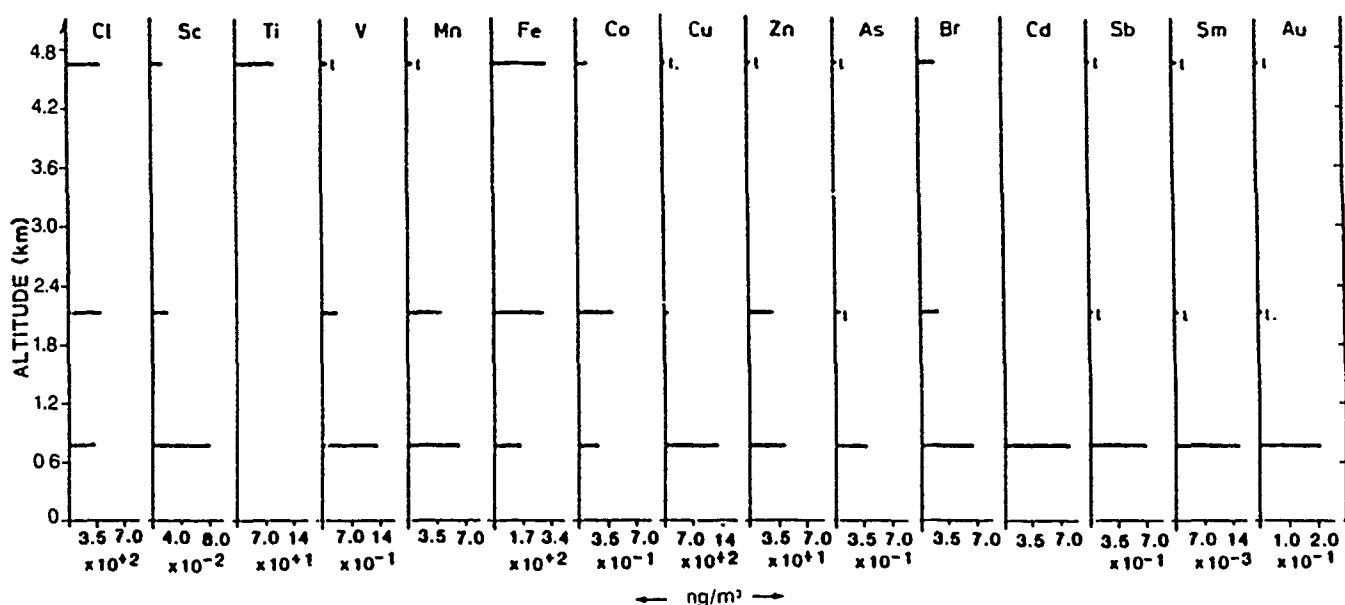


Figure 3. Chemical composition of aerosols measured at different altitudes during the 3 March 1984 flight. 1 = low concentrations.

introduction of the quasi-isentropic trajectory concept by Carlson [1981] and Iversen [1984]. Two interpretations of long-range transport of polluted air to the Arctic are offered. Iversen [1989] suggests that regional blocking is a basic flow phenomenon causing this transport. Regional blocking is conditioned by interference between stationary planetary waves, forced by orography and ground level heating, and low frequency transient waves created by baroclinic instability.

Raatz and Shaw [1984] suggested that anticyclones play the dominant role in providing the proper conditions for the transport of air pollutants to the Arctic. The authors suggest the following sequence of events: (a) a period of accumulation of aerosols over the source region, (b) a synoptic situation of accelerated air flow towards the Arctic, and (c) rapid transport across the Arctic.

Origin of the Arctic Air Pollution

Major progress in studying the origin of the arctic air pollution was made when the information on the chemical composition of the arctic aerosol became available. Rahn and colleagues [e.g., Lowenthal and Rahn, 1985] have developed the chemical fingerprinting system which uses the concentration ratios of various anthropogenic trace metals to distinguish between contributions from various source regions to the contamination of the arctic air.

Various dispersion and receptor models were used to determine the origin of arctic aerosols. A trajectory Lagrangian model of long-range transport of air pollutants has been applied to study the origin of the aerosols in the Norwegian Arctic [e.g., Pacyna et al., 1985]. A chemical transport model was developed to study the flux of anthropogenic sulfur into the Arctic from mid-latitudes using observed winds, precipitation and pollutant mixing depths as well as SO₂ emissions in Eurasia and North America [Barrie et al., 1989].

Maenhaut et al. [1989] applied the absolute principal component analysis (APCA) and the chemical mass balance (CMB) to assess the contribution of emissions from various source regions to the arctic aerosol. Further improvement of the receptor modeling method was obtained by applying APCA to aerosol elemental concentration measurements in separate particle size fractions [Li and Winchester, 1990b]. The APCA method was also applied to the sets of data obtained from the scanning electron microscope (SEM) analysis [e.g., Sheridan, 1989; Anderson et al., 1990]. The anthropogenic part of the arctic aerosol was studied with the help of information on the concentrations of not only trace metals but also radioisotopes [e.g., Sturges and Barrie, 1987], halogens [e.g., Sturges and Barrie, 1988], graphitic carbon [e.g., Heintzenberg, 1982; Rosen and Hansen, 1984] and organic compounds [Pacyna and Oehme, 1988].

Summarizing the results of the above studies, the following explanation of the origin of the arctic aerosol can be offered. Emissions from anthropogenic sources are the main contributors to the arctic haze observed up to 2–3 km of the atmosphere in the winter. The emissions from sources in the northern Soviet Union are a major source (at least two thirds) of the pollution measured in the Arctic during winter. Three major source regions in the northern Soviet Union include the Urals, the Kola Peninsula and the Norilsk area. The major source categories in these regions are non-ferrous

metal production, combustion of coal and oil to produce electricity and heat, and steel and iron manufacturing. Consumption of gasoline containing at least 0.4 g Pb l⁻¹ adds to the formation of small particles which are subject to long-range transport. The emissions from the Urals and the Norilsk area seem to be more important for the contamination of air over Alaska and the Canadian Arctic, while the sources on the Kola Peninsula contribute more to the Norwegian Arctic. The contribution of European emissions to the Arctic aerosol is lower than that from the Russian sources, particularly in Alaska and the Canadian Arctic. During sporadic summer transport of pollutants to the Arctic at altitudes below 2–3 km, emissions from sources in Europe seem to be more important than those from the Soviet Union. The North American source contribution in summer is also evident. Polluted air masses, carrying a mixture of anthropogenic and natural air pollutants from a variety of sources in different geographical areas, have been identified in the Arctic at altitudes of 4 to 5 km during both summer and winter. Pacyna and Ottar [1989] concluded that long-range transport of airborne loess from deposits in Asia and Africa can reach the Arctic at these altitudes. Further information summarizing the results of the arctic haze research is available from reports by Barrie [1985] and Shaw and Khalil [1989].

WHAT INFORMATION ON ARCTIC HAZE IS MISSING?

Although there has been significant progress in understanding the features of arctic haze, some aspects need further explanation. These unanswered questions can be grouped into three major subjects: (1) what happens to the haze-related pollutants in the Arctic?, (2) what is the contribution of natural sources to arctic haze?, and (3) what are local and global effects of arctic haze?

Removal of Haze-Related Pollutants in the Arctic

The meteorological conditions in the Arctic during winter do not favor the deposition of pollutants. There are fewer and smaller cloud droplets or ice crystals for the haze particles to collide with or to diffuse to and attach in the polar air mass. Dynamic stability in the arctic air mass is great and laminar flow is the rule. Washout of pollution is low throughout most of the polar air mass. Stable stratification in winter prevents strong vertical mixing. The lack of sunlight in mid-winter results in a greatly reduced rate of transformation of SO₂ to tiny droplets of sulfuric acid [e.g., Barrie, 1985]. Under such conditions, pollutants transported to the Arctic can be trapped there for several weeks and the residence time of aerosol in the atmosphere may be as long as several weeks. Indeed, the episode of "megahaze" in the Arctic in the late winter of 1986 seems to confirm this suggestion [Li and Winchester, 1989]. On some occasions, however, the episodes last not more than a few hours. Thus, is the deposition process efficient enough to retain small particles within the Arctic region, or are they carried out of the region with the air masses? Although the answer to this question has a fundamental meaning when assessing the impact of industrialization on the quality of the environment in polar regions, there are only a few measurements of wet deposition in the Arctic and even fewer of dry deposition. Summarizing the results obtained by Davidson for Green-

land [e.g., Davidson et al., 1985], Joranger and Semb for the Norwegian Arctic [e.g., Joranger and Semb, 1989], Dayan et al. [1985] for Alaska, and Shewchuk [1985] and Barrie et al. [1985] for the Canadian Arctic, it can be concluded that the arctic wet deposition is slightly acidic with pH ranging from 4.9 to 5.2. The high summer scavenging ratios for sulfates coincide with low concentrations. During summer the precipitation in the Arctic occurs mainly as fine drizzle from low stratiform clouds or during fog. Joranger and Semb [1989] explain that during winter, the relatively high concentrations of sulfates are confined to a shallow layer of the air next to the ground and that a significant part of the precipitation is derived from cleaner air above this layer during frontal precipitation. Generally, the process of wet deposition in the Arctic is not very well understood. The same applies to dry deposition. One of the poorly understood processes is deposition of small quantities of ice crystals, which tend to contain larger than normal aerosols as nuclei. The other problem is possible sublimation from snow or drifting. Davidson et al. [1989] suggest that the proportion of dry to wet deposition of sulfates in Greenland is 1:3. Extending this assumption for the whole arctic region, a mass budget of sulfur can be assessed (Table 1). This assessment suggests that only 2.5% of sulfur entering the Arctic is deposited in this region. This result is, however, very uncertain and more research should be carried out to improve or assure this estimate.

Natural Sources of Arctic Haze

The recent measurements at Barrow, Alaska [e.g., Li and Winchester, 1989] and Ny-Ålesund, Spitsbergen [e.g., Maenhaut et al., 1989] revealed that the impact of natural oceanic sources on the arctic haze can be appreciable. Natural compounds may also be transported to the Arctic from lower latitudes. According to Li and Winchester [1989], most of the carboxylic acid anions, accounting for 20% of the total aerosol mass, can be attributed to natural sources at lower latitudes. As much as 20% non-sea salt sulfates in aerosols can originate from gaseous marine sources. The sources and source regions for natural sulfates and other components of the arctic aerosol from natural sources are poorly recognized. It may be transport from lower latitudes, but may also be the sea-to-air flux of biogenic DMS in the

Area of arctic air mass*	44 x 10 ⁶ km ²
Mean concentration of sulfur in the atmosphere	470 µgm ⁻³
Deposition velocity	0.03 cm s ⁻¹
Arctic dry deposition	0.19 Tg S yr ⁻¹
Arctic wet deposition	0.57 Tg S yr ⁻¹
Northern hemisphere emission	30 Tg S yr ⁻¹
Fractional deposition in Arctic	2.5%
Snow acidity assuming H ₂ SO ₄ and water precipitation rate of 10 cm H ₂ O yr ⁻¹	10.3 µ eq l ⁻¹

Table 1. Mass budget of sulfur for the Arctic Basin [Shaw and Khalil, 1989]. *Area is taken to be that within the boundary of the arctic and represents 9% of the earth's surface. This represents an area about 30% larger than the African continent. ** Mean annual from data of Barrie [1985].

Arctic Ocean itself. Therefore, the role of natural products in the formation of arctic haze cannot be ignored and requires further investigation.

Local and Global Effects of Arctic Haze

The problem of possible climatic and ecological effects of arctic haze measured on a local and global scale is a very broad topic. Only major aspects of the problem will be outlined here. The potential for perturbation of the radiation budget in spring caused by highly absorbing soot and the acidic nature of arctic haze warrant our concern. According to Blanchet [1989], soot in aerosols is responsible for warming by 0.1 to 0.3 K per day during mid- and late spring. However, the warming of the Arctic may result in lowering surface pressure and thus create conditions of more cloud coverage and precipitation. Soot on the top of the snowpack is also responsible for warming, probably to the same extent as with the airborne particles. Sulfates, in contrast to soot, are responsible for cooling the arctic air due to a strong enhancement of solar radiation scattering. In summary, soot warming will dominate in the mid- and late spring, while sulfate cooling would be dominant in summer. The aircraft measurements of radiation by Valero and Ackerman [1986] showed the occurrence of radiative heating within the haze layers. Another area that needs our attention and more research is the connection between arctic air pollution and the microphysical properties of clouds [Borys, 1983]. There may be significant alteration in cloud albedo over the Arctic from the imported cloud condensation nuclei. Concerning the acidic nature of arctic haze and its chemical composition, an important question is to what extent does the transport of air pollution to the Arctic alter the geochemical cycles of various compounds? One measure of this problem is the enrichment of various air compounds in the arctic aerosol in relation to crustal material. Enrichment factors (EF) for aerosols in the Norwegian Arctic are shown in Table 2.

Element	Enrichment factor (Ti, earth crust)
Ag	200-1000
As	700-3000
Cd	500-6000
Cr	30-100
Cu	30-100
Ga	8-20
In	40-200
Mo	60-150
Ni	30-80
Pb	2500-4000
Sb	1000-3200
S	2500-15000
Se	3700-36000
V	35-50
W	20-130
Zn	300-900

Table 2. Enrichment factors of trace metals on particles <1.0 µm diameter in the Norwegian Arctic during winter episodes of long-range transport of air pollution.

There are several compounds having EFs over 100 thus their biogeochemical cycles are likely being perturbed by long-range transport from lower latitudes. What are the consequences of these alterations? Two examples can be given. The lead level in blood of Greenlanders is comparable to the level of Europeans living in industrial regions [e.g., Hansen, 1986]. The concentrations of PCBs in fish, seals and the human population in the Arctic are disturbingly high, exceeding 2–3 times the limits recommended by WHO [e.g., NILU, 1989]. Transport of these materials with waters to the Arctic cannot alone be responsible for their concentrations. Finally, particles in the Arctic are responsible for reduction of visibility. According to Barrie [1985], sulfate concentrations between 1 and 4 $\mu\text{g m}^{-3}$, result in visibility between 244 and 73 km in low relative humidity situations. The visibility measured in the Arctic is much lower than expected. The most likely reason is a combined effect of anthropogenic aerosols and ice crystals.

WHAT WE CAN DO TO IMPROVE OUR KNOWLEDGE OF ARCTIC HAZE AND ITS IMPACT ON THE ENVIRONMENT?

Two major issues may improve our knowledge about arctic haze and its influence on the quality of the environment in polar regions: establishment of a joint monitoring pro-

gram, and development of modeling of climatic and ecological impacts of arctic haze. In order to assess the effects of arctic haze on the environment in polar regions and to present the trends of these effects, a monitoring system is necessary. So far the measurements have not been correlated between research groups or nations. One exception could be the AGASP I measurement campaign in March 1983 when American, German and Norwegian planes participated. In the Autumn of 1989 representatives of eight Arctic nations—Canada, Denmark, Finland, Iceland, Norway, Sweden, USA, and the USSR—held a consultative meeting in Rovaniemi, Finland, and as one of the meeting results, the authorities in Norway and the USSR were asked to prepare a paper on the possibility of establishing a joint arctic monitoring program. The objectives of this programme are focused on the search for information on the climatic and pollution situations in the arctic environment (air, water, ice, sediments, vegetation, animals and humans), including documentation of levels of contaminants, effects, trends and transport processes of pollutants to the Arctic and within the arctic environment. The development of modeling of climatic and ecological impacts of arctic haze on the environment shall include the improvement of radiative transfer models as well as the adaptation of terrestrial models to arctic conditions.

REFERENCES

- Anderson, J. R., P. R. Buseck, D. A. Saucy, and J. M. Pacyna, Compositions, size distributions, and principal component analysis of individual fine-fraction particles from the Arctic aerosol at Spitsbergen, May–June, 1987, *Atmos. Environ.*, (submitted for publication).
- Barrie, L. A., Arctic air pollution: an overview of current knowledge, paper presented at International Conference on Atmospheric Sciences and Application to Air Quality, Seoul, Korea, May, 1985.
- Barrie, L. A., and R. M. Hoff, The oxidation rate and residence time of sulphur dioxide in the Arctic atmosphere, *Atmos. Environ.*, 18, 2711–2722, 1984.
- Barrie, L. A., and R. M. Hoff, Five years of air chemistry observations in the Canadian Arctic, *Atmos. Environ.*, 19, 1995–2010, 1985.
- Barrie, L. A., D. Fisher, and R. M. Koerner, Trends in Arctic air pollution revealed by glacial ice cores, *Atmos. Environ.*, 19, 2055–2063, 1985.
- Barrie, L. A., M. P. Olson, and K. K. Oikawa, The flux of anthropogenic sulphur into the Arctic from mid-latitudes in 1979/80, *Atmos. Environ.*, 23, 2505–2512, 1989.
- Benson, C. S., Problems of air quality in local arctic and sub-arctic areas, and regional problems of arctic haze, in *Arctic Air Pollution*, edited by B. Stonehouse, pp. 69–84, Cambridge University Press, Cambridge, 1986.
- Blanchet, J.-P., Towards estimation of climatic effects due to Arctic aerosol, *Atmos. Environ.*, 23, 2609–2625, 1989.
- Bodhaine, B. A., Barrow surface aerosol: 1976–1986, *Atmos. Environ.*, 23, 2357–2369, 1989.
- Borys, R. D., *Atmospheric Science Paper No. 367*, Department of Atmospheric Science, Colorado State University, Ft. Collins, Colorado, 1983.
- Carlson, T. N., Speculations on the movement of polluted air to the Arctic, *Atmos. Environ.*, 15, 1473–1477, 1981.
- Davidson, C. I., S. Santhanam, R. C. Fortmann, and M. P. Olson, Atmospheric transport and deposition of trace elements onto the Greenland Ice Sheet, *Atmos. Environ.*, 19, 2065–2081, 1985.
- Davidson, C. I., J. R. Harrington, M. J. Stephenson, M. J. Small, F. P. Boscoe, and R. E. Gandle, Seasonal variations in sulfate, nitrate and chloride in the Greenland Ice Sheet: relation to atmospheric concentrations, *Atmos. Environ.*, 23, 2483–2493, 1989.
- Dayan, U., J. M. Miller, W. C. Keene, and J. N. Galloway, An analysis of precipitation chemistry data from Alaska, *Atmos. Environ.*, 19, 651–658, 1985.
- Hansen, J. C., Exposure to heavy metals in Greenland from natural and man-made sources, in *Arctic Air Pollution*, edited by B. Stonehouse, pp. 249–258, Cambridge University Press, Cambridge, 1986.
- Heidam, N. Z., On the origin of the Arctic aerosol: a statistical approach, *Atmos. Environ.*, 15, 1421–1427, 1981.
- Heintzenberg, J., Size-segregated measurements of particulate elemental carbon and aerosol light absorption at remote Arctic locations, *Atmos. Environ.*, 16, 2461–2468, 1982.
- Heintzenberg, J., H.-C. Hansson, D. S. Covert, J.-P. Blanchet, and J. A. Ogren, Physical and chemical properties of arctic aerosols and clouds, in *Arctic Air Pollution*, edited by B. Stonehouse, pp. 25–35, Cambridge University Press, Cambridge, 1986.
- Herbert, G. A., J. M. Harris, and B. A. Bodhaine, Atmospheric transport during AGASP-II: the Alaskan flights (2–10 April 1986), *Atmos. Environ.*, 23, 2521–2535, 1989.
- Iversen, T., On the atmospheric transport of pollution to the Arctic, *Geophys. Res. Lett.*, 11, 457–460, 1984.
- Iversen, T., Some statistical properties of ground level air pollution at Norwegian Arctic stations and their relation to large scale atmospheric flow systems, *Atmos. Environ.*, 23, 2451–2462, 1989.

- Jaffe, D. A., R. E. Honrath, J. A. Herring, and S.-M. Li, Measurement of nitrogen oxides at Barrow, Alaska during Spring: Evidence for regional and northern hemispheric sources of pollution, *J. Geophys. Res.*, **96**, 7395-7405, 1991.
- Joranger, E., and A. Semb, Major ions and scavenging of sulphate in the Norwegian Arctic, *Atmos. Environ.*, **23**, 2463-2469, 1989.
- Larssen, S., and J. E. Hanssen, Annual variation and origin of aerosol components in the Norwegian Arctic-Subarctic region, paper presented at the WMO Technical Conference on Regional and Global Observation of Atmospheric Pollution Relative to Climate, Boulder, Colorado, 20-24 August, 1979.
- Lazrus, A. L., and R. J. Ferek, Acidic sulfate particles in the winter arctic atmosphere, *Geophys. Res. Lett.*, **11**, 417-419, 1984.
- Li, S.-M., and J. W. Winchester, Geochemistry of organic and inorganic ions of late winter arctic aerosols, *Atmos. Environ.*, **23**, 2401-2415, 1989.
- Li, S.-M., and J. W. Winchester, Particle size distribution of late winter Arctic aerosols, *J. Geophys. Res.*, **95**, 13897-13908, 1990a.
- Li, S.-M., and J. W. Winchester, Haze and other aerosol components in late winter Arctic Alaska, 1986, *J. Geophys. Res.*, 1797-1810, 1990b.
- Lowenthal, D. H., and K. A. Rahn, Regional sources of pollution aerosol at Barrow, Alaska during winter 1979-80 as deduced from elemental tracers, *Atmos. Environ.*, **19**, 2011-2024, 1985.
- Maenhaut, W., P. Cornille, J. M. Pacyna, and V. Vitols, Trace element composition and origin of the atmospheric aerosol in the Norwegian Arctic, *Atmos. Environ.*, **23**, 2551-2569, 1989.
- Mitchell, M., Visual range in the polar regions with particular reference to the Alaskan Arctic, *J. Atmos. Terr. Phys.* (Special supplement), 195-211, 1956.
- Nansen, F., *Blandt Sel og Bjørn*, Dywad, Oslo, 1924.
- NILU, Forurensningen av Arktis med klorerte pesticider og polyklorerte bifenyler, Norwegian Institute for Air Research, *Rept. RR 8/89*, (in Norwegian), May, 1989.
- Oden, S., Nederbordens och Luftens Forurning, dess Orsaker, Forlopp, och Verkan i Olika Miljoer. Statens Naturvetenskapliga Forskningsrad (Ekologikommitten, *Bull. No. 1*), (in Swedish), Stockholm, 1968.
- OECD, The OECD programme on long-range transport of air pollutants, measurements and findings, Organization for Economic Co-operation and Development, Paris, 1977.
- Ottar, B. and J. M. Pacyna, Origin and characteristics of aerosols in the Norwegian Arctic, in *Arctic Air Pollution*, edited by B. Stonehouse, pp. 53-67, Cambridge University Press, Cambridge, 1986.
- Ottar, B., Y. Gotaas, O. Hov, T. Iversen, E. Joranger, M. Oehme, J. M. Pacyna, A. Semb, W. Thomas, and V. Vitols, Air pollutants in the Arctic, *NILU OR Rept. No. 30/86*, The Norwegian Institute for Air Research, Lillestrøm, Norway, 1986.
- Pacyna, J. M., and M. Oehme, Long-range transport of some organic compounds to the Norwegian Arctic, *Atmos. Environ.*, **22**, 243-257, 1988.
- Pacyna, J. M., and B. Ottar, Vertical distribution of aerosols in the Norwegian Arctic, *Atmos. Environ.*, **22**, 2213-2222, 1988.
- Pacyna, J. M., and B. Ottar, Origin of natural constituents in the Arctic aerosol, *Atmos. Environ.*, **23**, 809-815, 1989.
- Pacyna, J. M., B. Ottar, U. Tomza, and W. Maenhaut, Long-range transport of trace elements to Ny Ålesund, Spitsbergen, *Atmos. Environ.*, **19**, 857-865, 1985.
- Raatz, W. E., and G. E. Shaw, Long-range transport of pollution aerosols into the Alaskan Arctic, *J. Climatol. Appl. Meteorol.*, **23**, 1052-1064, 1984.
- Radke, L. F., J. H. Lyons, D. A. Hegg, P. V. Hobbs, and I. H. Bailey, Airborne observations of Arctic aerosols. I. Characteristics of Arctic haze, *Geophys. Res. Lett.*, **11**, 392-396, 1984.
- Radke, L. F., C. A. Brock, J. H. Lyons, P. V. Hobbs, and R. C. Schnell, Aerosol and lidar measurements of hazes in mid-latitude and polar air masses, *Atmos. Environ.*, **23**, 2417-2430, 1989.
- Rahn, K. A., R. Borys, and G. E. Shaw, The Asian source of Arctic haze bands, *Nature*, **268**, 713-715, 1979.
- Rosen, H. and A. D. A. Hansen, Role of combustion-generated carbon particles in the absorption of solar radiation in the Arctic haze, *Geophys. Res. Lett.*, **11**, 461-464, 1984.
- Schnell, R. C., Arctic haze and the Arctic Gas and Aerosol Sampling Program (AGASP), *Geophys. Res. Lett.*, **11**, 361-364, 1984.
- Shaw, G. E., Evidence for a central Eurasian source area of Arctic haze in Alaska, *Nature*, **299**, 815-818, 1982.
- Shaw, G. E., and G. Wendler, Atmospheric turbidity measurements at McCall Glacier in northeast Alaska, paper presented at the Conference on Atmospheric Radiation, Fort Collins, Colorado. *Proc. Amer. Met. Soc.*, Boston, 181-187, 1972.
- Shaw, G. E., and M. A. K. Khalil, Arctic haze, in *The Handbook of Environmental Chemistry, Volume 4/Part B*, edited by O. Hutzinger, pp. 69-111, Springer, Berlin, 1989.
- Sheridan, P. J., Characterization of size segregated particles collected over Alaska and the Canadian High Arctic, ACASP-II flights 204-206, *Atmos. Environ.*, **23**, 2371-2386, 1989.
- Shewchuk, S. R., Acid deposition sensitivities within the Northwest Territories and current depositions to the snowpack and small lakes chemistry of a selected area of the Mackenzie District, *Proc. Int. Conf. on Arctic Water Pollut. Research: Applications of Science and Technology*, Yellowknife, 28 April-1 May, 1985.
- Sturges, W. T., and L. A. Barrie, Lead 206/207 isotope ratios in the atmosphere of North America as tracers of US and Canadian emissions, *Nature*, **329**, 144-146, 1987.
- Sturges, W. T., and L. A. Barrie, Chlorine, bromine and iodine in Arctic aerosol, *Atmos. Environ.*, **22**, 1179-1194, 1988.
- Valero, F. P. J., and T. P. Ackerman, Arctic haze and the radiation balance, in *Arctic Air Pollution*, edited by B. Stonehouse, pp. 121-133, Cambridge University Press, Cambridge, 1986.

AD-P007 356



A Polar Climate Iteration?

A. Hogan

U.S. Army Cold Regions Research and Engineering Laboratory, Hanover, New Hampshire, U.S.A.

D. Riley

Department of Natural Resources, Waterbury, Vermont, U.S.A.

B. B. Murphey

Whiteface Mountain Observatory, ASRC, Wilmington, New York, U.S.A.

S. C. Barnard and J. A. Samson

ASRC, State Univ. of New York, Albany, New York, U.S.A.

92-17860



ABSTRACT

The antarctic continental (cA) air mass is rarely displaced from the South Polar Plateau, but it is frequently modified by exchange with Antarctic maritime (mA) air advected from the ice shelves or frozen seas or with polar maritime (mP) air advected from the Southern Ocean. Because the cA air mass resides over an uninhabited and relatively static ice-covered surface, the concentration of aerosol particles in this unique air mass may reflect aerosol variation in the global atmosphere.

A continuous series of surface observations began at South Pole in 1974 and have continued to the present. Although a large seasonal variation in aerosol concentration is present, little year-to-year variation in mean seasonal aerosol concentration occurred prior to 1982. During the mid-1980s, a consistent diminution of mean annual aerosol concentration was observed, and a concurrent reduction in sodium concentration in snow and firn was reported. The decrease in aerosol concentration was greatest in late winter and spring, concurrent with decreases in mean air temperature and mean wind speed.

This paper describes concurrent aerosol and meteorological data collected at South Pole from 1974 through 1987 and presents several analyses attempting to verify if these changes do reflect a persistent variation in the properties of the cA air mass. Additional analyses, using upper air and automatic weather station data, attempt to identify circulation changes related to these changes in aerosol concentration.

INTRODUCTION

A cold dry air mass is permanently resident over the Antarctic Plateau. The elevation of the plateau, the radiation deficit afforded by its permanent snow cover, and the stability of the air, prevent the Antarctic continental (cA) air mass from being displaced by surrounding Antarctic maritime (mA) or polar maritime (mP) air masses. The cA air mass is warmed by advective exchange with these air masses, and

the aerosol properties of the cA air mass are modified coincidentally [Hogan et al., 1982; Riley, 1987; Hogan et al., 1990]. The uniformity of the surface of the polar plateau, the absence of continental antarctic aerosol sources, the unique stability of the cA air mass, and the relative slowness of Antarctic meteorological variation cumulatively provide Lettau's [1971] "test tube" for examining meteorological theories.

Surface and upper air meteorological observations have been continuously made at the South Pole since 1957. The station and observation site were relocated during December 1974, the anemometer environment varied at both sites, and the temperature sensor has frequently changed in relative height, due to snow drift accumulation about its base. Three automatic weather stations (AWS) [Stearns and Wendler, 1988] were operated in the vicinity of the South Pole in 1986 and 1987. Comparison of the official station observations with AWS records indicates that station observations are currently representative [Stearns, private communication] of the wind and temperature on the surrounding polar plateau. A comparison of official South Pole observations, obtained from the NOAA National Climatic Center, with those from an adjacent, and two 30-km-distant, AWS is shown in Figure 1. The mean values of observed temperatures are in agreement within 1°C, and track quite well in pseudo synoptic analyses. Official station winds are slightly greater than those measured at the outlying AWS. It is possible that the domed station slightly accelerates the surface wind in the vicinity, but there is no evidence from the AWS that the presence of the station diminishes the surface wind. A distinguished and dedicated series of meteorologists have obtained the South Pole climatic record; it now provides a unique data set for examining aerosol exchange and deposition theories.

DATA ANALYSIS AND DISCUSSION

The NOAA/GMCC program began systematic measurement [Pack, 1973] of aerosols, gases, and radiation at south pole in 1974, including a cooperative set of measurements of aerosol concentration [Pollak and O'Connor, 1955; Pollak and Metnieks, 1960; Skala, 1963], diffusion coefficient [Sinclair, 1972], and number of charged particles [Rich, 1966], which form the basis for this paper. These aerosol measurements are made once per day coincident with the 00 hrs Universal Time [00UT] upper air sounding and have provided more than 355 observation days per year since establishment of the Clean Air Facility in 1976. Analysis of the aerosol record [Hogan et al., 1982; Bodhaine et al., 1986; Riley, 1987; Samson et al., 1990; Hogan et al., 1990] indicates that particles and heat are simultaneously exchanged into the CA air mass. A comparison of aerosol concentration, surface temperature, and surface pressure, from Riley [1987] is given in Figure 2, to illustrate this unique relation among pressure, temperature and aerosol concentration on the Polar Plateau.

This transport of heat and particles can be traced meteorologically from the surrounding seas [Bodhaine et al., 1986; Murphey et al., 1991]. Sodium and other marine materials constitute a large fraction of the particle mass [Zoller et al., 1974; Maenhut et al., 1979; Parungo et al., 1979; Hogan et al., 1984a,b; Shaw, 1988], which increases during periods of surface warming.

Bodhaine and Shanahan [1990] and Samson et al. [1990] have made chronologies of different, but co-calibrated south pole aerosol data sets, and show the mean aerosol concentration decreased during the 1980 decade. Legrand and Kirchener [1988] measured sodium concentration in snow in a shallow snow pit near the south pole and found deposited sodium to be decreasing in a similar secular manner as particles in the air above. Comparison of the concentration of

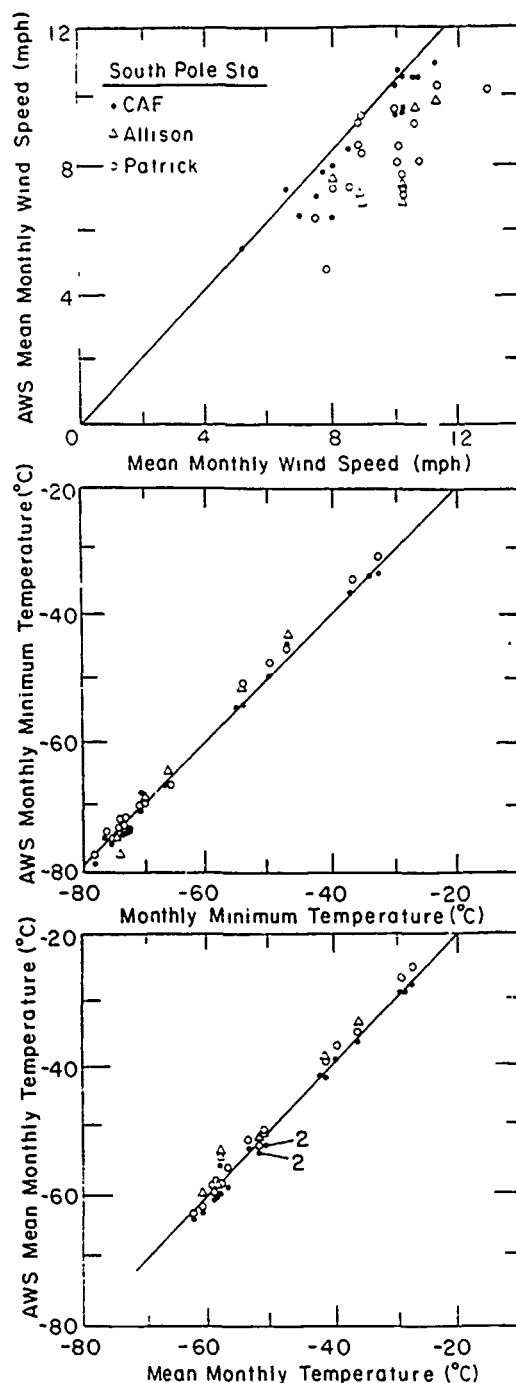


Figure 1. Temperatures and winds recorded at Automatic Weather Stations relative to official station observations at South Pole: (1) monthly minimum temperatures, (2) mean monthly temperatures, and (3) mean monthly wind speeds. Station "CAF" is adjacent to the official station; stations "Allison" and "Patrick" are 20 NM distant.

particles in air and concentration of sodium in snow for overlapping time periods are shown in Figures 3 and 4.

Figure 3 shows the mean monthly aerosol concentration from Samson et al. [1990], superimposed above the 10 slice per apparent glaciological year sodium analysis from Legrand and Kirchener [1988]. The similarly diminishing trend in concentration with time is apparent but the sodium concentration is almost exactly out of phase with the aerosol

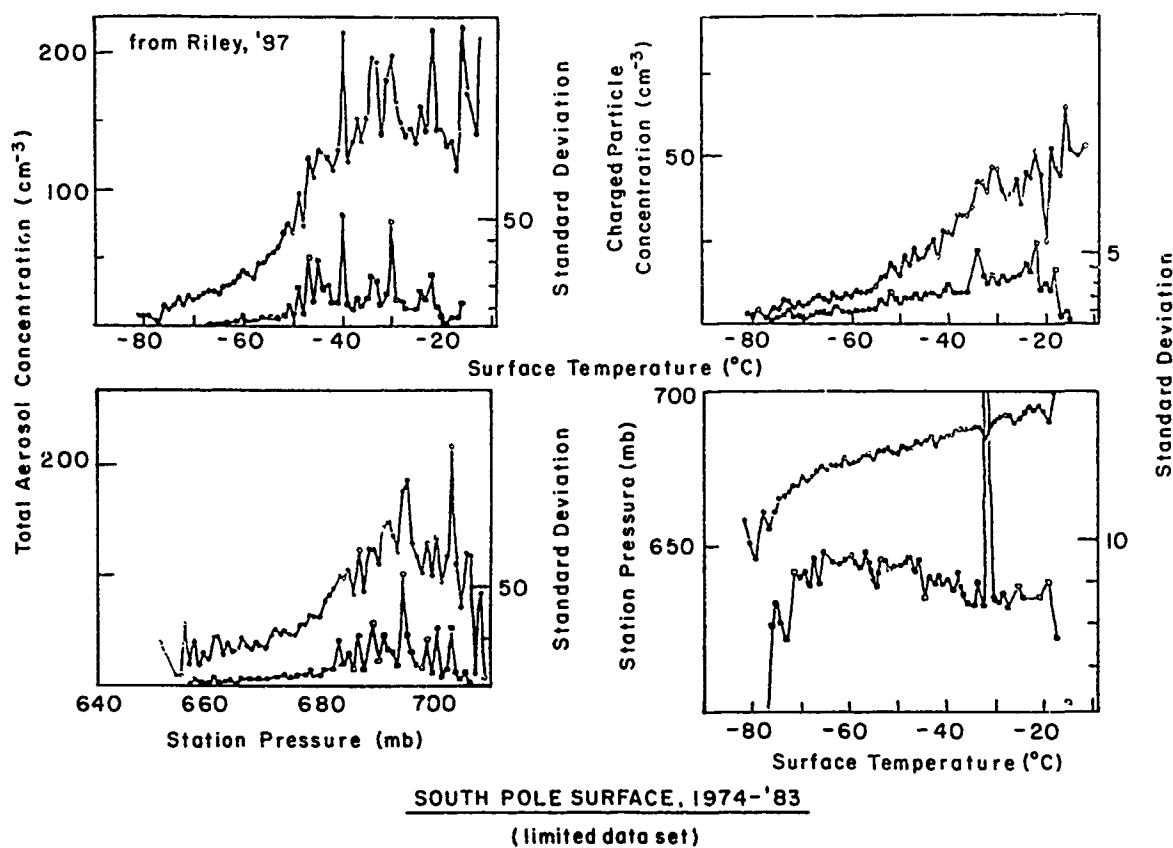


Figure 2. Relations among station pressure, surface air temperature, total aerosol concentration, and charged aerosol concentration, observed at South Pole, 1974-1983. The data set is limited to pressure and temperature observations made concurrently with aerosol observations. All data from Riley [1987].

concentration. This is due to formation of a winter crust following the summer winter transition and maximum snow-air temperature difference in March and April. Snow which falls in late winter (August) or during the winter-summer transition (September-October-November) does not adhere to this crust and drifts about the polar plateau, becoming the next season's winter layer [Gow, 1965]. Figure 4 shows a comparison of the mean "summer" (October through March) aerosol concentration with the integrated sodium concentration in the snow of the following winter. The number of data points is too few for statistical analysis, but both Figures 3 and 4 indicate sodium and aerosol have decreased in concentration during the decade of the 1980s.

Legrand and Kirchener [1988] attribute the decrease in sodium deposition to "reduced meridional transport"; aerosol has been shown to be transported to the antarctic plateau with warmer mP and mA air and these warm, enhanced aerosol events have been called "sodium storms" by Parungo et al. [1979, 1981] and Bodhaine et al. [1986]. Murphey et al. [1991] first traced salt particles measured during a storm at Ross Island to a warm aerosol event at South Pole in 1983, and similar advection of warm aerosol-enriched air across the Ross ice Shelf to the South Pole has been documented through analysis of AWS data since then. The "reduced meridional transport" proposed by Legrand and Kirchener [1988] may be deduced from the South Pole

Calendar Year Period	Mean Surface Air Temp. C	Mean Barometric Pressure mb	Mean Wind Speed m s ⁻¹
60/64	-49.3	680.7	6.1
65/69	-49.1	682.3	5.7
70/74	-49.1	681.3	4.7
80/84	-49.4	681.0	4.7
85/88	-50.0	681.0	4.3

Table 1. Time variation in temperature, pressure and wind observed at the South Pole.

temperature record as well as the aerosol and glacio-chemical records.

The pentadel mean temperature and wind speed observed at the surface at South Pole for the five pentads 1960-1984, and the partial pentad 1985-1988 are tabulated in Table 1. The mean annual temperature and wind speed and air temperature have diminished through the period, reflecting "reduced meridional transport." The monthly mean temperatures are plotted in Figure 5; the 1960-1988 mean values are shown as plotted lines, and the pentadel means are denoted by symbols. The summer months and mid-winter months show no systematic change. The summer to winter

transition (Mar^{ch}) is consistently warmer during the years 1975 through 1988 and the winter to summer transition (August–September–October) is consistently cooler during those years. The diminishing temperature trend shown in Table 1 is due to diminished August–September–October temperatures. A similar analysis of wind speeds shows mean summer (December–January) winds to be unchanged over the record period but all other months to have diminished speeds, and the winter to summer transition months of August–September–October to have wind speeds diminished by 3.5 mph, when the recent years are compared to those prior to 1974.

Analysis of the meteorological and aerosol records for August, September, and October show periods of warm advection that cause the surface temperature to increase from the -60°C to the -40°C range, and aerosol concentrations to increase by a factor of two or more in concert with these surface temperature increases. An analysis of twenty years of South Pole surface temperature records by Schwerdtfeger [1984] shows the mean daily temperature to

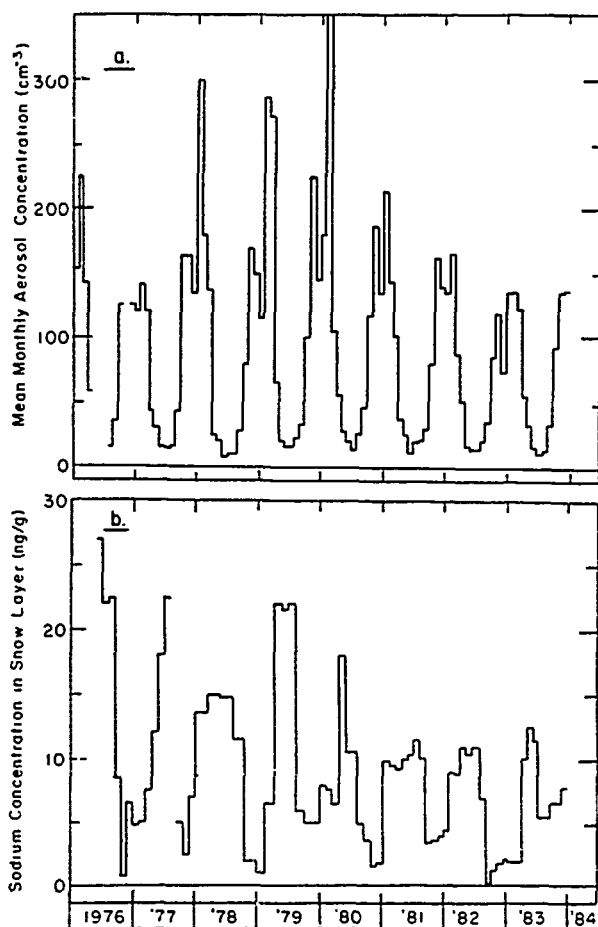


Figure 3. Chronology of (a) mean monthly aerosol concentration observed at South Pole, from Samson et al. [1990] and (b) sodium concentrations measured in a shallow snow pit near South Pole by Legrand and Kirchener [1988]. A time axis shift of 6 months, using the hypothesis that sodium precipitated to the polar plateau during the late winter and summer will be accumulated and stored in the following winter layer, similar to the accumulation of snow [Gow, 1965], places the decreasing trends in phase.

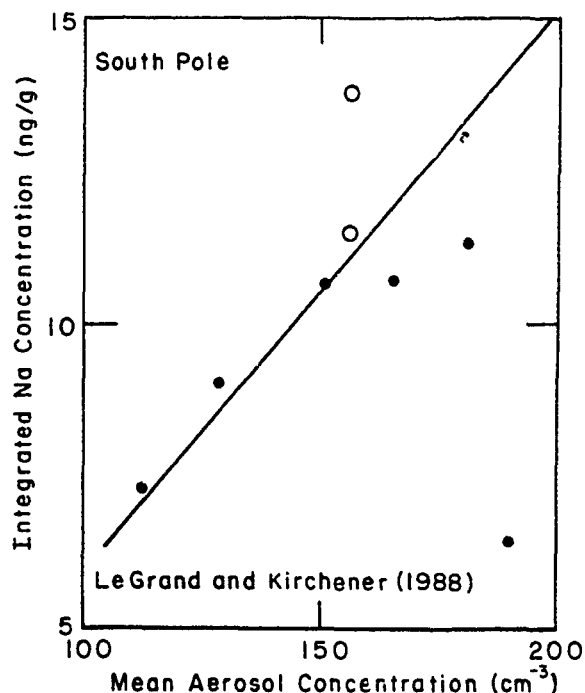


Figure 4. Comparison of the integrated Na concentration in "winter" snow layers collected from a shallow snow pit near South Pole by Legrand and Kirchener [1988] and the mean aerosol concentration observed during the previous October–March at South Pole.

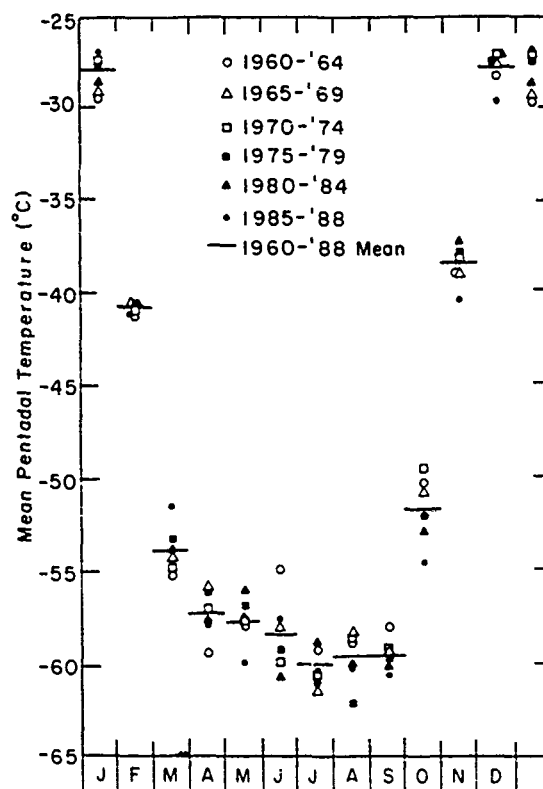


Figure 5. Mean monthly surface temperatures observed at the South Pole, 1960–1988. Pentadal mean temperatures are noted by symbols. The month of March has been consistently warmer since 1975; the months of August, September and October have been consistently colder.

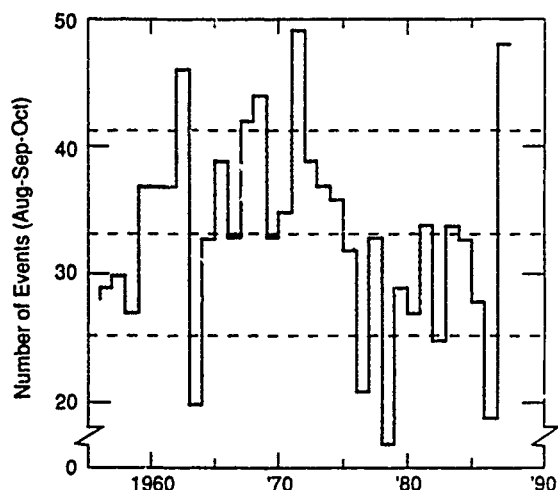


Figure 6. Frequency analysis of the number of days with temperatures exceeding -50°C during calendar months August, September, and October.

remain less than -50°C through late October. A daily maximum temperature of greater than -50°C is a strong indicator of warm advection or "meridional transport," and Riley's aerosol vs. surface temperature analysis in Figure 2 shows an inflection at -50°C . The number of days with maximum temperature greater than -50°C occurring in the months August, September, and October and the number of days with maximum temperature less than -50°C occurring in November were determined for each year, since establishment of the station. Only two November days colder than -50°C occurred prior to the decade of the 1980s, while seven occurred during the mid 1980s. The mean, median, and modal number of August, September and October days exceeding -50°C is 33, and the standard deviation is 8. All but one of the years in which the number of -50°C days exceeded the mean plus one standard deviation occurred before 1972; all but one of the years in which the number of days exceeding -50°C were less than the mean minus one standard deviation have occurred after 1977. It is quite apparent from examining this chronology, as shown in Figure 6, that the exchange of heat into the cA air mass during the winter-spring transition was much more vigorous during the period 1960–1975 than during 1976–1987 or 1957–1959, and that the winter-spring transition was delayed into November in some of these years.

It appears from examining these figures that we have recorded a "climatic iteration" at the South Pole in agreement with the tropospheric temperature variation reported by Angell [1988] and Jones [1988]. Figures 3 and 4 indicate that similar iterations occurred in aerosol concentration and sodium deposition. Some uncertainties remain which preclude establishing a calibration point in the meteorological and glaciological record. The reduced number of days of strong warm advection support the hypothesis of "reduced meridional transport," but the mean aerosol concentration and integrated deposition do not proportionally coincide with the frequency of warming events during these months. The vigor of spring warming actually diminished prior to the beginning of aerosol record. The reduction in wind

speed, which occurred simultaneously, complicates interpretation of the transport and exchange of heat and particles to the air at the polar surface and further complicates interpretation of precipitation and deposition processes for sodium.

CONCLUSION

We have had the good fortune to measure the variation of aerosol properties in a unique air mass during an identifiable climatic iteration. This series of observations is especially valuable, as most of our theories of aerosol transport to Antarctica propose increasing concentration with respect to time, while this circulation change resulted in diminishing concentrations. These findings indicate that we may be able to calibrate climatic changes recorded in polar snow and ice, but only through a broadened understanding of meteorological transport, exchange and precipitation processes.

The glaciological record remains available for additional analysis, as do the meteorological and aerosol records. It would be productive to date strata in several snow pits along a circle of 20-km radius about the South Pole, and compare the water and chemical accumulation with the 1957–1990 meteorological record. The winds observed 300 m above the station might supply a more precise record of changes in circulation, independent of surface modifications due to occupation of the polar plateau. An expanded AWS network is necessary to provide objective analysis of surface transport and exchange.

A dedicated research effort is necessary to identify and assess the processes that cause the precipitation of sodium or some other conservative aerosol tracer to the snow at the surface of the Polar Plateau. Identification of climatic or meteorologic variation from glaciological records will remain problematic until a quantitative precipitation and accumulation theory is established. It is of primary importance to investigate the influence of wind speed and direction on precipitation and accumulation of particulate matter in South Polar snow. It is also necessary to determine if the relations between aerosol, temperature, and pressure are source independent, or if it reflects changes in the properties of mP air over the Southern Ocean. The question mark in the title must remain.

ACKNOWLEDGMENTS

This research was supported by NSF-OPP, and NSF-DPP through grants to the Research Foundation of SUNY, over the period 1975–1988. USA CRREL supported the first author during preparation of this manuscript, and thanks are offered to K. Stoner, E. Perkins, M. Pacillo and Donna Harp for preparation of the text and figures. Dr. A. J. Gow read the first draft of the manuscript, and discussions with him and Dr. B. A. Bodhaine greatly improved several sections of the paper. Additional reviews were provided by E. Andreas and R. Melloh. Special thanks are offered to D. Pack, G. Herbert, M. Johnson and D. Nelson who established a long-term climatological aerosol observing program at South Pole, C. Jenkins who initiated the archiving of meteorological observations to support the program, and the entire sequence of station meteorologists and GMCC observers whose diligence in observation has produced this unique record. This paper is dedicated to Dr W. H. Zoller, the original South Polar aerosol scientist.

REFERENCES

- Angell, J. K., Variations and trends in tropospheric and stratospheric global temperatures, *J. Climate*, **1**, 1296–1313, 1988.
- Bodhaine, B. A., Aerosol measurements at four background sites, *J. Geophys. Res.*, **88**, 10753–10768, 1983.
- Bodhaine, B. A., J. J. DeLuise, J. M. Harris, P. Houmère, and S. Bauman, Aerosol measurements at the South Pole, *Tellus*, **38B**, 223–235, 1986.
- Bromwich, D. H., Snowfall in high southern latitudes, *Rev. Geophys.*, **26**, 149–168, 1988.
- Dalrymple, P., A physical climatology of the Antarctic plateau, in *Studies in Antarctic Meteorology*, pp. 195–231, AGU, 1966.
- Gow, A. J., On the accumulation and seasonal stratification of snow at the South Pole, *J. Glaciol.*, **40**, 461–477, 1965.
- Hogan, A. W., S. C. Barnard, J. A. Samson, and W. Winters, The Transport of heat, water vapour and particulate material to the south polar plateau, *J. Geophys. Res.*, **87**, 4287–4292, 1982.
- Hogan, A., et al., Particle concentrations at the South Pole, on meteorological and climatological time scales; is the difference important?, *Geophys. Res. Lett.*, **10**, 850–853, 1984a.
- Hogan, A. W., J. A. Samson, K. Kebschull, R. Townsend, S. Barnard, and B. Murphey, On the Interaction of Aerosol With Meteorology, *J. Rech. Atmos.*, **18**, 41–67, 1984b.
- Hogan, A. W., W. G. Egan, J. A. Samson, S. C. Barnard, D. M. Riley, and B. B. Murphey, Seasonal variation of some constituents of Antarctic tropospheric air, *Geophys. Res. Lett.*, **17**, 2365–2368, 1990.
- Jones, P. D., Hemispheric surface air temperature variations: recent trends and an update to 1987, *J. Climate*, **1**, 654–660, 1988.
- Legrand, M., and S. Kirchener, Polar atmospheric circulation and chemistry of recent (1957–83) south polar precipitation, *Geophys. Res. Lett.*, **15**, 879–882, 1988.
- Lettau, H. H., Antarctic atmosphere as a test tube for meteorological theories, in *Research in the Antarctic*, edited by L. O. Quam, pp. 443–476, AAAS Pub. 93, Washington, DC, 1971.
- Maenhut, W., W. H. Zoller, R. A. Duce, and G. L. Hoffman, Concentration and size distribution of particulate trace elements in the south polar atmosphere, *J. Geophys. Res.*, **84**, 2421–2431, 1979.
- Murphey, B. B., T. Hare, A. W. Hogan, K. Lieser, J. Toman, and T. Woodgates, Vernal atmospheric mixing in the Antarctic, *J. Appl. Meteorol.*, **30**, 494–507, 1991.
- Pack, D. H., Geophysical monitoring for climatic change, *Antarctic J. U.S.*, **1**, 253–254, 1973.
- Parungo, F., E. Ackerman, W. Caldwell, and H. K. Weickmann, Individual particle analysis of Antarctic aerosols, *Tellus*, **31**, 521–529, 1979.
- Parungo, F., B. A. Bodhaine, and J. C. Bortiniak, Seasonal variation of Antarctic aerosol, *J. Aerosol Sci.*, **12**, 491–504, 1981.
- Pollak, L. W., and A. L. Metnieks, Intrinsic calibration of the Photo Electric Nucleus Counter model 1957 with Convergent Light Beam, *Tech Note 9*, School of Cosmic Physics, Dublin Institute for Advanced Study, Dublin, Ireland, 1960.
- Pollak, L. W., and T. C. O'Connor, A Photo Electric Condensation Nucleus Counter of high precision, *Geof. Pura e Appl.*, **32**, 139–146, 1955.
- Rich, T. A., Apparatus and method for measuring the size of aerosols, *J. Rech. Atmos.*, **11**, 79–85, 1966.
- Riley, D. C., A study of the relationship between the variation of aerosol and meteorological parameters at South Pole on synoptic, seasonal, and climatological time scales, *ASRC Pub. 1122*, SUNY, Albany, NY, May 1987.
- Samson, J. A., Some characteristics of the south polar atmosphere, M.S. Thesis, SUNY Albany, Albany, NY, May 1983.
- Samson, J. A., S. C. Barnard, J. S. Obermski, D. C. Riley, J. J. Black, and A. W. Hogan, On the systematic variation of surface aerosol concentration at the South Pole, *Atmos. Res.*, **25**, 385–396, 1990.
- Schwerdtfeger, W., The climate of Antarctica, in *Climates of the Polar Regions*, edited by S. Orvig, pp. 253–322, Elsevier, New York, 1970.
- Schwerdtfeger, W., *Weather and Climate of the Antarctic*, Elsevier, New York, 1984.
- Shaw, G. E., Antarctic aerosols: A review, *Rev. Geophys.*, **26**, 89–112, 1988.
- Sinclair, D., A portable diffusion battery, *Am. Ind. Hygiene Assoc. J.*, **33**, 729–735, 1972.
- Sinclair, M. R., Record high temperatures in the Antarctic—A synoptic case study, *Mon. Wea. Rev.*, **109**, 2234–2242, 1981.
- Skala, G. F., A new instrument for measurement of condensation nuclei, *Anal. Chem.*, **35**, 702–705, 1963.
- Stearns C. R., and G. Wendler, Research results from Automatic Weather Stations, *Rev. Geophys.*, **26**, 45–61, 1988.
- Tuncell, G., N. K. Aras, and W. H. Zoller, Temporal variations and sources of elements in the south polar atmosphere: 1. Non enriched and moderately enriched elements, *J. Geophys. Res.*, **94**, 13025–13038, 1989.
- Vali, G., Nucleation terminology, *Bulletin AMS*, **66**, 1426–1427, 1985.
- Van Loon, H., Pressure in the Southern Hemisphere, in *Meteorology of the Southern Hemisphere*, edited by C. W. Newton, *Meteorol. Monographs*, **13**, 59–86, 1972.
- Voskresenskii, A. I., Condensation nuclei in the Mirnii region, (in Russian only, abstract translated in Antarctic bibliography), *Tr. Sov. Antarkt. Eksped.*, **38**, 194–198, 1968.
- Warburton, J. A., and G. O. Linkletter, Atmospheric processes and the chemistry of the snow on the Ross Ice Shelf, Antarctica, *J. Glaciology*, **20**, 149–162, 1978.
- Weller, G., Advances in antarctic geophysical sciences from the IGY to the present, *Antarctic J. U.S.*, **21**, 1–12, 1986.
- Zoller, W. H., E. S. Gladney, and R. A. Duce, Atmospheric concentrations and sources of trace metals at the South Pole, *Science*, **183**, 198–200, 1974.

AD-P007 357



92-17861



The Role of the Polar Regions in the Global Carbon Cycle and Related Climatic Changes

E. P. Borisenkov

Main Geophysical Observatory, Leningrad, U.S.S.R.

ABSTRACT

Empirical data are examined which characterize the role of the polar regions in the global carbon cycle, and the role of polar oceans as atmospheric carbon sinks is discussed. The dependence of the annual variation of atmospheric CO₂ content on latitude is analyzed. Natural and anthropogenic sources of CO₂ are studied, as well as their manifestation in polar regions. The results of carbon cycle numerical modeling with linear and non-linear box models for different scenarios of anthropogenic CO₂ growth are presented. The role of oceanic, biospheric and anthropogenic sources in carbon cycle dynamics is analyzed. The results of modeling the climate and its changes are discussed for different scenarios of energetics development with models of different complexity. Possible causes of climate warming and cooling are considered for the polar regions.

INTRODUCTION

The global carbon cycle and climate change are now the problems of prime importance. They are most completely described in the report prepared by WMO/UNEP [1990], but also in many other publications. A generalized description of the problem of the global carbon cycle relative to climate changes is presented in the monograph by Borisenkov and Kondratiev [1988], with an extensive bibliography.

It should be mentioned that despite the exceptional importance of the problem a quite simple assumption has been laid down so far that CO₂ concentration will double in the near future, resulting in global climate warming with maximum warming in the high latitudes of both hemispheres, and accompanied by a rise of the world ocean level by approximately 76 cm by the late 21st century.

Based on numerical experiments, Manabe and Wetherald [1975] determined that sudden CO₂ doubling would cause mean warming of approximately 2–3°C, and in polar areas of 6–8°C.

These results have been confirmed in many studies, although the range of temperature changes in different models was between 0.2°C and 9.6°C. It should be stressed that all these numerical experiments were made at a given temperature of sea surface (so-called swamp ocean) or with

approximate consideration of the dynamics of the ocean mixing layer.

A number of studies show an important role of deep ocean in the global carbon cycle. This effect is most fully described by Bacastow and Maier-Reimer [1990].

Feedbacks proved to be of no less importance, primarily in the case of lower cloud layer increase.

Polar regions are of special importance for studying the global carbon cycle. These regions, particularly the south polar region, are powerful sinks of carbon absorbed by oceanic water.

This flow in one direction can reach 80–100 Gigatons of carbon per year, which is far larger than the anthropogenic source due to fossil fuel combustion, which is equal to more than 5.5 Gt per year.

On the other hand, analysis of ice cores taken from the Greenland and Antarctica glaciers enables us to reconstruct the content of atmospheric carbon approximately for the past 160,000 years [Barnola et al., 1987]. Similar variation with time in paleodata is traced for another greenhouse gas, methane [Chappellaz et al., 1990].

Analysis of samples in the cores of continental ice shows periods of a considerable decrease in CO₂ content down to approximately 200 ppm and less, and periods of increased

CO₂ content reaching 300–310 ppm and, from the data of Shackleton et al. [1983], to 330–350 ppm. Glacial epochs with a cold climate approximately 20,000 and 150,000 years ago correspond to low CO₂ content. Warm epochs correspond to high CO₂ content.

The above CO₂ changes were by no means related to anthropogenic effects. Numerous data indicate that the periods of recession and extension of continental ice are well correlated with periods of change in the Earth's orbit parameters, and modeling results confirm this [Budd and Rayner, 1990]. It is natural to assume that, if we cannot simulate the CO₂ concentration variations with a numerical model of the carbon cycle, and cannot explain them, we have no reason to trust in modeling results when estimating future CO₂ concentrations and corresponding climate changes.

According to model estimates, the time of CO₂ concentration doubling varies between early in the next century and the middle of the 22nd century [Borisenkov and Kondratiev, 1988]. In view of the discussion of the greenhouse effect, it is also important to answer the question of whether paleo-analogues (warm periods of the middle Holocene, 5000–8000 years ago; the recent interglacial period–Mikhulinsky Optimum, 125,000 years ago; and Pliocene, 3–4 million years ago) could be used for constructing future climate scenarios. This problem is discussed in the scientific literature as well.

Since according to some results of model calculations CO₂ doubling will result in maximum warming in the polar regions, which should lead to the decrease of interlatitudinal temperature contrasts and circulation change, this problem is critical for future climate changes.

In view of the above the author made it his aim to give a critical analysis of the CO₂ problem and to propose several problems for discussion with an attempt to provide possible answers to them.

There is no reason to argue against the data on CO₂ content in the Greenland and Antarctica continental ice cores and the coincidence of warm climate periods with the continental ice minimum amount on the planet, extension of snow cover line to the poles, rise of world ocean level, and increase of incoming insolation due to the change of the Earth's orbit parameters as a result of gravitational interaction between the planets. Similarly the cold climate periods (ice epochs) are sufficiently well documented and are related to the increase of continental ice amount, extension of snow cover line to the equator of world ocean level, and decrease in incoming insolation.

There is some difference in the absolute values obtained for CO₂ content for the Mikhulinsky Optimum 125,000 years ago. According to the data in Shackleton et al. [1983] the CO₂ content then was about 330–350 ppm. The report of the WMO/UNEP working group [1990], referring to Barnola et al. [1987], gives the values 330–310 ppm.

PARAMETERIZATION OF THE RELATIONSHIP BETWEEN THE MECHANISM OF ATMOSPHERE-OCEAN CO₂ EXCHANGE AND TEMPERATURE

If one assumes that the experimental data providing answers to items 1 and 2 of Table 1 are reliable enough, we should be able to model the past changes in CO₂ concentration which are not of anthropogenic origin.

For simulating the carbon cycle, linear models of the following type are generally used:

$$\frac{dN_i}{dt} = \sum_{\substack{i=1 \\ j \neq i}} (K_{ij}N_j - K_{ji}N_i) + n_i \quad (1)$$

Here N_i is carbon content in i -th reservoir, K_{ij} and K_{ji} are coefficients of exchange between reservoirs characterizing the rate of carbon flux from i -th to j -th reservoirs (K_{ij}) and from j -th to i -th reservoirs (K_{ji}), n_i is the anthropogenic source in the i -th reservoir. This source exists now only for the atmosphere.

In this case at each time moment

$$N_1 + N_2 + N_3 + \dots + N_n = \sum_{i=1}^n N_{10} + N_i \quad (2)$$

Here N_{10} is carbon content in the i -th reservoir at the initial time moment. The beginning of the industrial period (1860) is usually taken as the initial time moment.

When linear models are integrated over a long period they come to a quasistationary regime depending on the rates of CO₂ exchange between reservoirs and the dynamics of the anthropogenic CO₂ source. In the absence of anthropogenic sources only the rates of exchange processes can change carbon cycle dynamics.

It is well known from theory and experiment that carbon flows between the ocean and the atmosphere depend to a considerable extent on ocean temperature, and carbon flows between the atmosphere and the biosphere depend also, though to a lesser extent, on atmosphere temperature.

Since the cumulative concentration of nonorganic carbon in the ocean (ΣC) is determined by carbon dioxide dissolved in the ocean (CO₂), carbonate ions (HCO₃⁻) and bicarbonate ions (CO₃²⁻), we have

$$\Sigma C = [\text{CO}_2] + [\text{HCO}_3^-] + [\text{CO}_3^{2-}] \quad (3)$$

The partial pressure of carbon dioxide dissolved in water which affects CO₂ exchange with the atmosphere depends in a complicated way on the process occurring in the ocean.

$$\text{Thus } P_{\text{CO}_2} = \frac{\Sigma C}{K_o + \frac{K_o K_1}{[\text{H}^+]} + \frac{K_o K_1 K_2}{[\text{H}^+]^2}} \quad (4)$$

In this case

$$\begin{aligned} [\text{CO}_2] + [\text{H}_2\text{O}] &\overset{K_1}{\rightleftharpoons} [\text{HCO}_3^-] \overset{K_2}{\rightleftharpoons} [\text{HCO}_3^-] + \\ &[\text{H}^+] + [\text{HCO}_3^-] \overset{K_2}{\rightleftharpoons} [\text{H}^+] + [\text{CO}_3^{2-}] \end{aligned} \quad (5)$$

where $[\text{H}^+]$ is hydrogen ion activity, α_o is the factor of carbon dioxide solubility in sea water, K_1 and K_2 are the first and the second constants of carbon dioxide dissociation supported by reaction (5).

$$\text{Denoting } \frac{1}{K_o + \frac{K_o K_1}{[\text{H}^+]} + \frac{K_o K_1 K_2}{[\text{H}^+]^2}} = \Phi$$

No. Question	Most probable answer (to be proven)
1. Are paleodata on CO ₂ content in the cores of Greenland and Antarctica continental ice sufficiently representative to judge the global CO ₂ concentration in different epochs?	YES
2. Is the coincidence between higher and lower CO ₂ content periods and those of warm and cold climate satisfactory enough?	YES
3. Can past warm climate periods be taken as a scenario for future warm climate due to the greenhouse effect?	NO
4. Can past climatic changes be explained by changes in atmospheric CO ₂ ?	ONLY SLIGHTLY; IN THE MAIN THEY CANT
5. Are the past CO ₂ content change periods the result of climate change due to external factors and primarily astronomical ones?	YES
6. Are CO ₂ content changes in polar ice cores for warm and cold climate periods the result of change in the CO ₂ exchange mainly between atmosphere and ocean and partly between atmosphere and biosphere due to temperature regime change caused by other factors?	YES
7. Is the viewpoint universally recognized that atmospheric CO ₂ doubling would increase mean global temperature near the earth's surface by 2-4°C, and the polar regions by 6-8°C?	NO
8. Do the empirical data obtained with models (temperature increase in the troposphere and decrease in the stratosphere, precipitation increase, water vapor content increase, sea level rise, glacier melting, etc.) confirm reliably enough the appearance of the greenhouse effect during the instrumental observation period?	MORE LIKELY NO THAN YES
9. Are there reasons to believe CO ₂ content doubling together with the increase of other greenhouse gases would cause maximum cooling in the north polar region rather than maximum warming?	YES
10. Do and will the polar regions and ocean processes play a key role in the global carbon cycle?	YES

Table 1. Key questions to the problem of global carbon cycle and climate and the role of polar regions.

based on (4) we have,

$$P_{CO_2} = \Phi \Sigma C \quad (6)$$

The carbon flux from ocean to atmosphere ($f_{O\alpha}$) would be proportional to P_{CO_2} . Then $f_{O\alpha} = K_{O\alpha} \Phi \Sigma C$ (7), where $K_{O\alpha}$ is a new constant characterizing the exchange rate. It is clear that accurate calculation of Φ and $K_{O\alpha}$ is difficult.

In this connection Revelle and Munk [1977] introduced a buffer factor characterizing the part of carbon absorbed by the ocean from the atmosphere.

Denoting the carbon content (partial pressure) at the initial state by $N_{mo} = \Phi_o(\Sigma C)_o$ and its deviation from initial state by $n_{mo} = \Phi \sigma(\Sigma C)$ based on (7) we have

$$f_{O\alpha} = K_{O\alpha}(N_{mo} + \xi n_{mo})$$

where $\xi = \frac{\delta P_{CO_2}/P_{CO_2}}{\delta \Sigma C/\Sigma C}$ is the buffer factor

$$\text{or } \xi = \left(1 + \frac{\delta \Phi}{\delta \Sigma C} \cdot \frac{\Sigma C}{\Phi}\right)$$

It is easy to see that dependence of parameter ξ on influencing factors is difficult to determine theoretically, but it has been found experimentally that ξ changes from about 7 at $t^\circ = 0^\circ\text{C}$ to 14 at 30°C . It is evident that with the past range of t° changes due to astronomical factors the change of carbon flux from ocean to atmosphere could reach tens of per cent.

THE RESULTS OF RECONSTRUCTING THE PAST CO₂ CONTENT WITH LINEAR BOX MODELS

Figure 1 presents the results of reconstruction with a box model of CO₂ content for the last 20,000 years [Borisenkov

and Kondratiev, 1988], using a 4-box linear model of Borisenkov and Altunin [1991] which includes atmosphere, biosphere, and active and deep oceanic layers. The model was integrated for 20,000 years back with a time step of 500 years. The exchange coefficient (the product of $K_{00}\alpha$ in formula (8)) was given in piecewise linear interpolation depending on paleotemperature. The Figure shows that the model reproduces quite well the minimum CO_2 content during the recent ice epoch. The CO_2 concentration variation follows that of paleotemperature.

Figure 2 gives the results of integrating the more sophisticated 8-box model of Altunin and Borisenkov [1991] for 140,000 years. The paleotemperatures were taken from Lorius et al. [1985].

The 8-box model of the global carbon cycle includes atmosphere, land biota, humus, oceanic inorganic carbon, phytoplankton, oceanic dissolved organic substance, oceanic sediment carbonate rock, and continental sediment rock. The rates of exchange between the atmosphere and land biota and humus depend to some extent on temperature. The rate of exchange between the atmosphere and the ocean, in particular the box of oceanic inorganic carbon, depends mainly on temperature. These exchange rates are taken from experimental data. The given version of box model was interpolated backward over 140,000 years with a time step of 100 years.

Since paleotemperature gives air temperature reproduction, and our calculations required ocean t° , it was assumed that ocean t° anomalies were 10% less than the corresponding air t° anomalies.

The water t° anomalies reconstructed in this way are shown in Figure 2a.

Numerical experimental data have shown that if the dependence of exchange coefficient t° is not considered, CO_2 concentration remains practically the same over the whole 140,000-year time interval, which should be expected.

If one disregards the dependence of CO_2 exchange between atmosphere and ocean (box of oceanic inorganic carbon) on t° , but includes that between atmosphere and biosphere (boxes of land biota and humus), weak variations in CO_2 content are observed which repeat t° variations (curve 2 in Figure 2b). However CO_2 variation amplitudes are far from real ones. When the dependence of CO_2 exchange coefficients between atmosphere and ocean on t° is considered, the agreement between measurements of CO_2 content (solid curve in Figure 2b) and values calculated from the model (dots with crosses) proves to be quite satisfactory.

This gives reason to assume that the past CO_2 content changes were determined most likely by natural processes and resulted from climate changes rather than vice versa.

In this connection one should very carefully estimate the possibilities of constructing scenarios of future climate caused by CO_2 content change on the basis of past warm epoch paleoclimates since absolutely different causes act here. It is worth mentioning that this conclusion does not contradict the conclusions of Broecker and Denton [1990] and of other authors that CO_2 changes could explain not more than 50% of climate changes which took place. What is more important is that climatic changes which were caused by astronomical factors determined CO_2 changes in the atmosphere.

To calculate ocean t° more exactly, the model of zero dimension can be accepted of the type,

$$\begin{aligned} C_1 \frac{d\Delta T_1}{dt} &= \Delta Q - \lambda_{12}(\Delta T_1 - \Delta T_2) - \lambda \Delta T_1 \\ C_2 \frac{d\Delta T_2}{dt} &= \lambda_{12}(\Delta T_1 - \Delta T_2) - \lambda_{23}(\Delta T_2 - \Delta T_3) \\ C_3 \frac{d\Delta T_3}{dt} &= \lambda_{23}(\Delta T_2 - \Delta T_3) \end{aligned} \quad (9)$$

here $C_1 = 0.45 \text{ W yr m}^{-2} \text{ }^\circ\text{C}^{-1}$ is the atmospheric heat capacity factor; $C_2 = 10 \text{ W yr m}^{-2} \text{ }^\circ\text{C}^{-1}$; $C_3 = 100 \text{ W yr m}^{-2} \text{ }^\circ\text{C}^{-1}$ are heat capacity factors of the active layer of ocean and of deep ocean respectively; $\lambda = 2.4 \text{ W m}^{-2} \text{ }^\circ\text{C}^{-1}$ is the parameter of climatic feedback; $\lambda_{12} = 45 \text{ W m}^{-2} \text{ }^\circ\text{C}^{-1}$ is the energy exchange factor between ocean and atmosphere; $\lambda_{23} = 4 \text{ W m}^{-2} \text{ }^\circ\text{C}^{-1}$ is the energy exchange factor between active and deep oceanic layers; ΔT_1 , ΔT_2 , ΔT_3 are anomalies of the mean t° of atmosphere, active and deep oceanic layers respectively. At the initial time moment (1860),

$$\Delta T_1 = \Delta T_2 = \Delta T_3 = 0$$

$$\text{with } t \rightarrow \infty \quad \Delta T_1 = \Delta T_2 = \Delta T_3 = \Delta T_{\text{eq}} = \frac{\Delta Q}{\lambda}$$

where ΔT_{eq} is the equilibrium atmospheric t° , and Q is the anthropogenic source. Figure 3 presents the results of model simulations described by the system of equations (9), for the scenario of anthropogenic source ΔQ using the data of Borisenkov and Kondratiev [1988]. It was taken that the equilibrium t°

$$\Delta T_{\text{eq}} = \frac{\Delta T(2 \times \text{CO}_2) \cdot \ln[N_1(t)/N_{10}]}{\ln 2} \quad (10)$$

It is clear that atmospheric t° is several decades behind the equilibrium t° due to the thermal inertia of the ocean. Further, behind CO_2 concentration variation are sea t° changes which influence the exchange between atmosphere and ocean. These time periods are tens of years, and considerable changes can take place in the ocean for this time.

Results mentioned in the WMO/UNEP report [1990] indicate that this is the case. This report contains much evidence showing that consideration of ocean leads to the lag of atmospheric and sea t° changes from respective equilibrium temperature. In the model under study for the atmosphere, model t° changes by 2000–2030 years are about 55% of equilibrium t° changes $\Delta T_{\text{eq}}(t)$. This conclusion is in good agreement with the results of other authors, in particular with the results of a recent study by Schlesinger and Jiang [1990].

DYNAMICS OF GREENHOUSE GAS ANTHROPOGENIC SOURCES

It is important to determine which dynamics of the anthropogenic source ΔQ should be prescribed in the model.

Many uncertainties and extremely high values of ΔQ corresponding to a maximum emission of anthropogenic carbon of up to 80–100 Gt yr⁻¹ in the near decades have led to overestimated values for Q . There several tens of scenarios at present for energetics development which are analyzed in Borisenkov and Kondratiev [1988].

The most realistic scenarios are determined by relationships of the type:

$$\begin{aligned} n_1(t) &= \frac{dQ}{dt} = R_0 \left(1 - \frac{Q}{Q_\infty}\right) \cdot Q \\ n_1(t) &= \frac{dQ}{dt} = R_0 \left[1 - \left(\frac{Q}{Q_\infty}\right)^n\right] \cdot Q \\ n_1(t) &= \frac{dQ}{dt} = R_0 \cdot Q^n \cdot e^{-mt} \end{aligned} \quad (11)$$

Here Q is the amount of carbon released to the atmosphere, Q_∞ is carbon reserves, R_0 is a parameter characterizing the rate of carbon growth, and n and m are some empirical parameters.

The scenarios of CO₂ emission dynamics determined from (11) depend first of all on the scenarios of energetics development. The maximum value $\frac{dQ}{dt}$ in some scenarios reached 80–100 Gt yr⁻¹, which is not realistic.

In most scenarios proposed, $\max \left(\frac{dQ}{dt}\right)$ amounts to 20–30 Gt of carbon per year, falling in the middle of the next century. The scenarios estimated in (11) depend to a considerable extent on parameters R_0 , n and m . The value Q_∞ corresponds to the forecasted supply of conventional fuel and was assumed equal to 600 Gt. The above three parameters were selected assuming that at $t=110$ (this corresponds to 1970) $Q=130$ Gt, and $\frac{dQ}{dt} = 5$ Gt yr⁻¹. These estimates are well confirmed experimentally. The parameter n was a varied one and was selected depending on scenarios of energetics development. In this case it was assumed that the maximum emission falls on 2030 and is 30 Gt yr⁻¹. Under these conditions $R_0=0.02$, $m_n=1.25$ and $n=1$.

Figure 4 gives the results of simulating the atmospheric carbon content on the basis of seven types of box models, beginning with a linear 9-box model and a nonlinear 7-box model and with sufficiently realistic scenarios for the dynamics of source $n_1(t)$, from Borisenkov and Altunin [1985]. This scenario is close to the scenario of the Institute of Applied System Analysis (Vienna).

The Figure shows that the range of possible CO₂ changes in the atmosphere is rather narrow. Maximum CO₂ concentrations in the atmosphere according to this model data would not exceed 2.0 to 2.5 times the pre-industrial level of 1860. Double CO₂ concentration is reached at the end of the 21st century or even the beginning of the 22nd century, not early in the 21st. This effect in the model is explained by considerable absorption by the ocean.

Bearing in mind that this model gives sufficiently good agreement between calculated CO₂ concentration for the industrial period of 1860–1960 and the past 130 years, one can hope that the above estimates should be relied upon.

It should be borne in mind that the greenhouse effect is influenced by other anthropogenic pollutants as well. As given in the WMO/UNEP report [1990], for the period 1765–1990 CO₂ yielded 61% of the contribution to the

greenhouse effect, methane 17%, stratospheric water vapor 6%, N₂O 4%, all freons CFCn 12%. The picture changed somewhat for 1980–1990 and this would characterize the future. Thus the CO₂ contribution was only 55%, the contributions of CH₄, stratospheric water vapor, N₂O and CFCn were 11, 4, 6 and 24% respectively. In other words, to consider completely the greenhouse effect, CO₂ growth of about 1% per year can be taken.

THE INFLUENCE OF DEEP OCEAN ON THE GREENHOUSE EFFECT

One approaches for modeling the carbon cycle and its CO₂ manifestations in the climate system seems to be prescribing a gradual increase of CO₂ at a rate of 1% per year, and its sudden doubling, as was done earlier. Besides, as we saw, the deep ocean processes should be included in the models. This should be done because, using real data, one cannot yet identify with assurance the global manifestation of the greenhouse effect in the climatic system components.

These manifestations of the greenhouse effect could be tropospheric t° rise and stratospheric t° fall, continental ice melting, sea level rise, and increase of atmospheric moisture content. Among these components we can best distinguish the really observed positive trend of mean t° near the earth's surface.

However, as is shown above, according to all model estimates the t° trend in the atmosphere and even more so in the ocean should be behind the CO₂ growth trend. Actually the reverse took place. The positive t° trend started at the beginning of the current century and reached its maximum in the 1930s. At that time the CO₂ trend was small. But in the 1940s when the positive trend of CO₂ concentration increased abruptly t° started falling. This gives reason to believe that the positive t° trend in the 1930s and 1940s was not related to CO₂ growth, and that it cannot be taken into account when attributing the observed t° trend to the greenhouse effect. Ellsaesser [1984] has the same viewpoint. This is even more evident if one takes into consideration that such warming periods in the history of climate took place several times, for example, in the first half of the 16th century [Borisenkov and Pasetsky, 1988]. These periods, including those in the 1930s and 1940s, were related to atmospheric circulation changes. If one subtracts the 1930s/1940s temperature trend from the total, the remaining trend shows a very weak component at noise level which does not correspond to temperature changes which should have taken place according to model (9). The actual t° trend after the 1930s and 1940s and up to the mid-1970s is opposite to the CO₂ trend. All this allows us to say that there are no reliable indications of greenhouse effect manifestations in the surface t° field. Nor are these indications found in other climate characteristics. Though some sections of the WMO/UNEP report [1990] are inconsistent, Wigley and Barnett [1990], the authors of section 8 of the report, state clearly that there are no reliable indications of greenhouse effect manifestations from observations.

This should not make the problem of the greenhouse effect and society's concern about its consequences less interesting. The question is whether we know reliably what the climatic consequences of a greenhouse effect would be and whether the future warming of climate with maximum warming in high latitudes is an accurate scenario.

One of these consequences, as mentioned above, is possible climate warming, on the average by 2–4°C, and in polar regions by 6–8°C. Although this viewpoint was most popular until recently, some scientists criticized it [Idso, 1982; Ellsaesser, 1984; Borisenkov and Kondratiev, 1988]. Recent numerical experiments made by Washington and Meehl [1989] and Washington [1989] have shown that this generally accepted scenario of future climate could hardly be considered reliable. Inclusion of deep ocean in model integration over 30 years with gradual yearly CO₂ increase of 1% leads to quite different scenarios of future climate compared to scenarios from models with sudden CO₂ doubling and disregarding deep ocean. These results are presented in Figure 5. When CO₂ increases by a factor of approximately 1.6–1.8 over the preindustrial level for 30 years the ocean is reconstructed so considerably that due to feedbacks weaker t° rise (by 2–3°C) occurred over continents. Over the north polar area, particularly in the Atlantic region, maximum t°C decrease by 6–8°C is observed (to 10–11°F) rather than maximum increase. In the southern hemisphere t° regime changes are insignificant. In this scenario the sea ice thickness increases by approximately 0.5 m. The southern boundary of polar ice shifts to the equator. Climate instability increases sharply.

This result radically changes the idea of climatic consequences of the greenhouse effect and recommendations on

taking preventive measures and is not unexpected in the light of the preceding discussion. Therefore all contrary scenarios of future climate relative to the greenhouse effect should be carefully analyzed and checked before planning preventive measures. For example, based on the scenarios of climate change toward warming, in the USSR suggestions were made to stop building ice-breakers since ice conditions in the Arctic would become less severe. Dangerous warnings are made regarding melting permafrost zones which occupy extensive areas in the USSR.

CONCLUSION

All the above gives reason to believe that science has not yet reliably provided conclusions on the manifestation of the greenhouse effect, and its climatic and social consequences. For this, further studies of the problem are necessary on an interdisciplinary basis. Society would have to pay a high price for ungrounded recommendations.

But in all cases it is evident that the focus of uncertainty in regional terms shifts to polar regions. In this connection the role of the polar regions in studying the given problem should be the leading one.

In conclusion it should be noted that the author did his best and tried to provide the answers to the questions in Table 1, understanding that the discussion of them cannot be considered finished.

REFERENCES

- Altunin, I. V., and E. P. Borisenkov, Description of atmospheric CO₂ dynamics on the time scale of 10 years (in Russian), *Acad. Sci. USSR Papers*, 316, 574–576, 1991.
- Bacastow, R., and E. Maier-Reimer, Ocean-circulation model of the carbon cycle, *Clim. Dynamics*, 4, 95–125, 1990.
- Barnola, J. M., D. Raynaud, Y. S. Korotkevich, and C. Lorius, Vostok ice core: 160000 year record of atmospheric CO₂, *Nature*, 329, 408–414, 1987.
- Borisenkov, E. P., and I. V. Altunin, Atmospheric CO₂ growth and its effect on climate (in Russian), *Acad. Sci. USSR Papers*, 281, 559–661, 1985.
- Borisenkov, E. P., and K. Ya. Kondratiev, Carbon cycle and climate. L., (in Russian), Gidrometeoizdat, 1988.
- Borisenkov, E. P., and V. M. Pasetsky, Thousand-year chronicle of extraordinary natural phenomena. M. (in Russian), *Mysl*, 1988.
- Broecker, W. S., and G. N. Denton, What drives glacial cycles?, *Scientific American*, 202, 1990.
- Budd W. F., and P. Rayner, Modelling global ice and climate changes through the ice ages, *Ann. Glaciol.*, 14, 1–17, 1990.
- Chappellaz, J. J., J. M. Barnola, D. Raynaud, E. C. Korotkevich, and C. Lorius, Ice core record of atmosphere methane over the past 160000 years, *Nature*, 345, 127–131, 1990.
- Ellsaesser, H. W., The climatic effect CO₂: a different view, *Atmos. Environ.*, 431–434, 1984.
- Idso, S. B., *Carbon Dioxide: Friend or Foe?* 92 pp., IBR Press, Tempe, Arizona, 1982.
- Lorius, C., et al., A 150000 year climate record from Antarctic ice, *Nature*, 316, 591–596, 1985.
- Manabe, S., and R. T. Wetherald, The effect of doubling the CO₂ concentration on the climate of a general circulation model, *J. Atmos. Sci.*, 32, 3–15, 1975.
- Revelle, R., and W. Munk, The carbon dioxide cycle and the biosphere, *J. Energy and Climate*, 140–158, 1977.
- Schlesinger, M. E., and X. Tiang, Simple model representation of atmosphere–ocean GCMs and estimation of the time scale, *J. Climate*, 3, 1297–1315, 1990.
- Shackleton, N. I., et al., Carbon isotope data in core V9-30. Confirm reduced carbon dioxide concentration in the age atmosphere, *Nature*, 306, 319–322, 1983.
- Washington, W. M. Where's the heat?, *Natural History*, No. 3, 69–72, 1990.
- Washington, W. M., and G. A. Meehl, Characteristics of coupled atmosphere–ocean CO₂ sensitivity experiments with different ocean formulations, 58 pp., Preprint, NCAR, Boulder, Colorado, 1989a.
- Washington, W. M., and G. A. Meehl, Climate sensitivity due to increased CO₂. Experiments with a coupled atmosphere and ocean general circulation model, *Clim. Dynamics*, 4, 1–38, 1989b.
- Wigley, T. M. L., and T. P. Barnett, Detection of the greenhouse effect in the observations. J. Rep. Scientific Assessment of Climate Change. Rep. for IPCC Work. Group 1. WMO/UNEP, 245–260, 1990.
- WMO/UNEP, Scientific assessment of climate change. Report prepared by working group 1, 1990.

The Influence of Arctic Haze and Radiatively Active Trace Gases on the Arctic Climate

J.-P. Blanchet

Canadian Climate Centre, Downsview, Ontario, Canada

ABSTRACT

Increasing fossil fuel consumption and industrial activities have raised concerns of possible man-induced climate changes. The changes result mostly from increased radiatively active trace gases (RAG) and anthropogenic aerosols in the atmosphere. Among the by-products of combustion, carbon dioxide is the leading RAG. Fossil fuel combustion also generates sulfates and soot, the principal constituents of the "Arctic haze." Both CO₂ and Arctic haze interact with radiative processes to produce external climate forcing. Due to their strong tendency to absorb visible solar radiation, soot particles result in strong diabatic heating in the Arctic. With a mixing ratio of 10-10, a concentration 1 million times less than H₂O, the solar radiative heating produced by particulate soot is still comparable to that of H₂O.

The Canadian Climate Centre (CCC) has recently completed a climate simulation with a double carbon dioxide scenario. Version II of the CCC-GCM includes a mixed-layer ocean and thermodynamic ice model. It allows for the evaluation of climate changes due to an external forcing. The aim of this paper is to compare the climate changes induced by increasing CO₂ and Arctic haze. Since both signals are occurring simultaneously, we must investigate the individual contributions with a climate model.

A preliminary sensitivity study of the Arctic haze (February to May) with interactive sea ice was done. The analysis suggests that the excess of solar radiative heating leads to increasing rates of snow and ice melt during spring and summer. The most sensitive regions are the Canadian Arctic Archipelago and the Greenland Sea. In both regions, the ice is substantially reduced. The anomaly of sea ice amount continues its propagation northward in June and July even though the Arctic haze is absent during that period. This result seems related to the reduction of the snow cover in the Spring. Another interesting result is the development of a systematic negative temperature anomaly in the lower stratosphere above the positive anomaly due to the Arctic haze in the lower troposphere. While the positive anomaly rapidly vanished after the removal of the haze (June-July), the negative stratospheric anomaly remains and propagates downward, resulting in a cooler summer at high latitudes. Those results are now investigated in a series of climate simulations.

AGASP-III, Polar Lows and CEAREX Norwegian Arctic Flight Program, Spring 1989

R. C. Schnell and P. J. Sheridan

Cooperative Institute for Research in Environmental Sciences, University of Colorado/NOAA, Boulder, Colorado, U.S.A.

J. D. Kahl

Department of Geosciences, University of Wisconsin-Milwaukee, Milwaukee, Wisconsin, U.S.A.

ABSTRACT

The third Arctic Gas and Aerosol Sampling Program (AGASP) intensive airborne research program was successfully conducted in the Norwegian Arctic, March–April 1989. Flying from Bodø, Norway, the NOAA WP-3D was utilized to study (1) two separate Polar Low systems that developed in the Greenland Sea; (2) the transfer of energy from the atmosphere to the ice over permanent pack ice north of Spitsbergen; (3) the transfer of wind and heat energy along the ice edge; and (4) Arctic haze (air pollution) and solar radiation distributions east of Spitsbergen. Participants were from three NOAA laboratories, three National laboratories, NASA, and nineteen universities, with representation from five countries.

These flights were coordinated with surface measurements at the Ny Ålesund Norwegian baseline station on Spitsbergen and the Office of Naval Research (ONR) Coordinated Eastern Arctic Experiment (CEAREX) "O" and "A" ice camps northwest of Svalbard.

In these latter flights, AGASP scientists continued their study of the photolytic destruction of tropospheric ozone in the Arctic spring boundary layer. A source for the Br molecule involved in the ozone destruction reaction has been suggested as being of under-ice origin released to the atmosphere as bromoform and bromodichloromethane. A marine or ice algae may be responsible.

From aircraft data on these flights, it was observed that the ozone destruction phenomenon may be capped by as little as a 0.2°C temperature inversion. Ozone destruction in the marine boundary layer over open water was not observed even on days when such destruction was observed 100 km further north over the Arctic ice pack.

	Mt C yr ⁻¹
Anthropogenic Influence	
Enteric Fermentation (domestic & wild animals)	60
Rice Paddies	80
Biomass Burning	40
Landfills	30
Coal Mining	30
Gas Prod. & Dist.	30
Subtotal	270
Natural Occurrence	
Termites	30
Wetlands	90
Oceans	8
Freshwaters	4
Methane Hydrates	4
Subtotal	136
TOTAL	406

Table 1. Annual methane carbon release rates (Mt yr⁻¹) from identified sources [adapted from Cicerone and Oremland, 1988]. Mt = 10¹² grams of methane carbon.

Sources of atmospheric methane have been qualitatively identified, and a candidate list has recently been constructed [Cicerone and Oremland, 1988]. Table 1, adapted from this list, gives estimates of the anthropogenically influenced and natural sources of atmospheric methane. The total annual methane release is estimated to be about 405 Mt (megatons = 10¹² g) of methane carbon. Of this amount, about one percent, or 4 Mt, of methane carbon is attributed to the decomposition of methane hydrates.

Methane hydrates are solid substances composed of rigid cages of water molecules that enclose mainly methane. The methane hydrate unit structure contains 46 water molecules and up to eight methane molecules, leading to a non-stoichiometric formula of CH₄·5.75 H₂O for a fully filled methane hydrate [Davidson, 1983]; a unit volume of methane hydrate can contain up to about 170 volumes of methane gas at standard conditions.

Besides requiring sufficient methane to stabilize the hydrate structure, methane hydrates can occur only under an appropriate set of pressure and temperature conditions (Figure 1). These conditions are found in continental sediments of permafrost regions and oceanic sediments of outer continental margins. The potential amount of methane in methane hydrates is very large, but estimates of the amount are speculative and range over about three orders of magnitude from 2 × 10³ to 4 × 10⁶ Gt of methane carbon [Trofimuk et al., 1977; Mciver, 1981; Dobrynin et al., 1981]. Recent estimates have converged on about 10⁴ Gt of methane carbon [Kvenvolden, 1988a; MacDonald, 1990] for oceanic gas hydrates and about 400 Gt of methane carbon for conti-

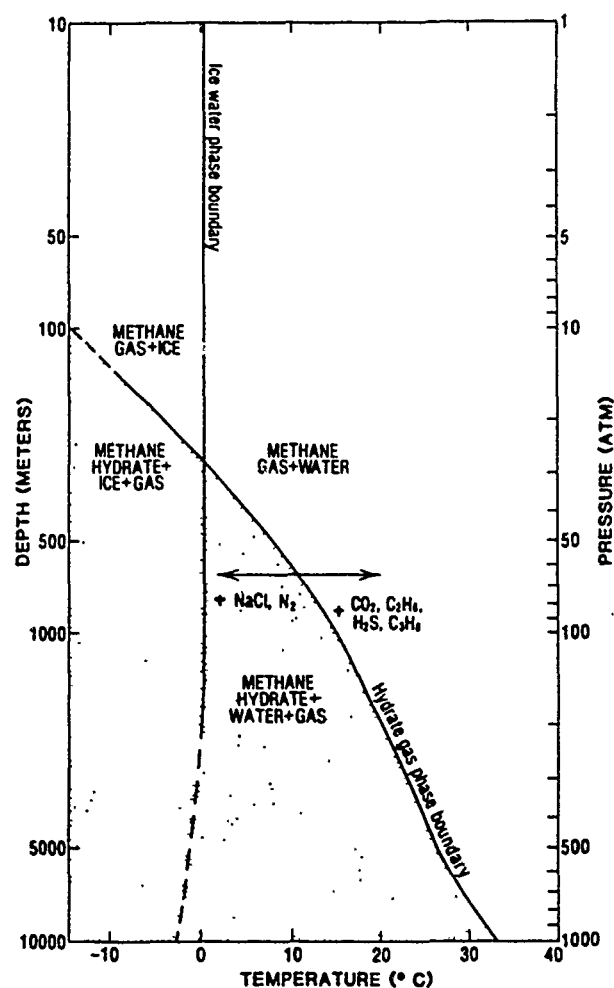


Figure 1. Phase diagram showing boundary between free methane gas (no stippling) and methane hydrate (stippling) for a pure water and pure methane system. Addition of NaCl to water shifts the hydrate-gas phase boundary to the left. Adding CO₂, H₂S, C₂H₆, and C₃H₈ to CH₄ shifts the boundary to the right, increasing the region of the gas hydrate stability field. For most naturally occurring gas hydrates, the effects approximately cancel each other. Depth scale assumes lithostatic and hydrostatic gradients of 0.1 atmospheres per meter. Drawn after Katz et al. [1959] and modified from Kvenvolden and McMenamin [1980].

mental gas hydrates [MacDonald, 1990]. This large reservoir of methane is located within 2000 m of the earth's surface.

Because methane hydrates are near to the surface, they are affected by surficial changes in pressure and temperature, and thus destabilized methane hydrates, which can potentially release enormous quantities of methane, are a likely candidate source of atmospheric methane. A question of current interest concerns the possible consequences of an addition of methane to the atmosphere from destabilized methane hydrates due to global change. Models of greenhouse warming predict that climate change will be accentuated in the Arctic [National Research Council, 1982]. Thus, gas hydrates of the Arctic will be most vulnerable to climate change. This paper examines gas hydrates of the Arctic and provides an estimate of the amount of methane being released from gas hydrates as a result of the present climatic regime.

GAS HYDRATES OF THE ARCTIC

Conditions for gas hydrate occurrence are met in three distinct environments in the Arctic Ocean region: (1) Offshore, in oceanic sediments of the outer continental margin where the combination of cold bottom water and high pressure from the water column establish the necessary stability conditions within the sediments beneath the sea floor to sub-bottom depths from about 300 to 700 m; (2) Onshore, in and beneath continuous permafrost, where surface temperatures are generally less than -5°C and the zone of methane-hydrate-stability ranges in subsurface depth from about 180 to 1200 m; and (3) On the nearshore continental shelf, where a comparable stability zone exists, and where relict permafrost has persisted since times of lower sea level when the present shelf, now covered with shallow sea water, was exposed to cold subaerial temperatures.

Offshore Oceanic Outer Continental Margins

Marine seismic reflection surveys conducted offshore from the northern coast of Alaska have shown the presence of an anomalous acoustic reflector that is located at depths which correspond to the base of the methane hydrate stability zone as determined by estimating temperatures and pressures [Grantz et al., 1976]. This anomalous seismic reflector is used to infer the presence of methane hydrates which extend over a region of more than 7200 km² offshore Alaska at water depths between 400 and 2800 m and within the oceanic sediments to subbottom depths ranging from 300 to 700 m. Kvenvolden and Grantz [1990] extrapolated this inferred occurrence of gas hydrates offshore northern Alaska to include the entire outer continental margin of the Arctic Ocean Basin, an area of about 700,000 km² (Figure 2). Using this area and estimates of sediment thickness, sediment porosity, and the yield of methane from gas hydrates, they calculated a total of 540 Gt of methane carbon in sediment at the outer continental margin of the Arctic Basin.

Onshore Continuous Permafrost Region

Since the 1940s, the pressure and temperature conditions of permafrost regions have been recognized as appropriate for gas hydrate occurrence [Katz, 1971]. The area of continuous onshore permafrost in the Arctic is approximately 7,000,000 km² (Figure 2); of this area about 700,000 km² is the potential region for gas hydrates, based on considerations of thermal gradients and the thickness requirements of permafrost. For example, in the Prudhoe Bay area of Alaska, gas hydrates can occur only where geothermal gradients are less than $3.7^{\circ}\text{C km}^{-1}$ and the base of permafrost is at depths greater than about 280 m [Collett, 1983]. These

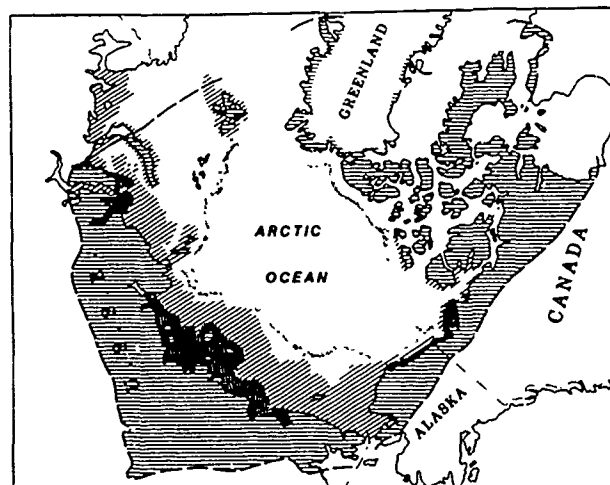


Figure 2. Map showing the Arctic regions where conditions for gas hydrate occurrences are possible: (1) region of continuous onshore permafrost (~7,000,000 km²) [horizontal lines]; (2) region of possible offshore permafrost (~2,200,000 km²) [diagonal lines]; (3) region of known offshore permafrost (~800,000 km²) [heavy stipple]; and (4) oceanic region of outer continental margin (~600,000 km²) [light stipple]. Within the regions of permafrost, the actual area where gas hydrates occur is probably one tenth of the area indicated as discussed in the text.

kinds of limitations reduce the potential region of gas hydrate occurrence by about a factor of ten in Alaska and, by inference, elsewhere. By the 1970s, well logging and formation tests had conclusively shown the presence of gas hydrates in the Messoyakha and Viluy fields of Siberia [Makogon, 1978] and in the Prudhoe Bay oil field of Alaska [reviewed by Kvenvolden and McMenamin, 1980]. Cherskiy et al. [1985] compiled geothermal data on four permafrost areas of the northern USSR, and MacDonald [1990] used this and other information to estimate that there are about 350 Gt of methane carbon stored in gas hydrates of Siberia (Table 2). In addition, MacDonald [1990] proposed that 50 Gt of methane carbon are present in the gas hydrates of the North American Arctic, for a total of 400 Gt of methane carbon in permafrost-associated gas hydrates of the Arctic, both onshore and offshore. This estimate is within the range of values of 75 to 1.8×10^4 Gt of methane carbon in gas hydrates as proposed by others [summarized by Kvenvolden, 1988b].

Region	Area of Gas Hydrate Stability (km ²)	Volume of Gas Stability Zone (m ³)	Methane Carbon in Gas Hydrates (Gt)
Timan-Pechora Province	6.7×10^4	2.7×10^{13}	10
West Siberian Platform	1.1×10^6	3.3×10^{14}	120
East Siberian Craton	1.8×10^6	8.1×10^{14}	150
Northeast Siberia	6.1×10^5	3.7×10^{14}	70

Table 2. Estimates of methane carbon (Gt) in gas hydrates of permafrost regions in Arctic USSR [MacDonald, 1990].

The presence of gas hydrates in the North American Arctic has been demonstrated. Well-log responses, consistent with the presence of gas hydrates, were obtained in the Mackenzie Delta [Bily and Dick, 1974; Judge, 1982]; Sverdrup Basin, Arctic Platform and Arctic Islands [Davidson et al., 1978; Judge, 1982]; and on the North Slope of Alaska [Collett, 1983]. Detailed reviews of well logs, well histories, drilling reports, core descriptions, and production tests from the North Slope of Alaska reveal gas hydrates in a restricted region of the Prudhoe Bay-Kuparuk River oil field area [Collett et al., 1989]. Most of the gas hydrates are patchy and occur in six laterally continuous sandstone and conglomerate units ranging in thickness from 2 to 28 m. The amount of methane present in the Prudhoe Bay-Kuparuk River area is estimated to be about 0.6 Gt of methane carbon.

Nearshore Continental Shelf Relict Permafrost Region

The amount of relict permafrost and associated gas hydrates beneath the shelf today depends upon the regression and transgression history, initial distribution of temperatures, ice content, gas content, and salinity in the sediment at the time of inundation. Offshore permafrost is known to occur on the Beaufort Sea shelf of Canada [Neave et al., 1978; Weaver and Stewart, 1982]. Also offshore permafrost occupies a part of the vast continental shelf of Siberia [Vigdorchik, 1980]. Studies by Rogers and Morack [1980] on subsea permafrost and sea level history lead to the inference that offshore permafrost may persist beneath any part of the Arctic shelf inshore from about the 90 m isobath. Based on this inference, the area of potential offshore permafrost is estimated to be about 3,000,000 km², and within this region there are about 800,000 km² where offshore permafrost is known to be present (Figure 2). About one tenth of these areas is assumed to contain gas hydrates based on constraints imposed by geothermal gradients and requirements for minimum thicknesses of permafrost, as discussed previously.

Evidence that gas hydrates are associated with offshore permafrost comes from the Mackenzie River delta area where well logs from offshore drilling indicated the presence of both permafrost and gas hydrates [Judge et al., 1987]. The observation of gas hydrates in this region suggests that gas hydrates are also present in other areas where offshore permafrost occurs. The distribution of gas hydrates associated with offshore permafrost is probably similar to that of gas hydrates associated with permafrost onshore; that is, the gas hydrates are restricted, patchy, and confined to porous sedimentary units as in the Prudhoe Bay-Kuparuk River area [Collett et al., 1989]. The amount of methane in gas hydrates associated with offshore permafrost can be estimated by utilizing the value of 400 Gt of methane carbon, determined by MacDonald [1990], as the total amount of methane in permafrost-associated gas hydrates, both onshore and offshore. The amount of methane in offshore gas hydrates is assumed to be proportional to the inferred area of gas hydrate occurrence in the known offshore permafrost region (80,000 km²) and the potential offshore permafrost region (300,000 km²) relative to the total potential area of gas hydrate occurrence in Arctic permafrost (1,000,000 km²). Thus, about 32 Gt of methane carbon is estimated to be present in gas hydrates associated with known offshore

permafrost and about 120 Gt of methane carbon to be present in the entire region where offshore permafrost is known or was possible in the recent past.

GLOBAL CHANGE

The total reservoir of methane carbon sequestered in gas hydrates of the Arctic is about 940 Gt, with 400 Gt [MacDonald, 1990] associated with permafrost and 540 Gt [Kvenvolden and Grantz, 1990] in outer continental margin sediments. Of the 400 Gt of methane carbon associated with permafrost, about 120 Gt are associated with offshore permafrost. Obviously these numbers are very speculative, but they provide a basis for attempting to judge the impacts of gas hydrates resulting from global change.

Because gas hydrates occur so near the surface, their stability is affected by pressure and temperature changes at the surface. Increases in pressure and decreases in temperature will tend to stabilize the gas hydrates, whereas the opposite changes, that is, a decrease in pressure and an increase in temperature, will destabilize the gas hydrate structure. Methane hydrates in each of the three distinct Arctic environments (offshore, onshore, and nearshore) are vulnerable to global change, but they are vulnerable to different extents depending on their settings.

Evidence already exists that warming of onshore permafrost is currently taking place. Lachenbruch and Marshall [1986] showed anomalous temperature profiles in the upper 100 m of permafrost in northern Alaska. They believe that these profiles indicate a varying but widespread secular warming of 2–4°C of the permafrost surface during the 20th century. These thermal changes will eventually penetrate deep enough to destabilize gas hydrates within and beneath the permafrost, but because of heat transfer properties as discussed in detail by MacDonald [1990], the time scale for these thermal changes is very large, requiring thousands of years before all gas hydrates are destroyed. For the present, however, gas hydrates associated with onshore permafrost have probably not felt the effect of permafrost warming.

Offshore, the outer continental margin sediments containing gas hydrates are under a column of very cold water (near 0°C) at pressures equivalent to 400–2800 m of water. Over the last 27,000 years the pressures on the offshore gas hydrates have probably slowly increased due to rising sea levels of about 100 m. Evidence for such a sea level rise has been obtained from boreholes in the Canadian Beaufort shelf [Hill et al., 1985]. Because circulation of Arctic Ocean water into the Canada Basin is restricted [Aagaard et al., 1985], this restriction may provide insulation against thermal changes in bottom waters at least for the present time. Therefore, these offshore gas hydrates, experiencing increased pressure and minimal temperature changes, are probably stable, and are a sink for methane and not a source. Even if small amounts of methane were being released from these gas hydrates, much of this gas would likely be dissolved in the water column or be oxidized to carbon dioxide.

The one environment of the Arctic where gas hydrates are currently vulnerable to global change is the region of offshore permafrost [Kvenvolden, 1988b]. Gas hydrates present within and under offshore permafrost are probably becoming unstable at least in part. The basic cause of the destabilization is the marine transgression that has taken place since the last ice age. On the Beaufort shelf, for exam-

ple, and probably on other continental shelves of the Arctic Ocean, sea level has risen significantly during the past 27,000 years [Hill et al., 1985] bringing cold water to an even colder surface. Before the marine transgression, the shelf was exposed to low subaerial temperatures of about -10°C [Lachenbruch, 1957], and these low temperatures promoted the development of permafrost. As the shelf is inundated by the advancing sea, the surface temperature of the shelf increases by about 10°C . The result is that the permafrost and any associated gas hydrates slowly degrade as a consequence of heat conducted downward from the sea floor and upward from the earth's interior at time scales measured in thousands of years. It is presumed, based on the work of Rogers and Morack [1980], that permafrost and gas hydrates were once present beneath the coastal shelf exposed during the last low-stand of sea level at about 90 m below present. Although rising sea level would have increased the pressure on the gas hydrates by about 9 atm, this pressure increase is more than offset by the 10°C temperature increase, leading to gas hydrate destabilization. Therefore, gas hydrates associated with offshore permafrost are currently being dissociated with a greater release of methane taking place farther offshore where the oceanic waters have warmed the colder shelf for a longer period of time. With global warming, the temperature of shelfal waters will likely increase and thus exacerbate the release of methane from gas hydrates associated with offshore permafrost. Clarke et al. [1986] suggested that cold plumes, seen on NOAA satellite photographs of Bennett Island in the Soviet Arctic shelf, resulted from methane released by the breakup of offshore permafrost and associated gas hydrates.

Given the present information concerning Arctic gas hydrates, it is not possible to calculate accurately the current rate of release of methane or to predict the future release expected due to global warming. Nevertheless, it is instructive to try to place some limits on gas hydrates as a source of atmospheric methane. It is assumed that gas hydrates associated with offshore permafrost are most vulnerable to global change and that about 120 Gt of methane carbon are available in these gas hydrates. Of this amount, 32 Gt of methane carbon are associated with known offshore permafrost. If during the last 27,000 years, 88 Gt (the difference between 120 and 32 Gt) of methane carbon were released from decomposing gas hydrates, then the rate of release would be about 3.3 Mt yr^{-1} of methane carbon. It is assumed

that the released methane is not trapped within the sediments but rather escapes to the atmosphere. This rate is slightly smaller than the "placeholder" estimate of 4 Mt yr^{-1} (Table 1) of Cicerone and Oremland [1988]. Although this amount of methane is small relative to most of the other candidate sources of atmospheric methane, the point to be emphasized is that this methane release is just the tip of an immense iceberg. That is, the large gas hydrate reservoir holds enormous quantities of methane which under accelerated temperature conditions could release amounts of methane that will contribute significantly to the atmosphere. If, for example, the time scale for release of methane from offshore permafrost-associated gas hydrates was only 2000 years instead of 20,000 years, then the calculated rate of release of methane would increase by an order of magnitude to about 30 Mt yr^{-1} . This value would place gas hydrates as one of the important candidate sources of atmospheric methane. With global warming, onshore gas hydrates will eventually be affected, creating a source of methane that is about a factor of two larger than that found in the nearshore environment. Even the gas hydrates in offshore outer continental margin sediments will ultimately experience the thermal effects of global warming, creating a larger potential source of methane.

SUMMARY

This paper contends that Arctic gas hydrates associated with offshore permafrost are presently more vulnerable to global climate change than are continental gas hydrates onshore or oceanic gas hydrates in outer continental margin sediments. Offshore permafrost-associated gas hydrates are undergoing significant global change caused by the transgression of marine waters over a previously exposed continental shelf. It is estimated that about 3 Mt yr^{-1} of methane carbon is released from these gas hydrates to the atmosphere. This rate of release of methane can be considered as the background contribution of methane hydrates to the atmosphere. With any increase in global warming, this contribution will increase, although at long time scales, until eventually all gas hydrates occurrences will be affected. Because the total amount of methane in the gas hydrate reservoir is so large, it is obvious that, wherever possible, efforts should be undertaken to minimize global trends which tend to destabilize these substances.

REFERENCES

- Aagaard, K., H. H. Swift, and E. C. Carmack, Thermohaline circulation in the Arctic Mediterranean Sea, *J. Geophys. Res.*, 90, 4833-4846, 1985.
- Bily, C., and J. W. L. Dick, Naturally occurring gas hydrates in the Mackenzie Delta, N.W.T., *Bull. Can. Petrol. Geol.*, 32, 340-352, 1974.
- Cherskiy, N. V., V. P. Tsarev, and S. P. Nikitin, Investigation and prediction of conditions of accumulation of gas resources in gas-hydrate pools, *Petrol. Geol.*, 21, 65-89, 1985.
- Cicerone, R. J., and R. S. Oremland, Biogeochemical aspects of atmospheric methane, *Global Biogeochem. Cycles*, 2, 299-327, 1988.
- Clarke, J. W., P. St. Amand, and M. Matson, Possible cause of plumes from Bennett Island, Soviet Far Arctic, *Am. Assoc. Petrol. Geol. Bull.*, 70, 574, 1986.
- Collett, T. S., Detection and evaluation of natural gas hydrates from well logs, Prudhoe Bay, Alaska, 78 pp., M.S. thesis, University of Alaska, 1983.
- Collett, T. S., K. J. Bird, K. A. Kvenvolden, and L. B. Magoon, The origin of natural gas hydrates on the North Slope of Alaska, in *Geologic Studies in Alaska* by the U.S. Geological Survey, 1988, edited by J. H. Dover and J. P. Galloway, pp. 3-9, *U.S. Geological Survey Bulletin* 1903, 1989.
- Davidson, D. W., Gas hydrates as clathrate ices, in *Natural Gas Hydrates: Properties, Occurrence and Recovery*, edited by J. Cox, pp. 1-16, Butterworth, Welbourn, Mass., 1983.
- Davidson, D. W., M. K. El-Defrawy, M. O. Fuglem, and

- A. S. Judge, Natural gas hydrates in northern Canada, in *Proceedings Third International Conference on Permafrost*, 1978, v. 1, pp. 938-943, National Research Council of Canada, Ottawa, Ontario, 1978.
- Dobrynin, V. M., Y. P. Korotajev, and D. V. Plyushev, Gas hydrates: a possible energy resource, in *Long-term Energy Resources*, v. 1, edited by R. F. Meyer and J. C. Olson, pp. 727-729, Pitman, Boston, Mass., 1981.
- Grantz, A., G. Boucher, and O. T. Whitney, Possible solid gas hydrate and natural gas deposits beneath the continental slope of the Beaufort Sea, *U.S. Geological Survey Circular 733*, 17 pp., 1976.
- Hill, P. R., P. J. Mudie, K. Moran, and S. M. Blasko, A sea-level curve for the Canadian Beaufort shelf, *Can. J. Earth Sci.*, 22, 1383-1393, 1985.
- Judge, A., Natural gas hydrates in Canada, in *Proceedings Fourth Canadian Permafrost Conference, 1981, Roger J. E. Brown Memorial Volume*, edited by M. H. French, pp. 320-328, National Research Council of Canada, Ottawa, Ontario, 1982.
- Judge, A. S., Permafrost base and distribution of gas hydrates, in *Marine Science Atlas of the Beaufort Sea—Geology and Geophysics*, edited by B. R. Pelletier, p. 39, *Geological Survey Canada, Misc. Report 40*, 1987.
- Katz, D. L., Depths to which frozen gas fields (gas hydrates) may be expected, *J. Petrol. Technol.*, 23, 419-423, 1971.
- Katz, D. L., D. Cornell, R. Kobayashi, F. H. Poettmann, J. A. Vary, J. R. Elenbass, and C. F. Weinaug, *Handbook of Natural Gas Engineering*, 802 pp., McGraw-Hill, New York, 1959.
- Kvenvolden, K. A., Methane hydrates—a major reservoir of carbon in the shallow geosphere?, *Chem. Geol.*, 71, 41-51, 1988a.
- Kvenvolden, K. A., Methane hydrates and global climate, *Global Biogeochem. Cycles*, 2, 221-229, 1988b.
- Kvenvolden, K. A., and A. Grantz, Gas hydrates of the Arctic Ocean region, in *The Arctic Ocean Region*, edited by A. Grantz, L. Johnson, and J. F. Sweeney, pp. 539-549, *The Geology of North America*, vol. 50, Geological Society of America, Boulder, Colorado, 1990.
- Kvenvolden, K. A., and M. A. McMenamin, Hydrates of natural gas: a review of their geological occurrences, *U.S. Geological Survey Circular 825*, 11 pp., 1980.
- Lachenbruch, A. H., Thermal effects of the ocean on permafrost, *Geol. Soc. Am. Bull.*, 68, 1515-1529, 1957.
- Lachenbruch, A. H., and B. V. Marshall, Changing climate: geothermal evidence from permafrost in the Alaskan Arctic, *Science*, 234, 589-696, 1986.
- MacDonald, G. J., Role of methane clathrates in past and future climates, *Climatic Change*, 16, 247-281, 1990.
- Makogon, Y. F., *Hydrates of Natural Gas* (Translated from Russian by W. Cieslewicz), 237 pp., Penn Well, Tulsa, Oklahoma, 1978.
- McIver, R. D., Gas hydrates, in *Long-term Energy Resources*, v. 1, edited by R. F. Meyer and J. C. Olson, pp. 713-726, Pitman, Boston, Mass., 1981.
- National Research Council, *Carbon Dioxide and Climate: A Second Assessment*, 72 pp., National Academy Press, Washington, DC, 1982.
- Neave, K. G., A. S. Judge, J. A. Hunter, and H. A. MacAulay, Offshore permafrost distribution in the Beaufort Sea as determined from temperature and seismic observations, *Geological Survey of Canada, Current Research, Part C, Paper 78-1C*, pp. 13-18, 1978.
- Rasmussen, R. A., and M. A. K. Khalil, Atmospheric methane in the recent and ancient atmospheres: concentrations, trends, and interhemispheric gradient, *J. Geophys. Res.*, 89, 11599-11605, 1984.
- Raynaud, D., J. Chappellaz, J. M. Barnola, Y. S. Korotkevich, and C. Lorius, Climatic and CH₄ cycle implications of glacial-interglacial CH₄ change in the Vostok ice core, *Nature*, 333, 655-657, 1988.
- Rogers, J. C., and J. L. Morack, Geophysical evidence of shallow nearshore permafrost, Prudhoe Bay, Alaska, *J. Geophys. Res.*, 85, 4845-4853, 1980.
- Stauffer, B., E. Lochbronner, H. Oeschger, and J. Schwander, Methane concentration in the glacial atmosphere was only half that of the pre-industrial Holocene, *Nature*, 332, 812-814, 1988.
- Trofimuk, A. A., N. V. Cherskiy, and kV. P. Tsarev, The role of continental glaciation and hydrate formation on petroleum occurrences, in *Future Supply of Nature-made Petroleum and Gas*, edited by R. F. Meyer, pp. 919-926, Pergamon, New York, 1977.
- Vigdorichik, M. E., *Arctic Pleistocene History and the Development of Submarine Permafrost* (Westview Special Studies in Earth Sciences), 286 pp., Westview Press, Boulder, Colorado, 1980.
- Weaver, J. S., and J. M. Stewart, In situ gas hydrates under the Beaufort Sea shelf, in *Proceedings Fourth Canadian Permafrost Conference, 1981, Roger J. E. Brown Memorial Volume*, edited by M. H. French, pp. 312-319, National Research Council of Canada, Ottawa, Ontario, 1982.

Methane and Nitrous Oxide in Arctic Permafrost

R. A. Rasmussen and M. A. K. Khalil

Institute of Atmospheric Sciences, Oregon Graduate Center, Beaverton, Oregon, U.S.A.

ABSTRACT

It is expected that, in the future, increasing levels of methane, nitrous oxide, and the chlorofluorocarbons (chlorotrifluoromethane and dichlorodifluoromethane) will together add significantly to global warming; perhaps as much as increasing levels of carbon dioxide. The present concentrations of methane are about 2.5 times more than normal interglacial levels, and concentrations of nitrous oxide are about 8% higher than during interglacial periods. According to our current understanding, these changes are caused primarily by increasing emissions due to human activities. The arctic permafrost is a large reservoir of methane and possibly also of nitrous oxide. In the future, as the polar regions warm from increasing CO₂ and trace gases, large quantities of methane and nitrous oxide may be released from the permafrost, causing a positive climatic feedback. We will show evidence for natural changes of CH₄ and N₂O during glacial and interglacial times. We will report our recent experimental results on the amount of methane and nitrous oxide in arctic permafrost and estimate the magnitude of the possible feedbacks.

AD-P007 359



92-17863



Depletion in Antarctic Ozone and Associated Climatic Change

M. Lal

Centre for Atmospheric Sciences, Indian Institute of Technology, New Delhi, India

ABSTRACT

Perhaps the most significant discovery in the atmospheric sciences in the last decade has been the observation of large decreases in ozone. These losses in ozone occur during austral spring, and from 1979 the severity of the depletion increased non-monotonically until September of 1987 when the lowest column ozone amounts ever recorded were observed in Antarctica. While the surprising "ozone hole" in the remote icy continent of Antarctica emphasizes the potential importance and complexity of processes in the high latitude stratosphere, it also motivated this study on the nature of greenhouse effect on polar climate due to perturbations in column ozone amount in association with observed increases in other trace gases in the Antarctic atmosphere. We have examined the potential climatic effects of changes in the concentration of greenhouse gases on thermal structure of the Antarctic atmosphere using both steady-state and time-dependent climate models. When we incorporate the greenhouse effect of increases in methane, nitrous oxide, carbon dioxide and chlorofluorocarbons in association with decrease in ozone at the levels of maximum concentration in our radiative flux computations for the Antarctic region, the net result is a surface warming which is in fair agreement with that inferred from mean Antarctic temperature series. Further, the stratospheric cooling due to the ozone hole phenomenon is not only restricted to low and middle stratosphere but also extends deep into the upper Antarctic stratosphere, particularly in the beginning of November. In view of this, it is possible that the polar stratospheric warming phenomenon associated with planetary wave events could be significantly disturbed by ozone depletion in the Antarctic atmosphere, leading to appreciable perturbations in the general circulation.

INTRODUCTION

Farman et al. [1985] were the first to show that an unprecedented depletion of the spring ozone column above Antarctica had taken place over the past decade. This intriguing phenomenon rapidly captured the attention of the international scientific community and a great deal has been learned in the past five years. The observed springtime ozone column amount in the Antarctic atmosphere has decreased by about 30% during the past decade, a magnitude far exceeding the climatological variability. These ozone changes are largely confined to the region at and below the altitudes where maximum number densities of ozone occur from about 10 to 20 km during the spring sea-

son and are generally associated with air within the polar vortex.

Several hypotheses on the causes of Antarctic seasonal decline in ozone have been advanced in recent years to explain the phenomenon [Solomon, 1990]. These include the idea that the hole is caused by upward atmospheric winds, that the resumption of high solar activity after polar night produces large amounts of ozone-destroying nitric oxide, or that the extreme cold temperatures and associated polar stratospheric clouds (that are most prevalent in the Antarctic atmosphere) lead to unusual chlorine chemistry due to anthropogenic halocarbon compounds, and eventual ozone destruction. While the Antarctic phenomenon may

not appear to be an immediate threat to worldwide ozone levels, there is concern that the ozone depletion may be a prelude to more widespread events. Of particular concern is that the observed changes in ozone could be linked to the observed increases in the trace gases that affect ozone, such as chlorofluorocarbons, methane and nitrous oxide. While this emphasizes the potential importance and complexity of processes in the high-latitude stratosphere, it also motivates a study on the nature of the greenhouse effect of polar climate due to perturbations in ozone amounts in Antarctica in association with observed changes in concentration of carbon dioxide, nitrous oxide and methane. It may be noted here that the Antarctic spring ozone decline is a unique event in both magnitude and persistence, thus inspiring both modeling and diagnostic studies.

We have examined the potential climatic effects of changes in trace gases at the surface and in the atmosphere over Antarctica using a local climate model described in Jain [1987] with inputs of Antarctic seasonal/monthly climatology. Both steady state and time-dependent calculations have been made to obtain the changes in surface temperature as well as the thermal structure of the Antarctic atmosphere.

MODEL DESCRIPTION

The model used for this study provides the requisite details in the radiation computations to account for the effects of perturbations in radiatively active trace constituents of the atmosphere in addition to several climatic feedback mechanisms. It has additional sources/sinks of energy from horizontal convergence (prescribed as seasonal meridional heat fluxes) due to climatological dynamics. This facilitates the applicability of the model to represent locally the polar atmospheres. For the Antarctic atmosphere, the local model extends from 60°S to 90°S with the underlying surface as snow/ice-covered land. The initial atmospheric composition, surface albedo and vertical distribution of temperature and clouds are prescribed in the model. The solar and thermal flux divergences averaged over clear and cloudy fractions are computed at 16 unequally spaced altitudes covering the lowest 54 km of the atmosphere. The surface boundary layer interacts with the snow/ice layer through the diffusion process to account for energy exchange between the surface and the atmosphere.

The vertical temperature profiles are computed by considering the two critical lapse rates to the local radiative-convective equilibrium, i.e., the lapse rate is constrained to be less than or equal to the appropriate temperature- and humidity-dependent adiabatic lapse rate at all levels and at the same time it is so constrained that its tropospheric mean value is less than the critical value calculated for baroclinic adjustment. For further details on computational aspects of the model, the reader is referred to Jain [1987] and Lal and Jain [1989].

THE INPUT DATA

The model requires climatological parameters which specify the seasonal mean zonally averaged climatic state. This input data serves as a basis for calculating zonally averaged temperature profiles for the atmosphere in radiative-convective equilibrium. In addition to this, we adopt the radiation budget of the Antarctic atmosphere from Ellis

[1978] to account for the net radiative imbalance due to the energy transported from the equator to the Antarctic region. Surface albedos are taken from Lian and Cess [1977]. For time-dependent numerical experiments, monthly mean climatology derived from various sources has been used [Ellis, 1978; Kukla and Robinson, 1980; Oort, 1983].

The atmospheric distributions of carbon dioxide, nitrous oxide, methane, water vapor, ozone and other radiatively active gases are compiled from a variety of sources [WMO, 1985; Bojkov, 1986; Ramanathan et al., 1987; GMCC, 1986, 1987; Komhyr et al., 1988] and prescribed in the model. The scenarios on trace gas perturbations are based on changes in their concentrations in the past decade (1978–1987).

Two sets of numerical experiments have been performed using the local climate model and the input data described above. In the first experiment, we examine the steady-state surface temperature changes due to the ozone loss in the Antarctic atmosphere without and with the observed perturbations in anthropogenic greenhouse gases. In another set of experiments, we have made a time-dependent simulation of the vertical temperature profile with standard ozone distribution (long-term monthly mean for the Antarctic atmosphere) and with the observed monthly ozone distribution for the year 1987. The findings of these numerical experiments are described in the following section.

RESULTS AND DISCUSSION

Table 1 summarizes the equilibrium surface temperature and its change for a uniform reduction of 30% ozone for levels of maximum concentration in the Antarctic atmosphere (between 10 and 30 km). The surface temperature obtained

Case	Antarctic Atmosphere (spring)
Equilibrium Surface temperature (unperturbed case)	232.19 K
a) Change in surface temperature $\Delta O_3/O_3 = -30\%$ ($10 \leq z \leq 30$ km)	-0.47 K
b) Change in surface temperature $\Delta O_3/O_3 = -30\%$ ($10 \leq z \leq 30$ km) $\Delta CH_4 = +1.94\%$	-0.09 K
c) Change in surface temperature $\Delta O_3/O_3 = -30\%$ ($10 \leq z \leq 30$ km) $\Delta CH_4 = 1.94\% + \Delta CO_2 = 3.64\%$	0.31 K
d) Change in surface temperature $\Delta O_3/O_3 = -30\%$ ($10 \leq z \leq 30$ km) $\Delta CH_4 = 1.94\% + \Delta CO_2 = 3.64\% + \Delta N_2O = 2.17\%$	0.37 K

Table 1. Model-computed surface temperature and its change due to perturbation in trace gases at Antarctica.

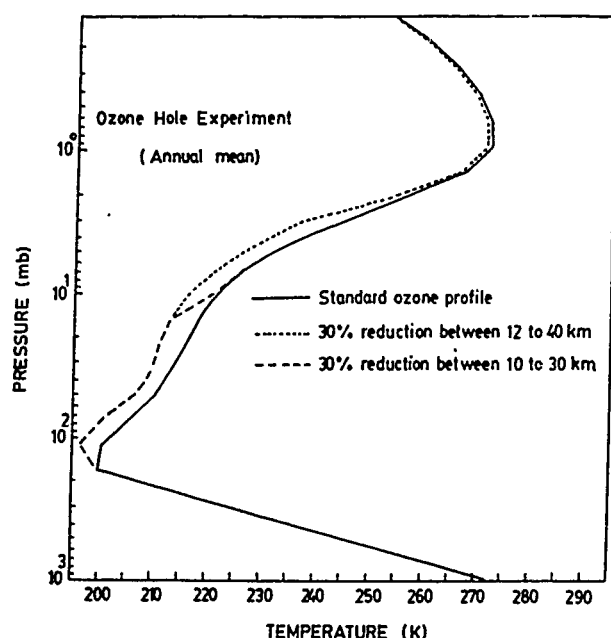


Figure 1. Model-simulated vertical temperature profiles for annual mean Antarctic atmosphere with and without ozone hole.

in model computations for the Antarctic atmosphere is in good agreement with climatology. The reduction of ozone between the levels of maximum concentration (10 to 30 km) leads to surface cooling on the order of 0.47 K. When observed increases in atmospheric methane are accounted for in our model calculations together with the ozone depletion, the surface cooling is reduced to only 0.09 K. When we incorporate the greenhouse effect of the observed increases in both methane and carbon dioxide in association with decrease in ozone at the levels of maximum concentration in our radiative flux computations, the result is a surface warming of about 0.31 K. The effect of observed increases in nitrous oxide with those of methane and carbon dioxide, together with the decline in ozone, is a net increase in surface temperature by 0.37 K. This model-computed surface warming of 0.37 K is in agreement with that inferred from the observed seasonal mean Antarctic temperature series [Raper et al., 1984], which shows a warming trend from about 1960 until the mid 1970s (a positive linear trend in temperature anomaly for the period 1955/58 to 1982 has been reported as 0.36 K for the spring season).

The surface temperature change is apparently sensitive to the altitude at which the decrease in ozone begins. A decrease in the stratospheric ozone, irrespective of the altitude of the decrease, would lead to an increase in the solar radiation reaching the troposphere. However, ozone also alters the longwave emission from the stratosphere in two ways. First, the decreased solar absorption (due to ozone decrease) cools the stratosphere; the cooler stratosphere emits less downward IR to the troposphere. Second, a decrease in ozone reduces the absorption (by the $9.6 \mu\text{m}$ band of ozone) of the surface-troposphere emission. This reduction causes an additional cooling of the stratosphere which in turn causes an additional reduction in the downward IR emission by the stratosphere. Thus the IR effects of ozone decrease tend to cool the surface. However, the IR

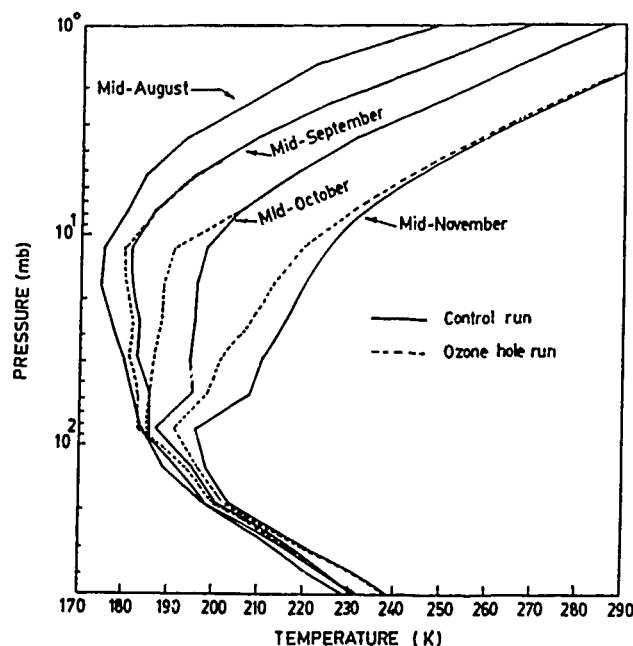


Figure 2. Model-simulated vertical temperature profiles for Antarctic atmosphere with monthly mean climatology (August to November).

opacity of the stratospheric carbon dioxide, water vapor and ozone is sufficiently strong that the impact of the reduction in IR emission (by the stratosphere) on the surface diminishes with an increase in altitude of ozone perturbation. On the other hand, the surface warming induced by the solar effect is independent of the altitude of ozone perturbations. Consequently, for a decrease in ozone in the upper stratosphere, the solar effect dominates, while for a decrease in the lower stratospheric ozone, the IR effect dominates. This can best be illustrated by the following: For the Antarctic atmosphere, the 30% reduction in ozone between 12 and 40 km causes a cooling of only 0.31 K, as compared to 0.47 K for the same ozone reduction between 10 and 30 km. Thus, lowering the altitude of stratospheric ozone reduction leads to enhanced cooling at the surface.

The annual mean temperature profiles of the Antarctic atmosphere simulated by the model for standard ozone distribution and for ozone distribution with 30% reduction in ozone mixing ratio between 10 to 30 km and 12 to 40 km are depicted in Figure 1. The 30% decline in ozone between 10 to 30 km causes about 5 K cooling in the lower stratosphere. However, if the ozone loss is shifted to higher levels (between 12 and 40 km), the stratospheric cooling extends to the middle and upper stratosphere also.

Figure 2 illustrates the vertical temperature profiles of the Antarctic atmosphere for standard ozone distribution (long-term monthly averages) as well as for the ozone loss observed in the months from August to November 1987. We observe that the Antarctic ozone hole observed in the year 1987 could have caused the lower stratosphere to cool by about 9 K in the month of October. This stratospheric cooling gradually extends to middle and upper stratosphere by mid-November. The magnitude of stratospheric cooling obtained in our model simulation as a result of ozone decline in the Antarctic atmosphere could lead to substantial perturbations in the dynamics of the polar atmosphere.

REFERENCES

- Bojari, R. D., The 1979–1985 ozone decline in the Antarctic as reflected in ground-based observations, *Geophys. Res. Lett.*, **13**, 1236–1239, 1986.
- Ellis, J. S., Cloudiness, the planetary radiation budget and climate, Ph.D. Thesis, 240 pp., Colorado State University, Ft. Collins, CO, 1978.
- Farman, J. C., B. G. Gardiner, and J. D. Shanklin, Large losses of total ozone in the Antarctic reveal seasonal ClO_x/NO_x interaction, *Nature*, **315**, 207–210, 1985.
- GMCC, Geophysical monitoring for climatic change, *NOAA/ERL Summary Report 1985*, No. 14, 146 pp., edited by R. C. Schnell, 1986.
- GMCC, Geophysical monitoring for climatic change, *NOAA/ERL Summary Report 1986*, No. 15, 155 pp., edited by R. C. Schnell, 1987.
- Jain, A. K., Climate sensitivity studies with radiative-convective models, Ph.D. Thesis, 199 pp., Centre for Atmospheric Sci., Indian Inst. of Technology, New Delhi, India, 1987.
- Komhyr, W. D., P. R. Franchois, S. E. Kuester, P. J. Reitelbach, and M. L. Fanning, ECC Ozone-sonde observations at South Pole, Antarctica during 1987, *NOAA Data Rep. ERL/APL-15*, 319 pp., 1988.
- Kukla, G., and D. Robinson, Annual cycle of surface albedo, *Mon. Wea. Rev.*, **108**, 56–68, 1980.
- Lal, M., and A. K. Jain, Increasing anthropogenic constituents in the atmosphere and associated climatic changes, in *Encyclo. Environ. Cont. Technol.*, Vol. 2, edited by P. N. Cheremisinoff, pp. 735–762, 1989.
- Lian, M. S., and R. D. Cess, Energy balance climate models: A reappraisal of ice-albedo feedback, *J. Atmos. Sci.*, **34**, 1058–1062, 1977.
- Oort, A. H., Global atmospheric circulation statistics: 1958–1973, *NOAA Prof. Paper 14*, 180 pp., 1983.
- Raper, S. C., T. M. L. Wigley, P. R. Mayer, P. D. Jones, and M. J. Salinger, Variations in surface air temperature, Pt. 3: The Antarctic; 1957–82, *Mon. Wea. Rev.*, **112**, 1341–1353, 1984.
- Ramanathan, V., L. Callis, R. Cess, J. Hansen, I. Isaksen, W. Kuhn, A. Lacis, F. Luther, J. Mahlman, R. Reck, and M. Schlesinger, Climate-chemical interactions and effects of changing atmospheric trace gases, *Rev. Geophys.*, **25**, 1441–1482, 1987.
- Solomon, S., Antarctic Ozone—progress towards a quantitative understanding, *Nature*, **347**, 347–354, 1990.
- WMO, Atmospheric ozone: Assessment of our understanding of the processes controlling its present distribution and change, *Rep. 16, Global Ozone Res. and Moni. Proj.*, pp. 88–100, Geneva, 1985.

Contamination of the Arctic Air During the Megahaze Vent in Late Winter, 1986

M. Djupström

Department of Physics, Chalmers University of Technology, Gothenburg, Sweden

J. M. Pacyna

Norwegian Institute for Air Research, Lillestrøm, Norway

G. E. Shaw

Geophysical Institute, University of Alaska Fairbanks, Fairbanks, Alaska, U.S.A.

J. W. Winchester

Department of Oceanography, Florida State University, Tallahassee, Florida, U.S.A.

S.-M. Li

National Center for Atmospheric Research, Boulder, Colorado, U.S.A.

ABSTRACT

The Arctic offers an opportunity to study the alterations of geochemical cycles of various compounds by human activity. The potential of the compounds to accumulate in the environment is a significant factor when studying these alterations.

Three measurement campaigns were carried out in various parts of the Arctic at Poker Flat, Alaska; Barrow, Alaska; and Ny Ålesund, Spitzbergen during the late winter of 1986. Enhanced concentrations of several components were measured at all these stations for periods lasting from a few days to several weeks. The chemical composition of aerosols and analyses of the meteorological conditions during these periods have revealed a coherent picture pointing to potential sources of these compounds in Eurasia, and particularly in the northern Soviet Union, and probable transport pathways. The pathways can be indicated by surge events across the Soviet Arctic coast towards Barrow and return flows towards Spitzbergen.

Evenly distributed concentrations of anthropogenic compounds suggest their rather limited en-route deposition in the arctic winter. However, due to the extended time of the episodes and their intensity, some compounds may accumulate in the Arctic environment. Very high enrichment factors of As, Cd, Pb, Sb, Se, and Zn in the Arctic seem to indicate that the geochemical cycles of these compounds have been altered on a global scale.

92-17864



AD-P007 360



Individual Particle Analysis of the Springtime Arctic Aerosol, 1983-1989

Patrick J. Sheridan and Russell C. Schnell

Cooperative Institute for Research in Environmental Sciences, University of Colorado/NOAA, Boulder, Colorado, U.S.A.

Jonathan D. Kahl

Department of Geosciences, University of Wisconsin-Milwaukee, Milwaukee, Wisconsin, U.S.A.

ABSTRACT

During the springs of 1983, 1986 and 1989, the Arctic Gas and Aerosol Sampling Program (AGASP) conducted major aircraft-based field experiments over much of the western Arctic. As part of the AGASP research efforts, several regions of the springtime Arctic atmosphere were probed by the NOAA WP-3D Orion research aircraft. These included the marine boundary layer over open water, the surface inversion layer over the pack ice, the "background" free troposphere, the frequently encountered Arctic haze layers, and the lower stratosphere.

Size segregated aerosol samples were collected from these air masses using a three-stage cascade impactor mounted on the aircraft. Individual particle analysis using analytical electron microscopy was performed on each collection substrate to reveal particulate morphology, size distribution and elemental composition information. Results of our studies show that (1) Arctic haze layers are composed largely of sulfates and anthropogenic particles, (2) the synoptic meteorology is an important factor which influences the magnitude of the pollution component in the haze, and (3) the stratospheric aerosols are predominantly H_2SO_4 droplets, with the exception of those collected in 1983, which showed relatively high crustal particle concentrations due to volcanic debris.

INTRODUCTION

Air pollution in the Arctic, especially during the springtime, is now a familiar and well-documented phenomenon, and one that has been intensively studied since the mid-1970s (see reviews by Rahn [1985] and Barrie [1986]). Results from many of these studies show that these Arctic haze aerosols undergo periodic fluctuations in concentration and composition, which have been linked to episodic transport from the middle latitudes [Barrie et al., 1981; Lowenthal and Rahn, 1985; Raatz, 1985]. Chemical analyses of the aerosols suggest a strong pollution component to the haze, one which may be capable of significantly disturbing the radiative balance in the Arctic [Valero et al., 1984; Wendling et al., 1985; Blanchet, 1989].

The major purpose of the international Arctic Gas and Aerosol Sampling Program (AGASP) research expeditions was to determine the distribution, transport, chemistry, aero-

sol physics and radiative effects of Arctic haze. The programs consisted of airborne gas, aerosol, radiation and meteorology measurements tied to similar baseline station measurements at Pt. Barrow, Alaska; Alert, Northwest Territories; and Ny Ålesund, Spitsbergen. During peak operations, the AGASP project included over 150 people from government research agencies and universities in the United States, Canada, Norway, Sweden, Denmark and the Federal Republic of Germany [Schnell et al., 1989].

The results presented in this paper focus primarily on the anthropogenic pollution component in Arctic haze layers. However, aerosol samples collected within the Arctic stratosphere, free troposphere (not in haze layers) and above-ice surface inversion layers are also discussed. When appropriate, meteorological analyses have been presented to show long-range transport of haze associated with mid-latitude sources.

METHODS

Atmospheric aerosols were sampled during the three AGASP field experiments using a three-stage, single orifice cascade impactor. The orientation and operation of this sampler have been described in detail elsewhere [Sheridan and Musselman, 1985; Sheridan, 1989a,b]. Typical sampling periods were 10–15 min., permitting sufficient temporal and spatial resolution of discrete air masses.

Particles were deposited onto thin formvar films supported by 200-mesh TEM grids, which were positioned directly behind the jet nozzle on each impactor stage. The manufacturer's stated aerodynamic cutoff diameters (ACDs) for the three stages are: Stage 1 - 4 mm; Stage 2 - 1 mm; Stage 3 - 0.25 mm. Under sampling conditions of flow and pressure similar to those encountered in the field, laboratory tests show that efficient collection of particles down to 0.1 mm in diameter was realized.

Particles were analyzed using a Japan Electron Optics Laboratory (JEOL) 200 kV analytical electron microscope (AEM) interfaced to an ultrathin window (UTW) x-ray spectrometer, multichannel analyzer and dedicated microcomputer. The positions of all particles in a given field-of-view (FOV) were recorded, so that subsequent x-ray analyses of all particles could be performed before continuing to another FOV. The UTW detector permitted elemental analysis down to B ($Z=5$); thus the interesting light elements C, N and O were detectable in individual particles. In addition to particulate chemistry information, the AEM also provided valuable morphological and mineralogical data, which were quite useful when proposing sources for the aerosol. As with the sampler, details of the analytical instrumentation and procedures have been reported previously [Sheridan and Musselman, 1985; Sheridan, 1989a,b].

RESULTS

The approximate flight tracks for the three AGASPs are shown in Figure 1. The AGASP-I (1983) field experiment was the largest of the three in terms of flight hours and areal coverage, spending significant time in both the North American and European Arctic. The AGASP-II (1986) project was based in Anchorage, Alaska and Thule, Greenland, and was conducted solely in the North American Arctic. The AGASP-III (1989) experiment was an extensive European Arctic mission conducted out of Bodo, Norway.

AGASP-I

Arctic haze layers encountered during AGASP-I flights generally showed a stronger and fresher pollution component than did those from the more recent missions (with the exception of haze observed on the first AGASP-II flight). Fine liquid (i.e., not significantly unneutralized) H_2SO_4 droplets were observed in numbers several orders of magnitude higher than other particle types. Both combustion (soot) and non-combustion (probably organic) varieties of carbonaceous particles were identified. Spherical particles and aggregates of probable combustion origin were encountered with likely sources (based on composition) being non-ferrous smelters, heavy industry, incinerators, coal- and oil-fired combustion, and possibly wood smoke. Other particle types, including crustal and marine particles, also suggested distant sources for the haze aerosol. Several types of particles observed in AGASP-I haze layers are shown in Figure

2, along with their respective x-ray spectra.

Meteorological and air trajectory analyses indicated that organized transport episodes occurred which moved air from within the Soviet Union and Central Europe to the Alaskan and Norwegian research areas prior to and during our operations there [Harris, 1984; Raatz, 1985]. The Eurasian areas targeted as source regions by the trajectories are consistent with the type of Arctic aerosol source areas we would expect, since they are highly industrialized with little pollution control and are usually situated north of the springtime Eurasian polar front. During most Arctic winters/springs, the synoptic meteorology responsible for this efficient tropospheric transport becomes a quasi-persistent feature [Raatz, 1989]. "Atypical" years (such as that of winter/spring 1989), and how they may affect atmospheric transport and Arctic aerosol concentrations, will be discussed below.

Stratospheric aerosol samples were collected anytime the aircraft flew above the relatively low Arctic tropopause. The stratospheric aerosols collected during AGASP-I showed a distinct bimodal size distribution. The fine particle mode, which dominated the number-size distribution, was centered at 0.3–0.4 μm diameter, and was composed almost totally of liquid H_2SO_4 droplets. The coarse particle mode was centered at 1–2 μm diameter, and the particles appeared by morphology and composition to be predominantly of crustal origin. Several researchers have attributed these coarse crustal-type particles in the stratosphere to the El Chichon volcanic eruption, which occurred approximately one year prior to AGASP-I sampling [Shapiro et al., 1984; Raatz et al., 1985; Winchester et al., 1985].

AGASP-II

The first three flights of the AGASP-II experiment were conducted in the Alaskan Arctic. The research areas for these flights were out over the Beaufort Sea, north and northeast of Barrow, Alaska. During the first flight, an extremely dense haze layer was encountered, heavier than those observed during any of the AGASP field experiments. Within this haze event, condensation nuclei (CN) counts exceeded $10,000 \text{ cm}^{-3}$, aerosol scattering extinction coefficients (b_{sp}) were $>80 \times 10^{-6} \text{ m}^{-1}$, and SO_2 concentrations reached 15 pptv [Herbert et al., 1989; Thornton et al., 1989]. Most of the fine aerosol particles were H_2SO_4 , probably being formed *in situ* during transport [Herbert et al., 1989]. Meteorological analyses, along with surface air quality measurements in Norway, suggest that the haze originated in Central Europe ten days earlier [Bridgman et al., 1989]. The transport pathway followed a pattern characteristic of spring haze transport in the Arctic [Raatz, 1989].

Haze layers observed on the second and third AGASP-II flights were much lighter and the pollution constituents less concentrated than on the first flight. Trajectories for these flights showed no direct, organized transport from the usual source regions. Instead, the trajectories originated or spent significant time over the Central Arctic Basin or the Canadian Archipelago [Herbert et al., 1989].

One aerosol sample collected in the troposphere over south-central Alaska was found to contain high concentrations of soil-derived particles, with little associated V_2SO_4 [Sheridan, 1989a]. This aerosol was probably a pocket of suspended ash from Mt. Augustine volcano in southern

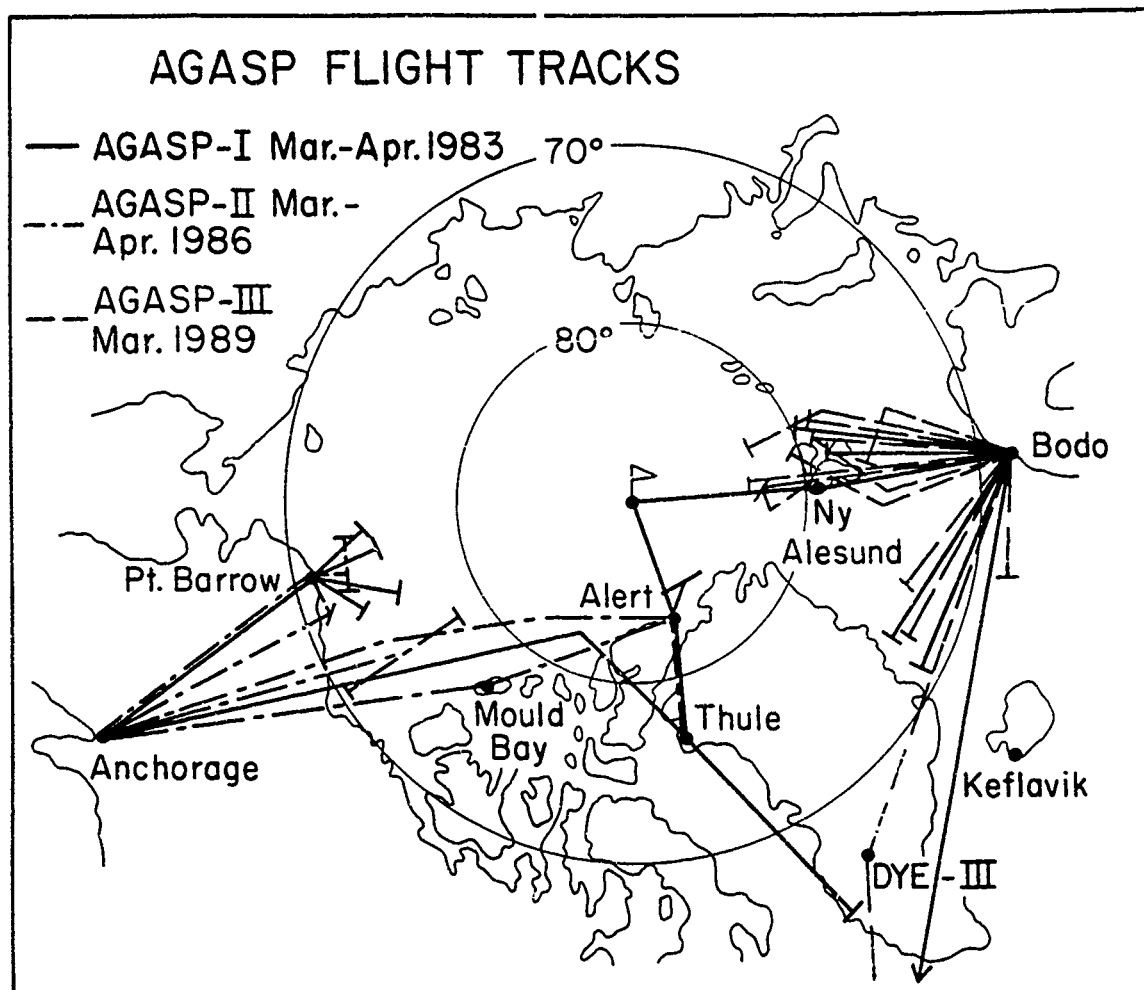


Figure 1. Approximate flights tracks for the three AGASP field experiments.

Alaska, which erupted 9–13 days earlier. Characterization of this sample using our AEM showed particles with compositions and morphologies closely resembling the bulk Mt. Augustine ash [Yount et al., 1987]. In Figure 3, photomicrographs and x-ray spectra representing this crustal material and several other types of particles observed in AEM analysis of AGASP-II samples are shown.

The final three flights of AGASP-II included ferry/research missions to and from Thule, Greenland, and a research mission based at Thule. The haze observed in the Canadian and Greenland Arctic was well-aged and mixed throughout the troposphere in concentrations below that of the haze observed in the Alaskan Arctic in previous weeks. Tropospheric samples collected on these flights may represent "background" springtime Arctic aerosol conditions [Sheridan, 1989b]. Stratospheric aerosol collected on these flights was characterized by a dominant fine H_2SO_4 component, with very few larger crustal-type particles. In contrast to the violent eruption of the El Chichon volcano which perturbed the stratospheric aerosol for several years, this suggests that the eruption of Mt. Augustine just prior to the start of AGASP-II was not powerful enough to inject significant quantities of crustal material into the stratosphere over the North American Arctic.

AGASP-III

Cascade impactor aerosol samples from the 1989 AGASP-III experiment in the Norwegian Arctic have been recently analyzed. Visual observations from the aircraft and electron microscope analyses of the samples suggest that the haze was consistently of the light, "background" variety (i.e., well-aged and mixed) rather than the concentrated type resulting from rapid transport from industrialized source regions.

Instead of finding high numbers of fine H_2SO_4 droplets as in previous AGASP missions, most AGASP-III haze samples contained more moderate concentrations of fine, solid (highly neutralized) sulfate particles. The neutralization of this sulfate supports the concept of a well-aged aerosol, in that the low ambient levels of NH_3 in the Arctic would suggest that the aerosol may have been present in the Arctic atmosphere for up to several weeks before becoming fully neutralized.

Most of the other observed types of aerosol particles could be classified as soil-derived or marine. An occasional combustion sphere or other pollution-derived particle was encountered in most samples, but not in numbers that would suggest they comprised a significant portion of the aerosol.

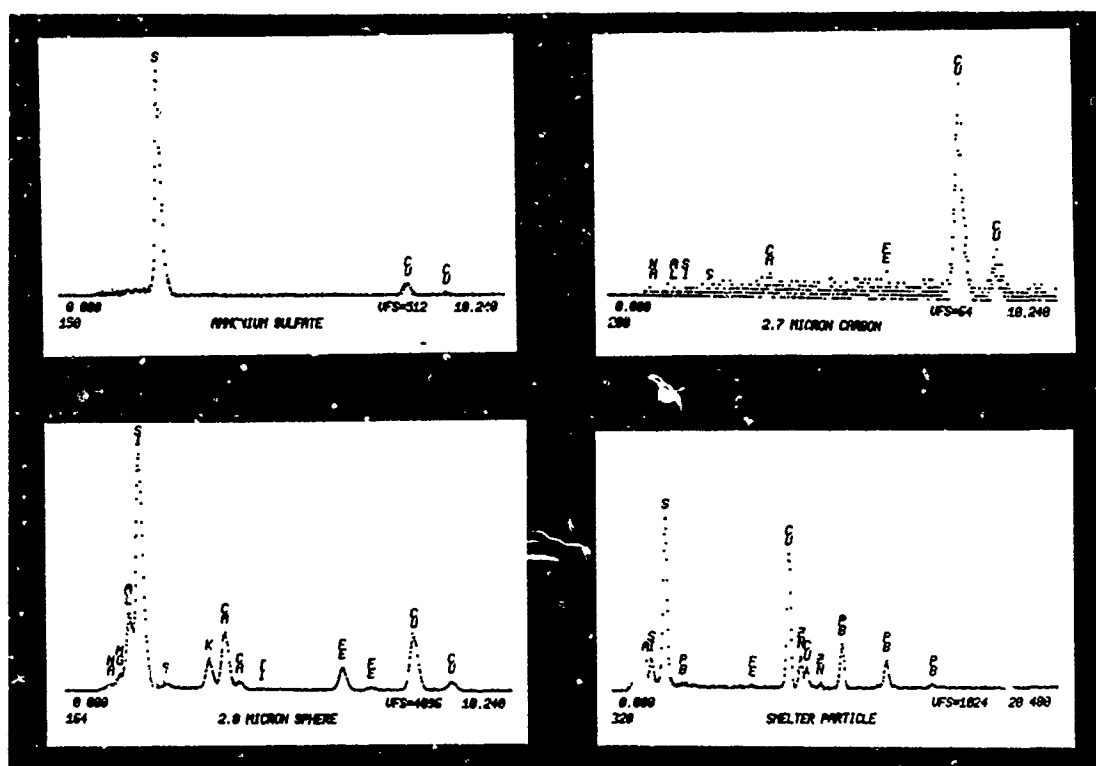
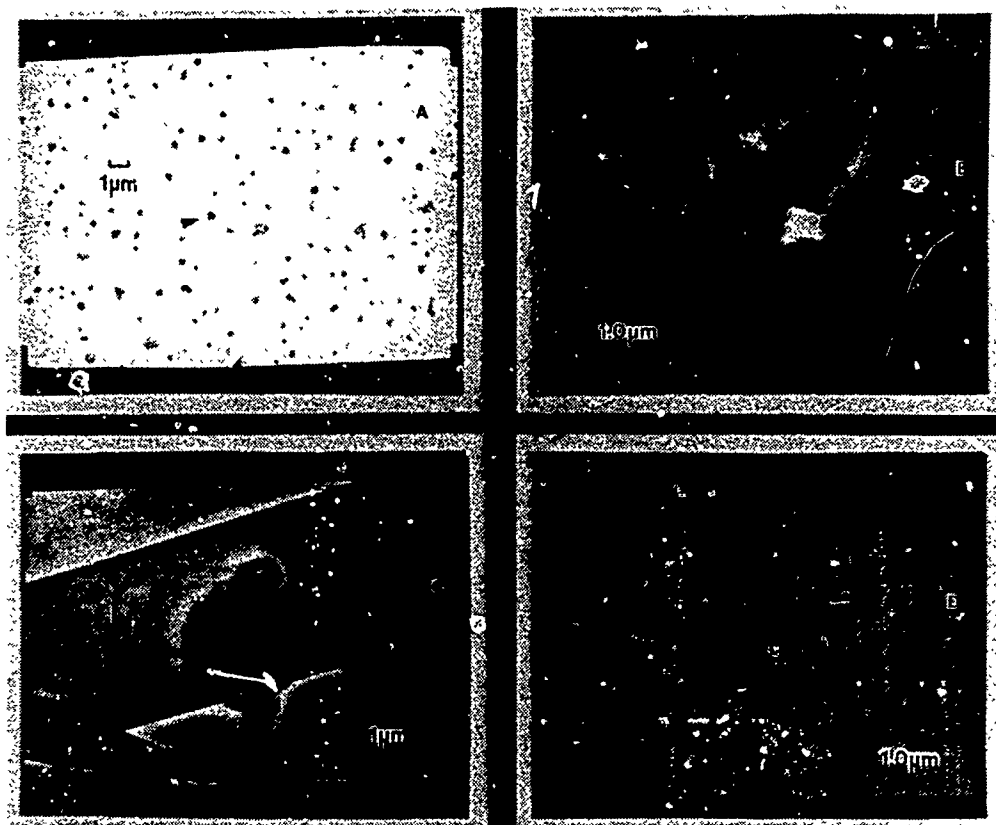


Figure 2. TOP: Photomicrographs of particles collected in AGASP-I Arctic haze layers. (A) Field of 0.6- μ m sulfate particles. At time of analysis, particles were solid $(\text{NH}_4)_2\text{SO}_4$; rings and residues around particles suggest they impacted as liquid H_2SO_4 . (B) A C-rich particle of the non-combustion class. (C) Joined combustion spheres. These particles, rich in Si, Al, Ca, Fe, and O, are believed to be from coal-fired combustion. (D) Small dark spheres (indicated by arrow) rich in Cu, Zn and Pb, surrounded by $(\text{NH}_4)_2\text{SO}_4$. These particles are of the types emitted by non-ferrous smelters. The sulfate appears to have impacted as a liquid. BOTTOM: X-ray spectra of the above particles collected in AGASP-I Arctic haze layers. The effective lower atomic number limit of detection is Na ($Z=11$). X-ray peaks resulting from the fluorescence of the Cu grid material are evident in each spectrum. (A) Spectrum from a typical Arctic haze sulfate particle. (B) X-ray spectrum from a C-rich particle showing no peaks from detectable elements in the particle. (C) Spectrum from one of the frequently encountered coal fly ash spheres. (D) X-ray spectrum from the small smelter-class spheres embedded in a larger sulfate particle.

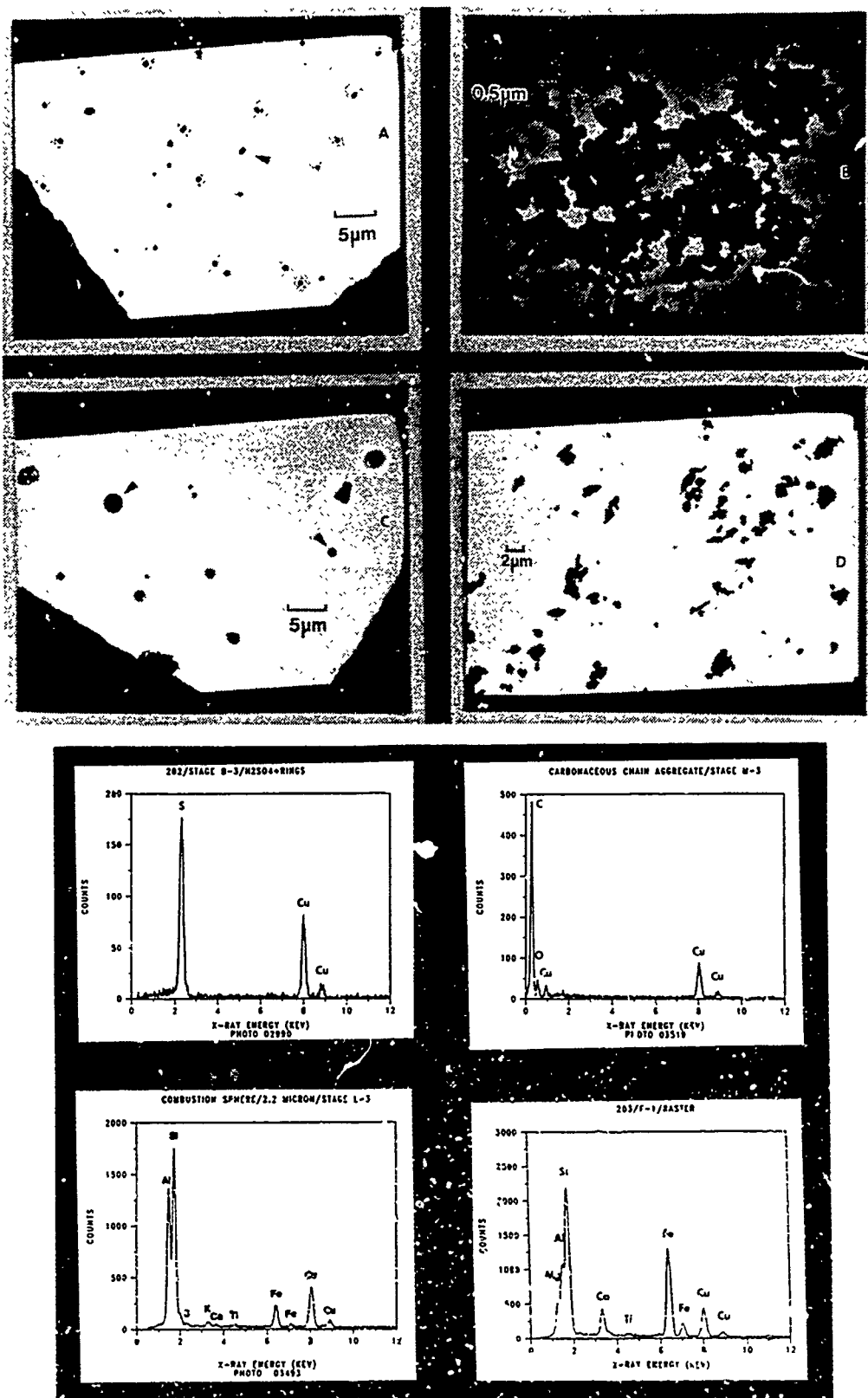


Figure 3. TOP: Photomicrographs of particles collected during flights of the AGASP-II mission. (A) Field of larger H_2SO_4 droplets, showing impaction satellite rings. (B) Combustion soot carbon showing characteristic chain spherical aggregate morphology. (C) Two of the frequently observed coal combustion spheres (indicated by arrows) with mostly sulfate particles. (D) Crustal material from over Alaska which probably is ash from the eruption of Mt. Augustine. BOTTOM: X-ray spectra of the above particles collected during flights of the AGASP-II mission. (A) X-ray spectrum from the indicated H_2SO_4 droplet above. (B) Ultra-thin window (UTW) x-ray spectrum of a portion of a carbon soot chain aggregate collected in Arctic haze. (C) Spectrum of the larger of the two indicated fly ash combustion spheres. (D) X-ray spectrum from a field of particles showing a crustal morphology and elemental signature. The particles were collected in the middle troposphere over south-central Alaska and were probably in a pocket of ash from the Mt. Augustine volcano.

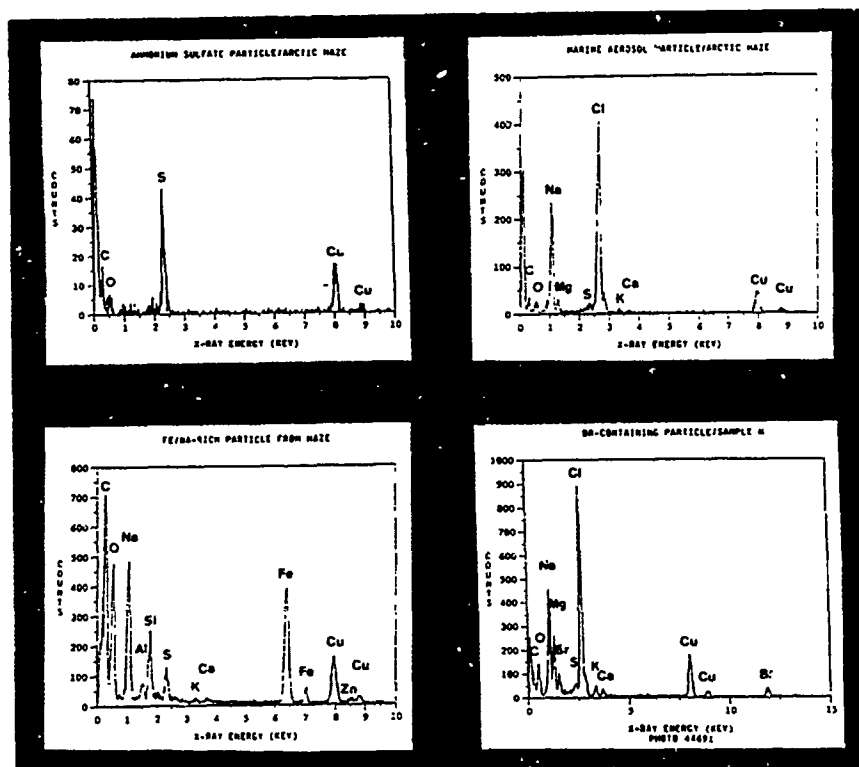
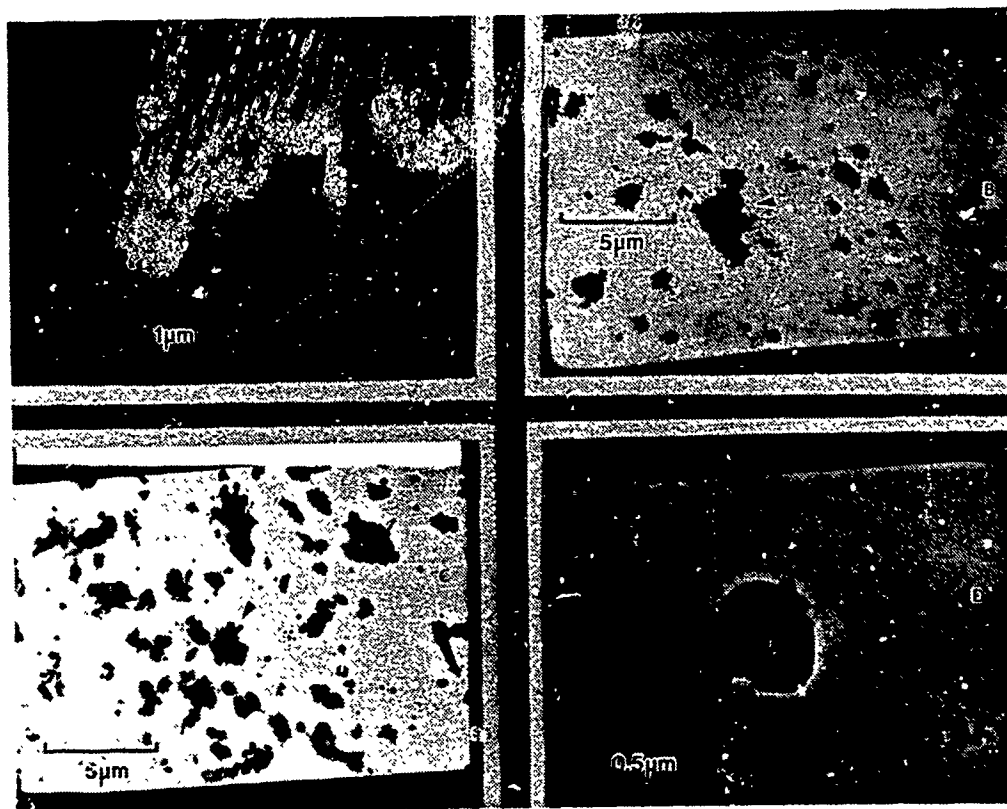


Figure 4. TOP: Photomicrographs of particles collected during the AGASP-III field experiment. (A) Field of solid sulfate particles of the type commonly observed in AGASP-III samples. (B) Crustal and marine particles associated with a liquid S-rich phase. (C) Field of terrestrial dust particles, showing free, liquid H_2SO_4 in the aerosol. (D) A Br-rich marine salt particle collected in the above-ice inversion layer near open leads. BOTTOM: X-ray spectra of the above particles collected during the AGASP-III field experiment. (A) X-ray spectrum from the indicated sulfate particle. (B) Spectrum from a marine aerosol particle collected in light haze. (C) Composition of a crustal-type particle collected at low altitude over DYE-III, Greenland. (D) Spectrum of a Br-containing marine aerosol particle collected below the Arctic surface temperature inversion over a lead-filled area of pack ice. Ozone concentrations in this region were essentially zero during aerosol sample collection.

Preliminary meteorological analysis attributes this relative lack of anthropogenic aerosol to two factors. First, the winter and spring of 1989 was an unusually warm one for all of Europe and much of the western Soviet Union. The higher-than-normal temperatures meant a diminished need to burn fossil fuels and wood. Second (and this may be related to the higher temperatures), the normal flow patterns from Eurasia to the European Arctic did not materialize, at least during our month-long operation there. These factors appear to be adequate to explain the lack of a clearly anthropogenic component in the 1989 Arctic aerosol.

When sampling under the surface inversion over the pack ice, we observed a total ozone depletion around leads in the ice. Aerosol samples collected at that time were composed primarily of marine salt particles, with many showing significant (2–10% mass fraction) amounts of elemental Br. The form of this Br in individual particles is at this time unknown, but this research supports the concept of a gas-phase Br/ozone reaction which forms particulate Br in the Arctic above-ice inversion layer [Barrie et al., 1988; Finlayson-Pitts et al., 1989]. Several classes of particles collected during flights of the AGASP-III field experiment are presented in Figure 4.

CONCLUSIONS

Measurements conducted on the three Arctic Gas and Aerosol Sampling Programs have shown the Arctic atmosphere, once thought of as pristine, to contain regions of high aerosol concentrations in the springtime. These concentrated aerosol layers are the result of (1) direct episodic transport over land, snow and ice to the Arctic from mid-latitude source areas; (2) the lack of precipitation in the Arctic to cleanse the atmosphere; (3) the relatively slow dry deposi-

tion of aerosols to the snow and ice surface; and (4) the limited vertical mixing of the stable Arctic atmosphere.

Individual particle analysis of aerosol samples from the three field experiments shows that the dominant class of particles for almost all samples is sulfate. In the 1983 and 1986 samples, the sulfate was present as fine liquid H_2SO_4 droplets, suggesting relatively rapid transport from its source and short residence times in the atmosphere. The AGASP-III samples showed neutralized sulfate (mostly $(\text{NH}_4)_2\text{SO}_4$) as the dominant aerosol constituent. Based on air trajectory analyses, much of this sulfate appears to be coming from industrialized source regions, although natural sulfate-precursor sources such as the oceans and volcanoes may contribute minor amounts of sulfate to the background tropospheric Arctic haze.

When organized transport from industrialized source regions occurs, extremely high concentrations of pollution aerosol are present in well-defined layers in the Arctic atmosphere. These layers typically contain fine sulfate, carbonaceous particles of both the combustion and non-combustion varieties, and several other classes of particles from anthropogenic combustion processes. Also present in these layers is terrestrial dust and (often) marine aerosol, confirming the distant nature of the sources.

When this organized transport does not occur for long periods of time (as was the case during AGASP-III), the haze in the Central Arctic Basin becomes a mixed background haze. The predominant constituent is (usually neutralized) sulfate, with lesser amounts of crustal, marine, and combustion aerosols. Even though the aerosol concentrations in this background haze are much lower than in "fresh" Arctic haze, the visibility reduction over the Arctic resulting from this aerosol can be dramatic.

REFERENCES

- Barrie, L. A., Arctic air pollution: an overview of current knowledge, *Atmos. Environ.*, **20**, 643-663, 1986.
- Barrie, L. A., R. M. Hoff, and S. M. Daggupaty, The influence of mid-latitude pollution sources on haze in the Canadian Arctic, *Atmos. Environ.*, **15**, 1407-1419, 1981.
- Barrie, L. A., J. W. Bottenheim, R. C. Schnell, P. J. Crutzen, and R. A. Rasmussen, Ozone destruction and photochemical reactions at polar sunrise in the lower Arctic atmosphere, *Nature*, **334**, 138-141, 1988.
- Blanchet, J.-P., Toward estimation of climatic effects due to Arctic aerosols, *Atmos. Environ.*, **23**, 2609-2625, 1989.
- Bridgman, H. A., R. C. Schnell, J. D. Kahl, G. A. Herbert, and E. Joranger, A major haze event near Point Barrow, Alaska: analysis of probable source regions and transport pathways, *Atmos. Environ.*, **23**, 2537-2549, 1989.
- Finlayson-Pitts, B. J., F. E. Livingston, and H. N. Berko, Ozone destruction and bromine photochemistry at ground level in the Arctic spring, *Nature*, **343**, 622-625, 1989.
- Harris, J. M., Trajectories during AGASP, *Geophys. Res. Lett.*, **11**, 453-456, 1984.
- Herbert, G. A., R. C. Schnell, H. A. Bridgman, B. A. Bodhaine, S. J. Oltmans, and G. E. Shaw, Meteorology and haze structure during AGASP-II, part 1: Alaskan Arctic flights, 2-10 April 1986, *J. Atmos. Chem.*, **9**, 17-48, 1989.
- Lowenthal, D. H., and K. A. Rahn, Regional sources of pollution aerosol at Barrow, Alaska during winter 1979-80 as deduced from elemental tracers, *Atmos. Environ.*, **19**, 2011-2024, 1985.
- Raatz, W. E., Meteorological conditions over Eurasia and the Arctic contributing to the March 1983 Arctic haze episode, *Atmos. Environ.*, **19**, 2121-2126, 1985.
- Raatz, W. E., An anticyclonic point of view on low-level tropospheric long-range transport, *Atmos. Environ.*, **23**, 2501-2504, 1989.
- Raatz, W. E., R. C. Schnell, M. A. Shapiro, S. J. Oltmans, and B. A. Bodhaine, Intrusions of stratospheric air into Alaska's troposphere, March 1983, *Atmos. Environ.*, **19**, 2153-2158, 1985.
- Rahn, K. A., Progress in Arctic air chemistry, 1980-1984, *Atmos. Environ.*, **19**, 1987-1994, 1985.
- Schnell, R. C., T. B. Watson, and B. A. Bodhaine, NOAA WP-3D instrumentation and flight operations on AGASP-II, *J. Atmos. Chem.*, **9**, 3-16, 1989.
- Shapiro, M. A., R. C. Schnell, F. P. Parungo, S. J. Oltmans, and B. A. Bodhaine, El Chichon volcanic debris in an Arctic tropopause fold, *Geophys. Res. Lett.*, **11**, 421-424, 1984.
- Sheridan, P. J., Analytical electron microscope studies of size segregated particles collected during AGASP-II, flights 201-203, *J. Atmos. Chem.*, **9**, 267-282, 1989a.
- Sheridan, P. J., Characterization of size segregated particles collected over Alaska and the Canadian high Arctic, AGASP-II flights 204-206, *Atmos. Environ.*, **23**, 2371-2386, 1989b.
- Sheridan, P. J., and I. H. Musselman, Characterization of aircraft-collected particles present in the Arctic aerosol; Alaskan Arctic, spring 1983, *Atmos. Environ.*, **19**, 2159-2166, 1985.
- Thornton, D. C., A. R. Bandy, and A. R. Driedger, III, Sulfur dioxide in the North American Arctic, *J. Atmos. Chem.*, **9**, 331-346, 1989.
- Valero, F. P. J., T. P. Ackerman, and W. J. Y. Gore, The absorption of solar radiation by the Arctic atmosphere during the haze season and its effects on the radiation balance, *Geophys. Res. Lett.*, **11**, 465-468, 1984.
- Wendling, P., R. Wendling, W. Renger, D. S. Covert, J. Heintzenberg, and P. Moerl, Calculated radiative effects of Arctic haze during a pollution episode in spring 1983 based on ground-based and airborne measurements, *Atmos. Environ.*, **19**, 2181-2193, 1985.
- Winchester, J. W., R. C. Schnell, S.-M. Fan, S.-M. Li, B. A. Bodhaine, P. S. Naegle, A. D. A. Hansen, and H. Rosen, Particulate sulfur and chlorine in Arctic aerosols, spring 1983, *Atmos. Environ.*, **19**, 2167-2173, 1985.
- Yount, M. E., T. P. Miller, and B. M. Gamble, The 1986 eruptions of Augustine Volcano, Alaska: hazards and effects, edited by T. D. Hamilton and J. P. Galloway, *U.S. Geological Survey Circular 998*, pp. 4-13, 1987.

AD-P007 361



Deposition of Metals from the Atmosphere at the North Pole Compared to Background Regions of the Northwestern USSR

V. N. Adamenko

Leningrad Higher Marine Engineering College of Admiral Makarov, Leningrad, U.S.S.R.

K. Ya. Kondratyev

Institute for Lake Research, Leningrad, U.S.S.R.

S. A. Sinyakov

Pacific Oceanography and Fishery Institute, Petropavlovsk-Kamchatsky, U.S.S.R.

ABSTRACT

An intercomparison of dry and wet deposition of heavy metals and a number of trace elements has been made on the basis of the analysis of snow samples for Ladoga and Onega lakes as well as for the central Arctic. A comparative assessment of contributions to lake pollution (Great Lakes included) due to atmospheric deposition and river runoff has been given. Annual variations in the deposition of heavy metals due to the varying air transport and industrial emissions have been analyzed.

INTRODUCTION

Despite the biological activity of trace elements and heavy metals (HM) received by natural waters, the HM input from the atmosphere as a result of dry and wet deposition has been studied poorly, so far. In this connection, a study has been made to assess this input in the Arctic and on the water basins of northwestern Europe, bearing in mind a determination of global, regional and local levels of the HM deposition from the atmosphere.

Based on observational studies performed simultaneously at the North Pole, on lakes Ladoga and Onega, in the suburbs of Leningrad, and watersheds of the Onega-Ladoga system, the Neva Bay, a quantitative estimate has been made of the fallout of dust and some metals from the atmosphere, most of which are either heavy metals or trace elements. These assessments have been made using X-ray-fluorescence analysis in the Laboratory for Nuclear Reactions of the Cooperative Institute for Nuclear Studies (Dubna, USSR) of the filters (Vladipore 0.45- μ m pore diameter membrane filters) on which a solid deposit from snow cover had been filtered.

RESULTS AND DISCUSSION

Table 1 shows data on relative concentrations of conditionally insoluble forms of HM, calcium and potassium in snow cover on the ice of Ladoga and Onega lakes, at the station North Pole-28 during the annual drift in the northeastern Arctic north of 84°N, as well as relationships between preindustrial and present-day concentrations of some chemical elements.

Analysis of these data suggests the following:

(1) In the background regions of the Arctic and northwestern Europe a combination of almost the same chemical elements falls out from the atmosphere—the same elements can be identified whose concentrations in snow cover are from hundredths of a microgram to tens and even hundreds of micrograms per liter of water solution.

(2) These elements are located, by order of priority, in the following successions:

Ladoga (concentrations in μ g l⁻¹ are given in parentheses): Fe (155), K (82), Ti (17), Ca (13), Mn (2), Zn (2), V(1), Cr (0.8), Zr (0.7), Ca (0.6), Pb (0.6), Sr (0.4), Ni (0.2), Rb (0.2), Br (0.1), dust (2.6 mg l⁻¹).

Element	C_L/C_O	C_L/C_{ns}	C_L/C_{nw}	C_O/C_{ns}	C_O/C_{nw}	C_O/C_p
K	2.9	12.1	-	4.2	-	-
Ca	1.1	5.6	-	5.0	-	9.8
Ti	3.4	19.6	9.4	5.8	2.8	-
V	3.0	6.0	2.0	2.0	0.7	-
C	1.1	6.2	1.9	5.4	1.6	-
Mn	1.6	25.0	8.5	15.0	5.2	-
Fe	1.8	27.0	15.8	14.7	8.6	10.6
Ni	0.9	5.2	3.0	6.1	3.5	-
Cu	1.3	9.1	7.8	7.1	6.1	18.3
Rb	1.2	2.7	3.3	2.1	2.6	15.4
Pb	2.7	21.8	-	8.2	-	-
Sr	1.6	26.3	10.2	16.8	6.5	-
Zr	1.5	45.5	14.3	29.7	9.3	-
Br	-	-	-	-	-	-
Zn	1.3	10.7	8.2	8.1	6.3	20.4
Dust	1.9	12.6	6.8	6.5	3.5	-

Table 1. The ratios of concentrations of chemical elements and dust in snow cover on Lakes Ladoga (C_L) and Onega (C_O); at the North Pole in winter (C_{nw}), summer (C_{ns}); and preindustrial (C_p) [Pakarinen et al., 1983] and current (C_c) in the northwestern part of the USSR.

Onega (in $\mu\text{g l}^{-1}$): Fe (84), K (29), Ca (11), Ti (5), Mn (1), Zn (1), Cr (0.7), Pb (0.5), Cu (0.5), V (0.4), Zr (0.4), Ni (0.3), Sr (0.3), Rb (0.1), Br (0.1), dust (1.36 mg l^{-1}).

North Pole (summer, $\mu\text{g l}^{-1}$): K (7), Fe (6), Ca (2), Ti (0.9), Pb (0.2), V (0.2), Zn (0.1), Cr (0.1), Mn (0.09), Cu (0.07), Ni (0.05), Br (0.020), Sr (0.017), Zr (0.015), Rb (0.010), dust (0.21 mg l^{-1}).

(3) The wintertime deposition in the Arctic exceeds 2–3-fold that in the summer, which is explained both by winter duration and by difference in atmospheric stratification, which is more stable in winter than in summer.

(4) For almost all elements the deposition on Ladoga is 20–40% greater than on Onega, which is explained by the proximity of Ladoga to relatively large sources of atmospheric pollution, compared to Onega, as well as by prevailing winds with the southern or western components in the northwestern USSR in cold seasons.

(5) Analysis of available data on the fallout of chemical elements from the atmosphere in the cities with multi-million population and with diversified industry suggests that in these cities the deposition of some chemical elements exceeds by one to two orders of magnitude the fallout for the background regions in the northwest (Ladoga and Onega) and exceeds by three to four orders of magnitude the input of metals at the North Pole. The latter data can be considered a measure of the HM deposition for the global background conditions of the Northern Hemisphere.

(6) The HM fallout on Ladoga is 3–45 times more intensive than at the North Pole in summer and 2–16 times more intensive than in the central Arctic in winter.

(7) The background deposition of HM on relatively pure Onega is 2–30 times more intensive than at the summertime North Pole and 2–9 times stronger than in the central wintertime Arctic.

(8) The present fallout of such elements as Ca, Fe, Cu, Pb, and Zn exceeds by 10–20 times that of 150–200 years

ago from the estimates of the Finnish experts [Pakarinen et al., 1983].

(9) Differences between the background hemispheric (North Pole) values of dust concentrations and the background regional (Ladoga) values reach one order of magnitude, and for Onega are half as much.

(10) The concentration differences of the deposited HM are, on the average, the same as in the case of dust. However, the concentrations of lithophyll metals (metals with low enrichment coefficients in particles of atmospheric aerosols) (manganese, strontium, iron) are tens of times smaller in the arctic dust, whereas the concentration of atmophyll metals (metals with high enrichment coefficients in particles of atmospheric aerosols), for which the industrial contributions are significant, differ less.

(11) The atmospheric flux of lithophyll elements (calcium, magnesium, iron) during the industrial epoch has increased by a factor of 5–11, and that of atmophyll elements (lead, zinc, copper) by a factor of 15–20. This points to the fact that the present background level of atmospheric deposition assessed for the hemisphere from snow samples at the North Pole are of about the same order of magnitude as in the mid-latitude northwest in the pre-industrial epoch.

(12) There are qualitative differences between the present flux of trace elements from the atmosphere to the surface in the Arctic and the flux in the region of Ladoga in the pre-industrial epoch, expressed through different relationships between the concentrations of atmophyll and lithophyll elements: the present background flux of trace elements from the atmosphere in the Arctic is characterized by greater (with respect to the pre-industrial flux) concentration of atmophyll elements (3–6 times for copper, zinc, lead) and lower concentrations of lithophyll elements (by a factor of 1.5).

(13) In comparing the data obtained from temporal (cores of stratified media) and spatial sections, it is necessary to take into account the possible fractionation of atmophyll and lithophyll elements on particles characterized by different rates of deposition from the atmosphere on the ways of transport to the arctic regions. It should be borne in mind that an additional pollution of the arctic atmosphere by industrial emissions takes place. The conclusion follows from an analysis of data on the HM concentration in the snow cover in winter and in summer: in winter the concentrations of HM and dust grow markedly, the differences being observed even in the color of analyzed filters (in winter the filters are darker) as well as in the increasing weight of deposits on the filter (in winter by a factor of 1.5–2). These differences are explained by changes in prevailing directions of air transport in the troposphere from winter (prevailing southwest and south components) to summer (prevailing north and east components). Another reason for the winter–summer difference is the growing intensity, increasing frequency, and duration of temperature inversions which weaken the vertical air motions and, consequently, the diffusion of pollutants in the mixing layer.

An additional factor of the wintertime pollution of the arctic atmosphere is a decrease of washing-out of the pollutants in cold seasons on the routes of transport. The latter is determined by smaller rain rates and greater anthropogenic emissions due to fuel burning in winter. This is manifested through growing ratios of concentrations V/Pb, equal

Water Basins	Iron a/b	Copper a/b	Lead a/b	Manganese a/b	Cadmium a/b
Lakes:					
Ladoga	3424/194	32/2	93/5	83/5	2/0.08
Onega	1603/161	21/2	49/5	47/5	0.4/0.04
Baikal	-/16,318	-/0.4	-/-	-/2	-/-
Michigan	2770/48	120/2	640/11	640/11	11/0.19
Erie	-/-	206/8	645/25	-/-	39/1.5
Region:					
Gulf of Bothnia	-/-	-/-	180/2	-/-	7/0.06
Sweden	-/16	-/0.6	-/3	-/3	-/0.05
Ontario	-/76	-/1.8	-/11	-/5	-/0.19

Table 2. Total input of metals from the atmosphere (a, nominator, in $t\ km^{-2}\ yr^{-1}$) and its intensity (b, denominator, in $kg\ km^{-2}\ yr^{-1}$) on various water basins of the Northern Hemisphere from the data of the authors and others [Eisenreich, 1980; Burnes, 1985; Chan et al., 1986; Enckel-Sarcola, 1986; Ross, 1987]. A dash (-) indicates "no information."

to unity in summer, and in winter greater by a factor of 3 in the arctic samples of atmospheric aerosol (vanadium is the principal indicator of emissions by power stations operating on oil products). A considerable increase of the concentrations of nickel, chromium and manganese in winter samples can also illustrate the anthropogenic origin of pollutants connected with the burning of oil and coal (nickel), production of steel and ferro-alloys (manganese, chromium) in the northern regions of Eurasia and North America.

A study of the size distribution of filter samples of snow for the pure regions of Onega and in the Arctic using the quantitative electrosonde microanalysis technique revealed spherical ash particles characteristic of high-temperature (anthropogenic) emissions in both Onega and Arctic samples.

A comparison of electron microscope photographs of the filters reveals the pollution of deposits by metal-containing particles in the case of background regions in northwestern Europe, compared to the background regions of the Northern Hemisphere. The pollution is higher by an order of magnitude.

An analysis of the maps of deposition of each HM during winter over the water basins of Onega and Ladoga revealed an exponential decrease in the concentration in the west-to-east (Onega) and south-to-north (Ladoga) directions such that at a distance of tens of kilometers from large sources of emissions the level of HM fallout reaches a regional background level, and farther out it varies weakly, although on the average by an order of magnitude less than the global average level of HM deposition.

The total amount (Table 2) of iron falling out from the atmosphere on the Ladoga water basin ($3424\ t\ yr^{-1}$) is about half as much as on the water basin of Onega ($1603\ t\ yr^{-1}$) and is approximately equal to that falling out on Lake Erie ($2770\ t\ yr^{-1}$). The input of lead from the atmosphere to the American Great Lakes [Eisenreich, 1980; Burnes, 1985; Chan et al., 1986; Enckel-Sarcola, 1986; Ross, 1987] exceeds by a factor of 6-7 the input to Lake Ladoga (640 , 645 and $93\ t\ yr^{-1}$ for Lakes Michigan, Erie and Ladoga, respectively), though the input rate (in $kg\ km^{-2}\ yr^{-1}$) to Michigan (Table 2) is only 2 times, and to Erie 5 times, greater than to Ladoga. The total amount of all other HM

depositions onto the Great Lakes as well as their intensities (Table 2) exceed the HM fallout in northwestern Europe. This is explained, first of all, by differences in the anthropogenic emissions for these regions. The HM emissions are characteristic for Sweden.

The relationship C_a/C_r between the atmospheric input (C_a) and river runoff (C_r) transport (in percent) constitutes for some metals:

	Fe	Cu	Pb	Mn	Cd
Ladoga	7	10	40	2	-
Michigan	-	52	356	-	92
Erie	-	12	92	-	-
Gulf of Bothnia	-	-	91	-	-
Sweden	20	18	722	-	-

These estimates taken from published data [Eisenreich, 1980; Burnes, 1985; Chan et al., 1986; Enckel-Sarcola, 1986; Ross, 1987] show that the atmospheric contribution of lead to large lakes of the northwest is about half of all lead input to water basins, while in the Great Lakes of North America, in Sweden, and in the Gulf of Bothnia, the atmospheric input is either equal to or exceeds 3-7 times the input of lead from the river runoff. The input of cadmium to the Great Lakes is also determined, largely, by dry and wet depositions of HM from the atmosphere. The input of iron and copper from the atmosphere to the northwestern water basins is less than a fourth of the HM value from river runoff, whereas on Lake Michigan the atmospheric source is approximately equal to the input of copper from river runoff.

So, the following general conclusions can be drawn:

(1) The dry and wet HM deposition from the atmosphere differs by three orders of magnitude under global, regional and local background conditions.

(2) In the central regions of the Arctic and in the industrial regions of northwestern Europe one can identify similar combinations of HM coming from the atmosphere, differing in intensity by 1-2 orders of magnitude.

(3) The input of HM in the central Arctic is much greater in winter than in summer.

(4) The spatial variations of HM deposition follow the exponential law of reduction in the direction of prevailing transports from their principal sources.

(5) The present level of HM deposition in the north-western part of the USSR is about 1–2 orders of magnitude less than that observed 100–150 years ago and an order of magnitude more than that typical of the central Arctic.

(6) It is important to monitor HM deposition from the atmosphere because it constitutes from 25% to 300–700% of that entering the water basins through river runoff.

REFERENCES

- Burnes, N. M., *Erie: The Lake that Survived*, p. 320, Rowman and Allenheld, 1985.
- Chan, W. H., J. S. Tang, H. S. Chang, and M. A. Lusi, Concentration and deposition of trace metals in Ontario—1982, *Water, Air and Soil Pollution*, 29, 373–389, 1986.
- Eisenreich, S. J., Atmospheric input of trace metals to Lake Michigan, *Water, Air and Soil Pollution*, 13, 287–301, 1980.
- Enckel-Sarcola, E., The pollutant load imposed on the Gulf of Bothnia—A survey, *Proc. 3rd Finnish-Swedish Seminar on the Gulf of Bothnia*, Aug. 20–21, 1984, pp. 55–59, Helsinki, 1986.
- Pakarinen, P., K. Tolonen, S. Heikkinen, and A. Nurmi, Accumulation of metals in Finnish raised bogs, *Environ. Biogeochem. Proc. 5th Int. Symp. JSEB*, Stockholm, 1–5 June, 1981, pp. 377–382, Stockholm, 1983.
- Ross, H. B., Trace metals in precipitation in Sweden, *Water, Air and Soil Pollution*, 36, 349–363, 1987.

92-17866



AD-P007 362



Seasonal Change and Chemical State of Polar Stratospheric Aerosols

Y. Iwasaka and M. Hayashi

Solar Terrestrial Environment Laboratory, Nagoya University, Toyokawa, Japan

A. Nomura

Department of Engineering, Shinshu University, Wakasato, Nagano, Japan

Y. Kondoh

Solar Terrestrial Environment Laboratory, Nagoya University, Toyokawa, Japan

S. Koga and M. Yamato

Water Research Institute, Nagoya University, Chikusa-ku, Nagoya, Japan

P. Amedieu

Service d'Aeronomie, CNRS, Verrieres le Buisson, France

W. A. Matthews

DSIR/PEL Lauder, Central Otago, New Zealand

ABSTRACT

Winter enhancement of stratospheric aerosols was measured at Syowa Station, Antarctica by a lidar. Electron microscope observation of individual particles collected in the winter Arctic stratosphere with a balloon-borne impactor suggested that particles containing nitric acid were formed during the cold winter season, and the appearance of such particles was an important process causing the winter enhancement of polar stratospheric aerosols. An externally mixed state of nitric acid and sulfate particles was observed in the region of 18.8–19.6 km (the upper region of the sulfate particle layer) during the measurements of January 31, 1990. One possible explanation of this is nitric acid particle sedimentation, which has been speculated as being an important process causing denitrification of the polar stratosphere and polar ozone depletion.

INTRODUCTION

Dramatic ozone depletion during Antarctic spring (ozone hole) was first observed by Farman et al. [1985], who suggested an increase in chlorofluorocarbon content in the atmosphere as one of the most important processes causing the ozone hole. The potential contribution of heterogeneous processes to the ozone hole was pointed out by Solomon et al. [1986] and others, since such a large ozone depletion during Antarctic spring cannot be explained only by gas phase chemical reactions.

Lidar measurements showed noticeable enhancement of stratospheric aerosols during winter at Syowa Station, Ant-

arctica [e.g., Iwasaka et al., 1985]. Satellite measurements showed winter enhancement of stratospheric aerosols in the Antarctic and Arctic regions [e.g., McCormick et al., 1982]. Formation of ice particles and/or nitric acid trihydrate particles was suggested as the main cause of winter enhancement of polar stratospheric aerosols from thermodynamical studies [e.g., McElroy et al., 1986; Toon et al., 1986; Hansen and Mauersberger, 1988]. Formation of such particles can seriously dehydrate and denitrify the stratosphere [e.g., Crutzen and Arnold, 1986]. In addition, these particles' surfaces are expected to serve as catalysts for surface-catalyzed reactions, converting reactive nitrogen gases to HNO_3 and

chlorine reservoir gases to photolytically active chlorine-containing gases, from which chlorine atoms can easily be liberated after the sun returns to the polar region [e.g., Solomon et al., 1985; Molina et al., 1987].

According to recent observations these heterogeneous processes certainly produce a large disturbance in ozone in the Antarctic spring stratosphere [e.g., special issue of *J. Geophys. Res.* describing results during the Airborne Antarctic Ozone Experiment].

Most of the previous measurements of PSCs (Polar Stratospheric Clouds) were from remote sensing such as satellite and lidar [e.g., McCormick et al., 1982; Iwasaka et al., 1985], in situ measurement with a balloon-borne particle counter [e.g., Hofmann et al., 1988, 1989], and bulk sampling with an airborne filter [e.g., Gandrud et al., 1989]. From these measurements the chemical composition and/or the molecular state of individual particle cannot be known.

Electron microscope observation of individual particles collected on the surface of a vapor (calcium, carbon, and nitron) deposited thin film has been frequently made for

studies on the nature of particles near the ground surface [e.g., Bigg et al., 1974; Ono et al., 1983; Yamato et al., 1987; Weisweiler and Schwarz, 1990]. This chemical test technique is very effective in identifying the molecular state of individual particles and the mixing state of particulate chemical composition (externally or internally mixed). However, concerning the stratospheric particles, there were limited chemical tests since only a few collections of particles were made and these techniques are very tedious.

Here, we made electron microscope measurements of the particles collected with a balloon-borne impactor in the winter Arctic stratosphere, and discuss the effect of nitrate particle formation on the winter enhancement of polar stratospheric aerosols.

WINTER ENHANCEMENT OF POLAR STRATOSPHERIC AEROSOLS: MEASUREMENTS AT SYOWA, ANTARCTICA

In Table 1, the main characteristics of the lidar used here are summarized. The lidar system consists of a 694 nm

Transmitter	
Laser output	>1 J/pulse (694 nm) > 0.3 J/pulse (347 nm)
Laser pulse width	40 ns
Repetition rate	60 ppm (max)
Laser beam divergence	1.6 mrad
Transmitter optics	Galilean telescope (x 4)
Transmitter beam divergence	0.5 mrad (30 mm diameter)
Receiver	
Receiver optics	Cassegrain telescope
Receiver diameter	500 mm
F-number	F/4.0
Receiver field of view	0.5–2.0 mrad
Transmitter/receiver mount	
Vertical direction only (fixed type)	
Detection system	
3-channel detection (typical confirmation)	
A-channel PMT R-943-02	347 nm \pm 1.3 nm
B-channel PMT R-943-02	694 nm \pm 0.5 nm
C-channel PMT R-1333	694 nm \pm 1.3 nm
PMT R-1332	347 nm \pm 1.3 nm
Signal processing	
Analog method	
A–D converter	8-bit resolution Sampling speed 50 ns (max)
Photon counting method	
Multichannel counter	8-bit resolution Range resolution 100 m (min)
Data processing	
CAMAC data logging system with minicomputer (Melcom 70/10)	

Table 1. Main characteristics of the laser radar system.

pulse ruby laser, 50 cm ϕ telescope, dual 100-channel photon counters, A scope, and A/D converter processing. Lidar measurements on the stratospheric aerosols were made in 1983, 1984, and 1985 at Syowa (69°S, 40°E), Antarctica, as a part of the international project "Antarctic Middle Atmosphere (1982-1986)."

The scattering ratio, $R(z)$, is defined as follows [e.g., Russell et al., 1976],

$$R(z) = [B_1(z) + B_2(z)]/B_1(z) \quad (1)$$

where $B_1(z)$ and $B_2(z)$ are the molecular and particulate backscattering coefficients, respectively, at altitude Z . The usual matching of the lidar signal containing both molecular and particulate backscattering with the profile of molecular backscattering was made using the radiosonde measurements which were routinely made at Syowa. The mixing ratio of particulate matter is estimated by

$$R(z) - 1 = B_2(z)/B_1(z) \quad (2)$$

In Figure 1, some typical profiles of scattering ratio measured in early winter are compared with the profile of May, before the cold winter set in. The profiles in June have larger layer depth and a higher layer top compared to the layer in May.

The vertically integrated backscattering coefficient in the stratosphere is given by

$$I = \int \Delta Z B_2(z) dz \quad (3)$$

where ΔZ is the height range from the base of the layer top. We chose the tropopause instead of the bottom of the layer when tropospheric clouds disturbed the base of the layer near the tropopause. The integral I can be recognized as the parameter corresponding to the column mass concentration of particulate matter, although this is not fully quantitative [Northam et al., 1974; Hofmann et al., 1983]. The variation of I is shown in Figure 2. The integral reaches its maximum in winter.

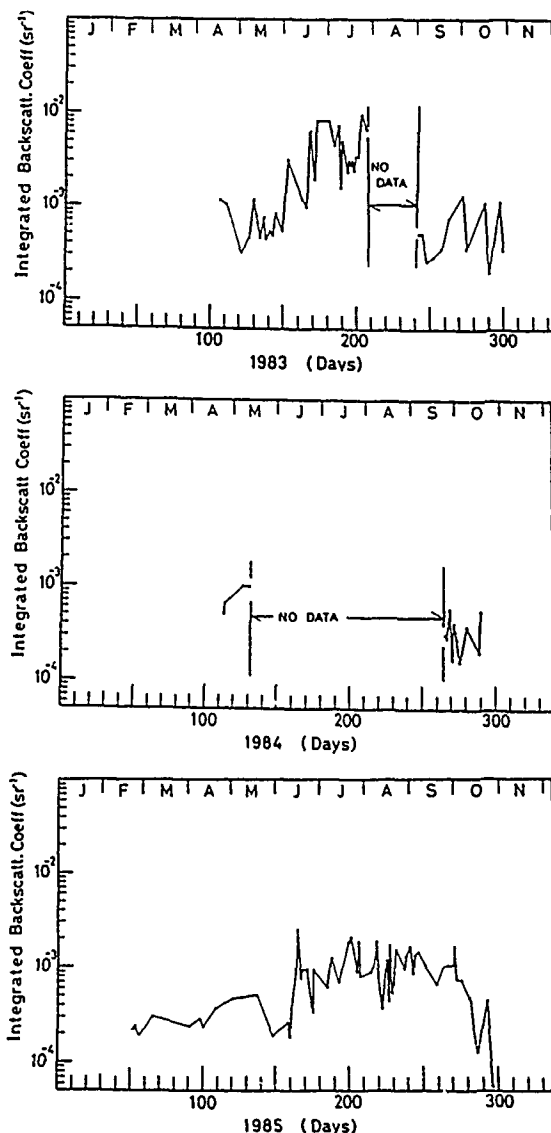


Figure 1. Vertical distribution of aerosol content, observed at Syowa (69°S, 40°E) with a lidar. "T" indicates the tropopause.

Sampling No.	Film	Height (km)	Temperature (°C)	Nitrate*	Sulfate**
5	C	15.5-16.1	-72.9- -69.7		Yes
6	N	16.1-16.7	-74.2- -71.6	No	
7	C	16.7-17.4	-74.7- -72.7		Yes
8	N	17.4-18.1	-77.9- -74.2	No	
9	C	18.1-18.8	-80.4- -75.8		Yes
10	N	18.8-19.6	-82.9- -78.7	Yes for a few particles	
11	C	19.6-20.2	-83.5- -80.8		Yes†
12	N	20.2-21.0	-84.9- -80.5	Yes	
13	C	21.0-21.6	-85.8- -80.8		Yes†
14	N	21.6-22.2	-85.6- -80.3	Yes	
15	C	22.2-22.9	-85.4- -80.3		No

Table 2. Molecular state of particulate matter collected in the winter stratosphere. Film C and N mean carbon thin film and nitron thin film used for collection of particles, respectively. *Test from needle-like crystals produced through reaction between nitron film and nitrate in particulate matter. **Detection from morphology of particles. †It is possible to detect nitrate particles collected on carbon film if nitrate particles are composed of nitric acid or ammonium nitrate, since these chemical constituents are volatile.

PARTICLE COLLECTION IN THE WINTER ARCTIC STRATOSPHERE

Stratospheric particles were collected on an electron microscope screen, the surface of which was coated with a thin film of carbon or nitron on January 18 and 31, 1990, at Kiruna, Sweden, with a balloon-borne impactor (from about 10 km to 23 km for measurements of January 18, and from about 13 km to 30 km for measurements of January 31). Thirty-one samples were collected during a balloon flight. The impactor used here had a 2-mm-diameter jet nozzle, and the flow rate of sampled air was 10 l min⁻¹. The 50% cut-off radius was 0.09 μ m at 15-km heights.

In measurements of January 31, many nitrate particles were collected. Figures 3, 4, 5, and 6 show vertical changes in the molecular state of individual particles collected at 18.1–21.0 km on January 31. Figure 3 is an electron micrograph of particles collected on carbon-deposited thin film at a height of 18.1–18.8 km. Most of the particles show typical features which have been frequently observed in sulfate particles [e.g., Gras and Laby, 1979; Yamato et al., 1987]. Some particles have "satellite structure," which has been recognized as characteristic of sulfuric acid morphology (see particles surrounded with a square). Sulfate particles and/or sulfuric acid droplets are considered to be major constituents of the stratospheric aerosol layer [e.g., Turco et al., 1982].

Figure 4 is an electron micrograph of particles collected on a nitron thin film at a height of 18.8–19.6 km. One particle only produced needle-like crystals through reaction between the nitron film and nitrate in particulate matter, and other the particle did not. Figure 5 is an electron micrograph of particles collected on carbon at 19.6–20.2 km. The particles in Figure 5 are very similar in morphology to the particles in Figure 3. Figure 6 shows an electron micrograph of particle collected on nitron thin film at a height of 20.2–21.0 km. All particles have a needle-like structure which forms through reaction between nitron and nitrate.

Few previous studies have described the existence of particles containing nitrate in the stratosphere on the basis of individual particle measurements. Present measurements clearly suggest that nitric acid particles form in the winter Arctic stratosphere.

DISCUSSION

Electron microscope observations on collected particles suggested the formation of nitrate particles in the winter Arctic stratosphere. From morphology of needle-like crystals surrounding the particles collected on a nitron thin film, these particles possibly contain nitric acid. In the cold winter polar stratosphere an extremely enhanced aerosol layer (Polar Stratospheric Clouds; PSCs) has been frequently observed [e.g., McCormick et al., 1982; Iwasaka et al., 1985]. From thermodynamical studies these particles were suggested to be ice crystals (type-II PSC particles) and nitric acid trihydrate crystals (NAT; type-I PSC particles) [e.g., Hansen and Mauersberger, 1988].

In Table 2 we summarize the molecular state of particles collected at 15.5–24.4 km during the measurements of January 31, 1990. Sulfate particles were dominant below 20.2 km, and this certainly corresponds to the stratospheric aerosol layer which is mainly composed of background sulfate particles. NAT particles were detected above this sulfate layer. Some investigators suggested that the preexisting sulfate particles acted as nuclei for PSC particles [e.g., Rosen et al., 1988; Fahey et al., 1989]. The clear separation of the sulfate particle layer and the NAT particle layer suggested that the nuclei of NAT particles were not always typical sulfate particles. According to Hofmann et al. [1989] there is a large increase in $r \geq 0.20 \mu$ m particles, reaching a concentration of more than 50% of the concentration of condensation nuclei in the cold layer at 19–22 km. Condensation nuclei distributed above the background sulfate layer can act as nuclei of NAT particles.

Lidar measurements suggested that the upper aerosol layer was enhanced in the early polar winter. This type of enhancement seems to correlate with the formation of NAT particles. Considering the usual distribution of HNO₃ and H₂O, it can be expected that freezing of the HNO₃-H₂O mixture first starts in the upper aerosol layer and/or above the background sulfate layer, since measurements at Syowa show that a cold air mass appeared above the usual height of the background aerosol layer [Iwasaka, 1986]. Figure 7 schematically shows the relation between the atmospheric frost point of water vapor, and the frost point of the HNO₃-H₂O mixture.

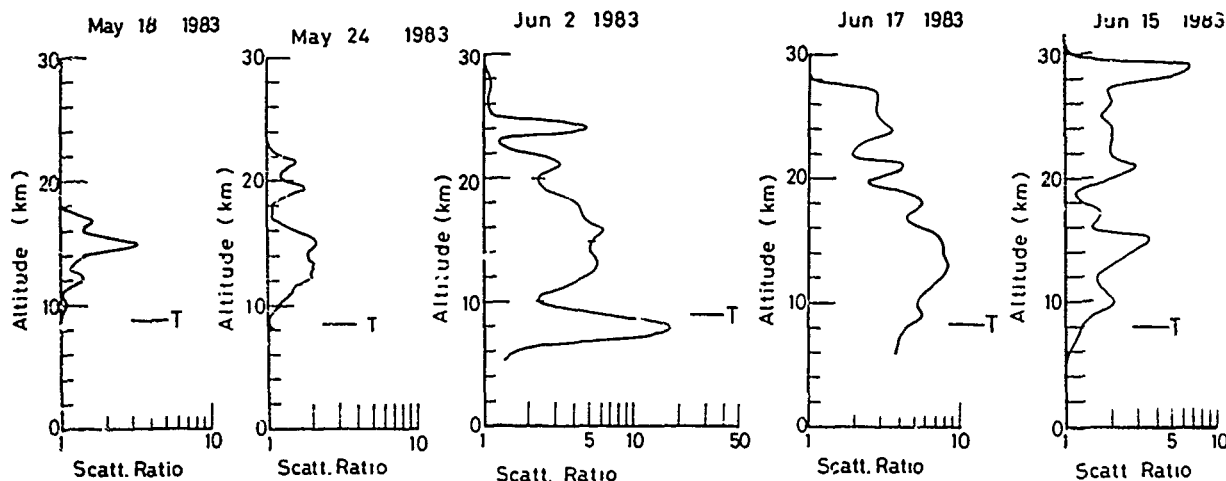


Figure 2. Integrated backscattering coefficient of stratospheric particulate matter measured at Syowa (69°S, 40°E).

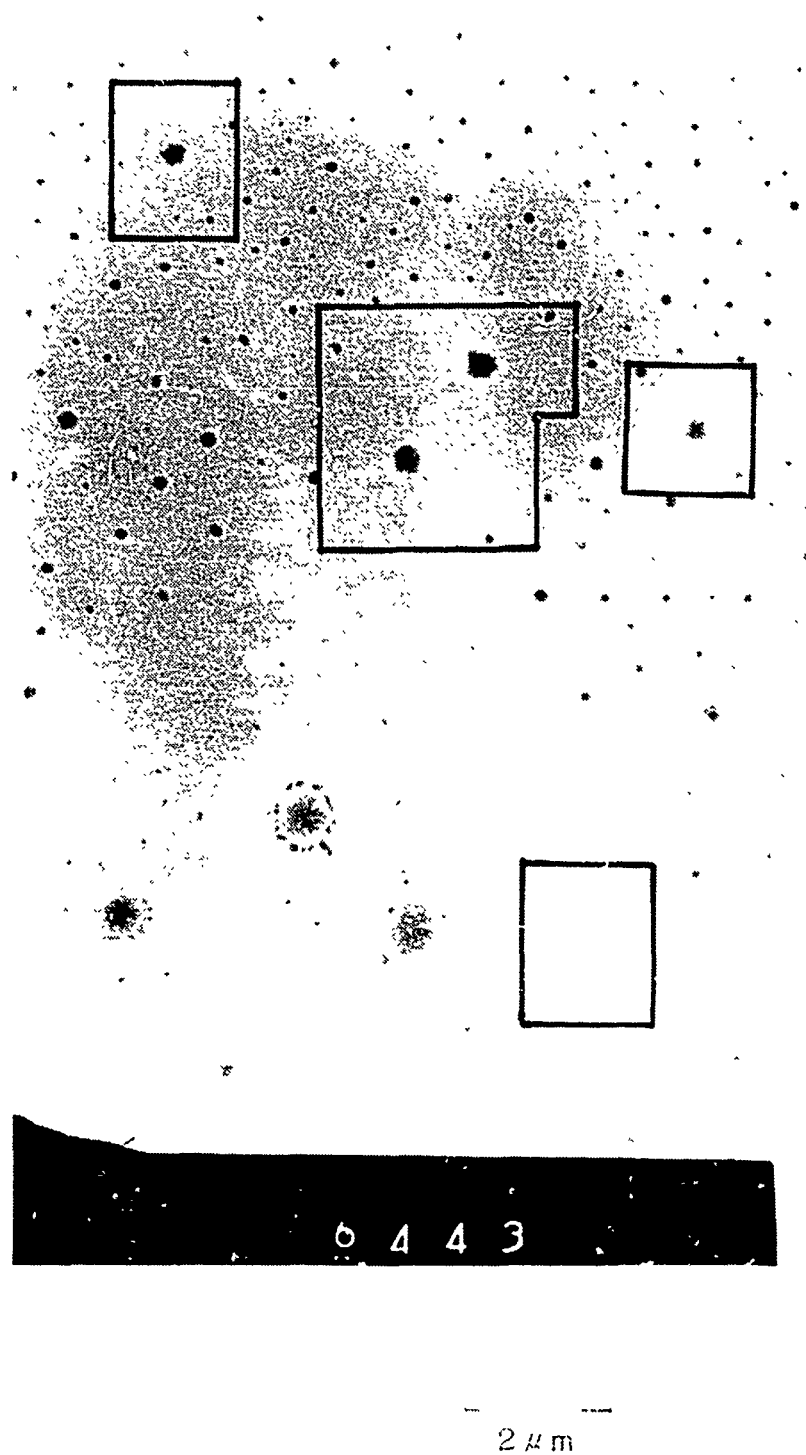


Figure 3. Electron micrograph showing the particles collected on carbon-deposited screen of electron microscope at 18.1–18.8 km, on January 31, 1990, at Kiruna (68°N, 21°E), Sweden.



5 μ m

Figure 4. Electron micrograph showing the particles collected on nitron-deposited screen of electron microscope at 18.8–19.6 km, on January 31, 1990, at Kiruna (66°N, 21°E), Sweden. Only the particle in the center of the figure has needle-like crystals formed by interaction between nitron film and nitrate-containing particulate matter.

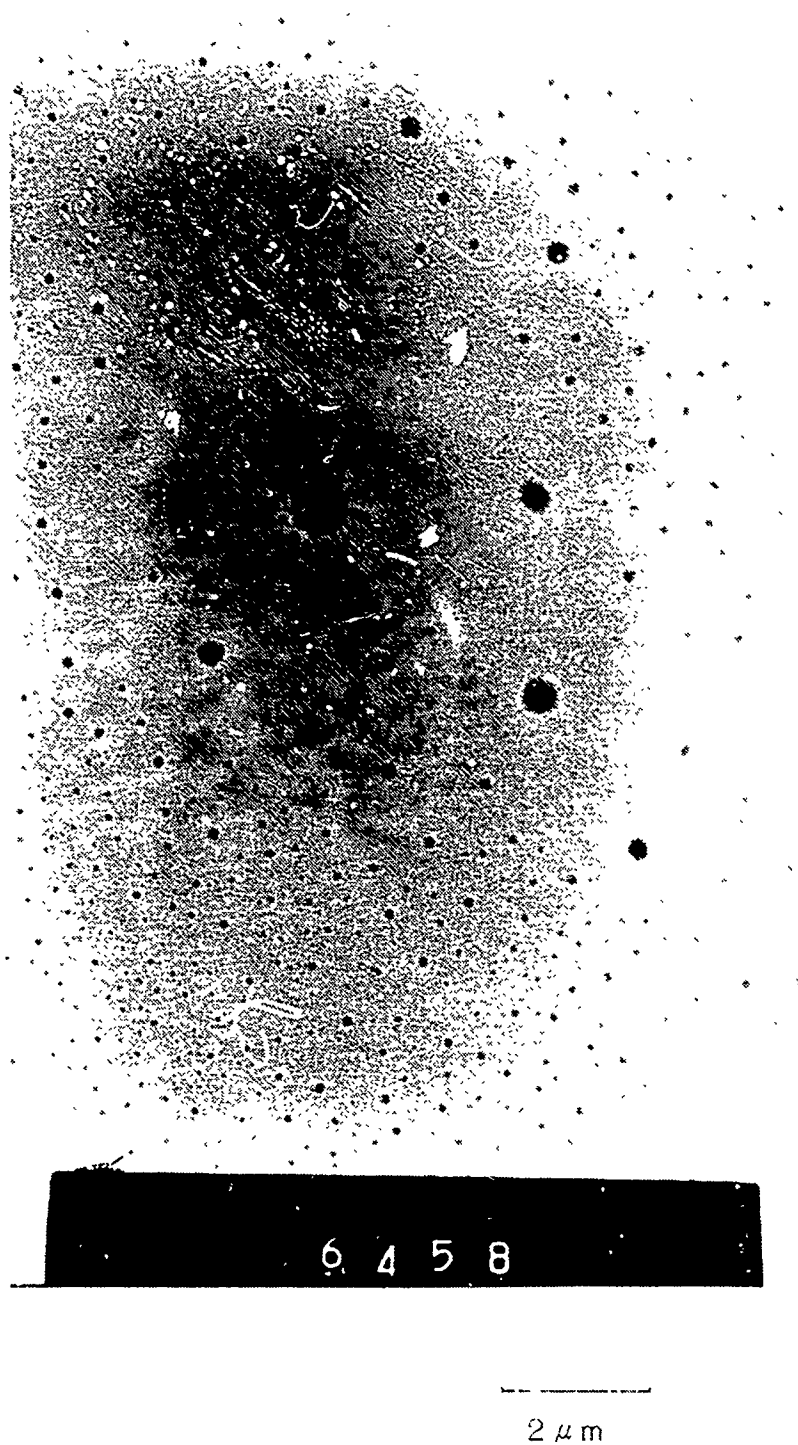


Figure 5. Electron micrograph showing the particles collected on carbon-deposited screen of electron microscope at 19.6–20.2 km, on January 31, 1990, at Kiruna (68°N, 21°E), Sweden. Particles show morphology very similar to those in Figure 3.



5 μ m

Figure 6. Electron micrograph showing the particles collected on nitron-deposited screen of electron microscope at 20.2–21.0 km, on January 31, 1990, at Kiruna (68°N, 21°E), Sweden. All particles in this figure have needle-like crystals.

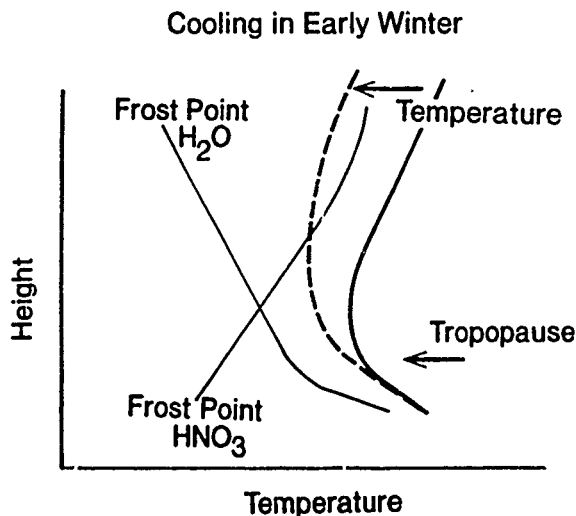


Figure 7. Schematic figure showing relation among temperature of early winter, frost point temperature of water vapor, and frost point of nitric acid vapor on NAT surface, assuming normal vertical profiles of water vapor and nitric acid vapor distribution.

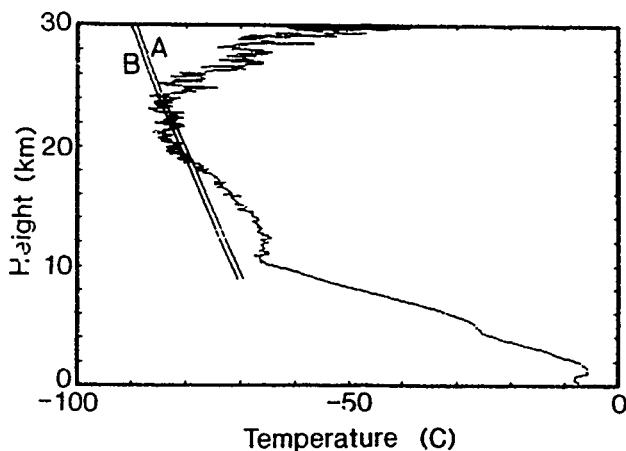


Figure 8. Temperature distribution and saturation point temperature of nitric acid trihydrate particles estimated on 3 ppmv water vapor and 10 ppbv nitric acid vapor mixing ratio (curve A) and on 3 ppmv water vapor and 5 ppbv nitric acid vapor mixing ratio (curve B).

When we assume the mixing ratio of 3 ppmv water vapor and 10 ppbv nitric acid vapor (or 5 ppbv nitric acid vapor) in the lower stratosphere, NAT particles can be expected to form in the region from 18 km to 24.5 km (Figure 8). The distribution of nitrate particles in Table 1 shows good correspondence with the estimated region where NAT particles can form. Summarizing these investigations it is reasonable to conclude that the particles shown in Figure 6 are possibly type-I PSC particles, and this good correspondence suggested that the concentration of the vapors of water and nitric acid were about 3 ppmv and 5–10 ppbv at 20–25 km during this period.

The externally mixed NAT particles with sulfate shown in Figure 4 is very interesting in regard to NAT particle behavior in the winter stratosphere. The following three

explanations are possible:

- (1) NAT particles formed in the region of 18.8–19.6 km.
- (2) A very thin NAT particle layer, with a thickness smaller than the vertical resolution of particle sampling, 700 m, was between 18.8 and 19.9 km, and
- (3) The NAT particle in Figure 4 had descended from the active NAT particle-forming region.

If we assume NAT particle formation in the region of 18.8–19.6 km, we are faced with a matter of great concern, that only a few sulfate particles can act as nuclei for NAT particles. Only when this region contained the particles, not sulfate particles, which can be activated as nuclei for NAT under the atmospheric conditions of January 31.

On the basis of particle concentration measurements, Hofmann et al. [1989] suggested that the cloud layer composed of PSCs had many tenuous layers. It is impossible to see whether the tenuous layer of PSCs is in the background sulfate particle layer or only from the particle concentration measurements. The particle mixing situation shown in Figure 4 suggests that the extremely tenuous layer of PSCs was in the sulfate particle layer (thickness of the PSC layer was possibly less than 22 m).

Of the three possibilities, process (3) seems to be most probable one since NAT particle can grow to several μm through condensation of nitric acid vapor, and coagulation of these NAT particles, in addition to this, can produce larger particles. Such size particles can easily descend from the NAT particle-forming region to the sulfate particle layer.

No nitrate particles were observed during the balloon measurements of January 18, 1990, although the temperature distribution of January 18 was very similar to that of January 31. Most particles collected on January 18 were sulfuric acid particles and sulfate particles (possibly ammonium sulfate or partially neutralized sulfate particles). This difference suggested the importance of studies on the whole evolution of PSC events. If we try to observe the denitrified atmosphere by severe PSC activity, it is impossible to detect NAT particles even if the atmosphere is very cold, since the atmosphere has no nitric acid vapor. The time lag between starting time of cooling and that of NAT formation also is an important factor. Too early particle collection cannot detect NAT particles.

CONCLUSION

Nitrate particles (possibly nitric acid particles) were detected in the winter Arctic stratosphere from electron microscope measurements on individual particles. The possible region of this type of particle is expected to be a little higher than the height of the usual background aerosol layer from temperature measured during the observation period. Most of the nitrate particles were detected above the sulfate aerosol layer. A high aerosol layer has been frequently observed in the early winter at Syowa. This may be due to formation of nitrate particles above the sulfate aerosol layer.

The externally mixed nitrate particles in the background sulfate particle layer suggests the possibility of NAT particle sedimentation.

REFERENCES

- Bigg, E. K., A. Ono, and J. A. Williams, Chemical tests for individual submicron aerosol particles, *Atmos. Environ.*, **8**, 1-13, 1974.
- Crutzen, P. J., and F. Arnold, Nitric acid cloud formation in the cold Antarctic stratosphere: A major cause for the springtime "ozone hole," *Nature*, **324**, 651-655, 1986.
- Fahey, D. W., K. K. Kelly, G. V. Ferry, L. R. Poole, J. C. Wilson, D. M. Murphy, M. Lowenstein, and K. R. Chan, In situ measurements of total reactive nitrogen, total water, and aerosol in a polar stratospheric cloud in the Antarctic, *J. Geophys. Res.*, **94**, 11299-11351, 1989.
- Farman, J. C., B. G. Gardiner, and J. D. Shanklin, Large losses of total ozone in Antarctica reveal seasonal ClOx/NOx interaction, *Nature*, **315**, 207-210, 1985.
- Gandrud, B. W., P. D. Sperry, L. Sanford, K. K. Kelly, G. V. Ferry, and K. R. Chen, Filter measurement results from the airborne Antarctic ozone experiment, *J. Geophys. Res.*, **94**, 11179-11738, 1989.
- Gras, J. L., and J. E. Laby, Southern hemisphere stratospheric aerosol measurements 1, Simultaneous impactor and in situ single-particle (light scatter) detection, *J. Geophys. Res.*, **83**, 1869-1874, 1979.
- Hansen, D., and K. Mauersberger, Laboratory studies of the nitric acid trihydrate: Implications for the south polar stratosphere, *Geophys. Res. Lett.*, **15**, 855-858, 1988.
- Hofmann, D. J., J. M. Rosen, J. W. Harder, and J. V. Hereford, Balloon-borne measurements of aerosol, condensation nuclei, and cloud particles in the stratosphere at McMurdo station, Antarctica, during the spring of 1987, *J. Geophys. Res.*, **94**, 16527-16536, 1989.
- Hofmann, D. J., J. M. Rosen, and J. W. Harder, Aerosol measurements in the winter/spring Antarctic stratosphere, 1, Correlative measurements with ozone, *J. Geophys. Res.*, **93**, 665-676, 1988.
- Hofmann, D. J., J. M. Rosen, R. Reiter, and H. Jager, Lidar and balloon-borne particle counter comparisons following recent volcanic eruptions, *J. Geophys. Res.*, **88**, 3777-3782, 1983.
- Iwasaka, Y., Non-spherical particles in the antarctic polar stratosphere—increase in particulate content and stratospheric water vapor budget, *Tellus*, **38B**, 364-374, 1986.
- Iwasaka, Y., T. Hirasawa, and H. Fukunishi, Lidar measurements on the Antarctic stratospheric aerosol layer, I, Winter enhancement, *J. Geomagn. Geoelectr.*, **37**, 1087-1095, 1985.
- McCormick, M. P., H. M. Steele, P. Hamill, W. P. Chu, and T. J. Swisler, Polar stratospheric cloud sightings by SAM II, *J. Atmos. Sci.*, **39**, 1387-1397, 1982.
- McElroy, M. B., R. J. Salawitch, and S. C. Wofsy, Antarctic O₃: Chemical mechanism for the spring decrease, *Geophys. Res. Lett.*, **13**, 1296-1299, 1986.
- Molina, M. J., T. Tso, L. T. Molina, and F. C. Y. Wang, Antarctic stratospheric chemistry of chlorine nitrate, hydrogen chloride, and ice release of active chlorine, *Science*, **238**, 1253-1257, 1987.
- Ono, A., M. Yamato, and M. Yoshida, Molecular state of sulfate aerosols in the remote Everest highlands, *Tellus*, **35B**, 197-205, 1983.
- Rosen, J. M., D. J. Hofmann, and J. W. Harder, Aerosol measurements in the winter/spring Antarctic stratosphere, 2, Impact on polar stratospheric cloud theories, *J. Geophys. Res.*, **93**, 677-686, 1988.
- Russell, P. B., W. Vezee, R. D. Hake, Jr., and R. T. H. Collis, Lidar observations of the stratospheric aerosol: California, October 1972-March 1974, *Q. J. Roy. Meteorol. Soc.*, **102**, 675-695, 1976.
- Solomon, S., R. R. Garcia, F. S. Rawland, and D. J. Waebles, On the depletion of Antarctic ozone, *Nature*, **321**, 755-758, 1986.
- Toon, O. B., P. Hamill, R. P. Turco, and J. Pinto, Condensation of HNO₃ and HCl in the winter polar stratospheres, *Geophys. Res. Lett.*, **13**, 1284-1287, 1986.
- Turco, R. P., R. C. Whitten, and O. B. Toon, Stratospheric aerosols: Observation and theory, *Rev. Geophys.*, **20**, 233-279, 1982.
- Weisweiler, W. K., and B. U. Schwarz, Nature of ammonium containing particles in an urban site of Germany, *Atmos. Environ.*, **24B**, 107-114, 1990.
- Yamato, M., Y. Iwasaka, A. Ono, and M. Yoshida, On the sulfate particles in the submicron size range collected at Mizuho station and in East Queen Maud Land, Antarctica, *Proc. NIPR Symp. Polar Meteorol. Glaciol.*, No. 1, 82-90, 1987.

92-17867



AD-P007 363



Tropospheric Nitrogen Oxide Measurements at Barrow, Alaska

D. A. Jaffe and R. E. Honrath

Geophysical Institute and Department of Chemistry, University of Alaska Fairbanks, Fairbanks, Alaska, U.S.A.

ABSTRACT

Nitrogen oxides play a critical role in the chemistry of the atmosphere and indirectly influence global warming through the production of ozone. At Barrow, Alaska, the NOAA long-term surface ozone record indicates an increase of about 2% per year during the summer months. Since NO_x ($\text{NO} + \text{NO}_2$) concentrations above about 30 ppt (parts per trillion) result in net ozone production in the presence of sunlight, we propose that the observed Barrow surface ozone increase is related to anthropogenic nitrogen oxide emissions.

A high-sensitivity chemiluminescent instrument for measurements of nitrogen oxides has been built to test this hypothesis. Measurement campaigns have been conducted during summer 1988 and spring 1989, and are continuing during spring and summer 1990.

Periods during which the NO_y concentrations measured at the GMCC site were unaffected by local (Barrow) emissions were selected from the data record. Observations during these periods suggest that nitrogen oxide concentrations are, at times, very elevated at Barrow and sufficient to account for photochemical O_3 production. Based on simultaneous collection of meteorological, sulfur, and NO_y data, several sources of nitrogen oxides have been tentatively identified at Barrow. These include (1) long-range transport of pollution from Eurasia; (2) Prudhoe Bay NO_x emissions; and (3) soil emissions.

INTRODUCTION

Nitrogen oxides play a critical role in the chemistry of the atmosphere [Crutzen, 1979]. By controlling the photochemical production of ozone and hydroxyl radicals in the troposphere, NO_x ($\text{NO} + \text{NO}_2$) plays a central role in atmospheric photochemistry. Additionally, NO_x is a precursor to nitric acid, a major constituent of acid rain [Galloway and Likens, 1981]. Other nitrogen oxides, such as peroxyacetyl nitrate (PAN), may play a significant role in the global distribution and lifetime of nitrogen oxides [Singh, 1987]. The concentration of total reactive nitrogen ($\text{NO}_y = \text{NO} + \text{NO}_2 + \text{HNO}_3 + 2\text{N}_2\text{O}_5 + \text{PAN} + \text{RONO}_2 + \text{particulate-NO}_3 + \dots$) can be used as a surrogate for the individual species and can provide valuable information on transport and removal processes, especially in situations where measurements of individual species are limited by resources or instrument sensitivities. In addition, it is possible that unknown and/or

unmeasured compounds make up a significant fraction of the total NO_y reservoir in remote areas [Singh, 1987].

The role that anthropogenic nitrogen oxides play in changes in arctic tropospheric ozone concentrations is not well understood. Surface ozone at Barrow during summer has shown a 2% per year increase since 1973 [Oltmans and Komhyr, 1986]. Industrial nitrogen oxides emissions from the Prudhoe Bay area could be responsible for the observed summer surface ozone increase, although to date the available summer NO_y data do not support this hypothesis. Alternatively, photochemical O_3 production resulting from lower-latitude NO_x sources could also contribute to the observed O_3 increase.

In this paper, we present NO_y data from two measurement campaigns conducted at the NOAA GMCC station near Barrow, Alaska, during the summer of 1988 and spring of 1989. These data constitute the longest and most complete data record for NO_y in the Arctic during spring and

support the general notion of "arctic haze": the long-range transport of pollution from distant anthropogenic sources. However, the NO_y observations additionally indicate the existence of a significant regional pollution source which should be taken into account in future arctic air pollution studies.

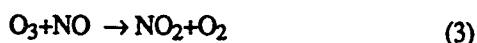
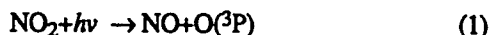
EXPERIMENTAL

NO and NO_y were measured using a high-sensitivity chemiluminescent detector built at the University of Alaska Fairbanks for this purpose [Honrath and Jaffe, 1990; Jaffe et al., 1991]. NO_y is detected as NO following reduction in a heated converter. During this period, there has been steady improvement in the accuracy and precision of low-level NO and NO_y measurements at Barrow. The current detection limit for this instrument is 5 ppt (parts per trillion) with an estimated uncertainty at concentrations well above the detection limit of approximately 15%.

Since NO_x is produced in virtually all combustion processes, it is necessary to carefully screen the data to eliminate local impacts on the data. In order to remove any possibility of the local sources impacting the measurements, the data were screened by wind direction and variability. Data shown here were obtained only when the winds were not from the direction of significant local sources and exhibited low variability.

Estimation of NO_x Concentrations

Although only NO and NO_y were measured, NO_x ($\text{NO} + \text{NO}_2$) concentrations can be estimated during the day using the photostationary state approximation [Leighton, 1961]. This approximation makes use of the rapid equilibrium achieved between the reactions



In the absence of oxidants other than ozone that convert NO to NO_2 , the steady-state concentration of NO_2 is given as

$$[\text{NO}_2]_{ss} = \frac{k_3[\text{NO}][\text{O}_3]}{J_1}$$

J_1 was not measured, but was estimated using the radiative transfer model of Stamnes et al. [1990], based on clear sky, no aerosol, and an 85% surface albedo.

RESULTS

Summer 1988 Measurements

A histogram of the background NO_y concentrations during the summer of 1988 is shown in Figure 1. These data have been screened by wind direction as well as ambient variability. The 175 values range from below 50 to 300 ppt. The median, mean, and standard deviation are 100, 120, and 60 ppt, respectively. NO concentrations were generally below our detection limit of 50 ppt, and the maximum observed was 100 ppt.

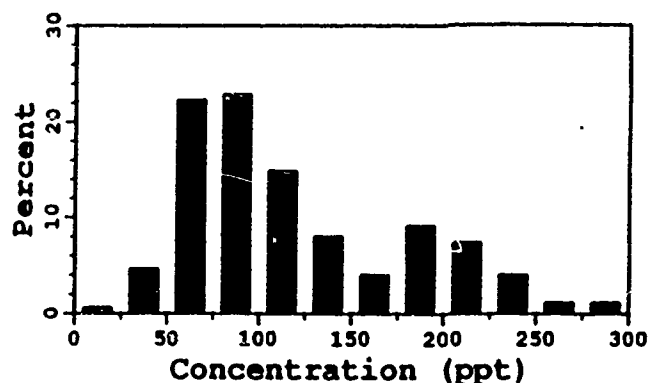


Figure 1. Histogram of background NO_y concentrations during summer, 1988.

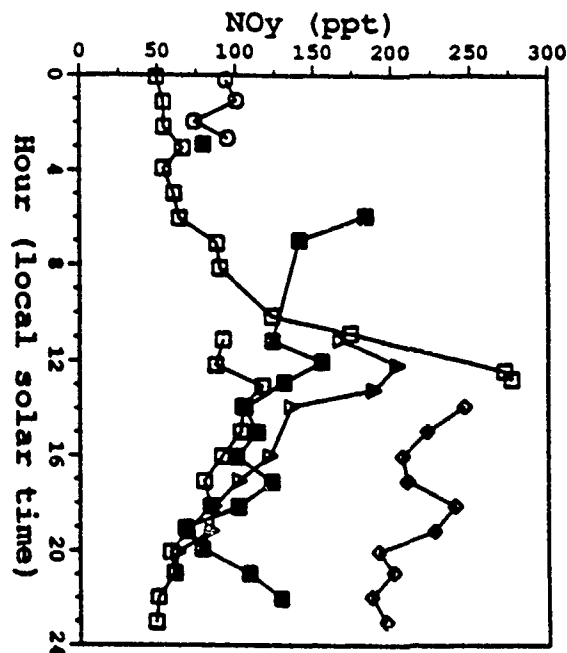


Figure 2. Diurnal variation in background NO_y during summer. Data points represent hourly averages. Data from different days are plotted with different symbols.

Hourly averages of the clean-air NO_y concentrations are shown in Figure 2 for each day, as a function of time of day. The concentrations exhibit a tendency to increase during midday, with lowest values near midnight. The mean day-time concentration of 140 ppt (6 a.m.–6 p.m. local solar time) is 40 ppt greater than that at night (6 p.m.–6 a.m. local solar time) (significant at the 99.9% confidence level). This diurnal cycle may be related to biological NO production, which increases with soil temperature [Williams et al., 1987], although diurnal boundary layer fluctuations could also produce a daily cycle.

Spring 1989 Measurements

Springtime concentrations of NO and NO_y were measured from March 2–April 7, 1989. After screening by wind direction and ambient variability, two types of periods were identified [Jaffe et al., 1991]: "background periods" and "events." Background periods correspond to times when NO

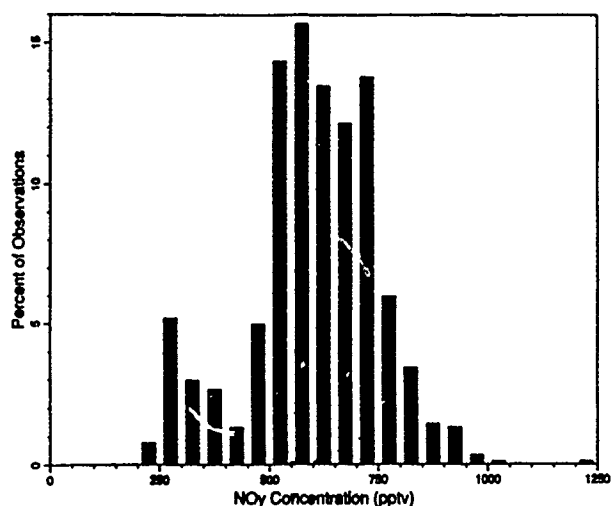


Figure 3. Histogram of background NO_y concentrations during spring, 1989.

and NO_y concentrations were relatively constant and were low (relative to the overall data record). Inspection of the raw data also revealed several "events," during which ambient concentrations changed smoothly and reached high values, and wind was generally from the clean sector (5° – 130°). Maximum NO_y levels exceeded 3 ppb during each event.

Background Periods

Eleven background periods were identified. Concentrations varied very little during individual periods, but larger differences were observed between periods. A histogram of all NO_y measurements during the springtime background periods ($N=885$) is shown in Figure 3. Median NO_y levels during each of the 11 background periods ranged from 280–850 ppt, with an overall median of 616 ppt. NO concentrations during background periods were all below our detection limit of 75 ppt. Based on the photostationary-state calculations described above, NO_x levels must have been below ~ 145 ppt, at least during clear midday periods.

An analysis of 850 mb back-trajectories [Harris, 1982; Jaffe et al., 1991] shows that these measurements are consistent with the understanding of a generally contaminated reservoir of air over the arctic basin during winter and spring, regenerated by episodic transport from source regions. The relatively constant and high NO_y levels during Arctic trajectories are indicative of a high- NO_y arctic reservoir. Lower levels during periods of transport from the south are likely due to enhanced scrubbing of air by the greater frequency and amount of precipitation in those regions. Interestingly, the springtime concentrations were higher than those in summer, even during southerly flow, consistent with the increased lifetime of NO_y reservoir compounds, such as PAN, during winter [Singh and Hanst, 1981].

Events

During this campaign, four identifiable pollution "events" were observed, lasting from 12–60 hours each as shown in Figure 4. NO_y reached a peak of 16.4 ppb, and NO reached 1.4 ppb. The suddenness with which these events occur and the extremely high NO_y concentrations observed for a back-

NO_y Concentration During Events

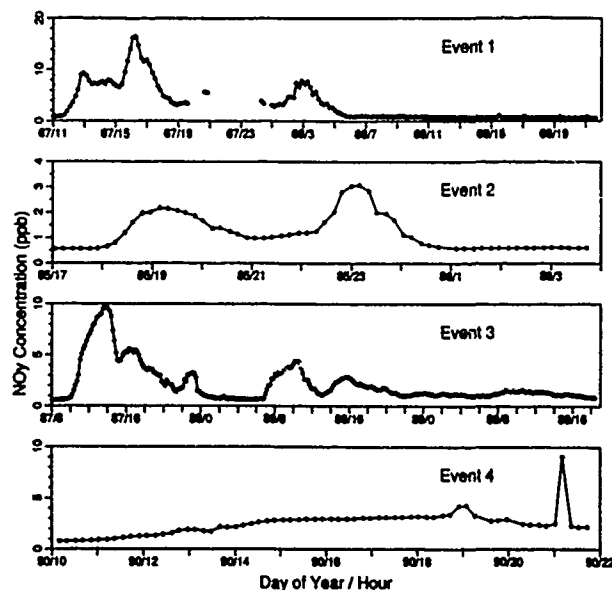


Figure 4. NO_y concentrations during events observed during spring, 1989.

ground site are not characteristic of "arctic haze." Moreover, the relatively smooth changes in NO_y concentration during the events contrast sharply with the well-characterized high-variability signatures of local (Barrow) pollution sources [Honrath and Jaffe, 1990].

Figure 5 shows a plot of the observed NO_y concentrations during events and background periods versus the local wind direction. The events were observed to occur when wind directions were in the range of 98° – 233° . Highest NO_y concentrations were observed when local winds were from 110° – 120° , suggesting that the nitrogen oxide source responsible for these events is located in that sector. The only major NO_x source in that direction is the Prudhoe Bay oil production complex, located at 111° from Barrow and approximately 300 km distant. The NO_x emissions from those facilities arise from natural gas combustion, and are estimated at 10,000–15,000 metric tons yr^{-1} [J. Coutts, personal communication, 1989]. It is interesting to note that Prudhoe Bay was first suggested as a possible influence on the Barrow record by Radke et al. [1976] based on measurements of condensation nuclei at Barrow during 1970.

During the four events, NO concentrations were always above the detection limit during sunlit hours, and were frequently a large fraction of NO_y . Estimated $\text{NO}_x:\text{NO}_y$ ratios during the events were very high, reaching a maximum value of 0.87, and were highly correlated with NO_y concentration. The large $\text{NO}_x:\text{NO}_y$ ratio indicates that the plumes were not aged. Since photochemical reactions transform NO_x to other NO_y compounds, the $\text{NO}_x:\text{NO}_y$ ratio can be used as a measure of the photochemical age of an air mass. Air sampled during background periods at Barrow had a low $\text{NO}_x:\text{NO}_y$ ratio and is photochemically well aged, while the air sampled during events 1–4 was relatively fresh.

Filter measurements of sulfur compounds support the hypothesis of a plume enriched primarily in NO_x and NO_y [Jaffe et al., 1991]. The sulfur (SO_4+SO_2) concentration during the events was not significantly different from the concentration during background periods. This indicates that the source responsible for NO_y enrichments did not sig-

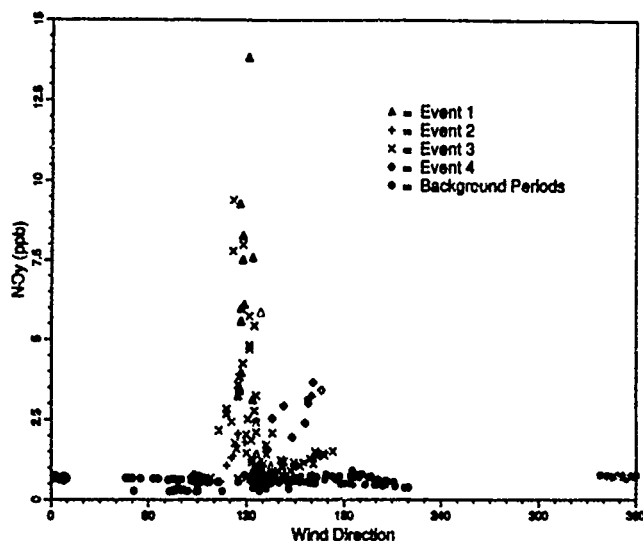


Figure 5. NO_y concentrations during events and background periods (spring, 1989) versus surface wind direction at the Barrow GMCC site.

nificantly affect the background arctic haze sulfur concentrations, consistent with the hypothesis that Prudhoe Bay emissions are responsible for the NO_y events at Barrow. Prudhoe Bay has a very large $\text{NO}_x:\text{SO}_2$ emission ratio (22–33 on a molar basis) [J. Coutts, personal communication, 1988].

SUMMARY

As a result of this measurement program, we have learned a great deal about nitrogen oxides in the arctic atmosphere. Some of the major conclusions based on this research to date include:

Arctic Background NO_y . NO_y concentrations in the arctic are significantly higher in spring than in summer. In springtime, surface NO_y levels at Barrow appear to be comparable to concentrations in the free troposphere outside of arctic haze layers [Dickerson, 1985] and about 50% of the levels in haze layers. In addition, springtime NO_y concentrations during southerly flow (as indicated by 850-mb trajectories) were ~50–70% of the levels observed when trajectories indicate arctic air was being sampled at Barrow. However,

springtime concentrations were higher than those in summer even during southerly flow, providing evidence for an increased NO_y lifetime during winter. NO_x concentrations in the Arctic during spring are estimated to be 0–20% of NO_y concentrations. In summer, NO_y levels at Barrow were very low and exhibited a diurnal cycle, which may be due to soil NO emissions.

NO_y "Events." Substantially elevated NO_y concentrations (to >16 ppb) were observed during spring 1989 in four events lasting from 12–60 hours. Substantial evidence indicates that emissions from the Prudhoe Bay industrial region are responsible: (1) Slow and smooth concentration variations during the events indicate that local (Barrow) sources were not the cause; (2) The correlation with local wind direction indicates that the source is in the 110° – 120° sector, consistent with Prudhoe Bay, which lies at a 111° bearing from Barrow; (3) The ratio of $\text{NO}_x:\text{NO}_y$ estimated during these events is very high (to 0.87) and indicates that the NO_y enrichment is almost entirely due to NO_x . This implies that very fresh NO_x emissions were responsible for the events; (4) Filter measurements of SO_4^{2-} and SO_2 do not indicate enrichment of sulfur compounds during the events. This is consistent with a source, such as Prudhoe Bay, which is rich in NO_x .

Although the GMCC site at Barrow is in a remote region, it is affected by local-, regional-, and global-scale pollutant sources. In order to differentiate between these sources, data collected at such a site must be selected with great care so that measurements are representative of specific, identifiable air masses. These data indicate that atmospheric transport processes can bring different air masses to the Barrow site on a time scale of hours. Daily, weekly, or monthly means may therefore not be adequate to discriminate between different air masses. In general, measurement systems which provide high time resolution data will provide greater insight into complex atmospheric processes at a site such as Barrow.

ACKNOWLEDGMENTS

Trajectories were calculated by Joyce Harris (NOAA GMCC, Boulder, Colorado). W. T. Sturges, S.-M. Li, and the staff of the Barrow GMCC station helped with sample collection. We are also thankful for assistance from the North Slope Borough Department of Wildlife Management. This work was supported by NSF grant ATM 88-14518.

REFERENCES

- Crutzen, P. J., The role of NO and NO₂ in the chemistry of the troposphere and stratosphere, *Ann. Rev. Earth Planetary Science*, 7, 443-472, 1979.
- Dickerson, R. R., Reactive nitrogen compounds in the Arctic, *J. Geophys. Res.*, 90, 10739-10743, 1985.
- Galloway, J. N., and G. E. Likens, Acid precipitation: the importance of nitric acid, *Atmos. Env.*, 15, 1081-1085, 1981.
- Harris, J. M., The GMCC atmospheric trajectory program, *NOAA technical memo ERL ARL-116*, Air Resources Laboratory, Rockville, Maryland, 1982.
- Honrath, R. E., and D. A. Jaffe, Measurements of nitrogen oxides in the arctic, *Geophys. Res. Lett.*, 17, 611-614, 1990.
- Jaffe, D. A., R. E. Honrath, J. A. Herring, and S.-M. Li, Measurement of nitrogen oxides at Barrow, Alaska during Spring: Evidence for regional and northern hemispheric sources of pollution, *J. Geophys. Res.*, 96, 7395-7405, 1991.
- Kahl, J. D., J. M. Harris, G. A. Herbert, and M. P. Olson, Intercomparison of three long-range trajectory models applied to arctic haze, *Tellus*, 41B, 524-536, 1989.
- Leighton, P. A., *Photochemistry of Air Pollution*, Academic Press, New York, 1961.
- Oltmans, S., and W. P. Komhyr, Surface ozone distributions and variations from 1973-1984: measurements at the NOAA Geophysical Monitoring for Climatic Change baseline observatories, *J. Geophys. Res.*, 91, 5229-5236, 1986.
- Radke, L. F., P. V. Hobbs, and J. E. Pinnons, Observations of cloud condensation nuclei, sodium-containing particles, ice nuclei and the light-scattering coefficient near Barrow, Alaska, *J. Appl. Met.*, 15, 982-995, 1976.
- Singh, H. B., Reactive nitrogen in the troposphere, *Env. Sci. Tech.*, 21, 320-327, 1987.
- Singh, H. B., and P. L. Hanst, Peroxyacetyl nitrate (PAN) in the unpolluted atmosphere: an important reservoir for nitrogen oxides, *Geophys. Res. Lett.*, 8, 941-944, 1981.
- Stamnes, K., and S.-C. Tsay, Optimum spectral resolution for computing atmospheric heating and photodissociation rates, *Planet. Space Sci.*, 38, 807-820, 1990.
- Williams, E. J., D. D. Parrish, and F. C. Fehsenfeld, Determination of nitrogen oxide emissions from soils: results from a grassland site in Colorado, United States, *J. Geophys. Res.*, 92, 2173-2179, 1987.

Observation of Ozone and Related Quantities by the Japanese Antarctic Research Expedition

H. Kanzawa and S. Kawaguchi
National Institute of Polar Research, Tokyo, Japan

ABSTRACT

Total ozone observations with a Dobson spectrophotometer, routinely carried out at Syowa Station (69°S, 40°E) since 1966, contributed to the discovery and confirmation of the Antarctic ozone hole. Routine meteorological sonde observations since the IGY period and ozone sonde observations since 1966 at Syowa Station gave useful information on the cause of the formation of the Antarctic ozone hole. Other observations at Syowa Station during the Middle Atmosphere Program period (1982–1985) also gave much information on the Antarctic ozone layer.

The "spring" total ozone at Syowa Station showed record low values in 1987 and 1989. In 1988, the following phenomenon was observed over Syowa Station. There occurred a large, sudden stratospheric warming in late winter 1988, competing in suddenness and size with major mid-winter warmings in the northern Hemisphere. Associated with the dynamical phenomenon of the sudden warming, total ozone suddenly increased. The sudden warming, as well as other warmings, which followed it made "spring" total ozone amount higher.

Meridional distributions of ozone were obtained with ozone sonde observations made by the Japanese Antarctic Research Ship, *Shirase*, on the way from Japan to Syowa Station, at intervals of about every 5 degrees for November through December in 1987 and 1988. Characteristics of interest may be summarized as follows: south of about 60°S, partial pressure of ozone shows low values in the altitude range of 10–18 km, while large values occur at 20–25 km; there was a tropopause gap around 30–35°S through which ozone seems to intrude from the stratosphere to the troposphere.

One or two balloons will be launched under the Polar Patrol Balloon (PPB) project in September 1991 at Syowa Station to measure in situ ozone, aerosol, and temperature for about two weeks along the track of the balloon on the 50 mb level over Antarctica. Data acquisition and balloon positioning will be made using the ARGOS system. Since the PPB observation is a Lagrangian type observation, the ozone measurement can detect the chemical source/sink of ozone more directly than other types of observation, and the aerosol measurement will give much information on the role of Polar Stratospheric Clouds (PSCs) in the formation of the Antarctic ozone hole.



Ozone Evolution Peculiarities in the Polar Regions: Analysis of Observational Data and Results of Modeling

Igor I. Mokhov

Institute of Atmospheric Physics, Academy of Sciences of the U.S.S.R., Moscow, U.S.S.R.

ABSTRACT

Analysis of ozone evolution peculiarities in intra-annual evolution of latitude-altitude and latitude-longitude atmospheric ozone concentration fields was carried out using a special method of amplitude-phase characteristics. The TOMS satellite ozone data for the period 1978-1987 were used in the analysis. Comparison was made with results of analysis of total ozone evolution based on data obtained from the World Data Center for Ozone (Toronto) and from the Main Geophysical Observatory (Leningrad) for the period 1973-1985 at 133 Northern and Southern hemisphere stations. Latitude-altitude peculiarities of the evolution of ozone concentrations from different satellite data are compared with results of simulations using a two-dimensional photochemical model of the atmosphere. There are large differences in ozone evolution in polar latitudes of the Northern and Southern hemispheres in different stratospheric layers and for different seasons. Particularly it was noted that the "ozone hole" phenomenon is more pronounced in the Antarctic than in the Arctic. Comparison with results of standard harmonic analysis was also carried out.

There have been many climatological studies of atmospheric ozone distribution, a number of which have been based on a harmonic analysis of ozone annual variations. However, a formal separation by certain modes does not always give a clear understanding of the real processes.

Analysis of the ozone evolution peculiarities in the intra-annual evolution for latitude-longitude and latitude-altitude ozone concentration fields in the atmosphere was carried out using a special method of amplitude-phase characteristics [Mokhov, 1985; Gruzdev and Mokhov, 1988]. The purpose of using this method is to minimize our prescription (for example, by the fixed mode representation) of the evolution of different fields.

TOMS (The Total Ozone Mapping Spectrometer) satellite data from Nimbus 7 [Bowman, 1989] for the total ozone content (TO) in the atmosphere during 1979-1987 were analyzed. (TOMS ozone data were provided by the National Space Science Data Center at Goddard Space Flight Center. The original TOMS data processing was carried out by A. J. Fleig, D. Heath, A. J. Krueger and the Nimbus Ozone Pro-

cessing Team. The 5°x5° ozone data set was prepared by K. Bowman.) The results of this analysis are interesting to compare with results of the standard harmonic analysis of the TOMS data for 4 years [Bowman and Krueger, 1985].

Study of the amplitude characteristics [Mokhov, 1985; Gruzdev and Mokhov, 1987] of the TO seasonal evolution revealed changes of boundaries of regions with the TO (X) decrease of $\Delta X = 20$ DU compared with March and September (Figure 1). In the high NH latitudes on the TOMS data the largest values of TO occurred in March (>480 DU) and the smallest values in September-October (<260 DU). In the SH high latitudes the smallest values of TO were noted in March-April (<260 DU) and the largest values in October (>400 DU) in subantarctic latitudes. So the ozone changes in the annual cycle compared with March are characterized in the NH high latitudes by a TO decrease (in the SH by an increase) on the whole. The appropriate ozone changes compared with September are characterized in the NH high latitudes by a TO increase (in the SH by a decrease) on the whole.

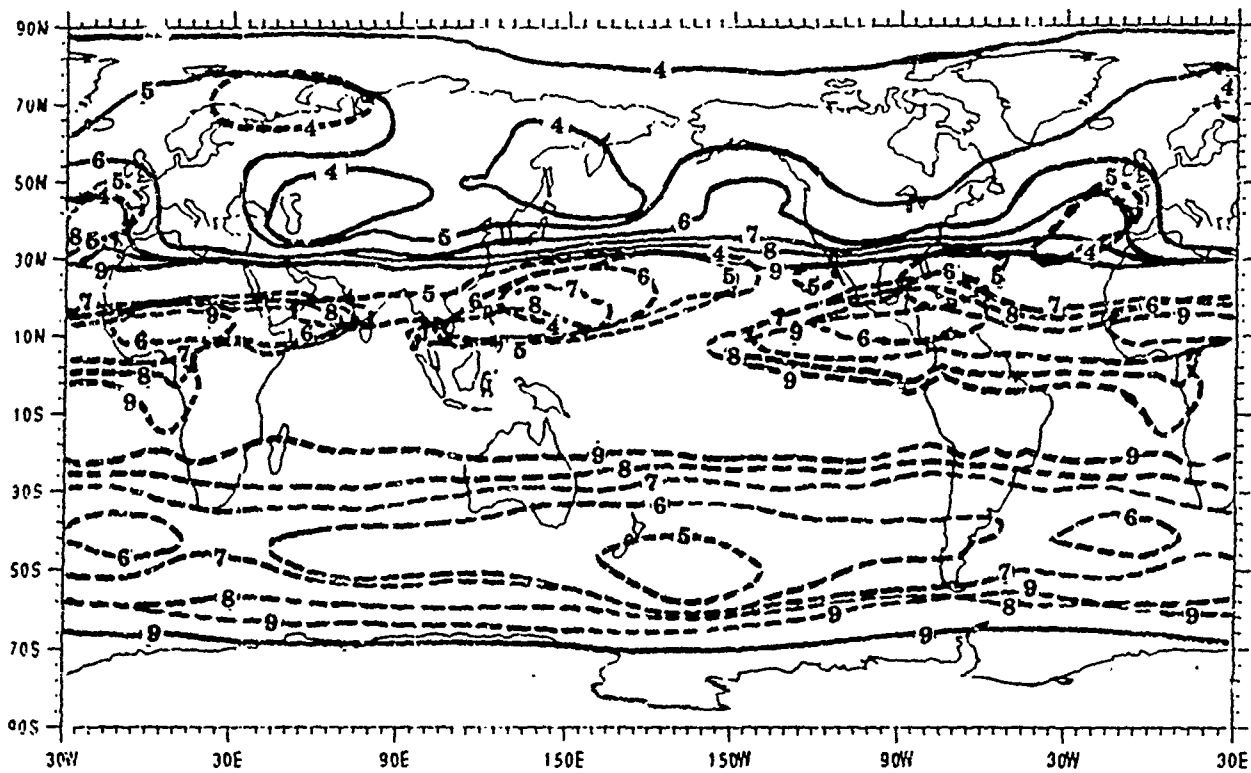


Fig. 1a

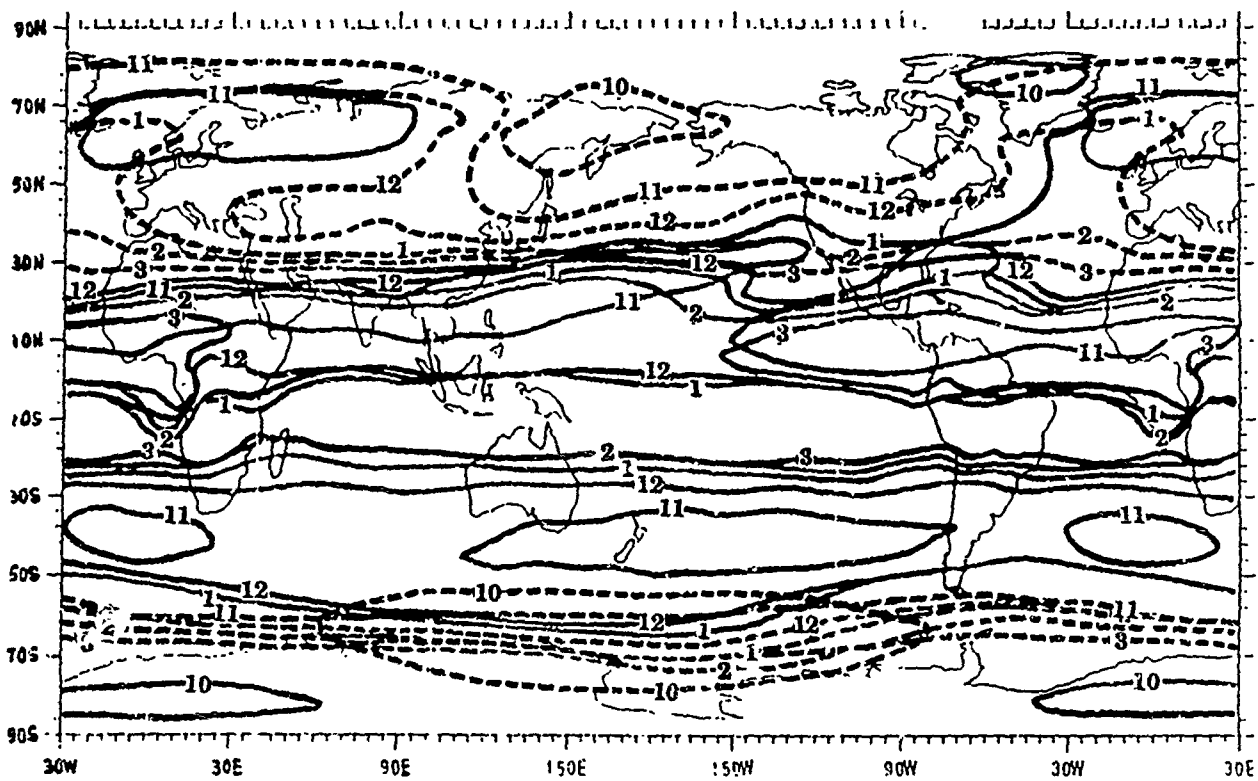


Fig. 1b

Figure 1. Successive isochrone boundaries (time in months) of areas with: (a) total ozone decrease (full isochrones) and increase (dotted isochrones) by 20 DU relative to March, (b) total ozone increase (full isochrones) and decrease (dotted isochrones) by 20 DU relative to September on TOMS data.

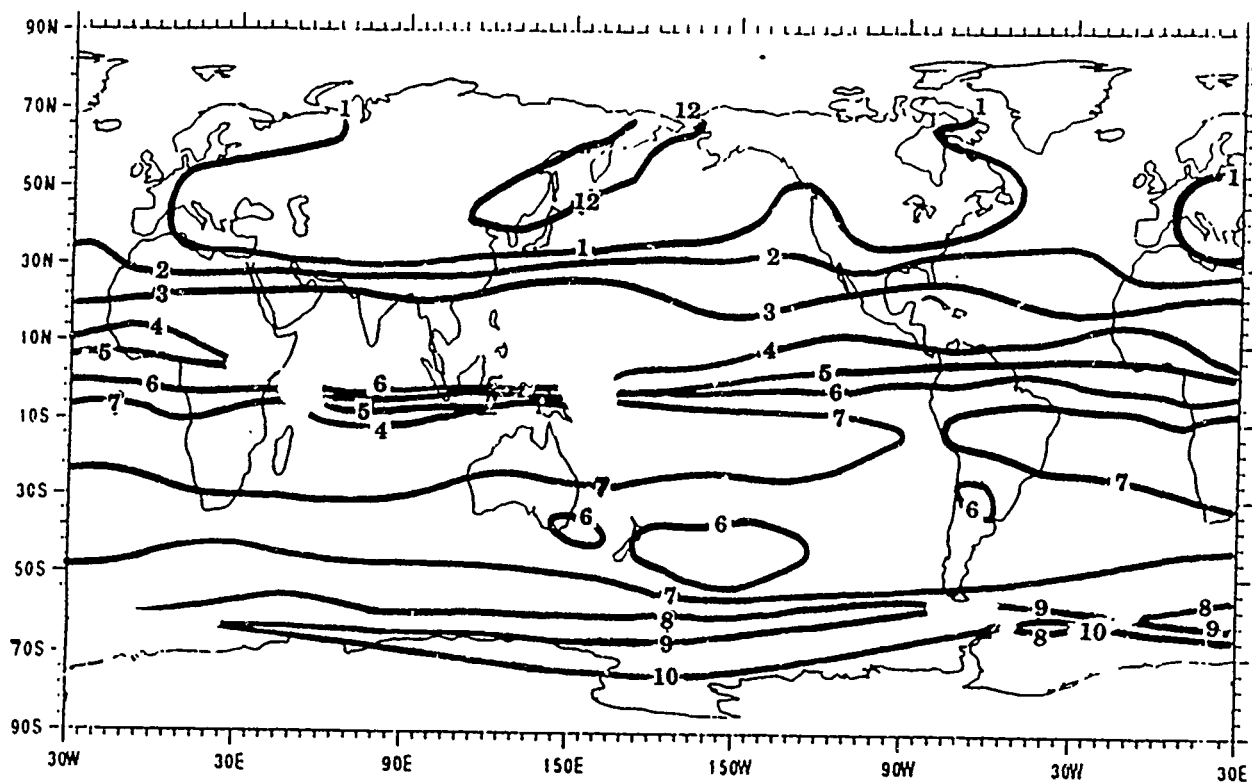


Fig. 2 a

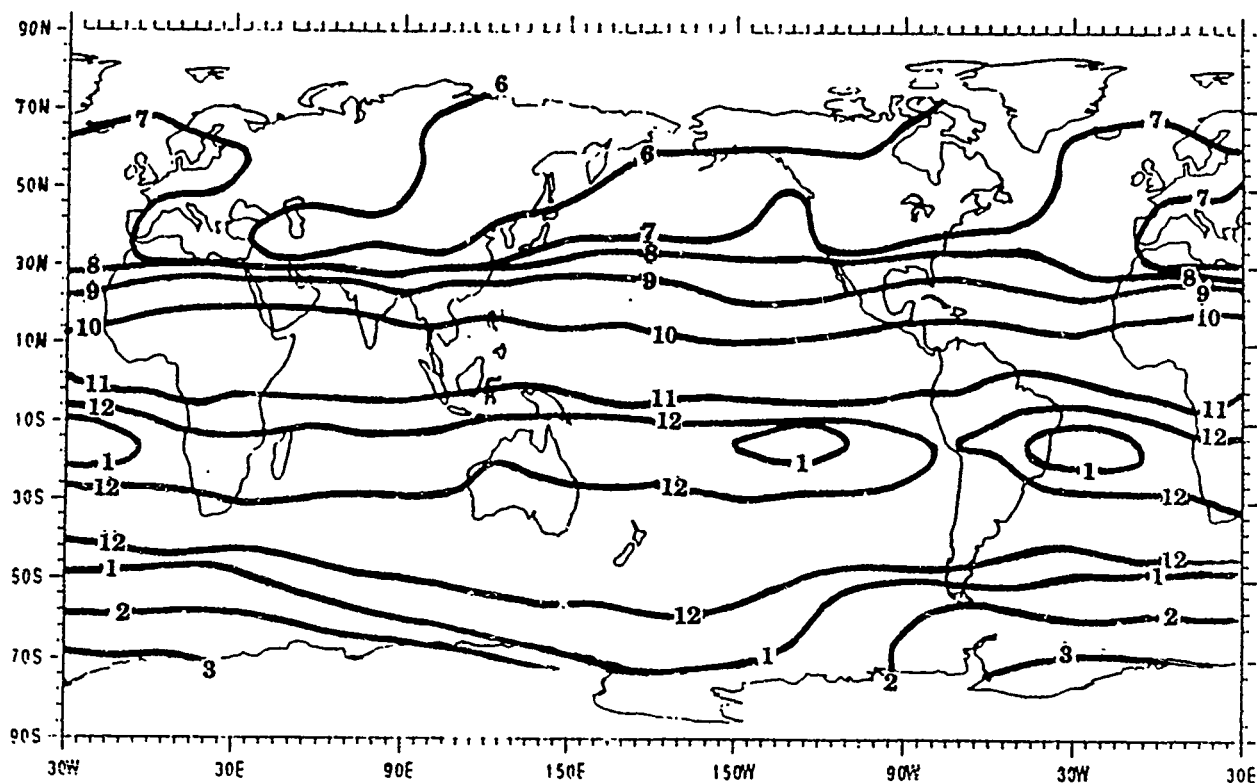


Fig. 2 b

Figure 2. Successive isochrones of O-phase (a) and π -phase (b) for total ozone in the annual cycle on TOMS data.

The general tendencies of TO evolution in the annual cycle against March and September on Figure 1 correspond in the NH on the whole to the shift of the appropriate successive isochrones (with time in months) from high to tropical latitudes. Peculiarities were noted over the Far East and over Middle Asia, with the most rapid decrease of TO relative to the March state. It should be noted that the spreading of successive isochrones on Figure 1a from higher to lower latitudes for the process of TO decrease in the NH (from March to September) is slower over oceans. At the same time in the tropics the TO was larger compared to March.

For the SH the TO is increased on the whole with respect to March during the next six months. In April there is a small region in Antarctica with a TO decrease of 20 DU relative to March. In September such changes were marked over all Antarctica. The most rapid increase of $\Delta X=20$ DU in the SH was exhibited over oceanic regions of $30^\circ-50^\circ$ latitudes (at first over the Pacific ocean). Then successive isochrones of an appropriate TO increase spread to polar and tropical latitudes.

According to Figure 1 there are significant differences in ozone evolution in the annual cycle for the NH and the SH. There are also some differences between the global evolution of processes of TO decrease and increase, particularly relative to March and September.

The most rapid increase of TO of 20 DU compared to September was noted for the NH over northeast Asia and Alaska (Figure 1b). As was the case for TO decrease, the spreading of successive isochrones on Figure 1b from higher to lower latitudes showing TO increase in the NH (from September to March) is slower over the oceans. Note the difference in TO evolution over Middle Asia during spring and fall. For the fall evolution there is also peculiarity. This is a region with relatively rapid TO changes; however, in fall the process is relatively late compared to the eastern part of Asia.

The process of TO increase (on Figure 1b of 20 DU) relative to September in the SH begins near 60°S over the Australian (Pacific and Indian oceans) sector. Then the appropriate successive isochrones spread to higher polar latitudes. It should be noted that in October, along with the region of TO increase in the Australian sector in Figure 1b, there is a region of TO decrease relative to September over polar Antarctica latitudes in the Atlantic sector. This phenomenon is connected with an "ozone hole" over Antarctica.

It should be noted that in the polar latitudes of the NH there are regions with negative changes of TO of 20 DU relative to September: in October over Greenland and in November over the northern Atlantic, Europe and Western Siberia. These regions with delayed TO decrease are characterized by relative values of TO during these periods. In the NH this region should be further from pole than in the SH because the process of TO increase is going toward the pole in the SH and away from the pole (on the whole) in the NH.

From 60°S to the equator in the SH there were marked negative changes of TO relative to September during half a year (up to March). The most rapid decrease of TO of 20 DU was noted in the $30^\circ-40^\circ$ latitudes over the Pacific and Atlantic oceans (by mid-November) with subsequent spreading of the appropriate successive isochrones to higher

and lower latitudes. During this period the negative changes of TO were marked also in the tropical latitudes of the NH (Figure 1b).

Comparison with a similar analysis of the global ozone evolution in the annual cycle on ground-based data for TO [Gruzdev and Mokhov, 1990] exhibits similar general tendencies and peculiarities (Figure 2 for NH). Gruzdev and Mokhov [1990] used data from the World Data Center for Ozone (Toronto) and from the Main Geophysical Observatory (Leningrad) for the period 1973–1985 at 133 stations in the NH and 1 SH.

The tendency of a shift of boundaries for regions with TO changes (decrease compared with March or increase compared with September) by ΔX from high to tropical latitudes is exhibited also by the analysis of ground-based data for TO in the NH. In the NH, TO increases by mid-October by $\Delta X=20$ DU compared with September over a considerable part of the Far East and the Sea of Okhotsk, and by mid-November the TO increases over most of Canada. The TO increases by $\Delta X=50$ DU compared with September earlier (in November) over the Sea of Okhotsk, to the north of Scandinavia and Kola Peninsula (over the Barents Sea) and by December over Canada. By analysis of TO seasonal evolution relative to March it was determined that the decrease of TO, in addition to spreading from polar latitudes (earlier over North America), is rather rapid (by $\Delta X=20$ DU by mid-April) over Middle Asia and the Sea of Okhotsk [Gruzdev and Mokhov, 1990].

A special TO evolution is exhibited through analysis of amplitude characteristics in the tropics. Here the tendencies of the TO change of 20 DU relative to the September and March states are opposite on the whole to tendencies for nontropical latitudes of NH. The regions with an increase and decrease of the TO of 20 DU over these latitudes compared with September and March are bounded not only by latitude, but also by longitude. In the SH the spreading of successive isochrones occurs in a northerly direction (in the Australian sector to the southeast) with a relative stabilization of their position in the tropical latitudes.

Also analyzed from TOMS data were the phase characteristics of the ozone annual cycle. Figure 2 presents the isochrones of O-phase and π -phase, which characterize the moments (t_λ and t_π) of simultaneous reaching of a local annual mean TO value with positive (O) and negative (π) time derivatives [Mokhov, 1985; Gruzdev and Mokhov 1988]. (The value of $\Delta t = t_\pi - t_\lambda$ is not equal to half a period (year)).

The spreading of successive isochrones for O-phase in Figure 2a reflects to some extent the interseasonal TO evolution, exhibited in Figure 1b for the NH nontropical latitudes. The same tendencies as in Figure 1a were exhibited in Figure 2a for the SH nontropical latitudes. Significant peculiarities in the high SH latitudes are connected with the role of the semi-annual harmonic.

For isochrones of π -phase on Figure 2b, as for isochrones of O-phase, there was a slower spreading over oceans than over continents in the NH from high latitudes to the tropics. In the high latitudes of the SH, the direction of isochrone spreading is of opposite sign (to the pole).

Similar tendencies on the whole were found for isochrones of the O-phase and π -phase for the TO annual cycle on ground-based data [Gruzdev and Mokhov, 1990]. The

boundaries of π -phase and minimum-phase (m-phase) for the TO annual cycle over North America according to [Gruzdev and Mokhov, 1990] extend on the whole from high to low latitudes. In Eurasia there were regions over the Far East and Middle Asia with an earlier reaching of the appropriate phases. The peculiarities of these regions were noted also for the maximum-phase (M-phase) and O-phase. Over North America the earlier reaching of the M-phase and O-phase states was marked in the vicinity of 50° – 60° latitudes. In Gruzdev and Mokhov [1990] it was noted that O-phase, π -phase, M-phase and m-phase states of the TO intra-annual evolution differ considerably over certain regions. Some of these peculiarities of evolution are difficult to exhibit by analysis using the fixed mode decomposition (specifically, by the standard harmonic analysis).

The phase characteristics on different satellite data [Keeting and Young, 1985] were also determined for the zonal mean TO [Gruzdev and Mokhov, 1990]. On the whole all the phase isochrones have a tendency to shift with time from the north to the south. In the SH there is a tendency of the isochrones to shift from $\sim 40^{\circ}$ S to the equator. For the m-phase there are discontinuities at $\sim 10^{\circ}$ S and at 60 – 65° S. The forming of the "ozone hole" structure over Antarctica in the SH spring is connected with noted peculiarity. The spring TO minimum forms first (in August) at $\sim 60^{\circ}$ S and then in higher latitudes (occurring at 75° S in the middle of September). The sequence of the TO maximum isochrone shift (and the sequence of "hole" filling) also has a direction from lower to higher latitudes. This corresponds to "ozone hole" filling at the middle stratosphere levels.

The noted peculiarities of the TO evolution in polar regions are connected with peculiarities of the ozone content (q) evolution in different atmospheric layers and latitudinal belts [Gruzdev and Mokhov, 1988, 1989]. Gruzdev et al. [1988] compared the intra-annual evolution of the ozone latitude–longitude fields from satellite data with results of a two-dimensional photochemical model of the atmosphere. On the whole there was qualitative agreement, although there are also the remarkable quantity differences.

In the nontropical SH latitudes both for the model (with $[q]=\text{mol}/\text{cm}^3$) and on the basis of satellite data (with $[q]=\text{ppmv}$) there was a descent of the O-phase and π -phase isochrones in the middle and lower stratosphere. On satellite data [Keeting and Young, 1985] the O-phase isochrones are shifted from the middle stratosphere layers higher than 35 km, while the level of the π -phase isochrones forming in March is remarkably lower (near 30 km). For the model, as for the data, there is a shift of the successive O- and π -phase isochrones in the lower SH stratosphere from lower to polar latitudes. The boundary of the π -phase reaches the tropopause by October. The boundary of the O-phase reaches by October the level near 22 km in the 60° SH latitudes and by March–April the tropopause level.

Unlike the SH, in the NH stratosphere for q there is no general delay of reaching of the O- and π -phase states in comparison with lower latitudes. The region with reaching of the O-phase state is extended from polar latitudes in the lower NH stratosphere above 20 km and below 16 km the tendency of the shift to pole is exhibited.

The appropriate peculiarities of the ozone content evolution in the SH and NH stratosphere are exhibited also by an analysis of the amplitude characteristic of the q annual cycle. In Gruzdev et al. [1988] the peculiarities for isochrones of boundaries of regions with increase and decrease of the ozone content in the annual cycle relative June and December are noted.

The noted peculiarities of the ozone annual cycle characterize, in particular, the mechanisms of forming and filling of the atmospheric ozone deficit ("ozone holes") in the polar atmosphere. As shown by the direction of latitudinal displacement of successive isochrones, different ozone regimes are reached later in Antarctica than in neighboring latitudes, due to relative dynamical isolation of the Antarctic atmosphere. On the other hand, the seasonal ozone evolution in the Arctic is characterized on the whole by displacement of successive isochrones from high latitudes. These results indicate that the "ozone hole" phenomenon is more pronounced in the Antarctic than in the Arctic.

REFERENCES

- Bowman, K. P., Global patterns of the quasi-biennial oscillation in total ozone, *J. Atmos. Sci.*, **46**, 3328–3343, 1989.
- Bowman, K. P., and A. J. Krueger, A global climatology of total ozone from Nimbus 7 total ozone mapping spectrometer, *J. Geophys. Res.*, **90**, 7967–7976, 1985.
- Gruzdev, A. N., and I. I. Mokhov, Diagnostics of stratospheric and mesospheric dynamics in annual cycle with amplitude–phase characteristics method, *Preprint of the Institute of Atmospheric Physics*, Moscow, 1987.
- Gruzdev, A. N., and I. I. Mokhov, Evolution of stratospheric ozone annual dynamics from satellite data, *Issledovanie Zemli iz Kosmosa*, **2**, 3–10, 1988.
- Gruzdev, A. N., and I. I. Mokhov, Peculiarities of intra-annual global dynamics of total ozone content, *Meteor. i Geofiz.*, **7**, 1990.
- Gruzdev, A. N., I. L. Karol, A. P. Kudryavtsev, and I. I. Mokhov, Diagnostics of atmospheric ozone dynamics in annual cycle from empirical data and in photochemical model, *Conf. on Atmospheric Ozone (2–6 October, 1988, Suzdal)*, CAO, Dolgoprudny, 1988.
- Keeting, G. M., and D. F. Young, Interim reference ozone models for the middle atmosphere, *Handbook for MAP*, **16**, 205–229, 1986.

Uncertainties in Total Ozone Amounts Inferred from Zenith Sky Observations: Implications for Ozone Trend Analyses

K. Stamnes and S. Pegau

Geophysical Institute and Department of Physics, University of Alaska Fairbanks, Fairbanks, Alaska, U.S.A.

J. Frederick

Department of Geophysical Sciences, University of Chicago, Chicago, Illinois, U.S.A.

ABSTRACT

In an effort to determine ozone measurement uncertainties associated with zenith sky radiation observations we have used radiative transfer calculations to simulate ozone inference by the Dobson procedure. Synthetic zenith sky charts are computed for the commonly used AD wavelength pairs by a procedure that simulates the construction of empirical charts. By using a comprehensive radiative transfer algorithm, a model atmosphere and a suitable set of ozone absorption cross sections, we may simulate the effects of cloud optical depth, cloud altitude, vertical distribution of ozone, temperature profile and surface albedo on the total amount of ozone inferred by the Dobson procedure from zenith sky observations. Our simulations indicate that attempts to determine small changes in total ozone amounts from measurements of zenith sky intensity are fraught with difficulties. These findings imply that what appears to be a trend in total ozone could conceivably be due to changes in (1) ozone profile, (2) effective temperature, or (3) incorrect estimates of the effects of clouds or surface albedo. We discuss possible means of rectifying this ozone measurement problem by invoking computer simulations to determine possible sources and magnitudes of errors incurred in zenith sky measurements to infer total ozone. In particular, we suggest that construction and use of synthetic correction tables for any particular station may alleviate difficulties encountered in the creation of empirical correction tables, since it avoids problems related to (1) time lapse between measurements, and (2) diffuse radiation from forward scattering in clouds influencing the direct sun measurements. Instrumental effects can be accounted for by comparing the theoretical charts with direct sun measurements under clear sky conditions.

Permafrost-Associated Gas Hydrates of Northern Alaska: A Possible Source of Atmospheric Methane

T. S. Collett

U.S. Geological Survey, Menlo Park, California, U.S.A.

ABSTRACT

Atmospheric methane, a potential greenhouse gas, is increasing at such a rate that the current concentrations (≈ 1.7 ppm) will probably double in the next 50 years. Analysis of gases trapped in ice cores indicates that the contemporary atmospheric methane concentrations and their rate of increase are unprecedented over the last 160,000 years. Numerous researchers have suggested that destabilized gas hydrates may be contributing to this buildup in atmospheric methane. Little is known about the geologic or geochemical nature of gas hydrates, even though they are known to occur in numerous arctic sedimentary basins.

Because of the abundance of available geologic data, our research has focused on assessing the distribution of gas hydrates within the onshore regions of northern Alaska; currently, onshore permafrost-associated gas hydrates are believed to be insulated from most atmospheric temperature changes and are not at this time an important source of atmospheric methane. Our onshore gas hydrate studies, however, can be used to develop geologic analogs for potential gas hydrate occurrences within unexplored areas, such as the thermally unstable nearshore continental shelf.

On the North Slope, gas hydrates have been identified in 36 industry wells by using well-log responses calibrated to the response of an interval in one well where gas hydrates were recovered in a core by an oil company. Most gas hydrates we identified occur in six laterally continuous Upper Cretaceous and lower Tertiary sandstone and conglomerate units; all these hydrates are geographically restricted to the area overlying the eastern part of the Kuparuk River Oil Field and the western part of the Prudhoe Bay Oil Field. Stable carbon isotope geochemical analysis of well cuttings suggests that the identified hydrates originated from a mixture of deep-source thermogenic gas and shallow microbial gas that was either directly converted to gas hydrate or first concentrated in existing traps and later converted to gas hydrate. We postulate that the thermogenic gas migrated from deeper reservoirs along the faults thought to be migration pathways for the large volumes of shallow, heavy oil found in the same area.

The Role of Natural Gas Hydrates in Global Changes

Y. F. Makogon

Oil and Gas Research Institute, Academy of Science U.S.S.R., Moscow, U.S.S.R.

ABSTRACT

Natural gas hydrates, a mineral widely spread on earth and on many space bodies in the Universe, have been known since the 1960s. The hydrates made a considerable contribution to the formation of the earth's atmosphere and hydrosphere at the early period of existence. They presently play a great role in accumulation of hydrocarbons in the sedimentary cover of the earth's crust on land and under the sea. Hydrates exert considerable influence on the thermal balance of the earth's surface, its climate, ecology and geography of the arctic shores.

The main features of gas hydrates which produce global changes are: structure and composition of hydrates, heat of the phase transition and of accumulation and decomposition (about 420 kJ kg⁻¹), the change of the water specific volume (26–32%) under its transition to the hydrate state, and the electric impulse formation between the two phases during the phase transitions of systems. One volume of water contains 70–200 volumes of gas in hydrate state. Gas pressure in the crystal lattice of hydrate is hundreds, even thousands MPa.

The hydrate formation zone is associated with frigid areas of Earth sedimentary rocks; on the land, near the polar regions, in the sea, at any latitude at depths >200–500 m. Methane hydrate resources make up about 10⁴ Gt, 99% of them under the sea. The explored resources are 500 Gt.

Hydrate methane is, undoubtedly, the energy potential of mankind for the next century, but the rates of the free methane outflow into the atmosphere and their influence on the global climate, ecology, geography, etc. need to be taken into account. The current amount of methane in the atmosphere is about 4.8 Gt. Thus, the average Earth surface temperature is increased by 1.3 K. The annual increase of methane in the atmosphere is 1%.

Natural gas hydrates, their spreading and features may cause blowouts of free methane to the atmosphere, much greater than the current biochemical and technogenic sources. Methane may flow from the top and from the bottom of the layer as well under changing thermodynamic conditions, such as decreasing pressure, increase of the geothermal gradient, neotectonic shifts, changing of the hydrate deposits, electric potential. The free methane provides for an increase of CO₂, H₂O, O₃ concentration. The heating effect of methane can be equal to or exceed that of CO₂.

92-17869



AD-P007 365



Volcanic Eruption Events and the Variations in Surface Air Temperature over High Latitude Regions

Jia Pengqun

Polar Meteorological Laboratory, Academy of Meteorological Science, State Meteorological Administration, Beijing, Peoples' Republic of China

ABSTRACT

The numerical experiments of our study suggest that volcanic eruptions cause a cooling of the surface temperature. Special attention will be given to the climatic fluctuation tied to the cooling in summer in high latitudes resulting from the eruptions occurring in spring or summer in high latitudes in the Northern Hemisphere.

INTRODUCTION

Volcanic eruptions are magnificent natural phenomena. The early studies on volcanic dust by Humphreys [1940] suggested that there is some relation between the pollution of the atmosphere envelope and climate variation. In the late 1950s, a perennial aerosol layer—the Junge Layer—was found in the lower stratosphere. It has been shown that the Junge Layer is substantially increased for a couple of years following major eruptions [WMO, GARP, 1975]. Based on these facts, some authors suggested volcanic eruptions to be one of the reasons for climatic variation [Mitchell, 1975; Pollack et al., 1976; Xiangon et al., 1985; Angell et al., 1985; Pengqun, 1989].

Climate modeling is useful in estimating the climatic effect of volcanic eruptions. Sellers [1973] and Pollack et al. [1976] separately used an energy balance model and a radiative-convective model to simulate the climatic effects of a stratospheric aerosol layer and the volcanic dust. In their studies the changes of the aerosol layer were indicated only by allowing the optical depth of the air to vary, but the changes in the other optical properties were neglected. The analyses by King et al. [1984] concluded that the stratospheric aerosol layer undergoes some important changes following major volcanic eruptions. The resulting variations of the optical and radiative properties of the stratospheric aerosol layer were discussed and a radiative parameterization for the stratospheric aerosol layer was developed by King et al. [1984].

In this study the radiative parameterization is used to force a one-dimensional global climate model based on the energy balance of the earth-atmosphere system, to present some interesting results. In the model the effect of the vol-

canic dust is expressed as a function of the optical depth and aerosol size distribution and a simple model of the latitudinal distribution of aerosol optical thickness as a function of time is developed. The sensitivity experiment results concerning the high latitude regions are described below, followed by a discussion of the reasons for these results.

THE MODEL

The Climate Model

The climate model used in this study is an improvement of the one first developed by Sellers [1973]. The latitude-mean surface temperature T_s is determined by the energy-balance equation for each 10° band with a 6-day time step:

$$C \frac{\partial T_s}{\partial t} = Q(1-\alpha) - \Delta I - \text{div}(F) + L \frac{dM}{dt} \quad (1)$$

where t is time, C is the thermal inertia, Q is the incident radiation, α is the planetary albedo, ΔI is the net loss caused by long-wave radiation, $\text{div}(F)$ is the energy dissipation and $L \frac{dM}{dt}$ is the latent heat change due to phase transformation of ice and snow where M is the amount of ice and snow, L is the latent heat of condensation.

The characteristics of our model that are different from the early one are as follows: (a) The time of the latent heat change by phase transformation of ice and snow is added to describe the effect of the phase transformation process on the surface temperature field over high latitude regions. This is done also to try to improve the early model in fitting with the observations over high latitude regions which are not as good as over low and middle latitude regions. (b) In our model, the land temperatures and the sea temperatures in one latitude band are not distinguished but are substituted by

latitude-mean temperatures. So it is not necessary to iterate and the integral time is reduced. (c) The parameterization given by King et al. [1984] is used to determine the planetary albedo to include the effect of the volcanic dust.

As a test of the model, Figure 1 gives the results of the controlled experiment. Also the observed values and the results from the original model are shown in the figure. Except at high latitude, both simulated temperature fields are compatible with the observations, but at high latitudes the improved model is better.

The Radiative Parameterization for the Stratospheric Aerosol Layer

The detailed description of the parameterization procedure is given by King et al. [1984]. In the model, any radiative quality for short- and long-wave radiation is the function of optical depth and aerosol size distribution. For instance, the albedo of the aerosol layer $R(\tau, \phi)$ may be expressed as a quadratic function of optical depth (τ):

$$R(\tau, \phi) = a(\phi)\tau + b(\phi)\tau^2 \quad (2)$$

where the coefficients a and b not only change with latitude (ϕ), but also have different values for the background aerosol model (the result marked by BK in equation (3)) or for the volcanic aerosol model (EC). When eruption occurs, $R(\tau, \phi)$ consists of two parts:

$$R(\tau, \phi) = R^{EC}(\tau, \phi) \exp(-\Delta t/T_a) + R^{BK}(\tau, \phi) [1 - \exp(-\Delta t/T_a)] \quad (\Delta t > 0) \quad (3)$$

where $\Delta t = t - t_e$ is the difference of the operative time (t) from the eruption time (t_e) and T_a is a time constant.

Simple Diffusion Model of the Spatial and Temporal Distribution of the Volcanic Stratospheric Aerosol Layer

In the climate model the optical depth of the atmospheric envelope consists of two parts:

$$\tau(\Delta t, \phi) = \tau_0 + \Delta\tau(\Delta t, \phi) \quad (4)$$

τ_0 is a constant ($\tau_0 = 0.144$, after King et al. [1984]), expressing the optical depth of the troposphere and unperturbed stratosphere. $\Delta\tau(\Delta t, \phi)$ is the added optical depth due to eruptions.

Besides being controlled by diffusion, the volcanic dust suffers the effects of many stochastic factors. The average results from these factors are assumed to make the distribution of the volcanic dust more smooth and symmetrical which may be approximately expressed by a normal distribution. The coordinate in proportion to the area of the latitude belt (the abscissa is sine of latitude: $x = \sin \phi$, the global integral $\int_{-1}^1 dx$ is equal to the area-weighted sum of the whole earth) is used. Based on diffusive transport in latitude and exponential decay in time [Robock, 1981; King et al., 1984] we have:

$$\Delta\tau = \bar{\tau} \left[\frac{1}{\sqrt{2\pi}\sigma(\Delta t)} \exp\left(-\frac{(x-x_0)^2}{2\sigma^2(\Delta t)}\right) \right] \exp(-\Delta t^2/T_b) \quad (\Delta t > 0) \quad (5)$$

where $x_0 = \sin \phi_e$, ϕ_e is the volcanic latitude, $\bar{\tau}$ and T_b are

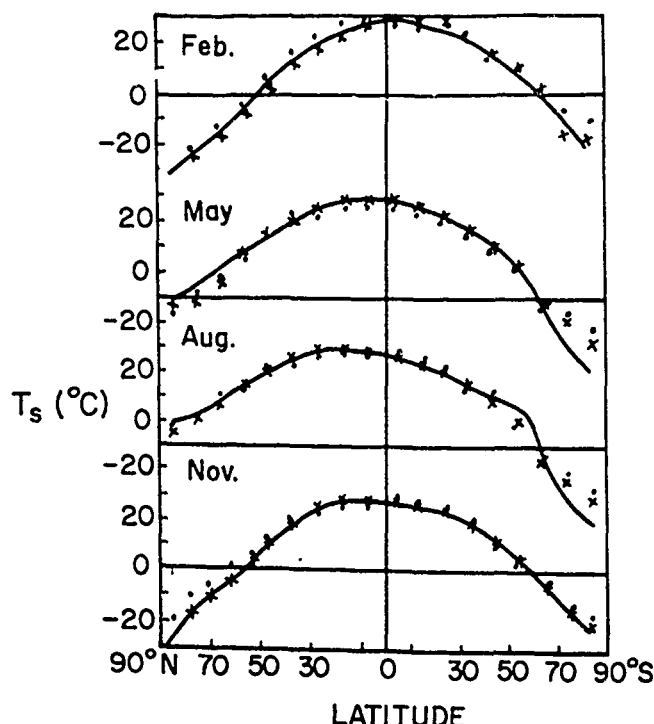


Figure 1. The observed latitudinal distribution of the mean surface temperature (solid lines) for February, May, August and November [after Sellers, 1973]. The values computed using our model and Sellers's model are indicated by crosses and dots, respectively.

the constants related only to the magnitude of the eruption. The variance $\sigma(\Delta t)$ increases with Δt to describe the volcanic-induced area symmetrically diffuse to two poles centered on the volcanic latitude. As the diffusive distance is in direct proportion to the square root of the time, we have:

$$\sigma(\Delta t) = a + b\sqrt{\Delta t} \quad (6)$$

The constant a is determined according to the diffusive range of the dust when it has moved once around the earth. From the observed results for Mount St. Helens and El Chichón [Robock, 1982, 1983], a is about 0.025, that is corresponding to the range of the dust diffusing southward and northward separately by 5 degrees of latitude when the dust has circled the earth once. The constant b and time constant T_b are determined in terms of getting the best fitting results with the observations. They are about 0.027 and 210 days respectively. In Figure 2 the results simulated by equations (5) and (6) are compared with the observations for El Chichón.

THE RESULTS OF THE SENSITIVITY EXPERIMENT

The sensitivity experiments using the model described above are designed to estimate the volcanic effect on surface temperature. The volcanic sources are added to the climate model, already operating at different seasons (15 March, 15 June, 15 Sept., and 15 Dec.) and latitudes (every 10 degrees). The complete results are given in another paper [Pengqun, 1989]. Here only the results concerning high latitude regions are described, as follows.

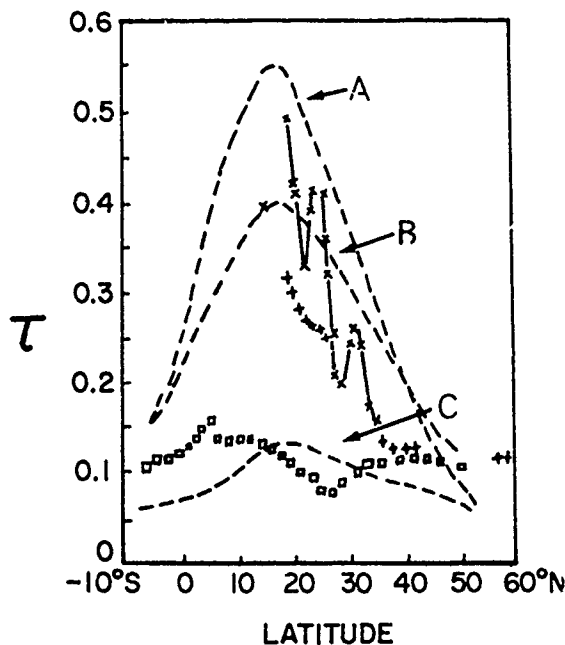


Figure 2. The latitudinal distribution of aerosol optical thickness two months (x's), four months (pluses) and nine months (boxes) following the eruption of El Chicón [after Shah et al., 1984]. The results of the diffusion model described in the text are indicated by lines A, B and C.

(A) There is almost no temperature change over high latitude regions when the eruption occurs at low latitude. That is more true in the Southern Hemisphere (SH).

(B) When the volcanic source is located at 25°N, the high latitude regions are effected. Especially in the Northern Hemisphere (NH), along with an increase of the eruption latitude, a cooling in summer is more clearly apparent in the high latitudes.

(C) When the volcanic source is located at high latitude, the situation is somewhat complicated. There are different cases for eruptions in NH or in SH. The biggest temperature change appears when the volcanic source is located at 65°N and the eruption is on 15 June. There are continuous colder summers and warmer winters following the eruption over the high latitude regions in NH. The amplitude of a decrease in summer temperature is larger than that of an increase in winter temperature.

(D) The volcanic eruptions in SH also give similar temperature changes. But there is a larger area of increasing temperature in winter in SH than that in NH and the area of main temperature decrease appears in middle and lower latitude regions instead of in high latitude regions as is the case for the NH.

DISCUSSIONS ON THE TEMPERATURE CHANGE OVER HIGH LATITUDE REGIONS

In the model, the temperature changes over high latitude regions are decided by many factors. When the volcanic source is added, it will act together with the internal factors

in the model, such as the seasonal variation of solar radiation and the changes of the thermal and optical properties of the surface resulting from the advance/retreat of the polar ice sheet, to affect the temperature field. Some feedback processes as showing in Figure 3 are then important in determining the energy variation over high latitude regions. In the figure, a-b-c is the process for the surface temperature change due to radiative effect. In summer, a-b₁-c is the leading case and the temperature drops, while in winter, a-b₂-c is more important and the temperature increases. All these general processes over high latitude regions are affected by feedback of c-d-e-c. The processes e-c are complicated, the effects of e_1 , e_2 , and e_3 are variable at different sites and times. The experiments show that the changes of ice/snow areas are mainly taking place at the edge of the ice sheet and are also correlated with seasonal changes of the edge. In summer, the processes of a-b₁-c bring about the temperature drop, the feedback of c-d-e₂-c will be more important because solar radiation is strong. That results in the strong cooling in summer.

The results of the sensitivity experiment and the mechanism responsible for the temperature change over high latitude regions described above may have great climatic importance. In the 1940s, Milankovitch advanced an astronomical hypothesis for climate change [Watts, 1984]. He held that the depletion of solar radiation due to variations of the parameters of earth's orbit leads to a cooling in summer in high latitude areas and then the melting process of the polar ice is restrained. This is the mechanism that triggered the ice age. We can gain a good deal of enlightenment from his hypothesis. The Milankovitch theory may also be used to explain the climate change for a shorter time, but the orbit parameter change must be substituted by volcanic eruptions. It seems reasonable to suppose that when a high level of volcanic activity is sustained over a long period of time, the polar ice sheet will be advanced equatorward due to the continuously cooling summers caused by volcanic eruptions. The effect of warm winters is not important because it is centered in polar areas which are covered by snow and ice year-round. So the extent of the polar ice sheet will increase accompanied by the volcanic eruptions and the feedback of snow/ice-albedo-temperature which will intensify as the temperature drops.

The results of our computations of the change in surface temperature suggest that the main driving force for climatic change due to volcanic eruptions arises from the radiative effects of volcanic aerosols on the energy balance of the earth-atmosphere system. Besides the magnitude, the site and time of a volcanic source are important for the simulated cases of these effects. Our models, of course, are too simple in terms of including full physical processes to be used for a thorough study of the problem. But it is clear from our study that the role of volcanic activity in causing large climatic variation is coming into play from high latitude areas.

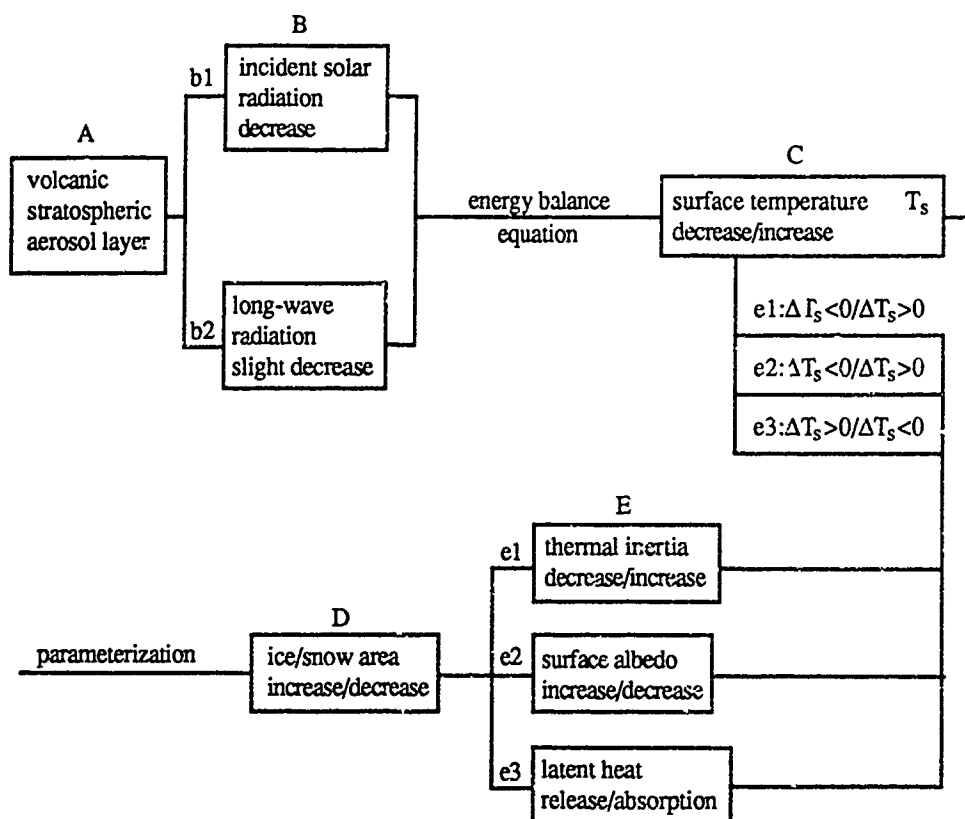


Figure 3. The energy change processes over high latitude regions in the model.

REFERENCES

- Angell, J. K., and J. Korshover, Surface temperature changes following the six major volcanic episodes between 1780 and 1980, *J. Clim. Appl. Met.*, 23, 1121-1137, 1985.
- Humphreys, W. J., *Physics of the Air*, McGraw-Hill, New York, 1940.
- King, M., D. Harshvardhan, and A. Arking, A model of radiative properties of the El Chichón stratospheric aerosol layer, *J. Clim. Appl. Met.*, 23, 1121-1137, 1984.
- Mitchell, J. M., Jr., A reassessment of atmospheric pollution as a cause of long-term changes of global temperature, in *The Changing Global Environment*, edited by Singer and Freed, pp. 149-173, D. Reidel Publishing Company, 1975.
- Pengqun, Jia, Sensitivity study on the effect of stratospheric volcanic aerosol layer on the global surface temperature, *Journal of Academy of Meteorological Science*, 4, 50-59 (in Chinese), 1989.
- Pollack, J. B., O. B. Toon, C. Sagan, A. Summers, J. M. J. Van der Pijl, and W. Van Camp, Volcanic explosions and climate change: a theoretical assessment, *J. Geophys. Res.*, 81, 1071-1083, 1976.
- Robock, A., A latitudinal dependent volcanic dust veil index and its effect on climate simulation - I, *Volcanol. Geotherm. Res.*, 11, 67-80, 1981.
- Sellers, M. D., A new global model, *J. Appl. Meteor.*, 12, 241-254, 1973.
- Shah, G. M., and W. F. J. Evans, Aircraft latitude survey measurement of the El Chichón eruption cloud, *Geophys. Res. Lett.*, 11, 1125-1128, 1984.
- WMO, GARP, The physical bases of climate and climate modelling, GARP, *P.S. No. 16*, 1975.
- Xiangon, Zhang, and Zhang Fuguo, Volcanic activity and its relation to the cold/warm and dry/wet weather in China, *ACTA Met. SINICA*, 43, 195-207 (in Chinese), 1985.

92-17870



AD-P007 366



Satellite and Slow-Scan Television Observations of the Rise and Dispersion of Ash-Rich Eruption Clouds from Redoubt Volcano, Alaska

Juergen Kienle

Geophysical Institute, University of Alaska Fairbanks, Fairbanks, Alaska, U.S.A.

A. W. Woods

Institute of Theoretical Geophysics, Dept. of Applied Mathematics and Theoretical Physics, Silver Street, Cambridge, England

S. A. Estes, K. Ahlhaes, K. Dean, and H. Tanaka

Geophysical Institute, University of Alaska Fairbanks, Fairbanks, Alaska, U.S.A.

ABSTRACT

✓ Polar-orbiting NOAA 10 and 11 weather satellites with their Advanced Very High Resolution Radiometer (AVHRR) imaging sensors and the Landsat 4 and 5 satellites have provided over 30 images of the 1989/90 eruptions of Redoubt Volcano. Between December 14 and April 21, about 20 major explosive eruptions occurred with ash plumes rising to heights of 10 km or more, most of them penetrating the tropopause. The ash severely impacted domestic and international air traffic in Alaska with a near disaster on December 15, 1989, when a KLM 747-400 jet aircraft with 247 people aboard intercepted an ash plume and temporarily lost all four engines. Fortunately, the engines were eventually restarted after several attempts and the plane landed safely in Anchorage. We have used satellite and also slow-scan television (TV) observations to study the dynamics and thermodynamics of rising eruption plumes in order to better understand plume dispersal.

SATELLITE DATA

We have used satellite imagery of eruption plumes to map ash dispersal into the far field from the volcano. The pervasive snow cover that existed near Redoubt Volcano from December 1989 to April 1990 preserved even micron-thin ash layers. For example, a NOAA 10 satellite image of April 21, 1990 shows three ash trajectories on the snow to distances of over 400 km from the vent. Dispersal areas for these three plumes of Redoubt eruptions of March 23, April 12 and April 15 range from about 4000 to 21,000 km². A numerical simulation of the ash dispersal involving calculations of the 3-D windfield, 3-D diffusion, and gravitational fallout and satellite images of the ash dispersals suggest that diffusion was not an important process. The ash on the snow formed three narrow undispersed fallout patterns that looked like spokes radiating from the volcano.

Satellite imagery of eruptive plumes was also used to map radiometric plume top temperatures. By convolving

these data with radiosonde measurements of atmospheric temperature versus altitude we could derive details of plume top topography, important for the study the dynamics of plume rise and dispersion in the atmosphere.

The infrared (IR) bands of the AVHRR of the NOAA 10 and 11 satellites have proven especially useful to detect eruptions at night or in overcast conditions, a common condition for the 1989/90 eruptive cycle of Redoubt Volcano, which occurred in mid-winter. Even though the volcano was often not visible from the ground, we could still track the high altitude plumes above overcasts or at night, using the IR channels.

SLOW-SCAN TELEVISION OBSERVATIONS

Real-time slow-scan TV observations of volcanic eruptions at Redoubt Volcano have also been most useful for supplementing the satellite observations for warnings to the public. On December 16, 1989, within 48 hours of the first

eruption of Redoubt's latest eruptive cycle, a slow-scan TV camera was installed at Kasilof, 30 km east of the volcano (Figure 1). Kasilof is the closest location with a view of Redoubt, AC power and an established microwave telecommunication link with the geophysical laboratory of the Alaska Volcano Observatory (AVO) at the Geophysical Institute of the University of Alaska Fairbanks, 530 km from Kasilof.

On April 15, 1990 and April 21, 1990, two explosive eruptions occurred, lasting about 4 and 8 minutes respectively, based on seismicity. On both occasions the erupted material traveled as a pyroclastic flow down an ice canyon on the north flank of the volcano. Using slow-scan TV recordings of the eruption and the seismic record from both near and far field stations, Wood and Kienle [1992] deduced that on each occasion, after a few minutes, the upper part of this pyroclastic flow became buoyant and a large, hot and dusty ash cloud rose from the flow. These thermals ascended to a height of about 12 km, at which point they began to spread laterally, as umbrella clouds. Thus, initially dome-shaped eruption plume tops collapsed to form top hat-shaped plumes, as material surged radially outward at the level of neutral buoyancy.

TV monitoring of volcanic eruptions in Alaska by ultra-low light cameras is particularly useful during the winter season when daylight drops to as little as 5 hours. We were able to clearly observe eruptions at local midnight under starlight conditions. For future monitoring, we plan to install such TV systems on two other active volcanoes that lie near Alaskan population centers in the Cook Inlet area, at Mt. Spurr and Mt. St. Augustine.

RESULTS

Using predictions of a new model for the dynamics governing the ascent of coignimbrite thermals and comparing them with the slow-scan TV observations of April 15, 1990, Wood and Kienle [1992] predict that the cloud initially ascended rather sluggishly, since it is only just buoyant on rising from the pyroclastic flow. However, as it ascends, it entrains and heats up more air, and hence generates more buoyancy. Therefore it accelerates upwards (this process is called super-buoyant plume rise). Only much higher in the cloud does the velocity decrease again, as the thermal energy of the plume becomes exhausted. The model also predicts that the height of rise of such coignimbrite thermals is a function of the initial mass and temperature of the cloud, but is almost independent of the initial velocity.

During the April 21 eruption, a sequence of photographs recorded the lateral spreading of the umbrella cloud during an interval of about 10 minutes after the eruption (Figure 2). Wood and Kienle [1992] analyzed these photographs and successfully compared the observed growth with a simple

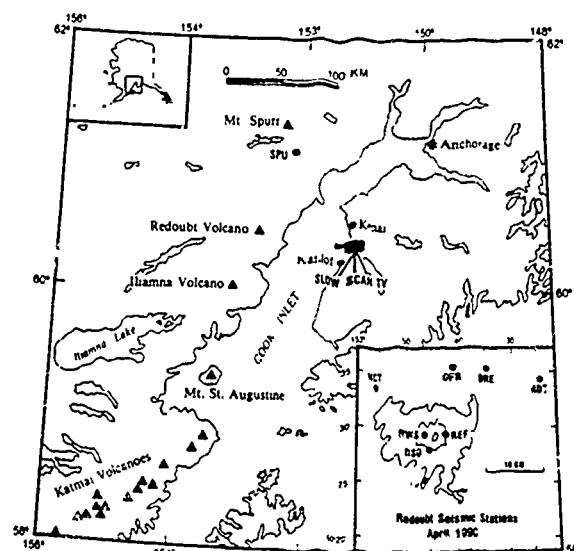


Figure 1. Map of Cook Inlet, showing location of active or Holocene volcanoes (solid triangles), location of the three seismometers REF, RSO and RWS (near the Redoubt vent) and SPU (far from vent), and also the location of the slow-scan television camera at Kasilof. The photographs shown in Figure 2 were taken at Kenai, 20 km north of Kasilof.

model for the spreading of the umbrella cloud as a gravity current in a stratified environment.

Using these simple thermodynamic models, Wood and Kienle [1992] estimated that the clouds had a temperature in the approximate range 600-700 K as they rose buoyantly from the flow after entraining and heating ambient air and melting and vaporizing ice. They also estimated that in each eruption approximately 10^9 kg of fine ash was injected into the atmosphere.

It is well known that fine volcanic ash and H_2SO_4 droplets in the stratosphere can affect climate for months, and even years, following eruptions that eject SO_2 and fine ash high into the stratosphere. Our studies help track particles in the troposphere and stratosphere and contribute to the understanding of the physics of their dispersal.

KEY REFERENCE

Woods, A. W., and J. Kienle, The dynamics and thermodynamics of volcanic clouds: Theory and observations from the April 15 and April 21, 1990 eruptions of Redoubt Volcano, Alaska, *Bull. of Volcanology (Redoubt Volume)*, in press, 1992.

16:16:45 GMT

16:22:09

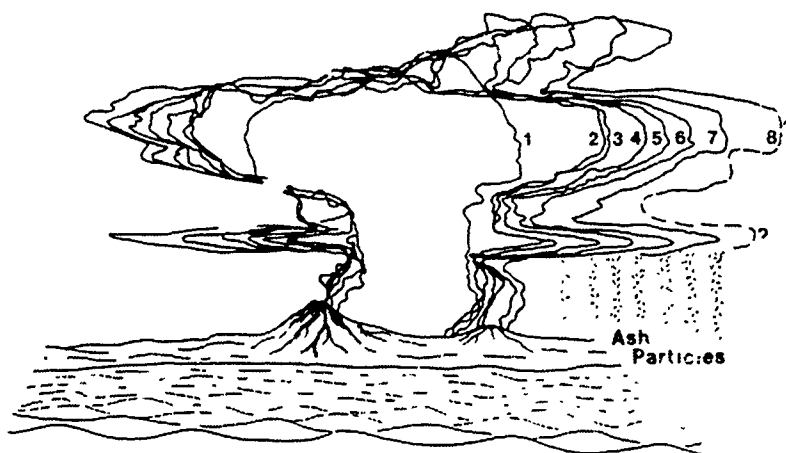
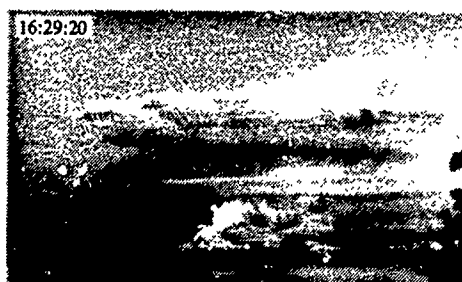


Figure 2. Sequence of eight photographs showing the development of the umbrella cloud on April 21, 1990. These photographs were taken by Mark and Audrey Hodgins from Kenai at the times (in GMT) noted (subtract 10 hours to obtain local time). The bottom drawing shows the growth of the plume and umbrella cloud based on these photographs.

AD-P007 367



92-17871



Bromine and Surface Ozone Atmospheric Chemistry at Barrow, Alaska During Spring 1989

W. T. Sturges and R. C. Schnell

Cooperative Institute for Research in Environmental Sciences, University of Colorado, Boulder, Colorado, U.S.A.

S. Landsberger

Department of Nuclear Engineering, University of Illinois, Urbana, Illinois, U.S.A.

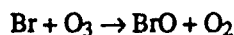
ABSTRACT

Measurements were made of surface ozone, particulate bromine and organic gaseous bromine species at Barrow, Alaska during March and April 1989 with a view to examining the causes of surface ozone destruction during the arctic spring. It was found that during major ozone depletion events ($O_3 < 25$ ppbv) concentrations of particulate bromine and the organic brominated gases bromoform and dibromochloromethane were elevated. A fast production rate of particulate bromine was shown by irradiating ambient nighttime air at Barrow in a chamber with actinic radiation that simulated midday conditions for that season and latitude. Such rapid reactions are not in keeping with gas phase photolysis of bromoform, but further studies showed evidence for a substantial fraction of organic bromine in the particulate phase, thus heterogeneous reactions may be important.

INTRODUCTION

It has been well documented that following first light in the Arctic, ozone concentrations measured at ground level begin to exhibit large negative excursions from wintertime maximum values [Barrie et al., 1988; Oltmans et al., 1989]. Ozone levels can be reduced to effectively zero within a matter of hours. These destruction events occur mostly during March and April and cease around May or June. Aircraft measurements [Oltmans et al., 1989] have shown that the ozone loss occurs entirely below the low level inversion, which forms a temporary barrier to downmixing of ozone-rich air.

The cause of this ozone loss remains a mystery. There are currently two favored hypotheses, both of which rely on monatomic bromine radicals attacking ozone, which can be simplified to:



The hypotheses differ in the origin of the bromine radicals. In the version put forward by Barrie et al. [1988], photolysis of bromoform gas ($CHBr_3$) releases bromine radicals. This is supported by the observation of high wintertime bromo-

form in the Arctic (perhaps the highest atmospheric concentrations measured anywhere in the world to date), which declines in antiphase to increasing solar flux following polar sunrise [Oltmans et al., 1989]. At the same time large quantities of filterable (presumably particulate) bromine are formed, suggesting that some conversion process of bromoform is indeed operating. Filterable bromine levels (f-Br) are observed to be strongly anticorrelated with ozone. The origin of the bromoform is thought to be biogenic, possibly from arctic ice microalgae [Sturges et al., 1991a].

In the second hypothesis [Finlayson-Pitts et al., 1990], dinitrogen pentoxide reacts with sea salt particles, releasing nitryl bromide which then photolyses to bromine atoms. This hypothesis requires the presence of sea salt aerosols transported from non-frozen oceans south of the ice margins, and pollution-derived oxides of nitrogen. Indeed, both sea salt aerosol and long range transported pollution are at a maximum in the late winter in the Arctic [Sturges and Barrie, 1988].

The measurement of the key nitrogen species required to evaluate the dinitrogen pentoxide route to ozone loss was beyond the scope of this work: we focus here on an exam-

ination of the plausibility of the bromoform photolysis mechanism.

METHODOLOGY

Sample Collection and Analysis

Measurements were made at the National Oceanic and Atmospheric Administration/Climate Monitoring and Diagnostics Laboratory (NOAA/CMDL, formerly GMCC) background monitoring station at Point Barrow on the north Alaskan coast, about 8 km from the village of Barrow. The "clean air sector" is normally defined as 5–130° but, since combustion sources are the only likely influence on the chemistry examined here, we have used less stringent limits and instead defined a "local combustion sector" of 215–320° to include areas of habitation, power generation and waste burning, plus 20° either side of these sources.

Surface ozone measurements are made routinely at the station by NOAA/CMDL using a Dasibi ultraviolet monitor. Ozone data consisting of consecutive hourly average concentrations were made available to us by CMDL, as were meteorological data.

Particulate bromine was collected on 90-mm-diameter, 1- μ m pore Nuclepore "Filinert" PTFE membranes in open-face Teflon filter holders at flow rates of around 15 dm³ min⁻¹ over twelve hours, with changeover at around 10 a.m. and 10 p.m. LST. Organic halogen gases were collected by absorption onto Tenax GC chromatography absorbent in 4-mm-ID glass tubes, with a filled length of 100 mm. Two tubes were placed in series to account for breakthrough. Particles were removed from the air with a quartz filter in a 10-mm fritted glass filter holder. Oxidants, which may decompose the collected hydrocarbons, were removed by passage through a plug of ferrous sulfate in a 6-mm-ID PTFE tube. Parallel samples with and without the ferrous sulfate plugs showed no consistent differences. Air was drawn through these assemblies at approximately 200 cm³ min⁻¹. Sampling times were synchronized to the filter pack sampling. The samples were returned frozen to the laboratory and stored at -20°C.

Filter samples were analyzed by neutron activation analysis (NAA). Tenax tubes were thermally desorbed into a gas chromatograph and organic halogenated species measured with an electron capture detector. Details of both measurement techniques are given in Sturges et al. [1991b].

Photochemical Experiment

A simple experiment was performed at the Barrow station to determine if filterable bromine formation could be induced in the ambient nighttime atmosphere by illumination with long wavelength ultraviolet (actinic) light. Air was drawn in to the building through PTFE tubing. This air stream was split through two identical Pyrex glass tube chambers, 60 cm long and 5 cm ID with a 2-mm wall. One of the chambers was surrounded by four actinic fluorescent tubes (Phillips TL 30W 05 color) which have a spectral emission distribution which approximates the actinic spectrum of natural sunlight. The other chamber was blacked out and acted as a control for the illuminated chamber results. Both chambers were connected to filter packs of similar construction to those described above, but designed to accept 47-mm-diameter filters. Air was drawn through the chamber and filter pack systems with a small pump, whose

flow rate was adjusted from 0.4 to 1.7 dm³ min⁻¹ to give different residence times of the air in the chambers. A timer was used to turn the lights and pump on only during the hours of total darkness. Temperature in the chambers remained at a few degrees below room temperature (about 25°C) in both the lit and unlit chambers. This may have influenced the measured reaction rates. Experiments were conducted only when the air was from off the Arctic Ocean so that the key bromine species should be present, but not at times when ozone was already almost completely removed so as to prohibit further reactions.

RESULTS AND DISCUSSION

Ambient Measurements

The surface ozone record for the period during which air samples were collected is shown in the top panel of Figure 1. Day 70 corresponds to 11 March and day 100 to 10 April. Several large negative excursions in ozone can be seen. Five depletion "events" are identified by the numbers 1–5. We may consider that the high ozone concentration periods (labeled A–C) represent the ozone concentration of a well-mixed lower troposphere at this time of year. It is then apparent that ozone was depleted throughout most of the study period, not only during the depletion events. The figure also shows the times of potential impact of local com-

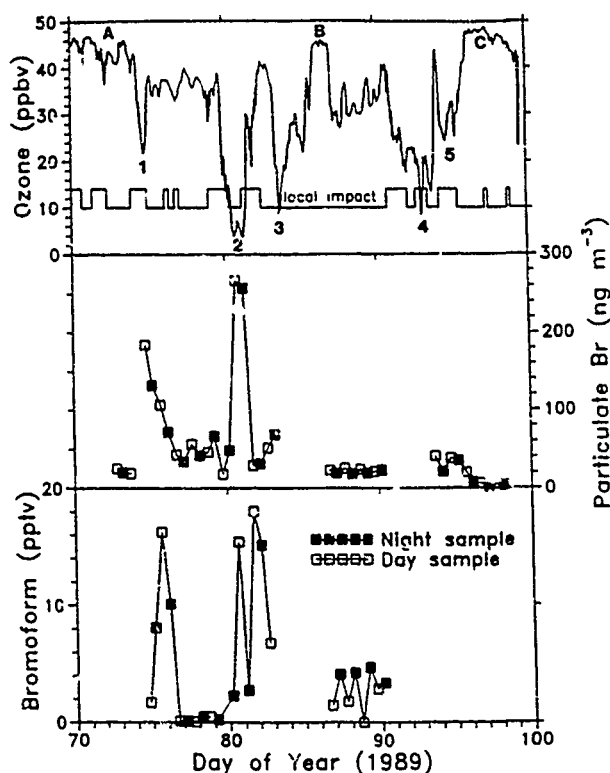


Figure 1. Ozone, particulate bromine (f-Br) and bromoform gas measurements from 11 March to 10 April (LST) 1989 at Barrow. Ozone depletion events are marked 1–5 in the upper panel and high ozone episodes A–C. The horizontal bars in the upper panel indicate periods when the sampling site was impacted with possible combustion sources from the town of Barrow. Open symbols in the lower two panels are samples collected from 10 a.m.–10 p.m. LST and filled symbols were collected 10 p.m.–10 a.m. LST.

bustion sources. There is no consistent evidence for an impact of local sources on ozone measured at the station. Although there was flow from the town during depletion events 1, 2, 4 and 5, the air was from the clean sector during event 3. We cannot rule out the possibility that local ozone production may have slightly compensated ozone loss on some occasions, but overall we believe that local combustion plays a very minor role in determining ozone concentrations at Barrow.

In keeping with Barrie et al. [1988] we refer to bromine collected on the filters as "filterable bromine" (f-Br), which may include some adsorbed gaseous species such as HBr. The f-Br results are shown in the center panel of Figure 1. The largest ozone depletion event (number 2) coincided with the highest f-Br values. Event 1 also coincided with high f-Br, but f-Br continued to decrease after ozone had recovered, although ozone was still depleted relative to the well-mixed tropospheric concentrations during this time. Unfortunately the second and third largest ozone depletion events (3 and 4) were not covered by air samples due to adverse weather conditions prohibiting access to the station. However there is evidence that f-Br was rising as event 3 began and was elevated as event 4 was ending. After event 5 f-Br dropped to near zero values, and ozone recovered to the highest concentrations observed during the study period. This coincided with a vigorous North Pacific airstream, whereas all the air masses throughout the rest of the period originated in the Arctic (as determined from 5-day back air mass trajectories [J. M. Harris, NOAA, personal communication]). It therefore appears that all of the f-Br concentrations in arctic air were elevated relative to North Pacific air.

Bromoform concentrations are plotted in the lower panel of Figure 1. For clarity these data have been replotted in Figure 2 to show the relationship with dibromochloromethane. The trends in concentrations of the two

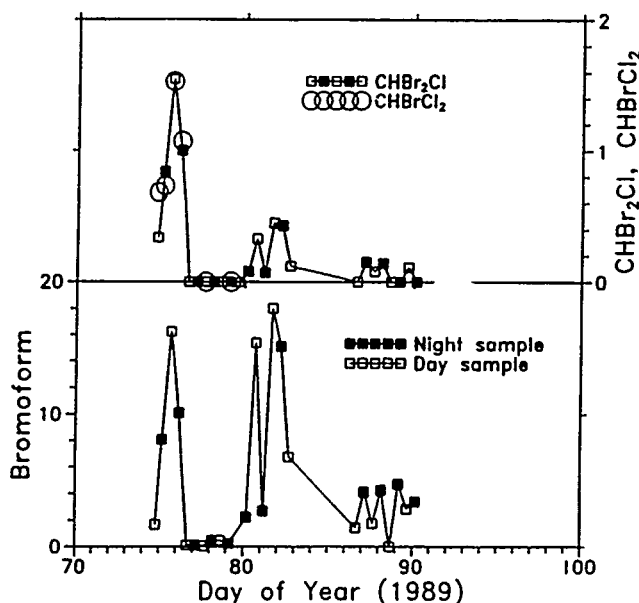


Figure 2. Organic bromine gases measured at Barrow (pptv). Open symbols are samples collected from 10 a.m.–10 p.m. LST and filled symbols were collected 10 p.m.–10 a.m. LST.

gases track each other closely, but dibromochloromethane concentrations were about an order of magnitude lower. Six measurements of bromodichloromethane were in very close agreement with dibromochloromethane. It would appear that all three bromine species have a common origin. Since there are virtually no known anthropogenic sources of these gases we suspect that this source is biogenic. Similar correlations between gaseous organic bromine species have been observed at Alert, NWT [Bottenheim et al., 1990]. Returning to Figure 1, bromoform appears to peak at around the same time as f-Br, approximately coinciding with ozone depletion events 1 and 2. Again measurements are missing for the other ozone events.

Photochemical Experiment at Barrow

Figure 3 shows the amount of f-Br formed in the lit chamber in excess of that measured in the (dark) control chamber. Chemical actinometry measurements of the actinic energy emitted from the fluorescent lights [G. S. Brown, University of Colorado, personal communication] were similar to computed total actinic irradiance figures provided by J. Frederick of the University of Chicago [personal communication] using a clear sky model [Frederick et al., 1989] for noon at Barrow on 6 April (53 and 79 J s⁻¹ m⁻² respectively). The UV cutoff of the Pyrex chambers is 310 nm, very close to that computed for ambient solar irradiation flux at Barrow (approximately 305 nm).

There appears to be a remarkably good correlation between f-Br formed and the length of irradiation: the correlation coefficient r is 0.89. The gradient of the line implies a rate of formation of f-Br of 7.85 ng Br m⁻³ min⁻¹, i.e., it would take just 34 minutes to form the highest ambient f-Br

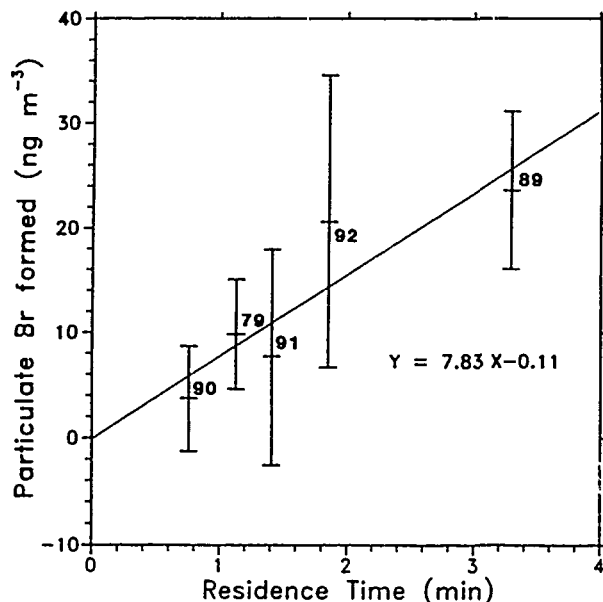


Figure 3. Results of the photochemistry experiment at Barrow. The amount of f-Br formed in the illuminated chamber is shown after subtracting the amount in the control (dark) chamber. The error bars are analytical uncertainty (1 sigma). Residence time is the average time the air spends in the chamber. The data point labels refer to the start day number of the night that the experiment was conducted.

concentration of 267 ng m⁻³ recorded in this study. Subsequent analysis of ambient bromoform samples collected at the time of the photochemical experiments (days 79 and 89–92) showed relatively low levels (1–4 pptv) (Figure 1). We might expect higher rates of formation during peak bromoform periods.

Some preliminary studies at Barrow in 1990 [unpublished data] have shown that ozone in similar illuminated chambers, under static conditions, was depleted from ambient concentrations of around 20 ppbv to zero within 30 min. More work is needed to confirm these findings, but the evidence is at least highly suggestive of the existence of fast reactions that both deplete ozone and form particulate bromine.

One further caveat is that, although wall losses are not a concern, since these are accounted for by comparison with the control chamber, wall reactions are a potential influence and could conceivably have speeded reactions. Our attempts to deactivate the glass walls with fluorocarbon wax, PTFE sprays, and so on, all caused unacceptable attenuation of the actinic light.

Comparison of Total Particulate Bromine with Bromide Ion

If, as suggested above, f-Br originates from the photolysis of bromoform, then the apparent speed of the reaction reported here is in serious disagreement with the only laboratory measurement of the UV cross section of bromoform reported to date [Barrie et al., 1988]. The same authors modeled the bromine-ozone chemistry in the Arctic and deduced that it would take on the order of weeks to produce the pronounced ozone loss observed if gas phase photolysis is the primary source of bromine radicals.

Can the two sets of observations be reconciled? One clue to a possible explanation comes from a comparison of our NAA measurements of particulate bromine (a measure of the total elemental bromine) with results from a parallel study [S. M. Li, Environment Canada, unpublished data] in which particulate samples collected on 47-mm, 0.45- μ m pore size Nuclepore filters were extracted in deionized water and the bromide ion in solution determined by ion chromatography (IC). The results are shown in Figure 4. Total bromine was higher than bromide ion in every case, an effect also reported in an entirely separate study [Sturges and Barrie, 1988]. This indicates that some of the bromine in the particulate phase did not form bromide ions when placed in water: obvious candidates are organic bromine compounds such as bromoform. What is particularly noticeable is that the discrepancy is greater at night, and the diurnal cycle of bromide ion is much more pronounced than that of total elemental bromine. This suggests the rapid conversion of organic bromine to inorganic bromide ion within particles during daylight. A reverse reaction to non-ionic bromine at night is highly unlikely; some replenishment from marine sources must be invoked to explain this. A possible source of such bromine-enriched particles may be marine aerosols which, during the process of generation by bubble-bursting, entrain substantial amounts of the sea surface microlayer: an organic-rich layer in which many compounds and elements are greatly enriched [Duce and Hoffman, 1976].

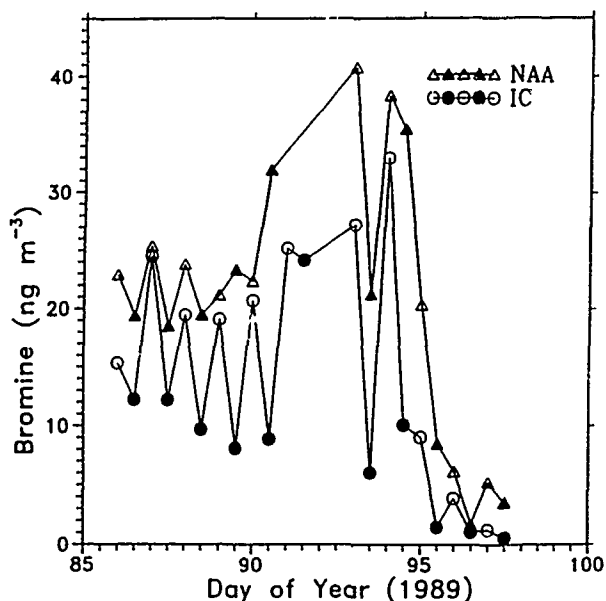


Figure 4. Comparison of total elemental bromine measured on PTFE filters by NAA with bromide ion extracted from Nuclepore filters and measured by IC. Open symbols are day samples, filled symbols are night samples.

SUMMARY AND CONCLUSIONS

The following tentative conclusions can be drawn from this study:

(1) Dramatic surface ozone destruction events at Barrow in the spring are accompanied by elevated levels of filterable bromine (f-Br) and the organic bromine gases bromoform and dibromochloromethane. The correlation between the two later compounds, which have no known anthropogenic sources in the arctic atmosphere, suggests a common source (which we believe to be from marine biota).

(2) Photochemical experiments showed a rapid formation potential for f-Br in the arctic spring atmosphere: sufficiently fast to account for observed ambient f-Br concentrations on the order of minutes.

(3) If bromoform is the precursor to ozone loss and f-Br formation then the problem remains that simple gas phase photolysis is evidently too slow to account for the apparently fast reactions. However, we have shown evidence that organic bromines may exist in the particulate phase and take part in unknown photolytic processes resulting in the observed conversion to inorganic bromide ions during the daytime. Consideration of possible heterogeneous processes should be given to future modeling and field efforts.

ACKNOWLEDGMENTS

WTS acknowledges the support of the National Research Council. We also thank NOAA-CMDL for permission to use the Barrow observatory and also for ozone and meteorological data; the Barrow observatory staff; and the North Slope Borough Department of Wildlife Management.

REFERENCES

- Barrie L. A., J. W. Bottenheim, R. C. Schnell, P. J. Crutzen, and R. A. Rasmussen, Ozone destruction and photochemical reactions at polar sunrise in the lower Arctic atmosphere, *Nature*, 334, 138-141, 1988.
- Bottenheim, J. W., L. A. Barrie, E. Atlas, L. E. Heidt, H. Niki, R. A. Rasmussen, and P. B. Shepson, Depletion of lower tropospheric ozone during Arctic spring: The Polar Sunrise Experiment 1988, *J. Geophys. Res.*, 95, 18555-18568, 1990.
- Duce, R. A., and E. J. Hoffman, Chemical fractionation at the air-sea interface, *Ann. Rev. Earth Planetary Sci.*, 4, 187-228, 1976.
- Finlayson-Pitts B. J., F. E. Livingstone, and H. N. Berko, Ozone destruction and bromine photochemistry at ground level in the Arctic spring, *Nature*, 343, 622-625, 1990.
- Frederick, J. E., H. E. Snell, and E. K. Haywood, Solar ultraviolet radiation at the Earth's surface, *Photochem. Photobiol.*, 50, 443-450, 1989.
- Oltmans, S. J., R. C. Schnell, P. J. Sheridan, R. E. Peterson, S. M. Li, J. W. Winchester, P. P. Tans, W. T. Sturges, J. D. Kahl, and L. A. Barrie, Seasonal surface ozone and filterable bromine relationship in the High Arctic, *Atmos. Environ.*, 23, 2431-2441, 1989.
- Sturges, W. T., and L. A. Barrie, Chlorine, bromine and iodine in Arctic aerosols, *Atmos. Environ.*, 22, 1179-1194, 1988.
- Sturges W. T., R. C. Schnell, S. Landsberger, S. J. Oltmans, J. M. Harris, and S.-M. Li, Chemical and meteorological influences on surface ozone destruction at Barrow, Alaska, during spring 1989, *Atmos. Environ.*, 1991, In press.
- Sturges, W. T., C. W. Sullivan, R. C. Schnell, L. E. Heidt, W. H. Pollack, and D. J. Hoffman, Biogenic bromine gases at McMurdo: Ice algal production, atmospheric concentrations, and potential influence on surface ozone, Symp. Tropospheric Chemistry of the Antarctic Region, June 3-6, 1991, Boulder, Colorado, *U.S. Army Cold Regions Research and Engineering Laboratory, Special Report 91-10*, and *Tellus*, 1991, submitted.

PANEL DISCUSSIONS

PANEL DISCUSSIONS: SUMMARY AND RECOMMENDATIONS

On the final day of the conference three panels met to discuss problems and priorities in polar research.

Panel 1 (chaired by Luis Proenza), dealing with research coordination, identified the following top priorities: better international cooperation involving scientists from all countries with polar interests; establishment of joint observational systems and networks, including satellites and long-term monitoring sites; information exchange through a common clearinghouse; addressing education and manpower needs; and closer ties between arctic and antarctic researchers.

Panel 2 (chaired by Oran Young), addressing societal problems of global change, recommended the establishment of an international program of social sciences in global change; a reexamination of the scenarios of climate change in the polar regions, as they affect social change; the inclusion of social scientists to a greater extent in future global change planning efforts; and the development of suitable curricula on global change at all educational levels.

Panel 3 (chaired by Douglas Posson), addressing polar data and information problems, recommended the establishment of a well-organized polar data directory building on present efforts of all the countries; free exchange of data with other countries having polar data sets; use of improved technologies, e. g., CD-ROM; retrieval of endangered data sets of retiring scientists through funding to the latter, perhaps through sabbatical leaves; and improving the quality of data sets.

Specific recommendations were made as follows:

Panel 1:

- (1) Develop Arctic-wide observational systems and networks which can guarantee the availability of long-term data sets.
- (2) Foster international cooperation.
 - (a) Find mechanisms to ensure that cooperation is sufficiently inclusive of interested scientists throughout the world. It was recognized that polar science efforts exist within a highly distributed system of resources across nations and within nations. Neither countries nor scientists should be excluded.
 - (b) Develop a truly bi-polar approach to science to facilitate coordination of appropriate problems, comparison of contrasts between the two polar regions, and integration of resources.
 - (c) Integrate and coordinate logistical resources to create a visible polar research system that is larger than the sum of the parts. This includes joint planning for the next generation of polar research platforms.
 - (d) Combine informational resources, and create an international information clearinghouse, or international data directories.
 - (e) Focus attention on educational issues to ensure the development of a new cadre of polar scientists, and the development of a new academic curriculum of global change.
 - (f) Erase disciplinary lines and develop mechanisms to move students and scientists across national, institutional, and disciplinary boundaries.
- (3) Develop a set of new "tools" essential to the scale of global change problems. This included satellites, ground-truth observatories and automated stations, and numerical models.

- (4) Keep the research priorities on polar problems in global change flexible to allow new avenues of research to be pursued as we learn about the earth system (e.g., antarctic ozone hole).
- (5) Organize an International Polar Year some time in the future.

Footnote: Several panelists stressed the need to be comprehensive when dealing with the topic of global change, not overlooking the need for social science research, nor forgetting that the upper atmosphere is part of the earth system. Some felt strongly, and the audience agreed, that there is too much emphasis on planning and reports and that we need more time for actual science. Linkages between scientists and policy makers was seen as a difficult area that needed attention. One opinion was that two "conceptual revolutions" were underway and converging—one dealing with the emerging science of global change, the other a bureaucratic revolution by which agency "cross-cuts" are beginning to enable agencies and budget offices to work together on large and complex program elements.

(Editor's Note: International mechanisms for global change research coordination in the polar regions are beginning to emerge for both the Antarctic and the Arctic. In the Antarctic, SCAR, the Scientific Committee on Antarctic Research, has established a global change committee and is in the process of defining a regional program for Antarctica. In the Arctic, IASC, the newly formed (1990) International Arctic Science Committee is pursuing a similar course).

Panel 2:

- (1) Structure future conferences and discussions of the role of the polar regions in global change deliberately to improve communications between scientists and policy makers at all levels, including those in grass-roots organizations.
- (2) Establish an international program of joint collaborative studies on the social impacts of global change in the polar regions, and on the role of the polar regions in shaping human responses to global change.
- (3) Organize future discussions of the role of the polar regions in global change around cross-cutting themes (for example, indicators of global change, feedback mechanisms, etc.) rather than conventional disciplinary categories, to enhance interactions among physical scientists, life scientists, and social scientists.
- (4) Modify the curricula of schools at all levels to incorporate concepts, tools, and analytical skills relevant to understanding the earth as an interactive system, and to increase understanding of the interactions between physical, biological, and social phenomena.
- (5) Critically reexamine models and scenarios of future climate changes in the polar regions, in order to be able to assess realistically the likely consequences to humans.

Panel 3:

- (1) Establish a well-supported polar data directory (or directories) linked with global change directories, which will be the main source for information on the polar regions.
- (2) Initiate a data set cataloging process that will identify endangered data and information (e.g., retiring scientists' data). This could be done through sabbatical leave programs or through other formal links to the library community.
- (3) Ask agencies giving grants and contracts to scientists to request a plan on data disposition as part of the grant or contract.
- (4) Build on successes (e.g., the Canadian ocean data) to improve the quality of data set documentation.
- (5) Increase data managers' participation in conferences, interaction between scientists and data managers, and user feedback.

- (6) Publicize information about data sets and investigate innovative methods to distribute data and metadata (e.g., digital data serial publications).
- (7) Prepare selected polar area CD-ROMs with actual data.
- (8) Seek opportunities for programmatic exchanges of data and information with other nations working in the Arctic (particularly USSR, Canada, etc.).
- (9) Insist on citations and connecting names of the original data collector with any data set, as a recognition of the work done.
- (10) Define the types and quantities of numerical model data input and output that the data systems must organize, document, and preserve.



3



4



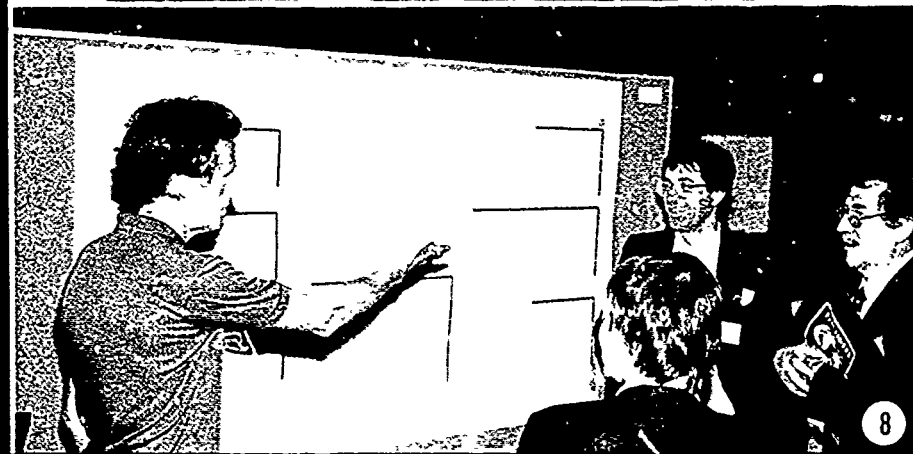
5



6



7



8

Photo Captions.

1. Prof. Garth Paltridge from the University of Tasmania sent 11 Australian graduate students to the conference, shown here with Cindy Wilson (second from left, front row), chair of the local organizing committee.
2. Baerbel Lucchitta of the USGS explains her poster to Juergen Kienle of the University of Alaska Fairbanks.
3. Two wise old polar hands, Joe Fletcher of Fletcher's Ice Island fame, and Ned Ortenso, both from NOAA, talk with Gunter Weller during the riverboat cruise on the Tanana River.
4. Doug Posson (USGS) chairs the panel on polar data and information.
5. Prof. Juan Roederer, chairman of the U.S. Arctic Research Commission, and Prof. V. Borisenkov of the Main Geophysical Observatory in Leningrad renew their acquaintance.
6. Victor Romanowsky, a permafrost researcher from Moscow State University, with an unidentified friend.
7. Prof. V. M. Kotlyakov from Moscow talks with Gunter Weller, the conference chairman, during the opening reception.
8. "Fritz" Koerner of the Geological Survey of Canada comments on the poster of Jesse Ford (back to the camera) while Ben Bantz and another participant look on.

ADDRESSES OF PRIMARY AUTHORS

(For countries other than the U.S. and Canada, country codes are in parentheses before telephone numbers)

Aagard, K.
NOAA/PMEL
7600 Sand Point Way N.E.
Seattle, Washington 98115-0070, U.S.A.
Phone 206-526-6806
GTE Telemail: K.Aagard

Adamenko, V. N. (SEE Kondratyev)

Alekseyev, G. V.
The Arctic and Antarctic Research Institute
Department of Ocean/Atmosphere Interaction
Leningrad, U.S.S.R.

Anderson, J. H.
Institute of Arctic Biology
University of Alaska Fairbanks
Fairbanks, Alaska 99775-0180, U.S.A.
Phone 907-474-7640

Anderson, L. G.
Department of Analytical and Marine Chemistry
University of Göteborg
and Chalmers University of Technology
S-412 96 Göteborg, Sweden
Omnet: L.Anderson.Goteborg

Anderson, P. M.
Quaternary Research Center AK-60
University of Washington
Seattle, Washington 98195, U.S.A.
Phone 206-543-0570

Anikiev, V. V.
Pacific Oceanological Institute
Far East Branch of the U.S.S.R. Academy of Sciences
7 Radio St.
Vladivostok 590032, U.S.S.R.

Anisimov, O. A. (SEE Nelson)

Barker, P. F.
British Antarctic Survey
High Cross
Madingley Road
Cambridge, England CB3 0ET
Phone (44) 223-61188; Fax (44) 223-62616

Antonov-Druzhinin, V. P.
Laboratory of the Geotechnical Systems of the Cold Regions
Monitoring Trust
626718, Novy Urengoy, 3-56-60, U.S.S.R.

Baranova, N. A.
Department of Geocryology, Geological Faculty
Moscow University
Moscow 119899, U.S.S.R.

Barnett, B.
Water Research Center
University of Alaska Fairbanks
Fairbanks, Alaska 99775-1760, U.S.A.
Phone 907-474-7115

Barrera
Department of Geological Sciences
1006 C. C. Little Building, The University of Michigan
Ann Arbor, Michigan 48109-1063, U.S.A.
Phone 313-764-1435; Fax 313-763-4690

Barrie, L. A.
Atmospheric Environment Service
4905 Dufferin Street
North York, Ontario M3H 5T4, Canada
Phone 416-739-4368; Fax 416-739-4224

Begét, James E.
Dept. Geology and Geophysics
University of Alaska Fairbanks
Fairbanks, Alaska 99775-9760, U.S.A.
Phone 907-474-7565

Belchansky, G. I.
Institute of Evolutionary Animal Ecology and Morphology
U.S.S.R. Academy of Science,
Lenin Avenue, 33
Moscow 117071, U.S.S.R.

Bentley, C. R.
Geophysical and Polar Research Center
Department of Geology and Geophysics
University of Wisconsin-Madison
Madison, WI 53706-1692, U.S.A.
Phone 608-262-1921; Fax 608-262-0693

Berkman, Paul Arthur
Byrd Polar Research Center
The Ohio State University
103 Mendenhall Laboratory
Columbus, Ohio 43210-1308, U.S.A.
Phone 614-292-6639; Fax 614-292-4697

Bessis, Jean-Luc
Service Argos, Inc.
1801 McCormick Dr., Suite #10
Landover, Maryland 20785, U.S.A.
Phone 301-925-4411; Fax 301-925-8995
Telemail: A. SHAW/CCI

Bigelow, N. H.
Dept. of Anthropology
University of Alaska Fairbanks
Fairbanks, Alaska 99775-0160, U.S.A.
Phone 907-474-6756

Blanchet, J.-P.
Canadian Climate Centre/CCRN
4905 Dufferin St.
Downsview, Ontario M3H 5T4, Canada
Phone 416-739-4414; Fax 416-739-4521

Böcher, J.
Zoological Museum, University of Copenhagen
Universitetsparken 15
DK 2100 Copenhagen, Denmark
Phone (45) 31354111

Bölter, M.
Institute for Polar Ecology
University of Kiel
Olshausenstr. 40
D-2300 Kiel 1, Germany
Phone (49) 431-880-4561; Fax (49) 431-880-4284

Bonan, Gordon B.
National Center for Atmospheric Research
P.O. Box 3000
Boulder, Colorado 80307, U.S.A.
Phone 303-497-1000; Fax 303-497-1137

Borisenkov, E. P.
Main Geophysical Observatory
Kaarbysheva Street, 7
Leningrad 194018, U.S.S.R.
Phone (812) 247-01-03

Bowling, S. A.
Alaska Climate Research Center, Geophysical Institute
University of Alaska Fairbanks
Fairbanks, Alaska 99775-0800, U.S.A.
Phone 907-474-7456; Fax 907-474-7290

Breitenberger, E.
Geophysical Institute
University of Alaska Fairbanks
Fairbanks, Alaska 99775-0800, U.S.A.
Phone 907-474-7360; Fax 907-474-7290

Brigham-Grette, Julie
Department of Geology & Geography
University of Massachusetts
Amherst, Massachusetts 01003-0026, U.S.A.
Phone 413-545-4840; Fax 413-545-1200
E-Mail: Brigham-Grette@GeolGeog.UMass.EDU

Bromwich, D. H.
Byrd Polar Research Center
The Ohio State University
Columbus, Ohio 43210, U.S.A.
Phone 614-292-6531; Fax 614-292-4697
Omnet: Byrd.Polar

Brugman, Melinda M.
National Hydrology Research Institute, Environment Canada
11 Innovation Blvd.
Saskatoon, Saskatchewan, S7N 3H5 Canada
Phone 306-975-5143

Budd, W. F.
Department of Meteorology
University of Melbourne
Parkville, Victoria 3052, Australia
Phone (61) 3-344-6912; Fax (61) 3-347-2091

Calkin, Parker E.
Department of Geology
University at Buffalo
415 Fronczak Hall
Buffalo, New York 14260, U.S.A.
Phone 716-636-6100; Fax 716-636-3999

Carter, L. D.
U.S. Geological Survey
4200 University Drive
Anchorage, Alaska 99508-4667, U.S.A.
Phone 907-786-7441

Cheng Guodong
Lanzhou Institute of Glaciology and Geocryology
Academia Sinica
Lanzhou 730000, Peoples Republic of China

Clew, G. D.
U.S. Geological Survey
345 Middlefield Rd., MS 946
Menlo Park, California 94025, U.S.A.
Phone 415-329-5179

Cohen, S. J.
Canadian Climate Centre
Atmospheric Environment Service
4905 Dufferin St.
Downsview, Ontario M3H 5T4, Canada
Phone 416-739-4389; Fax 416-739-4521

Collett, T. S.
U.S. Geological Survey
345 Middlefield Road, MS 999
Menlo Park, California 94025, U.S.A.
Phone 415-354-3009

Colony, R.
Polar Science Center, University of Washington
Seattle, Washington 98105, U.S.A.
Phone 206-543-6615
Telemail: polar science

Crame, J. A.
British Antarctic Survey
High Cross
Madingley Road
Cambridge CB3 0ET, United Kingdom
Phone (44) 223-61188; Fax (44) 223-62616

Dean, K. G.
Geophysical Institute
University of Alaska Fairbanks
Fairbanks, Alaska 99775-0800, U.S.A.
Phone 907-474-7364; Fax 907-474-5195

DjupstrHom, M. (SEE Pacyna)

Domack, E. W.
Geology Department
Hamilton College
Clinton, New York 13323, U.S.A.
Phone 315-859-4711

Doronin, N. Yu.
Arctic and Antarctic Research Institute
Leningrad, U.S.S.R.

Droessler, Terry D.
ManTech Environmental Technology, Inc.
US EPA Environmental Research Lab
200 SW 35th St.
Corvallis, Oregon 97333, U.S.A.
Phone 503-757-4664; Fax 503-757-4799

Eastland, Warren G.
Institute of Arctic Biology
University of Alaska Fairbanks
Fairbanks, Alaska 99775-0180, U.S.A.
Phone 907-474-7028

Edwards, M. E.
Department of Geology and Geophysics
University of Alaska Fairbanks
Fairbanks, Alaska 99775-0760, U.S.A.
Phone 907-474-5014

Elliot, D. H. (SEE Bromwich)

Ferrigno, J. G.
U.S. Geological Survey
Reston, Virginia 22092, U.S.A.
Phone 703-648-6360

Fletcher, J. O.
NOAA Environmental Research Laboratories
Boulder, Colorado 80303-3228, U.S.A.
Telemail: J.Fletcher

Ford, Jesse
NCASI, c/o U.S. EPA Environmental Research Laboratory
200 SW 35th St.
Corvallis, Oregon 97333, U.S.A.
Phone 503-753-6221; Fax 503-757-4335

Furmanczyk, K. (SEE Prais)

Garagula, L. S.
Department of Geocryology, Faculty of Geology
Moscow State University
Moscow, 119899, U.S.S.R.
Phone (7) 939-1459

George, Tom
Alaska SAR Facility, Geophysical Institute
University of Alaska Fairbanks
Fairbanks, Alaska 99775-0800, U.S.A.
Phone 907-474-7621; Fax 907-474-5195
Omnet: T.George

Gloersen, Per
Laboratory for Oceans, Code 971
NASA Goddard Space Flight Center
Greenbelt, Maryland 20771, U.S.A.
Phone 301-286-6362; Fax 301-286-2717
Omnet: P.Gloersen

Gordon, Arnold L.
Lamont-Doherty Geological Observatory
Palisades, New York 10964, U.S.A.
Phone 914-359-2900, ext. 325; Fax 914-365-0718
Omnet: A.Gordon

Graumlich, Lisa J.
Laboratory of Tree-Ring Research
University of Arizona, Bldg. #58
Tucson, Arizona, 85721 U.S.A.
Phone 602-621-6469; Fax 602-621-8229

Groves, J. E.
Geophysical Institute
University of Alaska Fairbanks
Fairbanks, Alaska 99775-0800, U.S.A.
Phone 907-474-7870; Fax 907-474-5195

Hakkinen, S.
Princeton University
P.O. Box CN 710
Princeton, New Jersey 08544-0710, U.S.A.
Phone 609-258-1317

Harrison, W. D.
Geophysical Institute
University of Alaska Fairbanks
Fairbanks, Alaska 99775-0800, U.S.A.
Phone 907-474-7706; Fax 907-474-7290

Harritt, R. K.
U.S. National Park Service, Alaska Region
2525 Gambell St., Rm. 106
Anchorage, Alaska 99503-2892, U.S.A.
Phone 907-257-2546

Hempel, G.
Alfred Wegener Institute for Polar and Marine Research
P.O. Box 12 61
D-2850 Bremerhaven, Germany
Phone (49) 471-4831-100; Fax (49) 471-4831-149
Telemail: Alfred.Wegener

Herbert, Gary
Climate Monitoring and Diagnostics Laboratory
Environmental Research Laboratories, NOAA
325 Broadway
Boulder, Colorado 80303-3328, U.S.A.
Phone 303-497-6842; Fax 303-497-6290

Higuchi, Kaz
Climate Diagnostic Research Group
Atmospheric Environment Service
4905 Dufferin St.
Downsview, Ontario M3H 5T4, Canada
Phone 416-739-4452; Fax 416-739-5704

Hinzmar, Larry D.
Water Research Center
University of Alaska Fairbanks
Fairbanks, Alaska 99775, U.S.A.
Phone 907-474-7331

Hobbie, J. E.
The Ecosystems Center
Marine Biological Laboratory
Woods Hole, Massachusetts 02543, U.S.A.
Phone 508-548-3705; 508-457-1548
Omnet: J.Hobbie

Hogan, A.
Atmospheric Research, Geochemical Sciences Branch
U.S.A. CRREL
72 Lyme Rd.
Hanover, New Hampshire 03755-1290, U.S.A.
Phone 603-646-4364; Fax 603-646-4644
Telemail: A. Hogan

Holt, Benjamin
Jet Propulsion Laboratory
California Institute of Technology, MS 300-323
Pasadena, California 91109, U.S.A.
Phone 818-354-5473; Fax 818-393-6720
UN:BHOLT, SITE:NASAMAIL

Hunkins, Kenneth
Lamont-Doherty Geological Observatory
Palisades, New York 10964, U.S.A.
Phone 914-359-2900, ext. 383

Hus, L.
Department of Remote Sensing and Marine Cartography
University of Szczecin
71-412 Szczecin, Felczaka 3A, Poland
Telemail: L.Hus

Iwasaka, Y.
Research Institute of Atmospherics
Nagoya University
Honohara, Toyokawa 442, Japan
Phone (81) 5338-6-3154; Fax (81) 5338-5-0811

Jacka, T. H.
Australian Antarctic Division
Channel Highway
Kingston, Tasmania 7050, Australia
Phone (61) 2-29-0209; Fax (61) 2-29-3335

Jacoby, G. C.
Tree-Ring Laboratory
Lamont-Doherty Geological Observatory
Palisades, New York 10964, U.S.A.
Phone 914-359-2900; Fax 914-365-3046
Omnet: G.Jacoby
E-mail: druid@LAMONT.LDGO.COLUMBIA.EDU

Jaffe, D. A.
Geophysical Institute and Department of Chemistry
University of Alaska Fairbanks
Fairbanks, Alaska 99775-0800, U.S.A.
Phone 907-474-7610; Fax 907-474-7290
Bitnet: FFDJ@ALASKA

Jakobsen, Bjarne Holm
Institute of Geography
University of Copenhagen
Oster Voldgade 10
DK-1350 Copenhagen K, Denmark
Phone (45) 33 132105; Fax (45) 33 148105

Jeffries, Martin O.
Geophysical Institute
University of Alaska Fairbanks
Fairbanks, Alaska 99775-0800, U.S.A.
Phone 907-474-5257; Fax 907-474-5195

Jenne, Roy L.
Scientific Computing Division, Data Support Section
National Center for Atmospheric Research
P.O. Box 3000
Boulder, Colorado 80307, U.S.A.
Phone 303-497-1215; Fax 303-497-1137
Omnet: r.jenne

Jezek, Kenneth C.
Byrd Polar Research Center
The Ohio State University
Columbus, Ohio 43210, U.S.A.
Phone 614-292-6531
Omnet: K.Jezek

Jones, E. Peter
Department of Fisheries and Oceans
Bedford Institute of Oceanography
P.O. Box 1006
Dartmouth, Nova Scotia B2Y 4A2, Canada
Phone 902-426-3869

Jones, John E.
U.S. Geological Survey
521 National Center
Reston, Virginia 22092, U.S.A.
Phone 703-648-4138; Fax 703-648-5585

Juday, G. P.
School of Agriculture and Land Resources Management
University of Alaska Fairbanks
Fairbanks, Alaska 99775, U.S.A.
Phone 907-474-6717

Judge, Alan
Terrain Sciences Division
Geological Survey of Canada
601 Booth St.
Ottawa, Ontario K1A 0E8, Canada
Phone 613-996-9323; Fax 613-992-2468

Kahl, Jonathan D.
Department of Geosciences
University of Wisconsin-Milwaukee
Milwaukee, Wisconsin 53201, U.S.A.
Phone 414-229-4561

Kanzawa, H.
National Institute of Polar Research
1-9-1 Higashi, Itabashi-ku
Tokyo 173, Japan
Phone (81) 3-962-4611; Fax (81) 3-962-2529
Telemail: C32581@JPNKUDPC.BITNET

Karakin, V. P.
Pacific Geography Institute
Far East Division of the U.S.S.R. Academy of Sciences
7 Radio St.
Vladivostok 690032, U.S.S.R.

Kienle, Juergen
Geophysical Institute
University of Alaska Fairbanks
Fairbanks, Alaska 99775-0800, U.S.A.
Phone 907-474-7467; Fax 907-474-7290

King, R. H.
Department of Geography
University of Western Ontario
London, Ontario N6G 1T4, Canada
Phone 519-679-2111, ext. 5006; Fax 519-661-3868
E-mail: King@VaxR.sscl.uwo.ca

Kirts, Carla A.
School of Agriculture and Land Resources Management
301 O'Neill Resources Building
University of Alaska Fairbanks
Fairbanks, Alaska 99775-0100, U.S.A.
Phone 907-474-7471; Fax 907-474-7439

Kodama, K.
Institute of Low Temperature Science
Hokkaido University
Sapporo 060, Japan
Phone (81) 11-716-2111

Koerner, R. M.
Terrain Sciences Division
Geological Survey of Canada
601 Booth St.
Ottawa, Ontario K1A 0E8, Canada
Phone 613-996-7623; Fax 613-996-9990

Kolchugina, T. P.
Department of Geocryology, Faculty of Geology
Moscow State University
Moscow, 119899, U.S.S.R.
Phone (7) 939-2961; Fax (7) 939-0126

Konstantyev, K. Ya.
Institute for Lake Research
U.S.S.R. Academy of Science
Sevastyanov str., 9
196199 Leningrad, U.S.S.R.
Phone (812) 231-77-73

König-Langlo, G.
Alfred-Wegener-Institute
Columbustrasse
2850 Bremerhaven, Germany
Fax (49) 471-4831149

Kotlyakov, Vladimir M.
Institute of Geography
U.S.S.R. Academy of Sciences
Staromonety Per. 29
109017 Moscow, U.S.S.R.
Phone (7) 238-86-10

Kubisch, M.
GEOMAR, Research Center for Marine Geosciences
Wischhofstr. 1-3
D-2300 Kiel, Germany
Phone (49) 431-7297191; Fax (49) 431-725650

Kvenvolden, Keith A.
U.S. Geological Survey
345 Middlefield Rd., M/S 999
Menlo Park, California 94025, U.S.A.
Phone 415-354-3213; Fax 415-354-3191

Lal, M.
Centre for Atmospheric Sciences
Indian Institute of Technology
New Delhi 110 016, India
Phone (91) 656197

Lange, M. A.
Alfred-Wegener-Institute for Polar- and Marine Research
Postfach 12 01 61
Columbusstrasse
D-2850 Bremerhaven, Germany
Phone (49) 471-4831-217/349; (49) 471-4831-149

Ledley, Tamara Shapiro
Department of Space Physics and Astronomy
Rice University
P.O. Box 1892
Houston, Texas 77251, U.S.A.
Phone 713-527-8101, ext. 3594; Fax 713-285-5143
E-mail: Internet: LEDLEY@SPACVAX.RICE.EDU

Letréguilly, A.
Alfred Wegener Institute for Polar and Marine Research
Columbusstrasse
D-2850 Bremerhaven, Germany
Phone (49) 471-4831-194; Fax (49) 471-4831-149

Lingle, Craig S.
Geophysical Institute
University of Alaska Fairbanks
Fairbanks, Alaska 99775-0800, U.S.A.
Phone 907-474-7679; Fax 907-474-5195

Livingston, Gerald P.
TGS Technology, Inc., NASA Ames Research Center
Earth Systems Science Division, SGE:239-20
Moffett Field, California 94035-1070, U.S.A.
Phone 415-604-3232; Fax 415-604-3954

Lorius, C.
Laboratoire de Glaciologie et Géophysique de
l'Environnement
B.P. 96
38402 St Martin d'Hères cedex, France
Phone (33) 76 82 42 00; Fax (33) 76 82 42 01

Lucchitta, B. K.
U.S. Geological Survey
2255 North Gemini Dr.
Flagstaff, Arizona 86001, U.S.A.
Phone 602-527-7176

McKendrick, J. D.
School of Agriculture and Land Resources Management
Agriculture and Forestry Experiment Station
University of Alaska Fairbanks
533 East Fireweed
Palmer, Alaska 99645, U.S.A.
Phone 907-745-3257

McLaren, A. S.
University of Colorado/CIRES
Campus Box 449
Boulder, Colorado 80309, U.S.A.
Phone 303-492-1272

Makogon, Y. F.
Oil and Gas Research Institute
Academy of Science U.S.S.R.
Moscow, U.S.S.R.

Marchant, Harvey J.
Australian Antarctic Division
Channel Highway
Kingston, Tasmania 7050, Australia
Phone (61) 2-32-3209; Fax (61) 2-32-3351

Martinson, Douglas G.
Lamont-Doherty Geological Observatory
Palisades, New York 10964, U.S.A.
Phone 914-359-2900; Fax 914-365-0718
Omnet: D.Martinson
Internet: dgm@lamont.columbia.edu

Mason, Owen K.
Alaska Quaternary Center
University of Alaska Fairbanks
Fairbanks, Alaska 99775, U.S.A.
Phone 907-474-6293

Milkovich, Mary F.
Institute of Marine Science
University of Alaska Fairbanks
Fairbanks, Alaska 99775-1080, U.S.A.
Phone 907-474-7931

Mokhov, I. I.
Institute of Atmospheric Physics
3, Pyzhevsky
Academy of Sciences of the U.S.S.R.
Moscow 109 017, U.S.S.R.
Phone (7) 231-64-53; Fax (7) 200-22-16, 200-22-17

Molnia, Bruce F.
U.S. Geological Survey
917 National Center
Reston, Virginia 22092, U.S.A.
Phone 703-648-4120

Mosley-Thompson, Ellen
Byrd Polar Research Center
The Ohio State University
103 Mendenhall Laboratory
Columbus, Ohio 43210-1308, U.S.A.
Phone 614-292-6531; Fax 614-292-4697
Omnet: E.Mosley.Thompson

Mudie, P. J.
Geological Survey Canada, Atlantic Geoscience Centre
Box 1006
Dartmouth, Nova Scotia B2Y 4A2, Canada
Phone 902-426-8720; Fax 902-426-4104

Mysak, L. A.
Centre for Climate and Global Change Research
and Dept. of Meteorology
McGill Univ.
805 Sherbrooke St. W.
Montreal, P.Q. H3A 2K6, Canada
Phone 514-398-3759; Fax 514-398-6115

Naborov, I. V.
1st Moscow Medical Institute
GTK
Moscow, U.S.S.R.
Phone (7) 284-75-33

Nelson, Frederick E.
Department of Geography
Rutgers University
New Brunswick, New Jersey 08903, U.S.A.
Phone 201-932-4103; Fax 201-932-2175

Nishio, Fumihiko
National Institute of Polar Research
9-10, Kaga, Itabashiku
Tokyo 173, Japan
Phone (81) 3-962-4711; Fax (81) 3-962-2529

Oechel, W. C.
Department of Biology
San Diego State University
San Diego, California 92182-0057, U.S.A.
Phone 619-594-4818; Fax 619-594-5642

Olausson, Eric
Hultvägen 9
S-440 06 Gråbo, Sweden
Phone (46) 0302-400 82

Olmsted, Coert
Alaska SAR Facility, Geophysical Institute
University of Alaska Fairbanks
Fairbanks, Alaska 99775-0800, U.S.A.
Phone 907-474-7475; Fax 907-474-5195

Osterkamp, T. E.
Geophysical Institute
University of Alaska Fairbanks
Fairbanks, Alaska 99775-0800, U.S.A.
Phone 907-474-7548; Fax 907-474-7290

Pacyna, J. M.
Norwegian Institute for Air Research
P.O. Box 64
2001 Lillestrom, Norway
Phone (47) 6-814170; Fax (47) 6-819247

Pagels, U.
GEOMAR, Research Center for Marine Sciences
Wischhofstr. 1-3
D-2300 Kiel 14, Germany
Phone (49) 431-7202114

Parish, T. R.
Department of Atmospheric Sciences
University of Wyoming
Laramie, Wyoming 82071, U.S.A.
Phone 307-766-5153

Parkinson, Claire L.
Oceans and Ice Branch, Code 971
Goddard Space Flight Center
Greenbelt, Maryland 20771, U.S.A.
Phone 301-286-6507
Omnet: C.Parkinson

Pengqun, Jia
Polar Meteorological Laboratory
Academy of Meteorological Science
State Meteorological Administration
Beijing, 100081, Peoples Republic of China
Phone (86) 8312277-2296

Pettré, P.
Centre National de Recherches Météorologiques
42 Av. Coriolis
31057 Toulouse Cedex, France
Phone (33) 61 07 93 62; Fax (33) 61 07 96 00

Pfeffer, W. T.
University of Colorado/INSTAAR
Campus Box 450
Boulder, Colorado 80309, U.S.A.
Phone 303-492-3480
email: pfeffer@prince.colorado.edu

Pinney, DeAnne S.
Dept. of Geology and Geophysics
University of Alaska Fairbanks
Fairbanks, Alaska 99775-9760, U.S.A.
Phone 907-474-7565

Polyakova, A. M.
Pacific Oceanological Institute
Far Eastern Branch U.S.S.R. Academy of Sciences
7 Radio St.
Vladivostok 590032, U.S.S.R.

Posson, D. R.
U.S. Geological Survey, MS 801
Reston, Virginia 22091, U.S.A.
Phone 703-648-7106
Omnet: D.Posson

Prajs, J.
Department of Remote Sensing and Cartography
University of Szczecin
Felczake 3A
71-412 Szczecin, Poland
Telemail: J.Prajs

Proshutinsky, A. Yu.
The Arctic and Antarctic Research Institute
Leningrad, U.S.S.R.

Radok, Uwe
University of Colorado/CIRES
Campus Box 449
Boulder, Colorado 80309, U.S.A.
Phone 303-492-5562

Rasmussen, R. A.
Institute of Atmospheric Science
Oregon Graduate Center
19600 N.W. Von Neumann Drive
Beaverton, Oregon 97006, U.S.A.
Phone 503-690-1093

Reeburgh, W. S.
Institute of Marine Science
University of Alaska Fairbanks
Fairbanks, Alaska 99775-1080, U.S.A.
Phone 907-474-7830
Telemail: W.Reeburgh

Reeh, N.
Alfred Wegener Institute for Polar and Marine Research
Columbusstrasse
D-2850 Bremerhaven, Germany
Phone: (49) 471-483-1174

Rogachev, K. A.
Pacific Oceanological Institute
Far Eastern Branch of the U.S.S.R. Academy of Sciences
Vladivostok 690032, U.S.S.R.

Romanovsky, V. E.
Department of Geocryology, Faculty of Geology
Moscow State University
Moscow, 119899, U.S.S.R.
Phone (7) 939-1453

Royer, T. C.
Institute of Marine Science
University of Alaska Fairbanks
Fairbanks, Alaska 99775, U.S.A.
Phone 907-474-7835
Telemail: T.ROYER

Sand, K.
SINTEF Norwegian Hydrotechnical Laboratory
Klaebuveien 153
N-7034 Trondheim, Norway
Phone (47) 7-592300; Fax (47) 7-592376
Omnet: J. Saetnan

Sandberg, D. V. (SEE Slaughter)

Schell, D. M. (SEE Barnett)

Schnell, R. C.
Cooperative Institute for Research in Environmental Sciences
University of Colorado/NOAA
Boulder, Colorado 80309-0449, U.S.A.
Phone 303-497-6661

Scvortzov, I. D.
State Scientific-Research and Design Institute of Oil and Gas
Industry
Respubliki St., 62
Tyumen 625000, U.S.S.R.

Seko, Katsumoto
Water Research Institute, Nagoya University
Chikusa-ku
Nagoya 464, Japan
Phone (81) 52-781-5111, ext. 5727; Fax (81) 52-781-5998

Semiletov, I. P.
Pacific Oceanological Institute
Far Eastern Branch of the U.S.S.R. Academy of Sciences
7 Radio St.
Vladivostok 690032, U.S.S.R.

Sharratt, B. S.
USDA-ARS
309 O'Neill Building
University of Alaska Fairbanks
Fairbanks, Alaska 99775, U.S.A.
Phone 907-474-7187

Shasby, M. B.
U.S. Geological Survey/EROS Field Office
Anchorage, Alaska 99503-4664, U.S.A.
Phone 907-271-4065

Sheridan, Patrick J.
Cooperative Institute for Research in Environmental Sciences
University of Colorado/NOAA
Boulder, Colorado 80309-0449, U.S.A.
Phone 303-497-6672; Fax 303-497-6290

Simmonds, Ian
Department of Meteorology
University of Melbourne
Parkville, Victoria 3052, Australia
Phone (61) 3-344-6912; Fax (61) 3-347-2091

Slaughter, C. W.
Institute of Northern Forestry
Pacific Northwest Research Station
USDA Forest Service
308 Tanana Drive
Fairbanks, Alaska 99775, U.S.A.
Phone 907-474-3311

Stamnes, K.
Geophysical Institute
University of Alaska Fairbanks
Fairbanks, Alaska 99775-0800, U.S.A.
Phone 907-474-7368; Fax 907-474-7290

Stearns, Charles R.
Department of Meteorology
University of Wisconsin-Madison
1225 West Dayton St.
Madison, Wisconsin 53706, U.S.A.
Phone 608-262-2828
Omnet: AWS.MADISON

Steele, Michael
Polar Science Center, Applied Physics Lab
University of Washington
1013 NE 40th St.
Seattle, Washington 98105, U.S.A.
Phone (206) 543-6586

Stephens, Graeme L.
Department of Atmospheric Science
Colorado State University
Ft. Collins, Colorado 80523, U.S.A.
Phone (303) 491-8541; Fax (303) 491-8449
Omnet: G.STEPHENS

Stewart, R. E.
Cloud Physics Research Division
Atmospheric Environment Service
4905 Dufferin St.
Toronto, Ontario M3H 5T4, Canada
Phone 416-739-4608; Fax 416-739-4211
Omnet: R.Stewart.AES

Stocker, Thomas F.
Lamont-Doherty Geological Observatory
Palisades, New York 10964, U.S.A.
Phone 914-359-2900, ext. 705; Fax 914-365-3183

Stone, Robert S.
Cooperative Institute for Research in Environmental Sciences
University of Colorado
Boulder, Colorado 80306, U.S.A.
Phone 303-497-6056

Sturges, W. T.
University of Colorado/CIRES
Campus Box 216
Boulder, Colorado 80309-0126, U.S.A.
Phone 303-492-1143; Fax 303-492-1149

Sturm, Matthew
U.S.A. CRREL-Alaska
Building 4070
Ft. Wainwright, Alaska 99703-7860, U.S.A.
Phone 907-353-5149; Fax 907-353-5142

Sullivan, C. W.
Department of Biological Sciences
University of Southern California
Los Angeles, California 90089-0371, U.S.A.
Phone 213-743-6904
Omnet: C.Sullivan

Tanaka, H. L.
Institute of Geoscience
University of Tsukuba
Tsukuba, Ibaraki 305, Japan

Taylor, Alan
Terrain Sciences Division
Geological Survey of Canada
601 Booth St.
Ottawa, Ontario K1A 0E8, Canada
Phone 613-996-9324

Turner, J.
British Antarctic Survey
High Cross
Madingley Road
Cambridge CB3 0ET, U.K.
Phone (44) 223-61188; Fax (44) 223-62616

Untersteiner, N.
Department of Atmospheric Sciences AK-40
University of Washington
Seattle, Washington 98195, U.S.A.
Phone 206-543-4250
Telemail: N.Untersteiner

Vaikmäe, Rein
Institute of Geology
Estonian Academy of Sciences
7 Estonia puistee
200 101 Tallinn, Estonia
Phone 7-0142-444189; Fax 7-0142-523624

Vinje, Torgny
Norwegian Polar Research Institute
Post Office Box 158
1330 Oslo Lufthavn, Norway
Phone (47) 2-123650; Fax (47) 2-123854

Vlasova, T. M.
Far North Institute for Agricultural Research
Reindeer Department
663302 Noril'sk, U.S.S.R.

Wadhams, Peter
Scott Polar Research Institute
University of Cambridge
Lensfield Road
Cambridge CB2 1ER, England
Phone (44) 223-336542; Fax (44) 223-336549
Telemail: P.Wadhams

Walsh, John E.
Dept. of Atmospheric Sciences
University of Illinois
Urbana, Illinois 61801, U.S.A.
Phone 217-333-7521

Way, JoBea
Jet Propulsion Laboratory
4800 Oak Grove Dr., MS 300-233
Pasadena, California 91109, U.S.A.
Phone 818-354-8225

Weaver, R. L.
National Snow and Ice Data Center, CIRES
University of Colorado, Boulder
Boulder, Colorado 80309-0449, U.S.A.
Phone 303-492-7624
Omnet: R.WEAVER

Weidner, George A.
Department of Meteorology
University of Wisconsin-Madison
Madison, Wisconsin 53706, U.S.A.
Phone 608-262-4882

Wendler, Gerd
Geophysical Institute
University of Alaska Fairbanks
Fairbanks, Alaska 99775-0800, U.S.A.
Phone 907-474-7378; Fax 907-474-7290

Wettlaufer, J. S.
Polar Science Center and Geophysics Program
University of Washington
Seattle, Washington 98105, U.S.A.
Phone 206-543-2824; Fax 206-543-0308
Omnet: Polar.Science

Wharton, R. A., Jr.
Biological Sciences Center
Desert Research Institute
Reno, Nevada 89506, U.S.A.
Phone 702-673-7323

Williams, R. S., Jr.
U.S. Geological Survey
927 National Center
Reston, Virginia 22092, U.S.A.
Phone 703-648-6388; Fax 703-648-4227

Wollenburg, I. R.
GEOMAR, Research Center for Marine Geosciences
Wischhofstr. 1-3, Bdg. 4
D-2300 Kiel 14, Germany
Phone (49) 431-7202114

Yanitsky, P. A.
Institute of Northern Development
Box 3004
Tyumen-31, 625031 U.S.S.R.
Phone 296818 or 290172

Yarie, J.
Forest Soils Laboratory
Agricultural and Forestry Experiment Station
University of Alaska Fairbanks
Fairbanks, Alaska 99775
Phone 907-474-6714
Internet: jyarie@forest.liter.alaska.edu
bitnet: FFJAY@ALASKA

Zimov, S. A.
Pacific Institute of Geography
Far East Branch of the U.S.S.R. Academy of Science
Radio St. 7
Vladivostok 590032, U.S.S.R.

Zwally, H. Jay
Oceans and Ice Branch
NASA Goddard Space Flight Center
Greenbelt, Maryland 20771, U.S.A.
Phone 301-286-8239

AUTHOR INDEX

AUTHOR INDEX

Aagaard, K.	248	Choclov, D. A.	452
Adamenko, V. N.	716	Christensen, N.	93
Ahlnaes, K.	748	Chuprynin, V. I.	411
Aimediou,	720	Clow, G. D.	502, 533
Alekseev, A. V.	451	Cohen, S. J.	200
Alekseyev, G. V.	158, 317	Colinvaux, P. A.	628
Alt, B. T.	576	Collett, T. S.	7429
Andersen, D. T.	502	Colony, R.	290
Anderson, J. H.	453	Comiso, J. C.	22
Anderson, L. G.	340, 355	Crame, J. A.	396
Anderson, P. M.	557, 628	Crushin, P. N.	468
Andreev, A. A.	628	Crux, J. A.	663
Anikiev, V. V.	451, 452	Curlander, J.	80
Anisimov, O. A.	534		
Antonov-Druzhinin, V. P.	553	D'Arrigo, R. D.	599
		Davidson, A.	397
Baranova, N. A.	641	Davydov, S. P.	416
Barker, P. F.	586	Davydova, A. I.	416
Barnard, S. C.	681	Dean, K.	133, 338, 748
Barnett, B.	417	Déqué, M.	236
Barrera, E.	666	DiMarzio, J. P.	35
Barrie, L. A.	673	DjupstrHom, M.	707
Begét, J. E.	594, 634, 658	Dobson, C.	93
Belchansky, G. I.	47, 112	Domack, E. W.	643
Benson, C. S.	519	Doronin, N. Yu.	205, 310
Bentley, C. R.	481	Dreyer, N. N.	477
Berkman, P. A.	440	Droessler, T. D.	431
Berntsen, E.	525	Dudachev, O. V.	452
Bessis, J.-L.	126		
Bigelow, N. H.	658	Eastland, W. G.	460
Binnian, E. F.	46	Echelmeyer, K. A.	517
Blanchet, J.-P.	693	Edwards, M. E.	633, 644
Böcher, J.	582	Eisner, W. R.	628
Bodhaine, B. A.	695	Elliot, D. H.	508
Bölter, M.	418	Estes, S. A.	748
Bonan, G. B.	391		
Borisenkov, E. P.	627, 687	Federova, I. N.	628
Bourgeois, J. C.	576	Fedosova, S. P.	549
Bourke, R. H.	79	Fei, T.	505
Boukvareva, E. N.	112	Ferrigno, J. G.	44, 88, 518
Bowling, S. A.	206	Field, W. O.	519
Breitenberger, E.	320	Filipchuk, A. N.	423
Brigham-Grette, J.	644	Fisher, D. A.	576
Brenner, A. C.	35	Fletcher, J. O.	149
Breus, T. K.	469	Ford, J.	102
Bromwich, D. H.	190, 237, 508	Frederick, J.	741
Brubaker, L. B.	628	Fujii, Y.	664
Brugman, M. M.	500	Funder, S.	644
Budd, W. F.	63, 256, 489	Furmanczyk, K.	532
Burgess, M.	504	Furukawa, T.	238
Burkley, L.	643		
		Garagula, L. S.	90, 536, 543
Calkin, P. E.	617	Gard, G.	663
Campbell, W. J.	28	George, T.	133
Carmack, E. C.	248	Giovinetto, M. B.	481
Carsey, F.	80	Gloersen, P.	28
Carter, L. D.	593	Gordon, A. L.	249
Cavalieri, D.	43	Gosink, J. P.	338, 505
Cheng, G.	243	Graumlich, L. J.	565
Chernenky, B. I.	628	Groves, J. E.	357

Hagen, J. O.	525	Kondoh, Y.	720
Hakkinen, S.	339	Kondratyev, K. Ya.	3, 716
Hall, D. K.	519	König-Langlo, G.	325
Hansen, A. D. A.	695	Kotlyakov, V. M.	477
Hanson, C. S.	120	Kotova, L. N.	628
Harrison, W. D.	517	Kovalev, B. I.	423
Harritt, R. K.	401	Kubisch, M.	667
Harwood, D. M.	508	Kutzbach, J.	644
Hayashi, M.	720	Kvenvolden, K. A.	696
Hedley, A.	504	Kwok, R.	80, 93
Hempel, G.	450		
Herbert, G. A.	159	Lal, M.	703
Higuchi, K.	164, 412	Lachenbruch, A. H.	533
Hinzman, L. D.	503	Landers, D. H.	102
Hobbie, J. E.	378	Landsberger, S.	751
Hogan, A.	681	Lange, M. A.	275, 668
Holt, B.	80	Larter, R. D.	586
Honrath, R. E.	730	Ledley, T. S.	321
Hopkins, D. M.	628	Letréguilly, A.	495, 626
Huber, B. T.	666	Li, S.-M.	707
Humphrey, N.	517	Lin, C. A.	164, 227
Hunkins, K.	304	Lingle, C. S.	35
Hus, L.	87	Livingston, G. P.	372
Huybrechts, P.	495	Lomakin, A. F.	319
		Lorius, C.	570
Illangasekare, T. H.	499	Lozhkin, A. V.	628
Ishikawa, N.	199	Lucchitta, B. K.	88, 518
Ivanov, B.	325		
Iwasaka, Y.	720	MacDonald, T. R.	518
		MacInnes, K.	504
Jacka, T. H.	63	McDonald, K.	93
Jacoby, G. C.	599	McKay, C. P.	502, 533
Jaffe, D. A.	730	McKendrick, J. D.	430
Jakobsen, B. H.	406	McLaren, A. S.	79
Jeffries, M. O.	332	Makogon, Y. F.	743
Jenn ^o R. L.	107	Maher, L.	644
Jr C.	43	Manak, D. K.	284
J	340	Marchant, H. J.	397
Jones, J. E.	524	Marsden, R. F.	284
Jones, M. O.	106	Martinson, D. G.	269
Jordan, J. W.	649	Mason, O. K.	649
Juday, G. P.	45	Matthews, J. V., Jr.	644
Judge, A.	504	Matthews, W. A.	720
		Maximova, L. N.	537
Kahl, J. D.	119, 184, 694, 695, 708	Maxwell, J. B.	200
Kane, D. L.	503	Medvedev, A. N.	451
Kanzawa, H.	735	Meier, M. F.	499
Kapustin, V. N.	695	Mellor, G. L.	339
Karakin, V. P.	429	Milkovich, M. F.	210
Kawaguchi, S.	735	Miller, G. H.	644
Khalil, M. A. K.	702	Miller, H.	626
Khroutsky, S. F.	641	Miller, J.	133
Kienle, J.	748	Miller, M. C.	628
King, R. H.	384	Mokhov, I. I.	176, 736
Kirts, C. A.	470	Molnia, B. F.	88, 89, 524
Knox, J. L.	164	Morgan, A.	644
Kobayashi, D.	199	Morrissey, L. A.	372
Kodama, K.	199	Mosley-Thompson, E.	606
Koerner, R. M.	576	Mudie, P. J.	669
Koga, S.	720	Murphey, B. B.	681
Ku ^u der, S.	585	Musgrave, D.	338
Kolchugina, T. P.	549	Mysak, L. A.	284, 291

Naborov, I. V.	469	Seko, K.	238
Nakawo, M.	664	Semiletov, I. P.	356, 665
Narita, H.	664	Seregina, N. V.	536, 537, 543
Nedashkovski, A. P.	452	Shabbar, A.	164
Nelson, F. E.	534	Sharratt, B. S.	465
Nishio, F.	501, 664	Shasby, M. B.	46
Nomura, A.	720	Shaver, G. R.	378
O'Brien, W. J.	378	Shaw, G. E.	674, 707
Oechel, W. C.	369	Sheinhouse, A. S.	429
Oerter, H.	626	Sheridan, P. J.	119, 694, 708
Olausson, E.	496	Shoji, H.	664
Olmsted, C.	141	Shymilin, E. M.	451
Osterkamp, T. E.	505	Simmons, G. M., Jr.	502
Pacyna, J. M.	674, 707	Simmonds, I.	256, 489
Pagels, U.	585	Sinyakov, S. A.	716
Parish, T. R.	191	Slaughter, C.	93, 435
Parkinson, C. L.	17, 71	Smith, I. R.	384
Pasetsky, V. M.	627	Spielhagen, R. F.	667
Pegau, S.	741	Stamnes, K.	741
Pengqun, J.	744	Stearns, C. R.	58, 220, 223
Pervushin, A. V.	452	Steele, M.	330
Peterson, B. J.	378	Stephens, G. L.	151
Pettré, P.	236	Stewart, R. E.	227
Petrosyan, V. G.	112	Stocker, T. F.	291
Pfeffer, W. T.	499	Stone, P. S.	184
Pfirman, S. L.	668	Stringer, W. J.	357
Pichugin, A. P.	47	Sturges, W. T.	751
Pinney, D. S.	634	Sturm, M.	519
Polujan, A. I.	628	Sullivan, C. W.	371
Polyakov, I. V.	347	Tanaka, H. L.	170, 748
Polyakova, A. M.	318	Tarnocai, C.	644
Posson, D. R.	106	Taylor, A.	642
Prais, J.	532	Thompson, L. G.	606
Proshutinsky, A. Yu.	296, 310, 347	Trivett, N. B. A.	412
Prosyannikov, S. F.	416	Troisi, V. J.	120
Prosyannikova, O. V.	416	Tumeo, M. A.	470
Pudsey, C. J.	586	Turner, J.	14
Radok, U.	192	Untersteiner, N.	247, 331
Rasmussen, R. A.	702	Vaikmäe, R.	611
Reeburgh, W. S.	370	Van Cleve, K.	390, 436
Reeh, N.	495, 626	Vance, E.	390
Repp, K.	525	Vernal, A. de	644
Rogachev, K. A.	319	Viereck, L.	93
Roujansky, V. E.	90	Vincent, J.-S.	644
Reynolds, G.	133	Vinje, T.	23
Riley, D. GI03		Vlasova, T. M.	423
Romanovsky, V. E.	536, 537, 543	Voropaev, U. V.	416
Rovako, L. G.	628	Voropaeva, Z. V.	416
Royer, T. C.	150	Wadhams, P.	4
Rutter, N. W.	644	Wakahama, G.	199
Sagalaev, S. G.	452	Walsh, J. E.	22, 263
Samson, J. A.	681	Watanabe, O.	238, 664
Sand, K.	525	Way, J.	93
Sandberg, D. V.	435	Weatherly, J. W.	263
Schell, D. M.	417	Weaver, R. L.	79, 120
Schnell, R. C.	119, 694, 695, 708, 751	Webb, P.-N.	508
Schweger, C.	644	Weidner, G. A.	58, 220, 223
Scvortzov, I. D.	468	Weingartner, T.	338

Wendler, G.	192, 231, 320
Wettlaufer, J. S.	331
Whalen, S. C.	370
Wharton, R. A., Jr.	502
White, R. G.	460
Wiles, G. C.	617
Williams, R. S., Jr.	44, 88, 518
Winchester, J. W.	707
Wollenburg, I. R.	668
Woods, A. W.	748
Wright, D. G.	291
Xie, Z.	243
Yamato, M.	720
Yanitsky, P. A.	535
Yarie, J.	390, 436
Yarosh, V. V.	452
Young, R. B.	384
Zablotsky, G. A.	205
Zachek, A.	325
Zadonskaya, T. A.	452
Zhang, T.	505
Zimov, S. A.	411, 416
Zimova, G. M.	416
Zwally, H. J.	22, 35, 263